OCS Study
BOEM 2022-XX

Passive Acoustic Monitoring Program for the Northern Gulf of Mexico – Project Report (Draft)

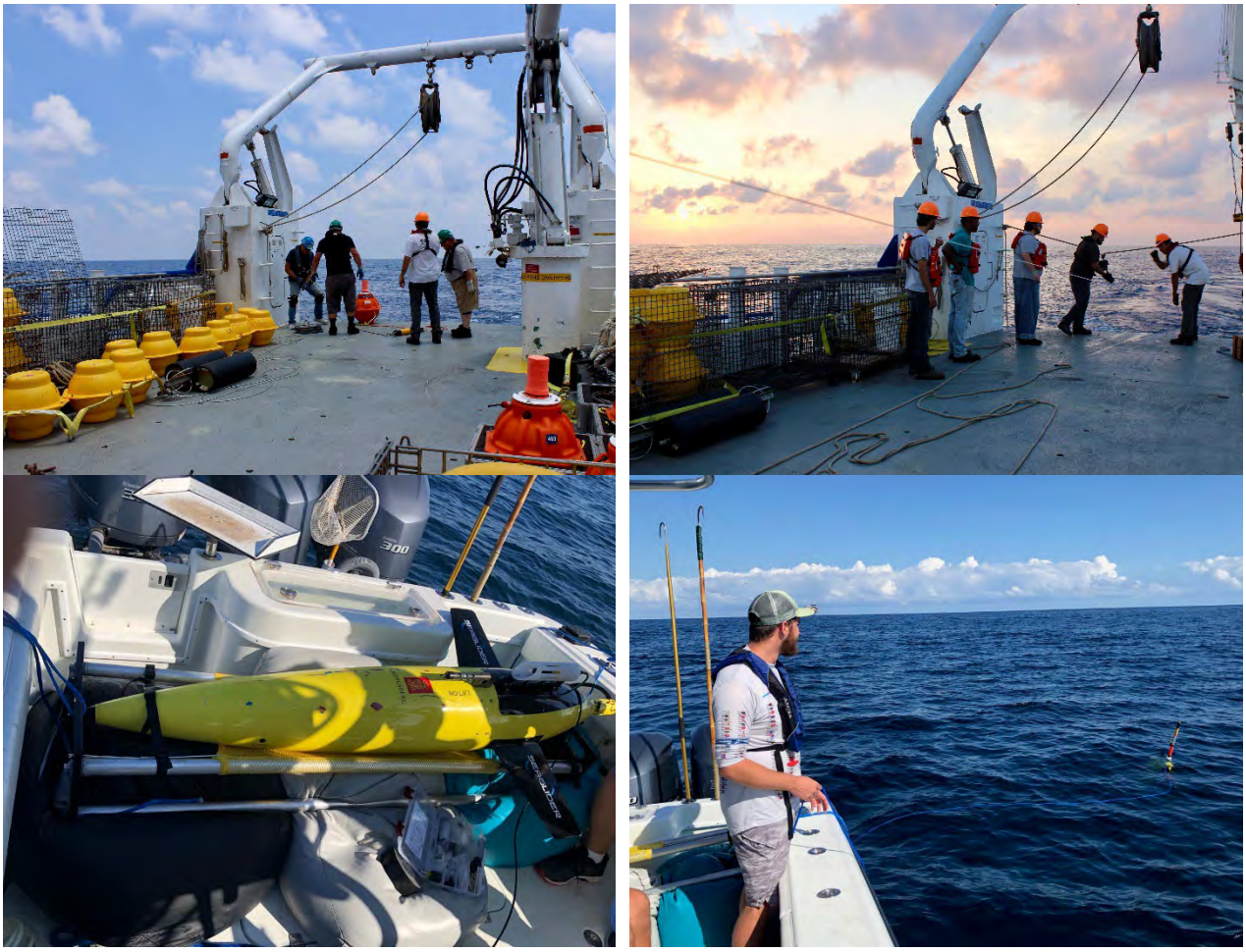

U.S. Department of the Interior
Bureau of Ocean Energy Management
Office of Renewable Energy Programs

BOEM
Bureau of Ocean Energy Management

OCS Study
BOEM 2022-XX

Passive Acoustic Monitoring Program for the Northern Gulf of Mexico – Project Report (Draft)

January 2022

Authors (in alphabetical order):
Jennifer Amaral
Kristen Ampela
Helen Bailey
Robert Bell
Keshab Bhattarai
Mark Deakos
Peter Dugan
Adam Frankel
Selene Fergosi
Anwar Khan
Holger Klinck
Naomi Mathew
James Miller
David Mellinger
Aaron Rice
Dimitri Ponirakis
Gopy Poty
Natalia Sidorovskaia
Ying-Tsong Lin
Lora Van Uffelen

Prepared under BOEM Award
Contract No. M17PC00001
Task Order Nos. M17PD00011 and 140M0119F0001
By
HDR
300 N. Madison Street
Athens, AL 35611

U.S. Department of the Interior
Bureau of Ocean Energy Management
Office of Renewable Energy Programs

BOEM
Bureau of Ocean Energy Management

DISCLAIMER

Study concept, oversight, and funding were provided by the U.S. Department of the Interior, Bureau of Ocean Energy Management (BOEM), Environmental Studies Program, Washington, DC, under Contract Number M17PC00001, Task Order Nos. M17PD00011 and 140M0119F0001. This report has been technically reviewed by BOEM, and it has been approved for publication. The views and conclusions contained in this document are those of the authors and should not be interpreted as representing the opinions or policies of the U.S. government, nor does mention of trade names or commercial products constitute endorsement or recommendation for use.

REPORT AVAILABILITY

To download a PDF file of this report, go to the U.S. Department of the Interior, Bureau of Ocean Energy Management Data and Information Systems webpage (http://www.boem.gov/Environmental-Studies-EnvData/), click on the link for the Environmental Studies Program Information System (ESPIS), and search on 2022-xxx. The report is also available at the National Technical Reports Library at https://ntrl.ntis.gov/NTRL/.

CITATION

HDR. 2022. Passive Acoustic Monitoring Program for the Northern Gulf Of Mexico – Project Report, Prepared for the U.S. Department of the Interior, Bureau of Ocean Energy Management, Office of Renewable Energy Programs. Xx p. Report No.: OCS Study BOEM: 2022-XX. Contract No.: M17PC00001.

ABOUT THE COVER

Cover Photos: Deployment of acoustic sensors and environmental monitors in the northern GOM. Courtesy of HDR GOM PAM Program Team.

ACKNOWLEDGMENTS

As the BOEM Contracting Officer's Technical Representative, Dr. Tre Glenn provided important guidance and critical support to the HDR Project Delivery Team throughout the contract period. His support and assistance are gratefully acknowledged.

The contractor Project Delivery Team was led by HDR Program Manager Anwar Khan. The following Principal Investigators directed and guided monitoring and data analyses:

Rockhopper	Dr. Holger Klinck, Director, K. Lisa Yang Center for Conservation Bioacoustics, Cornell Lab of Ornithology, Cornell University
EARS	Dr. Natalia Sidorovskaia, Coca-Cola/BORSF Endowed Professor of Physics and Chairperson, Director of Littoral Acoustic Demonstration Center – Gulf Ecological Monitoring and Modeling Consortium, Physics Department, University of Louisiana at Lafayette
SHRU VLAs	Dr. Ying-Tsong Lin, Associate Scientist with Tenure, Applied Ocean Physics & Engineering Department, Woods Hole Oceanographic Institution
Playback Experiment	Dr. Ying-Tsong Lin, Associate Scientist with Tenure, Applied Ocean Physics & Engineering Department Woods Hole Oceanographic Institution
Seaglider™	Dr. David Mellinger, Professor (Senior Research), Oregon State University
Seaglider™	Dr. Lora Van Uffelen, Assistant Professor, Ocean Engineering, University of Rhode Island
Field Team Leader	Sean Griffin, Proteus Technologies LLC
Phase 1 Data Analyses	Dr. James Miller and Dr. Gopu Potty, Professors, Department of Ocean Engineering, University of Rhode Island
Phase 2 Data Analyses	Dr. Adam Frankel, Marine Acoustics, Inc.
Reporting and Data Archiving	Dr. Helen Bailey, Research Professor, University of Maryland Center for Environmental Science

Each PIs was supported by a team of scientists and technical experts. Institutional affiliations for key team members are shown on the next page.

Cruise vessels were provided by the Louisiana Universities Marine Consortium's DeFelice Marine Center, Cocodrie, Louisiana.

Assistance and support from all Principal Investigators and team members are greatly appreciated.

Project Delivery Team Member Affiliations	
Jennifer Amaral	Marine Acoustics, Inc.
Kristen Ampela	HDR EOC
Helen Bailey	University of Maryland Center for Environmental Science
Robert Bell	University of Maryland Center for Environmental Science
Keshab Bhattarai	University of Louisiana at Lafayette
Mark Deakos	HDR EOC
Peter Dugan	K. Lisa Yang Center for Conservation Bioacoustics, Cornell Lab of Ornithology, Cornell University
Adam Frankel	Marine Acoustics, Inc.
Selene Fergosi	Oregon State University
Anwar Khan	HDR EOC
Holger Klinck	K. Lisa Yang Center for Conservation Bioacoustics, Cornell Lab of Ornithology, Cornell University
Naomi Mathew	University of Louisiana at Lafayette
James Miller	University of Rhode Island
David Mellinger	Oregon State University
Aaron Rice	K. Lisa Yang Center for Conservation Bioacoustics, Cornell Lab of Ornithology, Cornell University
Dimitri Ponirakis	K. Lisa Yang Center for Conservation Bioacoustics, Cornell Lab of Ornithology, Cornell University
Gopu Potty	University of Rhode Island
Natalia Sidorovskaia	University of Louisiana at Lafayette
Ying-Tsong Lin	Woods Hole Oceanographic Institution
Lora Van Uffelen	University of Rhode Island

Contents

List of Figures

List of Photographs

List of Tables

List of Abbreviations and Acronyms

3D	three-dimensional
ADEON	Atlantic Deepwater Ecosystem Observatory Network
AIS	Automatic Identification System
BIAS	Baltic Sea Information on the Acoustic Soundscape
BOEM	Bureau of Ocean Energy Management
BSEE	Bureau of Safety and Environmental Enforcement
CF	center frequency
CPA	closest point of approach
CSAC	Chip Scale Atomic Clock
CTD	Conductivity/Temperature/Depth
dB	decibel(s)
dB re 1 µPa	decibels referenced to 1 microPascal
EA	environmental assessment
EARS	Environmental Acoustic Recording System
EEZ	Exclusive Economic Zone
ESA	Endangered Species Act
FFVS	free field voltage sensitivity
FLAC	Free Lossless Audio Codec
ft	foot
GAM	generalized additive models
GB	gigabyte
GOM	Gulf of Mexico
GPS	Global Positioning System
GUI	Graphic User Interface
HF	high frequency
Hz	Hertz
IF	intermediate frequency
kHz	kilohertz
km	kilometer(s)
LADC	Littoral Acoustic Demonstration Center
LED	light-emitting diode
L_{eq}	equivalent sound level
LF	low frequency
LTSA	long-term spectral average
m	meter(s)
MF	mid frequency
MMPA	Marine Mammal Protection Act
MP	Monitoring Project
M/V	Motor Vessel
NCEI	National Centers for Environmental Information
nm	nautical mile(s)
NMFS	National Marine Fisheries Service

NOAA	National Oceanic and Atmospheric Administration
NUWC	Naval Undersea Warfare Center
PAM	Passive Acoustic Monitoring
PK	Peak Sound Pressure Level
Program	GOM PAM Program
PSD	power spectral density
psi	pounds per square inch
QA/QC	Quality Assurance/Quality Control
RH	Rockhopper
RL	received level
rms	root-mean square
R/V	Research Vessel
SEL_{cum}	Cumulative Sound Exposure Level
SHRU	Several Hydrophone Recording Unit
SL	source level
SPL	Sound Pressure Level
TB	terabyte
TL	transmission loss
µPa	microPascal
U.S.	United States
VHF	very high frequency
VLA	vertical line array

Executive Summary

Results from analyses of an approximately 24-month underwater Passive Acoustic Monitoring (PAM) dataset collected from a strategically delineated 100- by 200-kilometer study area in the northern Gulf of Mexico (GOM) are presented and discussed in this report. Recommendations for continuing the two-year monitoring in future years and expanding program objectives to beyond soundscape characterization are also presented.

Underwater acoustic data were collected using a mix of stationary and mobile platforms under Bureau of Ocean Energy Management's (BOEM) GOM PAM Program (Program), the primary objective of which was to design and field test implementation of a large-scale, multi-year, underwater PAM program in the region. The primary purpose of the 2-year data collection and analyses was to characterize the existing soundscape (including sounds contributed by both natural and anthropogenic sources) in the GOM. Since the northern GOM is characterized by complex bathymetry, it was important to better understand the influence of prominent geological features such as canyons on the soundscape. Therefore, a site-specific three-dimensional (3D) underwater sound propagation numerical model was setup. Simulation outputs were used to assess sound focusing and defocusing effects caused by 3D variations in underwater bathymetry.

The experimental design targeted collection of underwater acoustic data in the 10 Hertz (Hz) to 96 kilohertz (kHz) frequency range. This frequency range encompassed the most common anthropogenic and natural sounds that contribute to the existing soundscape in the GOM; namely, those related to weather, the oil and gas industry, shipping, marine mammals, and fish. Given the potential for follow-on marine mammal studies, this bandwidth also allows for detection of sounds produced by mysticete whales and most odontocetes, including deep diving whales such as pygmy (*Kogia breviceps*) and dwarf (*Kogia sima*) sperm whales and beaked whales, and lower frequency components of *Kogia* spp.

The study area included portions of the underwater Mississippi and DeSoto Canyons. Both canyons are populated by deep diving marine mammals and exhibit unique acoustic propagation features. While both canyons were determined to be viable candidates for data collection, the Mississippi Canyon was preferentially selected as the focus area for monitoring primarily because it provided broad industrial source representation, including seismic exploration surveys, oil production platforms, remotely operated vehicle maintenance, and pipeline installation along axis and on both eastern and western slopes.

A systematic random design, which ensured that survey effort was evenly distributed over the study area while avoiding underwater infrastructure, was selected for placement of data recorders. Data were collected at depths ranging from 53 to 2,148 meters (m) within the main habitat types in the region, including the continental shelf (less than 200 m deep), continental slope (200 to 1,600 m deep), and the abyssal plain (greater than 1,600 m deep).

Three different types of stationary moorings equipped with sensors (hydrophones) and recording systems were used, namely Rockhoppers and Environmental Acoustic Recording Systems, both with effective recording bandwidth ranging from 10 Hz to 96 kHz; and Chip Scale Atomic Clock-Several Hydrophone Recording Unit vertical line arrays, with effective recording bandwidth of 10 Hz to 4.5 kHz. Additionally, two separate mobile autonomous platforms (Seaglider™), with an effective recording bandwidth of 10 Hz to 62.5 kHz, were also deployed within selected portions of the study area to collect data in between the stationary moorings within the Mississippi Canyon and to cover selected areas in the DeSoto Canyon. A shipboard playback experiment for measuring sound transmission loss was also conducted to gather data for characterization of underwater sound propagation properties.

Data were analyzed using standardized software packages and acoustic metrics to provide data products consistent with guidelines adopted by the Baltic Sea Information on the Acoustic Soundscape Project as well as the Atlantic Deepwater Ecosystem Observatory Network Project. Results indicated that the key dominant sound sources recorded during this study varied seasonally and primarily consisted of seismic surveys, shipping, storms, and marine mammal calls. Key observations from the data analyses are summarized below:

- There was a noticeable difference in recorded low frequency levels (less than 100 Hz) between the recorders deployed at the shelf break versus offshore locations. Low-frequency levels observed at offshore sites were significantly higher and appear to be driven by seismic airgun activities that occurred in closer proximity. Also, high frequency levels (greater than 1,000 Hz) were higher and more variable during the winter months. This was likely related to higher variability in weather conditions and associated sea states.
- Observed noise levels at the deep-water sites were comparable to those previously reported and are indicative of extensive industry-related sound from oil and gas operations in the northern GOM. Seismic airgun noise contributed to elevated sound levels across multiple years.
- The deep-water monitoring locations exhibited similar sound pressure level distributions in values and frequencies and in general are consistent with the levels previously measured in this region of the GOM.
- In general, deeper locations appeared to have the highest sound pressure levels at the low frequency bands (below 100 Hz) and the lowest sound pressure levels at the mid frequency bands (500 to 10,000 Hz).
- On a seasonal basis, levels at frequencies greater than 1,000 Hz were higher and more variable during the winter months. This was likely related to higher variability in weather conditions and associated sea states.
- While airgun noises were the most dominant anthropogenic sound source in the acoustic environment, other sources, including vessel-related noise, also contributed to the levels below 1 kHz.
- Biological sounds (dolphin whistles, sperm whale clicks, Risso's dolphin clicks, and beaked whale clicks) were present throughout all deployments.
- As expected, the analyses also revealed a strong relationship between a vessel's closest point of approach and measured low-frequency sound levels, indicating that ship Automatic Identification System (AIS) data is useful for predicting low-frequency noise in the GOM. There was a strong seasonal pattern in vessel activity, with most vessel detections occurring in summer months. Month and year for airgun signal detections had similar patterns to that of vessel detections. Latitude and longitude effects for airgun signals were borderline statistically significant, with a dip in the frequency of airgun detections in the middle latitudes and a higher frequency of signal detection in the middle longitudes.
- There were also notable differences between the soundscapes of the Mississippi and DeSoto Canyons, largely as a result of the generally lower anthropogenic activity in the latter.
- The multi-year study spanned from 2018 to 2020, documenting interannual variation and changes in the soundscape that occurred likely as a result of anthropogenic activity restrictions related to the COVID-19 pandemic.

The 3D underwater sound propagation model established by this study provided valuable data for capturing and understanding focusing and defocusing effects due to 3D variations in bathymetry. These effects can meaningfully intensify or decrease local ambient noise levels, potentially influencing localized

impacts to marine mammals. Incorporation of advanced 3D sound propagation modeling is recommended for future Program phases, particularly within complex topographic regions; this would provide valuable data to better understand and account for important acoustic effects. Model simulation output would help answer important questions such as "Do marine mammals preferentially occupy (in the sense of vocal activity) high transmission loss (lower intensity) regions to avoid potential anthropogenic sounds?"

An important legacy of the GOM PAM Program is the robust, 2-year underwater calibrated acoustic dataset that was collected in the field and some of the analytical tools that were developed to further the soundscape characterization data analysis. Approximately 250 terabytes of raw data were collected during the Program, and these were appropriately packaged and submitted to the National Oceanic and Atmospheric Administration's National Centers for Environmental Information (NCEI) for archiving. After NCEI completes archiving of the raw data on its servers, it is anticipated that they will provide public access to the data along with searching and visualization tools.

Since the primary Program objective was to collect data for underwater soundscape characterization, field data collection protocols (especially placement of recorders) were customized to collect data to meet the defined objective. However, if BOEM's overall goal is to generate comprehensive data that will be useful for managing present and future anthropogenic activities in the region, future Program initiatives should be expanded beyond soundscape characterization to also include collecting and analyzing data for the following purposes:

- Evaluation of marine mammal vocalization data for characterizing spatial and temporal distribution of selected mammalian species and modeling spatial and temporal patterns of marine mammal acoustic activity and density estimations for selected species of interest.
- Estimation of impacts of anthropogenic sounds on marine mammals and other species.
- Monitoring long-term trends in soundscapes and marine mammal density.

Conceptual ideas for achieving these additional Program objectives are presented in this report.

The data, results, conclusions, and recommendations presented in this report were generated for BOEM by the HDR Program Team under IDIQ Contract M17PC00001, Task Order Nos. M17PD00011 and 140M0119F0001.

1 Introduction

This report contains results and recommendations from an evaluation of underwater acoustic data that were collected and analyzed under the Bureau of Ocean Energy Management's (BOEM) Passive Acoustic Monitoring (PAM) Program for the northern Gulf of Mexico (GOM). The northern GOM is a highly industrialized environment with multiple anthropogenic sound sources, including shipping, oil and gas activities, and military operations. Noise impacts to protected species (primarily cetaceans) may occur as a result of oil and gas exploration companies undertaking activities (e.g., seismic surveys, platform decommissioning, drilling, vessel noise) licensed by BOEM and the Bureau of Safety and Environmental Enforcement (BSEE). However, characterizing the impacts and trends is difficult without comprehensive baseline data on the noise environment in the GOM.

Also, BOEM and BSEE are required to assess potential impacts on protected species, specifically under the Marine Mammal Protection Act (MMPA), Endangered Species Act (ESA), and National Environmental Policy Act to assist and guide their decision making. The future BOEM MMMPA rulemaking for seismic activities in the GOM will have a monitoring requirement associated with it, including data collection on ambient noise and on noise associated with seismic activities. **In short, there was an urgent need to implement a systematic and comprehensive underwater acoustic data collection effort in the northern GOM. BOEM's GOM PAM Program (Program) was intended to collect and analyze data to meet this need.**

1.1 GOM PAM Program Objectives

The primary objective of the Program was to **design and field test** implementation of a large-scale, multi-year, PAM effort in the northern GOM. The Program was initiated in 2017 and the first two years of data collection (mid-2018, 2019, and mid-2020) and analyses were focused on collecting data primarily for soundscape characterization (including sounds contributed by both natural and anthropogenic sources). This 2-year dataset will serve as a reference point for follow-on efforts to characterize changes in the soundscape of the area over time.

Also, the underwater soundscape is significantly influenced at different scales by three-dimensional (3D) sound propagation (Duda et al. 2011; Ballard et al. 2015; Heaney and Campbell 2016; Reilly et al. 2016; Oliveira and Lin 2019; Reeder and Lin 2019; and Oliveira et al. 2021). Physical oceanographic and geological conditions associated with continental shelves and shelf break areas can cause horizontal heterogeneity in medium properties, so horizontal reflection/refraction of sound can occur and produce significant 3D sound propagation effects. These propagation effects can constructively or destructively interfere with sound as it travels from source to receiver. Constructive interference can lead to areas of focused sound energy and extended propagation/detection ranges, while destructive interference can result in areas of shadowing and reduced ranges.

Since the northern GOM is characterized by two large canyons (Mississippi and DeSoto), it was important to better understand the influence of these prominent geological features on the soundscape. Therefore, data collected during the first 2 years were also used to establish a site-specific 3D underwater sound propagation numerical model. Model simulation outputs were used to assess sound focusing and defocusing effects caused by 3D variations in underwater bathymetry.

In the future, besides continuing data collection and analyses for soundscape characterization, Program objectives could be expanded to include collecting and analyzing data for estimating current marine mammal occupancy and (call) density, supporting the estimation of impacts of anthropogenic sounds on

marine mammals and other species of concern, and monitoring long-term trends in soundscapes and marine mammal density.

The initial 2-year Program was implemented as two back-to-back 12-month Monitoring Projects (MP):

- **2018 MP** – Acoustic monitoring was conducted within a 100- by 200-kilometer (km) study area box located in the northern GOM for the 12-month period from May 2018 to April 2019. Two separate deployments were conducted, the first from May to October 2018 (designated as Deployment 1) and the second from November 2018 to April 2019 (Deployment 2). The 2018 MP is also referred to as the Program Pilot Study in other Program documentation.[1]
- **2019 MP** – Monitoring initiated under the 2018 MP was continued for an additional 12 months (May 2019 to April 2020) under this MP.[2] Lessons learned from the 2018 MP were used to guide delineation of the study area boundaries and placement of sensors for the 2019 MP. The study area for this MP was a subset of the 2018 MP study area and measured approximately 100- by 140 km. Two separate deployments were conducted, the first from May to October 2019 (designated as Deployment 3) and the second from November 2019 to April 2020 (Deployment 4).

This report contains results and recommendations from evaluation of the approximately 24 months of data collected under the two MPs.

1.2 2018 and 2019 Monitoring Project Objectives

The experimental data collection and analysis design for both MPs targeted collection of underwater acoustic data in the 10 Hertz (Hz) to 96 kilohertz (kHz) frequency range (HDR 2018, 2019). This frequency range encompasses the most common anthropogenic and natural sounds that contribute to the existing soundscape in the GOM; namely, those related to weather, the oil and gas industry, shipping, marine mammals, and fish. Given the potential for follow-on marine mammal studies using data collected under the two MPs, this bandwidth also allows for detection of sounds produced by mysticete whales and most odontocetes, including deep diving whales such as pygmy (*Kogia breviceps*) and dwarf (*Kogia sima*) sperm whales and beaked whales, and lower frequency components of *Kogia* spp.

A suite of underwater acoustic sensors and recorders were deployed at strategically selected locations within the delineated study area(s) to collect data for meeting Program objectives. Data were analyzed using standardized software packages to provide data products consistent with guidelines adopted by the Baltic Sea Information on the Acoustic Soundscape (BIAS) Project as well as the Atlantic Deepwater Ecosystem Observatory Network (ADEON) Project (Ainslie et al. 2017). Data analyses were focused on producing outputs to support the primary objective (i.e., soundscape characterization). In future Program phases, data and data products from the two MPs may also be used for other purposes, such as:

- Guide continuation of soundscape characterization data collection and analyses in the northern GOM
- Expand data collection outside of the study area covered under the two MPs

[1] Implementation of the 2018 MP was covered under BOEM Contract No. M17PC00001, Task Order No. M17PD00011.

[2] Implementation of the 2019 MP was covered under BOEM Contract No. M17PC00001, Task Order No. 140M0119F0001.

- Develop and test additional approaches for synthesizing and evaluating data collected across different types of PAM platforms (both stationary and mobile)
- Identify strategies to optimize and increase robustness of the data collection and analyses methods during future years of monitoring
- Characterize spatial variations and contribution to soundscapes in the enclosed and surrounding Mississippi Canyon habitats, including the continental shelf, continental slope, and abyssal plain
- Characterize variations in soundscapes over multiple temporal scales, including diel, lunar, and seasonal periods
- Estimate contributions of anthropogenic sounds to the Mississippi Canyon and vicinity soundscape
- Describe biological sources of sound present in the Mississippi Canyon and vicinity across the frequency spectrum from 10 to 100 kHz
- Evaluate marine mammal vocalization data
- Establish how sound propagation influences soundscapes in the various Mississippi Canyon habitats

1.3 Study Area

The GOM is a semi-enclosed ocean basin that narrowly connects to the Atlantic Ocean through the opening between Cuba and the Yucatán Peninsula and the Florida Straits. The presence of the Loop Current and warm water eddies separated from the Loop Current are dominant oceanographic features of the GOM that considerably influence the GOM ecosystem/seascape. The Western Planning Area lies 17 km (9 nautical miles [nm]) offshore of Texas and extends to the United States (U.S.) Exclusive Economic Zone (EEZ), which is the jurisdictional limit over the continental shelf (**Figure 1**). The EEZ limit is 370 km (200 nm) from the U.S. coast. The Central Planning Area lies offshore of Alabama, Mississippi, and Louisiana from 6 km (3 nm) to the U.S. EEZ. The Eastern Planning Area lies 17 km (9 nm) offshore of the Gulf Coast of Florida and extends to the EEZ. The water depths in the Western, Eastern, and Central Planning Areas extend up to approximately 3,346 meters (m) (BOEM 2013).

When monitoring the natural environment because of time and resource limitations it is usually not possible to exhaustively survey the entire area of interest. Therefore, in consultation with BOEM, a representative subset of the northern GOM, which was centered on the underwater Mississippi and DeSoto Canyons, was delineated for data collection and analyses. Both shallow and deeper areas within the delineated study area were targeted for data collection.

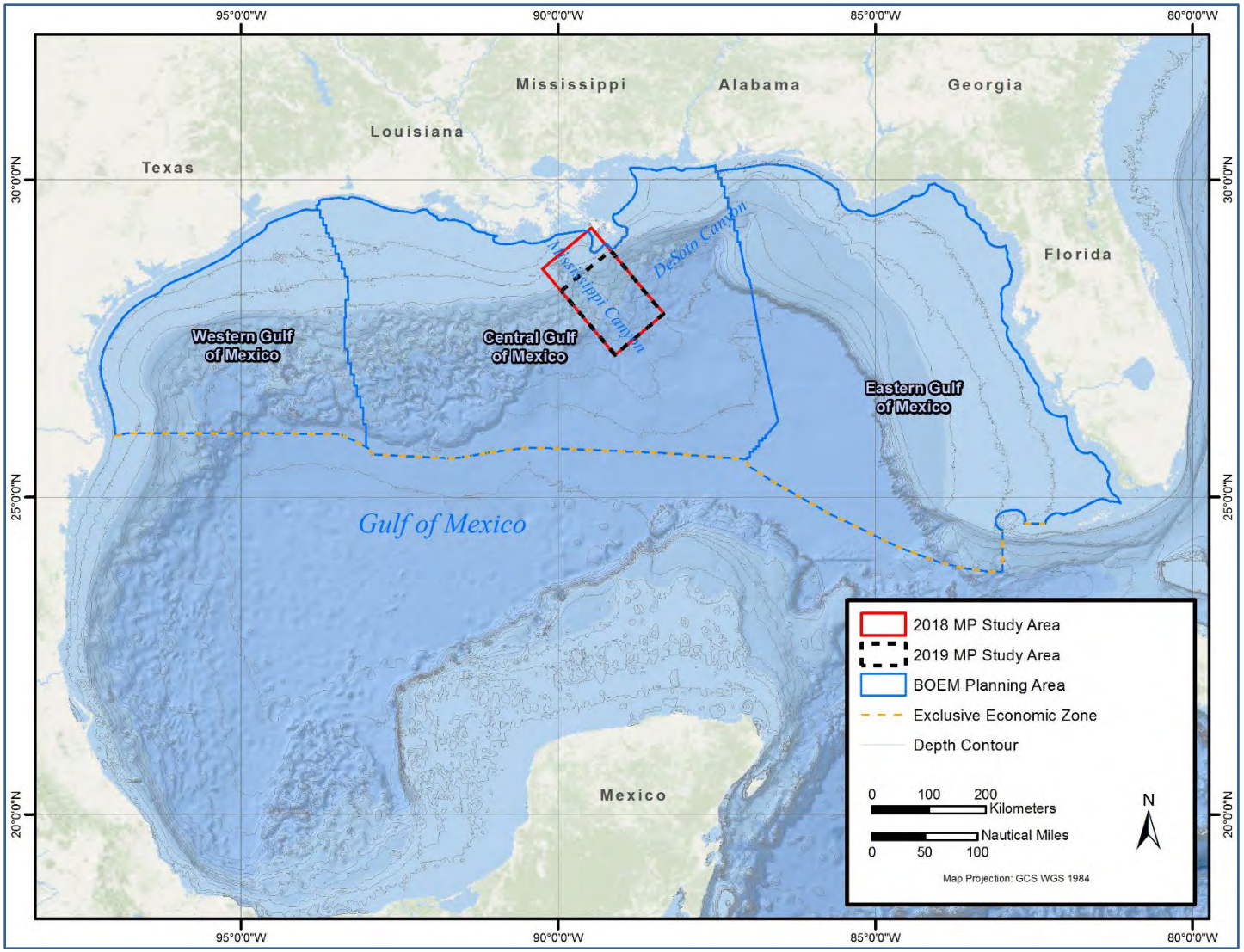

Figure 1. Northern GOM BOEM's Planning Areas and GOM Program 2018 and 2019 MP study areas

The Mississippi Canyon is located directly south of New Orleans within BOEM's Central Gulf Planning Area. The DeSoto Canyon, which straddles the Central and Eastern Planning Area boundaries, is located south of Mobile and Pensacola Bays. Both canyons are populated by deep diving marine mammals and exhibit unique acoustic propagation features. Each canyon is characterized by three separate and unique ecosystems, namely the continental shelf (less than 200 m deep), the continental slope (200 to 1,600 m deep), and the abyssal plain (greater than 1,600 m deep).

While both canyons were determined to be viable candidates for data collection to meet the overall Program and Project objectives, the Mississippi Canyon was preferentially selected as the focus area for both MPs for the following reasons:

- The Mississippi Canyon provides broad industrial source representation, including seismic exploration surveys, oil production platforms, remotely operated vehicle maintenance, and pipeline installation along axis and on both eastern and western slopes. The DeSoto Canyon has some limited industrial activity along its western slope, but almost none towards the center and eastern half.
- PAM has been active in the Mississippi Canyon since 2001 by Cornell University, the Littoral Acoustic Demonstration Center (LADC), the GOM Research Initiative, the National Oceanic and Atmospheric Administration (NOAA), the Sperm Whale Acoustic Monitoring Program, and the Sperm Whale Seismic Study. Availability of these historical multi-decadal datasets was important because they served to validate data collected under the Program.
- The DeSoto Canyon is larger in dimensions than the Mississippi Canyon and would require additional bottom moorings for equivalent planned sensor coverage. The smaller canyon dimension of the Mississippi Canyon also implies a more localized and therefore more targetable concentration of deep-diving whales.
- The Mississippi Canyon experiences a significantly greater exposure to shipping noise than the DeSoto Canyon.
- Given the proximity to elevated anthropogenic noise, the Mississippi Canyon is expected to deliver a more spectrally uniform soundscape. The anthropogenic contribution to the DeSoto Canyon soundscape likely will be dominated by the lower frequencies because of distant source propagation. Mid- and high-frequency anthropogenic sources (such as oil platform remotely operated vehicle control/communication) are expected to be less prevalent in the DeSoto Canyon.
- There is an extensive network of meteorological buoys and industrial platforms in the Mississippi Canyon, which can provide corroborative data for analyses and interpretation of weather-related noise trends.
- The Mississippi Canyon experiences a greater influx of fresh water from the Mississippi River. This may play a role in biological soundscapes.

For the 2018 MP, an approximately 100- by 200-km study area box overlapping the Mississippi Canyon was delineated as the 2018 MP study area (**Figure 1**). One of the key lessons learned from analyses of data collected and evaluated under the 2018 MP was that collecting underwater acoustic data using stationary platforms in coastal, shallow-water areas entailed a high risk of expensive monitoring platforms (and accompanying data) being accidently damaged and/or permanently lost due to heavy shipping traffic, including fishing trawlers and/or industrial activities.

In consultation with BOEM, it was therefore decided that for the 2019 MP, shallow-water areas within the 2018 MP study area box less than 100 m would be avoided. The 2019 MP study area was therefore delineated by truncating the shallow-water areas to the north, as shown in **Figure 1**. The 2019 MP study area box measured approximately 100- by 140-km. The goal was to ensure that, barring unforeseen

circumstances and to the extent practicable, a complete data set would be generated for the second 12-month monitoring period.

Marine mammals known to inhabit the study area and its surrounding environment include the Atlantic spotted dolphin (*Stenella frontalis*), bottlenose dolphin (*Tursiops truncatus*), Clymene dolphin (*Stenella clymene*), Fraser's dolphin (*Lagenodelphis hosei*), pantropical spotted dolphin (*Stenella attenuata*), rough-toothed dolphin (*Steno bredanensis*), spinner dolphin (*Stenella longirostris*), striped dolphin (*Stenella coeruleoalba*), false killer whale (*Pseudorca crassidens*), killer whale (*Orcinus orca*), melon-headed whale (*Peponocephala electra*), long- and short-finned pilot whale (*Globicephala melas* and *G. macrorhynchus*), Risso's dolphin (*Grampus griseus*), beaked whales (Ziphiidae), pygmy and dwarf sperm whale, sperm whale (*Physeter macrocephalus*), and fin whale (*Balaenoptera physalus*).

Additionally, the DeSoto Canyon is home to a genetically distinct resident population of Bryde's whales (*Balaenoptera edeni*), which appears to have fewer than 100 individuals remaining (NOAA Fisheries 2018). This species was listed as endangered in May 2019 under the ESA (84 *Federal Register* 15446). Because the DeSoto Canyon is a Biologically Important Area for Bryde's whales, data collection under the 2018 MP was extended to include selected portions of the DeSoto Canyon.

1.4 Literature Review

Prior to developing an experimental design for the 2018 MP implementation, a comprehensive literature review was conducted to identify and evaluate available relevant data from previous GOM underwater soundscape characterization efforts (Latusek-Nabholz et al. 2020). The search also included assessment of existing tools and methodologies for acoustic source detection, localization, tracking, and classification. For the literature data review, low, medium, and high underwater noise frequencies were defined as follows:

- **Low frequency** (**LF**)generally includes sounds in the bandwidths between 10 and 500 Hz. This category is primarily composed of anthropogenic sources, including commercial shipping, followed by seismic sources. However, fish also generate low-frequency sound and can make up a large part of this spectrum for natural ambient noise. The most common way fish produce sounds is by grinding or strumming using musculoskeletal anatomy around the swim bladder. Fish can chorus together and increase the amount of noise in the low-frequency band by as much as 30 decibels (dB) (Hildebrand 2009). Under the right conditions, low-frequency sounds can travel across ocean basins because they propagate over long ranges. Shipping noise has increased more than 12 dB as shipping across the globe has expanded. Over the years, oil exploration and construction has expanded into deeper waters and increased the production of seismic sounds.
- **Medium frequency** (**MF**)generally includes sounds from 500 Hz to 25 kHz. This category includes natural sources of sound such as sea-surface agitation, including breaking waves, spray, bubble formation and collapse, and rainfall. Heavy precipitation can increase noise levels in this range by as much as 14 dB. Biological sources in the medium-frequency range include snapping shrimp. When snapping shrimp (*Alpheus* spp.) are present and actively producing sound, they can also increase the amount of noise by 20 dB. Medium-frequency sounds are more local or regional in nature, as they do not propagate over long distances. Noise associated with military and small vessels also fall in this range.
- **High frequency** (**HF**)generally includes sounds above 25 kHz and are generally located close to the receiver. Mapping sonars and thermal noise, the result of particles moving close to the hydrophone for instance, are included in this category.

Appendix A contains a copy of the *Literature Synthesis Report*. Key findings from the review are summarized below:

- Over 30 PAM projects have been conducted in the GOM since 1991. Nine of these studies were specifically designed to gather data on noise in the GOM, while the other 21 studies were designed to gather information on marine mammals. Most data collection efforts focused primarily upon the eastern and central GOM. Additionally, PAM surveys have tended to focus on waters of the continental shelf and slope down to approximately 2,000 m deep; only two surveys covered the abyssal plain, which is also an important biological habitat, extending to approximately 3,200 m.
- The GOM soundscape is characterized by a mix of sounds from both anthropogenic and natural sources. Anthropogenic sounds are primarily associated with navigation, industrial, and military activities. Major sources are categorized logarithmically in **Table 1**. Natural sources include bio-acoustic sounds, earthquakes, wind/waves, rainfall, and thermal agitation of the seawater. Of all the natural sounds, marine mammal calls are of particular interest. Frequency ranges of marine mammal calls in the GOM are shown in **Table 2**. The two different types of sound sources are quantitatively compared in **Figure 2**.
- There are three major anthropogenic contributors to the underwater soundscape in the GOM, namely ship traffic, seismic surveys, and oil drilling activity. Noise from ship traffic is one of the major anthropogenic sources of sound in the GOM, and it includes a variety of sources, including noise related to engines, thrusters, civilian commercial sonar, and other equipment in commercial shipping. Within the delineated study area (**Figure 1**), there are two dominant shipping lanes that form an inverted Y to the north of the Mississippi Canyon. The northeast/southwest-aligned lane runs perpendicular to the shallow northwest canyon origin. The northwest/southeast lane is offset northeast from the canyon and runs nearly parallel to the canyon alignment.

  Seismic surveys are typically conducted using an array of airgun releases that introduce compressed air into the water and create a bubble that generates a pulse of sound sufficiently energetic to penetrate deep beneath the seafloor. A seismic airgun array produces a single, downward-directed, high-energy impulse that is primarily directed downward to map the composition of the seafloor (Gisiner 2016).

  Drilling and production platforms generate a continuous-type sound through transmission of the vibrations of the machinery and drilling equipment such as pumps, compressors, and generators that are operating on the platform. Noise resulting from the drilling operation may include machinery noise, such as that from the drill's drive machinery, including drilling, engine and exhaust, and generator noise. Noise originates from vibration associated with the grinding of rock in the seabed, which can either radiate directly from the drill bit through the rock into the water, or can conduct upwards through the drill shaft, radiating into the surrounding water. Additional noise originates from drill ships and other semi-submersibles that maintain position using dynamically positioned thrusters.
- The Eastern and Central Planning Areas within the GOM have been extensively covered by PAM studies; no stationary sensor deployments have been made in the Western Planning Area. Seventeen distinct sites in the Central Planning Area, and more than 50 distinct sites in the Eastern Planning Area, have been covered. Locations of PAM deployments and studies generally have covered the continental shelf and continental slope waters. The majority of PAM studies in the GOM have been conducted in waters between 0 and 1,500 m and only a few have focused on the deeper waters of the GOM, which include the abyssal plain. Additional data gaps were identified concerning differences in sound propagation modeling predictions and field measurements. For instance, academic researchers have theorized that modeling sound propagation from seismic arrays may overestimate propagation losses (Kearns & West 2015).

More information is also needed to address whether there are discrepancies between modeled and actual propagation losses as measured in the field.

Table 1. Anthropogenic sound sources categorized by logarithmic bandwidth

Frequency Range	Representative Acoustic Sources
1–10 Hz	Ship propellers[1]; explosives
10–100 Hz band	Shipping activities[1]; explosives; seismic surveying sources[1]; construction activities; industrial activities; naval surveillance sonar systems
100–1,000 Hz	Shipping activities[1]; explosives; seismic surveying sources[1]; construction activities; industrial activities; naval surveillance sonar systems
1,000–10,000 Hz	Nearby shipping activities[1]; seismic airguns[1]; underwater communication; naval tactical sonars; seafloor profilers; depth sounders
10,000–100,000 Hz	Underwater communication; naval tactical sonars; seafloor profilers; depth sounders; mine-hunting sonars; fish finders; some oceanographic systems (e.g., acoustic Doppler current profilers)
Above 100,000 Hz	Mine hunting sonar; fish finders; high-resolution seafloor mapping devices (e.g., side-scan sonars, some depth sounders, some oceanographic sonars, and research sonars for small-scale oceanic features)

Key: Hz = Hertz
[1] These sources represent the major noise contributors in the GOM.
Sources: NRC 2003 and Hildebrand 2009

Table 2. Frequency range of marine mammal calls in the GOM

Frequency Range	Mammalian Species
1–10 Hz	
10–100 Hz	Bryde's whale (5), other baleen whales (3, 10, 13, 16, 17, 23)
100–1,000 Hz	Bryde's whale (5), other baleen whales (3, 10, 13, 16, 17, 23)
1,000–10,000 Hz	Sperm whale (26), large delphinid whistles and partial (low-end) clicks (4, 9, 14,15,19, 21, 24), humpback whale (13), minke whale (16), manatee (29)
10,000–100,000 Hz	Beaked whales (2, 7, 12, 25), sperm whale (26), delphinid whistles and clicks (most energy) (1, 4, 6, 11, 14, 15, 18, 19, 21, 22, 24, 27, 28), partial (low-end) clicks, dwarf and pygmy sperm whale (8, 20)
Above 100,000 Hz	Partial (high-end) delphinid clicks, dwarf and pygmy sperm whale (8, 20)

Sources: Rice et al. 2014a; Širović et al. 2014b; Johnson et al. 2006; NOAA Fisheries 2018; Scripps Whale Acoustics Laboratory 2022; Discovery of Sound in the Sea 2022.)
Key: Hz = Hertz

1. Atlantic spotted dolphin – *Stenella frontalis*
2. Blainville's beaked whale – *Mesoplodon densirostris*
3. Blue whale – *Balaenoptera musculus*
4. Bottlenose dolphin – *Tursiops truncatus*
5. Bryde's whale – *Balaenoptera edeni*
6. Clymene dolphin – *Stenella clymene*
7. Cuvier's beaked whale – *Ziphius avirostris*
8. Dwarf sperm whale – *Kogia simus*
9. False killer whale – *Pseudorca crassidens*
10. Fin whale – Balaenoptera physalus
11. Fraser's dolphin – *Lagenodelphis hosei*
12. Gervais' beaked whale – *Mesoplodon europaeus*
13. Humpback whale – *Megaptera novaeangliae*
14. Killer whale – *Orcinus orca*
15. Melon-headed whale – *Peponocephala electra*

16. Minke whale – *Balaenoptera acutorostrata*
17. North Atlantic right whale – *Eubalaena glacialis*
18. Pantropical spotted dolphin – *Stenella attenuata*
19. Pygmy killer whale – *Feresa attenuata*
20. Pygmy sperm whale – *Kogia breviceps*
21. Risso's dolphin – *Grampus griseus*
22. Rough-toothed dolphin – *Steno bredanensis*
23. Sei whale – *Balaenoptera borealis*
24. Short-finned pilot whale – *Globicephala macrorhynchus*
25. Sowerby's beaked whale – *Mesoplodon bidens*
26. Sperm whale – *Physeter macrocephalus*
27. Spinner dolphin (long-snouted) – *Stenella longirostris*
28. Striped dolphin – *Stenella coeruleoalba*
29. West Indian manatee – *Trichechus manatus*

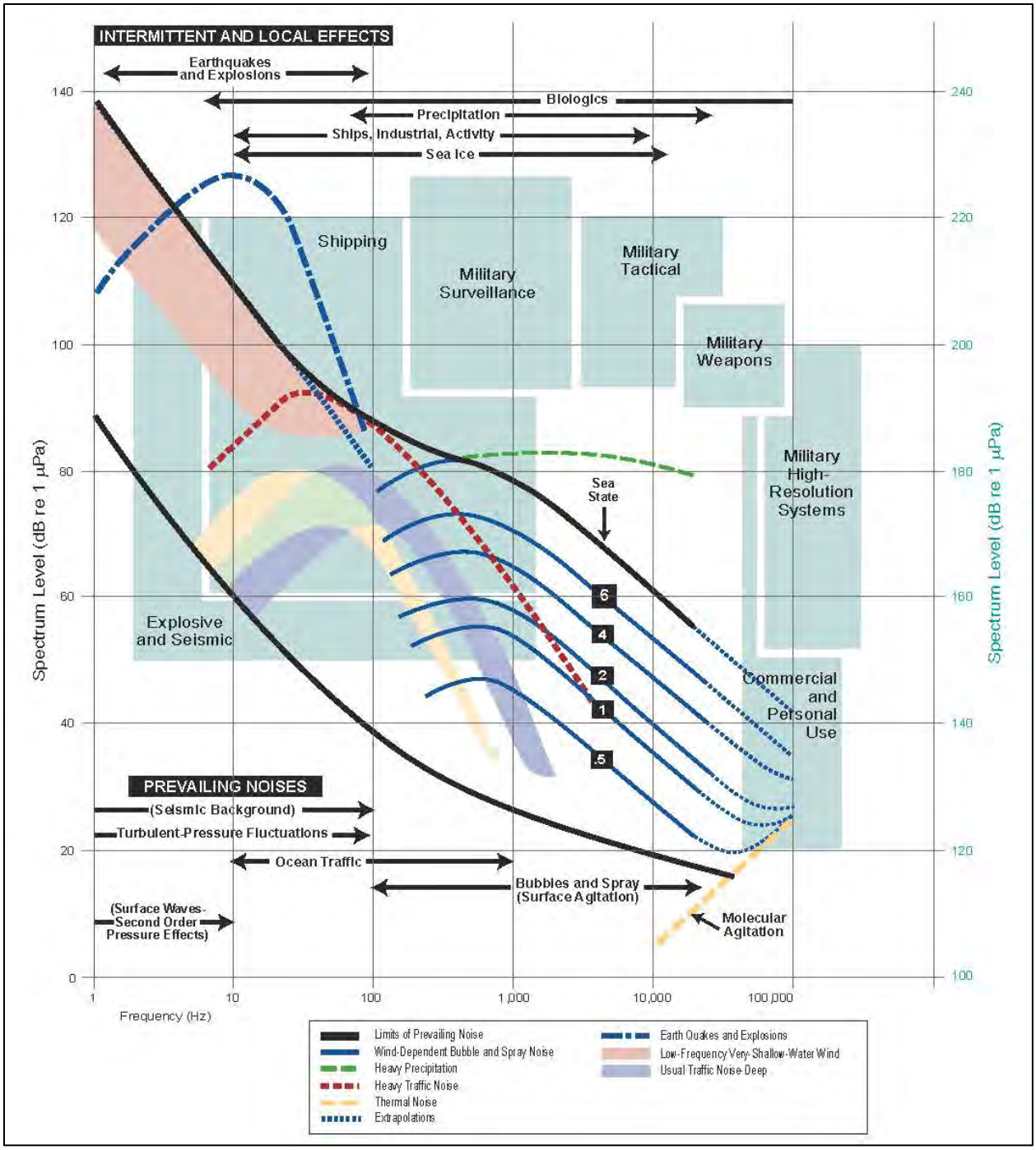

Figure 2. Sources of noise

Notes: Shipping, military, commercial, and personal uses are shown in blue and use the blue spectrum level values on the right axis. These values are 100 dB greater than the values used on the left axis for intermittent, local effects, and prevailing noises. 100 dB corresponds to five orders of magnitude.

Source: Bradley and Stern 2008(based on Wenz 1962; reprinted with permission, *Journal of the Acoustical Society of America*)

1.5 Basic Underwater Acoustic Terminology and Key Metrics

A variety of metrics are used to describe sounds, and these different metrics are not directly comparable. The most common term used to define underwater sound is "sound pressure," which in underwater acoustics is expressed as a basic unit in Pascals. Sound pressure is measured by a hydrophone and recorded using connected electronics. The most common unit used to express sound pressure is the microPascal (µPa).

The pitch of a sound wave is characterized by a frequency content of the wave, which is measured in Hz or thousands of kHz. Frequency is often expressed as low (less than 1 kHz), medium (1 to 10 kHz), and high (greater than 10 kHz). Sounds levels are often presented as dB, which can be defined as:

$$dB = 10 \times \log10 (\text{Sound Pressure}^2 / \text{Reference Sound Pressure}^2)$$

It is critical that the value of the reference pressure be specified. This is the "re" in the common unit decibels referenced to 1 microPascal (dB re 1µPa^2). Sound pressure is often used to characterize continuous sounds in terms of risk of damage to marine animals, such as fish, turtles, and mammals. The root-mean-square (rms) sound pressure and peak sound pressure are the most commonly used sound pressure metrics (Popper et al. 2014). Peak sound pressure is often used to characterize impulsive sounds, is measured as the maximum absolute value of an instantaneous sound pressure during a specific time period and is expressed as dB re 1µPa. The sound exposure level metric is an index of the total energy in a sound received over a chosen time interval and is usually expressed as Sound Pressure Level (SPL) (peak to zero) in dB re 1 µPa^2. This metric can be used to assess risk from exposure to multiple sound sources, as it is an index for accumulated sound energy (Popper et al. 2014).

To assess the exposure of marine mammals to anthropogenic sounds, NOAA's National Marine Fisheries Service (NMFS) recommends specific metrics for establishing acoustic thresholds and predicting impacts of sound sources on marine mammal hearing (NMFS 2016, 2018). NMFS includes both the Cumulative Sound Exposure Level (SEL_{cum}) and Peak Sound Pressure Level (PK) metrics in their recent technical guidance recommendations for determining permanent threshold shift onset acoustic thresholds. The SEL_{cum} metric is typically normalized to a single sound exposure of 1 second and considers both received level and duration of exposures. This metric is applied to a single source to estimate impacts of exposure to an animal but is not considered appropriate for assessing exposures resulting from multiple activities/sources occurring within the same area or over the same time period (NMFS 2016).

Additionally, the SEL_{cum} metric is not always sufficient for assessing the effects of impulsive sounds (e.g., seismic airguns, impact pile drivers). Therefore, NMFS recommends the concurrent use of the PK metric for impulsive sounds, with PK thresholds. Because NMFS considers dual metric acoustic thresholds for impulsive sounds, the onset of permanent threshold shift is assumed to occur when either the SEL_{cum} or PK metric is exceeded (NMFS 2016). Additional information on frequency weighting and additional metrics is presented in Popper et al. (2014).

All noise measurements performed for this Project, and the metrics and units derived from those measurements, are consistent with, and directly comparable to, guidelines adopted by the BIAS Project and ADEON Project (Ainslie et al. 2017).

2 Underwater Acoustic Data Collection Methods

2.1 Monitoring Instrumentation

During both MPs, acoustic data were collected using a mix of stationary and mobile platforms that were deployed at strategically selected locations within the respective study areas (**Figure 1**). Data were collected at depths ranging from 53 to 2,148 m within the main habitat types in the region, including the continental shelf (less than 200 m deep), continental slope (200 to 1,600 m deep), and the abyssal plain (greater than 1,600 m deep).

Three different types of stationary moorings equipped with sensors (hydrophones) and recording systems were used, namely Rockhoppers (RH) and Environmental Acoustic Recording Systems (EARS), both with effective recording bandwidth ranging from 10 Hz to 96 kHz; and Chip Scale Atomic Clock-Several Hydrophone Recording Unit (CSAC)-Several Hydrophone Recording Unit (SHRU) vertical line arrays (VLA), with effective recording bandwidth of 10 Hz to 4.5 kHz. Additionally, two separate mobile autonomous platforms (Seaglider™), with an effective recording bandwidth of 10 Hz to 62.5 kHz, were also deployed within selected portions of the study area to collect data in between the stationary moorings within the Mississippi Canyon and cover selected areas in the DeSoto Canyon.

RHs, EARS, and Seaglider data were primarily used for soundscape characterization. SHRU data collection was geared towards establishment of a 3D sound propagation model and supporting soundscape characterization. **Table 3** contains additional information on the various recording systems used for monitoring.

Table 3. Data recording systems summary

Monitoring System	Number of Units Placed Within the Study Area During Each Deployment	Total Number of Deployments	Servicing and Data Recovery
RH	5	4 (6 months each)	6 months
EARS	5	4 (6 months each)	6 months
CSAC-SHRU	2	2 (6 months each)	No interim servicing
2018 MP Seaglider	1	1 (6 weeks)	No interim servicing
2019 MP Seaglider	1	1 (2 weeks1)	No interim servicing

Key: CSAC = Chip Scale Atomic Clock; EARS = Environmental Acoustic Recording System; MP = monitoring project; RH = Rockhopper; SHRU = Several Hydrophone Recording Unit

[1] Planned period of data collection; due to adverse weather conditions, data could be collected over 2 weeks only.

2.1.1 Instrumentation System Specifications

The different data recording systems differed in detail such as depth rating, battery capability, data storage capability, sampling rates, and type of data stored. Between the different systems, there was a trade-off between the schedule, power, and storage under similar conditions. There was also a trade-off between using stationary and mobile data collection platforms. Sensors and data recording systems specifications are summarized in **Table 4**. **Appendix B** presents additional technical specifications and instrument calibration details.

Table 4. Data recording system specifications

Monitoring System	Sample Rate/Bits/ No. of Channels	Monitoring Bandwidth	Duty Cycle	Design Depth (m)
RH	192 kHz 24 bits 1 channel	10 Hz – 96 kHz	Continuous	3,500
EARS	192 kHz 16 bits 1 channel	10 Hz – 96 kHz	Continuous	6,000
CSAC-SHRU	9.8 kHz 24 bits 4 channels	10 Hz – 4.5 kHz	Continuous	500
2018 MP Seaglider	125 kHz	10 Hz – 62.5 kHz	Continuous	0–1,000
2019 MP Seaglider	128 kHz 24 bits 1 channel	20 Hz – 64 kHz	Continuous	0–1,000

Key: CSAC = Chip Scale Atomic Clock; EARS = Environmental Acoustic Recording System; Hz = Hertz; kHz = kilohertz; m = meter(s); MP = monitoring project; No. = Number; RH = Rockhopper; SHRU = Several Hydrophone Recording Unit

2.2 Monitoring Locations

An in-depth analysis was conducted to develop a defensible strategy for selecting locations within the study area box for data collection (HDR 2018, 2019). While a totally random placement of moorings in the survey area would ensure that data were collected within an objective subsample of the study area, selecting a random design also meant that every location in the study area would have a known (typically equal) chance of being selected for monitoring. Adopting a completely random design. On the other hand, could end up placing monitoring points next to one another, while leaving other parts of the study area uncovered (unsurveyed).

One of the key experimental design challenges was the presence of a large number of oil platforms and underwater pipelines in the GOM. Fixed instruments could not be deployed near these structures. Oil platforms typically have a 2-km exclusion zone around them. For pipelines, a 500-m buffer on either side was assumed to be off limits for placing a mooring. Also, moorings could not be placed in close proximity of existing meteorological towers and/or NOAA data collection buoys, because collocation could potentially introduce noise from the non-project anchoring/mooring equipment.

2.2.1.1 2018 MP Stationary Mooring Locations

For the 2018 MP, three alternative design strategies were evaluated for placement of RHs and EARS stationary moorings, namely systematic randomized grid construct, space-filling algorithm grid construct, and stratified grid construct. Additional details and pros and cons about the three different design strategies are discussed in the GOM PAM experimental design report (HDR 2018). With input from BOEM, a systematic random design, which ensured that survey effort was evenly distributed over the study area while avoiding the underwater infrastructure, was selected. Final deployment coordinates for RHs and EARS under the 2018 MP are listed in **Tables 5** and **6** and shown in **Figure 3**. Between the 10 moorings, the 2018 MP covered a depth range of 53 to 1,772 m.

2.2.1.2 2019 MP Stationary Mooring Locations

For placement of EARS and RHs during the 2019 MP, five locations were retained from the 2018 MP, and five new locations were added within the delineated study area (**Tables 7** and **8** and **Figure 4**). Between the 10 moorings, the 2019 MP covered a depth range of 440 to 2,148 m.

2.2.2 SHRUs Locations

Since SHRU data were intended primarily for establishment of a 3D sound propagation model, a different strategy was adopted to select locations for placement of two custom designed SHRU VLAs. These locations were determined based on analyses of simulation output from a preliminary 3D underwater sound propagation model, which compared acoustic coverage strength at several candidate stations within the Mississippi Canyon and surrounding slopes and plateaus. Additional details regarding the preliminary 3D sound propagation modeling are also discussed in the GOM PAM experimental design report (HDR 2018).

The preliminary model simulation showed that locations within the canyon plateau provided better acoustic listening coverage, specifically more uniform and extended. Areas inside the canyon were found to have shadow zones with up to 25 dB variation, and the transmission loss (TL) was stronger. The maximum range considered in the "inside canyon" computation was found to be 30 km. As compared to this, maximum range at areas on the plateaus were estimated at greater than 100 km. Based on this analysis, one station for an "inside the canyon" SHRU (i.e., on the canyon floor) and one station for a Slope SHRU were finalized. The SHRU deployment locations did not change between the two MPs (**Tables 5** through **8**, and shown in **Figures 3** and **4)**.

2.2.3 Seaglider Flight Paths

2.2.3.1 2018 MP Seaglider Flight

For the 2018 MP, the Seaglider path consisted of three contiguous segments to cover approximately 2 weeks of data collection in the DeSoto Canyon and 2 weeks in the Mississippi Canyon (**Table 9** and **Figure 2**). The unit was programmed to cover approximately 20 km per day, during which the unit would record both acoustic and metocean data.

The glider was deployed near the top of DeSoto Canyon on May 10, 2018, from where it transited out of the canyon along its southern slope, diving as deep as possible to follow the seafloor bathymetry. During the second half of the deployment period, the glider traveled westward, reaching the top of the Mississippi Canyon from where it was retrieved on June 18, 2019. During deployment, the flight path was modified as necessary to stay close to the programmed path based on transit speeds and oceanographic currents that were reported back to the pilot via satellite in real time.

Table 5. 2018 MP stationary mooring locations, RHs and EARS

Monitoring Station No.	Data Recording System	Monitoring Bandwidth	Deployment 1 (May to October 2018)				Deployment 2 (November 2018 to April 2019)			
			Latitude (deg)	Longitude (deg)	Water Depth (m)	Data Recorded (hours)	Latitude (deg)	Longitude (deg)	Water Depth (m)	Data Recorded (hours)
S1	RH	10 Hz – 96 kHz	27.64300	-89.24300	1,413	3,141	27.64300	-89.24300	1,413	4,368
S2	EARS	10 Hz – 96 kHz	27.65000	-88.82000	1,772	4179	27.65000	-88.82000	1,772	3,745
S3	RH	10 Hz – 96 kHz	28.01100	-89.67500	712	3,106	28.01100	-89.67500	712	4,359
S4	EARS	10 Hz – 96 kHz	28.02000	-89.25100	1,280	1,678	27.98713	-89.27067	1,280	3,820
S5	EARS	10 Hz – 96 kHz	28.02600	-88.82700	1,672	4,227	27.99418	-88.80950	1,672	3,703
S6	RH	10 Hz – 96 kHz	28.38900	-89.68500	685	3,065	28.38900	-89.68500	685	3,052
S7	RH	10 Hz – 96 kHz	28.49000	-89.25800	440	3,030	28.49000	-89.25800	440	4,415
S8	EARS	10 Hz – 96 kHz	28.40200	-88.83200	1,262	1,332	28.40200	-88.83200	1,262	3,960
S9	RH	10 Hz – 96 kHz	28.86100	-89.82400	53	1,108	28.66000	-88.83000	1,067	4,491
S10	EARS	10 Hz – 96 kHz	28.77100	-89.26600	131	4,128	28.77180	-89.26640	131	3,808

Key: deg = degree; EARS = Environmental Acoustic Recording Systems**;** Hz = Hertz; kHz = kilohertz; m = meter(s); No. = Number; RH = Rockhopper; S = Site
Notes:

1. Primary data collection objective was underwater soundscape characterization.
2. RH and EARS were deployed for a total of 24 months (four separate deployments, each lasting 6 months).
3. During Deployment 1, the RH at site 9 was dragged up by a fishing trawler and therefore the location was moved to deeper waters during Deployment 2.
4. Approximately 2 weeks into the second deployment, the RH at S3 developed an issue with one of the two 4-terabyte hard drives. The unit successfully switched over to the second hard drive. However, the capacity of the second Solid State Drive alone was not quite enough to store recordings for the entire deployment period. The data storage limit was reached approximately 4 months after the start of the deployment.

Table 6. 2018 MP stationary mooring locations, SHRU VLAs

Monitoring Station ID	Data Recording System	Monitoring Bandwidth	Latitude (deg)	Longitude (deg)	Water Depth (m)	Data Recorded (hours)
Canyon	SHRU VLA	10 Hz – 4.5 kHz	28.40991	-89.78438	4 hydrophones at 175, 200, 250, and 275	3,648
Slope	SHRU VLA	10 Hz – 4.5 kHz	28.52531	-89.29874	4 hydrophones at 175, 200, 250, and 275	624

Key: deg = degree; Hz = Hertz; ID = Identification; kHz = kilohertz; m = meter(s); SHRU = Several Hydrophone Recording Units; VLA = vertical line array
Notes:

1. Primary data collection objective was setting up a 3D underwater sound propagation model.
2. The SHRU data collection period was only 6 months during each deployment, totaling 12 months over 2 years.
3. During Deployment 1, the Slope SHRU had an electrical malfunction due to seepage of salt water into the sensor housing, and the recording systems failed after 26 days of data collection.

Table 7. 2019 MP stationary mooring locations, RHs and EARS

Monitoring Station No.	Data Recording System	Monitoring Bandwidth	Deployment 3 (May to October 2019)				Deployment 4 (November 2019 to April 2020)			
			Latitude (deg)	Longitude (deg)	Water Depth (m)	Data Recorded (hours)	Latitude (deg)	Longitude (deg)	Water Depth (m)	Data Recorded (hours)
S1	RH	10 Hz – 96 kHz	27.92710	-89.56040	2,148	4,390	27.92710	-89.56040	2,148	Unit lost
S2	EARS	10 Hz – 96 kHz	27.64837	-88.82111	1,777	1,048	27.64837	-88.82111	1,777	5,077
S3	RH	10 Hz – 96 kHz	27.80900	-89.27890	1,375	4,396	27.80900	-89.27890	1,375	5,096
S4	EARS	10 Hz – 96 kHz	27.98871	-89.26963	1,332	5,057	27.98871	-89.26963	1,332	4,682
S5	EARS	10 Hz – 96 kHz	27.99373	-88.80897	1,671	5,160	27.99373	-88.80897	1,671	4,371
S6	RH	10 Hz – 96 kHz	28.38520	-89.68530	685	4,375	28.38520	-89.68530	685	5,276
S7	RH	10 Hz – 96 kHz	28.49160	-89.25810	440	3,973	28.49160	-89.25810	440	2,881
S8	EARS	10 Hz – 96 kHz	28.24345	-89.27747	830	5,223	28.24345	-89.27747	830	5,071
S9	RH	10 Hz – 96 kHz	28.17980	-88.83490	1,526	4,388	28.17980	-88.83490	1,526	5,171
S10	EARS	10 Hz – 96 kHz	27.43412	-89.07278	1,797	5,159	27.43412	-89.07278	1,797	4,680

Key: deg = degree; EARS = Environmental Acoustic Recording Systems; Hz = Hertz; kHz = kilohertz; m = meter(s); No. = Number; RH = Rockhopper; S = Site
Notes:

1. Primary data collection objective was underwater soundscape characterization.
2. RH and EARS were deployed for a total of 24 months (four separate deployments, each lasting 6 months).
3. Approximately 2 weeks into the second deployment, the RH at S3 developed an issue with one of the two 4-terabyte hard drives. The unit successfully switched over to the second hard drive. However, the capacity of the second Solid State Drive alone was not quite enough to store recordings for the entire deployment period. The data storage limit was reached approximately 4 months after the start of the deployment.
4. During Deployment 4, the RH at S1 was lost and could not be recovered due to a communication system failure.

Table 8. 2019 MP stationary mooring locations, SHRU VLAs

Monitoring Station ID	Data Recording System	Monitoring Bandwidth	Latitude (deg)	Longitude (deg)	Water Depth (m)	Data Recorded (hours)
Canyon	SHRU VLA	10 Hz – 4.5 kHz	28.77150	-89.78500	4 hydrophones at 175, 200, 250, and 275	3,480
Slope	SHRU VLA	10 Hz – 4.5 kHz	28.4124	-89.29920	4 hydrophones at 175, 200, 250, and 275	3,480

Key: deg = degree; Hz = Hertz; ID = Identification; kHz = kilohertz; m = meter(s); SHRU = Several Hydrophone Recording Units; VLA = vertical line array
Notes:

1. Primary data collection objective was setting up a 3D underwater sound propagation model.
2. SHRU data collection period was only 6 months during each deployment for a total of 12 months over 2 years.

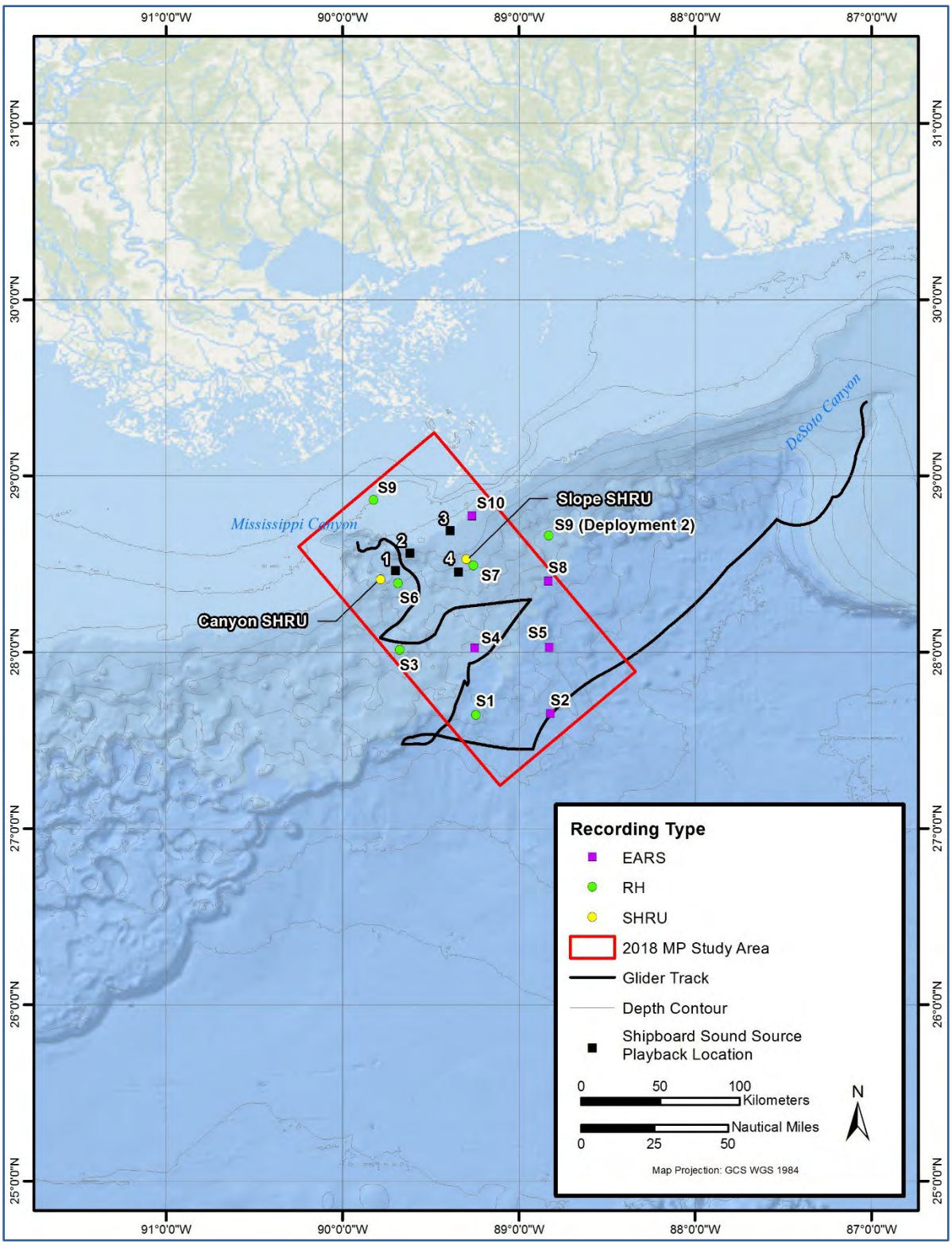

Figure 3. 2018 MP – stationary and mobile platform deployment locations (Deployments 1 and 2)

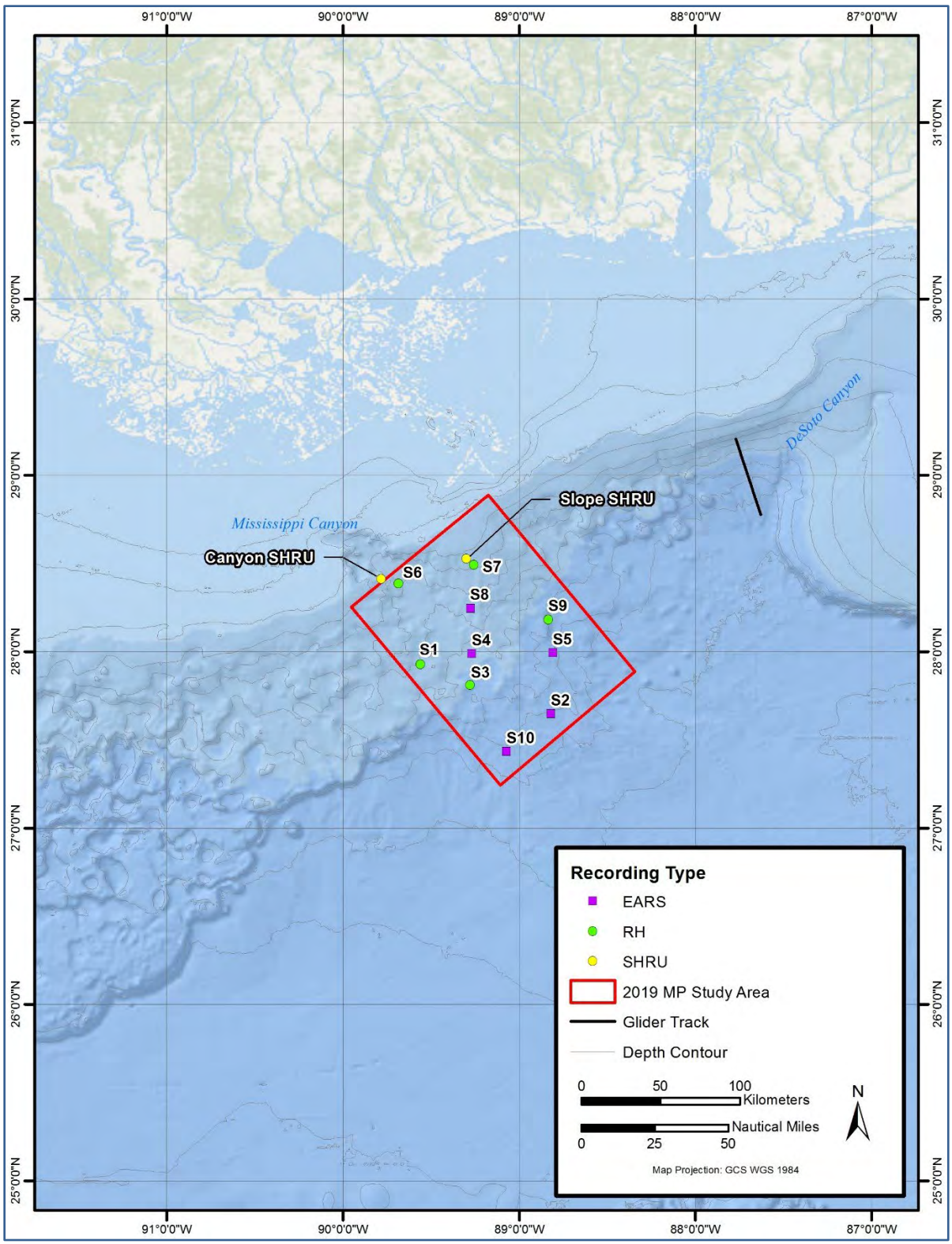

Figure 4. 2019 MP – stationary and mobile platform deployment locations (Deployments 3 and 4)

Table 9. 2018 MP Seaglider flight path segment coordinate

Flight Path Segment No.	Flight Path Segment ID	Data Collection Dates	From		To	
			Latitude (deg)	Longitude (deg)	Latitude (deg)	Longitude (deg)
1	DeSoto Canyon	05/10/2018 – 5/19/2018	29.419722	-86.995378	28.705587	-87.574675
2	Deep Slope	05/19/2018 – 05/30/2018	28.676265	-87.601155	27.518300	-89.415167
3	Mississippi Canyon	05/30/2018 – 06/20/2018	27.519063	-89.415153	28.640717	-89.894550

Key: deg = degree; ID = Identification; No. = Number

2.2.3.2 2019 MP Seaglider Flight

For the 2019 MP, an initial attempt to launch the Seaglider within the DeSoto Canyon was made on July 23, 2019. The glider was able to complete only four dives and attain a maximum depth of only approximately 10 m, utilizing all the available thrust of the instrument. This was due to prevailing very strong density gradient at the surface, which prevented the glider from attaining deeper depths. These strong density gradients, particularly in the upper 10 m, were caused by a massive influx of freshwater inflow from the Mississippi River due to heavy rains throughout the basin in the prior weeks.

The Seaglider was recovered after four dives and redeployed on July 24, 2019, after modifying the ballast by adding additional lead weight and recalculating flight parameters. The glider was able to achieve approximately 90 m depth, but this utilized the full range of the vehicle's available thrust, and it was unable to penetrate any deeper. Additional weight was added by the Program Field Team, but the additional weight caused the Seaglider to sit low in the water, so the full antenna was not above the water line. The Argos tag, which is the backup method of locating the instrument if communication is lost, was also partially submerged with the additional weight. It was determined that addition of this weight would compromise the ability of the instrument to surface and communicate effectively. The Team corresponded with the manufacturer, Kongsberg Maritime; it was their opinion that the density gradients experienced in this region of the GOM under the current conditions were too extreme for the Seaglider platform to function effectively. During this deployment, the Seaglider instrumentation was functioning properly, and it was able to collect environmental and underwater acoustic data.

During the second attempt in September 2019, the Team was able to deploy the Seaglider successfully. However, after approximately 2 weeks, the glider reported errors with the internal compact flash, which disabled the unit's ability to read and write mission-critical data, and the glider stopped diving and remained floating on the surface. It did continue to communicate and periodically send position updates, which allowed the Team to recover the unit and download the data collected during the 2-week period. Internal inspection of the instrument after recovery revealed that the compact flash card had become dislodged, possibly due to impact of the glider with a hard surface. High quality environmental and acoustic data were collected during the 2-week flight path (**Table 10** and **Figure 3**).

Table 10. 2019 MP Seaglider flight path segment coordinate

Flight Path Segment No.	Flight Path Segment ID	Data Collection Dates	From		To	
			Latitude (deg)	Longitude (deg)	Latitude (deg)	Longitude (deg)
1	DeSoto Canyon	09/24/2019 – 10/05/2019	29.2043882	-87.769433	28.776567	-87.630433

Key: deg = degree; ID = Identification; No. = Number

2.3 Field Deployments

Each of the four deployments was guided by a BOEM-approved Field Deployment Plan. All field activities were conducted in accordance with a customized, project-specific Health and Safety Plan, which defined safety and health requirements, designated project safety responsibilities, and described protocols to be followed by the team during field activities. Through careful planning and implementation of corporate and site-specific health and safety protocols, the Project Delivery Team was able to record zero accidents and incidents on this multi-year and challenging project.

2.3.1 Data Collection Timelines

Data were collected during four separate deployments over a 24-month period.

- **Deployment 1**, which extended from May to October 2018, covered data collection during the spring and summer seasons of 2018 (**Table 11** and **Figure 5**). Twelve stationary moorings (five RHs, five EARS, and two SHRU VLAs) were deployed at selected locations within the study area over an 8-day period (**Table 5** and **Figure 3**). This deployment also included data collection using a Seaglider.
- **Deployment 2**, which extended from November 2018 to April 2019, covered data collection during the fall and winter seasons of 2018 and 2019 (**Table 11** and **Figure 5**). Nine of the ten stationary moorings (four RHs and five EARS) were serviced and redeployed at the same locations within the study area (**Table 5** and **Figure 3**). One RH was relocated to deeper waters to avoid shallow, heavy traffic areas.
- **Deployment 3**, which extended from April to October 2019, covered data collection during the spring and summer seasons of 2019 (**Table 12** and **Figure 6**). Twelve stationary moorings (five RHs, five EARS, and two SHRU VLAs) were put in place at the selected locations within the study area over an 8-day period (**Table 6** and **Figure 4**). This deployment also included data collection with a Seaglider.
- **Deployment 4**, which extended from November 2019 to April 2020, covered data collection during the fall and winter seasons of 2019 and 2020 (**Table 12** and **Figure 6**). Ten stationary moorings (five RHs and five EARS) were serviced and redeployed at the same locations within the study area (**Table 6**, and **Figure 4**). The final mooring retrieval cruise had to be postponed to June 2019 due to lockdown restrictions imposed by the various state government and partner academic institutions during the COVID-19 pandemic. During the final cruise, nine stationary moorings were successfully retrieved at the end of Deployment 4; the RH deployed at Site 1 could not be recovered during the final recovery cruise due to a malfunction of the acoustic release communication system.

At the end of each deployment, hard drives from each stationary mooring were returned to the laboratory for data extraction, Quality Assurance/Quality Control (QA/QC), pre-processing, and data analyses. Five cruises were undertaken during each MP (**Tables 11** and **12**).

Table 11. 2018 MP data collection timelines

Deployment No.	Cruise No.	Start Date	End Date	Key Activities Completed
1 (May to October 2018)	1	05/10/2018	05/10/2018	• Deployed one Seaglider
	2	05/17/2018	05/24/2018	• Deployed 12 stationary moorings (5 RHs, 5 EARS, and 2 SHRU VLAs)
	3	06/18/2018	06/18/2018	• Seaglider retrieved
2 (November 2018 to April 2019)	4	10/28/2018	11/06/2018	• Retrieved the stationary moorings deployed in May 2018 • Deployed a fresh set of 10 moorings (5 RHs and 5 EARS)
	5	04/04/2019	04/08/2019	• Retrieved stationary moorings deployed in October 2018

Key: EARS = Environmental Acoustic Recording System; MP = monitoring project; No. = Number; RH = Rockhopper; SHRU = Several Hydrophone Recording Unit; VLA = vertical line array

Table 12. 2019 MP data collection timelines

Deployment No.	Cruise No.	Start Date	End Date	Key Activities Completed
3 (April to October 2019)	1	04/04/2019	04/08/2019	• Deployed a fresh set of 10 stationary moorings (5 RHs and 5 EARS)
	2	07/23/2019	07/24/2019	• Attempted to deploy the Seaglider • Deployment was unsuccessful due to ambient buoyancy issue created by heavy influx of freshwater from the Mississippi River
	3	09/24/2019	10/06/ 2019	• Seaglider was retrieved early due performance issues, which could not be addressed on site
	4	11/04/2019	11/11/2019	• Deployed 12 stationary moorings (5 RHs, 5 EARS, and 2 SHRU VLAs)
	5	03/10/2020	03/12/2020	• Retrieved the SHRUs VLAs
4 (November 2019 to April1 2020)	6	06/17/2020	June 2020	• Retrieved 9 out of 10 stationary moorings • RH deployed at Site 1 could not be recovered during the final recovery cruise due to a malfunction of the acoustic release communication system

[1] Cruise no.1 of Deployment 3 overlapped with Cruise no. 5 of Deployment 2.

[2] Even though the Deployment 4 data collection ended in April 2020, the moorings could not be recovered until June 2020 due to lockdown restrictions imposed by the various state government and partner academic institutions during the COVID-19 pandemic.

Key: EARS = Environmental Acoustic Recording System; No. = Number; RH = Rockhopper; SHRU = Several Hydrophone Recording Unit

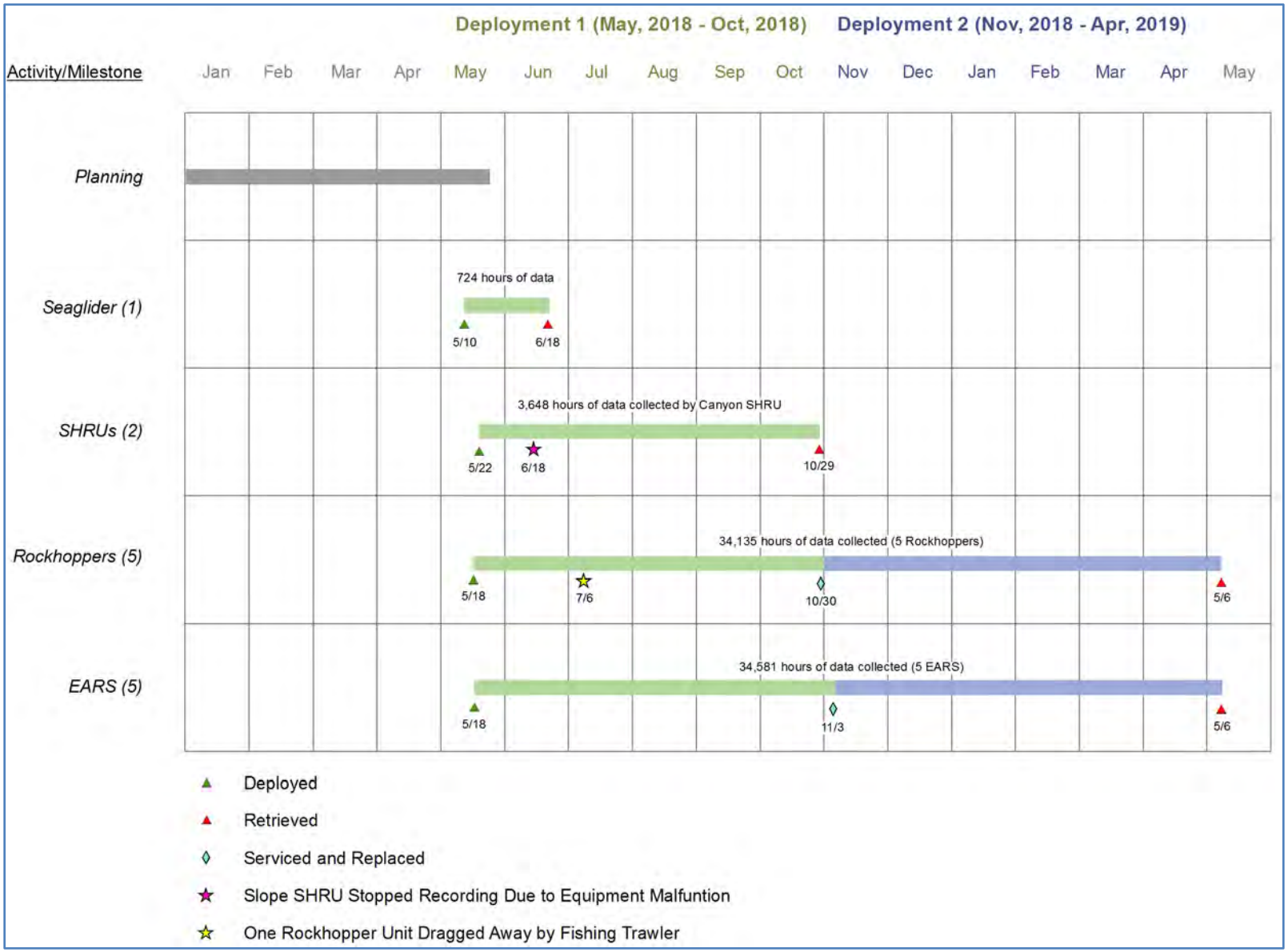

Figure 5. 2018 MP monitoring platform deployment timelines

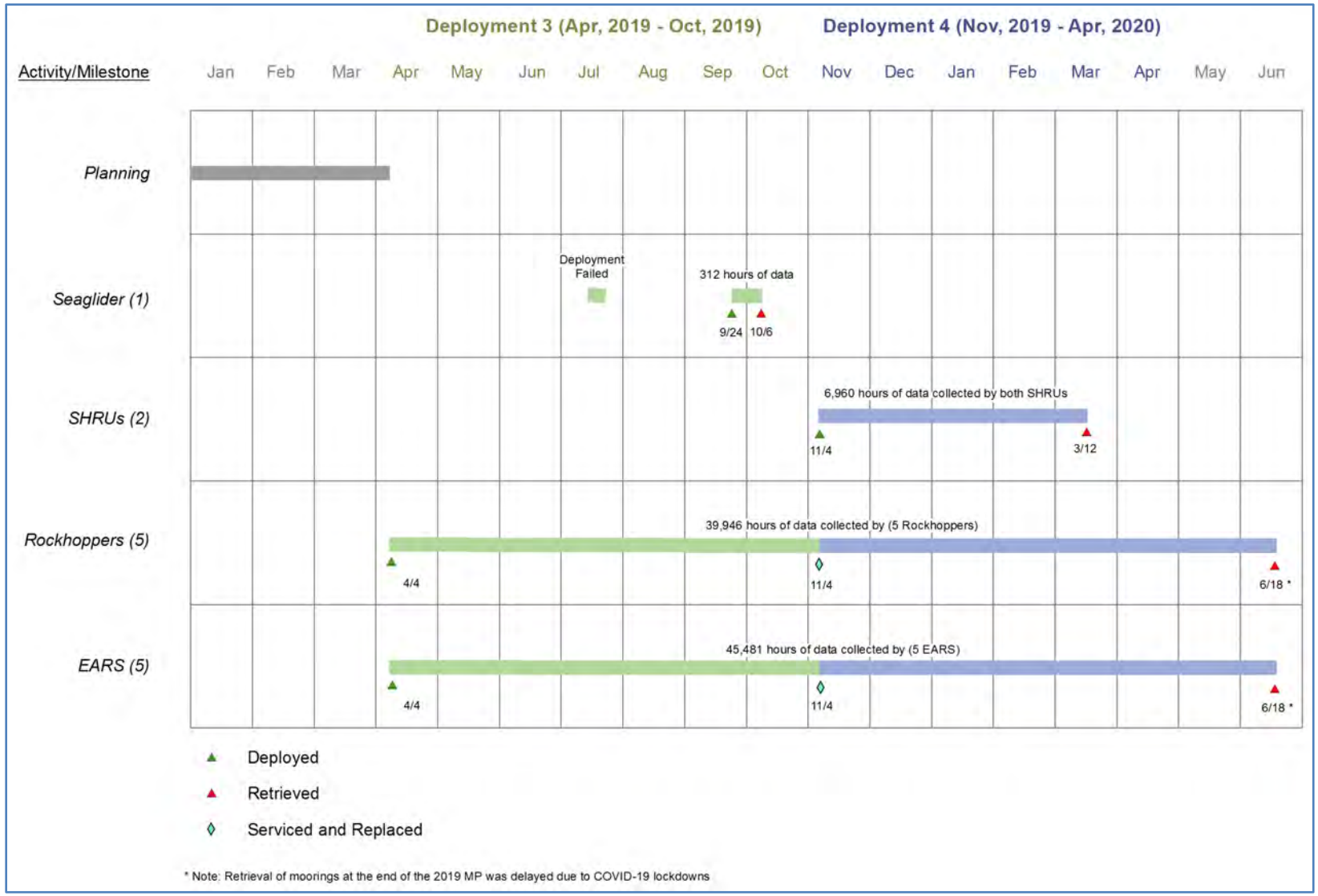

Figure 6. 2019 MP monitoring platform deployment timelines

2.3.2 Deployment Protocols

Field activities were staged from Cocodrie, Louisiana, a fishing village 31 miles south of Houma on Terrebonne Bay. Located approximately 145 km (78 nm) southwest of New Orleans, this location was convenient to provide support for field data collection efforts in both the Mississippi and DeSoto Canyons.

All stationary moorings were deployed and retrieved from the 116-foot (ft) Research Vessel *(R/V) Pelican*, which was leased from the Louisiana Universities Marine Consortium. The vessel is based at the Louisiana Universities Marine Consortium's DeFelice Marine Center in Cocodrie, Louisiana, and it is equipped to handle a variety of scientific and laboratory operations, including buoy deployment and recovery and hydrographic casts with Conductivity/Temperature/Depth (CTD)-rosette systems. A 30-ft, locally chartered, day vessel was used to deploy and retrieve the mobile platform.

A Field Sampling Plan was developed prior to each cruise to guide all field activities. The Field Sampling Plan included a customized Health and Safety Plan, which defined safety and health requirements, described onboard safety protocols, and identified safety responsibilities for all field staff. The goal was to ensure that field activities generally complied with applicable federal and state occupational safety and health laws and regulations. **Appendix C** presents specific steps followed during each cruise for deployment and recovery of individual monitoring platforms. **Appendix D** shows a photograph log of field activities.

2.4 Metocean Data Collection

For robust underwater soundscape characterization and interpretation, it was necessary to collect and analyze not only acoustic data but also meteorological and physical oceanography data during each cruise. Conductivity, temperature, and pressure of seawater to support sound speed profiling were collected by CTD casts from the research vessel. Time and weather permitting, expendable bathythermograph sensors were also deployed during selected cruises. Instrumentation onboard the Seaglider collected and transmitted data on temperature, salinity, dissolved oxygen, nutrients, and currents. In addition to metocean data collected by the deployed sensors, additional ancillary data were also obtained from reliable external sources to support data analyses.

2.5 Playback Experiment

During the 2018 MP, a shipboard playback experiment for measuring sound transmission loss (TL) was also conducted after the fixed sensors were deployed to gather data for characterization of underwater sound propagation properties. The purpose of the playback experiment was to obtain acoustic TL data for 1) studying propagation of industrial sound sources, 2) ground-truthing the localization abilities within the canyon versus outside the canyon, and 3) validating the underwater sound propagation model.

Two autonomous sound sources were deployed to transmit sound signals at four stations (**Figure 3**). The center frequencies (CF) of these two sources were 550 Hz and 750 Hz, respectively, and the bandwidths for both were 200 Hz. The source level (SL) was 158 dB rms re 1 µPa at 1 m, and the source signal type was a linear frequency modulated chirp. The source system also had monitoring hydrophones. **Table 13** lists playback source signal specifications. **Figure 7** shows the system design and a deployment photograph.

Table 13. Playback experiment source signal specifications

	Signal 1 HF Downchirp	Signal 2 IF Downchirp
Bandwidth	850 to 650 Hz	500 to 650 Hz
Chirp Length	5 sec	6 sec
Source Level	158 dB rms	158 dB rms
Transmission Pattern	At every 0, 10, 20, 30, 40, and 50 sec mark	At every 4, 14, 24, 343, 44, and 54 sec mark

Key: dB = decibel; HF = high frequency; Hz = Hertz; IF = intermediate frequency; rms = root-mean square; sec = second.

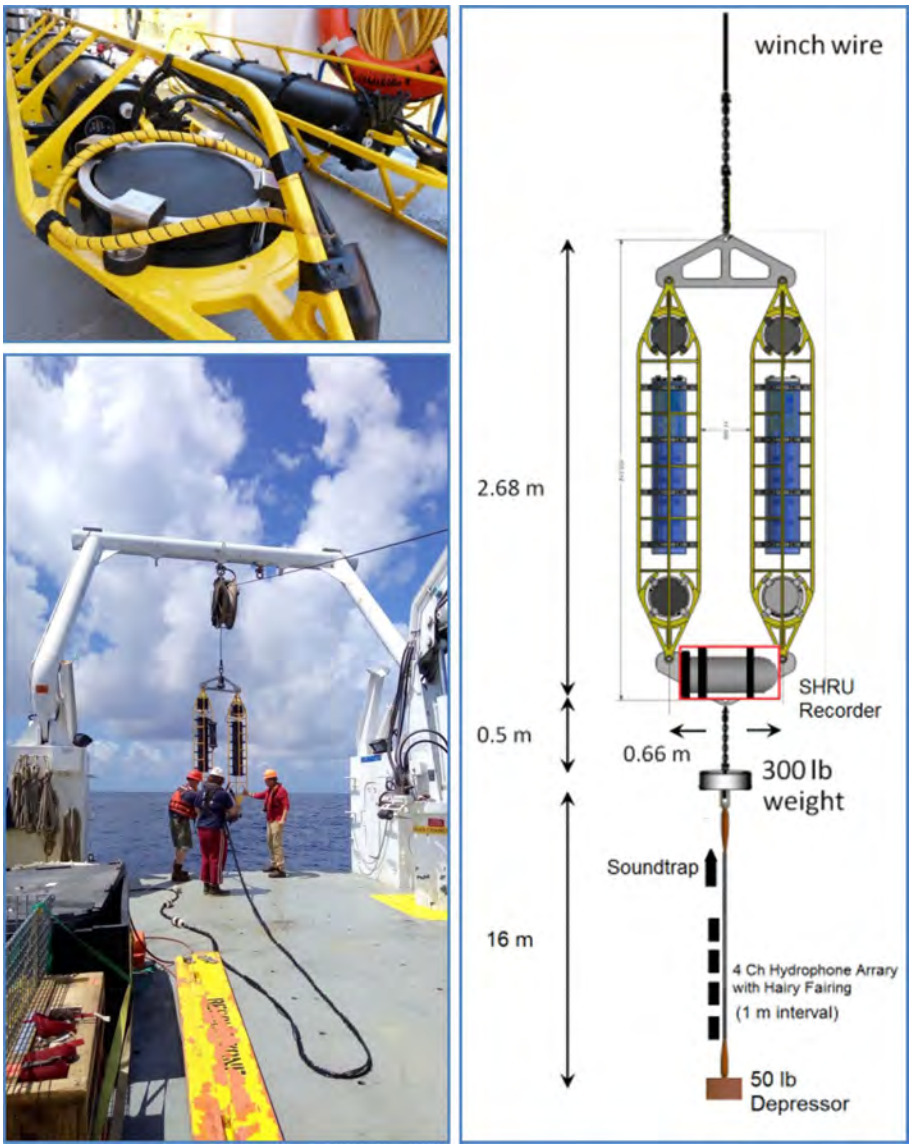

Figure 7. Transmission experiment shipboard source design (right panel) and photographs of the transducer (upper left) and the deployment on site (lower left)

Note: The design and deployment of these sound sources and monitoring hydrophone array were done by the Woods Hole Oceanographic Institution group.

2.6 Field Data Collection Challenges

Deploying unattended, expensive instrumentation underwater in the marine environment, especially over long durations (months), was an inherently risky undertaking. Major risks included equipment and data loss due to damage from collision with ship traffic, industrial activity (such as unmanned vehicles servicing oil and gas infrastructure), equipment dislodging due to trawling, and storm events (hurricanes). Instruments (and data) may also be damaged and lost due to equipment malfunction, the most common cause of which is seawater encroachment into the sealed chambers, which can corrode electrical connections and damage the recording system.

The following preemptive measures were implemented during the monitoring Program to minimize potential loss of equipment and data:

- Instruments and systems with a long and successful track record of underwater PAM were selected.
- Hydrophones, recording systems, and power supplies were secured in sealed, watertight compartments, and the entire assembly was coupled with customized, heavy moorings.
- Moorings were deployed underwater by trained and experienced personnel from a large research vessel (*R/V Pelican*) that was properly equipped for these types of deployments.
- Moorings were generally deployed during calm weather to avoid equipment damage due to accidental mishandling because of rough seas.
- Moorings were not placed adjacent to underwater infrastructure to avoid damage from oil and drilling industry service vessels.
- Areas known to be active trawling grounds and designated navigation channels were generally avoided.
- State-of-the-art beacons were installed on the moorings to ensure quick detection, response, and recovery in case the equipment surfaced prematurely:
    - SHRU VLA moorings were equipped with the XEOS KILO location beacons[3].
    - XEOS Onyx beacons[4] were installed on the RHs.
    - Novatech Iridium beacons[5] were fitted on the EARS.
    - The Seaglider was equipped with 1) a primary Iridium satellite connection, 2) a secondary smart position and temperature 6 Argos locating tag from Wildlife Computers[6], and 3) an acoustic transponder. During each recovery cruise, an acoustic deck box was available on the vessel, which would be used to locate the glider if it did not surface as planned.
- RHs were also equipped with an onboard very high frequency (VHF) radio transmitter.
- Both RHs and EARS were equipped with a light-emitting diode (LED) flasher for night recovery, if necessary.

[3] http://www.xeostech.com/product/kilo

[4] http://www.xeostech.com/product/onyx

[5] https://ocean-innovations.net/companies/metocean/novatech-beacons-flashers/satellitebeacons/novatech-ibcn/

[6] https://wildlifecomputers.com/data-products/argos/

Notwithstanding all the preemptive measures taken, some equipment and data loss were incurred. The following issues were dealt with during Deployment 1:

- One RH (RH402), which was deployed at Site 9 at a relatively shallow depth of 53 m, was apparently trawled and damaged by a shrimping vessel on July 6, 2018. Evaluation of audio recordings form the partially recovered unit and the Global Positioning System (GPS) track of the surfaced equipment indicated that the mooring was brought on board a fishing vessel (most likely the 148-ton shrimper, *Sea Dolphin*); after several hours on deck, it was likely tossed overboard until it was discovered and reported to the Project Team by a sport fisherman a week later. Only the recording unit (glass sphere) was recovered; the acoustic release was missing. For the second deployment, this station was moved to deeper waters (28.660°North, 88.830°West; depth of 1,067 m) to avoid similar loss.
- One of the EARS was also accidently dislodged from its mooring and floated to the surface. Upon receiving an alert from the dislodged unit, a Field Team was immediately dispatched on a search and recover mission. The unit was located and safely retrieved after 2 days. Apparently, the line had been cut, and it appeared that most likely an oil industry underwater infrastructure servicing robot was responsible for the accident. Data were recovered from the dislodged unit and used in the analyses.
- The Slope SHRU VLA also suffered an equipment malfunction during the first deployment. The power cable manufactured by SubConn, Inc., which connected the second battery housing on the SHRU, failed completely. Post-recovery investigations confirmed that the cause of the malfunction was a defective connector. Apparently, water had intruded into the connector from the base of the pings. Significant corrosion was observed along the connector body, and the plastic protection sleeve had cracked due to pressure of the accumulated water. The water damage shorted the connector, leading to a series of chain effects on the electronics until the recorder stopped working completely at the end of July. This VLA only collected and recorded data for a total of 26 days.
- Also, one of the four hydrophones (SN 238078) on the Slope SHRU VLA, which was deployed at a depth of 250 m, suffered damage during the deployment. The data recorded by this hydrophone showed that the sensitivity was approximately 20 dB lower than the calibrated value. The hydrophone was calibrated and tested before the array assembly, and one likely cause is static electronic damage at some time before the deployment.

At the end of Deployment 4 one RH (Site 10) could not be recovered due to malfunction of the release mechanism.

During the 2019 MP, the first Seaglider deployment, undertaken on July 23, 2019, had to be aborted due to presence of strong density gradients at the surface, which prevented the glider from diving beyond 10 m depths. These strong density gradients, particularly in the upper 10 m, were caused by a massive influx of freshwater sent down the Mississippi River due to heavy rains throughout the basin. The Seaglider was recovered after four dives and redeployed on July 24, 2019, after modifying the ballast by adding additional lead weight and recalculating flight parameters. The instrument was able to achieve approximately 90 m depth, but this utilized the full range of the vehicle's available thrust and it was unable to penetrate any deeper. Additional weight added to the unit caused the Seaglider to sit low in the water, so the full antenna was not above the water line. The Argos tag, which is the backup method of locating the instrument if communication is lost, was also partially submerged due to the additional weight.

A second successful deployment attempt was made on September 24, 2019. However, within approximately 2 weeks of being deployed, the unit had to be retrieved due to a malfunction of the internal compact flash card. This malfunction disabled the unit's ability to read and write mission-critical data, and the Seaglider was not able to dive to the programmed depths. A third deployment attempt was planned for spring 2020; however, that could not be undertaken due to COVID-19-pandemic-related lockdowns.

Also, COVID-19 pandemic related lockdowns at various team partner institutions created serious challenges for completing the field work safely and on time and consequently led to a significant delay in conducting data analyses and reporting. Another significant challenge was the delay in acquisition of the AIS data, which is the backbone of the vessel soundscape analysis. The 2018 AIS data were not available until 2020, and the last part of the 2019 AIS data were not available until mid-2021.

3 Data Analyses and Archiving Methods

3.1 Data Analyses

A two-step data analyses approach was adopted, as described in the following sections.

3.1.1 Phase 1 (Basic) Data Analyses

Data collected under the two MPs by each instrument type were separately processed, analyzed, and reported. RH data were analyzed using the noise analysis tools within the Raven-X toolbox for MATLAB, developed by the Cornell University Center for Conservation Bioacoustics. A subset of EARS data was analyzed using the EARS MATLAB noise analysis software as a quality control check. The data standards for the analyses were generally consistent with guidelines adopted by the BIAS Project and ADEON Project (Ainslie et al. 2017). The single-hydrophone statistics, as described in the following sections, were generated.

3.1.1.1 Long-term Spectral Average Plots

Long-term spectral average (LTSA) plots were calculated for each site for visualization purposes. The duration of the LTSA can span from hours to months, to show different acoustic events such as ships, storms, seismic surveys, sperm whale click trains, or fish choruses.

3.1.1.2 Equivalent Sound Levels

To examine the variation in sound levels as a function of time, the metric of equivalent continuous SPL, or equivalent sound levels (L_{eq}) (dB re 1 µPa), which represents the average flat frequency-weighting sound pressure of a continuous time-varying signal (ANSI 1994) over specified time intervals, was used. L_{eq} were calculated for one or both sets of the following frequency bands:

- 10 Hz to 1 kHz (low frequency [LF] band), 1 kHz to 10 kHz (mid-frequency [MF] band), and 10 kHz to 96 kHz (high frequency [HF] band): Each of these bands will contain acoustic signatures from a variety of anthropogenic, biological, and geophysical sources. Noise levels in the LF band are expected to be primarily driven by shipping and seismic airguns. The MF band will cover the frequency range of sperm whale echolocation clicks. Signals in the HF band will include vocalizations of a wide variety of delphinids and beaked whales.
- One-third octave frequency bands covering the entire frequency range from 10 Hz to 96 kHz: For sound analysis in a biological context, one-third octave bands are commonly used, since the function of the mammalian ear can be approximated as a set of band-pass filters with a resolution of approximately one-third octave.

3.1.1.3 Cumulative Percentage Distribution

A cumulative percent distribution was computed for each recording site and selected frequency band, which represents the percentage of time that SPLs reached a particular L_{eq}, averaged over 1-second time

intervals. The cumulative percent distribution allows for a direct comparison of the statistical noise characteristics of each site within selected frequency bands.

3.1.1.4 Power Spectral Density Levels

To statistically evaluate the SPLs across the entire frequency spectrum at each recording site, power spectral density (PSD) plots were created. The PSD captures long-term variation in ambient noise across the measured frequency domain by representing power spectra (dB re 1 $\mu Pa^2/Hz$) as a function of frequency using linearly averaged 1 second sound data and a 1 Hz frequency resolution. PSD levels from the entire recording period for each sensor type were represented using the median percentiles of the PSD.

Because the SHRU VLAs have a 100-m depth aperture, two cross-channel statistics, described in the following sections, were also computed using only SHRU data.

3.1.1.5 Cross-spectral Probability Density Plots

Cross-spectral probability density plots illustrating the statistical distribution of PSD levels were generated for each site.

3.1.1.6 Noise Coherence

Coherence of sound data between two channels of a SHRU VLA were computed to identify highly coherent noise sources, such as noise emitted from surface ships passing near the hydrophone array. Coherence is an important soundscape measurement to ensure accuracy of passive acoustic localization.

3.1.1.7 3D Underwater Sound Propagation Model

Data collected by the SHRU VLA under the 2018 MP was used to initiate establishment and testing of an underwater sound propagation model for assessing sound focusing and defocusing effects caused by 3D variations in underwater bathymetry. Model development and validation continued during Phase 2.

3.1.2 Phase 2 (Advanced) Data Analyses

In Phase 2, RH and EARS data collected under the two MPs were combined to create a 24-month dataset for more detailed analyses, which included the following:

- **Power Spectral Density Analysis of Raw Data**: Raw data had been collected using different instruments, each one of which used a different data format. Therefore, a project-customized module of Raven-X was developed and used to generate summary statistics for the raw acoustic data in 1-Hz, 1-second resolution. These Raven X summary statistics outputs served as inputs for the Phase 2 data analysis. Since the Raven X outputs are ADEON-guidelines compliant, the Phase 2 outputs are also considered ADEON-guidelines compliant by extension.
- **Detector Band Creation**: Known acoustic sources have specific frequency characteristics. Candidate frequency bands that are likely to be able to indicate the presence of different sources were identified. Some of these frequency bands were determined from the literature, while the remaining bands (defined as empirical bands) were identified through a review of the data. While these frequency bands were observed, they are not inferred to be associated with any particular source(s).
- **Detection of Acoustic Events in Candidate Bands**: The hourly mean received level in each band is calculated and subtracted from each candidate band to produce a “normalized” band. The detection threshold was taken as the sum of standard deviation of the normalized band plus 3 dB. Any level exceeding this threshold is taken as a detection.

- **AIS Data**: 2018 and 2019 AIS data were obtained[7] and incorporated into the analyses to identify specific acoustic sources.
- **Statistical Analysis**: The bandstats output, the cumulative acoustic power in a 1-hour band in each of the source candidate frequency bands, were analyzed with two predictor variables, namely AIS metrics and windspeed values. The resulting analyses clarified the relative power of these metrics to predict acoustic levels. Graphical representations of the candidate frequency bands were used to identify spatiotemporal patterns.
- **Stationary Mooring and Seaglider Data Comparison**: This comparison was performed to determine how far data from a single stationary buoy could be extrapolated.

During Phase 2, SHRU data were used to advance and validate the 3D sound propagation model that had been initiated under Phase 1. These data were also used to conduct noise coherence and source correlation analyses and soundscape fingerprint analyses. As appropriate and relevant, metocean data collected during the MPs or acquired from external sources were also incorporated into the analyses to support data interpretation.

3.1.2.1 Phase 2 Data Analysis Challenges

COVID-19 pandemic related lockdowns at various team partner institutions created serious challenges for completing the field work safely and on time and consequently led to a significant delay in conducting data analyses and reporting. Another significant challenge was the delay in acquisition of the AIS data, which is the backbone of the vessel soundscape analysis. The 2018 AIS data were not available until 2020, and the last part of the 2019 AIS data were not available until mid-2021.

3.2 Data Archiving

Approximately 250 terabytes (TB) of raw underwater acoustic data were collected during the two MPs over a roughly 24-month period (**Table 14**). These data were appropriately packaged and submitted for archiving to NOAA's National Centers for Environmental Information (NCEI). NCEI is the nation's leading authority for environmental data, and it manages one of the largest archives of atmospheric, coastal, geophysical, and oceanic research in the world. After NCEI completes archiving of the GOM PAM Program's raw data on its servers, it is anticipated that it will provide public access to the data along with searching and visualization tools.

Q for BOEM/Tre/Erica, should we state in the report that we had coordinated with Navy on the locations of the sensors prior to sending the data to NCEI? If yes, need some politically correct language to state this?

All data submitted to NCEI for archiving are unprocessed to the degree that it is still usable by the public (i.e., formats that do not require proprietary applications to be read). The data are replete with metadata and reports describing collection techniques used by each principal investigator. NCEI will be responsible for backups, data integrity, and standard industry practices for maintaining access to the data objects.

Key steps in the data packaging for archiving consisted of the following:

- Raw acoustic files from each sensor were collated. These files ranged from 2 minutes to 4 hours in length. Per NCEI request, small files were concatenated to create files with durations of 4 hours.

[7] https://marinecadastre.gov/

- All files were converted to the Free Lossless Audio Codec (FLAC), providing compression of the acoustic data files without any loss of information. FLAC is an open-source format released by the Xiph.org Foundation under the BSD license. The libraries used for conversions are libFLAC version 1.3.3 (August 4, 2019).
- After conversion, data were packaged with version 3.1.0 of PassivePacker (NCEI). PassivePacker is an NCEI-provided Python script for packaging acoustic data with metadata and ancillary environmental data in an archive-friendly format. This script also verifies that required NCEI metadata fields were included.
- Where available, additional environmental and ancillary data were also packaged with the acoustic data. For example, Seaglider monitoring data included corresponding temperature, salinity, and dive profiles for each deployment.
- Formatted data were transferred to sets of portable 8 TB hard drives and shipped to NCEI for archiving.

Table 14. Summary of data, sampling rate, and file size for each sensor type

Sensor Type	Original Format	Number of Files (Approximate)	Data Size	Included Ancillary Data
Rockhopper	FLAC	18,520	147.0 TB	
EARS	Proprietary	13,410,066	107.3 TB	
SHRU	WAV	3,114	3.1 TB	
2018 MP Seaglider	FLAC	21,840	891.3 GB	Dive profile, conductivity, temperature, depth
2019 MP Seaglider	FLAC	527	49.5 GB	Dive profile, conductivity, temperature, depth

Key: FLAC = Free Lossless Audio Codec; GB = gigabyte; TB = terabyte; WAV = Waveform Audio

4 Results

Approximately 250 TB of raw underwater acoustic data were collected during the two MPs over a roughly 24-month period and analyzed per a BOEM approved Data Analyses Plan. Key results from the analyses are summarized in this section. Information is presented on the different types of analyses conducted and observations made from interpretation of the results, including soundscape characterization, spatial and temporal trends assessment, anthropogenic and biological sound detection, statistical modeling of vessel received levels, fixed and mobile sensor comparison, 3D underwater sound propagation modeling, noise coherence and source correlation analyses, and soundscape fingerprint analysis.

4.1 Soundscape Characterization

4.1.1 Rockhoppers

Between May 2018 and June 2020, a total of 74,081 hours of continuous acoustic data were collected by the RHs during four back-to-back deployments (**Figures 5** and **6**). The units were programmed to collect data continuously at a 197 kHz sampling rate and 24-bit resolution. Data quality was excellent, and no issues (e.g., electronic noise, drop-outs) were detected during the manual QA/QC performed as part of the post-processing.

RH data collected under the two MPs were processed, analyzed, and reported using the noise analysis tools within the Raven-X toolbox for MATLAB developed by the Cornell University's Bioacoustics Research Program package (Dugan et al. 2018). This MATLAB-based package features parallelized data processing capabilities, which enables processing of large audio archives at significantly improved throughput rates. Raven-X features a Noise Analyzer module (Ponirakis et al. 2015), which was used to generate multiple data outputs, including long-term spectral average plots, L_{eq}, cumulative percentage distribution, temporal trends, PSD levels, and spectral probability density plots. The analysis methods and units followed established standards outlined in Ainslie et al. (2017).

Comprehensive results from the RH data analyses were detailed in two separate sensor reports (one per MP) (Klinck et al. 2019, 2020). Key results from interpretation of data outputs are:

- Data collected from 2018 through 2020 indicate that the majority of seismic surveys are being conducted further offshore in the GOM. There was a noticeable difference in recorded low frequency levels (less than 100 Hz) between the two units deployed at the shelf break (Sites 6 and 7) and the offshore sites (Sites 1, 3, and 9).
- There was a noticeable difference in recorded low frequency levels (less than 100 Hz) between the recorders deployed at the shelf break versus offshore locations. Low-frequency levels observed at offshore sites were significantly higher and appear to be driven by seismic airgun activities that occurred in closer proximity (compared to Sites 6 and 7; **Figure 8**). Also, high frequency levels (greater than 1,000 Hz) were higher and more variable during the winter months. This was likely related to higher variability in weather conditions and associated sea states.
- Observed noise levels at the deep-water sites were comparable to those previously reported by Estabrook et al. (2016) and Wiggins et al. (2016) and are indicative of extensive industry-related sound from oil and gas operations in the northern GOM (**Figures 9** and **10**). Seismic airgun noise contributed to elevated sound levels across multiple years.
- On a seasonal basis, levels at frequencies greater than1,000 Hz were higher and more variable during the winter months. This was likely related to higher variability in weather conditions and associated sea states.

- While airgun noises were the most dominant anthropogenic sound source in the acoustic environment, other sources, including vessel-related noise, also contributed to the levels below 1 kHz.
- During the period of July 11 through 15, 2019, Tropical Storm Barry moved across the hydrophone array. As indicated in **Figure 11**, this corresponded with a significant drop in one-third octave frequency band levels with the CF of 63.1 Hz as all airgun surveys ceased due to hazardous weather conditions. The occurrence of tropical storms seemed to allow measurement of low-frequency levels in the absence of major anthropogenic contributors (i.e., baseline assessment).

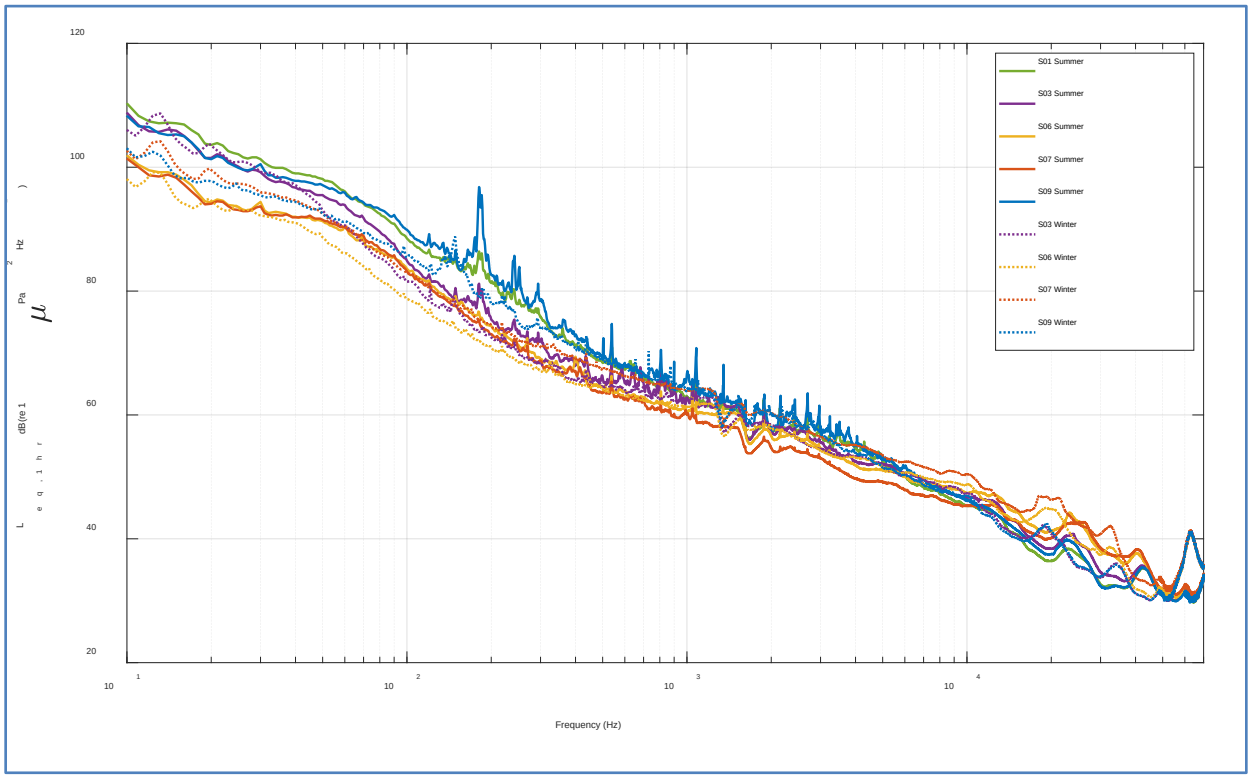

Figure 8. Average PSD levels by site for Deployment 3 (May 2019 – November 2019) representing summer months, and Deployment 4 (November 2019 – June 2020) representing winter months

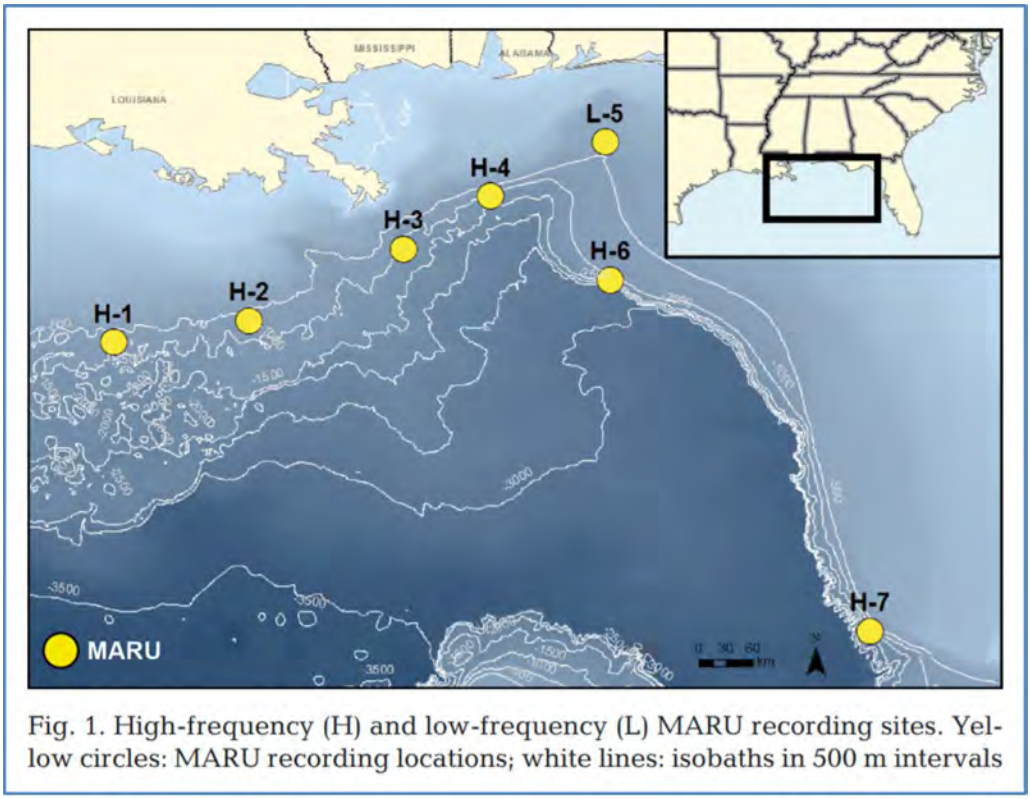

Fig. 1. High-frequency (H) and low-frequency (L) MARU recording sites. Yellow circles: MARU recording locations; white lines: isobaths in 500 m intervals

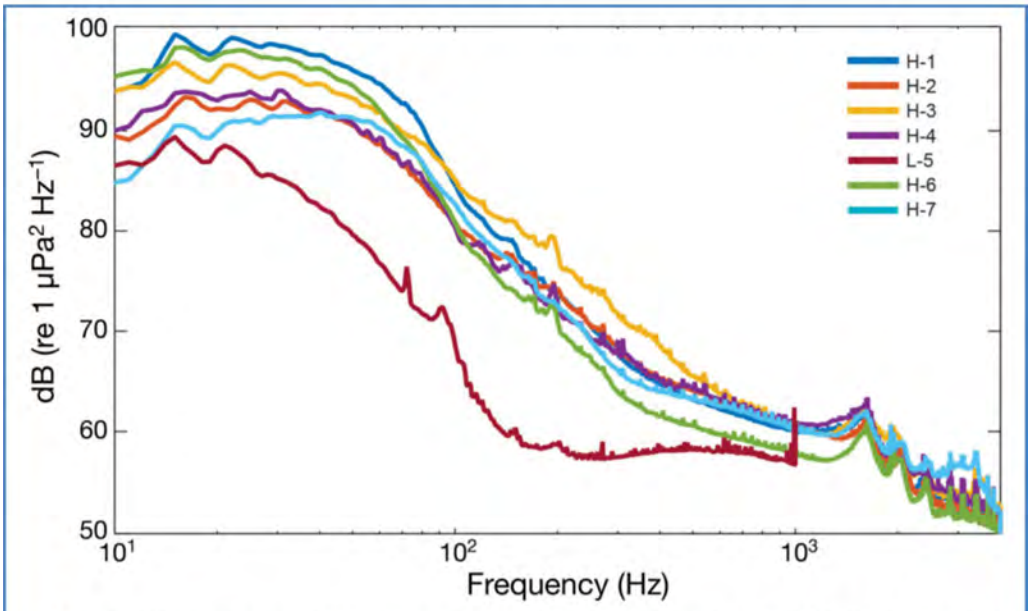

Fig. 5. Power spectral density of sound levels (dB re 1 µPa^2 Hz^{-1}) of the 50th percentiles for the 7 study sites throughout the recording period averaged over 1 s time intervals

Figure 9. Previous Cornell recorder locations in the GOM (top panel) and corresponding spectrum levels (bottom panel)

808 Source: Estabrook et al. (2016)

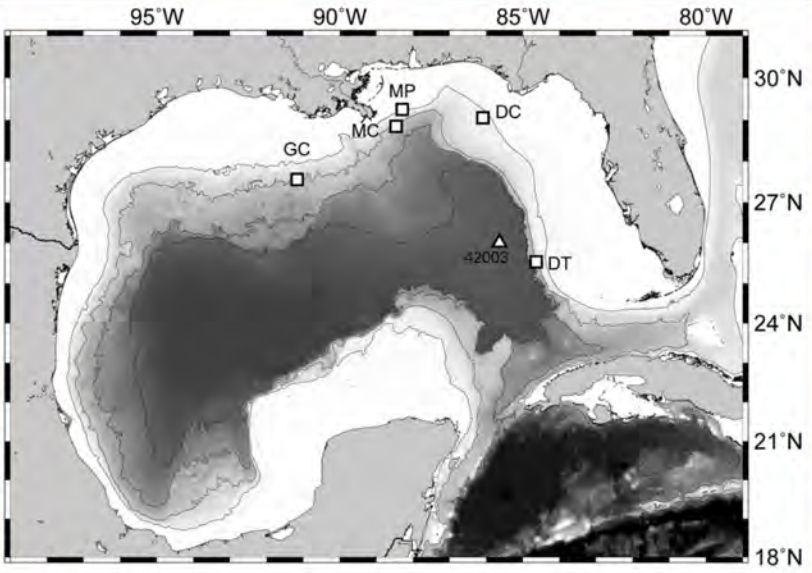

FIG. 1. HARP locations (see Table I) shown as squares with site names. NOAA NDBC weather buoy station 42003 shown as triangle northwest of site DT. GOM bathymetric map with contours at 100, 1000, 2000, and 3000 m depth.

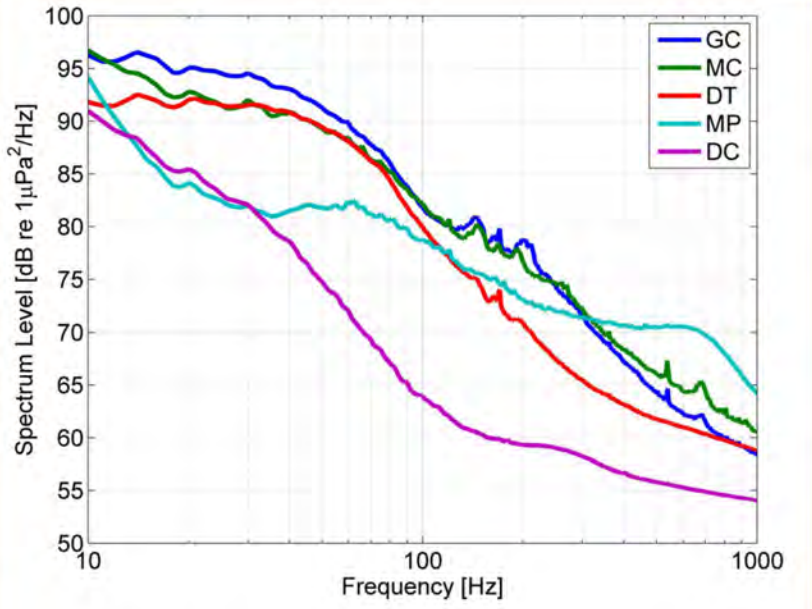

FIG. 3. (Color online) Average sound pressure spectrum levels by site over entire deployment period. See Table I for total number of days used for each average.

Figure 10. Previous Scripps Institution of Oceanography recorder locations in the GOM (top panel) and corresponding spectrum levels (bottom panel)

809 Source: Wiggins et al. (2016)

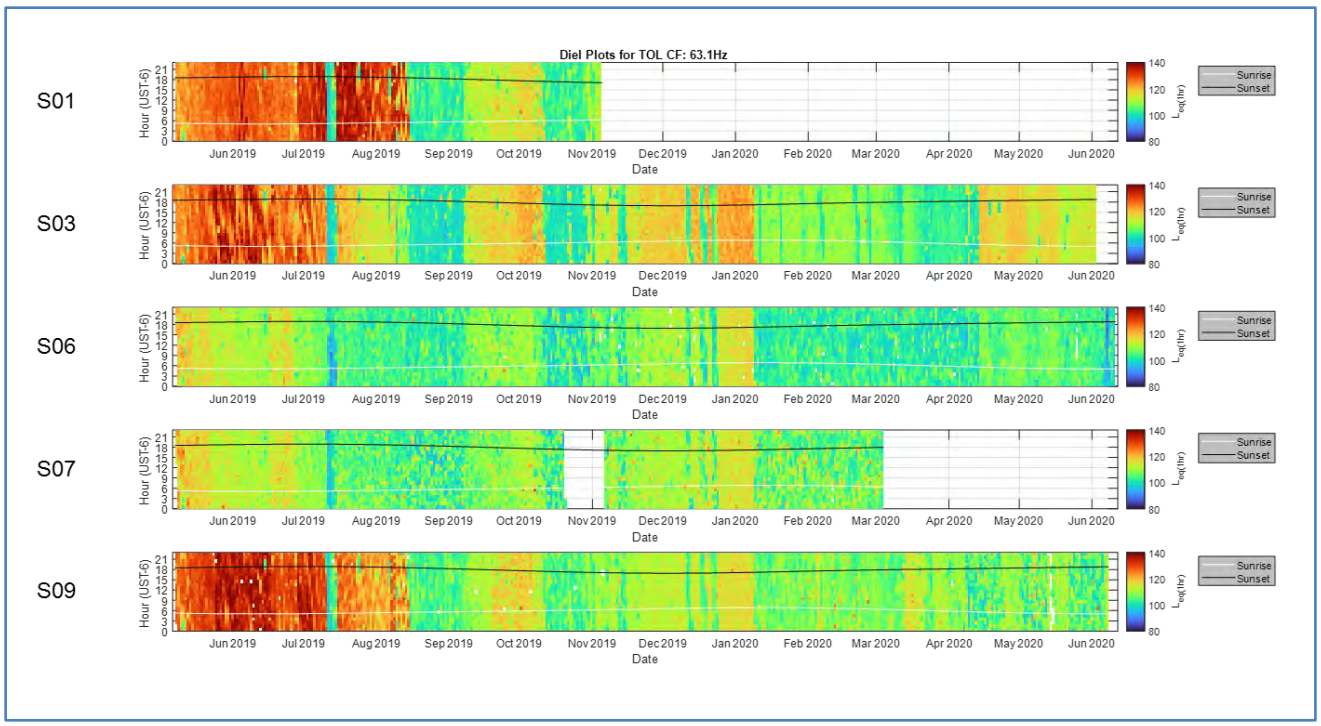

Figure 11. Hourly L_{eq} levels for the on-third octave frequency band with a 63.1 Hz center frequency for each deployment site

Note: Increased levels in this band are indicative of airgun activity

4.1.2 Environmental Acoustic Recording System

Between May 2018 and June 2020, a total of 80,061 hours of continuous acoustic data with a sample rate of 192,000 samples per second were collected by the EARS moorings during the four back-to-back deployments (**Figures 5** and **6**). The units were programmed to collect data continuously at a 192 kHz sampling rate and 24-bit resolution. Data quality was excellent, and no issues (e.g., electronic noise, drop-outs) were detected during the manual QA/QC performed as part of the post-processing.

EARS data collected under the two MPs were processed and analyzed using a noise analysis package developed by the University of Louisiana at Lafayette. The software and data processing workflow are based on the standards developed for previous large-scale ocean ambient noise monitoring projects (Betke et al. 2015; Ainslie et al. 2017). The analyses methods and units followed established standards outlined in Ainslie et al. (2017). Extracted acoustic field characteristics are directly comparable to ones measured in previous and ongoing studies in the Baltic Sea (BIAS Project) and the North Atlantic (ADEON Project). Data analyses outputs included long-term spectral average plots, L_{eq}, cumulative percentage distribution, temporal trends, PSD levels, and spectral probability density plots.

Comprehensive results from the EARS data analyses are presented in four separate sensor reports (two per MP) (Sidorovskaia and Bhattarai 2019a, 2019b, 2020; Sidorovskaia and Griffin 2020). Key results from interpretation of data outputs are:

- The measured SPL monitored by the EARS buoys were comparable to levels previously reported in the northern GOM (Wiggins et al. 2016; Sidorovskaia and Li 2016) and were similar to the simultaneously deployed RHs. The 50th percentiles (medians) of one-third octave band SPLs for all sites monitored are shown in **Figures 12** through **14**.

- The LF soundscape was dominated by distant seismic surveys.
- On a seasonal basis, the low-frequency noise curves at deep sites, which are dominated by oil and gas industry activities and service shipping, were lower during the winter months as compared to the summer months. This was an expected finding since the industrial activity in the GOM generally declines during the colder months due to harsh marine weather.
- Biological sounds (dolphin whistles, sperm whale clicks, Risso's dolphin clicks, and beaked whale clicks) were present throughout all deployments.
- The deep-water monitoring locations (Sites 2, 4, 5, and 8) exhibited similar SPL distributions in values and frequency and in general are consistent with the levels previously measured in this region of the GOM.
- In general, deeper locations appeared to have the highest sound pressure levels at the low frequency bands (below 100 Hz) and the lowest sound pressure levels at the mid frequency bands (500 to 10,000 Hz).
- The MF band highest SPLs were observed during Deployments 3 and 4 at Site 8 (830 m), which is located at the edge of the study area just outside the Mississippi Canyon.
- There were anthropogenic pauses in the soundscapes due to impacts of the COVID-19 pandemic; exploration surveys and industrial activities were present across all COVID-19-pandemic-impacted months (March through June). However, the decidecade band associated with seismic exploration (63 Hz central frequency) had the lowest observed levels in April 2020 followed by a quick recovery in the activity levels in May and June 2020.

4.1.3 Comparison of Data from EARS and RH Recorders

Data from each deployment of the RH and EARS recorders were compared against each other (**Figures 15** through **18**). The two datasets were comparable above 100 Hz and a systematic difference in the data below 100 Hz was observed. This deviation appears to begin at 100-200 Hz and increases in magnitude as frequency decreases. At 40 Hz, the difference seems to exceed 10 dB. These differences were seen in the monthly temporal and spatial spectral data.

The experimental design adopted for placement of recorders and data generated under this project do not readily lend themselves to directly answering the Q as to which of these two types of recorders is closer to the "truth". In order to make that determination, a laboratory test will have to be performed under controlled conditions during which representative and comparably calibrated units of the two recorders are tested side-by-side along with a standard reference hydrophone.

4.1.4 Several Hydrophone Recording Unit Vertical Line Arrays

Approximately 11,280 hours of acoustic data were collected by the SHRU VLAs at a sample rate of 9,800 samples per second during two separate, approximately 6-month deployments (May to October 2018 and November 2019 to March 2020). The VLAs were placed at the same location (one on the floor of the Mississippi Canyon and the other on the slope) during both deployments (**Tables 3** and **4** and **Figures 6** and **8**) to better capture temporal soundscape variability. Data quality was excellent, and no issues (e.g., electronic noise, drop-outs) were detected during the manual QA/QC performed as part of the post-processing.

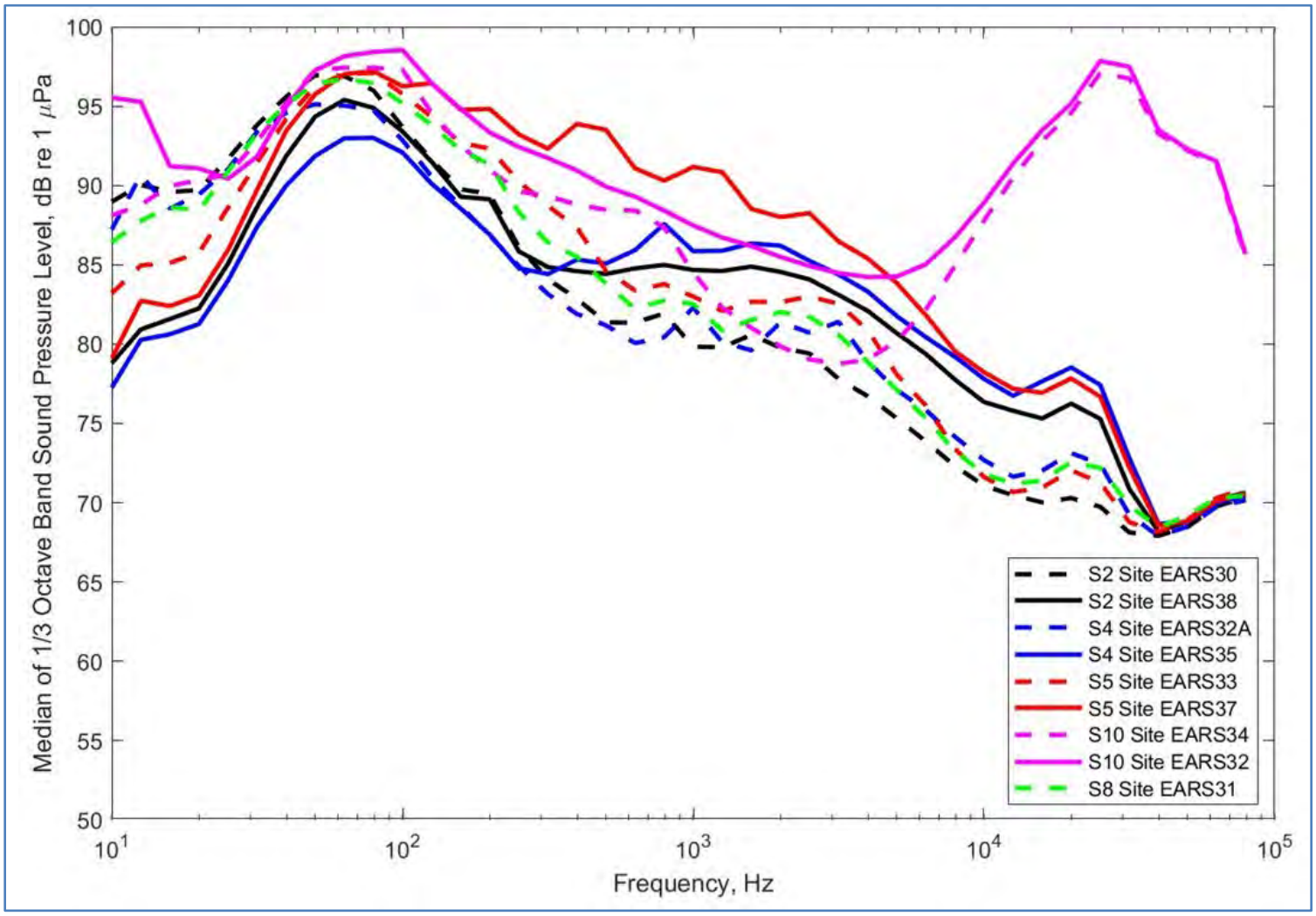

Figure 12. Medians of one-third octave band spectrum (1 second equivalent) for all monitored sites between May 2018 and April 2019 (Deployments 1 and 2) for EARS

Note: The solid lines correspond to the winter deployment, dashed lines correspond to the summer deployment, and colors are associated with deployment sites.

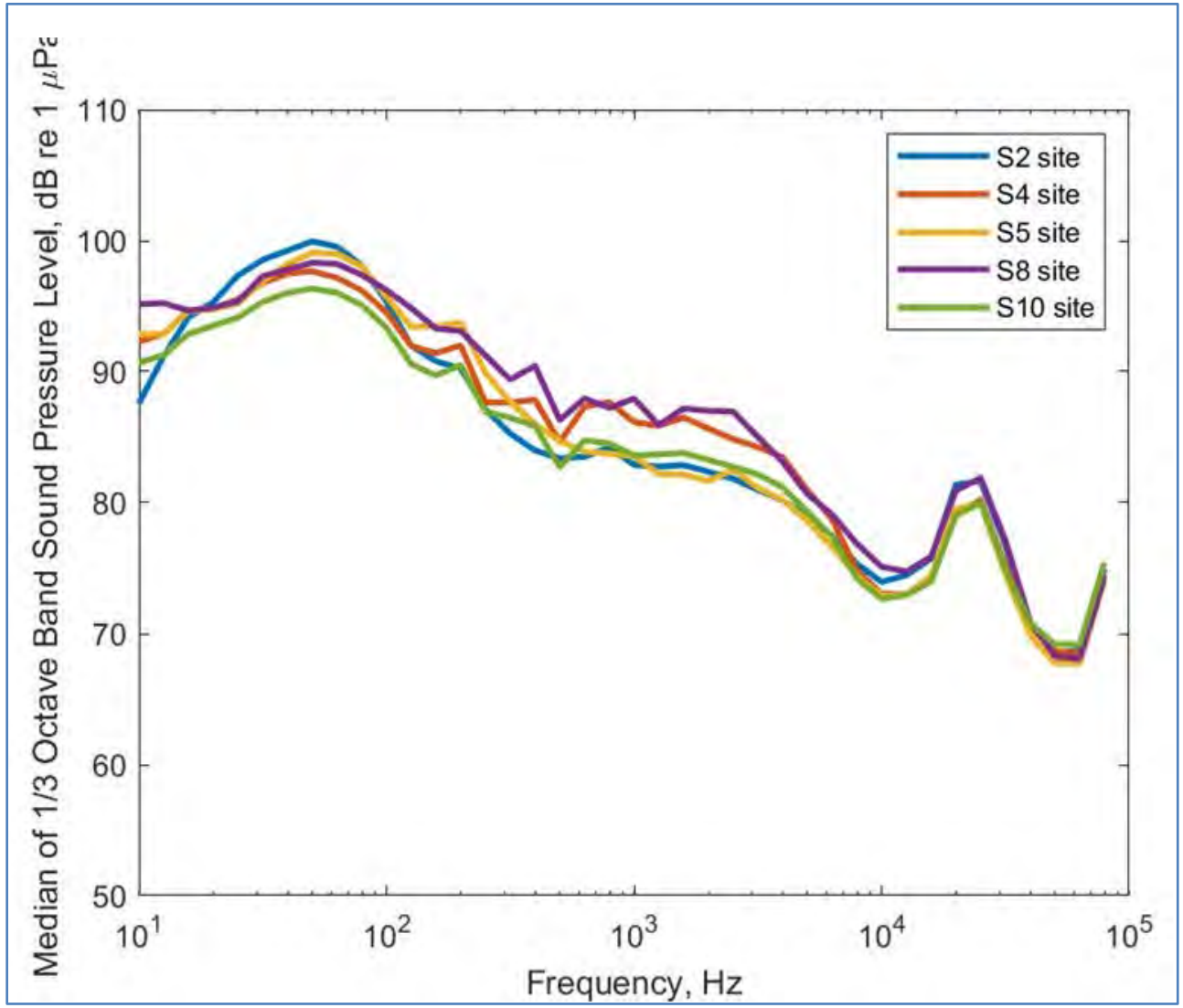

Figure 13. Medians of one-third octave band spectrum (1 second equivalent) for all five monitored sites between April 6 and November 11, 2019 (Deployment 3) for EARS

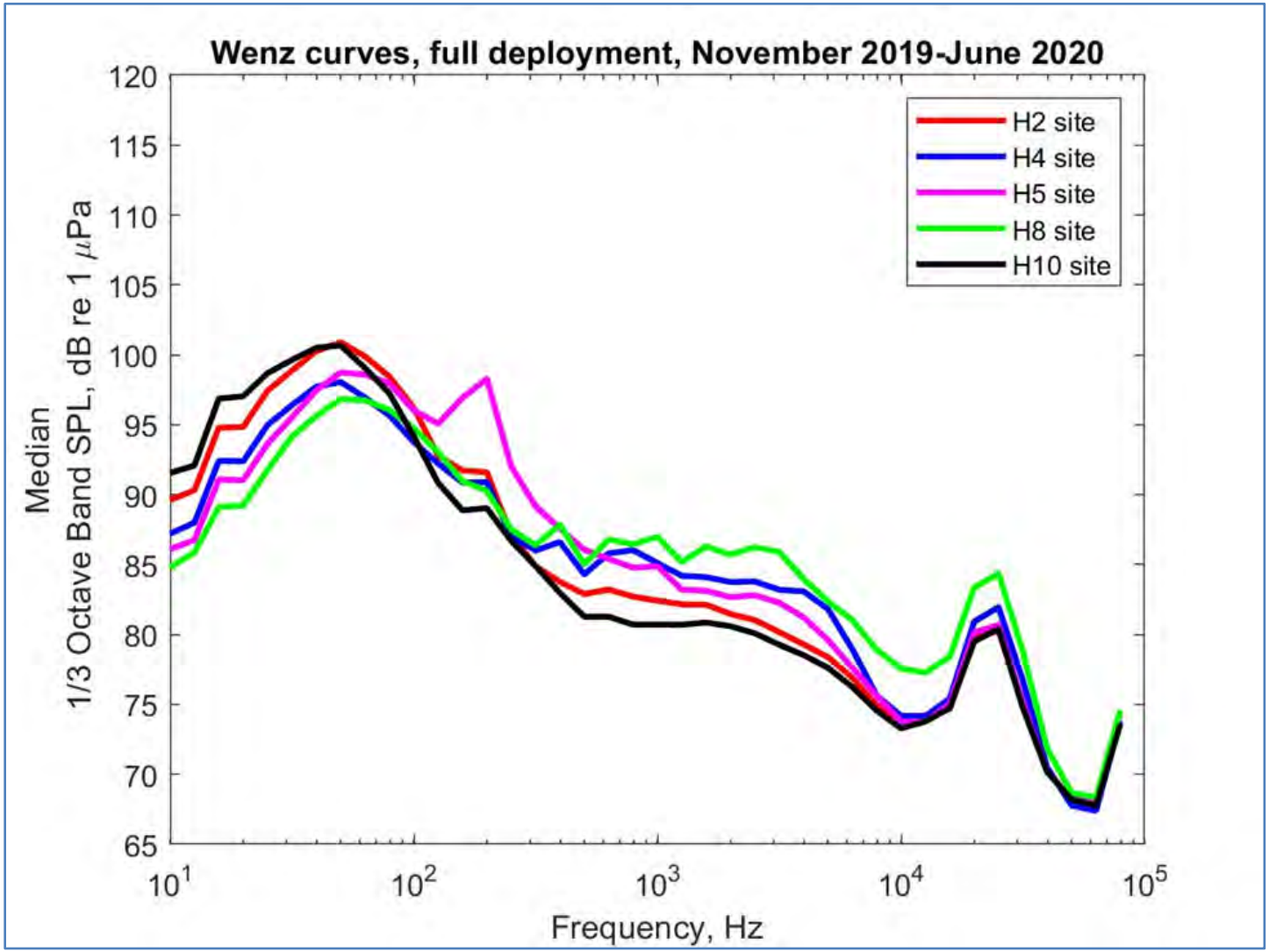

Figure 14. Medians of one-third octave band spectrum (1 second equivalent) for all five monitored sites between November 11, 2019, and June 15, 2020 (Deployment 4) for EARS

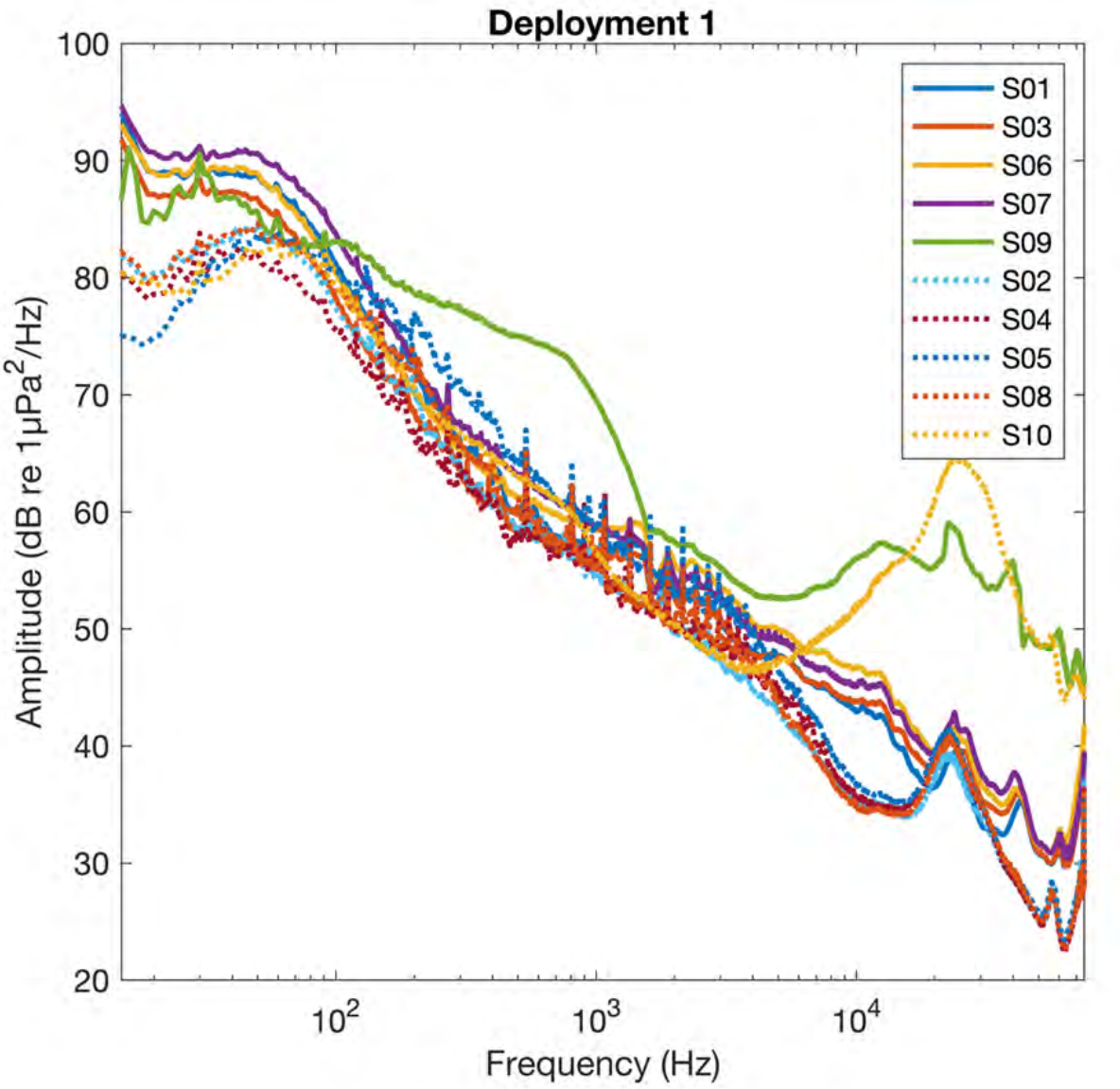

Figure 15. Comparison of RH and EARS median spectra for data collected during Deployment 1

Note: RH data are shown as solid lines, and EARS are shown as dotted lines. Stations 9 and 10, which were the shallowest water recorder locations, show elevated HF noise.

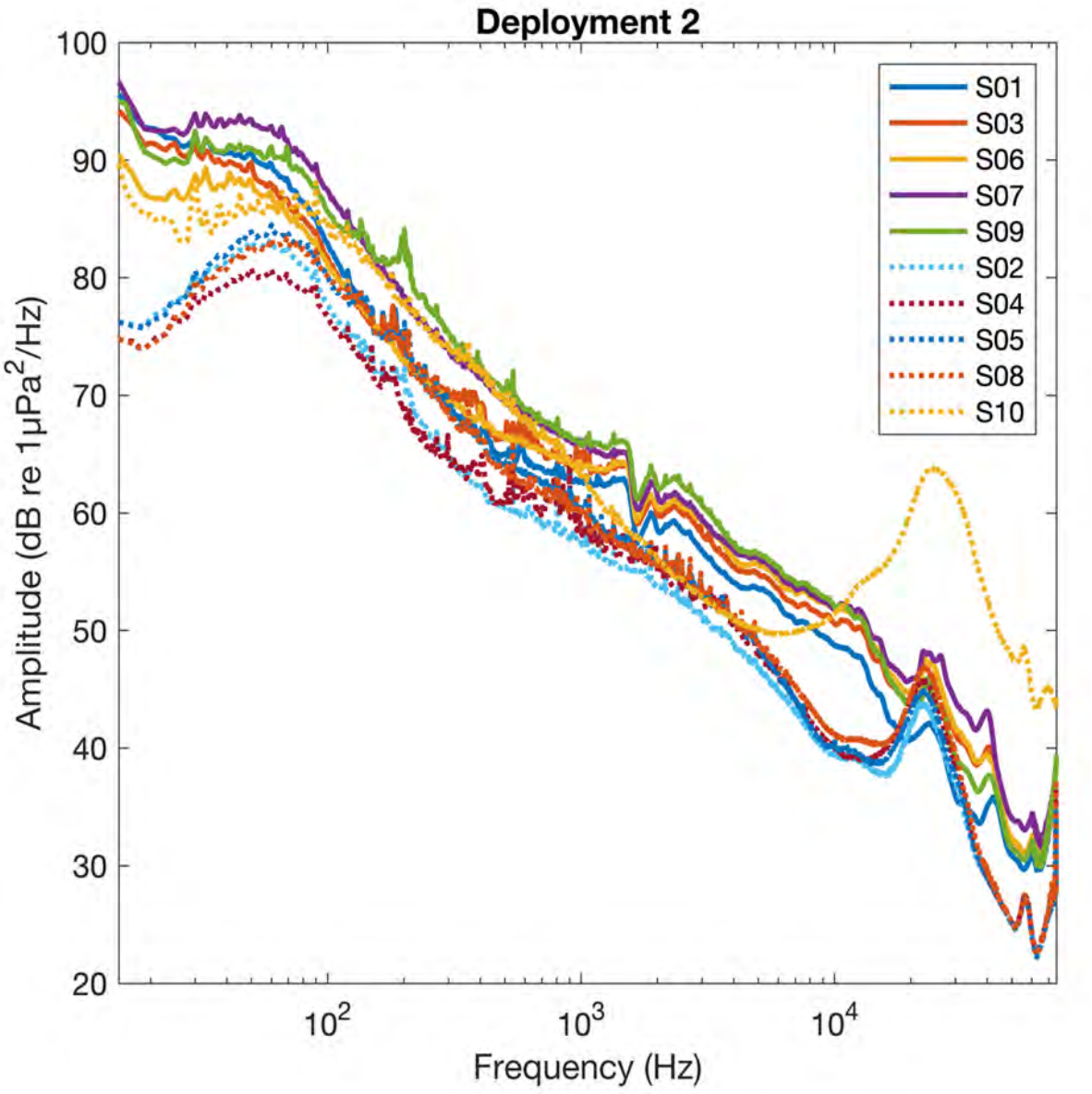

Figure 16. Comparison of RH and EARS median spectra for data collected during Deployment 2

Note: RH data are shown as solid lines, and EARS are shown as dotted lines.

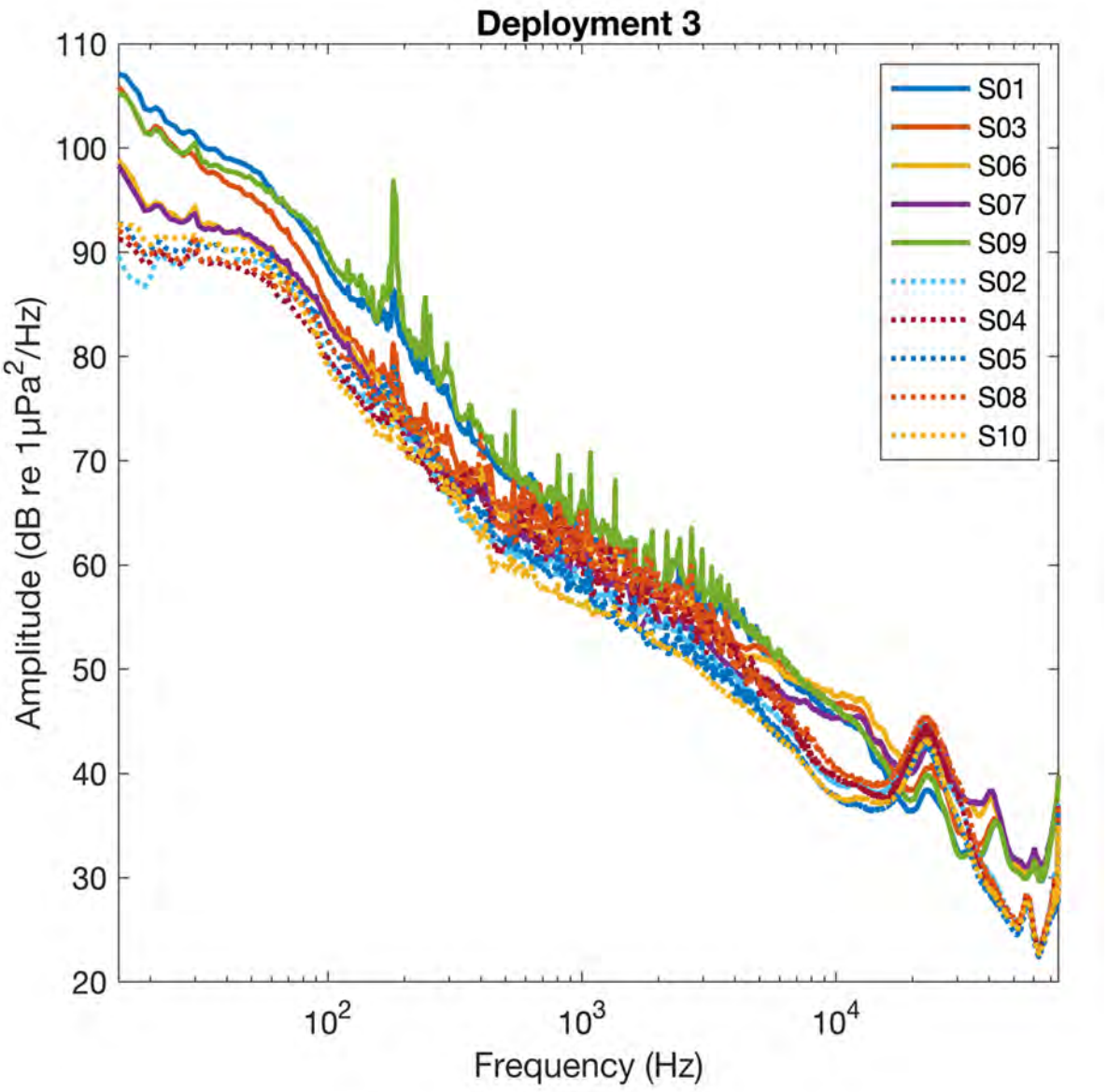

Figure 17. Comparison of RH and EARS median spectra for data collected during Deployment 3

876 Note: RH data are shown as solid lines, and EARS are shown as dotted lines.

877

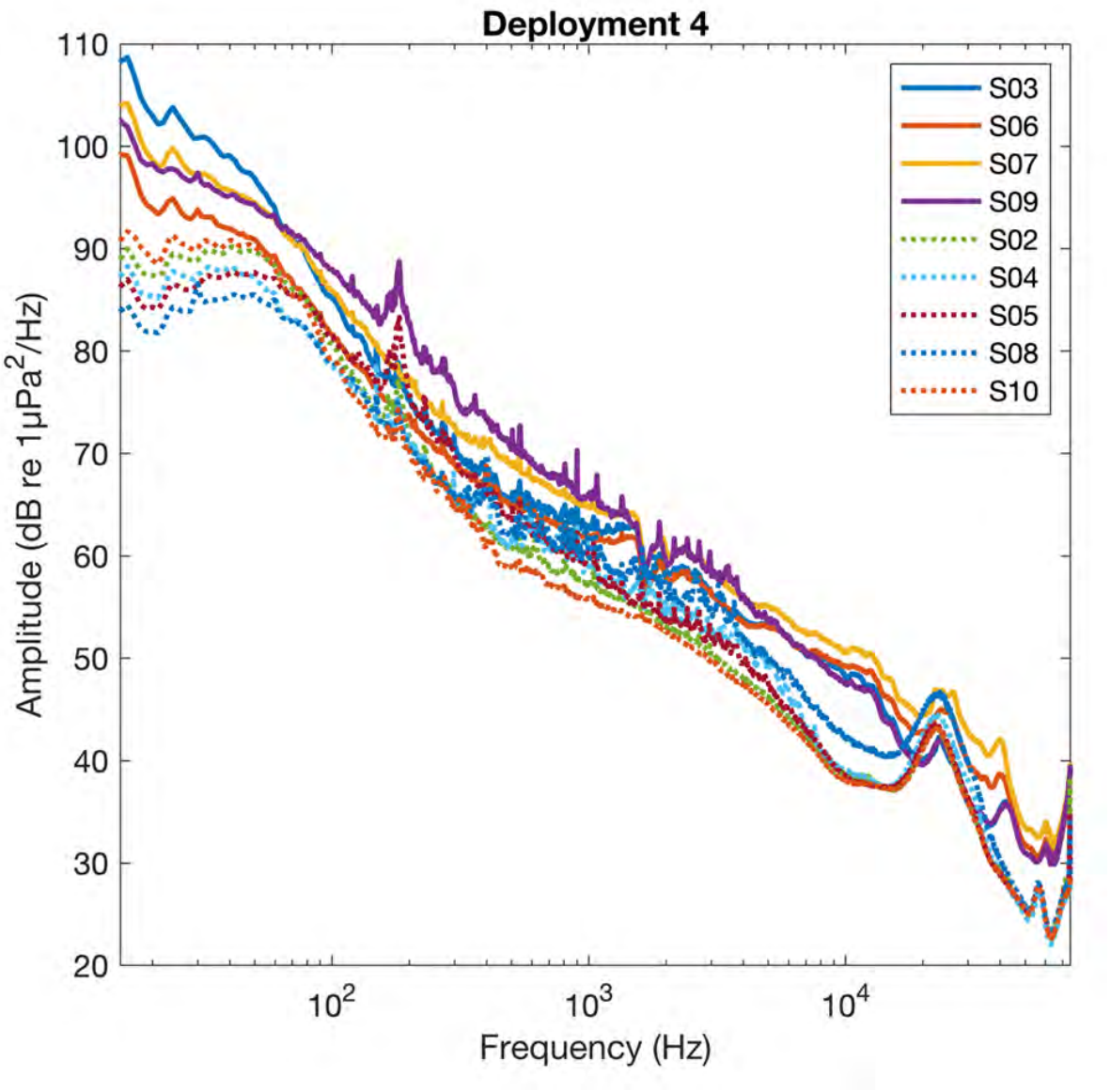

Figure 18. Comparison of RH and EARS median spectra for data collected during Deployment 4

878 Note: RH data are shown as solid lines, and EARS are shown as dotted lines.

879

SHRU VLA data were analyzed using standardized acoustic data analysis protocols following standards outlined in Ainslie et al. (2017) for average sound pressure spectrum levels, L_{eq}, PSD levels, cross-spectral density levels, and noise coherence over the entire deployment period. Site-specific physical oceanography data collected from CTD casts conducted during each cruise and sensors mounted on the VLAs were used to derive sound speed profiles for underwater soundscape characterization and sound propagation modeling. SHRU data were also used for conducting 1) noise coherence and source correlation analyses, and 2) soundscape fingerprint analyses. These analyses are discussed in **Sections 4.8** and **4.10**.

During the 2018 MP, an acoustic playback experiment was conducted to obtain LF broadband acoustic transmission data as a function of distance. These data were used to assess sound propagation from selected anthropogenic sources, ground-truth localization abilities of the SHRU VLA inside and outside a canyon environment and validate the underwater sound propagation model.

Comprehensive results from the SHRU VLA data analyses are presented in individual sensor reports (Lin 2019, 2021). Key results from these analyses are:

- Soundscape characterization results were consistent with those observed from RHs and EARS data analyses.
- LF soundscapes were dominated by seismic airgun surveys.
- VLA data analyses indicated that the average SPLs measured from 2019 to 2020 were substantially higher than those measured in 2018. This was most probably related to frequent seismic exploration activities conducted during the 2019 deployment period.
- LTSA plots for the Canyon and Slope SHRUs based on L_{eq} measured in one-third octave frequency bands are shown in **Figure 19** (May through October 2018) and **Figure 20** (September 2019 through March 2020).
- The acoustic playback experiment was successfully completed. Transmitted and received signals are shown in **Figure 21**.
- Noise coherence results were correlated with a subset of relevant AIS data (see **Section 4.8**). These results demonstrate the utility of collecting PAM data when AIS data are not available.

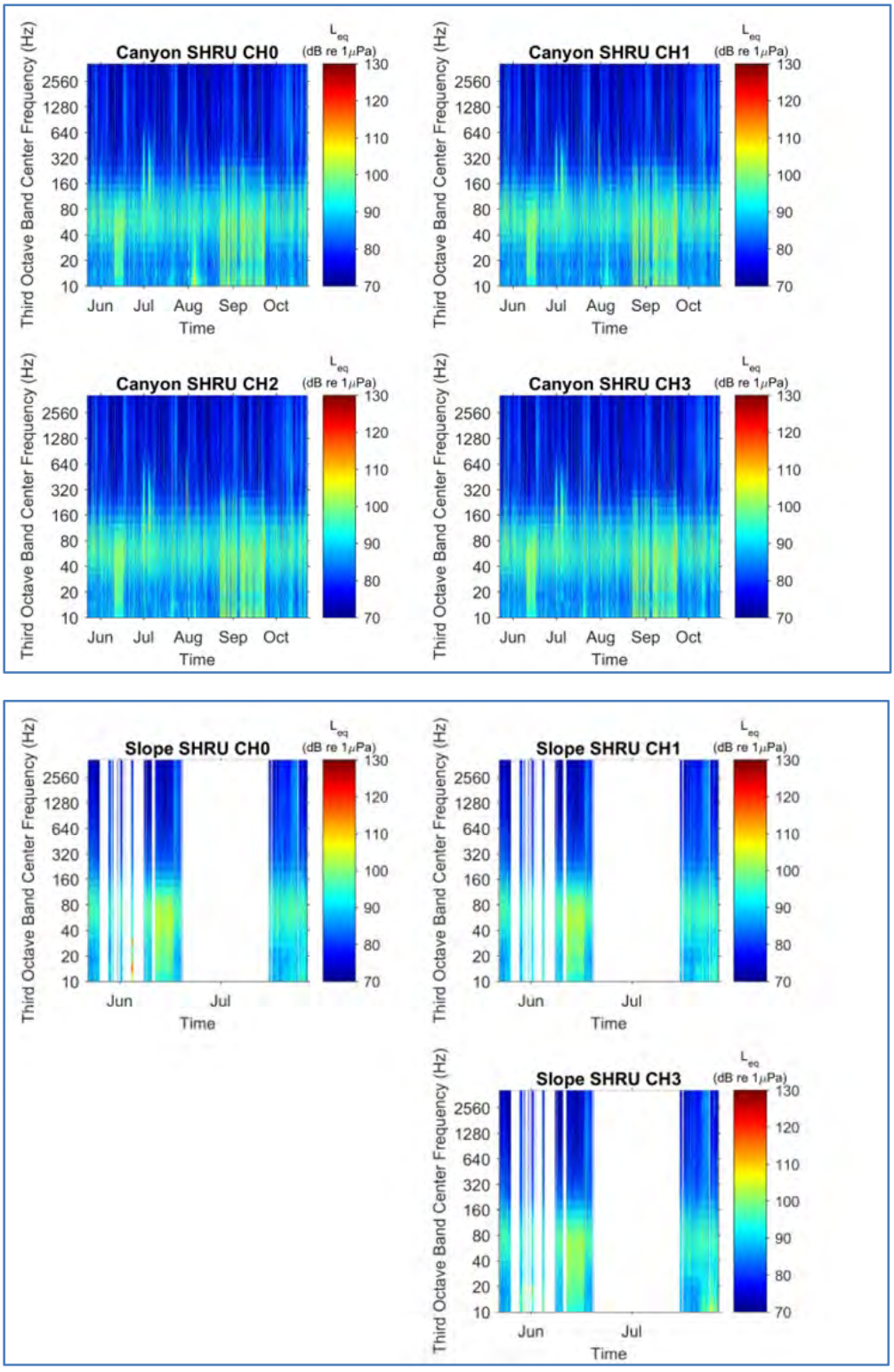

Figure 19. LTSA plots for the Canyon and Slope SHRUs based on L_{eq} measured in one-third octave frequency bands

908 Note: Data shown are from Deployments 1 and 2 (May to October 2018).

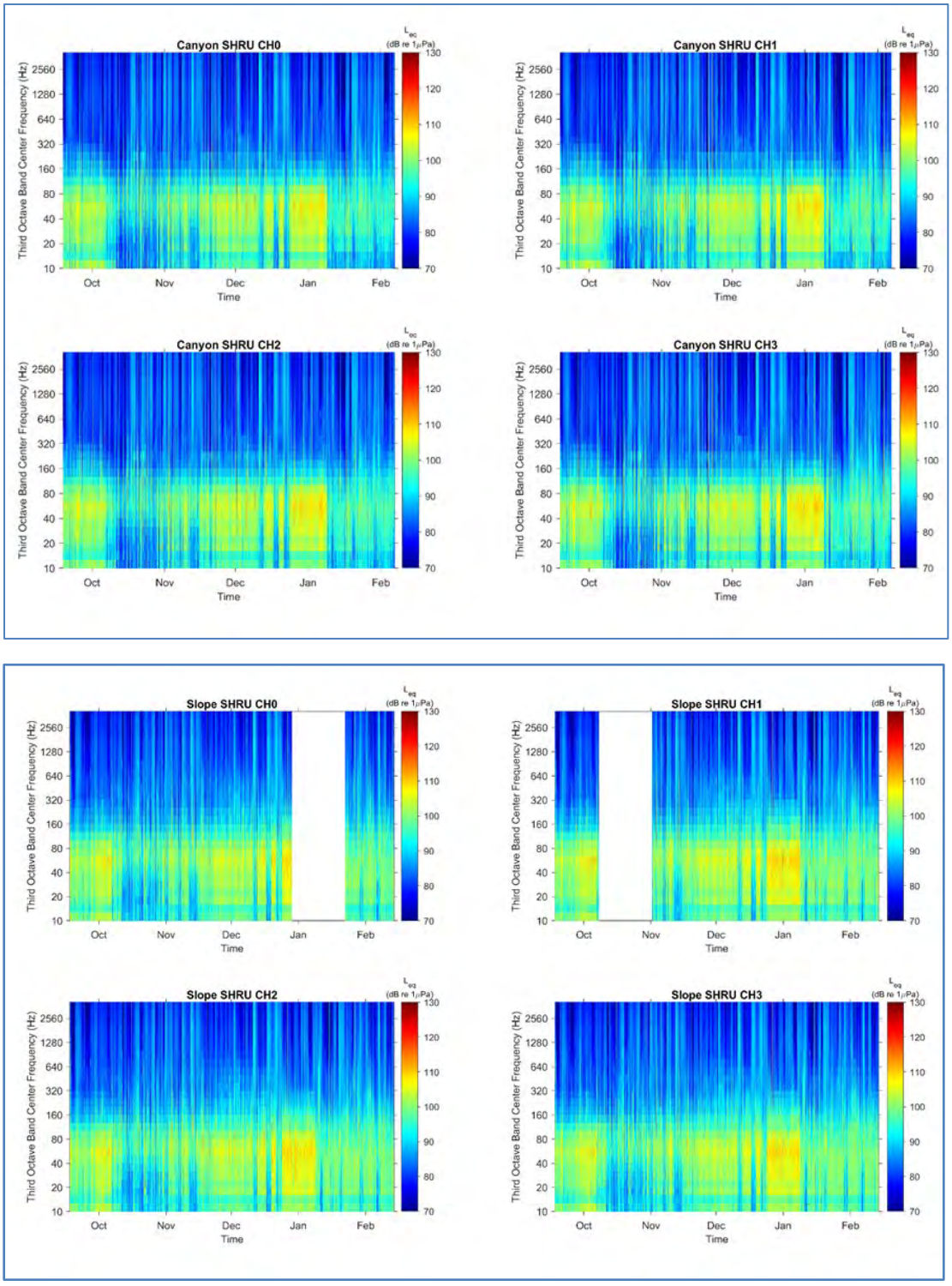

Figure 20. LTSA plots for the Canyon and Slope SHRUs based on L_{eq} measured in one-third octave frequency bands

909 Note: Data shown are from Deployments 3 and 4 (September 2019 to March 2020).

910

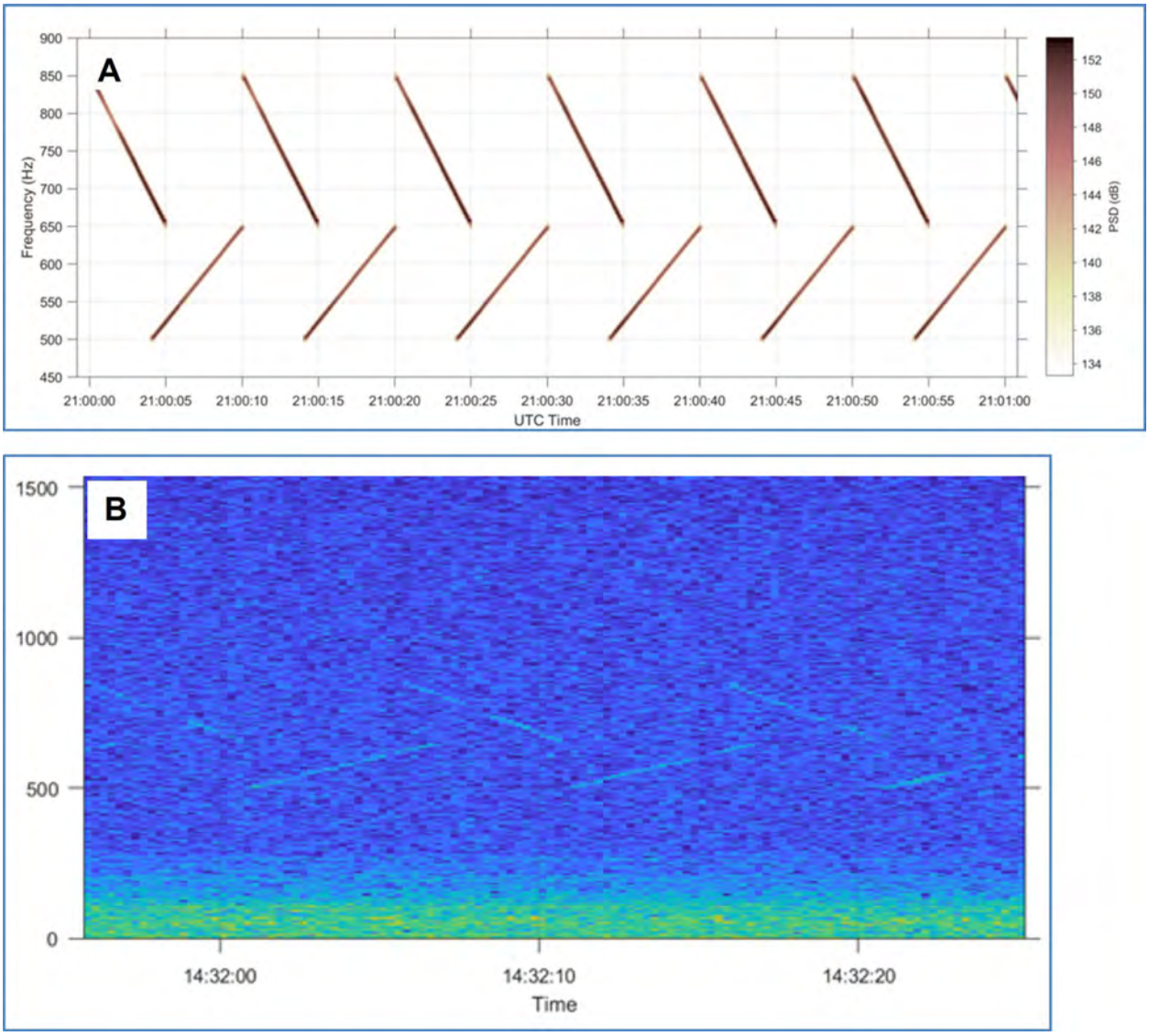

Figure 21. Source signal samples (a) and received signals (b) on the Canyon SHRU during the acoustic playback experiment conducted in May 2018

911

4.1.5 2018 MP Seaglider

In May through June 2018, the Seaglider collected approximately 724 hours of continuous data at a sample rate of 125,000 samples per second. Data were collected in the DeSoto Canyon area, through a deep-water area near the base of the continental slope, and into the Mississippi Canyon. Data quality was excellent, and no issues (e.g., electronic noise, drop-outs) were detected during the manual QA/QC performed as part of the post-processing.

Data were analyzed using the Raven-X software package (Dugan et al. 2018). The analysis methods and units followed established standards outlined in Ainslie et al. (2017). PSD levels (1 Hz, 1-second resolution) and spectral probability densities (Merchant et al. 2013) were calculated for each region using the 1-hour mean levels. The levels were calibrated and seconds containing glider motor noise detections were removed. Mean hourly PSDs were calculated from the noise-removed data and noise spectra percentiles were calculated from the hourly means.

LTSAs were determined for all three frequency range datasets (full bandwidth, 125 kHz sampling rate, down sampled to 10 kHz, and down sampled to 1 kHz). Noise was removed from each LTSA. Noise spectra percentiles and spectral probability density plots were separately prepared for three flight segments. Additionally, hourly mean PSDs were compared across three glider depth bins (50 to 250 m, 400 to 600 m, and 800 to 1,000 m).

Comprehensive results from the 2018 MP Seaglider data analyses are presented in an individual sensor report (Mellinger and Fregosi 2019). Key results from these analyses are:

- The Seaglider effectively recorded sounds from a greater than or equal to 500-km-long path over a span of approximately 6 weeks, covering both highly industrialized (Mississippi Canyon) and lightly industrialized (DeSoto Canyon) areas and found large differences (greater than 10 dB) in sound levels between them.
- DeSoto Canyon had the lowest surface sound speeds, while Mississippi Canyon had the fastest surface sound speeds, likely due to the influx of warmer waters from the Mississippi River. The difference was not large, however; mean sound speed difference between the two areas was only approximately 6 m/second. What was notably different between the areas was the presence of a surface duct in the Mississippi Canyon caused by a non-decreasing sound speed profile in a layer shallower than 20 m. This duct has the potential to keep a larger fraction of acoustic energy generated in that shallow layer near the surface than in regions without the duct (Urick 1984).
- Noise levels follow the general pattern of ocean noise elsewhere, with highest levels at low frequencies and a steady decline with increasing frequency to approximately 10 kHz.
- Noise levels in the deepest waters are higher than those in shallower water, possibly due to the ability of sound to propagate farther in deep water.
- Noise levels were quietest in DeSoto Canyon, likely due to lower levels of industrialization, and loudest in the deep-water area, possibly due to longer sound propagation distances.
- DeSoto Canyon also had the greatest differences in sound levels with depth (**Figure 22**). This was most pronounced at 300 Hz, where the median levels of the shallowest (50- to 250-m) recordings were approximately 8 dB quieter than the mid-depth (400- to 600-m) ones, which in turn were approximately 8 dB quieter than the deepest ones. Differences in median levels with depth were present, though to a lesser extent, from 10 Hz up to 40 kHz, above which the median levels converged. This effect existed for the quieter levels (10th percentile) as well, and was more pronounced for those levels, with nearly a 20 dB difference between the shallowest (50- to 250-m) and deepest (800- to 1,000-m) regions.

- The Deep Slope region had the least differences by depth, with the median 10th and 90th percentile levels showing little difference across the three depth bands measured at most frequencies (**Figure 23**). A difference was observed from approximately 15 to 40 kHz, with the median sound levels at deeper depths (800- to 1,000-m) 2 to 4 dB louder than those at shallower depths (50- to 250-m and 400- to 600-m).
- Mississippi Canyon also had differences in median sound levels with depth, though to a lesser degree (**Figure 24**). Median sound levels at the shallow (50- to 250-m) and middle (400- to 600-m) depths were nearly equal, while the deepest depths (800- to 1,000-m) were approximately 5 dB louder in the 70 to 300 Hz band. At quiet (10th percentile) and loud (90th percentile) sound levels, there were few differences with depth.

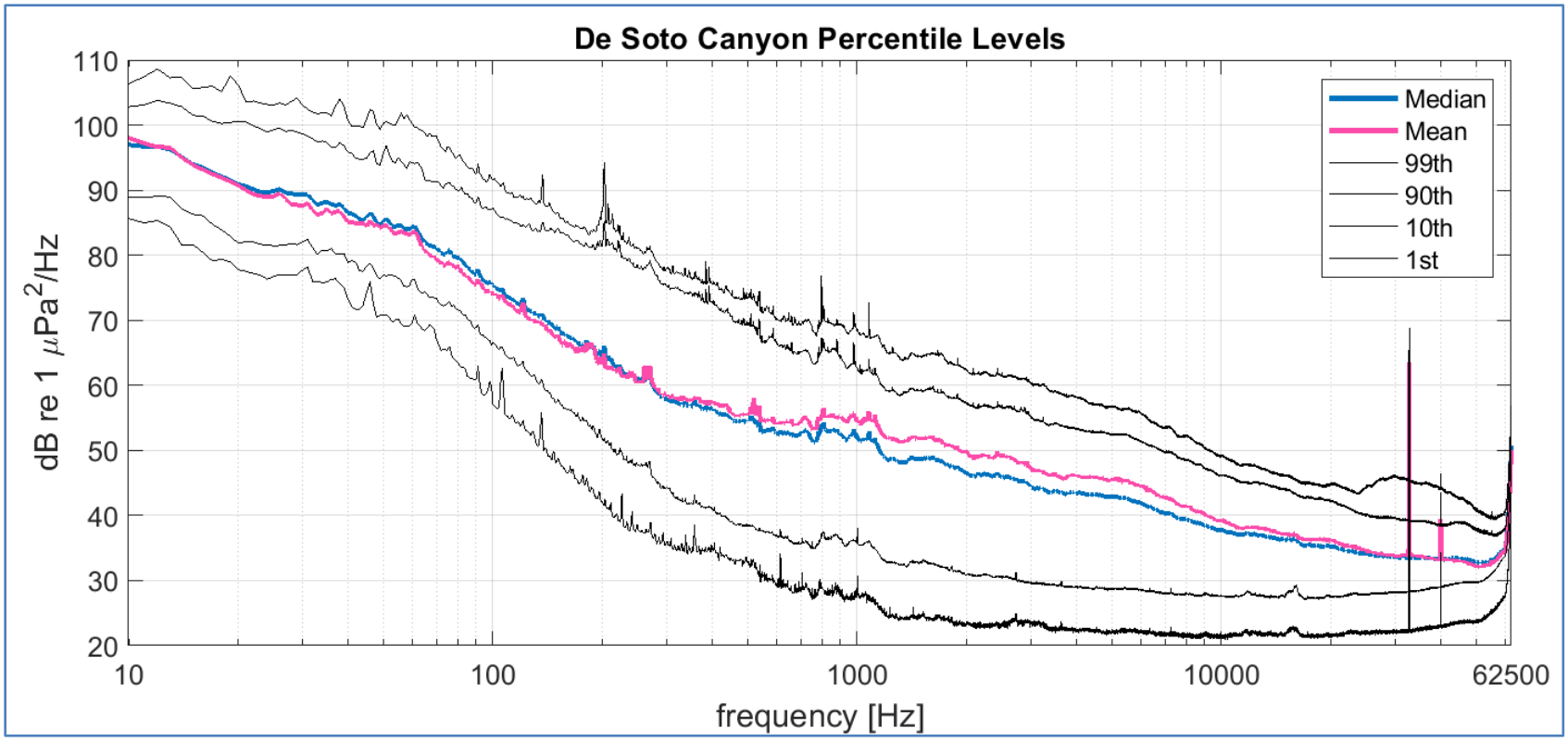

Figure 22. DeSoto Canyon percentile levels

Note: Noise levels at the 99th, 90th, 50th (blue), 10th, and 1st percentiles for the three segments of the glider track from east to west. The mean is shown in pink.

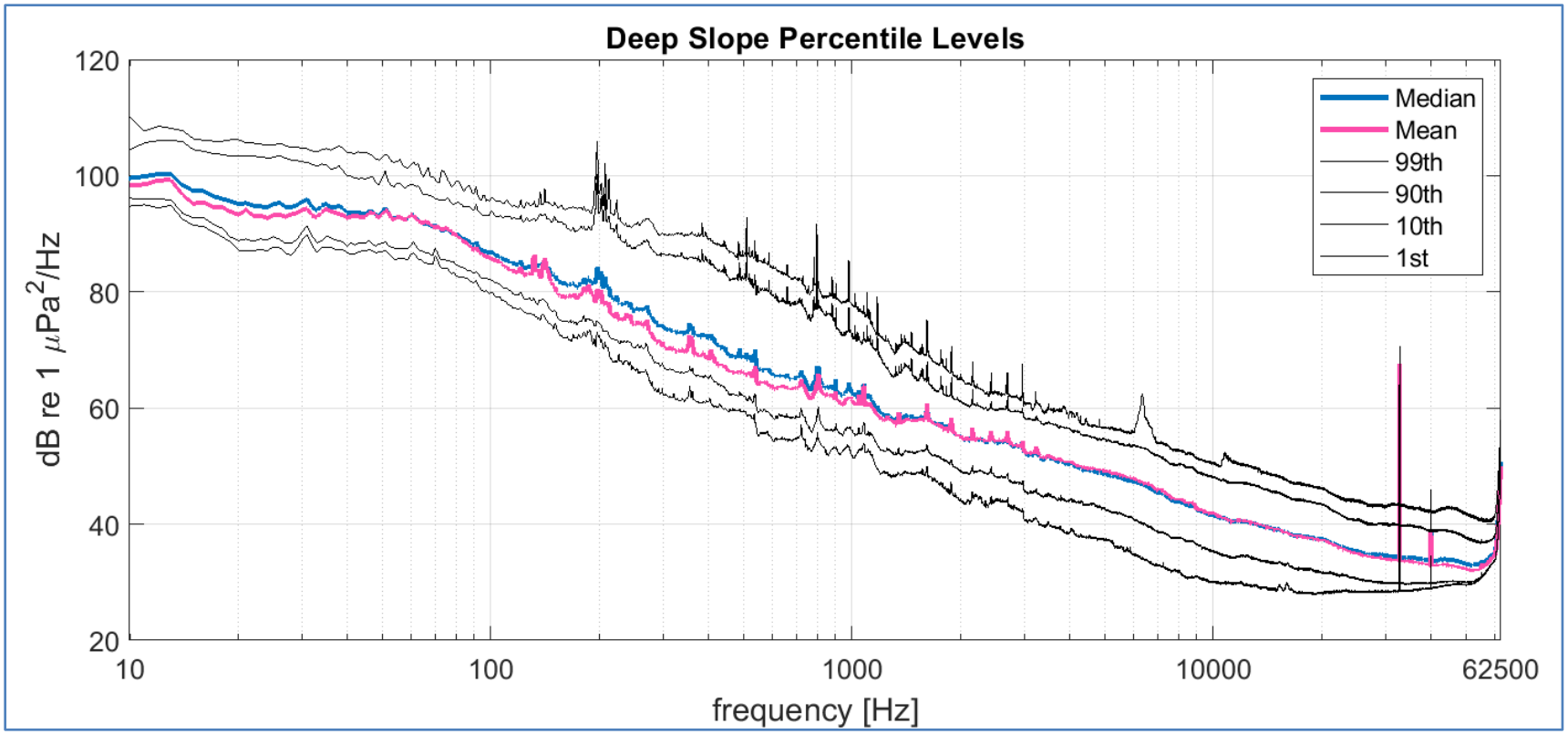

Figure 23. Deep Slope Canyon percentile levels

Note: Noise levels at the 99th, 90th, 50th (blue), 10th, and 1st percentiles for the three segments of the glider track from east to west. The mean is shown in pink.

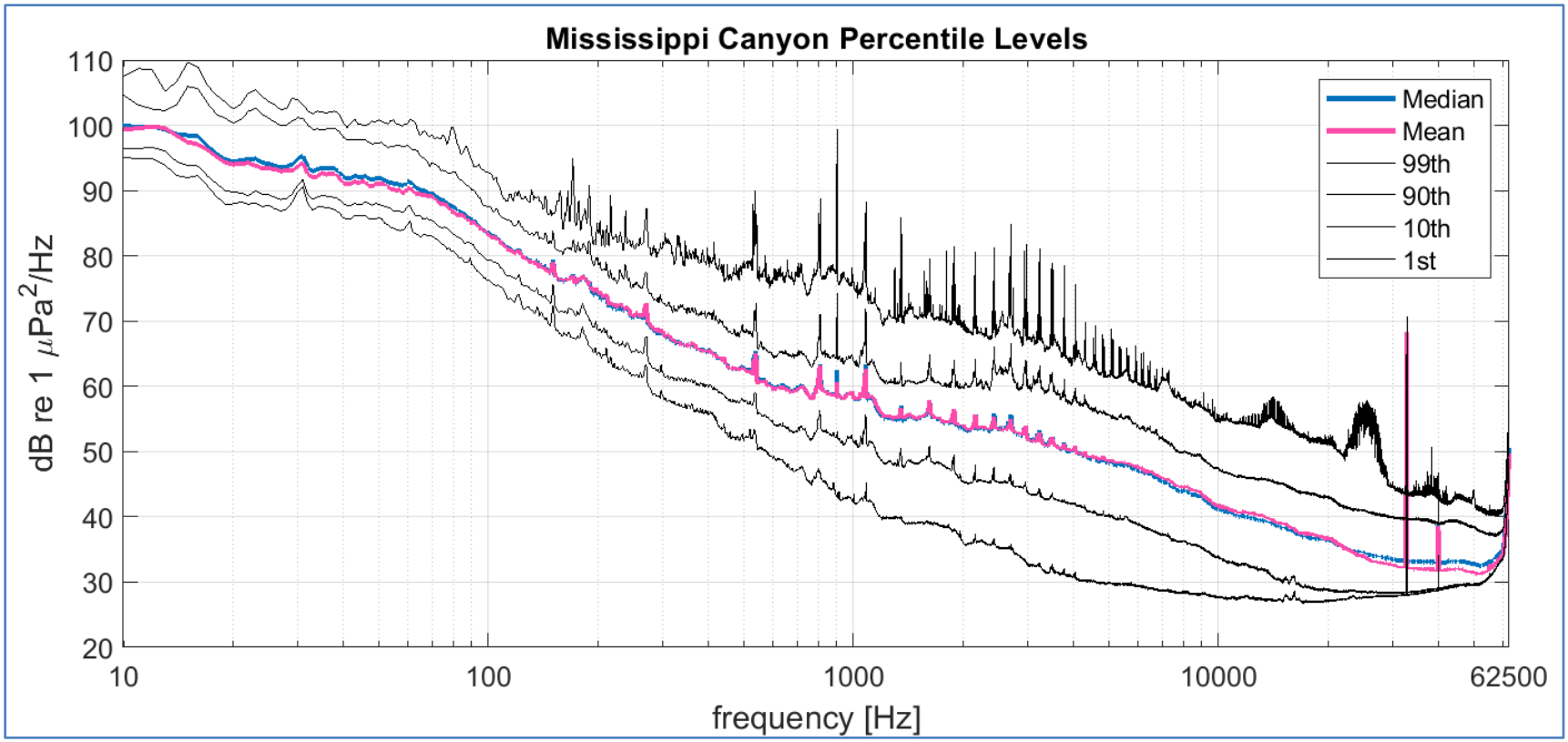

Figure 24. Mississippi Canyon percentile results

Note: Noise levels at the 99th, 90th, 50th (blue), 10th, and 1st percentiles for the three segments of the glider track from east to west. The mean is shown in pink.

4.1.6 2019 MP Seaglider

Under the 2019 MP, a Seaglider was deployed on September 24, 2019, near DeSoto Canyon and recovered on October 6, 2019, during which time it completed 63 dives (**Figure 25**).

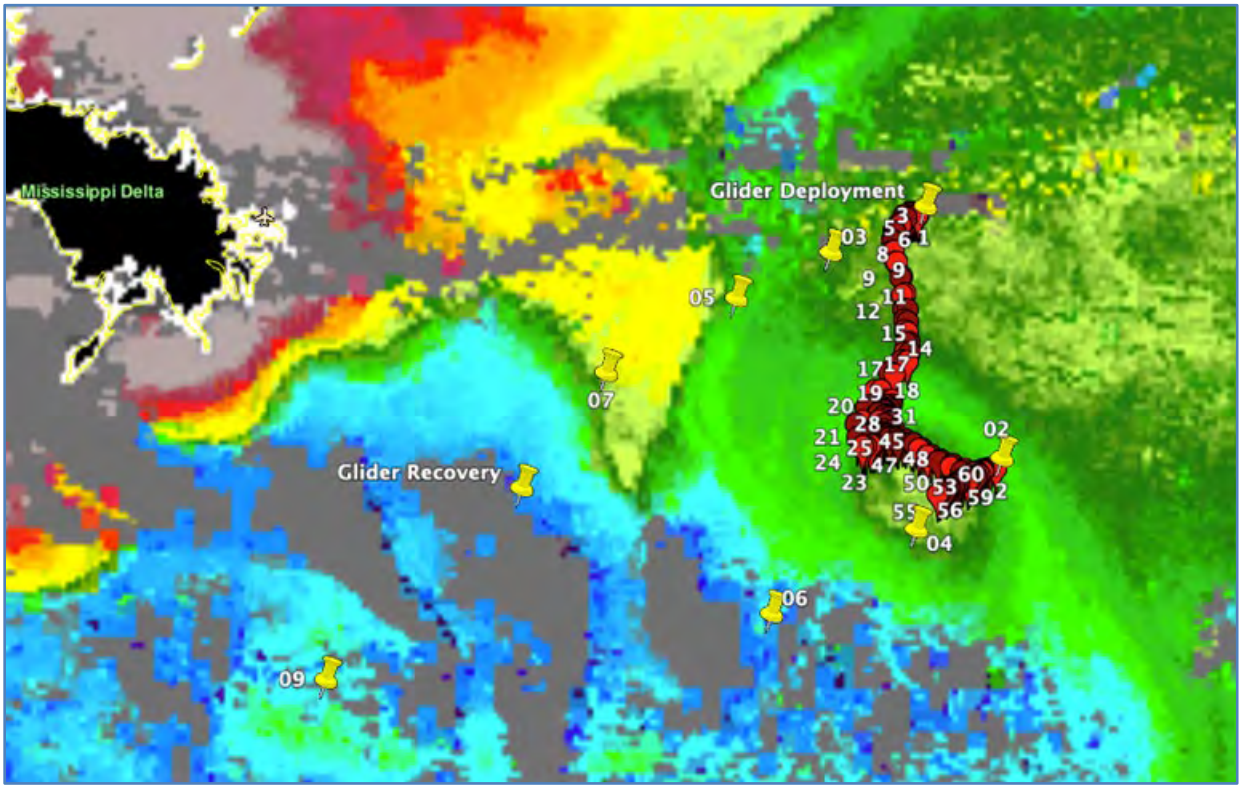

Figure 25. Seaglider track (in red with dive count number) and the mission targets (yellow tacks) overlaid on satellite image of chlorophyll-a index color

Note: Satellite image courtesy of the Optical Oceanography Laboratory at the University of South Florida.

Passive acoustic data as well as temperature and salinity profiles were collected throughout the deployment. **Figure 26** shows temperature, salinity, and sound speed profile data collected during three different phases of the mission. These data demonstrate that the density difference is primarily due to differences in surface salinity, as the temperature is fairly consistent at the sea surface.

The PAM system recorded continuously during the descent and ascent portions of the Seaglider dives (63 dives) at a sample rate of 128 kHz. PAM data were available for all dive segments except for the descent portions of Dives 36 and 57. Cursory inspection of the acoustic data identified marine mammal vocalizations, particularly dolphin whistles, throughout the mission.

Sample spectrograms (**Figure 27**) show whistles and clicks as well as LF pulses, below 100 Hz, likely attributable to oil and gas activity. A large number of echolocation clicks were visible and audible throughout much of the deployment, notably in the last few acoustic data files of the mission (Uffelen et al. 2019).

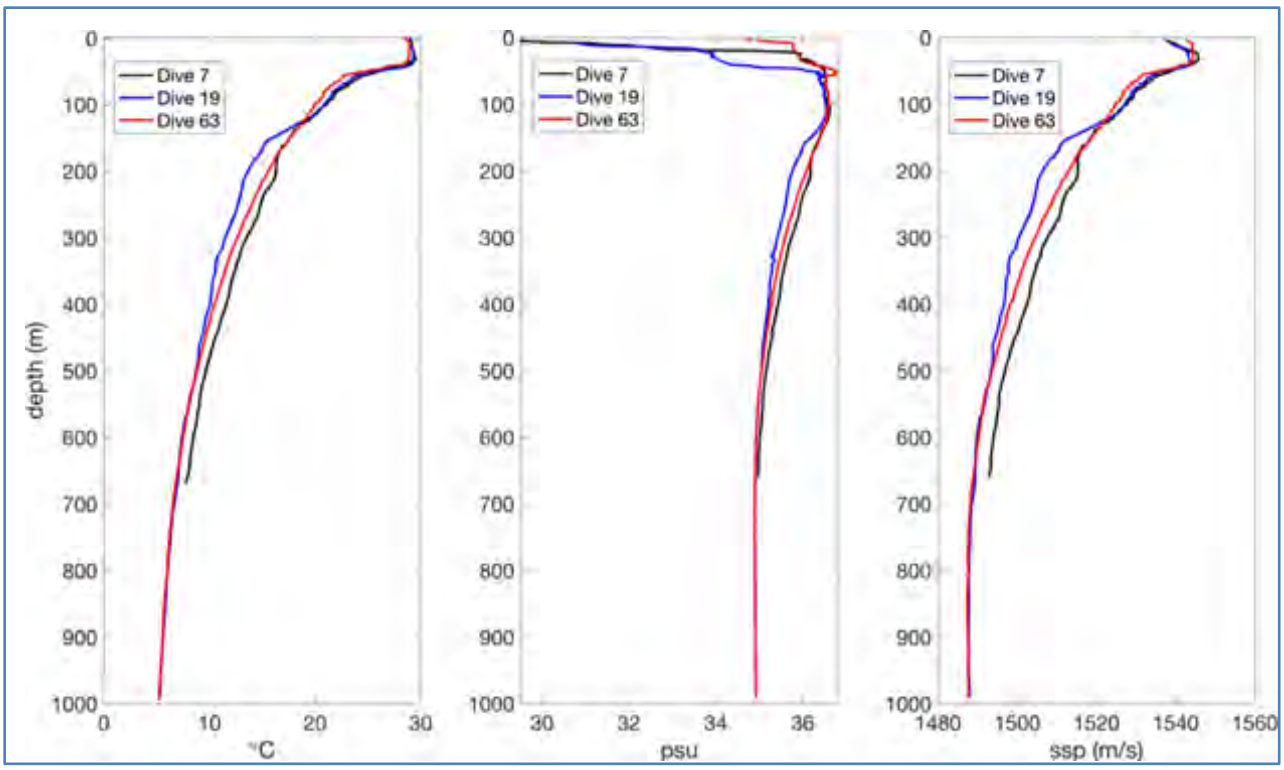

Figure 26. Temperature, salinity, and sound speed profiles observed during three different phases of the September/October 2019 Seaglider mission in the GOM

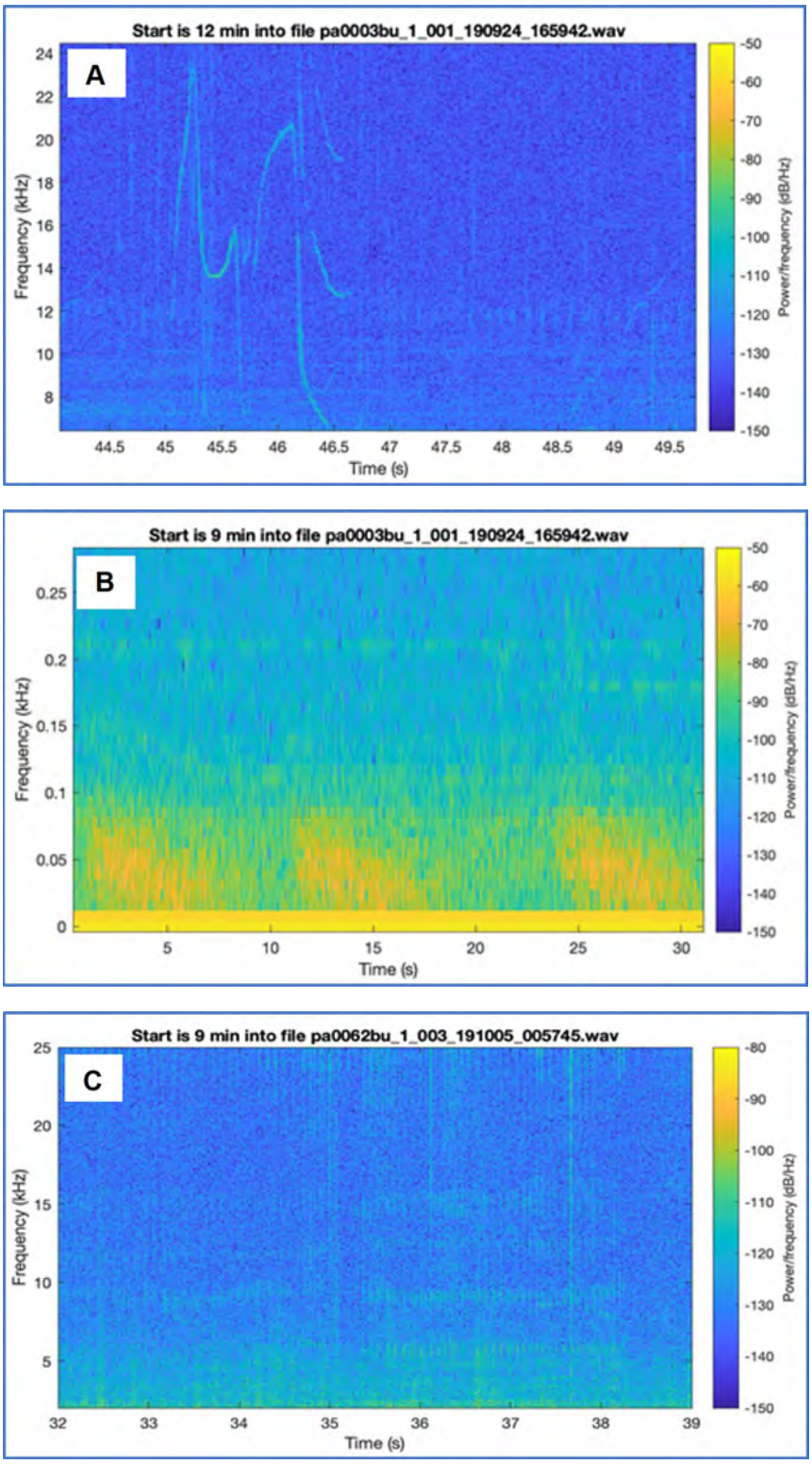

Figure 27. Sample spectrograms from acoustic data collected by the 2019 MP Seaglider deployment showing whistles (a), LF pulses (Dive 3) (b), and clicks (Dive 62) (c)

4.2 Soundscape Spatial and Temporal Trend Analyses

4.2.1 2018 MP Spatial and Temporal Trend Analyses

Spatial and temporal trend analyses were conducted using data collected by the four sensor types during Deployments 1 and 2 under the 2018 MP. For assessment of temporal trends, Wenz curves, which describe average noise levels in deep waters for varying noise sources such as ship traffic, wind waves, and other sources, were used as the basis for the comparison (**Figure 28**) (Bradley 2003).

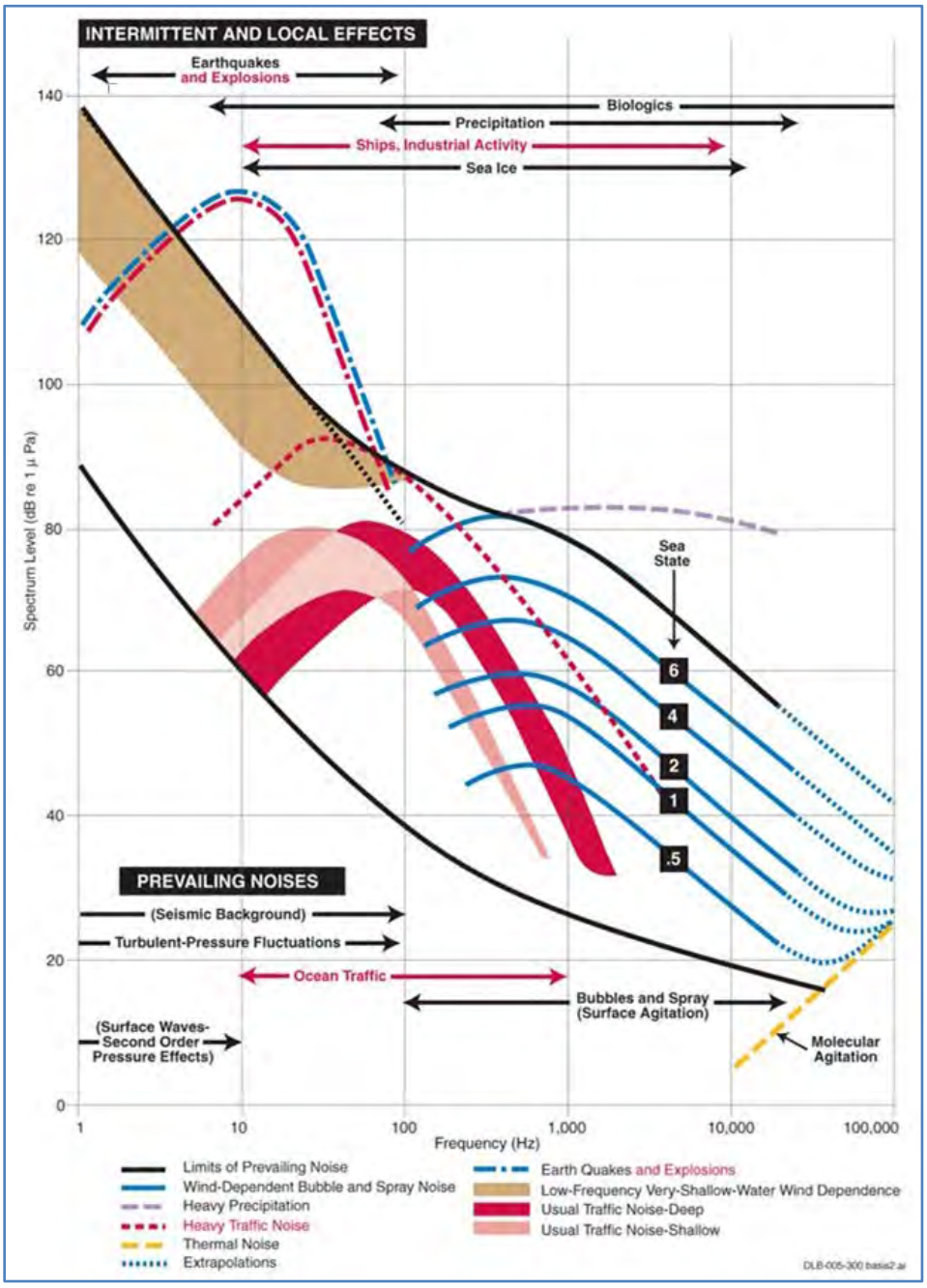

Figure 28. Historical ambient noise Wenz curves

Note: Plot of Wenz curves abridged from Bradley (2003)

In **Figure 29,** average noise spectrum levels from data collected by RHs, EARS, SHRU VLAs, and Seaglider over the entire spring and summer 2018 deployment period (Deployment 1) are plotted side-by-side with previously reported Wenz curves of historical typical ambient noises in the marine environment. The average noise spectrum levels are in dB re 1 μPa^2/Hz and shown in 1 Hz wide bands for 10, 100, 1,000, and 10,000 Hz from each of the three systems. Key observations/conclusions from **Figure 29** are:

- The average soundscape characteristics for the study area fall within the Wenz curve bands and are consistent with prior reporting (Latusek-Nabholz et al. 2020).
- In general, the average noise levels were almost centered between the upper and lower noise limit ranges shown in the Wenz curves.
- HF (10 kHz) levels were consistent with lower sea states except for Site 9, in shallow water where the noise was dominated by snapping shrimp. Note that Wenz curves were derived from historical deep-water measurements, and shallow noise is typically higher than deep water for frequencies at or above 1,000 Hz.
- The Mississippi Canyon levels are slightly (but consistently across platforms) quieter than the slope nearby. For example, the SHRU VLAs measured a 1 to 2 dB difference between the canyon and slope. This finding is corroborated by the TL predictions from preliminary simulation runs of the 3D sound propagation model. The model simulations predict a slightly higher transmission loss to similar ranges from the canyon site compared to the slope site. The biological significance of the difference in noise levels between the canyon and slope sites needs further evaluation.
- Measurements recorded by the Seaglider indicate that the noise levels in the DeSoto Canyon are significantly lower than the Mississippi Canyon. This finding is consistent with the known difference in the extent of industrialization of the two canyon areas.
- Seismic exploration dominated measurements recorded by most of the sensors placed in deep waters at frequencies at or below 100 Hz.
- Different sensor systems reported approximately 20 dB or more of variability on a daily basis. In the 1 to 10 kHz band, there was 30 dB of variability. This variability is likely due to a combination of anthropogenic and natural sound sources. Marine mammals, specifically beaked whales, appear to be a significant contributor to the noise field above 30 kHz. The shallow-water site measured with one of the RHs showed the highest levels of noise above 100 Hz and some of the lowest levels at 10 Hz.
- The Seaglider levels are lowest of all the sensors for almost all the bands and are especially low in the DeSoto Canyon. This may be because the Seaglider spent so much time in the shallower water where propagation of natural and anthropogenic sounds received at the sensor may not be as good. Therefore, the average noise levels were lower as compared to the moored sensor systems that recorded at greater depths.

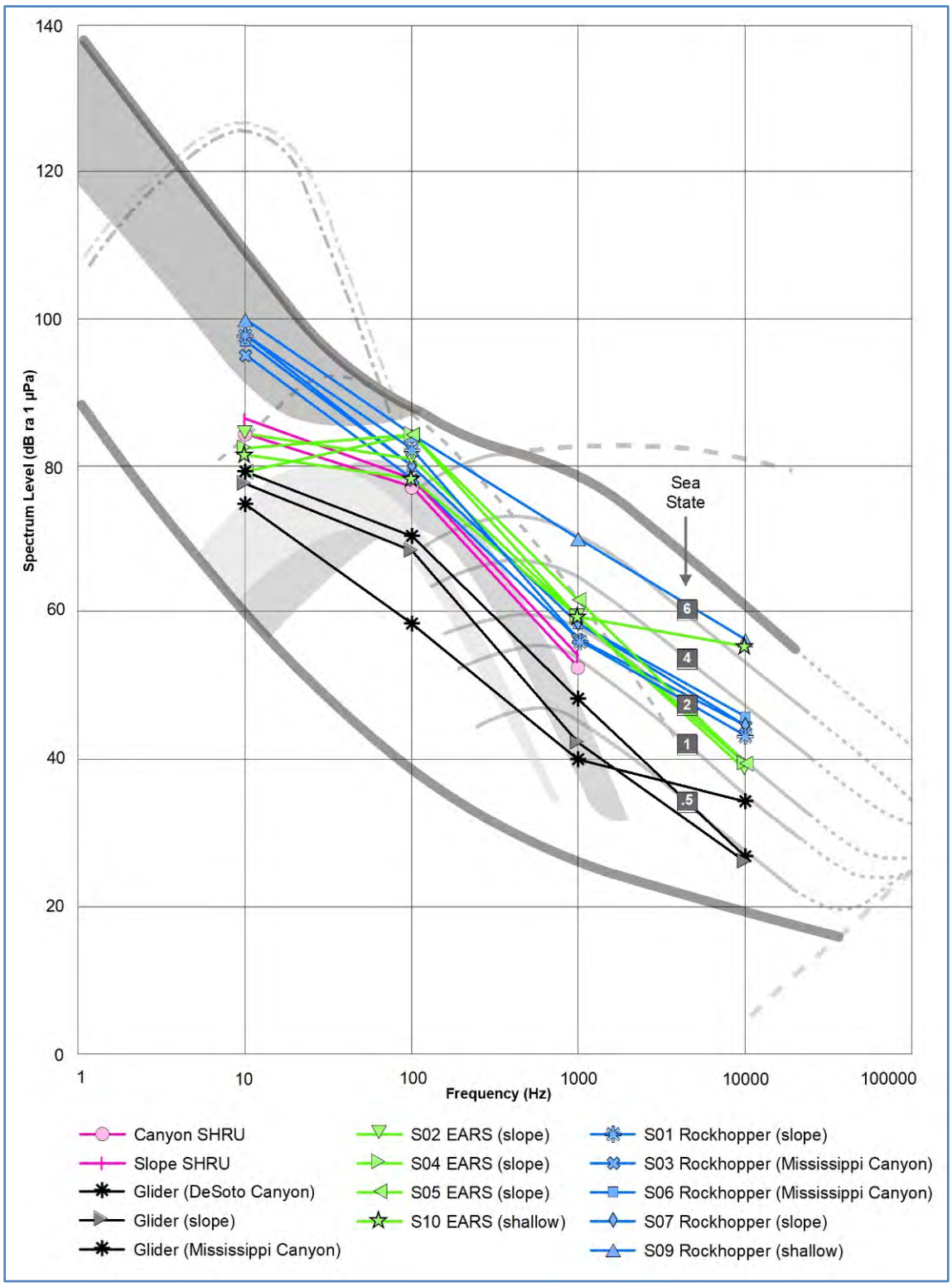

Figure 29. Comparison of the average spectral levels from the four sensor systems deployed under the GOM PAM 2018 MP with historical ambient noise Wenz curves

Note: Plot of Wenz curves abridged from Bradley (2003)

In **Figure 30,** average noise spectrum levels from data collected by RHs and EARS over the entire fall 2018 and winter 2019 deployment period (Deployment 2) are plotted side-by-side with previously reported Wenz curves of historical typical ambient noises in the marine environment. The average noise spectrum levels are in dB re 1 μPa^2/Hz and shown in 1-Hz-wide bands (for 10, 100, 1,000, and 10,000 Hz) from each of the three systems. Various factors such as presence of anthropogenic noise sources (e.g., shipping, airgun surveys, oil platforms), weather (e.g., wind, waves, rain, sediment disturbance), propagation regimes (e.g., shallow versus deep water, canyon) appear to have a significant influence in the spatial and temporal variations in the noise characteristics. Key observations/conclusions from **Figure 30** are:

- Average noise spectrum levels from measurements made in fall and winter are louder than measurements from spring and summer, most likely due to seasonal variation in airgun surveys activity. This seasonal variation is evident across all frequency bands.
- Shallow-water noise spectrum levels are quieter at 10 Hz, most likely due to greater interaction with the seafloor as compared to deeper waters.
- Shallow-water levels are louder at 10,000 Hz, most likely due to biological noise sources, specifically snapping shrimp.
- Noise spectrum levels in the Mississippi Canyon are lower than on the slope due to propagation/shielding effects.

Overall, SPLs during the fall and winter months were consistently lower than during the spring and summer months, especially in the LF band below 500 Hz. This is likely correlated to a decline in industrial activities during the colder winter months. Noise levels at higher frequencies (500 Hz to 10 kHz) driven by weather were higher during the winter months. Only during the February to March 2019 period were the LF soundscapes dominated by distant seismic surveys, unlike across the entire deployment period during summer.

To investigate the spatial aspects of the measured noise levels, **Figures 29** through **32** show the noise spectrum levels at each of the measurement sites for data collected during the second deployment under the 2018 MP. These figures correspond to the average spectrum levels from various systems at frequencies of 10, 100, 1,000, and 10,000 Hz, respectively. These figures demonstrate the spatial as well as the frequency structure of the ambient noise spectrum.

In general, shallow-water noise spectrum levels (Sites 9 and 10 in **Figure 29**) are quieter compared to deeper sites at 10 Hz. Shallow-water propagation is highly complex because of modal cut-off effects and boundary interactions, but this most likely could be due to greater interaction with the seafloor as compared to deep waters and the absence of LF noise from distant sources (e.g., shipping, airgun surveys).

It is interesting to note that this trend is reversed for HF (10,000 Hz; **Figure 30**), which indicates nearby sources that may possibly be biological in nature (snapping shrimp). The levels measured by the SHRU VLAs increased by 2 dB (10 Hz and 100 Hz) and by 4.5 dB (1,000 Hz) during the fall and winter seasons compared to the spring and summer seasons. A detailed modeling of canyon propagation is needed to explain whether this increase is driven by weather-related events, biological sources, or waveguide effects.

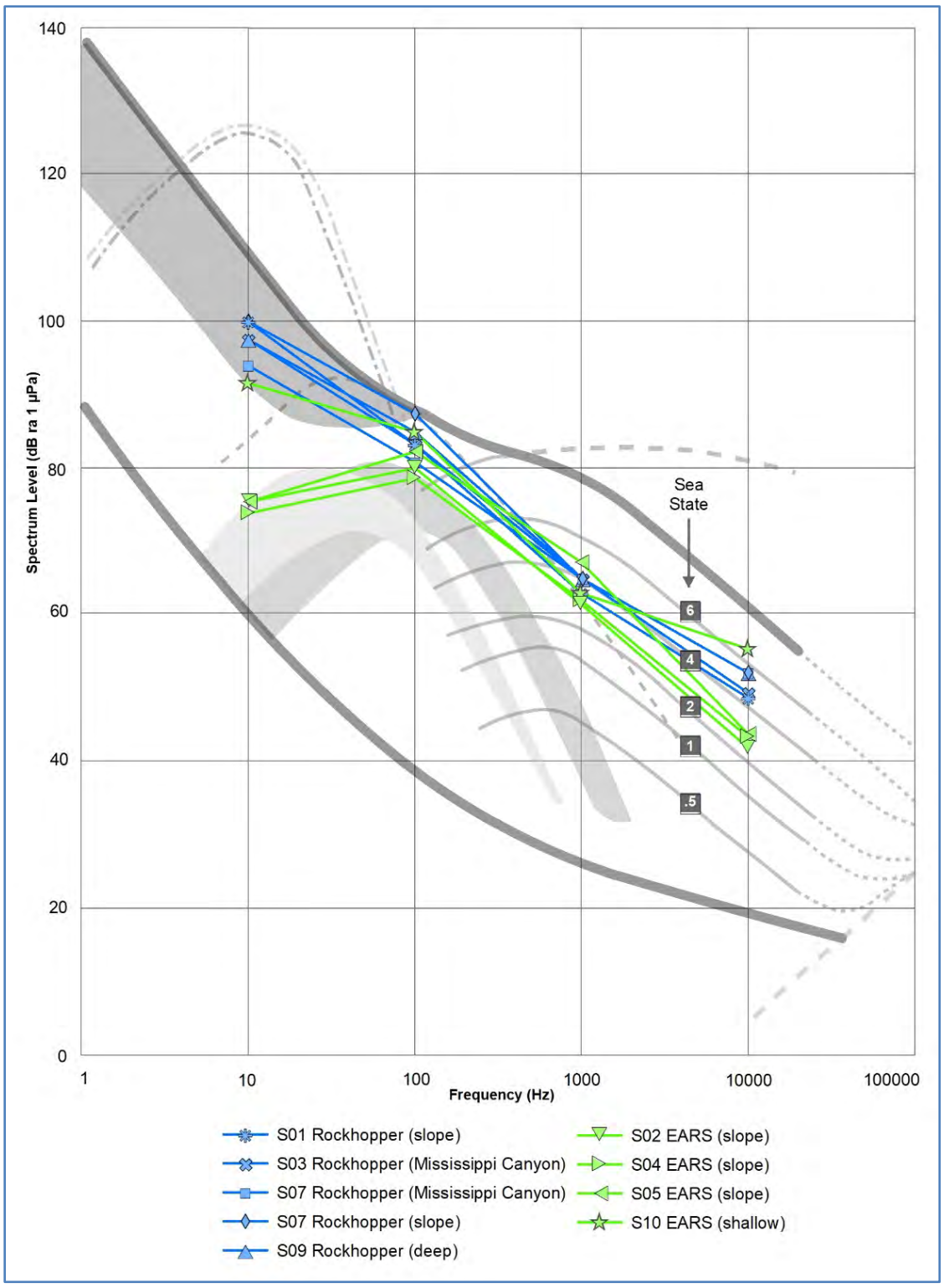

Figure 30. Comparison of the average spectral levels from EARS and RHs under the GOM PAM 2018 MP

Note: Deployment 2 measurements plotted side-by-side with historical ambient noise Wenz curves.

4.2.2 2019 MP Spatial and Temporal Trend Analyses

Spatial and temporal trend analyses were conducted using the complete 24-month RH and EARS dataset as part of which monthly spectral levels of the ten RH and EARS recorders were assessed to determine whether any spatial or temporal trends were evident in the data. **Figures E-C1** through **E-C26** in **Appendix E** present the monthly median spectral levels of the ten RHs and EARS recorders over the 24-month data collection duration. In each monthly figure, the top spectrum represents the entire frequency range, while the bottom panel presents the LF band (10 to 1,000 Hz) in more detail. These figures illustrate the temporal variability at each recorder sensor location, as well as an apparent difference in the data recorded by the RH and EARS recorders, particularly below 100 Hz.

4.3 Anthropogenic Sound Detection Analysis

The 24-month RH and EARS dataset were analyzed for detection of the two major anthropogenic contributors to the underwater soundscape in the GOM, namely ship traffic (vessels) and airguns used in seismic surveys. The technical report presented in **Appendix E (Section E.3.2.1)** contains detailed information on these analyses and data outputs; key information from the technical report is summarized and discussed below.

4.3.1.1 Vessel Detection Analysis

Vessels were present within the study area almost every day at every receiver location (**Figure 31**). The effects of spatial and temporal variables on vessel detection rates were explored with a generalized additive models (GAM). Significant patterns by year and month were observed. Numbers of vessel detection increased from 2018 to 2019 but decreased again in 2020. This may be a side effect of the sampling period and the markedly strong monthly pattern where the number of vessels was highest in the summer months and lower in the winter months. The patterns observed for latitude and water depth were also significant and indicated more contradictory patterns of increased vessel detection rates as latitude and water depth increased (**Figure 32**). The number of vessel detections was greatest in the middle longitudes and decreased strongly to the east, probably related to the location of port facilities (**Figure 33**).

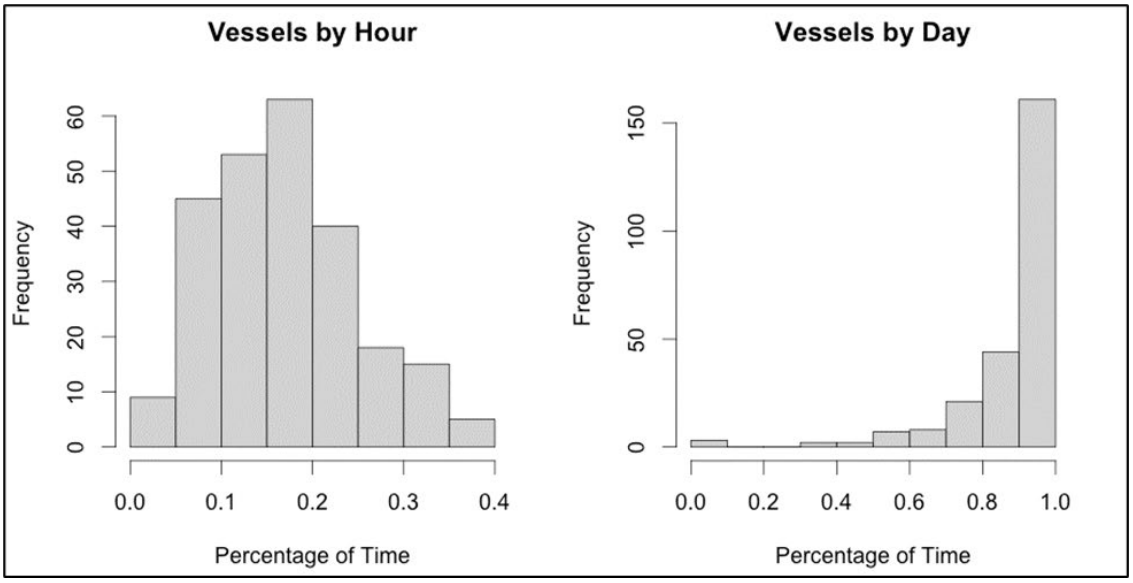

Figure 31. Comparison of monthly values for vessel detection based on hourly inputs (left) and daily inputs (right)

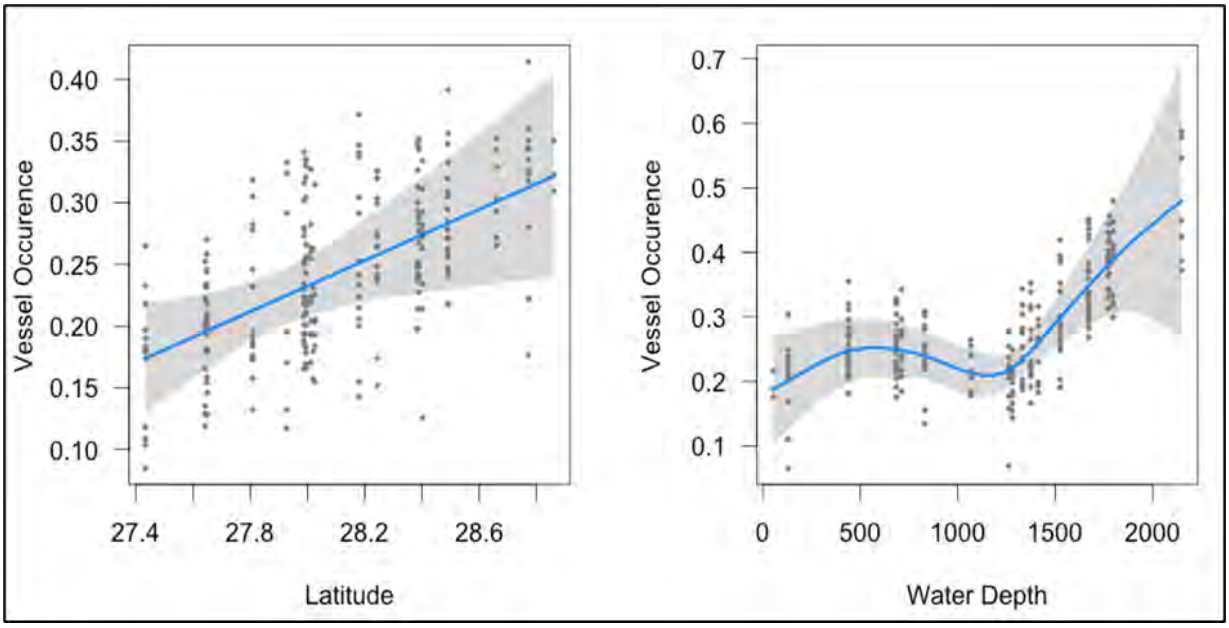

Figure 32. GAM smoothing functions for latitude (left) and water depth (right) effects on vessel detections

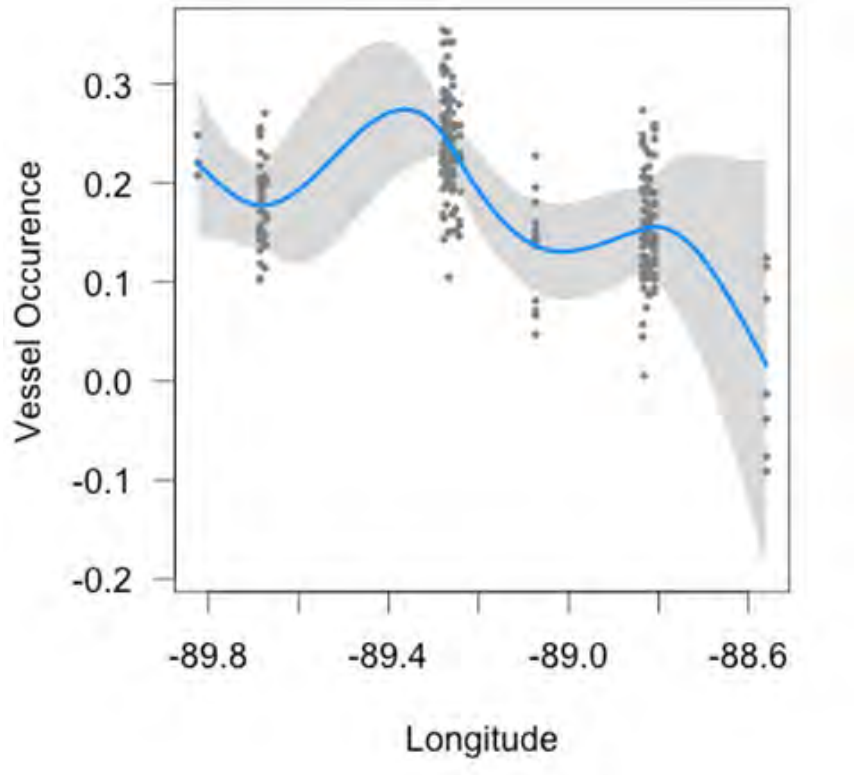

Figure 33. GAM smoothing functions for longitude effects on vessel detections

4.3.1.2 Airgun Detection Analysis

The approach described in **Section 4.3.1.1** for vessel detection was also adopted airgun signal detections. Month and year for airgun signal detections had similar patterns to that of vessel detections (**Figure 34**). Latitude and longitude effects for airgun signals were borderline statistically significant, with a dip in the frequency of airgun detections in the middle latitudes and a higher frequency of signal detections in the middle longitudes (**Figure 35**).

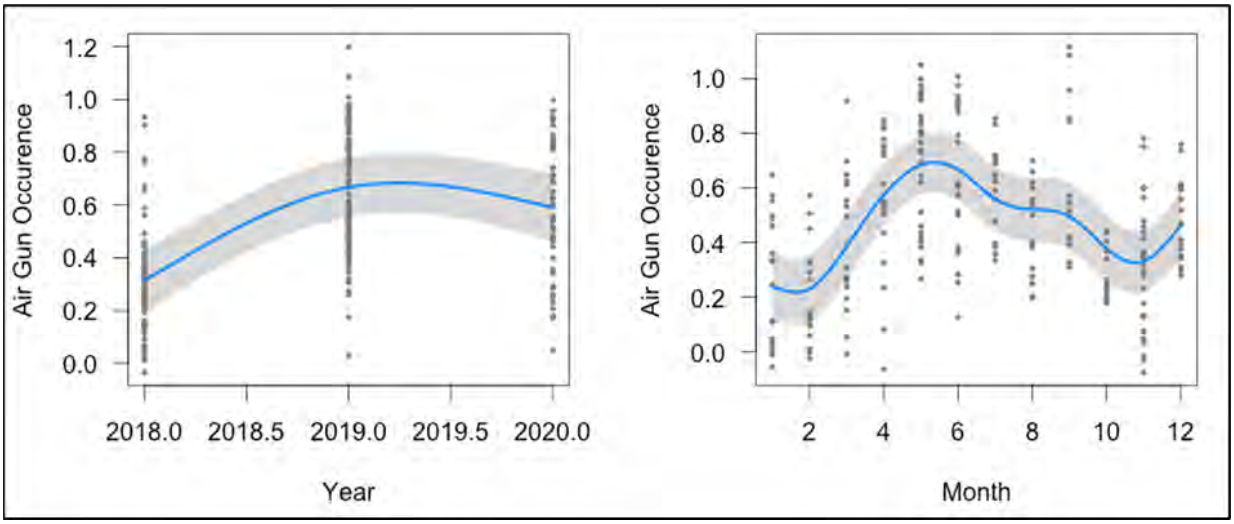

Figure 34. GAM smoothing functions for year (left) and month (right) effects on airgun signal detections

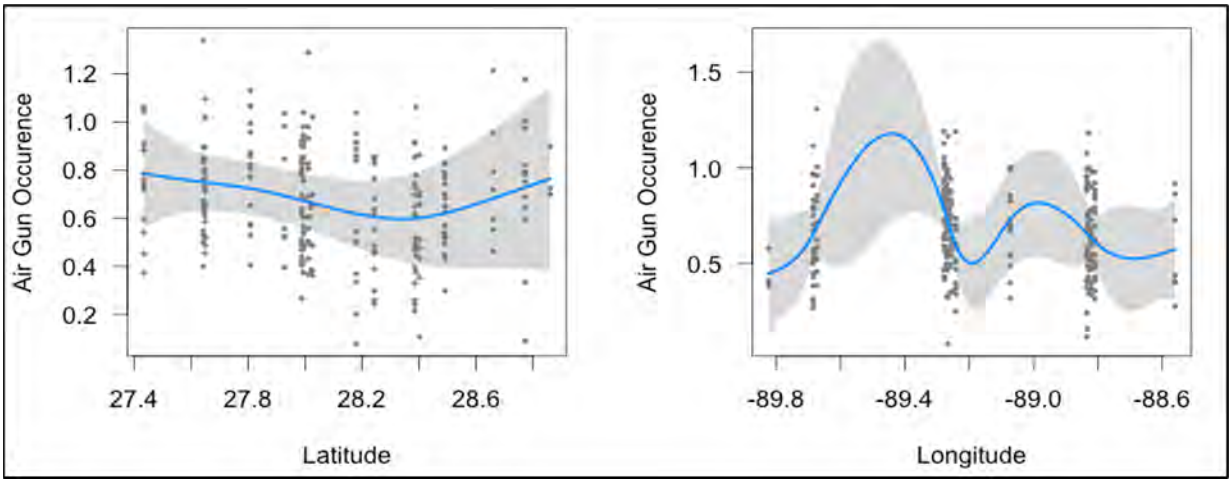

Figure 35. GAM smoothing functions for latitude (left) and longitude (right) effects on airgun signal detections

4.4 Biological Detection Analysis

To differentiate some of the most common sound-producing marine mammals in the northern GOM that may contribute to the soundscape, frequency bands were identified for the following species/species groups: Rice's whale, beaked whales, and dolphins. The technical report presented in **Appendix E** contains detailed information on these analyses; key information from the technical report is summarized and discussed below.

4.4.1 Rice's Whale (*Balaenoptera ricei*) Detections

The frequency overlap between the signals of Rice's whales and the prevalent anthropogenic noise made it difficult to reliably detect the calls of Rice's whales using only the spectrally analyzed data. A better approach would be to use a matched-filter detection process that operates on the waveform data.

4.4.2 Dolphin Band Detections: Low-frequency Clicks

Throughout the first deployment, dolphin band detections rose from May until September and then fell precipitously, both in rate and number of detections, in November (**Figure 36**). Detection rates peaked in nearshore shallow waters as well as in offshore water deeper than 1,000 m (**Figure 36**). This may be due to the detection function being triggered by multiple species. Detection rates appeared to increase with latitude. Peak rates were seen in the middle longitudes and decreased to the east and west (**Figure 37**).

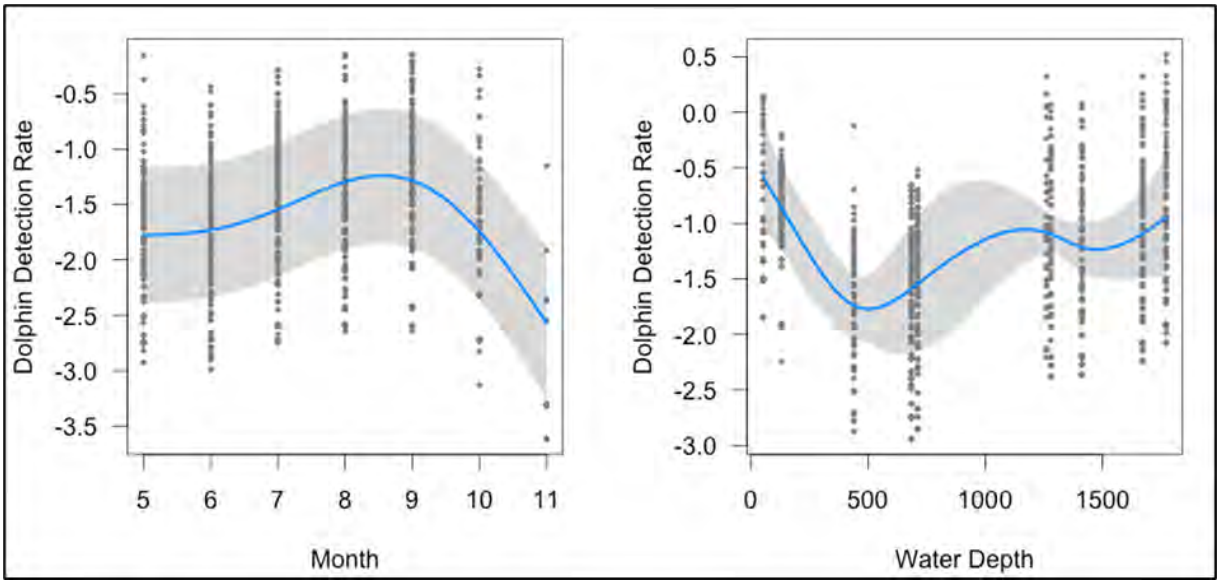

Figure 36. Month (left) and water depth (right) prediction functions for dolphin band detection rates

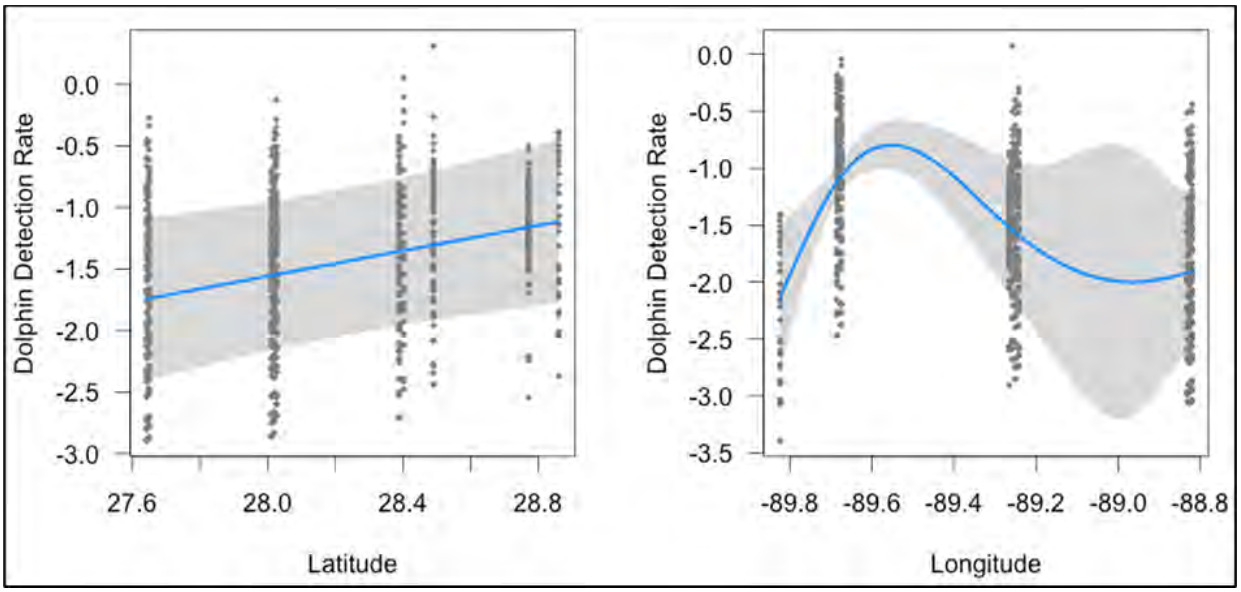

Figure 37. Latitude (left) and longitude (right) prediction functions for dolphin band detection rates

4.4.3 Beaked Whale Band Detections: Mid-frequency Clicks

Detections in the beaked whale frequency band increased from May through September and then began to decline in October (**Figure 38**). The peak of beaked whale detections appeared to occur at intermediate water depths of 500 to 1,000 m and declined in the very shallow and very deep depths (**Figure 38**), which may indicate a habitat preference for slope environments. Detection rates appeared to be highest in lowest latitudes and decreased as latitude increased. The effect of longitude here appears to be the opposite of that for the dolphin band results, with highest values to the west and east (**Figure 39**).

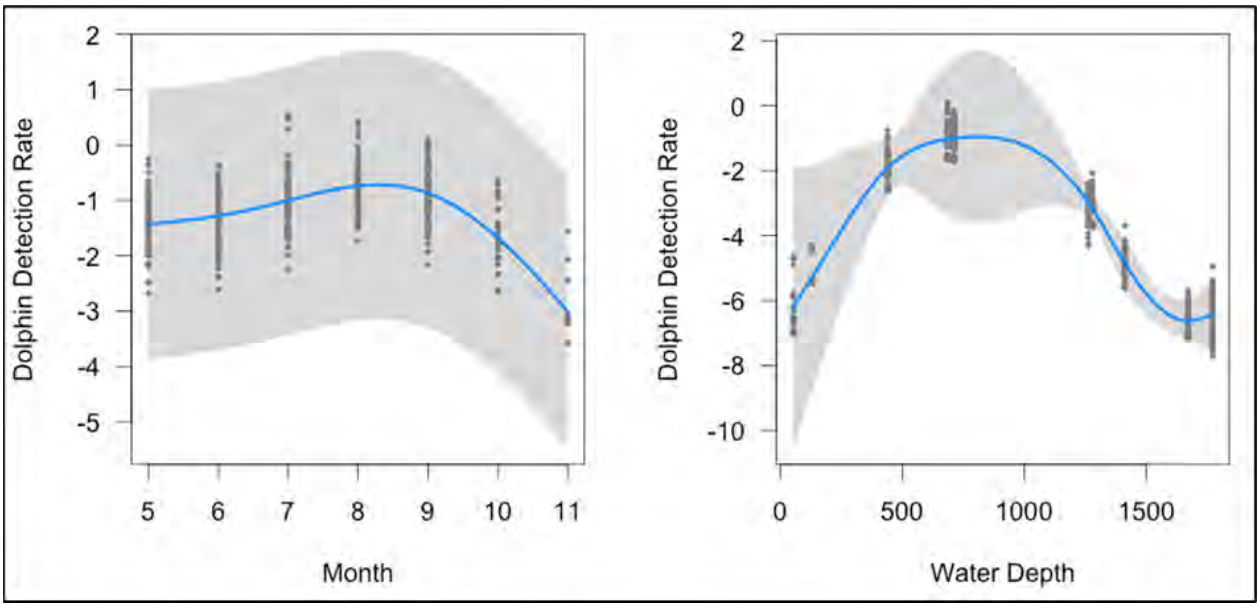

Figure 38. Month (left) and water depth (right) prediction functions for Beaked Whale Band detection rates

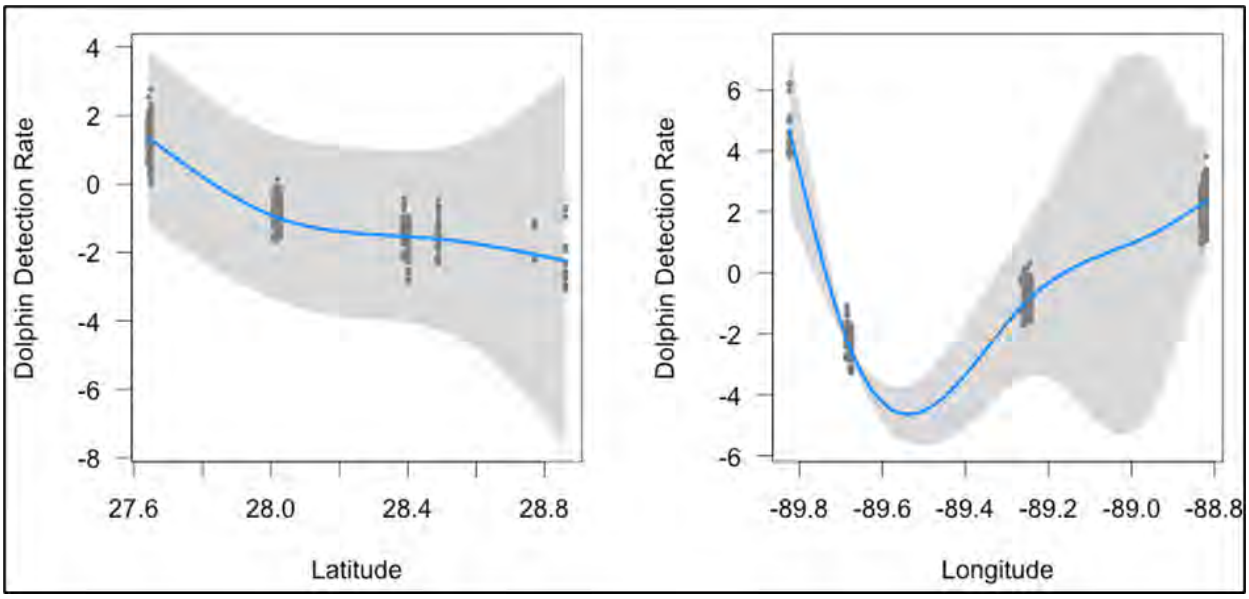

Figure 39. Latitude (left) and longitude (right) prediction functions for beaked whale band detection rates

4.5 Statistical Modeling of Vessel Received Levels

The individual analyses of the ten receivers produced several common patterns. First the R-squared for most of the analyses was quite high, exceeding 0.5 in some cases. This indicates that a good amount, if not most of the variance in the measured received levels (RL), could be explained by the statistical models. One of the most common patterns in the data was a strong relationship between closest point of approach (CPA) distance and measured LF sound level. In almost all analyses, this relationship was very similar, with a near linear increase in RL as vessels approached within 10 km. This relationship was much stronger than any of the predicted RL values. Based on this finding, it is recommended that future efforts to predict LF noise in the GOM should rely directly upon AIS data as predictor variables.

In most of the receivers, there was also the expected positive relationship between windspeed and wave height with increased measured LF noise. **Sections E-3.4** and **E-3.5** of the technical report presented in **Appendix E** present detailed results and discussion.

In evaluating the spectrograms of the 24 hours of data before and after the CPA of the Seaglider to the Site 2 EARS recorder, the expectation was that the acoustic characteristics of the collected data would be similar at CPA but would diverge as the range between the recorders increased (**Figure 41**). However, the spectrograms from the 2018 MP Seaglider and Site 2 EARS data show minimal similarity at any point.

Furthermore, the monthly spectra (**Figures E-B1** through **E-B6** in **Appendix E**) showed that in some months, the spectral profiles for individual recorders in deep water were almost identical. However, in other months, the spectral differences exceeded 20 dB. This indicates that the glider-static receiver comparison is not generalizable to the full range and temporal scale of the Project.

4.6 Extrapolation Capability of Acoustic Data: Seaglider/Fixed Sensor Comparison

In order to answer the question "How far can data from a single buoy be extrapolated?", acoustic data from the stationary EARS buoy recorders at Site 2 was compared to data from the 2018 MP Seaglider as it approached, nearly flew over, and departed from that buoy location. Specifically, the Seaglider approached within 1,500 m of the EARS buoy at Site 2 during the first deployment (**Figure 40**).

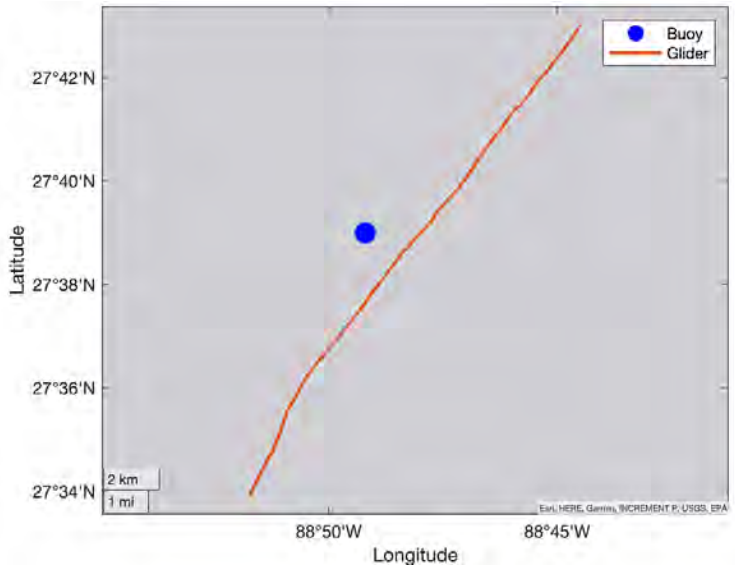

Figure 40. Path of the 20189 MP Seaglider past the Site 2 EARS recorder during Deployment 1

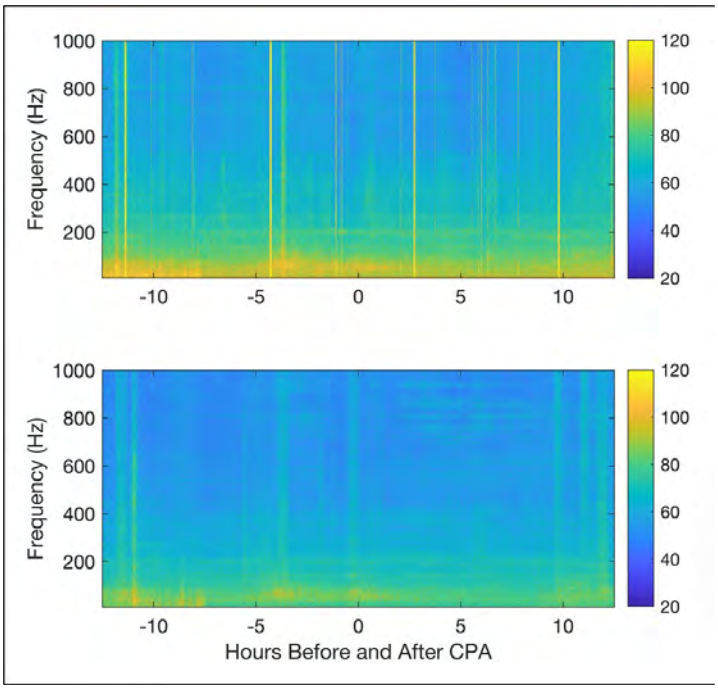

Figure 41. Comparison of spectrograms from the 2018 MP Seaglider (top panel) and the Site 2 EARS recorder (bottom panel) for the 12 hours before and after the Seaglider's CPA

4.7 3D Underwater Sound Propagation Modeling

The underwater soundscape in the GOM is significantly influenced at different scales by 3D sound propagation (Duda et al. 2011; Ballard et al. 2015; Heaney and Campbell 2016; Reilly et al. 2016; Oliveira and Lin 2019; Reeder and Lin 2019; and Oliveira et al. 2021). Physical oceanographic and geological associated with continental shelves and shelf break areas can cause horizontal heterogeneity in medium properties, so horizontal reflection/refraction of sound can occur and produce significant 3D sound propagation effects. These propagation effects can constructively or destructively interfere with sound as it travels from source to receiver. Constructive interference can lead to areas of focused sound energy and extended propagation/detection ranges, while destructive interference results in areas of shadowing and reduced ranges. Since the northern GOM is characterized by two large canyons (Mississippi and DeSoto), it was important to better understand influence of these prominent geological features on the soundscape.

Accordingly, the SHRU VLA data were used to establish a 3D underwater sound propagation model, which is capable of capturing sound focusing and defocusing effects due to the 3D variation in bathymetry (**Figure 42**). These focusing and defocusing effects can intensify or decrease local ambient noise levels, potentially influencing noise impacts to marine animals.

This model was used to assess 3D propagation of seismic airgun sounds produced during an oil and gas survey conducted by two survey ships on September 29, 2019, the Motor Vessel (*M/V) Artemis Angler* and *M/V Artemis Arctic*. The ship positions in the signal analysis time window around 08:57 Coordinated Universal Time on September 29, 2019, are shown in **Figure 43** (panels (a) and (b)), and the mooring locations of the two vertical hydrophone arrays that recorded the airgun data are shown in **Figure 43** (panels (c) and (d)). The two seismic survey ships were fairly close (5 km) to one another within the time window analyzed, and the distances from them to the two hydrophone arrays were in the range of 135 and 164 km.

Cross-correlation analysis was performed to pair up two sets of airgun pulse arrivals emitted from the two seismic survey ships separately (annotated by yellow and red arrows with sequential numbers in **Figure 43** panels (c) and (d)). The airgun pulses received at the Slope SHRU (**Figure 43** panel c) were up to 7.7 dB stronger than those received at the Canyon SHRU (**Figure 43** panel (d)**)**, even though the Slope SHRU was farther away from the noise source. These differences in received levels were likely caused by horizontal reflection and 3D focusing effects due to canyon and slope bathymetry (**Figure 44**).

Propagation of 50 Hz sound from the seismic survey ships *M/V Artemis Arctic* and *M/V Artemis Angler* were simulated with the 3D sound propagation model. In order to identify 3D propagation effects, Nx2D simulations that constrained sound from propagating across different azimuths were also conducted. The model output from each simulation is shown in **Figure 44**, where panels (a) and (b) are 3D models, and panels (c) and (d) are Nx2D models. To better illustrate horizontal reflection and focusing, depth integrated energy levels are shown.

In future phases of the GOM Program, the 3D model output may be used to address scientific questions such as “Do marine mammals preferentially occupy (in the sense of vocal activity) high TL (low intensity) regions to avoid potential effects from manmade sounds, such as masking?”

Additional details on the 3D sound propagation modeling and simulation data analyses are presented in Lin (2019, 2021).

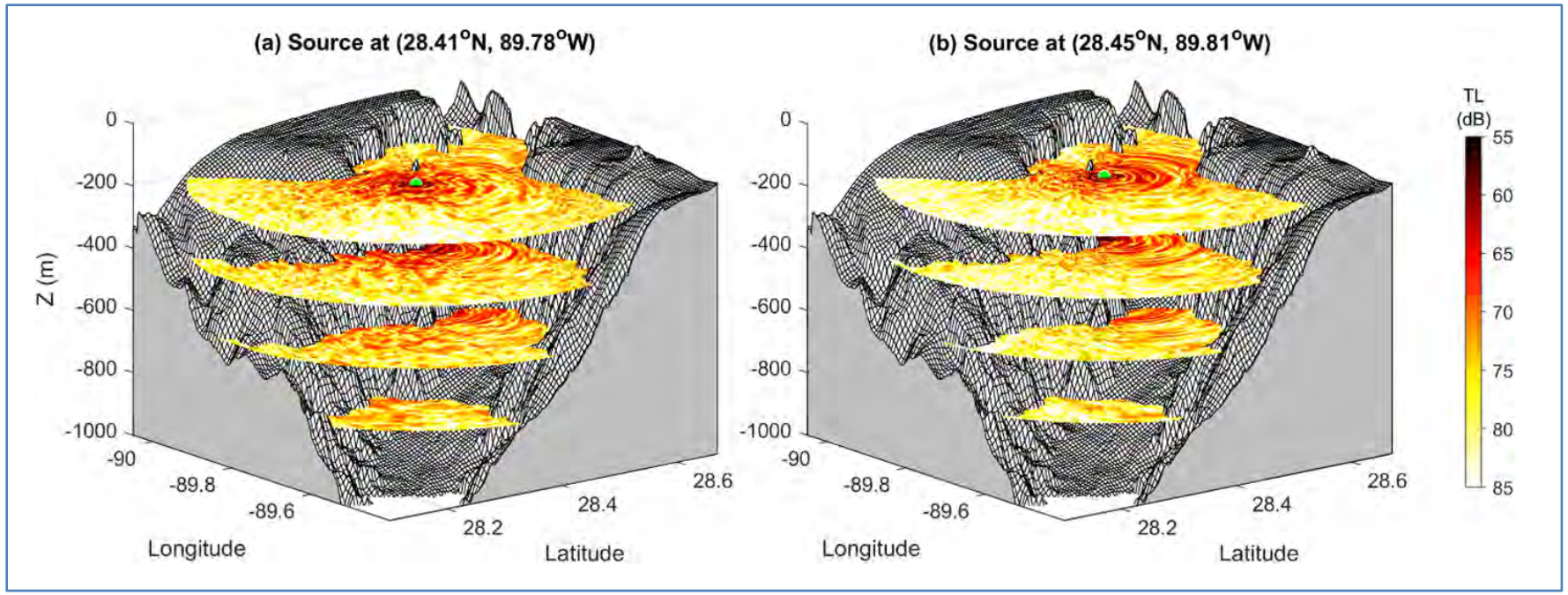

Figure 42. TL output of the 3D underwater soundscape model in the Mississippi Canyon

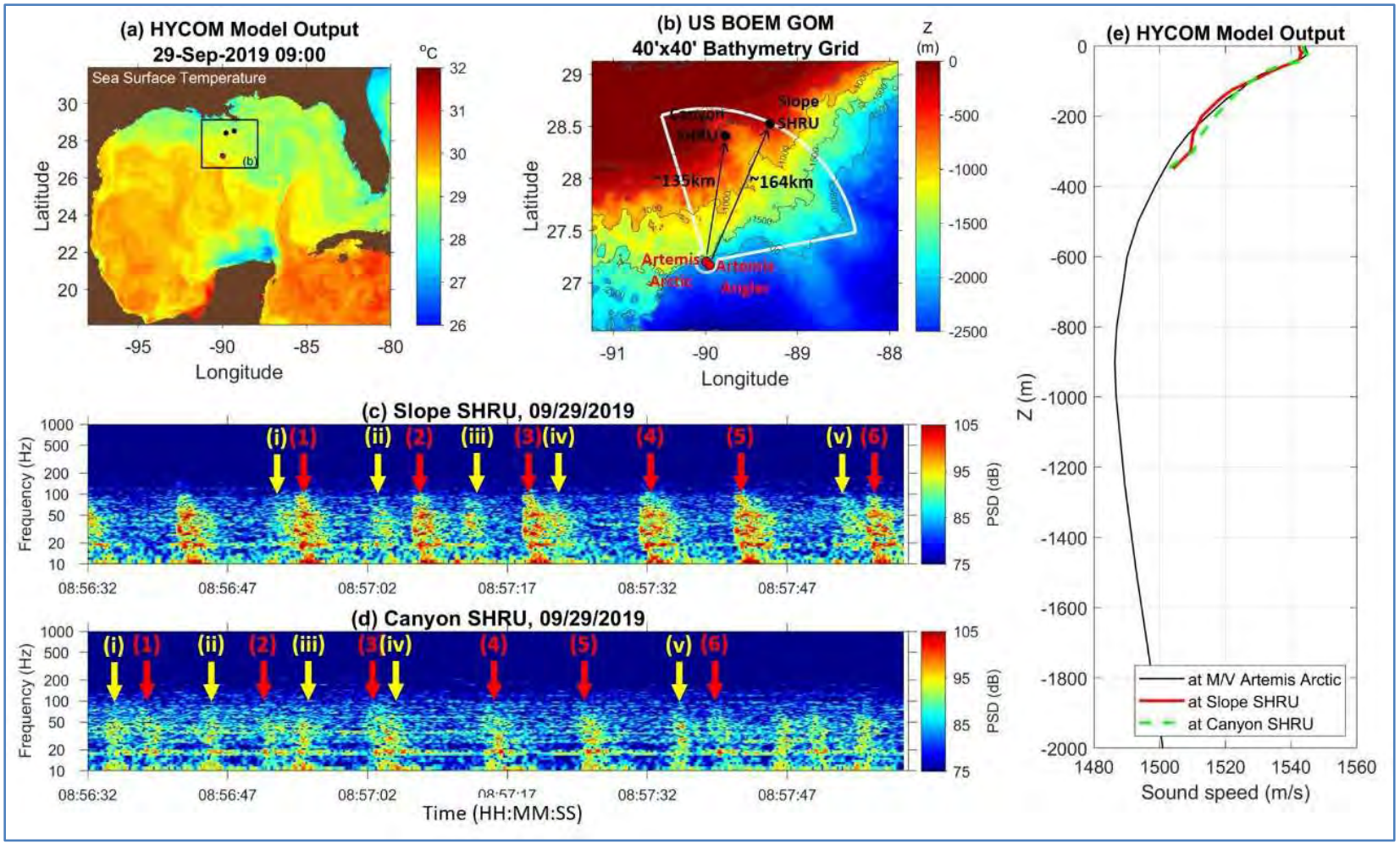

Figure 43. (a) HYCOM sea surface temperature (SST) output in the GOM

Note: The 3D propagation model area is indicated by the box around the Mississippi Canyon. (b) A high-resolution bathymetry map in which the ship and hydrophone array locations are marked. (c) and (d) Spectrograms of received airgun pulses on the two hydrophone arrays. The airgun pulses emitted from each of the two survey ships are annotated by yellow and red arrows, respectively. (e) Sound speed profiles calculated using the HYCOM temperature and salinity output.

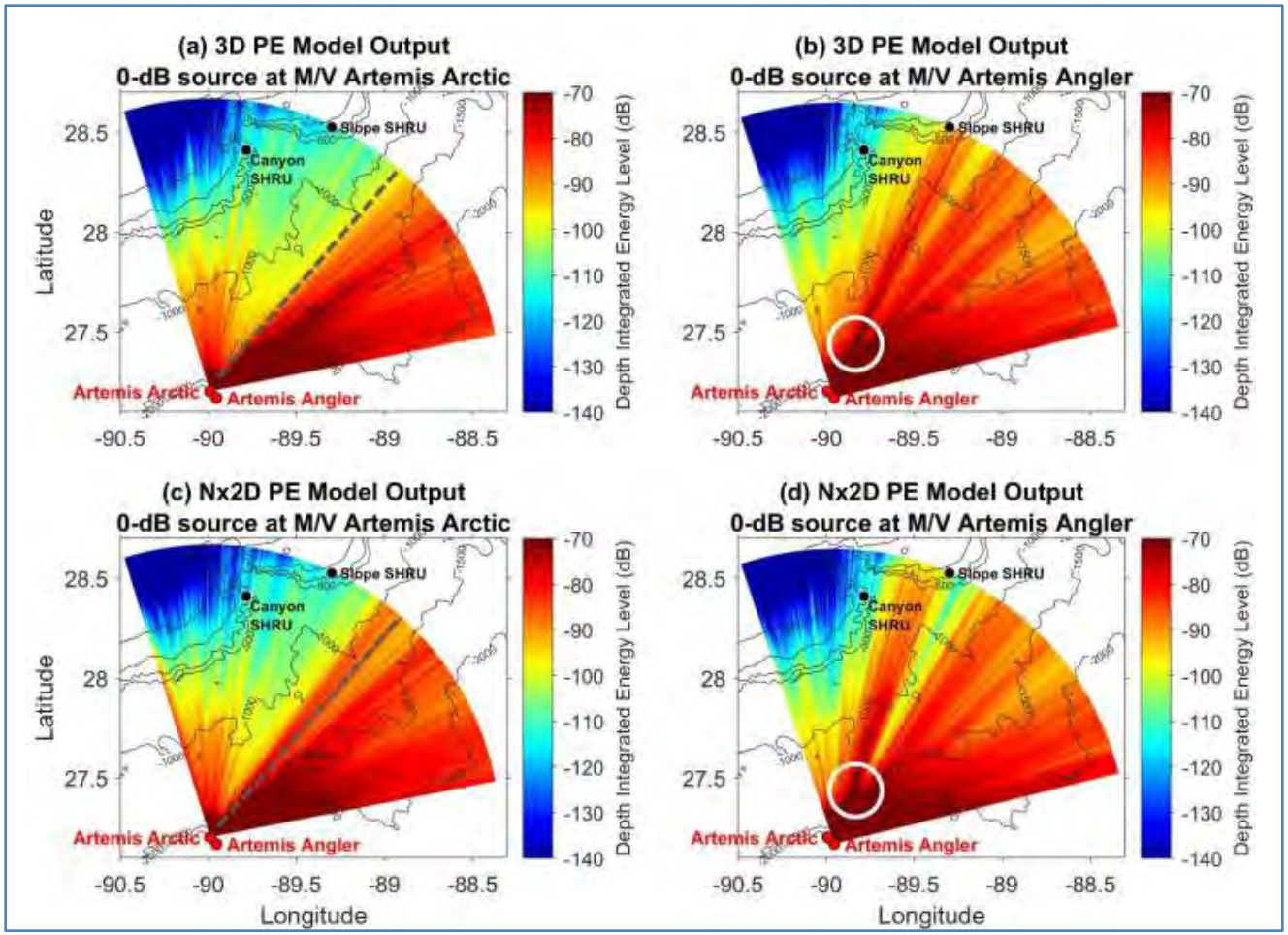

Figure 44. (a) and (b) 3D and (c) and (d) Nx2D sound propagation (50 Hz) model output for the airgun pulse propagation study

4.8 Noise Coherence and Source Correlation Analyses

Noise source correlation with available marine traffic data was conducted using the SHRU VLA data, which, among the four sensor types, is the only dataset that lends itself to this type of analyses. AIS data overlapping with the period of SHRU VLA deployment were obtained from a commercial vendor. **Figure 45** shows an example of correlation between soundscape statistics and AIS data. This example clearly shows the potential of using passive acoustic data, especially noise coherence, for monitoring marine traffic when AIS data are not available. Additional information on these analyses and results are presented in Lin 2021.

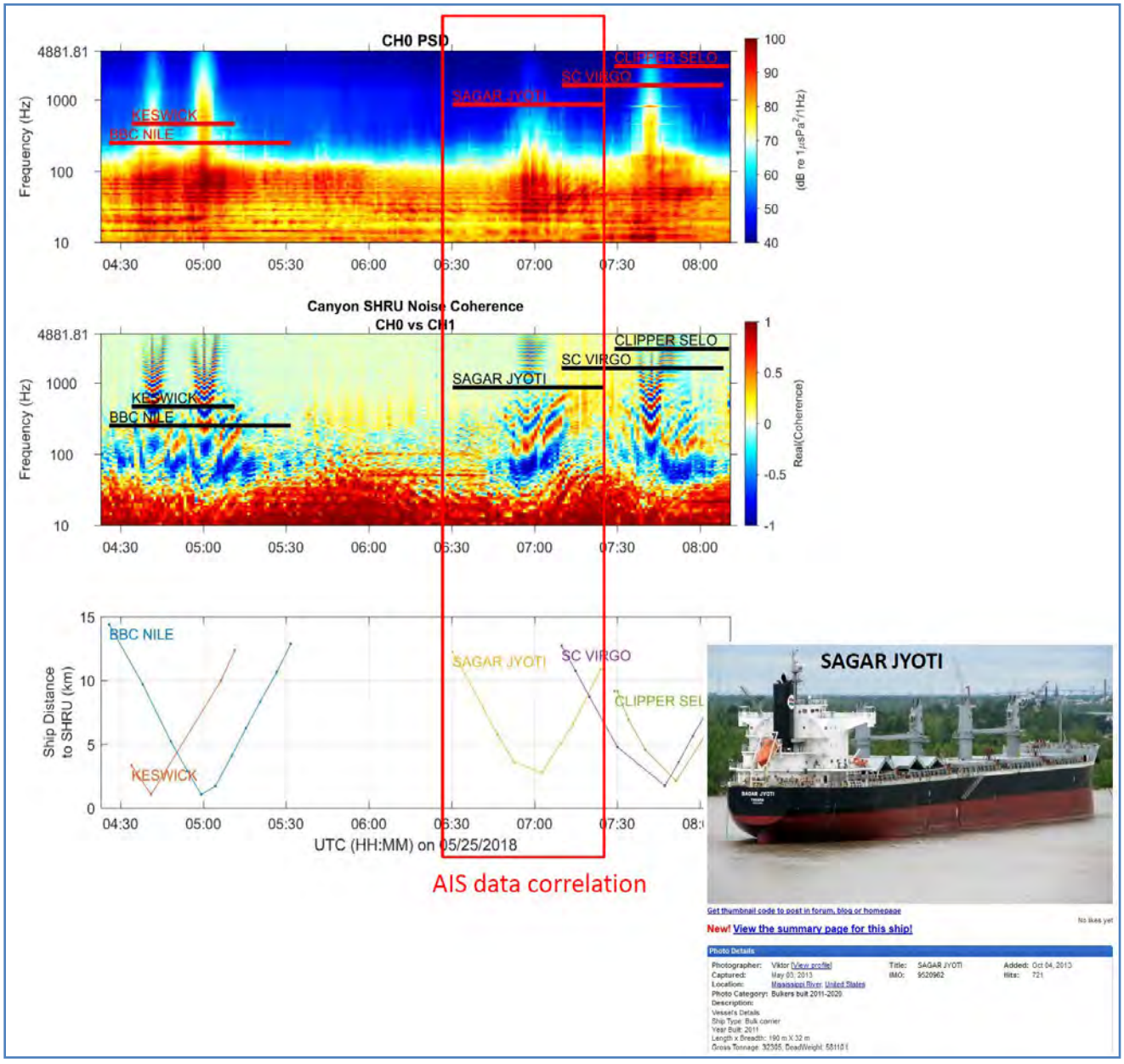

Figure 45. An example of correlation between soundscape statistics and AIS data

4.9 Mississippi Canyon Soundscape Characterization Analyses Using SHRU VLA Data

4.9.1 SPL Time Series Comparison

As part of the soundscape characterization, in addition to the six standard soundscape statistics, a time series of 12-hour average SPLs in the LF (10 to 1,000 Hz) and MF (1,000 to 4,883 Hz) bands at the Canyon SHRU array location were also computed with the SHRU VLA data. The outputs from these analyses are shown in **Figure 46**. The measurement shows that +/- 5 dB average pressure changes are seen in the LF band, while the MF band has larger deviation (up to +/- 10 dB).

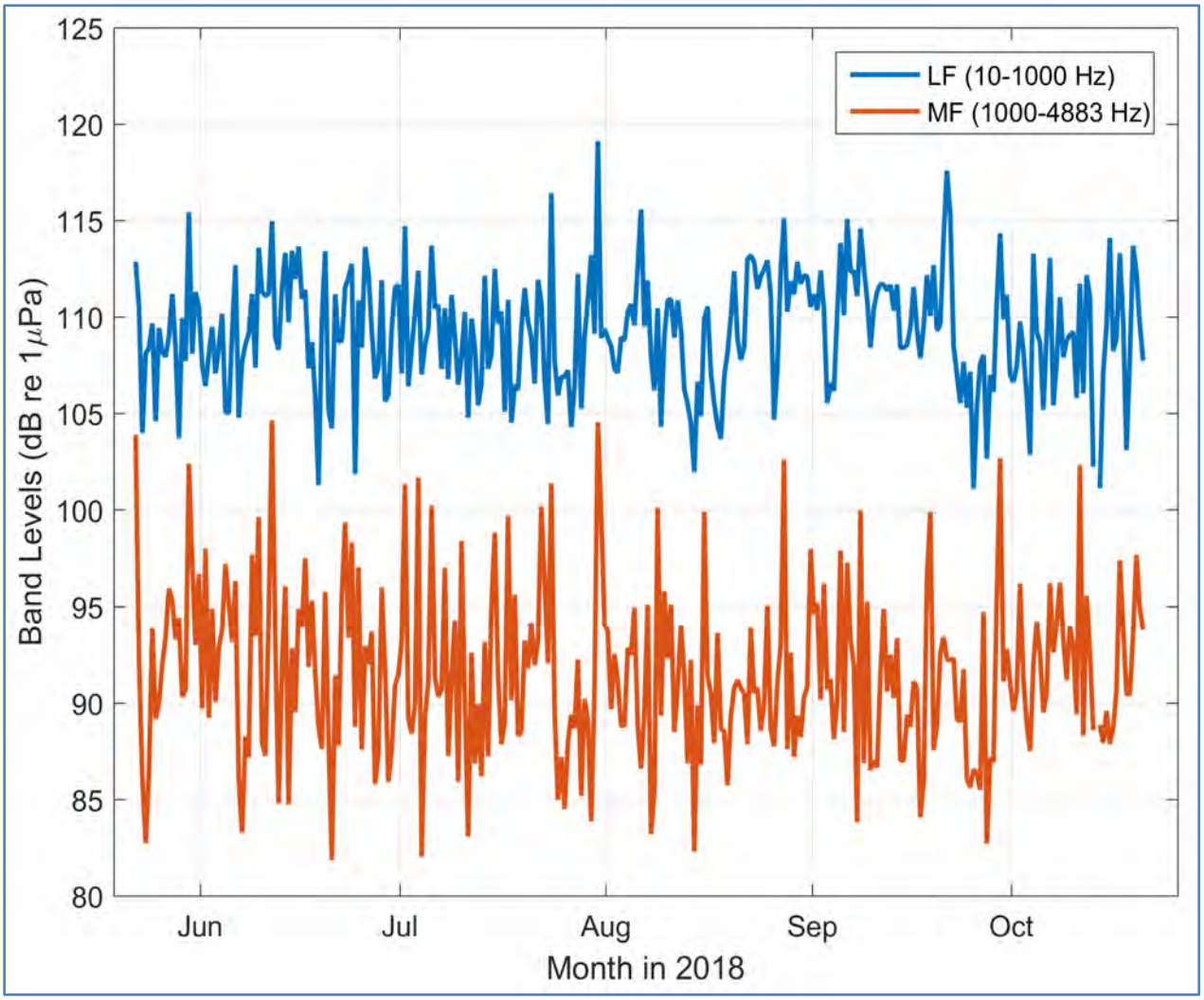

Figure 46. Time series of 12-hour average SPLs in the LF (10–1,000 Hz) and MF (1,000–4,883 Hz) bands at the Canyon SHRU array

4.9.2 Soundscape Differences Between the Mississippi Canyon Floor and Slope

Soundscape statistics computed for the SHRU VLA data showed significant differences between the Mississippi Canyon floor and slope based on comparison of long-term percentile levels (**Figure 47**) and average PSD levels (**Figure 48**). In the next phase, these outputs will be compared to outputs from similar analyses performed with the 2019 MP SHRU VLA data to determine if the statistical difference between the canyon floor and slope are consistent over time.

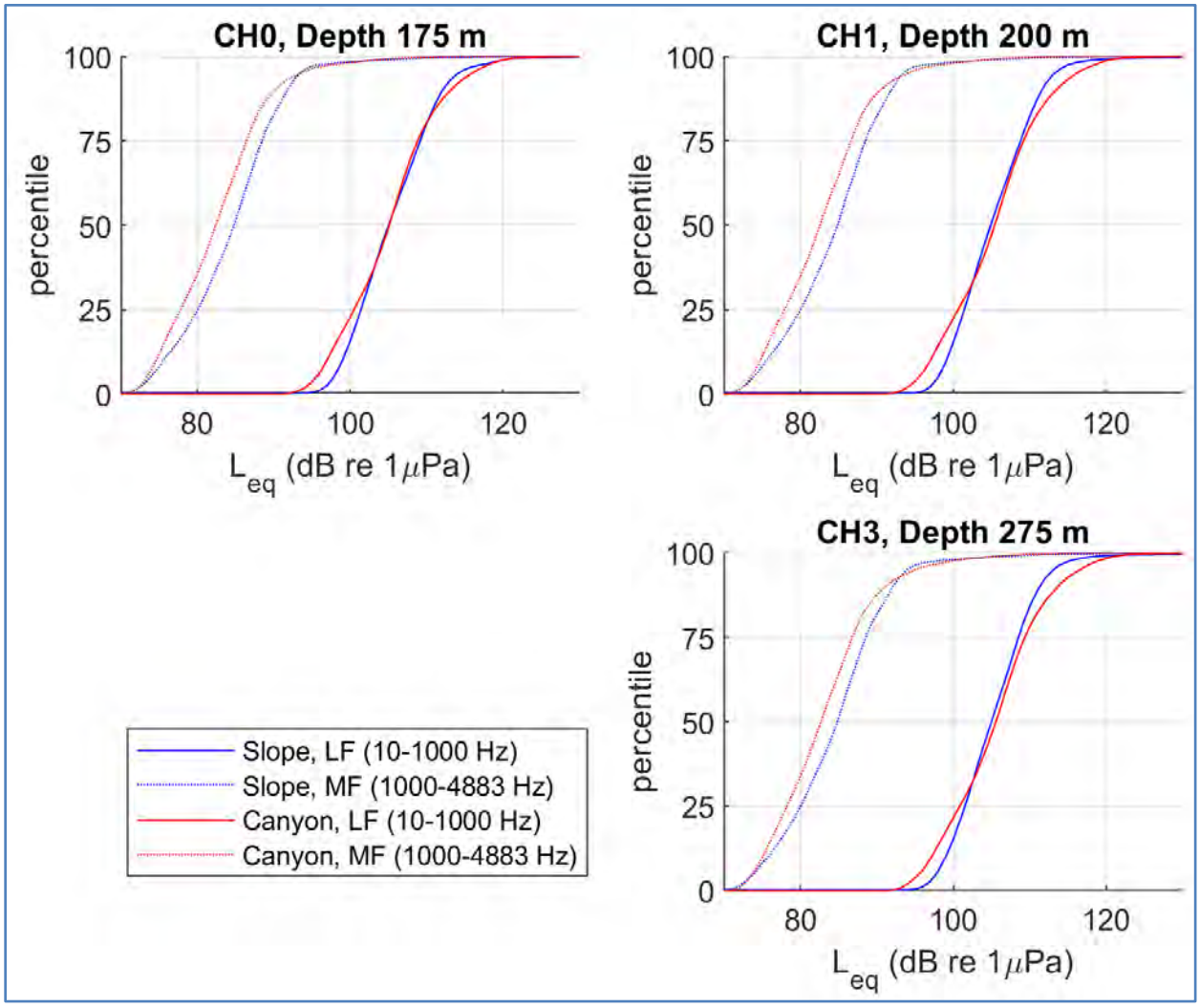

Figure 47. Comparisons of long-term percentile levels measured at the Slope (blue curves) and Canyon (red curves) SHRU sites

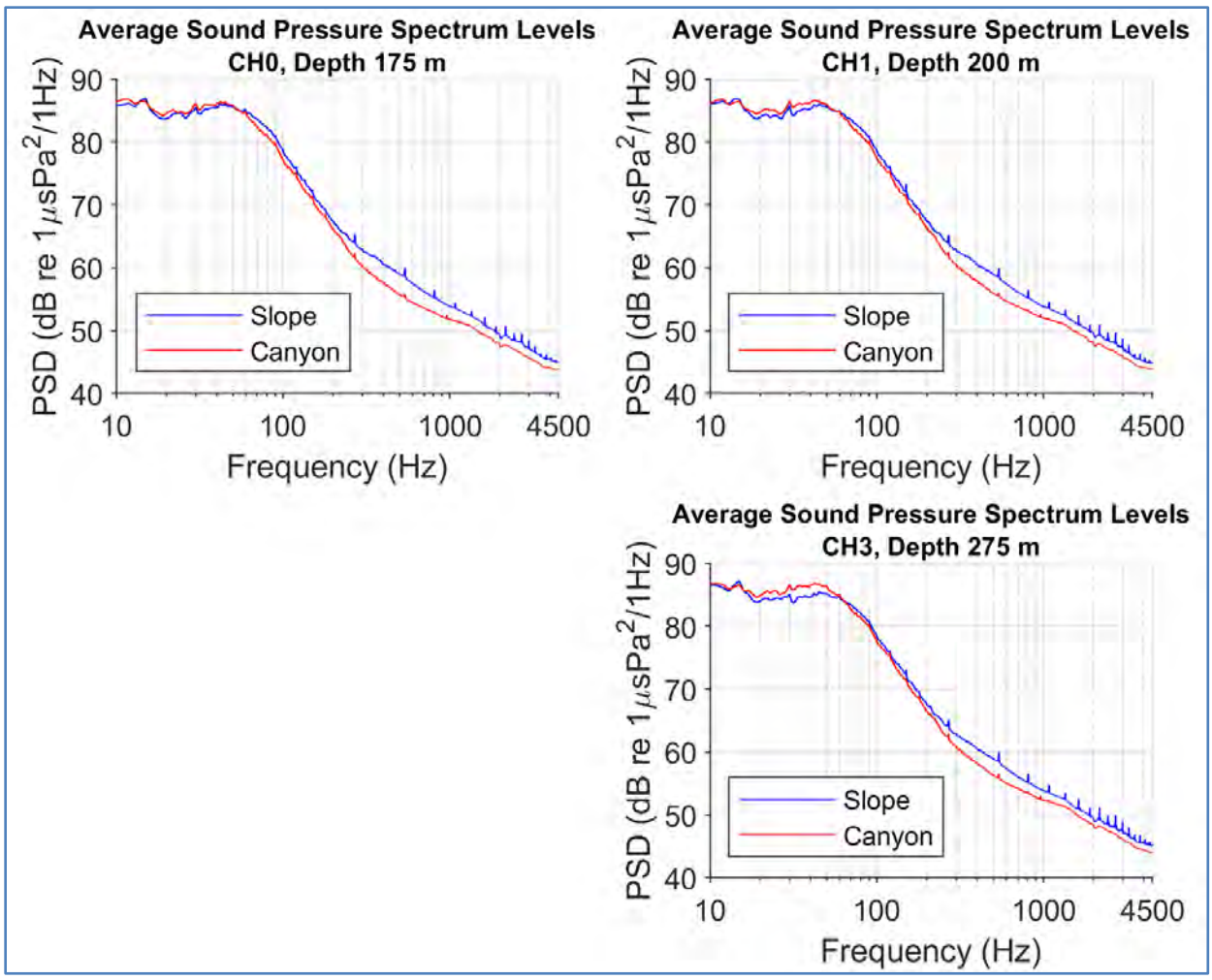

Figure 48. Comparisons of average PSDL measured on the Mississippi Canyon slope (blue curves) and floor (red curves)

4.9.3 Annual Soundscape Variability between the Mississippi Canyon Floor and Slope

To better understand the annual soundscape variability between the Mississippi Canyon floor and its slope, SPLs computed from the 2018 MP SHRU VLA data were compared with SPLs computed with the 2019 MP data. **Figure 49** shows comparison of the average SPL measured on the floor of the Mississippi Canyon during 2018 and 2019.

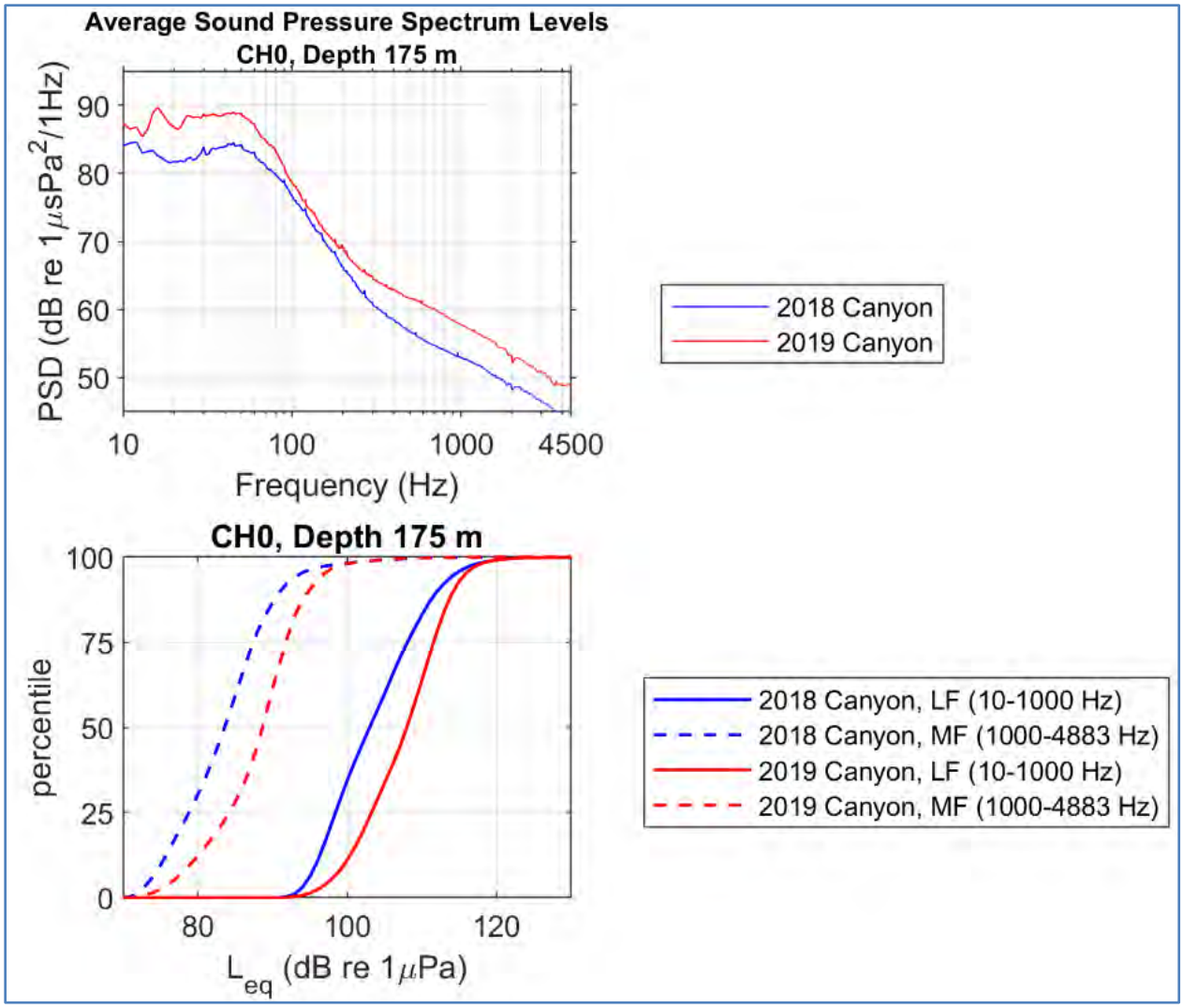

Figure 49. Comparison of average SPL measured in 2018 and 2019 on the Mississippi Canyon floor

4.10 Soundscape Fingerprint Analysis

The noise coherence and source correlation analysis presented in **Section 4.8**. was further developed to generate a "soundscape fingerprint" by computing ship noise coherence across discrete frequency bands. A 3D model adopting realistic ocean environmental data in the Mississippi Canyon was used to simulate spatial noise coherence distributions across the canyon area. Because the coherence distribution highlights the acoustic influence of bathymetric features that can be unique at different locations, the distribution is referred to as a "soundscape fingerprint." In fact, the pattern of the coherence distribution resembles the impression of a human fingerprint (**Figure 50**).

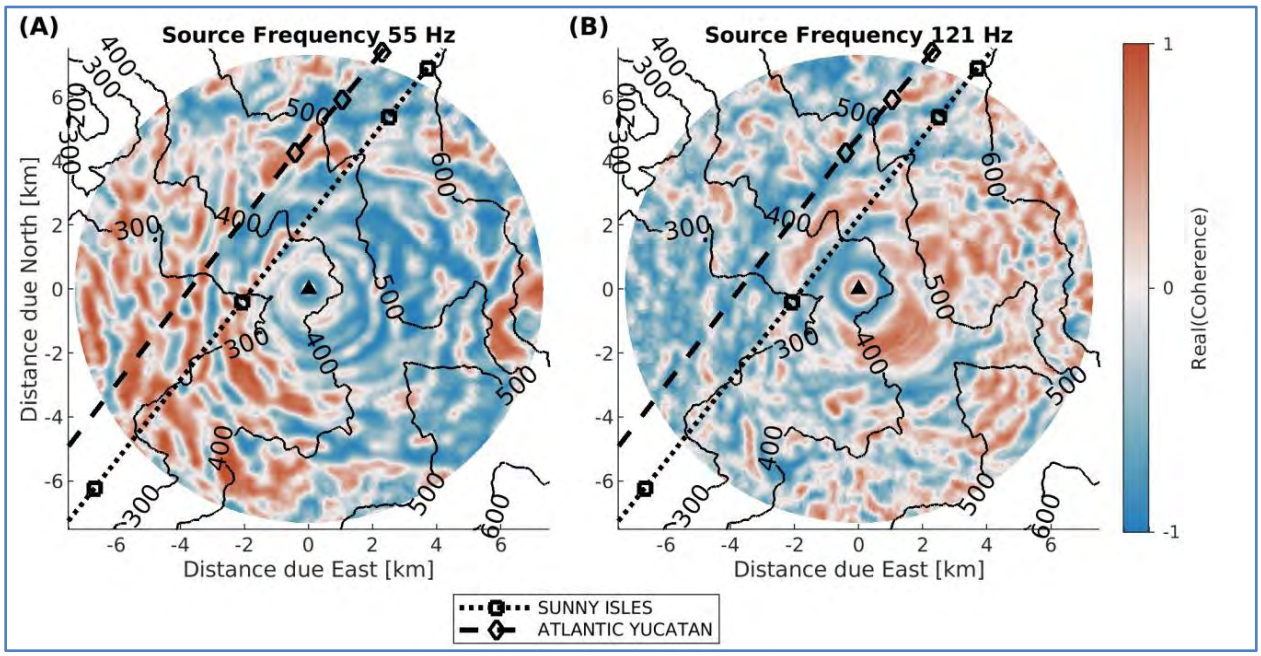

Figure 50. Acoustic fingerprint for the Canyon SHRU at 55 Hz (A) and 121 Hz

Note: Black contours 224 are constant bathymetry depths at 100-meter intervals and labeled in meters. Estimated ship tracks 225 are denoted by dotted (SUN) or dashed (ATL) lines connecting open squares (SUN) or open 226 diamonds (ATL). Squares and diamonds in the ship tracks denote known AIS locations. (A) The 227 range-variable bathymetry forces a positive (red) coherence at 55 Hz west of the SHRU and negative 228 (blue) to the east. (B) At 121 Hz the coherence sign is flipped to negative (blue) to the west and 229 positive (red) to the east.

Ship noise recorded by the canyon SHRU array was shown to contain the acoustic influence of bathymetric features, and noise coherence was demonstrated to be an effective metric for identifying ship traffic in recorded data. Comparison of the data and the model showed a promising agreement for lower frequencies which are less susceptible to temporal environmental changes, suggesting an avenue for source localization efforts in strongly range-dependent environments. Furthermore, seasonal variability in the soundscape fingerprint was examined, with models suggesting a strong influence of seasonal changes to near-surface ocean properties (**Figures 51** and **52**).

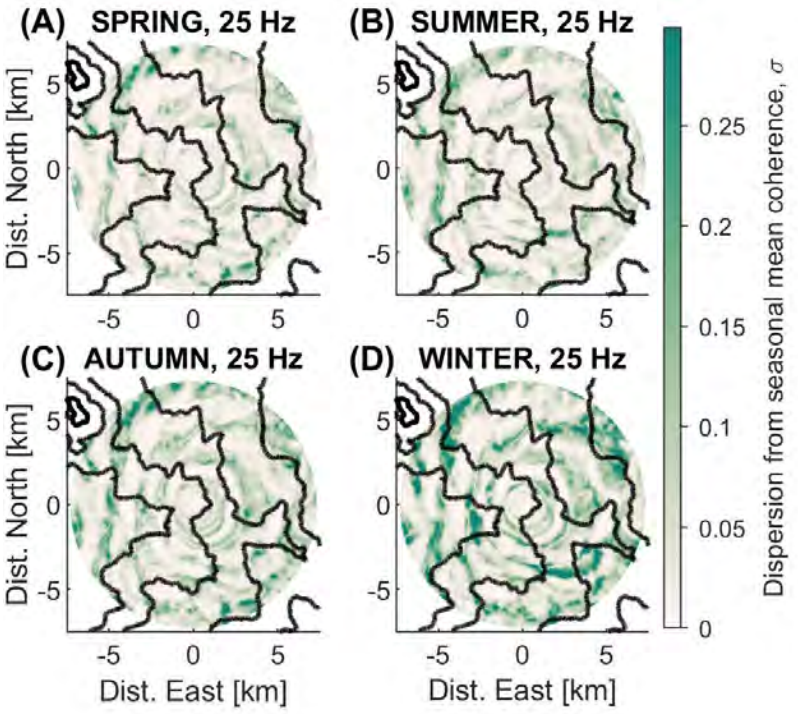

Figure 51. Dispersion of soundscape fingerprints from seasonal means, represented by one standard 296 deviation across seasonal samples. Source frequency 25 Hz.

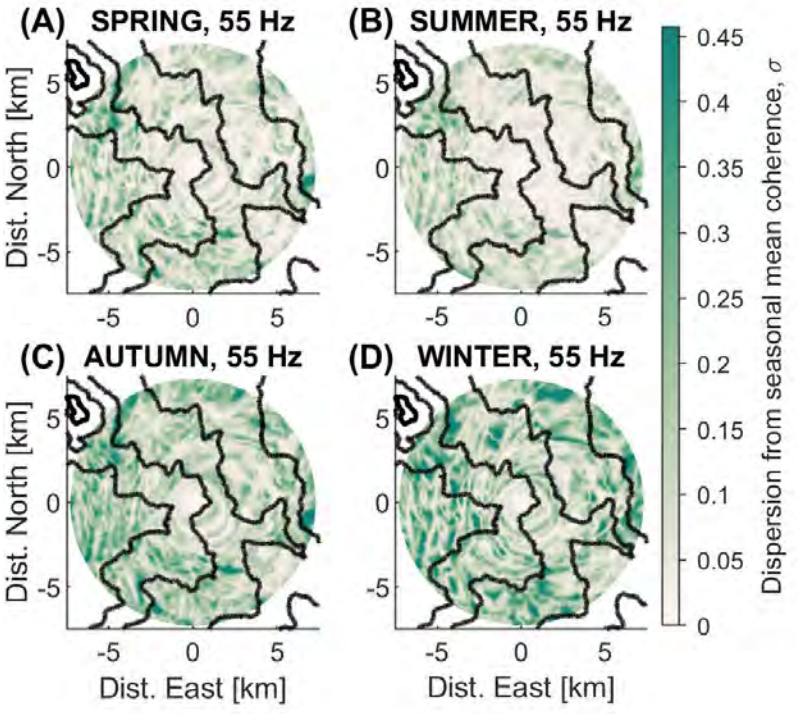

Figure 52. Dispersion of soundscape fingerprints from seasonal means, represented by one standard 299 deviation across seasonal samples. Source frequency 55 Hz

5 Discussion

Soundscapes are created from the interaction of the spatial-temporal patterning of natural and anthropogenic sounds in the environment (Pijanowski et al. 2011). The Northern GOM is a productive subtropical region that supports a variety of vocally active species, including fish and marine mammals (Wall et al. 2013, Roberts et al. 2016, Boyd et al. 2021). It is also a major area for oil and gas exploration and extraction, military operations, fishing, and tourism. The GOM PAM Program study area was focused on the central portion of the northern GOM where the flow of freshwater from the Mississippi River creates strong ecological gradients. The underwater soundscape described in this study provides valuable information on the current environment that can be used to inform assessments of future changes in ambient sound caused by restoration and human activities (such as increased shipping, future renewable energy development), species occurrence and density, and potential impacts of elevated noise to protected species.

5.1 Ambient Sound Levels

The northern GOM has very high average ambient sound levels at 10 to 100 Hz and moderately high levels at frequencies up to 1 kHz and above, relative to other locations around the world (Dahl et al. 2007). SPLs recorded under the GOM PAM Program were similar to those previously recorded in this region in 2010 to 2013 (Estabrook et al. 2016; Wiggins et al. 2016), indicating persistently high levels of LF noise over the decade. Human-caused sound (anthrophony) has been increasing globally because of shipping, resource exploration and exploitation, and infrastructure development (Duarte et al. 2021). The northern GOM is one of the most industrialized parts of the ocean; therefore, this ecosystem has experienced long-term, chronic exposure to LF noise pollution.

In addition to these anthropogenic sources of sound, wind, and storm events (geophony) periodically elevate ambient sound levels at higher frequencies (500 Hz and above). Wind speeds from storms have been found to be correlated with SPLs at 900 Hz in the GOM (Wiggins et al. 2016). During this study, Tropical Storm Barry moved through the study area in mid-July 2019. Although this storm created underwater sound, there was a reduction in the one-third octave frequency band levels, with the center frequency of 63.1 Hz as seismic surveys and shipping transits ceased due to the adverse weather conditions. This reduction in LF sound (less than 100 Hz) was similarly found during Hurricane Isaac in August 2012 (Wiggins et al. 2016) and Tropical Storm Barry in 2001 (Newcomb et al. 2002).

5.2 Detection of Anthropogenic Sounds

As in 2010 to 2013 (Estabrook et al. 2016; Wiggins et al. 2016), monitoring conducted under the GOM PAM Program from 2018 to 2020 found that the LF soundscape was dominated by distant seismic survey and vessel traffic sounds. Seismic surveys produce loud, LF sounds created by airguns. In this LF range (below 100 Hz), elevated sound levels occurred nearly continuously during the summer months. Although the activity creates an impulsive sound, the multiple paths it propagates in deep water means the duration of the sound increases with distance to form a nearly continuous signal (Greene and Richardson 1988; Guerra et al. 2011).

Airgun occurrence had strong annual and monthly patterns. Latitude and longitude predictors were both only marginally significant, and water depth had no statistically significant effect. This likely reflects the greater distance over which airgun operations could be detected. The same temporal pattern of airgun activity was seen on many of the recorders.

Despite seismic surveys not occurring in proximity to the recorder locations in this study, the sounds were detected, and SPLs elevated for months. A similar elevation of LF (10 to 100 Hz) ambient sound levels

was found in the polar waters of the North Atlantic (Klinck et al. 2012) and the Chukchi Sea (Roth et al. 2012), where seismic surveys occurred. Airguns in the Chukchi and Beaufort Seas elevated average sound levels by 2 to 8 dB re 1 μPa^2/Hz at 20 to 50 Hz, depending on distance from the source (Roth et al. 2012). Along the Mid-Atlantic Ridge, airgun sounds were detected on hydrophones at a depth of approximately 900 m in the Deep Sound Channel up to 4,000 km away during at least 9 months per year at all 12 recording locations (Nieukirk et al. 2012). The main sources of these airgun sounds were Newfoundland, northeastern Brazil, and Senegal and Mauritania in West Africa, which personified the LF soundscape in the Atlantic Ocean almost year-round (Nieukirk et al. 2012).

The northern GOM is well-positioned to support a transition to a renewable energy future, as much of the infrastructure already exists to support offshore wind development in the region. As part of the current administration's goal of permitting 30 gigawatts of offshore wind power development by 2030, BOEM recently announced that it is preparing a draft environmental assessment (EA) to consider the impacts of potential offshore wind leasing in federal waters of the GOM. The area that will be reviewed in the EA includes almost 30 million acres just west of the Mississippi River to the Texas/Mexican border. This is the same area for which BOEM recently requested public input in a Call for Information and Nominations. BOEM plans to narrow the area that is advanced for Wind Energy Area delineation, which are offshore locations that appear most suitable for wind energy development, based on stakeholder and ocean user input received as through this call.

While the GOM PAM Program study area lies to the east of the area that the EA will consider, findings and recommendations from the GOM PAM Program monitoring are relevant to guiding future offshore wind energy development in this region. For example, impulsive sounds from pile-driving of turbine foundations have their main energy below 2 kHz, with the peak generally at 100 to 500 Hz (Bailey et al. 2010; Amaral et al. 2020). Impact pile driving usually occurs in waters up to approximately 50 m depth (Bailey et al. 2014), with greater TL and lower corresponding received sound levels at greater ranges (10 km from source) than seismic surveys occurring in deeper water. Although similar, these two different sound sources are expected to have different contributions to the soundscape, and their classification as impulsive or non-impulsive sounds for EAs will depend on the range and bathymetry (Hastie et al. 2019). If seismic surveys ceased, and even if offshore wind energy development moved forward, a reduction in the average LF ambient sound levels would be expected because of the shorter time period and shallower water location of the activity.

5.3 Vessel Sound Levels

The second major source of anthropogenic noise detected in the northern GOM was vessel traffic, which is prevalent in this region. In contrast to seismic survey sounds that were persistent in time, vessel passages were more transitory. Received sound levels tend to depend on the proximity and size of the vessel (Bassett et al. 2012). Daily detections of vessel activity, reported for close passbys to the receivers (i.e., close enough to create a Lloyd mirror interference pattern), varied from below 10 percent to near constant or daily occurrences. There was a strong seasonal pattern, with most vessel detections occurring in the summer months (May to June). The annual pattern indicated an increase in vessel traffic from 2018 to 2019, and a subsequent decrease in 2020. However, the sampling within the first and last year only covered a portion of the years 2018 and 2020. Monitoring in 2018 began in late May, and most recording was completed by May 2020. Therefore, these partial years may have missed a portion of the peak in vessel traffic. Another possibility is that the decline in vessel numbers in 2020 may reflect reduced vessel traffic due to the COVID-19 pandemic.

The effects of latitude and longitude on the distribution of vessel detections were both statistically significant. Vessel detection rates increased with both water depth and latitude. However, the magnitudes of these effects were not equivalent. Water depth appeared to be the stronger predictor, and this may

reflect better acoustic propagation in deeper waters, or all these effects could reflect the prominent shipping routes into the Port of New Orleans.

Program data showed vessel noise contributed to the underwater sound levels below 1 kHz year-round almost every day at all the recorder locations. High vessel traffic off the U.S. coast in the northeast Pacific (McDonald et al. 2006) and western Atlantic (Rice et al. 2014) similarly caused increased ambient sound levels. Off California, ambient sound levels were higher by 10 to 12 dB re 1 μPa^2/Hz at 30 to 50 Hz in 2003 to 2004 compared to 1964 to 1966, which is thought to have been caused by an increase in commercial shipping (McDonald et al. 2006). Off the U.S. East Coast, the Mid-Atlantic coastal areas had the highest ambient sound levels, and these were mainly attributable to vessel noise in proximity to high-use shipping ports (Rice et al. 2014). New Jersey had the most hours above 120 dB re 1 µPa within the 71 to 224 Hz frequency band in the region spanning the Gulf of Maine to off the coast of Georgia (Rice et al. 2014), but these levels were still generally lower than recorded in the northern GOM study area.

Statistical analysis of Received Vessel Band noise focused on predicting the actual RL at the recorders. This involved 1) measurement of distance from each vessel to the recorder, 2) estimation of the SL of the vessel, and 3) prediction of the TL between the two. Modeled vessel noise level was most often a good predictor of measured levels. However, on occasion these functions curiously showed a negative relationship with measured noise levels. Such an occurrence may be due to overprediction of noise levels at this location.

The most important vessel predictor for measured sound level was the CPA. This variable is relatively easy and quick to calculate when AIS data are available. A significant challenge in the analysis was the delay in acquisition of the AIS data, which is the backbone of the vessel soundscape analysis. The 2018 AIS data were not available until 2020, and the last part of the 2019 AIS data were not available until 2021. In the future, analysis of collected and archived data should consider focusing on the AIS metrics. This is particularly the case where studies are focusing on large, commercial vessels, and the analysis is occurring more than 12 months after data collection. However, if propagation predictions are needed, then 3D modeling should be conducted along with a comparison of simpler propagation models. Additionally, if a future study involves near real-time data and analyses or aims to include sound emissions from smaller, recreational vessels that may not be using AIS, then propagation modeling is beneficial.

5.4 Detection of Biological Sounds

The main source of biological sounds (biophony) detected were marine mammal calls. More than 20 species of marine mammals occur in the waters of the northern GOM, with species of dolphins, including the bottlenose dolphin, predominantly populating continental shelf waters, and deeper diving species such as beaked whales and the sperm whale inhabiting offshore waters (Fulling et al. 2003). One baleen whale, the newly named Rice's whale (formerly GOM Bryde's whale), is a year-round resident of northeastern GOM waters, with a very small population (50 to 100 whales) listed as endangered under the ESA (Hayes et al. 2021).

To differentiate some of the most common sound-producing marine mammals that may contribute to the ambient soundscape, frequency bands for the known vocalizations of five marine mammal species or species groups (Rice's whale, beaked whales, and dolphins) were identified. The recorded acoustic data were assessed to determine which characteristics informed the spatial and temporal patterns of these marine mammal species or groups.

The frequency overlap between the signals of Rice's whales and the prevalent anthropogenic sound environment made reliably detecting the calls of Rice's whales difficult using only the spectrally analyzed

data. A potentially better approach to test in the future would be a matched-filter detection process that operates on the waveform data.

The detection rate results from the "dolphin" and "beaked whale" frequency bands had similar temporal patterns. Detection rates increased from May to September and began to decline in October. November rates were generally lower. Note data from November 2018 (under deployment 1) were sparse, as some recorders had stopped recording early due to either recording system failures, severed moorings, trawled recorders, or data compression issues (Klinck et al. 2019; Sidorovskaia and Bhattarai 2019). All these issues were addressed in subsequent deployments.

The effect of water depth on detection rates had the opposite effects for the two frequency bands. In the dolphin band, peaks were seen in both shallow and deep waters, while the values from approximately 400 to 700 m were lower. This pattern is perhaps most easily explained by multiple species being detected with differing habitat preferences (Roberts et al. 2016). The peak of beaked whale band detections appeared to occur at intermediate water depths of 500 to 1,000 m and then declined in the very shallow and very deep depths. This may indicate a habitat preference for slope environments.

Latitude also had contrasting effects between the two frequency band results. For the dolphin band, the detection rates were lowest in the southernmost waters and increased over the more northerly recorders. For beaked whale band detections, the rates were highest in the south and decreased to the north. Finally, longitude also had opposite trends for these two bands. The highest dolphin band detection rates were found in the central longitudes, while the highest beaked whale band detection rates were found to the far west and east of the study area.

5.5 Use of Multiple Sensor Platforms

A variety of stationary and mobile sensor types and platforms were deployed in this study that allowed a broad characterization of the ambient soundscape as well as detailed modeling of the temporal and spatial patterns of the anthrophony and biophony. It is recognized that it may not be feasible to deploy such a comprehensive suite of sensors in all future studies. Selection of the most appropriate type of monitoring platform will depend on the stated goals and objectives of the data collection and analyses. Benefits and potential applications of single and multiple stationary arrays of acoustic recorders and mobile platforms are summarized in **Table 15** to guide future study planning.

Table 15. Summary of sensor platforms, benefits, and potential applications for future monitoring

Platform	Example Benefits	Potential Applications
Stationary – Single Depth	• Long-term (several months to a year) recordings at a specific location • Compare sound levels and characteristics over time	• Further characterize the soundscape in DeSoto Canyon, which had lower sound levels recorded in the present study • Long-term baseline recordings within potential lease areas for offshore wind energy in the western GOM
Stationary – Multiple Depths in a Vertical Line	• Mid-term (weeks to months) recordings at multiple depths • Compare sound levels over time and between depths	• Localization ability for sound sources, such as vessel traffic • Validate sound propagation models and received sound levels within areas of interest
Mobile	• Potentially large spatial coverage over short-term (weeks) periods • Recordings throughout the water column and derived sound speed profiles	• Sample the soundscape within the western GOM, particularly within the call area for offshore wind energy, where there is currently a lack of data

Key: GOM = Gulf of Mexico

6 Recommendations

Recommendations for continuing the monitoring in future years; expanding data collection, analyses, and interpretation beyond soundscape characterization; and advancing data analyses using the existing 2-year dataset are presented in this section for BOEM's consideration.

6.1 Future Monitoring in the Northern GOM

Key lessons learned and recommendations from the monitoring and data analyses conducted under the GOM PAM Program are listed below; these could serve to guide planning for future monitoring and data analyses that may be conducted under this Program:

- The primary objective of the 2-year data collection and monitoring was to characterize the existing soundscape (including sounds contributed by both natural and anthropogenic sources) in the GOM:
    - This 2-year dataset will serve as an important reference point for similar monitoring conducted in the future. In future years, the Program could be expanded to cover other important objectives such as estimating marine mammal occupancy and (call) density, supporting estimation of impacts of anthropogenic sounds on marine mammals and other species of concern, and monitoring long-term trends in soundscapes and marine mammal density.
- The data collection and analysis experimental design provided an effective approach and framework for collecting and analyzing a robust dataset for soundscape characterization in the northern GOM:
    - The experimental design adopted for the two MPs can be used to guide continuation of monitoring in future years.

- A variety of stationary and mobile sensor types and platforms were deployed in this study that allowed a broad characterization of the ambient soundscape as well as detailed modeling of the temporal and spatial patterns of the anthrophony and biophony. The selected mix of monitoring platforms and sensors (RHs, EARS, SHRUs, Seaglider) was well suited for collecting data to support the overall GOM PAM Program objectives:
    - It is recognized that it may not be feasible to deploy such a comprehensive suite of sensors in all future studies. Selection of the most appropriate type of monitoring platform will depend on the stated goals and objectives of the data collection and analyses. Benefits and potential applications of single and multiple stationary arrays of acoustic recorders and mobile platforms were summarized in **Table 15** to guide future study planning.
- An important legacy of this Program is the robust, 2-year underwater acoustic dataset that was collected in the field within the delineated study areas:
    - For future years of monitoring, it is recommended that data collection be focused on the western portion of the northern GOM, and within the proposed offshore wind energy call area as a first priority and the DeSoto Canyon as a second priority.
- The multi-hydrophone SHRU VLAs provided a unique dataset that allows for analyses of parameters that cannot be evaluated using data from single hydrophone moorings. Because of schedule and resource constraints, only two stations could be monitored using the SHRU VLAs during each monitoring year of this study:
    - For future years of monitoring, additional locations should be considered for placement of SHRU VLA monitors.
- Use of a mobile platform was effective in ensuring that data were also collected between the stationary moorings, allowing for the soundscape in the entire study area to be adequately characterized:
    - Use of one or more mobile platforms are recommended in future years in which sampling over a large area is of interest. Use of a multiple glider fleet could also be considered in future years to provide a large coverage area and data redundancy.
- The effective frequency range of the monitoring instrumentation (10 Hz to 96 kHz) was appropriate to encompass the most common anthropogenic and natural sounds likely to be encountered in the GOM:
    - For future years of monitoring, it is recommended that a similar frequency range is used to encompass low- to high-frequency sounds for robust and useful comparison of spatial and temporal trends in the soundscape over the years.
- Monitoring under both MPs began in early summer (late April to early May). The power packs for the instrumentation used in the monitoring last approximately 6 months; therefore, the equipment needed to be serviced in late fall/early winter (around November), by which time weather and sea conditions had deteriorated in the GOM. Handling of heavy moorings, even from large vessels, is not recommended during rough seas to ensure personnel health and safety and to minimize equipment damage:
    - For future years of monitoring, it is recommended that monitoring start no later than late March to early April so the 6-month servicing can be completed before the end of October.
- To ensure personnel health and safety, mobile platforms are best deployed and retrieved from smaller fishing vessels. Typically, deployment and retrievals take no more than a 1-day cruise:

- For future years, monitoring with mobile platforms should be avoided during the November to March timeframe, when conditions in the GOM are not conducive to operating at far offshore locations from smaller vessels.

- Notwithstanding all the preemptive measures that were implemented to avoid equipment and data loss, a few stationary platforms were either damaged or lost during the deployments. One SHRU VLA also suffered some data loss due to seawater seepage into the recorder casing:
  - Mitigation plans, such as satellite trackers on sensors, together with redundancy (multiple units) should be used when possible, to reduce the impact of any equipment or data loss on the project outcomes.

- Very little relevant data are currently available about ocean sound levels in the deeper waters of the central GOM and in the western portion of the northern GOM:
  - Acoustic data collection in the ultra-deep areas of the northern GOM is strongly recommended for future years, especially as the industry is now operating farther offshore (e.g., Shell Oil's Stone Project). Once this area is commercially developed, the opportunity for measuring and determining a true natural acoustic baseline will be lost. Another priority area is the western GOM offshore of Texas and Louisiana, within the call area (and future lease areas) for offshore wind, to provide a baseline prior to construction.

- The northern GOM shallow-water soundscapes are extremely complex in nature and poorly understood. There is an urgent need to collect and analyze data in the shallow waters of the GOM. However, expensive monitoring equipment cannot be deployed in shallow-water areas because these areas carry a high-risk for losing moorings due to heavy industrial, shipping, and fishing activities:
  - Risk-benefit analysis should be conducted if long-term monitoring of the shallow-water areas is a priority. Commercial, off-the-shelf, trawl-resistant housings are available. These could be outfitted with low-cost acoustic recorders (e.g., sound traps) for shallow water recording systems.

- Both MPs were focused on collecting and analyzing data to meet the stated Program objective, which was ambient soundscape characterization. Data analyses results indicated that the region is biologically active, and numerous marine mammal vocalizations also were recorded:
  - During future phases of the GOM PAM Program, data from the two MPs may be further analyzed in detail to support other Program objectives such as estimating current marine mammal occupancy and (call) density in the study area; projecting potential impacts of anthropogenic sounds on marine mammals, fish, and other protected species; and developing long-term trends in the soundscape and marine mammal occurrence/density.

- Due to resource and field time limitations, a playback experiment could be conducted only under the 2018 MP, and it included transmitting signals at only four stations. Additionally, the SL had to be minimized so it could be considered de minimis to satisfy environmental compliance:
  - During future program phases, more detailed and longer-duration playback experiments should be considered to determine sensor detection ranges and sound propagation, and to assist with localization of sounds. Use of a calibrated source can also assist in improving understanding of differences in levels recorded across different platforms.

- The 3D underwater sound propagation model was used during the planning phase to optimize selection of SHRU VLA stations by maximizing the hydrophone listening coverage. Results of the data analyses showed that presence of a 3D undersea environment (canyons and slopes) makes the acoustic propagation complex and challenging. To dissect the soundscape components

for extracting environmental information or monitoring anthropogenic noise, sound propagation effects in the soundscape measurements must be removed. Without doing this, noise source signatures cannot be clearly observed, and the true soundscape environment information or anthropogenic noise level may be deviated by sound propagation effects, including multipath arrivals, focusing and defocusing, scattering, and sound signal phase dispersion:

    - Incorporation of advanced 3D sound propagation modeling is recommended for future data analyses phases, particularly within complex topographic regions; this would provide valuable data to better understand and account for important acoustic effects. Model simulation output would help answer important questions such as "Do marine mammals preferentially occupy (in the sense of vocal activity) high TL (low intensity) regions to avoid potential anthropogenic sounds, such as masking?"

- Sensors often store data in different formats, some open and some proprietary. This may create some challenges in creating a cohesive public database for future researchers:
    - Establishing a common, open format (e.g., FLAC) for all data submissions will make large data collections more accessible in the future.
- The magnitude of data collected during this Program required significant effort to prepare and format for archiving at NOAA's NCEI:
    - In the future, incremental formatting and archiving of collected acoustic data with a repository, such as NCEI, would help to reduce some of the challenges associated with processing large volumes of data. This should be detailed within a Data Management Plan, including required formats and methods of data transfer, although the challenge should be recognized that archiving practices and requirements for passive acoustic data continue to evolve over time. Assigning a Program Data Manager early in the process for multi-sensor and multi-institutional projects could also assist with data conformity and sharing.

6.2 Expanding Program Objectives

Since the primary Program objective was to collect data for underwater soundscape characterization, field data collection protocols (especially placement of recorders) were customized to collect data to meet the defined objective. However, if BOEM's overall goal is to generate comprehensive data that will be useful for managing present and future anthropogenic activities in the region, future Program initiatives should be expanded beyond soundscape characterization to also include collecting and analyzing data for the following purposes:

1. Evaluation of marine mammal vocalization data for characterizing spatial and temporal distribution of selected mammalian species and modeling spatial and temporal patterns of marine mammal acoustic activity and density estimations for selected species of interest.
2. Estimation of impacts of anthropogenic sounds on marine mammals and other species.
3. Monitoring long-term trends in soundscapes and marine mammal density.

Conceptual ideas for achieving these additional Program objectives are discussed below.

6.2.1 Program Objective 1: Characterize the spatial and temporal distribution (including density) of select marine mammal species

Marine mammals are common in the GOM and occupy a range of habitats, from shallow coastal waters to the deep abyssal plain. They also have a high potential for being negatively impacted by anthropogenic noise. Under this objective, the spatial and temporal distribution of marine mammals in the GOM will be

further investigated in order to provide information about ecological areas of importance for these animals, and also to serve as a baseline metric to better understand potential changes in marine mammal distribution over time.

To address this objective, acoustic data previously collected under the 2018 and 2019 MPs could be further analyzed to characterize occurrence and distribution of select marine mammal species similar to previous acoustic studies conducted in the area (Li et al, 2020 and 2021). This could be accomplished by applying available automated species detection algorithms to the data where possible, as well as performing manual data processing and review where needed. Because of the potential influence of high levels of anthropogenic noise (e.g., vessel traffic) and biological masking noise (e.g., snapping shrimp), it is possible that conventional automated detectors for marine mammals will be ineffective or perform poorly on data obtained from shelf waters. In these cases, a manual approach will be necessary to identify periods of marine mammal presence. This manual analysis approach would involve trained analysts processing multi-band, long-term spectral averages and/or examine recordings individually, annotating the presence of all cetacean calls encountered.

The resulting detections would be plotted over multiple temporal scales (diel, lunar, seasonal) to characterize the existing trends in bio-acoustic activity at each monitored location. Information provided by these analyses would include, but is not limited to, time and date of detection, spatial location of the sensor that recorded the animal vocalization, identification of species/species groups where possible, and relative frequency of detections by species/species group and sensor location. Because of the experimental design adopted for the 2018 and 2019 data collection efforts, these analyses would likely not provide precise animal locations or abundance/density of calling animals.

Suggested target species/species groups and associated sampling rates are as follows:

- Rice's whale (*Balaenoptera ricei*) (would require a 2 kHz sampling rate)
- Sperm whales (*Physeter macrocephalus*) (would require >20 kHz sampling rate)
- Pygmy and dwarf sperm whales (*Kogia* spp.) (would require 384 kHz sampling rate)
- Beaked whales (>100 kHz sampling rate)
- Other large and small delphinids (>32 kHz sampling rate)
- Vocalizing fish species (would require a 2 kHz sampling rate)

Some delphinid species produce individually identifiable calls, known as signature whistles (Janik and Sayigh 2013, Bebus and Herzing 2015, Fearey et al. 2019). These can be used to determine the minimum number of individuals present and track those individuals through the time series of detections (Bailey et al. 2021). Such information can be valuable to identify how frequently individuals are detected as an indication of how resident or transient the animals are. It can also be used to determine expected exposure levels for individuals given how frequently they occur in an area and whether it is the exposed animals that return after a disturbance event, or whether it is naïve animals entering from outside the area affected.

In order to determine the actual locations of vocalizing marine mammals, and derive estimates of animal density (number of animals per unit area), the following sub-objectives could potentially be pursued as part of the follow-on monitoring program:

- Develop estimates of species-specific detection probabilities (as a function of range) for occupancy and call density estimation. Call density estimation is based on the detection of animal calls, not individual animals, because animals can be present but not calling.
- Describe spatial and temporal trends in occupancy and call density.

- Develop estimates of call production rates1 necessary to convert call density into animal density and abundance.
- Construct species-specific spatio-temporal habitat models that explain patterns in species density as a function of environmental covariates.
- Develop empirical or model-based spatial maps of animal densities for different areas of the northern GOM.
- Combine call density measurements with call production rates to calculate species-specific density and abundance estimates.

Regarding survey design, it will be necessary to specify the spatial and temporal resolution at which abundance and density estimates are required before a design can be finalized. For example, fixed sensors will be preferable if the main objective is to assess temporal trends, while mobile sensors might be ideal if spatial coverage is key. An ideal design might in fact be comprised of a combination of sensors. Finally, drifting sensors are also a possibility.

If there is a desire to obtain spatially explicit density surface models for some species, then the best option may be a network of sensors spaced over the entire area of interest in a systematic manner. Many aspects will have to be considered, in particular the spatial coverage of a given sensor, which influences the probability of detection of a sound by a sensor. As noted above, if some sensors provide the ability to locate animals this task is considerably simplified using distance sampling methods or their modifications; if not, methods that by-pass location might be considered (e.g., spatially explicit capture-recapture, SECR).

It is unlikely that a single design will allow collection of reliable data in an optimal way for multiple species. Hence hybrid designs, in which different nodes might occur at different scale grids, should be considered. In particular, a sensible multi-purpose design might be achieved essentially with overlapping designs, where a small number of sensors, perhaps more expensive but capable of providing localization of close-range sounds, are placed within a network of coarser but cheaper sensors which essentially collect information on spatial distribution (Figure X). Additionally, these could potentially allow for matching of sounds which can travel larger distances, allowing the estimation of animal density using SECR approaches (e.g., Martin et al. 2012). Smaller scale experiments might be conducted using additional sensors and gliders/drifting buoys.

6.2.2 Program Objective 2: Support the Estimation of Impacts of Anthropogenic Sounds on Marine Mammal and Other Species

Determining the effects of anthropogenic sounds on marine mammals is a complex task requiring multifaceted information about the occurrence, distribution, ecology, behavior, and hearing sensitivities of target species, as well as knowledge about the anthropogenic sounds involved, how the sound propagates through the environment, and the received levels. It is important at the outset to identify the time scales of interest, i.e., long-term changes in population densities, medium-term changes in local densities associated with sounds over the period of days, associated with animals leaving an area, or short-term acoustic or other behavioral response over the period of seconds or minutes. It is also important to distinguish between inferences that can be obtained from controlled experimental and observational studies. Broadly, observational studies can identify correlation, but not causation.

With these challenges in mind, data collected under the GOM PAM Program could be used to inform studies of behavioral impacts on marine mammals. For example, the GOM PAM effort will produce data that will be used to build time series and 3D sound propagation models, which could help inform anticipated predictive studies of anthropogenic impacts on marine mammals. The 3D variation in bathymetry creates focusing and defocusing regions, which can correlate with animal behavior.

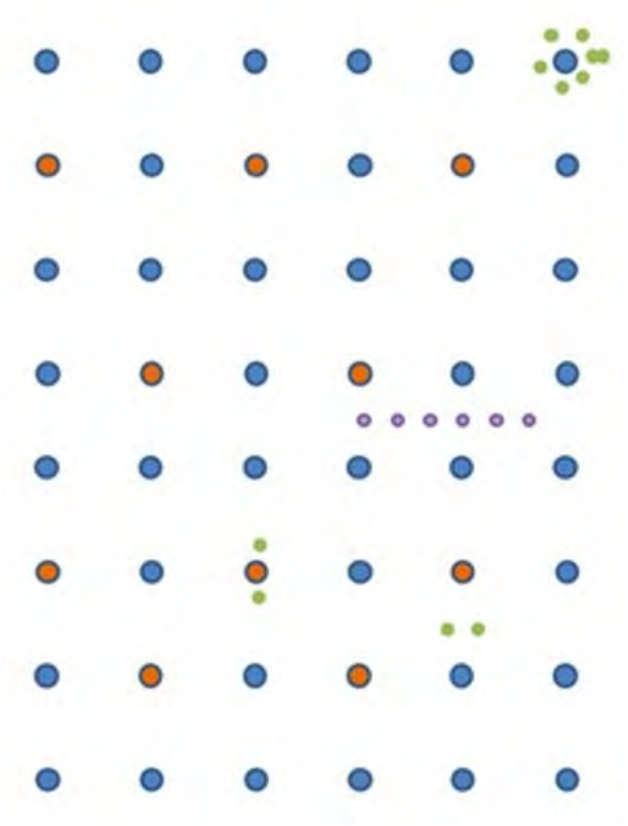

Figure 53. An example of a hybrid design with different sensor types

Note: Hypothetically, blue sensors would be standard sensor nodes, orange would represent ranging capable sensors, while green sensors might be redundant or dedicated to small scale studies/experiments, and purple sensors might be involved in specific sound propagation experiments/calibrations

The collected information on ambient sound levels is also important for determining when a sound source will no longer be distinguishable above the background noise level as this will occur at shorter ranges when the ambient levels are inherently noisy.

Future studies could focus on collecting data on specific variables of interest in impact studies (e.g., sound intensity in a band of interest, or occurrence of target species, or density), as well as leveraging previously collected data where possible. Regarding study design, large-scale observational studies of population change could leverage existing designs that capture both sound levels of potential stressors and animal acoustic activity. Another approach would be to design dedicated smaller scale experiments aimed to answer questions about animals' reactions to specific sound sources, such as seismic surveys.

6.2.3 Program Objective 3: Monitor Long-term Trends in Soundscapes and Marine Mammal Density

Objective 3 focuses on characterizing long-term (multi-year) temporal trends in the phenomena being studied, namely soundscape and animal density. To meet this objective, information obtained through Objectives 1 and 2 can be integrated to develop an advanced understanding of how changes in marine mammal density correlate with changes in the anthropogenic sound field they experience. Data will be collected over a multi-year time frame, possibly adjusting spatial and or temporal coverage depending on the spatial and temporal precision required in trend estimation. Specific sub-objectives may include the following:

- Statistically evaluate the feasibility of reducing the number of sensors required for continued monitoring in follow-on years to capture changes in soundscape and marine mammal density.
- Statistically evaluate whether natural temporal variations in soundscapes and marine mammal occurrence in the GOM will permit intermittent monitoring efforts to capture long-term trends, and if so, at what interval (e.g., 3, 5, 10 years?).
- Implement an adjusted sampling plan for long-term monitoring of soundscapes and marine mammal trends based on guidance from the findings of the first two sub-objectives.
- Estimate long-term trends in soundscape and marine mammal occurrence and density and how these vary over space.

It should be noted that the evaluation of trends over time is slightly more complex than joining a set of points in time, because there are different ways in which such point joining exercise could take place. The spatial-temporal models of variables of interest (be it soundscape, e.g., sound intensity in a band of interest, or occurrence of species, or density), will likely be an intrinsically statistical problem. An optimal survey design for obtaining a density in each time point might not be optimal to evaluate trend in said density over a longer time period. As an example, if evaluating trend over multiple years is key, then a fixed network of sensors over years would be preferable, while to get a mean density in each year, a rotating set of sensors providing wide spatial coverage might be optimal. With conflicting objectives, a design that represents a compromise between these might be required (e.g., a set of fixed locations for trend over time, and some rotating sensors / moving platforms to provide ample spatial coverage.

A wide variety of soundscape metrics have been developed, mostly for terrestrial systems, that provide information on the spatiotemporal patterns of biodiversity and environmental sounds (Pieretti and Danovaro 2020). These metrics have the advantage that they can provide a holistic and time efficient approach to synthesizing large acoustic data sets and providing a measure of biodiversity and anthropogenic activity that will complement ongoing species specific detection studies. Metrics that identify the contribution of different components of the soundscape are also highly beneficial for ecosystem-based management. Depending on the environment, pre-processing of recordings and the application of some metrics, or weighted combinations of metrics, have proved more useful for indicating biological patterns and ecosystem changes (Parks et al. 2014, Towsey et al. 2014). These metrics could be applied and further refined to the collected acoustic data to determine if they perform better with adaptations that take into account the GOM's unique ambient soundscape.

6.3 Advancing the Modeling and Data Analyses

A robust dataset is now available from the two MPs. Due to time and resource constraints, only selected analyses were conducted under this study. Several different aspects of the soundscape could be further evaluated and explored using the available dataset, preferably supplemented with collection of some limited additional field data. For example, measurements and modeling of the GOM 3D soundscape could be advanced further as discussed below.

One of the distinct features revealed by the 3D acoustic propagation modeling study conducted under this Program is the non-negligible seasonal variability of the 3D soundscape. This outcome warrants further assessment for the purpose of generating a soundscape metric that can be referenced to characterize ambient sound signatures and their temporal variability. Advanced modeling study and data analyses are suggested, along with inter-seasonal sound transmission experiments.

A necessary feature of a regional environment soundscape metric is a relative stability over some specified time interval. Stability in the soundscape can be represented by a constraint on the allowed noise coherence variability. This is a desirable trait as it allows a single metric to be used over a longer period

of time, reducing the need to continuously update 3D acoustic propagation models, and locking in ambient sound signatures that can be further ping-pointed, investigated, and explored to characterize the surrounding environments for shipping density, oil and gas exploration and extraction activities, marine mammal habitats, and other activities. To demonstrate the seasonal variability of the GOM soundscape, a seasonal mean of the noise coherence model at 25 and 55 Hz is displayed in **Figures 54** and **55**, respectively.

The noise coherence can range from -1 to +1, so a seasonal dispersion of 0.25, as apparent in **Figure 54** panel (D) during winter at 25 Hz, is significant, and the dispersion displayed at 55 Hz (**Figure 55**) is even more so. Of importance is that the LF displays smaller dispersion when compared to the HF. This suggests that the temporal variability of the soundscape is frequency-dependent, with LFs remaining stable over longer time frames. Additionally, the range of dispersion over the computational environment suggests that certain spatial locations are "acoustic hot spots," which are also sensitive to source frequency and require more frequent updates to the underlying soundscape metric.

Further development of the modeling effort could be supported by more ocean temperature and salinity data, which would allow a finer handling of the temporal variability study of the soundscape metric. Besides that, the collected PAM data under this Program can be further analyzed to study variability in different time scales shorter than seasons and most importantly to reconstruct the 3D soundscape "fingerprint." It is also suggested to use playback transmission experiments with controlled sources to validate 3D sound propagation models and PAM techniques for environmental characterization, especially passive acoustic localization of marine mammals.

To summarize, three main pathways to improvement of the 3D soundscape study in the GOM are immediately identifiable:

- **Advanced data analyses and modeling study of identifying time intervals of soundscape stability at varying source frequencies:** Currently, it is evident that a season defined by roughly three calendar months is too long to capture a stable soundscape. It is also evident that the duration of soundscape stability varies with source frequency. Additionally, it is recommended to increase environmental data resolution for the acoustic modeling. Currently, a single vertical mean sound speed profile is translated horizontally across the entire computational domain, therefore placing all range variability in the bathymetry.
- **Identification of ship signatures in the PAM data by cross-referencing AIS data to create a library of ship signatures:** This library would map ship signals with known ship locations and would provide the opportunity to incorporate machine learning techniques to train a system for identifying ship location from new signals. This method will benefit greatly from the first bullet above, which can provide appropriate constraints to apply on selecting proper training data to avoid identification errors due to the time-dependent nature of the ocean state and consequently any received ship noise.

Playback transmission experiments with controlled sources: A short playback experiment was conducted during the 2018 MP, which provided critical TL data for the 3D modeling. Additional playback experiments could be conducted to generate high-resolution TL maps, complementing the soundscape coherence maps. Four playback experiments per year (one in each season) are recommended to capture seasonal as well as annual variability. To capture temporal variability in a shorter time scale, each of these four playback experiments should last for a few weeks.

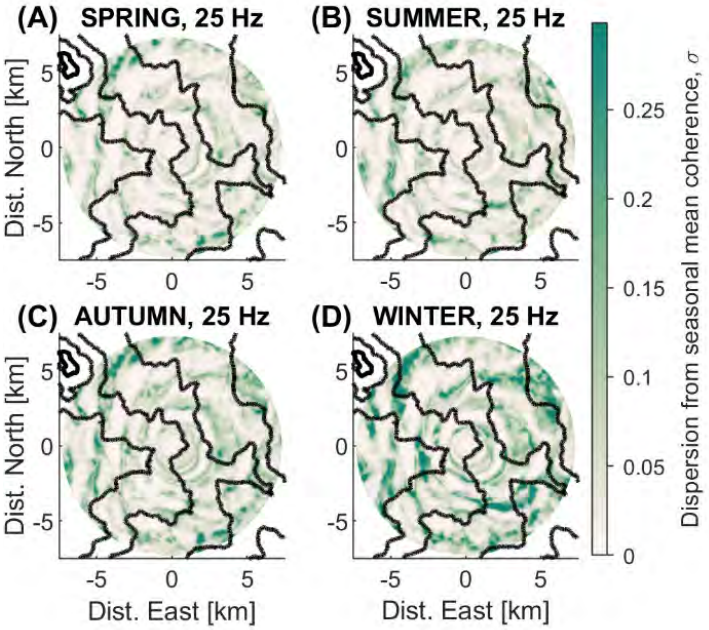

Figure 54: Seasonal variability at 25 Hz

Note: The standard deviation of the noise coherence at each spatial location is plotted for four 3-month periods.

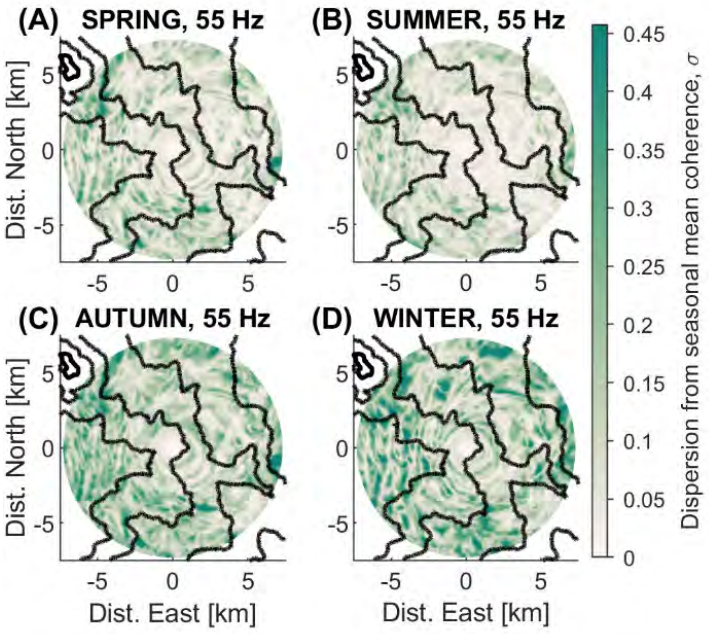

Figure 55: Seasonal variability at 55 Hz

Note: The standard deviation of the noise coherence at each spatial location is plotted for four 3-month periods.

7 References

(GOM PAM interim deliverables highlighted in bold font)

Ackleh AS, Ioup GE, Ioup JW, Ma B, Newcomb JJ, et al. 2012. Assessing the Deepwater Horizon oil spill impact on marine mammal population through acoustics: endangered sperm whales. J Acoust Soc Am. 131(3):2306–2314. doi: 10.1121/1.3682042.

Ainslie MA, Miksis-Olds JL, Martin B, Heaney K, de Jong CAF, von Benda-Beckman AM, Lyons AP. 2017. ADEON soundscape and modelling metadata standard. Version 2.0 DRAFT. Netherlands Organization for Applied Scientific Research (TNO). 41 p. ADEON Prime Contract No. M16PC00003.

Amaral J, Vigness-Raposa K, Miller JH, Potty GR, Newhall A, Lin YT. 2020. The underwater sound from offshore wind farms. Acoust Today 16:13–21.

[ANSI] American National Standards, Inc. 1994. Procedures for outdoor measurement of sound pressure level. Acoustical Society of America. ANSI S12.18:1994.

Ballard MS, Goldsberry BM, Isakson MJ. 2015. Normal mode analysis of three-dimensional propagation over a small-slope cosine shaped hill. J Comput Acoust. 23:1550005. doi: 10.1142/s0218396x15500058.

Bailey H, Senior B, Simmons D, Rusin J, Picken G, Thompson PM. 2010. Assessing underwater noise levels during pile-driving at an offshore windfarm and its potential impact on marine mammals. Marine Pollution Bulletin 60:888–897.

Bailey H, Brookes KL, Thompson PM. 2014. Assessing environmental impacts of offshore wind farms: Lessons learned and recommendations for the future. Aquatic Biosyst. 10:8.

Bailey H, Fandel AD, Silva K, Gryzb E, McDonald E, Hoover AL, Ogburn MB, and Rice AN. 2021. Identifying and predicting occurrence and abundance of a vocal animal species based on individually specific calls. Ecosphere 12: e03685.

Bassett C, Polagye B, Holt MM, Thomson J. 2012. A vessel noise budget for Admiralty Inlet, Puget Sound, Washington (USA). J Acoust Soc Am 132:3706–3719.

Bebus, SE., and DL. Herzing. 2015. Mother-offspring signature whistle similarity and patterns of association in Atlantic spotted dolphins (*Stenella frontalis*). Animal Behavior and Cognition 2: 71-87.

Betke K, Folegot T, Matuschek R, Pajala J, Persson L, Tegowski J, Tougaard J, Wahlberg M. 2015. BIAS standards for signal processing: aims, processes and recommendations. Amended version. 2015. Editors: U.K. Verfuß, P. Sigray.

[BOEM] Bureau of Ocean Energy Management. 2013. GOM OCS oil and gas lease sales: 2014 and 2016; eastern planning area lease sales 225 and 226—final environmental impact statement. Volume I: chapters 1–8. New Orleans (LA): Bureau of Ocean Energy Management, GOM Region. 710 p. OCS EIS/EA BOEM 2013-200. https://www.boem.gov/sites/default/files/boem-newsroom/Library/Publications/2013/BOEM-2013-200-v1.pdf.

1193 Boyd AD, Gowans S, Mann DA, Simard P. 2021. Tropical Storm Debby: soundscape and fish sound
1194 production in Tampa Bay and the Gulf of Mexico. PLOS ONE 16: e0254614.

1195 Bradley D. 2003. Wenz curves describing pressure spectral density levels of marine ambient noise from
1196 weather, wind, geologic activity, and commercial shipping in ocean noise and marine mammals.
1197 Washington (DC): The National Academies Press. p. 195. https://doi.org/10.17226/10564.

1198 Bradley, DL, Stern R. 2008. Underwater sound and the marine mammal acoustic environment: A guide to
1199 fundamental principles. Bethesda (MD): Marine Mammal Commission.

1200 Calupca TA, Fristrup KM, Clark CW. 2000. A compact digital recording system for autonomous
1201 bioacoustic monitoring. J Acoust Soc Am. 108(5):2582. doi: 10.1121/1.474359.

1202 Christensen MG, Jakobsson A. 2009. Multi-pitch estimation. Synthesis Lectures on Speech and Audio
1203 Processing 5(1):1–160. https://doi.org/10.2200/s00178ed1v01y200903sap005.

1204 Dahl PH, Miller JH, Cato DH, Andrew RK. 2007. Underwater ambient noise. Acoust Today 3:23-33.

1205 DeCourcy BY, Lin T. in review. Spatial and temporal variation of three-dimensional ship noise coherence
1206 in a submarine canyon. J. Acoust. Soc. Am.

1207 Discovery of the Sound in the Sea. 2022. Manatee. Discovery of the Sound in the Sea (DOSITS)
1208 [accessed 28 January 2022]. https://dosits.org/galleries/audio-gallery/marine-
1209 mammals/sirenians/manatee/.

1210 Duarte CM, Chapuis L, Collin SP, Costa DP, Devassy RP, Eguiluz VM, Juanes F. 2021. The soundscape
1211 of the Anthropocene ocean. Science. 371(6529).

1212 Duda TF, Lin YT, Reeder DB. 2011. Observationally constrained modelling of sound in curved ocean
1213 internal waves: examination of deep ducting and surface ducting at short range. J Acoust Soc Am
1214 130:1173–1187. doi: 10.1121/1.3605565.

1215 Dugan PJ, Zollweg JA, Helble T, Roch MA, Clark CW, Klinck H. 2018. The Raven-X software package
1216 - a scalable high performance computing framework for the analysis of large bioacoustic sound
1217 archives. In: Proceedings of the 8th International Conference on Detection, Classification,
1218 Localization, and Density Estimation of Marine Mammals using Passive Acoustics, Paris, France, p.
1219 34.

1220 Estabrook BJ, DW Ponirakis, CW Clark, AN Rice. 2016. Widespread spatial and temporal extent of
1221 anthropogenic noise across the northeastern GOM shelf ecosystem. Endanger Species Res. 30:267–
1222 282. doi:10.3354/esr00743.

1223 Fearey J, Elwen SH, James BS, and Gridley T. 2019. Identification of potential signature whistles from
1224 free-ranging common dolphins (*Delphinus delphis*) in South Africa. Animal Cognition 22: 777-789.

1225 Fulling GL, Mullin KD, Hubard CW. 2003. Abundance and distribution of cetaceans in 1010 outer
1226 continental shelf waters of the U.S. Gulf of Mexico. Fishery Bulletin. 101:923-932.

1227 Gisiner RC. 2016. Sound and marine seismic surveys. Acoust Today. 12:10-18.

Greene CR, Richardson WJ. 1988. Characteristics of marine seismic survey sounds in the Beaufort Sea. J Acoust Soc Am 83: 2246.

Guerra M, Thode AM, Blackwell SB, Macrander AM. 2011. Quantifying seismic survey reverberation off the Alaskan North Slope. J Acoust Soc Am 130:3046–3058.

Hastie G, Merchant ND, Götz T, Russell DJF, Thompson P, Janik VM. 2019. Effects of impulsive noise on marine mammals: investigating range-dependent risk. Ecol Applications. 29:e01906.

Hayes SA, Josephson E, Maze-Foley K, Rosel PE, Turek J. 2021. U.S. Atlantic and Gulf of Mexico marine mammal stock assessments - 2020. Washington DC: U.S. Department of Commerce. 403 p. NOAA Tech Memo NMFS-NE 271.

HDR. 2018. Experimental design for the passive acoustic monitoring pilot study in the northern GOM. Final report. Washington DC: Bureau of Ocean Energy Management (BOEM), Office of Renewable Energy Programs. OCS Study BOEM 2018.

HDR. 2019. Experimental design for the passive acoustic monitoring pilot study in the northern GOM. Final Report. Washington DC: Bureau of Ocean Energy Management (BOEM), Office of Renewable Energy Programs. OCS Study BOEM 2019.

Heaney KD, Campbell RL. 2016. Three-dimensional parabolic equation modelling of mesoscale eddy deflection. J Acoust Soc Am. 139:918–926. doi: 10.1121/1.4942112.

Hildebrand JA. 2009. Anthropogenic and natural sources of ambient noise in the ocean. Marine Ecol Progress Ser. 395:5–20.

Janik VM, and Sayigh LS. 2013. Communication in bottlenose dolphins: 50 years of signature whistle research. Journal of Comparative Physiology A 199: 479-489.

Johnson M, Madsen PT, Zimmer WMX, Aguilar de Soto N, Tyack PL. 2006. Foraging Blainville's beaked whales (*Mesoplodon densirostris*) produce distinct click types matched to different phases of echolocation. J Exp Biol 209(Pt 24):5038–5050.

Klinck H, Ponirakis DW, Dugan PJ, Rice AN (Cornell University, Ithaca, NY). 2019. Assessment of ocean ambient sound levels in the northern GOM, May 2018 – May 2019. Preliminary report. Washington DC: Bureau of Ocean Energy Management (BOEM). Contract No. M17PC00001, Task Orders M17PD00011.

Klinck H, Ponirakis DW, Dugan PJ, Rice AN. 2020. Assessment of ocean ambient sound levels in the northern GOM, May 2019 – June 2020. Preliminary report. Washington DC: Bureau of Ocean Energy Management (BOEM). Contract No. M17PC00001, Task Order 140M0119F0001.

Klinck H, Nieukirk SL, Mellinger DK, Klinck K, Matsumoto H, Dziak RP. 2012. Seasonal presence of cetaceans and ambient noise levels in polar waters of the North Atlantic. J Acoust Soc Am. 132:EL176.

Kearns & West. 2015. Synthesis report: stakeholder webinars to inform development of a monitoring plan for marine mammals in the GOM. Washington DC: Bureau of Ocean Energy Management (BOEM). 24 p. https://www.boem.gov/Synthesis-Report-Stakeholder-Webinars/.

Li K, Sidorovskaia NA, Guilment T, Tiemann CO. 2021. Decadal Assessment of Sperm Whale Site-Specific Abundance Trends in the Northern Gulf of Mexico Using Passive Acoustic Data. J. Mar. Sci. Eng. 2021, 9, 454. https://doi.org.10.3390/jmse9050454.

Li K, Sidorovskaia NA, Guilment T, Tiemann CO. 2020. Model-based unsupervised clustering for distinguishing Cuvier's and Gervais' beaked whales in acoustic data. Ecological Informatics, vol 58, 19p. https://doi.org.10.1016/jecoinf.2020.101094.

Latusek-Nabholz JN, Whitt AD, Fertl D, Gallien DR, Ampela K, Khan AA, Sidorovskaia N. 2020. Literature synthesis on passive acoustic monitoring projects and sound sources in the GOM. Washington DC: Bureau of Ocean Energy Management (BOEM). 104 p. OCS Study BOEM 2020-009. Contract No. M17PC00001.

Lin YT. 2019. GOM PAM 2018 program monitoring project SHRU report. Washington DC: Bureau of Ocean Energy Management (BOEM). Contract No. M17PC00001, Task Order M17PD00011.

Lin YT. 2021. GOM PAM program 2019 monitoring project SHRU report. Washington DC: Bureau of Ocean Energy Management (BOEM). Contract No. M17PC00001, Task Order No. 140M0119F0001.

McDonald MA, Hildebrand JA, Wiggins SM. 2006. Increases in deep ocean ambient noise in the Northeast Pacific west of San Nicholas Island, California. J Acoust Soc Am. 120:711–718.

Newcomb J, Fisher R, Field R, Rayborn G, Kuczaj S, Ioup G, Ioup J, Turgut A. 2002. Measurements of ambient noise and sperm whale vocalizations in the northern Gulf of Mexico using near bottom hydrophones. OCEANS'02 MTS/IEEE 3:1365–1371.

[NRC] National Research Council. 2003. Ocean noise and marine mammals. Washington (DC): National Academies Press. 204 p.

Merchant ND, Barton TR, Thompson PM, Pirotta E, Dakin DT, Dorocicz J. 2013. Spectral probability density as a tool for marine ambient noise analysis. Proc. Meetings Acoust. 19:010049. doi:10.1121/1.4799210.

Mellinger DK, Fregosi S. Assessment of ocean ambient sound levels in the northern GOM, May - June 2018. Final Report. Washington DC: Bureau of Ocean Energy Management (BOEM). Contract No. M17PC00001.

Nieukirk SL, Mellinger DK, Moore SE, Klinck K, Dziak RP, Goslin J. 2012. Sounds from airguns and fin whales recorded in the mid-Atlantic Ocean, 1999-2009. J Acoust Soc Am. 131:1102–1112.

[NMFS] National Marine Fisheries Service. 2016. Technical guidance for assessing the effects of anthropogenic sound on marine mammal hearing: underwater acoustic thresholds for onset of permanent and temporary threshold shifts. Silver Spring (MD): National Marine Fisheries Service, Office of Protected Resources. 189 p. NOAA Tech Memo NMFS-OPR-55.

[NMFS] National Marine Fisheries Service. 2018. 2018 revisions to: Technical guidance for assessing the effects of anthropogenic sound on marine mammal hearing (Version 2.0): underwater thresholds for onset of permanent and temporary threshold shifts. Silver Spring (MD): National Marine Fisheries Service. 167 pp. NOAA Tech Memo NMFS-OPR-59.

[NOAA Fisheries] National Oceanic and Atmospheric Administration Fisheries. 2018. GOM Bryde's whales. http://sero.nmfs.noaa.gov/protected_resources/brydes_whale/index.html.

Oliveira TCA, Lin YT. 2019. Three-dimensional global scale underwater sound modelling: the T-phase wave propagation of a Southern Mid-Atlantic Ridge earthquake. J Acoust Soc Am. 146:2124–2135. doi: 10.1121/1.5126010.

Oliveira TCA, Lin YT, Porter MB. 2021. Underwater sound propagation modelling in a complex shallow water environment. Frontiers in Marine Science. doi: 10.3389/fmars.2021.751327.

Parks SE, Miksis-Olds JL, and Denes SL. 2014. Assessing marine ecosystem acoustic diversity across ocean basins. Ecological Informatics 21: 81-88.

Pijanowski BC, Villanueva-Rivera LJ, Dumyahn SL, Farina A, Krause BL, Napoletano BM, Gage SH, Pieretti N. 2011. Soundscape ecology: the science of sound in the landscape. BioScience. 61:203–216.

Pieretti N., and Danovaro R. 2020. Acoustic indexes for marine biodiversity trends and ecosystem health. Philosophical Transactions of the Royal Society B 375: 20190447.

Ponirakis DW, Dugan PJ, Zollweg JA, Porter MB, Clark CW. 2015. A Matlab based HPC toolset for noise analysis of large acoustic datasets. Proceedings of the 7th International Conference on Detection, Classification, Localization, and Density Estimation of Marine Mammals using Passive Acoustics, San Diego, CA, USA, page 85.

Popper A, Hawkins A, Fay R, Mann D, Bartol S, Carlson T, Coombs S, Ellison W, Gentry R, Halvorsen M, Løkkeborg S, Rogers P, Southall B, Zeddies D, Tavolga W. 2014. Sound exposure guidelines. doi:10.1007/978-3-319-06659-2_7.

Reeder DB, Lin YT. 2019. 3D acoustic propagation through an estuarine salt wedge at low-to-mid-frequencies: modelling and measurement. J Acoust Soc Am 146:1888–1902. doi: 10.1121/1.5125258.

Reilly SM, Potty GR, Thibaudeau D. 2016. Investigation of horizontal refraction on Florida Straits continental shelf using a three-dimensional Gaussian ray bundling model. J Acoust Soc Am. 140:EL269–EL273.

Rice AN, Tielens JT, Estabrook BJ, Muirhead CA, Rahaman A, Guerra M, Clark CW. 2014. Variation of ocean acoustic environments along the Western North Atlantic Coast: A case study in context of the right whale migration route. Ecol Inform. 21:89–99.

Rice AN, Palmer KJ, Tielens JT, Muirhead CA, Clark CW. 2014. Potential Bryde's whale (*Balaenoptera edeni*) calls recorded in the northern GOM. J Acoust Soc Am. 135:3066–3076.

Roberts JJ, Best BD, Mannocci L, Fujioka E, Halpin PN, Palka DL, Garrison LP, Mullin KD, Cole TVN, Khan CB, McLellan WA, Pabst DA, Lockhart GG. 2016. Habitat-based cetacean density models for the U.S. Atlantic and Gulf of Mexico. Scientific Reports. 6:22615.

Roth EH, Hildebrand JA, Wiggins SM, Ross D. 2012. Underwater ambient noise on the Chukchi Sea continental slope from 2006-2009. J Acoust Soc Am. 131:104–110.

Scripps Whale Acoustic Laboratory. 2022. Scripps Whale Acoustic Laboratory. Scripps Institute of Oceanography [accessed 28 January 2022]. https://www.cetus.ucsd.edu/.

Sidorovskaia NA, Li K. 2016. Decadal evolution of the northern GOM soundscapes. Proc Meet Acoust. 27(1):040014, doi: 10.1121/2.0000382.

Sidorovskaia N, Bhattarai K. 2019a. Assessment of ocean ambient sound levels in the northern GOM, May - October 2018: autonomous Environmental Acoustic Recording System (EARS) buoys. Preliminary data processing report. Washington DC: Bureau of Ocean Energy Management (BOEM). Contract No. M17PC00001, Task Order M17PD00011.

Sidorovskaia N, Bhattarai K. 2019b. Assessment of ocean ambient sound levels in the northern GOM, October 2018 – April 2019: autonomous Environmental Acoustic Recording System (EARS) buoys. Preliminary data processing report. Washington DC: Bureau of Ocean Energy Management (BOEM). Contract No. M17PC00001, Task Order M17PD00011.

Sidorovskaia N, Bhattarai K. 2020. Assessment of ocean ambient sound levels in the northern GOM, April - November 2019: autonomous Environmental Acoustic Recording System (EARS) buoys. Preliminary data processing report. Washington DC: Bureau of Ocean Energy Management (BOEM). Contract No. M17PC00001, Task Order 140M0119F0001.

Sidorovskaia N, Griffin S. 2020. Assessment of ocean ambient sound levels in the northern GOM, November 2019-June 2020: autonomous Environmental Acoustic Recording System (EARS) buoys. Preliminary data processing report. Washington DC: Bureau of Ocean Energy Management (BOEM). Contract No. M17PC00001, Task Order 140M0119F0001.

Širović A, Bassett HR, Johnson SC, Wiggins SM, and Hilderbrand JA. 2014. Bryde's whale calls recorded in the Gulf of Mexico. Marine Mamm Science. 30(1):399–409.

Towsey M, Wimmer J, Williamson I, and Roe P. 2014. The use of acoustic indices to determine avian species richness in audio-recordings of the environment. Ecological Informatics 21: 110-119.

Uffelen LV, Pomales L, Graupe C. 2019. GOM PAM program 2019 monitoring project Seaglider report. Washington DC: Bureau of Ocean Energy Management (BOEM). Contract No. M17PC00001.

Urick RJ. 1984. Ambient noise in the sea. Washington (DC): Naval Sea Systems Command. 194 p.

Wall CC, Simard P, Lembke C, Mann DA. 2013. Large-scale passive acoustic monitoring of fish sound production on the West Florida Shelf. Marine Ecol Progress Ser. 484:173–188.

Warren VE, Marques TA, Harris D, Thomas L, Tyack PL, Aguilar de Soto N, ... Johnson MP. 2017. Spatio-temporal variation in click production rates of beaked whales: Implications for passive acoustic density estimation. J Acoust Soc Am. 141(3):1962–1974.

Wenz GM. 1962. Acoustic ambient noise in the ocean: spectra and sources. J Acoust Soc Am. 34:1936–1956. doi: 10.1121/1.1909155

Wiggins SM, Hall JM, Thayre BJ, Hildebrand JA. 2016. GOM low-frequency ocean soundscape impacted by airguns. J Acoust Soc Am. 140:176–183. doi:10.1121/1.4955300.

Appendix A: GOM PAM Program Literature Synthesis Report

OCS Study
BOEM 2020-009

Literature Synthesis: Passive Acoustic Monitoring Projects and Sound Sources in the Gulf of Mexico

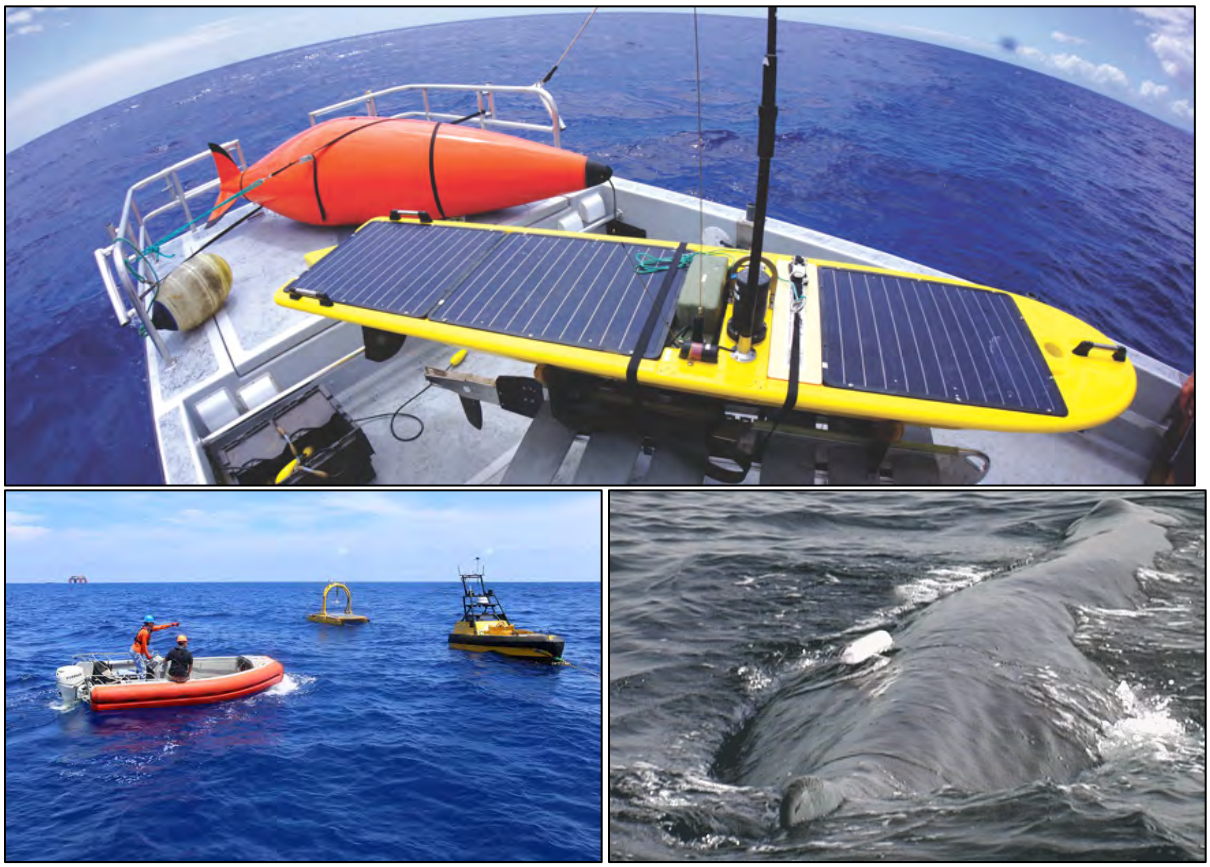

U.S. Department of the Interior
Bureau of Ocean Energy Management
New Orleans Office

OCS Study
BOEM 2020-009

Literature Synthesis: Passive Acoustic Monitoring Projects and Sounds Sources in the Gulf of Mexico

Authors

Jennifer N. Latusek-Nabholz
Amy D. Whitt
Dagmar Fertl
Dennis R. Gallien
Anwar A. Khan
Natalia Sidorovskaia

Prepared under BOEM Contract
M17PC00001
by
HDR, Inc.
300 N. Madison Street
Athens, Georgia 35611

Published by

U.S. Department of the Interior
Bureau of Ocean Energy Management
New Orleans Office

New Orleans, LA
January 2020

DISCLAIMER

Study concept, oversight, and funding were provided by the US Department of the Interior, Bureau of Ocean Energy Management, Environmental Studies Program, Washington, DC, under Contract Number M17PC00001, Task Order No. M17PD00011. This report has been technically reviewed by BOEM, and it has been approved for publication. The views and conclusions contained in this document are those of the authors and should not be interpreted as representing the opinions or policies of the U.S. government, nor does mention of trade names or commercial products constitute endorsement or recommendation for use.

REPORT AVAILABILITY

To download a PDF file of this report, go to the US Department of the Interior, Bureau of Ocean Energy Management Data and Information Systems webpage (http://www.boem.gov/Environmental-Studies-EnvData/), click on the link for the Environmental Studies Program Information System (ESPIS), and search on 2020-009. The report is also available at the National Technical Reports Library at https://ntrl.ntis.gov/NTRL/.

CITATION

Latusek-NabholzJN, Whitt AD, Fertl D, Gallien DR, Ampela K, Khan AA, Sidorovskaia N. 2020. Literature synthesis on passive acoustic monitoring projects and sound sources in the Gulf of MexicoNew Orleans (LA): US Department of the Interior, Bureau of Ocean Energy Management. Contract No.: M17PC00001. OCS Study BOEM 2020-009. 99 p.

ABOUT THE COVER

Photo credits: (Top) glider and towed acoustic transponder set for test deployment, Scripps Institution of Oceanography at University of California San Diego; (bottom left) sperm whale with DTAG (digital-recording acoustic tags) deployed during Sperm Whale Seismic Study (SWSS), Texas A&M University; (bottom right) autonomous surface vehicles getting ready to work in the Gulf of Mexico, Littoral Acoustic Demonstration Center.

Acknowledgements

Tre Glenn, PhD, served as the Bureau of Ocean Energy Management (BOEM) Contracting Officer's Technical Representative and provided guidance and support throughout the contract period.

This report is the first deliverable under the "Passive Acoustic Monitoring (PAM) Program for the Northern Gulf of Mexico (GOM)" IDIQ Contract No. M17PC00001, Task Order No. M17PD00011. The HDR BOEM PAM Program for the Northern GOM implementation team includes the following subcontractors:

- University of Rhode Island
- University of Louisiana, Lafayette
- Cornell University
- Oregon State University
- St. Andrews University
- Azura Consulting, LLC
- Oceanside Science Institute
- Marine Acoustics, Inc.
- Abakai International, LLC
- Woods Hole Oceanographic Institution
- Southall Environmental Associates, Inc.

Assistance and support from all team members are greatly appreciated.

Contents

List of Figures

List of Tables

List of Abbreviations and Acronyms

Short Form	Long Form
ADCP	acoustic Doppler current profiler
AFTT	Atlantic Fleet Training and Testing
AMAPPS	Atlantic Marine Assessment Program for Protected Species
ASV	autonomous surface vehicle
AUV	autonomous underwater vehicle
BIA	Biologically Important Area
BOEM	Bureau of Ocean Energy Management
BSEE	Bureau of Safety and Environmental Enforcement
CAAMP Monitoring Program	Coastal Alabama Acoustic Monitoring Program
CEE	controlled exposure experiment
CetSound	cetacean & sound mapping
CV	coefficient of variation
dB	decibel(s)
dB re 1 µPa/m	decibels referenced to 1 microPascal per meter
dB re 1 μPa^2	decibels referenced to 1 microPascal squared
dB re 1 µPa	decibels referenced to 1 microPascal per meter
dB re 1 µPa @ 1 m	decibels referenced to 1 microPascal at 1 m
dB re 1 μPA^2/Hz	decibels referenced to 1 microPascal squared per Hertz
dB re 1 µPa [rms] m	decibels referenced to 1 microPascal (root mean square) at 1 m
dB re 1 μPa^2 s	decibels referenced to 1 microPascal squared second
DIFAR	directional frequency analysis and recording
DoN	Department of the Navy
DP	dynamic positioning
DSG	Digital SpectroGram
DTAG	digital-recording acoustic tag
EARS	environmental acoustic recording system
EBRV	Energy Bridge™ Regasification Vessel
EEZ	Exclusive Economic Zone
EIS	environmental impact statement
ERMA	energy ratio mapping algorithm
GAM	generalized additive model
GCOOS	Gulf of Mexico Coastal Ocean Observing System
GEMM	Gulf Ecological Monitoring and Modeling
GMM	Gaussian mixture model
GOM	Gulf of Mexico
GoMRI	Gulf of Mexico Research Initiative
GRIIDC	GoMRI Information and Data Cooperative
GulfCet	Gulf of Mexico Cetacean Study
HARP	high-frequency acoustic recording package
Hz	hertz
IOOS	US Integrated Ocean Observing System
kHz	kilohertz
LADC	Littoral Acoustic Demonstration Center
LADC-GEMM	Littoral Acoustic Demonstration Center–Gulf Ecological Monitoring and Modeling
LIDO	Listening to the Deep Ocean Environment
LLC	limited liability company
LNG	liquefied natural gas
MARMAM	Marine Mammals Research and Conservation Discussion
MARU	marine autonomous recording unit
MMO	Marine Mammal Organisation

Short Form	Long Form
MMS	Minerals Management Service
NMFS	National Marine Fisheries Service
NMFS SEFSC	NMFS Southeast Fisheries Science Center
NOAA	National Oceanic and Atmospheric Administration
NSWC PCD	Naval Surface Warfare Center Panama City Division
OBIS-SEAMAP	Ocean Biogeographic Information System Spatial Ecological Analysis of Megavertebrate Populations
OCS	Outer Continental Shelf
ONR	Office of Naval Research
PAL	passive acoustic listening
PAM	passive acoustic monitoring
PK	peak sound pressure level
psu	practical salinity unit
ppt	parts per thousand
PTS	permanent threshold shift
RMS	root mean square
ROCCA	real-time odontocete call classification algorithm
R/V	research vessel
SEFSC	Southeast Fisheries Science Center
SEL	sound exposure level
SELcum	cumulative sound exposure level
SPL	sound pressure level
SST	sea surface temperature
SWAMP	Sperm Whale Acoustic Monitoring Program
SWSS	Sperm Whale Seismic Study
TL	transmission loss
T-POD	Timing Porpoise Detector
US	United States
USV	unoccupied surface vessel
WGH	Wave Glider HARP

Summary

Purpose

Available and relevant literature and data on previous and ongoing passive acoustic monitoring in the Gulf of Mexico (GOM) were compiled. This information was reviewed to characterize potential sound sources and their distribution in the GOM and to identify existing methodologies for acoustic source detection, localization, tracking, and classification. Acoustic sources encompass weather events, industrial and military activities (including the use of explosives), shipping, animal vocalizations, and geologic events. This review was conducted under the Bureau of Ocean Energy Management's (BOEM) Passive Acoustic Monitoring (PAM) Program for the Northern GOM. The primary objective of the program is to design and implement a multi-year acoustic data collection and monitoring plan for both the acoustic and the biotic environments in the GOM further defining the associated baseline soundscapes.

The objective of this literature synthesis was to collect and review published literature and available datasets of previous and ongoing PAM projects in the GOM for the following purposes:

1. Characterize potential sound sources in the GOM.
2. Summarize the state of current knowledge on GOM baseline acoustic noise levels.
3. Investigate existing methodologies for acoustic source detection, localization, tracking, and classification of marine mammals.
4. Identify by spatial mapping previous and current study areas.
5. Identify the most appropriate field methodologies and protocols for measuring the acoustic environment in the GOM.

Approach

Readily available literature and data on previous and ongoing PAM projects in the three BOEM planning areas in the GOM (Eastern, Central, and Western) were searched and compiled through the use of online databases and literature and World Wide Web. The search focused on gathering a variety of literature types on biological and physical ambient noise levels in the GOM. The review also focused on PAM projects for marine mammals in the GOM and on anthropogenic sound sources in the region. The focus was on collecting information from the last 15 years of studies; some research in the GOM as far back as 1991was included.

Commercial databases, search tools, and email list servers were used in the search for data on PAM projects in the GOM. Key search terms and phrases were used to conduct methodical queries of databases and the World Wide Web. The search included terms in all fields (title, abstract, etc.) referencing noise and/or sound, research method, marine mammal species of interest, specific BOEM planning areas and GOM features of interest, and/or specific researchers and/or institutions, funding sources, and monitoring programs. Studies generally pertained to PAM studies in the Northern GOM. Selected references on research methods and PAM studies were consulted that occurred outside the region because similar studies may be lacking or nonexistent in the Gulf , but may be useful either to characterize PAM work in general and/or to provide suggestions on the future BOEM PAM Program for the Northern GOM.

Key Findings and Recommendations

Since 1991, thirty-two projects have been conducted in the GOM using PAM. Eight of these reviewed studies were specifically designed to gather data on ambient noise in the GOM; the other 24 studies were designed to gather information on marine mammals using PAM. The majority of data collection efforts focused primarily upon the Eastern and Central GOM. Additionally, PAM surveys have tended to be in waters of the continental shelf and slope down to approximately 2,000 meters (6,562 feet) deep; only two surveys were in waters extending to approximately 3,200 meters (10,499 feet).

A preliminary experimental design has been proposed for the acoustic data collection under the BOEM PAM Program for the Northern GOM. This design has included deployment of a carefully selected network of stationary and mobile PAM platforms at strategically identified locations within Mississippi and De Soto canyons in the Northern GOM. Based on the findings from literature review, the following recommendations are made to enhance the preliminary experimental design for the BOEM PAM Program for the Northern GOM:

- Focus the first two-year deployment effort in areas of the Mississippi Canyon and/or valley where many ambient noise sources are present and the majority of previous baseline data collections were conducted. However, expand the sensor deployment to shallow water and abyssal plain.
- If possible, establish at least one stationary monitoring site in BOEM Western or Eastern planning areas to understand the differences in soundscapes among regions with at minimum two years of deployment.
- Investigate the using mobile PAM platforms (gliders and autonomous surface vehicles) for ambient noise measurements, where consistent with study goals and objectives.
- Investigate using oil and gas facilities as opportunistic platforms for data collection, particularly to characterize near-field anthropogenic noise features of drilling and construction activities.
- Conduct comprehensive oceanographic data collection simultaneously with acoustic measurements to assure proper input into propagation models to study their effectiveness in predicting acoustic energy distribution from different sources.
- Focus on long-term multi-year continuous calibrated PAM data collection over a broad frequency range while understanding a need for designing special requirements for the systems that will be monitoring different frequency bands (hydrophone sensitivities and dynamic range, system response curves, etc.).
- Implement rigorous unified hydrophone and/or system pre-deployment calibration protocols across different PAM instruments to ensure quantitative data compatibility and comparability across different PAM platforms.
- Develop common data processing workflows and reporting metrics across the program, in consultation with BOEM.
- Incorporate goals to design experimental data collection in a way that allows benchmarking modeling results for the GOM against newly collected data through the program for different propagation scenarios (range-independent, range-dependent, canyon propagation, etc.).
- Recommend appropriate PAM methodologies for different GOM regions (e.g., shallow water, continental slope, deep-water, industrially active) and for different study objectives (e.g., baseline noise measurements, anthropogenic soundscapes, species abundance, habitat use, etc.). Consider an ecosystem-based approach to PAM data gathering that would allow biological soundscapes relevant to species that have not been extensively studied in the GOM, such as fish and invertebrates.
- Make all data available to the stakeholders and public through NOAA, the GOM Research Initiative Information and Data Cooperative, and other data sharing databases after analyzing and vetting the data and data sharing databases.
- At a later date, support further effort into the comprehensive review of PAM information available for the GOM to include development and implementation of a scientific advisory group.
- Develop and implement protocols to determine acoustic detection ranges and false positive and negative rates within these ranges.
- Develop and implement protocols to determine acoustic sound production rates for species of interest.

1. Introduction

1.1 Study Background

Available and relevant literature and data on previous and ongoing passive acoustic monitoring in the Gulf of Mexico (GOM) were compiled. This information was reviewed to characterize potential sound sources and their distribution in the GOM and to identify existing methodologies for acoustic source detection, localization, tracking, and classification. This review was conducted under the Bureau of Ocean Energy Management's (BOEM) Passive Acoustic Monitoring (PAM) Program for the Northern GOM.

The primary objective of the program is to design and implement a multi-year acoustic data collection and analysis plan to characterize baseline noise level across the GOM. There is considerable concern about the potential effects of anthropogenic noise on marine mammals, sea turtles, and fish. Worldwide, the ocean becomes a very noisy habitat for marine animals when ambient noise levels rise as a result of anthropogenic activities and global warming. Cetaceans rely on sound as a primary sense for vital life functions, so increased noise levels may mask important sounds (including conspecific vocalizations), temporary threshold shift in an animal auditory system, and to direct permanent physical damage, including death. As ambient noise levels have increased in some areas, cetaceans have shifted the frequency band in which they vocalize in order to adapt to communication in a noisy environment (Parks et al. 2007).

In 2006, the National Oceanic and Atmospheric Administration (NOAA) conducted a National Passive Acoustics Workshop (Van Parijs et al. 2007), which recognized the need for a passive acoustic oceans observing system worldwide. This need is perhaps especially acute in places like the GOM, which is extensively industrialized. Cetaceans in the GOM inhabit a highly industrialized environment with multiple anthropogenic acoustic inputs including shipping, oil and gas activities, and military operations. Though a national program is still not in place, smaller scale PAM programs exist in some areas (e.g., Bering Sea, Stellwagen Bank National Marine Sanctuary). These programs have proven effective in measuring ambient noise levels, detecting marine mammal presence, and monitoring anthropogenic noise (e.g., seismic, vessel noise).

The Gulf of Mexico Coastal Ocean Observing System (GCOOS) was established in 2005 under the Global Ocean Observing System (GOOS) and the US Integrated Ocean Observing System (IOOS). GCOOS works under a member/partnership model, with data collected by partners (e.g., data from oceanographic buoys) that then stream the data to GCOOS. The GCOOS data portal is located online[1]; GCOOS can be a repository for data products and modeling (Kirkpatrick 2015).

Of additional interest for the GOM is the Southeast Regional Acoustics Consortium (SEAC), a working group initiated in 2012 that brings together academic institutions, federal and regional fisheries and environmental management agencies, and private industry that conduct acoustics research in the coastal environments of the US from North Carolina to Texas and the US Caribbean.

A recent Ocean Conservancy report (Love et al. 2015) provided a gap analysis for existing GOM monitoring programs for species and habitats negatively impacted by the 2010 *Deepwater Horizon* oil spill. The report highlighted the rare and disjointed nature of offshore monitoring and advocated for moving towards a Gulf-wide ecosystem monitoring network. In particular, monitoring was documented as limited and fragmented for marine mammals and fish and often absent for sea turtles. The need for such network and baseline data gathering becomes even more critical with several large coastal restoration projects underway in the Gulf Coast region. The coastal habitat alterations may also negatively impact deep water ecosystems (e.g., Bishop et al. 2017; Heery et al. 2017).

[1] See the Gulf of Mexico Coastal Ocean Observing System (GCOOS) portal: http://data.gcoos.org.

Data on ambient noise levels in the GOM are extremely limited. Other than some short-term recordings associated with previous studies and recent PAM work done as part of the Natural Resource Damage Assessment for the *Deepwater Horizon* oil spill event, few data exist (Hildebrand et al. 2015a; Estabrook et al. 2016; Snyder 2007, 2009; Newcomb et al. 2002, 2007, 2009).

Noise impacts to protected species (primarily cetaceans) may occur as a result of oil and gas exploration companies undertaking activities (e.g., seismic surveys, platform decommissioning, drilling, vessel noise, etc.) licensed by BOEM and the Bureau of Safety and Environmental Enforcement (BSEE); however, characterizing the impact and trends is difficult without comprehensive baseline data on ambient noise environment (or soundscape) in the GOM. BOEM and BSEE are required to assess potential impacts on protected species, specifically under the Marine Mammal Protection Act, Endangered Species Act, and the National Environmental Policy Act to assist and guide their decision-making. The future BOEM Marine Mammal Protection Act rulemaking for seismic activities in the GOM will have a monitoring requirement associated with it, and data collection on ambient noise and on noise associated with seismic activities. In short, there is an urgent need to implement a systematic and comprehensive acoustic data collection effort in the Gulf. The BOEM PAM Program for the Northern GOM is intended to meet this need.

1.2 Literature Review Goals, Purposes, and Objectives

The objective of the literature synthesis was to collect and review published literature and data about previous and ongoing projects measuring underwater sound in the GOM for the following purposes:

1. Characterize potential sound sources in the GOM and further define the soundscape.
2. Summarize the state of current knowledge on GOM baseline acoustic noise levels.
3. Investigate existing methodologies that have been employed for sound source detection, localization, tracking, and classification (including species vocalizations) for marine mammals.
4. Identify by spatial mapping previous and current study locations.
5. Identify the most effective field methodologies and protocols for measuring the acoustic environment in the GOM.

Observations, findings, and recommendations from the literature synthesis will guide the development of an experimental design for the multi-year acoustic data collection plan to be implemented under the BOEM PAM Program for the Northern GOM.

1.3 Report Organization

This literature synthesis report is divided into six chapters. Chapter 1 is an introduction. Chapter 2 presents the approach, including the boundaries and characteristics of the study area, and the literature and data search methods. Chapter 3 provides an overview of the past and current projects that involve PAM in the GOM. The information includes the locations of PAM projects and explanations of the various types of equipment and research conducted in this area. Chapter 4 provides the current state of knowledge on physical and biological ambient noise and on marine mammal acoustics. Chapter 5 provides recommendations to be considered in developing the experimental design for implementation of the BOEM PAM Program for the Northern GOM. Chapter 6 lists all the references cited in this document. Appendix 1 gives a list of keywords used in the search.

2. Approach

2.1 Identification of Study Area

The Gulf of Mexico (GOM) is a semi-enclosed ocean basin that narrowly connects to the Atlantic Ocean through the opening between Cuba and the Yucatán Peninsula and the Florida Straits. The presence of the Loop Current and warm water eddies separated from the Loop current are dominant oceanographic features of the GOM that considerably influence the Gulf ecosystem/seascape. To assess the information available on passive acoustic monitoring (PAM) in the GOM, a literature search and review was conducted across BOEM's Eastern, Central, and Western planning areas in the GOM (**Figure 1**).

The Western Planning Area lies 17 kilometers (9 nautical miles) offshore of Texas and extends to the United States (US) Exclusive Economic Zone (EEZ), which is the jurisdictional limit over the continental shelf. The EEZ limit is 370 kilometers (200 nautical miles) from the US. The Central Planning Area lies offshore of Alabama, Mississippi, and Louisiana from 6 kilometers (3 nautical miles) to the US EEZ. The Eastern Planning Area lies 17 kilometers (9 nautical miles) offshore of the Gulf Coast of Florida and extends to the EEZ. The water depths in the Western, Eastern, and Central Planning Areas extend up to approximately 3,346 meters (10,978 feet) (BOEM 2013).

2.1.1 Oceanographic and Other Features of the Study Area

In addition to a sound source characteristics, propagation of underwater sound depends upon many environmental factors, such as water depth, bathymetry, currents, salinity, temperature, and sediment composition. All have a part in the transmission of sound and formation of soundscapes. Therefore, a short description of the relevant features of the GOM is provided in the following paragraphs. It also is important to keep in mind that the GOM adjoins North America, which is one of the most industrially developed continents in the world. Thus, there is high magnitude and extent of anthropogenic underwater noise in the GOM.

The GOM is distinguished by an enormous river delta, limestone islands, expansive and relatively flat continental-shelf areas, submarine canyons, steep escarpments, sea fans, and a central deep, flat basin where bottom depths exceed 3,700 meters (12,139 feet). Bottom depths in the GOM range from <10 meters (<33 feet) in the Florida Keys to the maximum depth (3,700 meters [12,139 feet]) over the Sigsbee Abyssal Plain. In the GOM, continental shelf waters (i.e., less than 200 meters (656 feet) in depth) make up approximately 35 percent of the Gulf. Sediments here are made up of sand, silt, and clay. The shelf is quite broad in some places (e.g., offshore west Florida, Texas-Louisiana coast, and Campeche) and narrowly restricted in other places (such as near the mouth of the Mississippi River and offshore eastern Mexico).

The area in the US where deep water in the GOM comes closest to shore is off the Mississippi River Delta where deep waters are within 10 kilometers (5.4 nautical miles) of shore. Deep oceanic waters include only 25 percent of the GOM and are located mostly in the mid-western GOM. At the shelf break, the seafloor begins to slope steeply towards the abyssal plain of the deep GOM, often terminating in a near-vertical scarp or cliff-like formation that extends on down to the bottom. This region is called the continental slope and includes waters in the 200 to 3,000-meter (656- to 9,843-foot) range and covers 40 percent of the ocean basin. The area slopes steeply, and contains deep canyons, knolls and banks particularly in the western portion of the region. Sediments are generally calcareous here and came from shells of marine organisms.

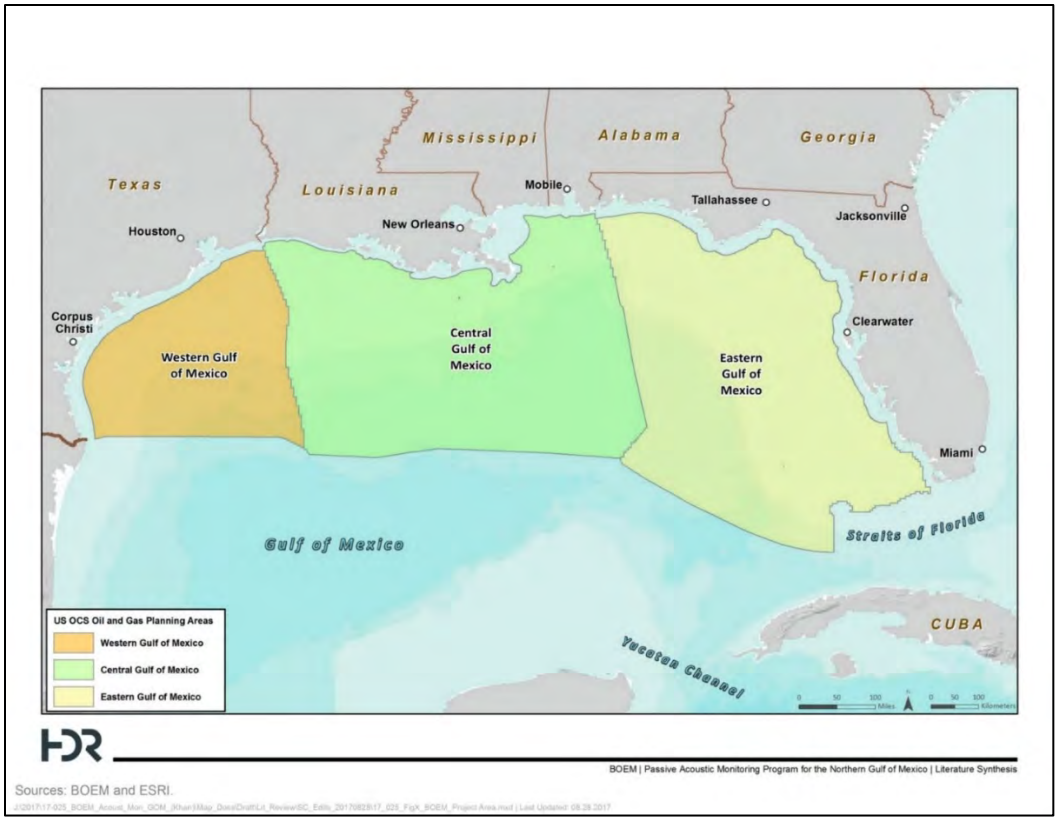

Figure 1. Study area for BOEM literature review of passive acoustic monitoring (PAM) work in the Gulf of Mexico.

Two major rivers discharge freshwater into the GOM: the Mississippi River in the southern US and the Rio Grande on the Mexico-US border. Warm, tropical water enters the GOM through the Yucatan Strait, circulates as the Loop Current, and then exits through the Florida Strait eventually forming the Gulf Stream. Portions of the Loop Current often break away forming eddies (also referred to as "rings" or "gyres") which affect regional current patterns. The Loop Current and associated eddies (both anticyclonic and cyclonic) dominate the upper-layer circulation.

Seasonal variations in sea surface temperature (SST) occur uniformly across the GOM with maximum temperatures occurring in summer (July through September) and minimum temperatures occurring in mid-winter (February through March). Temperature differences between the eastern and western GOM are attributed to the influx of warm Caribbean waters through the Yucatan Channel, which dominates the SST in the Eastern GOM. Sea surface salinities in the Northern Gulf vary seasonally and are heavily influenced by outflow from the Mississippi River. In months with little freshwater input, the salinities along the coast range from 29 to 32 practical salinity units (psu or parts per thousand [ppt]). During the spring and summer when the freshwater input volume from the Mississippi and other rivers is high, a strong salinity gradient forms with salinities typically less than 20 psu (or ppt) in shelf waters. The mixed layer in the central, open GOM extends from 100 to 150 meters (328 to 492 feet) with salinities between 36.0 and 36.5 psu (or ppt).

Sound propagation in the marine environment is influenced by a variety of physical properties of the ocean, including temperature, salinity, sediment type, and pressure. Influences on sound in the GOM include, but are not limited to, the following:

- Surface sound ducts, or channels, occur when the sound speed increases with depth below the surface, leading to a positive sound speed gradient, forming the local minimum of the sound speed near the surface. This can occur in the mixed layer when surface waters are cooler than

underlying waters. Sounds propagating in these channels are refracted upward and can become partially trapped near the surface, leading to enhanced sound propagation and higher near-surface sound levels. A weak surface sound channel is present during some months of the year in the GOM, with variations in the gradient and depth of the surface channel based on the month and zone (Zeddies et al. 2015). Acoustic tags placed on sperm whales (*Physeter macrocephalus*) in the GOM, that were part of controlled exposure experiments (CEEs), received peak pressures and sound exposure levels (SELs) that did not necessarily decrease monotonically as the distance between the whale and the seismic array increased (DeRuiter et al. 2013). The authors identified that selective high-frequency content (>500 Hz) was trapped near the surface when a surface duct occurred.

- As noted by Snyder (2007), energy from distant ships located in shallow water (e.g., shelf regions) may be able to travel long distances with little attenuation if the energy is trapped in the deep sound channel (or the deep ocean region where speed of sound decreases to a minimum value based on depth and then speed of sound increases due to pressure). The amount of noise received will depend on a variety of factors, including the slope of the shelf, the bottom properties of the slope, and the near-surface characteristics of the shelf waters.
- Noise enhancement can occur in frontal regions, such as across the Loop Current (refer to Urick 1984). The SST is warmer to the north of the Loop Current and colder to the south, which causes the surface sound speed to be higher to the north.
- Variations in oceanographic features may lead to changes in travel time and propagation paths for sounds produced underwater (e.g., Mellberg et al. 1990, 1991). For example, Rankin (1999) reported that preliminary studies of changes in the sound speed across the hydrographic features present in the GOMreport, "Cetaceans, sea turtles and seabirds in the Northern Gulf of Mexico: distribution, abundance and habitat associations" (GulfCet) II, (Davis et al. 2000) study area suggest that warm core rings may essentially offer a "shadowing effect" for sound created outside of the feature. In cold core rings, animals at depth and in surface waters may be exposed to increased levels of sound, while animals in a warm core ring may realize a lowered overall intensity level.

There are a number of significant features and important regions in the GOM. For instance, De Soto Canyon lies on the relatively flat continental slope. This canyon starts in approximately 450 meters (1,476 feet) of water and ends in approximately 950 meters (3,117 feet); it is a transition area where the sediments of the Mississippi River Delta meet the calcareous deposits of the easternmost GOM. De Soto Canyon is an area with a significant amount of hardbottom area. As relevant to this report, the area has been identified as important to marine mammals. National Oceanic and Atmospheric Administration (NOAA)'s Cetaceans and Sound Mapping (CetSound[2]) working group was formed to evaluate the impacts of anthropogenic noise on cetacean species and to develop geospatial tools to understand the long-term human activities that contribute to underwater noise throughout US waters (NOAA n.d.). Biologically Important Areas (BIAs) have been developed through this working group; CetSound identified one BIA that directly overlaps with the study area. The BIA identified for Bryde's whales (*Balaenoptera edeni*) has an area of 23,559 square kilometers (9,096 square miles) (LaBrecque et al. 2015) and extends along the northern reaches of the West Florida Escarpment. The Bryde's whale BIA begins near the De Soto Canyon area offshore from Pensacola, Florida, in the 100-meter (328-foot) depth range, and it extends into the 400-meter (1,312-foot) depth to offshore areas of Tampa, Florida. The area supports a small resident population of Bryde's whales (Rosel et al. 2016), that was listed in May 2019 as endangered under the Endangered Species Act (84 Federal Register 15446-15488).

Mississippi Canyon is another feature that is well-studied and known in the GOM. The Mississippi Canyon begins at the 200-meter (656-foot) isobaths and is located at the tip of the Mississippi Fan. This location has been a productive area for oil and gas exploration.

[2] NOAA's CetSound: http://cetsound.noaa.gov/cetsound

Flower Garden Banks is located offshore of Texas and Louisiana. Designated to protect the unique coral reef system that occurs here, Flower Garden Banks includes East Flower Garden Bank, West Flower Garden Bank, and Stetson Bank. The area includes salt domes. The area is the only known site that supports species of *Acropora* in the GOM.

2.1.2 Study Area Acoustic Zones

Recently, the Northern GOM was partitioned into seven acoustic zones (**Figure 2**) for the purposes of preparing "take" estimates for the annual marine mammal acoustic exposure caused by introduction of underwater noise from geological and geophysical exploration activity in the GOM for years 2016 to 2025 (see BOEM 2016a). The selected zone boundaries, patterned to conform to BOEM's planning areas where possible, considered geospatial dependence of acoustic fields (i.e., sound propagation conditions as affected by physical properties of the project area) and marine mammal species distribution to create regions of optimized uniformity in both acoustic environment and animal density. This resulted in three shelf zones, 1–3, (25 to 200 meters [82 to 656 feet]); three slope zones, 4–6, (200 to 2,000 meters [656 to 6,562 feet]); and 1 deep zone, 7, (> 2,000 meters [>6,562 feet]).

Zeddies et al. (2015) noted that the size and shape of acoustic footprints from exploration surveys in the GOM are influenced by many parameters, with the strongest being bottom depth and seabed slope. Bottom depth influences marine mammal species distribution in the GOM in that there are distinctions from Shelf to Slope and from Slope to Deep. Maps in Appendix A of Zeddies et al. (2015) depict marine mammal distribution information from the Marine Geospatial Ecology Laboratory (Duke University) model (Roberts et al. 2016) and the subdivision depth boundary contours.

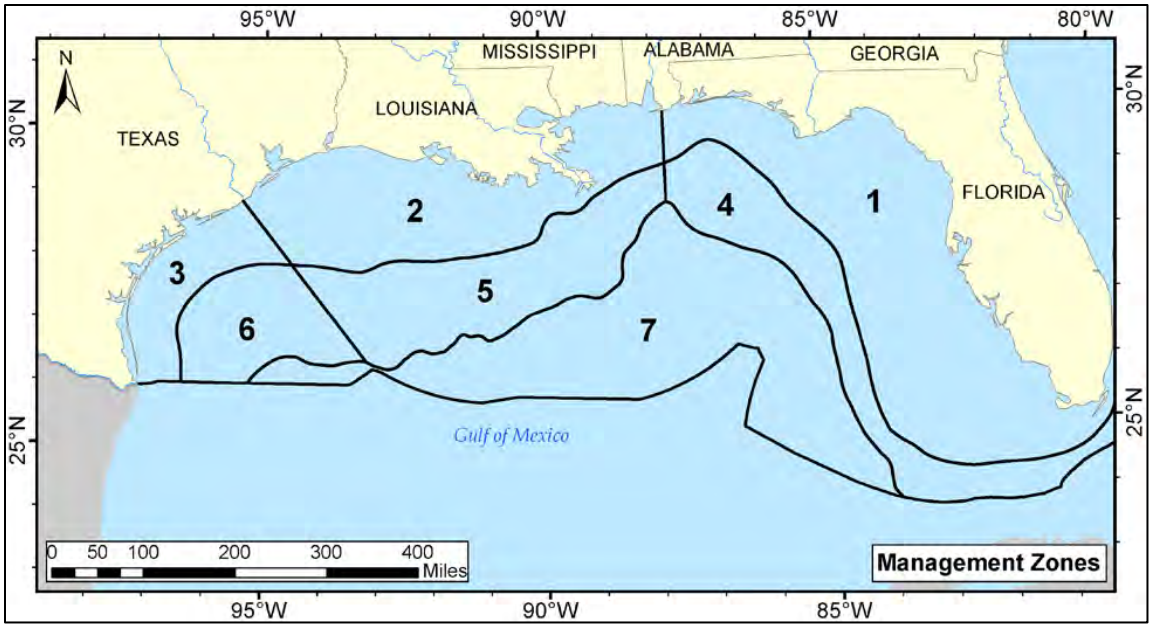

Source: BOEM (2016a)

Figure 2. Seven acoustic regions and representative model sites (zones) in the Gulf of Mexico.

2.2 Literature and Database Search Methods

The authors collected data through online databases and literature and the World Wide Web to gather information characterizing PAM projects in the GOM. The search focused on gathering a variety of literature types on biological and physical ambient noise levels in the GOM, on PAM projects focused upon marine mammals in the GOM, and on anthropogenic sound sources in the region. The authors focused on collecting information from the last 15 years of studies.

The following commercial databases, search tools, and email list servers were used in the search for data on PAM projects in the GOM: the Acoustical Society of America's meeting abstracts database, BOEM's Environmental Studies Program Information System, DataCite, Defense Technical Information Center, Google Scholar, MARMAM (Marine Mammals Research and Conservation Discussion) email list, and NOAA Central Library. Authors of this report also accessed private electronic libraries of HDR, Inc. and Azura, Limited Liability Company (LLC) staff members. Key search terms and phrases were used to conduct methodical queries of databases and the World Wide Web. The search included terms in all fields (title, abstract, etc.) referencing noise and/or sound, research method, marine mammal species of interest, specific BOEM planning areas and GOM features of interest, and/or specific researchers/institutions, funding sources, and monitoring programs.

This collaboration ensured a more complete list of terms was developed to capture all data and literature available on GOM PAM projects and sound sources. Examples of simple terms and phrases used in the search include the following:

"acoustic," "ambient noise/sound," "anthropogenic noise/sound," "biological sound sources," "detection," "passive acoustic monitoring," "Central Planning Area," Eastern Planning Area," "Western Planning Area," "Deepwater Horizon," "beaked whales," "Bryde's whales," "cetaceans," "dolphins," "marine mammals," "Risso's dolphins," "sperm whales," and "whales."

Authors of this report searched for information from a number of researchers and funders, including those individuals comprising the "Center for the Integrated Modeling and Analysis of the Gulf Ecosystem (C-IMAGE) institutions," "CetSound," "GOM Research Initiative," "Littoral Acoustic Demonstration Center –Gulf Ecological Monitoring and Modeling (LADC GEMM)," "Natural Resource Damage Assessment partners," and "Scripps Institution of Oceanography."

This list merely is meant to provide examples of search terms and key words. Appendix 1 contains a comprehensive list of keywords.

Studies generally pertained specifically to PAM studies in the GOM. Some references on research methods and PAM studies that were consulted occurred outside the region because similar studies may be lacking for the GOM, but may be useful either to characterize PAM work in general and/or to provide suggestions on the future BOEM plan for PAM in the GOM. The literature search focused on published, peer-reviewed studies written in English and indexed in scientific databases. Relevant government and industry technical reports, websites, presentations, and conference proceedings were also reviewed. Individuals involved in PAM projects were contacted when necessary and requests were made for particular references and recent publications.

Online shared databases are becoming more common and more advanced with improvements in web applications and online storage capacities. However, the integration of PAM data into existing databases is challenging due to the large volume of data storage required for long-term, high-frequency recordings. Additional challenges include the extensive data processing required for raw PAM data, the metadata standards required to document information about PAM data collection, and the difficulties in determining the meaning of a PAM record compared to a visual sighting record, for example (Fujioka et al. 2014). Despite these challenges, several online databases made successful attempts to integrate PAM data, so that researchers can store, manage, and disseminate their data to the public. During the literature search, the authors conducted a concurrent search of data online and examined the availability of PAM data in large, publicly accessible databases.

3. Current and Past Passive Acoustic Monitoring (PAM) Projects in the Gulf of Mexico and Related Research Approaches

3.1 Basic Underwater Acoustic Terminology and Metrics

A variety of metrics are used to describe sounds, and these different metrics are not directly comparable. The most common term used to define underwater sound is sound pressure, which in underwater acoustics is expressed as a basic unit in Pascals. This measurement is easily measured with a hydrophone and expresses the pressure, velocity, amplitude and direction of particle movement when the sound wave propagates away from the source. The most common unit used to express sound pressure is the microPascal (μPa).

The frequency of sound is the number of waves that pass a given point per second, which is measured in hertz (Hz). Frequency is often expressed as low (less than 1 kilohertz [kHz]), medium (1 kHz to 10 kHz), and high (greater than 10 kHz).

Sounds are generally impulsive or non-impulsive. Impulsive sounds include those sounds related to the use of explosives, seismic airguns, and pile-driving strikes. Non-impulsive sounds or pure tone generally include examples such as sonar pings, vessel noise, and drilling noise.

Sound pressure (referenced as 1 μPa) is often used to characterize continuous sounds in term of risk of damage to marine animals, such as fish, turtles, and mammals. The root-mean-square (rms) sound pressure and peak sound pressure are the most commonly used sound pressure level (SPL) metrics (Popper et al. 2014). Peak sound pressure is often used to characterize impulsive sounds and is measured as the maximum absolute value of an instantaneous sound pressure during a specific time period. The sound exposure level (SEL) metric is an index of the total energy in a sound and is usually expressed in dB re 1 $\mu Pa^2 \cdot s$. This metric can be used to assess risk from exposure to multiple sound sources; therefore, it is also an index for accumulated sound energy (Popper et al. 2014).

To assess the exposure of marine mammals to anthropogenic sounds, the National Oceanic and Atmospheric Administration's (NOAA's) National Marine Fisheries Service (NMFS) recommends specific metrics for establishing acoustic thresholds and predicting impacts of sound sources on marine mammal hearing (NMFS 2016; NMFS 2018). NMFS includes both the Cumulative Sound Exposure Level (SEL_{cum}) and Peak Sound Pressure Level (PK) metrics in their recent technical guidance recommendations for determining permanent threshold shift (PTS) onset acoustic thresholds. The SEL_{cum} metric is typically normalized to a single sound exposure of one second and takes into account both received level and duration of exposure. This metric is applied to a single source to estimate impacts of exposure to an animal but is not considered appropriate for assessing exposures resulting from multiple activities/sources occurring within the same area or over the same time period (NMFS 2016).

In addition, the SEL_{cum} metric is not appropriate for assessing effects of impulsive sounds (e.g., seismic airguns, impact pile drivers) of short duration and high amplitude which can cause greater risk to the inner ear compared to non-impulsive sounds (e.g., tactical sonar, vibratory pile drivers). Therefore, NMFS recommends the use of the PK metric for impulsive sounds with PK thresholds considered unweighted and/or flat-weighted within the frequency band of a hearing group. Because NMFS considers dual metric acoustic thresholds for impulsive sounds, the onset of PTS is assumed to occur when either the SEL_{cum} or PK metric is exceeded (NMFS 2016). See Popper et al. (2014) for more information on frequency weighting and additional metrics.

3.2 Field Methods to Measure and Assess Ambient and Anthropogenic Underwater Noise Levels in the Gulf of Mexico

3.2.1 Autonomous Acoustic Instruments

PAM of ambient noise in the GOM has been ongoing since 1996, when the first generation of Naval Oceanographic Office Environmental Acoustic Recording System (EARS) buoys was deployed (Snyder 2007). In 2001, the Littoral Acoustic Demonstration Center (LADC), which currently operates as the Littoral Acoustic Demonstration Center–Gulf Ecological Monitoring and Modeling (LADC-GEMM) consortium, was formed to make environmental measurements, particularly on ambient noise and marine mammals, using these EARS buoys (Ioup et al. 2016).

This consortium of scientists from universities and the US Navy has included representatives from the University of New Orleans, the University of Southern Mississippi, and the Naval Research Laboratory-Stennis Space Center; and the University of Louisiana at Lafayette, the Applied Research Laboratories at the University of Texas at Austin, and Oregon State University (Ioup et al. 2016). The consortium also collaborates with businesses such as Proteus Technologies, Limited Liability Company (LLC); R2Sonic, LLC; ASV; and Seiche Measurements Limited (Sidorovskaia and Li 2017). The LADC studies and additional monitoring and recording of ambient and anthropogenic noise in the GOM are summarized below.

3.2.1.1 Environmental Acoustic Recording System (EARS): Littoral Acoustic Demonstration Center (LADC) ambient noise studies in Mississippi Valley-Canyon region, 2001–2017

The LADC used EARS buoys to measure ambient noise and marine mammal sounds in the GOM in 2001, 2002, 2007, 2010, and 2015. They also used EARS to characterize seismic airgun array sounds in 2003 and 2007 in the Western GOM. Brief descriptions of these studies are provided below. EARS buoys were specifically developed for long-term recordings of ambient noise. The current Generation 2 EARS buoys can record one channel to 100 kHz or 4 channels to 25 kHz and are capable of sampling at rates up to 200 kHz (Ioup et al. 2016). The deployment design usually differs from other studies described here and allows receiving hydrophones to be placed in the water column at the pre-defined depths relevant to survey purporses. Each mooring consists of flotations, the EARS buoys, dual acoustic releases, and an anchor (**Figure 3**).

In 2001 (LADC 01), the LADC deployed three bottom-mounted EARS buoys in the Northern GOM in water depths of 600, 800, and 1,000 meters (1,969, 2,625, and 3,281 feet) along the continental slope (Newcomb et al. 2002). The hydrophones were placed 50 meters (164 feet) above the seafloor (Ioup et al. 2016). The EARS sampled at a rate of approximately 12 kHz and was capable of capturing sperm whale vocalizations (Newcomb et al. 2002; Paulos 2007). The 36 days of the deployment period, which was 18 July and 29 August 2001 overlapped with the Sperm Whale Acoustic Monitoring Program (SWAMP) shipboard surveys.

In 2002 LADC returned to the 2001 deployment area and re-deployed three EARS buoys in the Northern GOM in water depths ranging from 645 to 1,034 meters (2,116 to 3,392 feet) between 28 August and 23 October 2002 (Ioup et al. 2009, Newcomb et al. 2007). Buoys were moored 50 meters (164 feet) above the seafloor (Ioup et al. 2016). The sampling rate was approximately 12 kHz (Newcomb et al. 2007). This deployment overlapped with the second leg of sperm whale seismic studies (SWSS) that took place between 19 August and 15 September 2002, referred to as the “DTAG experiment” after the digital-recording acoustic tags (DTAGs) were used to obtain data on the movements and physiology of sperm whales.

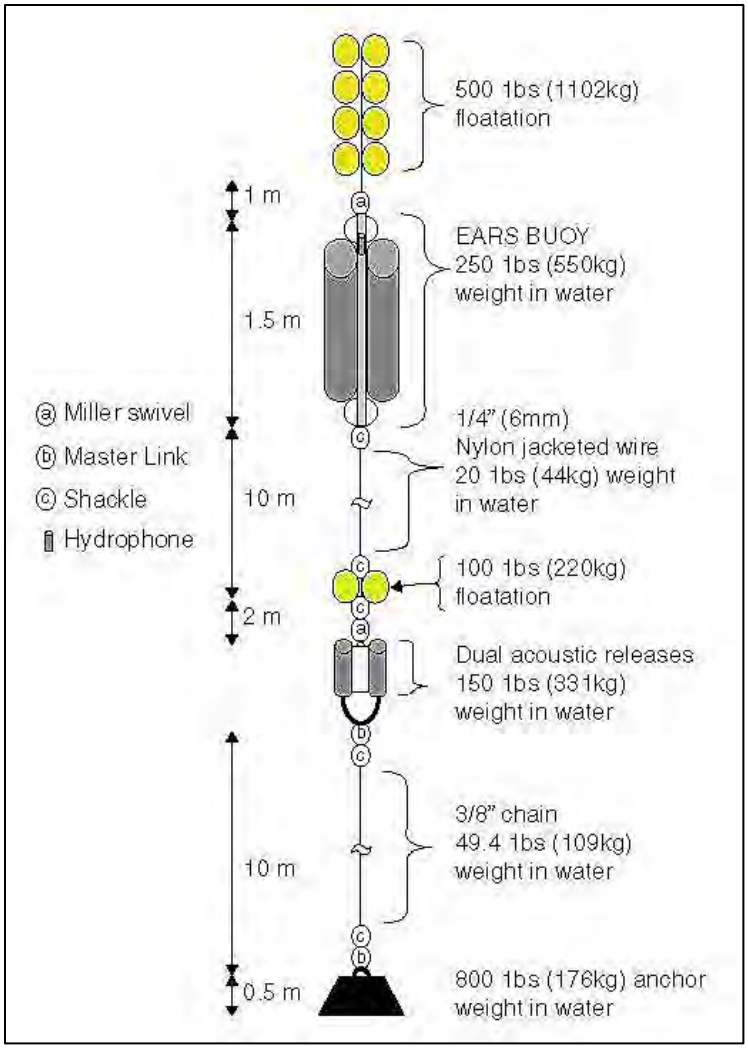

Source: Ioup et al. (2016).

Figure 3. Schematic of components of an environmental acoustic recording system (EARS) mooring.

The goal of these multiple deployments has been to quantify short-term and long-term changes in broadband baseline noise levels in the Mississippi Canyon region in order to direct future mitigation measures to decrease potential impacts of anthropogenic acoustic pollution (Sidorovskaia and Li 2017) and study the impacts of oil spills on deep-diving marine mammals using PAM methods. In addition to bottom-mounted EARS buoys, the 2015 and 2017 (to be conducted) acoustic data were collected using autonomous surface vehicles (ASVs) with towed hydrophone arrays and gliders. The LADC deployed the first set of EARS (LADC 07) between July 6 and 16, 2007 (active recording period was July 6 through 14), in deep waters (approximately 1,500 meters [4,921 feet]) (Ackleh et al. 2012; Sidorovskaia and Li 2017). These two sites were only 17 and 37 kilometers (9 and 20 nautical miles) from what would become, in April 2010, the *Deepwater Horizon* oil spill site.

The hydrophones of the EARS were positioned approximately 500 meters (1,640 feet) above the seafloor to target feeding depth of beaked whales and recorded continuously for 12 days at a sampling rate of 192 kHz (Ackleh et al. 2012; Sidorovskaia and Li 2017). The LADC 2007 dataset also provided first acoustic recordings of the GOM beaked whales. After the spill, the LADC deployed the second set of EARS (LADC 10) at the same sites, and they recorded between 10 and 24 September 2010. The third set of EARS were also deployed at the same sites and recorded between 26 June and 22 October 2015. LADC-GEMM is scheduled to operate three platforms in the region during summer-fall 2017.

3.2.1.2 High-frequency acoustic recording package (HARP): ambient noise in the Gulf of Mexico, 2010–2013

To assess the ambient noise in the GOM during and after the *Deepwater Horizon* oil spill, bottom-mounted high-frequency recording packages (HARPs) were deployed in the Northern and Eastern GOM between May 2010 and October 2013 (Wiggins et al. 2016).

Similar to EARS, a HARP was developed in response to the need for an instrument capable of recording long-term, high bandwidth acoustic data by researchers from Scripps Institution of Oceanography (Wiggins and Hildebrand 2007). These acoustic recorders consist of a hydrophone, data logger, battery power supply, ballast weight, acoustic release system, and flotation and have sampling rates up to 200 kHz. HARPs can be mounted to the seafloor or attached to devices such as Wave Gliders (see **Section 3.2.2**). The hydrophone is suspended 10 meters (33 feet) from the seafloor (Hildebrand et al. 2015b, Merkens 2013) (**Figure 4**).

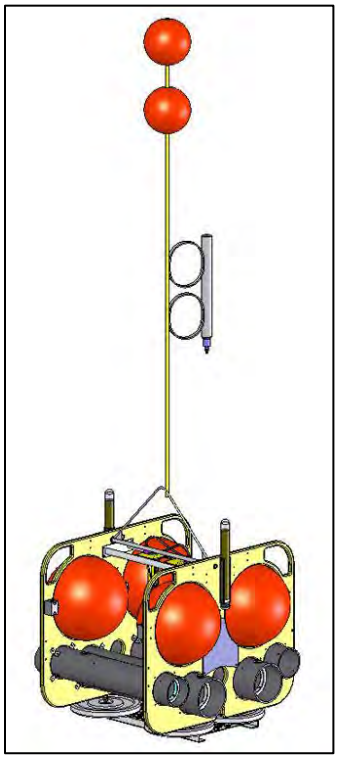

Source: Merkens (2013).

Figure 4. Schematic of a high-frequency acoustic recording package (HARP).

The maximum deployment depth is approximately 7,000 meters (22,966 feet) (Sousa-Lima et al. 2013). Bottom-mounted HARPs use EdgeTech acoustic releases which contain an electronic board and International Transducer Corporation transducer to receive acoustic commands from a support ship and then power a motor-activated release of the ballast weights. Because the HARP system is capable of recording mid- to high-frequency sound, it can record acoustic data from a variety of sources such as baleen and toothed whales, pinnipeds, sirenians, fish, vessels, seismic surveys, wind, and rain (Wiggins and Hildebrand 2007).

The GOM HARPs single deployment periods were for 2 to 9 months and sampled continuously at 200 kHz. The five deployment locations included three deep-water sites and two shallow-water sites. The deep sites ranged from 980 to 1,300 meters (3,215 to 4,265 feet) and were located in Green Canyon, Mississippi Canyon, and De Soto Canyon. The shallow sites were in Main Pass and Dry Tortugas at 90 and 260 meters (295 and 853 feet), respectively. Ambient noise recordings were calibrated and processed to produce monthly average noise spectral levels time series (Wiggins et al. 2016)[3].

3.2.1.3 Marine autonomous recording units (MARUs): anthropogenic noise across the Northeastern Gulf of Mexico shelf ecosystem, 2010–2012

Cornell conducted this post *Deepwater Horizon* oil spill study to record ambient noise in the northeastern GOM and identify major anthropogenic and abiotic noise contributors (Estabrook et al. 2016). Between western Louisiana and the West Florida shelf break, researchers deployed bottom-mounted marine autonomous recording units (MARUs) (Calupca et al. 2000) at seven sites between 39 and 461 kilometers [21 and 249 nautical miles] apart and ranging in depth from 250 to 1,370 meters (820 to 4,495 feet). Near year-round deployments allowed for acoustic coverage between July 2010 and February 2012, resulting in 79,440 hours of recordings. Most of the MARUs recorded using duty-cycles with sampling rates of 8 and 20 kilohertz (kHz); one low-frequency MARU was deployed three times and recorded continuously at sampling rates of 2 and 5 kHz (Estabrook et al. 2016).

[3] These spectral data are available for download at: https://data.gulfresearchinitiative.org/data/R4.x267.180:0009.

MARUs, also known as "pop-ups," are bottom-mounted autonomous recording buoys developed in the late 1990s by the Bioacoustics Research Program at the Cornell Laboratory of Ornithology (Calupca et al. 2000, **Figure 5**). MARUs used in this study consisted of a hydrophone, an 80-gigabyte hard drive, and a microprocessor.[4] They are battery-powered and float a few feet above the seafloor by a cable attached to an anchor. MARUs include an acoustic communication system which allows researchers to beam an acoustic signal into the water when they are ready to retrieve the unit.

The MARU hears the signal, severs its attachment to the anchor, and pops up to the surface for retrieval (Calupca et al. 2000). MARUs can be set for low or high frequency recordings are a capable of a maximum sampling rate of 64 kHz. They also can be set to operate continuously or on a set schedule (duty cycle). Maximum deployment depth is between 2,500 meters (8,202 feet) (acoustic release dependent) and 6,000 meters (19,685 feet) (on moorings) (Sousa-Lima et al. 2013).

Source: Rice et al. (2014b).

Figure 5. External and internal views of a marine autonomous recording unit (MARU).

3.2.1.4 EARS: source characterization study, 2007

From 2 September through 22 September 2007, LADC conducted this study to characterize the full three-dimensional acoustic field of the seimic airgun array in the northwestern GOM (Newcomb et al. 2009). Acoustic recording equipment for this study consisted of EARS moored array with Generation 2 four-channel EARS buoys (each channel measuring up to 25 kHz) and a total of 48 hydrophones with 16 hydrophones on the mid-water column bottom-moored array and 8 on the deeper (1,500-meter [4,921-foot]) bottom-moored array (Newcomb et al. 2009).

3.2.1.5 EARS: long-term ambient noise statistics in the Gulf of Mexico, 2004–2005

This study involved deployments of bottom-moored EARS buoys approximately 294 kilometers (159 nautical miles) south of Panama City, Florida, near a major shipping lane (Snyder 2007). The Naval Oceanographic Office deployed a total of seven buoys in water depths of 3,200 meters (10,499 feet) such that each hydrophone was positioned 265 meters (869 feet) above the sea floor. Sampling rate was 2,500 Hz with a useful bandwidth of 10 to 1,000 Hz (Snyder 2007, 2009) for ambient noise characterization.

3.2.1.6 Noise level effects on manatee habitat use, 2003–2004

To assess the affects of ambient and anthropogenic noise on West Indian manatee (*Trichechus manatus*) use of foraging habitat, PAM was conducted in two manatee habitats (grassbeds and dredged habitats) in Sarasota Bay, Florida, from April to September in 2003 and 2004 (Miksis-Olds et al. 2007b). Two different PAM methods were used. In 2003, recordings were made using a HTI-99-HF hydrophone with built-in preamplifier. The sampling rate was 200 kHz for all recordings. In 2004, ambient noise was recorded using a passive acoustic listening (PAL) buoy deployed for 3 to 4 days at each site in order to

[4] The Cornell Lab of Ornithology: http://www.listenforwhales.org/page.aspx?pid=456

provide better sampling of diurnal noise patterns. This bottom-mounted system was duty-cycled at 10-minute intervals and had a low-noise broadband hydrophone (100 Hz to 50 kHz) (Miksis-Olds et al. 2007b).

3.2.1.7 EARS: source characterization study, 2003

The LADC conducted an acoustic characterization study for a 21-element marine seismic exploration airgun array to investigate the potential impacts on marine mammals and fish and predict the exposure levels for future seismic surveys in other areas (Tashmukhambetov et al. 2008). The LADC deployed two single-channel EARS (25-kHz bandwidth) near Green Canyon during June 2003. The hydrophones were approximately 250 meters (820 feet) from the seafloor in a water depth of approximately 990 meters (3,248 feet).

3.2.1.8 PAM studies to detect, localize, and characterize marine mammals in the Gulf of Mexico

A variety of methods have been used to detect, localize, and characterize marine mammal sounds in the GOM. These methods have included the use of data collected by fixed acoustic recorders and/or systems and by mobile recorders that may be remotely controlled or towed. Mobile platforms have not been proven to be suitable for studying baseline ambient noise levels but have been successfully used to study marine mammals in the GOM. Relevant mobile platforms are described in this section (the bottom-moored platforms were introduced in **Section 3.1**) along with brief summaries of the study objectives.

3.2.2 Fixed Autonomous Acoustic Recording Devices

3.2.2.1 High-frequency acoustic recording package

3.2.2.1.1 HARP population densities, 2010–present

The Scripps Institution of Oceanography team used PAM data recorded from HARPs in the Northern and Eastern GOM to assess marine mammal populations after the *Deepwater Horizon* oil spill (Baumann-Pickering et al. 2013, Frasier 2015, Frasier et al. 2016, Hildebrand et al. 2015b). Three HARPs were deployed between 980 and 1,320 meters (3,215 and 4,331 feet) depths in Green Canyon and Mississippi Canyon in the Northern GOM and near the Dry Tortugas in the Eastern GOM (Hildebrand et al. 2015b). Two HARPs were deployed on the continental shelf in shallow waters near Main Pass and De Soto Canyon. At each site, the HARPs recorded continuously at a sampling rate of 200 kHz for two to nine months per deployment since 16 May 2010 (Hildebrand et al. 2015b). Continuous acoustic sampling is ongoing at five sites in the GOM as of the time of finalization for this report[5]. See **Section 3.2** for more information on methods used to measure and assess ambient and anthropogenic underwater noise levels. See **Section 4.2** for a summary of beaked whale and delphinid density estimates generated from these PAM data.

3.2.2.1.2 Assessing impacts of *Deepwater Horizon* on large whale species, 2010–2012

As part of the *Deepwater Horizon* oil spill assessment, 22 MARUs were deployed in the northeastern GOM between 16 June and 15 October 2010 and from 15 November 2011 to 29 February 2012 along the continental slope from Louisiana to Florida (Clark 2015, Rice et al. 2014a, Rice et al. 2015, Rice et al. 2014b). MARUs were deployed in the same area where previous visual surveys had observed Bryde's whales and sperm whales. MARUs were anchored at depths between 231 and 1,370 meters (757 and 4,494 feet), and the 22 deployment sites were 39 to 241 kilometers (21 to 130 NM) apart (Rice et al. 2014b). Most of the MARUs were set to record high frequencies; the high-frequency MARUs sampling rate was 8 or 20 kHz, while the low-frequency sampling rate was set to 2,000 Hz. To aid in density estimations of sperm and Bryde's whales, the last deployment included two arrays, each deployed in an area with high probability of sperm whale or Bryde's whale occurrence. The sperm whale array consisted of four high-frequency MARUs recording from 14 November 2011 through 13 December 2011. The

[5] Dr. John Hildebrand, Scripps Institution of Oceanography, confirmed the HARP study in GOM is ongoing.

Bryde's whale array included four low-frequency MARUs and recorded from 15 November 2011 through 29 February 2012 (Rice et al. 2014b).

3.2.2.1.3 HARP Bryde's whale study, 2010–2011

To identify Bryde's whale calls in the GOM, HARPs were used in conjunction with vessel-based recordings via a towed array and sonobuoys during the 2011 NMFS Southeast Fisheries Science Center's (SEFSC's) Atlantic Marine Assessment Program for Protected Species (AMAPPS) survey (NEFSC and SEFSC 2012, Širović et al. 2014). The sonobuoys and array were deployed from the NOAA Ship *Gordon Gunter* during this line transect survey following the 200-meter (656-foot) isobath from the southeastern edge of the GOM to Pascagoula, Mississippi between 28 July and 1 August 2011 (Širović et al. 2014).

Three HARPs provided long-term recordings in the Northern and Southeastern GOM: (1) Main Pass HARP (north-central GOM) deployed 29 June to 29 August 2010, 2 November 2010 to 19 February 2011, 20 March to 14 April 2011, and 2 May to 21 June 2011; (2) De Soto Canyon HARP (Northeastern GOM) deployed from 21 October 2010 to 17 January 2011 and 21 March to 6 July 2011; and (3) Dry Tortugas HARP (Southeastern GOM) deployed 20 July to 26 October 2010, 3 March to 15 May 2011, and 12 July to 14 November 2011. Depths ranged from 90 meters (295 feet) at Main Pass to 1,320 meters (4,331 feet) at Dry Tortugas. The sampling rate of all HARPs was 200 kHz, but the data were decimated to a 2-kHz rate for analysis (Širović et al. 2014).

3.2.2.2 Digital spectrogram recorders

Digital spectrogram (DSG) recorders are a type of autonomous acoustic recorder designed and manufactured by Loggerhead Instruments (Sarasota, Florida; **Figure 6**). Specifically referred to as the DSG-ST, these recorders are designed for long-term deployments of hundreds of days depending on the desired duty cycle and sampling rate (up to 288 kHz). They are also said to be the lowest power acoustic recorder on the market. The housings are rated from 300 meters (984 feet) depths (polyvinyl chloride) to 3,000 meters (9,843 feet) depths (aluminum).[6]

Figure 6. Image of a digital spectrogram recorder.

(Loggerhead Instruments, DSC-ST).

3.2.2.2.1 Dolphin distribution on the West Florida Shelf, 2008–2010

DSG recorders (DSG recorders, Loggerhead Instruments, Sarasota, Florida) were used in conjunction with visual surveys to determine the seasonal and spatial distribution of dolphins on the West Florida Shelf (Simard 2012, Simard et al. 2015). These recorders were deployed at 19 sites from June through September 2008. Spaced 25 kilometers (13.5 nautical miles) apart, the recorders formed a grid pattern between the shoreline and the 30-meter (98-foot) isobath.

During the second deployment from June 2009 through June 2010, the recorders were deployed at 63 stations in a grid pattern with 20-kilometer (11-nautical mile) spacing out to the 100-meter (328-foot) isobath. The sampling rate was set to 50 kHz for the first deployment and 37 kHz for the second deployment. Because this study was targeting high-frequency sounds (e.g., dolphin echolocation clicks above 130 kHz), the chosen sampling rates and duty cycles were a balance between sufficient recordings of high-frequency sounds and the digital memory constraints during long deployments (Simard et al. 2015).

[6] Loggerhead Instruments, DSG-ST Specification Sheet: https://static1.squarespace.com/static/57cf673c414fb5a80f7adf1c/t/5845d15be4fcb5c4ed91593e/1480970594125/DSG-ST-SPEC-SHEET.pdf

3.2.3 Mobile Acoustic Recording Systems

Mobile acoustic recording systems move through the water column or along the surface and may be autonomous or towed.

3.2.3.1 Gliders

Marine gliders equipped with acoustic equipment offer a low-cost approach to studying marine mammal sounds (Mellinger 2015). They can cover large areas over long periods of time and can simultaneously record environmental data, including temperature, salinity, dissolved oxygen, nutrients, and currents. They are relatively easy to deploy and can send data when at the surface. They are also capable of near-real-time detections of marine mammal species of interest when equipped with a glider-resident detection and/or classification system (Mellinger 2015).

A hybrid sea-surface and underwater autonomous vehicle, the Wave Glider uses wave energy for propulsion and solar energy via panels to continuously charge the batteries used for powering control, navigation, communication, and scientific instrumentation payloads (Manley and Willcox 2010). A Wave Glider consists of a submerged glider and a surface float which is equipped with real-time communications that allow remote control of its path. It can accommodate a variety of payloads, including an acoustic Doppler current profiler (ADCP), acoustic modems, and HARP systems (Manley and Willcox 2010).

The Seaglider™ is trademarked by Konsberg Maritime AS; the Slocum is built by Webb Research Corporation, as discussed in their respective descriptions. Each glider is described in the following respective paragraphs and there may be overlapping information since they are based on the same type of technology.

A deep-diving autonomous vehicle, the Seaglider™, currently produced by Kongsberg Maritime AS, was developed in the 1990s by Applied Physics Laboratory at University of Washington and the University of Washington's School of Oceanography with funding from the US Navy's Office of Naval Research (**Figure 7**).[7] The Seaglider™ controls its buoyancy via an external “bladder,” can control pitch and roll, and is capable of moving forward and steering without a propeller or movable rudder. When it surfaces, it connects to a remote base station via an iridium router based unique device identifier connectivity solution connection. The Seaglider™, used in the GOM, recorded at a sampling rate of 125 kHz (Sidorovskaia et al. 2015a).

Figure 7. Seaglider™ autonomous underwater vehicle.

Another type of glider that has been used in PAM studies in the GOM is the Slocum glider (manufactured by Webb Research Corp) (**Figure 8**). This class of glider includes buoyancy-driven electric autonomous underwater vehicles (AUVs), 1.8 meters (5.9 feet) in length and shaped like a winged torpedo. Slocum gliders move horizontally and vertically and have long range and duration capabilities. The Slocum glider

[7] Autonomous underwater vehicle, Seaglider: https://www.km.kongsberg.com/ks/web/nokbg0240.nsf/AllWeb/EC2FF8B58CA491A4C1257B870048C78C?OpenDocument

uses a pump that transfers mineral oil back and forth between the external and internal bladders. This changes the center of buoyancy of the instrument by which it either glides up or down.

The Slocum gliders then control the pitch and roll by shifting battery packs around. At the end of each dive the gliders come to the surface and transmit compressed science and/or engineering via Iridium calls. They can be deployed up to 18 months and can move horizontally up to 2 knots in speed. Slocum gliders can be outfitted with over 40 different types of sensors for sampling a wide variety of ocean conditions. Their operating depth range extends to 1,000 meters (3,280 feet).[8]

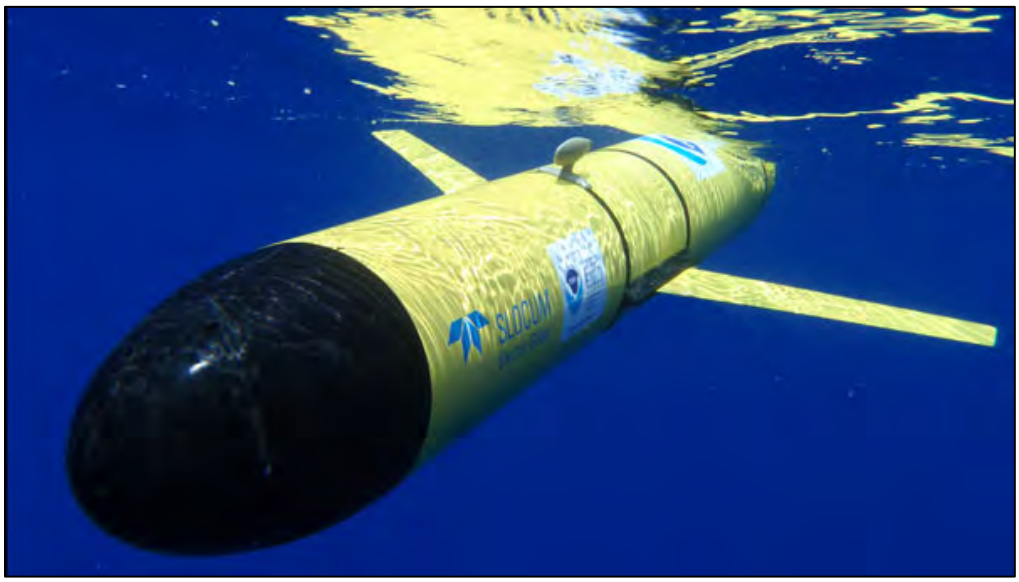

Figure 8. Slocum glider.

Image from http://www.teledynemarine.com/slocum-glider/ .

3.2.3.1.1 Littoral Acoustic Demonstration Center–Gulf Ecological Monitoring and Modeling (LADC-GEMM) glider studies in Mississippi Canyon, 2015

The LADC-GEMM (see **Section 3.2.1**) first deployed a Seaglider™ to record marine mammal sounds (Sidorovskaia et al. 2015a) and compare its performance in detecting different species with bottom-moored buoys and autonomous surface vehicles (ASVs). This study also included the simultaneous use of ASVs and EARS buoys (see **Sections 3.2.2**). The glider was programmed to move in a sawtooth pattern, diving down to 1,000 meters (3,280 feet) in depth and moving 4 kilometers per hour (~2 nautical miles per hour) horizontally.

Once deployed on 24 June 2015, it moved in a continuous clockwise triangle pattern around three waypoints (Sidorovskaia et al. 2015a). Attempts to recover the Seaglider™ on 4 August 2015 were unsuccessful; therefore, a Slocum Glider with two acoustic recording units was deployed on 12 October 2015 to collect relevant data for comparison over a 10-day period and complete the originally planned glider-portion of the study (Sidorovskaia et al. 2015b).

3.2.3.1.2 Wave Glider HARPs, 2011

In 2011, HARP electronics were installed in the surface floats of two Wave Gliders, and the hydrophones were towed behind each subsurface glider unit at approximately 8 meters (26 feet) in depth and used two sensors covering the band 10 Hz to 100 kHz (Hildebrand et al. 2013, Collins 1993).

[8] Slocum G3 Glider: http://www.teledynemarine.com/slocum-glider/

3.2.3.2 Autonomous surface vehicles and/or unoccupied underwater vehicles (with towed arrays)

ASVs (**Figure 9**) have been used to collect marine mammal PAM data throughout the GOM. ASV Global specifically designs ASVs as low impact vehicles for marine observations and data collection.[9] For example, the C-Enduro class of ASV can effectively gather data from the marine environment while also generating power via solar panels and wind turbines (**Figures 9 and 10**). They can also be outfitted with a diesel generator or fuel cell if longer missions are required. In addition to PAM, ASVs are capable of water quality monitoring, water sampling, wave monitoring, acoustic transponder tracking (fish), current profiling, meteorological monitoring, and more.[9]

Figure 9. AutoNaut® with towed array–wave propelled autonomous surface vehicle.

Source: Sidorovskaia et al. (2015a).

Figure 10. ASVs C-Worker (left) and C-Enduro (right).

[9] ASV Unmanned Marine Systems: https://www.asvglobal.com/marine-science/

With low self-noise ASVs coming to the market, they could potentially offer a low-cost solution for measuring soundscapes in real time. An ASV that could be deployed in the BOEM PAM Program for the Northern GOM is the recently developed AutoNaut® (**Figure 9**). This is a wave propelled unit and performs equally well on all headings including directly into wind and waves. The unit has zero emissions, and can roam the oceans for very long periods, transmitting data by satellite to shore. This extreme endurance coupled with a unique solution to the speed-payload-power balance for unmanned surface vessels (USVs) offers great new potential to all engaged in oceanic monitoring and surveillance.

3.3.2.1 ASV-towed arrays, LADC-GEMM PAM studies in Mississippi Canyon, 2015

As part of the LADC-GEMM consortium studies on the long-term impact of the *Deepwater Horizon* oil spill on deep-diving marine mammal populations, Autonomous Surface Vehicles, LLC provided two ASVs fitted with towed hydrophone arrays to record marine mammal sounds in the vicinity of the spill between 23 June and 2 July 2015 (Dyer et al. 2015; Sidorovskaia et al. 2015a; Ziegwied et al. 2016). The ASV C-Enduro™ is a 4.2-meter (13.8-foot) catamaran that is powered via solar panels, a wind turbine, and a diesel generator with two electric engines. It can cruise at 3 knots and be deployed up to 90 days. During this study, the C-Enduro™ towed a 55-meter (180-foot) two-element array.

The ASV C-Worker™ is 6 meter (20 feet) long, has an average speed of 4 knots, and can be deployed up to 30 days. It houses a fully redundant power propulsion and communication system and can integrate multiple offshore payloads. For this study, the C-Worker™ towed a 220-meter (722-foot), two-element array. Acoustic data were recorded as the ASVs were under autonomous power. Data were collected at a sampling rate of 500 kHz along with concurrent conductivity-temperature-depth and global positioning system data. The PAM systems were configured to detect a variety of species with vocalizations ranging from 20 to 160 kHz (Dyer et al. 2015, Ziegwied et al. 2016)[10].

3.2.3.3 PAM arrays towed from vessels

3.2.3.3.1 NMFS-SEFSC Shipboard Surveys, 2012–2016

As noted earlier, NMFS-SEFSC has conducted several recent shipboard surveys in the GOM aboard the NOAA Ship *Gordon Gunter*. These surveys include visual observations and PAM via a towed hydrophone array.

More recent PAM efforts by the NMFS SEFSC have targeted the Bryde's whale population in the Northeastern GOM. For example, in September 2015 a female Bryde's whale was tagged with an acoustic and kinematic data-logging, suction-cup tag in De Soto Canyon (Rosel et al. 2016). Also, with funding from NOAA Fisheries Office of Science and Technology Ocean Acoustics Program, in June 2016, NMFS SEFSC deployed five calibrated autonomous acoustic instruments along the 200-m isobath throughout the western GOM in predicted Bryde's whale habitat. The objectives of this study are to collect passive acoustic data for use in investigations of 1) Bryde's whale occurrence and distribution, and 2) ambient noise conditions in the western GOM. These units recorded through June 2017.

3.2.3.3.2 Airborne Mine Neutralization System Monitoring, 2011

HDR and Exploration and Production Environmental Services – RPS conducted monitoring surveys for protected species during an Airborne Mine Neutralization System live-inert explosives research, development, test, and evaluation event off the west coast of Florida (NSWC PCD 2012). Between 5 and 10 December 2011, the visual and acoustic monitoring efforts were conducted from a 50.3-meter (165-foot) research vessel within the Naval Surface Warfare Center Panama City Division (NSWC PCD) Study Area. The test area was approximately 22 kilometers (12 nautical miles) from shore in waters ranging from 20 to 40 meters (66 to 131 feet) in depth.

[10] The data are available for download at: https://data.gulfresearchinitiative.org/data/R4.x261.233:0001.

Acoustic monitoring was conducted using a towed hydrophone array built by Seiche Measurements Limited, and PAMGUARD software (Gillespie 2008) was used during data collection and to initially classify recordings. The frequency range and sampling rate were 0 to 96 kHz and 48 to 192 kHz, respectively (NSWC PCD 2012). These acoustic detection data are available on Ocean Biogeographic Information System Spatial Ecological Analysis of Megavertebrate Populations (OBIS-SEAMAP)[11] as part of the dataset "Acoustic Detections for Airborne Mine Neutralization System Passive Acoustic Monitoring in the NSWC PCD Study Area from December 2011."

3.2.3.3.3 NOAA *Pisces*: Protected Species Monitoring and Mitigation Measures during Trawling, 2011

Mid-water trawl sampling operations were conducted aboard the NOAA Ship *Pisces* during two cruises (21 June to 15 July and 7 to 29 September 2011) in the Northern GOM as part of NOAA's Natural Resource Damage Assessment following the *Deepwater Horizon* oil spill incident (Norris and Jacobsen 2015). Geo-Marine Inc. and Bio-Waves Inc. conducted visual observations and PAM during trawling operations to help researchers avoid potential capture and/or entanglement of marine mammals and sea turtles. PAM operations used a towed hydrophone array during the day and at night; the use of the array during nighttime was particularly important for data collection when visual observations were not possible.

3.2.3.3.4 Measuring Delphinid Whistle Characteristics and Source Levels on the West Florida Shelf, 2008–2009

As part of a larger study sponsored by the National Ocean Partnership Project conducted in cooperation with the University of South Florida, this study targeted bottlenose (*Tursiops truncatus*) and Atlantic spotted (*Stenella frontalis*) dolphins offshore of Sarasota, Florida (Frankel et al. 2014). A Transducers, Inc. ("squid") hydrophone array was towed from the Research Vessel (R/V) *Eugenie* during eight days in April 2008 and 11 days in April-May 2009. The main results obtained from the overall project included recordings of wild dolphins producing source level estimates of 164 and 161 dB re 1 µPa at 1 m for bottlenose and spotted dolphins. Marine Acoustics Incorporated also performed acoustic propagation predictions in order to estimate the detection range around individual bottom-mounted acoustic recorders. A total of approximately 33 hours of acoustic data were recorded during 11 days of effort in waters less than 50 meters (164 feet) in depth. The frequency response of the array system was limited to 32 kHz; the data were filtered at a sampling rate of 64 kHz (Frankel et al. 2014).

3.2.3.3.5 Low-frequency Sounds of Bottlenose Dolphins, 2003–2009

Acoustic data were recorded from bottlenose dolphins (*Tursiops truncatus*) at three sites in the Northeastern GOM: Mississippi Sound (May 2005 to June 2008); Tampa Bay, Florida (February 2006 to May 2008 and June 2008 to December 2009); and Sarasota Bay, Florida (July 2003) (Simard 2012, Simard et al. 2011). All sites were within 1 and 14 meters (3 and 46 feet) in depth. Acoustic recordings were collected continuously during boat-based visual surveys of bottlenose dolphins. A variety of acoustic recorders and hydrophones were used and were either towed or stationary. Recorder types included Fostex, Sony TCD-D8, NI-6062, M-Audio 24/96, M-Audio, TDT-RP2 A-D with sampling rates between 48 and 200 kHz (Simard 2012, Simard et al. 2011). Hydrophone types included Reson, Aquarian, and HTI-96-MIN. All recordings were analyzed for low-frequency narrow-band sounds which are thought to be correlated with dolphin socialization (Simard et al. 2011).

3.2.3.3.6 Assessing the Echolocation Pulse Rate of Bottlenose Dolphins, 2008

Visual and acoustic data on bottlenose dolphins were collected for the Dolphin Ecology Vocalizations and Oceanography Project and the Eckerd College Dolphin Project from April to September 2008 off west-central Florida (Simard et al. 2010). The survey area included Tampa Bay, Boca Ciega Bay, and Gulf waters extending 50 kilometers (27 nautical miles) offshore with bottom depths ranging from 1 to 30

[11] See "Acoustic Detections for Airborne Mine Neutralization System Passive Acoustic Monitoring in the NSWC PCD Study Area from December 2011": http://seamap.env.duke.edu/.

meters (3 to 98 feet). Two acoustic recording systems were used: (1) a 16-element towed array (Innovative Transducers, Inc., Fort Worth, Texas) with a 64-kHz sampling rate and (2) a single HTI-96-MIN omnidirectional hydrophone with a 96-kHz sampling rate (Simard et al. 2010).

3.2.3.3.7 The Sperm Whale Seismic Study (SWSS) Program, 2002–2005

Sperm whale research in the GOM continued during this three-year study to establish the baseline behavior of sperm whales in the Northern GOM, characterize sperm whale habitat use in the Northern GOM, and determine possible changes in behavior of sperm whales when subjected to man-made noise, particularly from seismic airgun arrays (Jochens et al. 2008). The overall study area covered Northern GOM offshore waters between Galveston, Texas and De Soto Canyon, at depths ranging from 800 to 1,200 meters (2,624 to 3,937 feet). Cruises were conducted during the summers of 2002, 2003, 2004, and 2005 and included passive acoustic monitoring, and some included a test of three-dimensional passive acoustic tracking. Surveys generally took place between June and early September. The acoustic tagging component of this study is discussed in **Section 3.2.3**. Acoustic surveys used towed arrays, typically stereo-towed hydrophones with 3-meter (10-foot) separation between elements. Recording systems had a fairly flat response between 0.1 and 15 kHz (Jochens et al. 2008).

3.2.3.3.8 NMFS SEFSC Shipboard Visual Surveys, 2003–2004

NMFS SEFSC conducts the majority of all marine mammal shipboard surveys in the GOM. These surveys are designed to collect data to assess marine mammal stocks occurring in US waters. Therefore, these surveys are conducted using line transect distance sampling methods (Buckland et al. 2001). In addition to visual observation data, PAM data are also recorded to provide a more complete representation of cetacean occurrence. The first shipboard offshore marine mammal surveys in the GOM were conducted aboard the NOAA Ship *Oregon II* during spring 1990 (Mullin et al. 1991; Würsig et al. 2000). Since then, NMFS SEFSC has conducted numerous marine mammal shipboard surveys in the GOM. The NMFS SEFSC surveys during 2003 and 2004 were related to the SWSS Program. From 12 June through 18 August 2003, the NOAA Ship *Gordon Gunter* cruise GU-03-02 (023) was conducted to monitor cetaceans in oceanic waters (>200 meters [656 feet]) from Brownsville, Texas, to Key West, Florida. Methods included visual and acoustic surveys.

The PAM surveys used a five-element acoustic array towed approximately 600 meters (1,969 feet) behind the ship (NMFS SEFSC 2003). A similar array was used on the NOAA Ship *Gordon Gunter* cruise GU-04-02 (027) survey from 13 April through 11 June 2004 in EEZ waters between Brownsville, Texas, and the Florida Straits (NMFS-SEFSC 2004a). During the NOAA Ship *Gordon Gunter* cruise GU-04-03 (028) survey from 22 June through 19 August 2004 from the Maryland/Delaware border into southern Florida waters, a five-element broadband array was towed 450 meters (1,476 feet) behind the ship in waters deeper than 100 meters (328 feet). Digital audio tape recordings of signals of interest were made using multi-channel digital tape recorders and were limited to a bandwidth of 10 Hz to 24 kHz (NMFS-SEFSC 2004b).

3.2.3.3.9 The Sperm Whale Acoustic Monitoring Program (SWAMP), 2000–2001

The MMS (now BOEM) funded this study to assess the behavior of sperm whales in the Northern GOM and their responses to anthropogenic noise (e.g., seismic activity) (Jochens et al. 2006; Lang 2000). Research techniques included shipboard visual surveys, photo-identification, satellite and acoustic tagging, biopsy sampling, and acoustic monitoring. The acoustic tagging component of this study is discussed in **Section 3.2.3**.

The acoustic monitoring was conducted via a towed hydrophone array deployed during shipboard surveys on the NOAA Ship *Gordon Gunter* during 28 June through 26 July 2000, 16 March to 3 April 2001, and 17 July through 22 August 2001 (Burks et al. 2001, Mullin 2001). Two arrays were used: a five-element towed array with five hydrophones spaced 2 meters (7 feet) apart along a 100-meter (328-foot) long Kevlar-reinforced cable and a passive two-element array with a 8-meter (26-foot) polyurethane tube filled

with Isopar M fluid and containing two Benthos AQ4 (mid-frequency) elements spaced 3 meters (10 feet) apart (Burks et al. 2001).

3.2.3.3.10 GulfCet II, 1996–1998

To continue the research from GulfCet I, GulfCet II shipboard and aerial surveys were conducted from the northwestern to the Northeastern GOM (Davis et al. 2000). Acoustic surveys were conducted via a towed hydrophone array in the Eastern Planning Area in late summer 1996 and mid-summer 1997 to identify and record cetacean and anthropogenic sounds. Similar to the array used in GulfCet I, the new array used in GulfCet II consisted of multiple hydrophone groups spaced along the cable. In contrast, this new array was spectrally flat (6 Hz to 18 kHz) and could be towed at faster speeds. Surveys ranged in depth from 50 to 3,000 meters (164 to 9,842 feet) (Davis et al. 2000).

3.2.3.3.11 GulfCet I, 1992–1994

Texas A&M University, operating under contract to the MMS (now BOEM) and the NMFS SEFSC, operating under an interagency cooperating agreement with MMS, conducted shipboard and aerial surveys to determine the distribution and abundance of cetaceans in the northwestern and north-central GOM (Davis and Fargion 1996). The 12 shipboard surveys, which were conducted seasonally between April 1992 and May 1994, included the use of towed hydrophone arrays to record marine mammal sounds, particularly sperm whale vocalizations. Developed by the Hubbs-Sea World Research Institute, the towed linear hydrophone array consisted of a 290-meter (951-foot) tow cable and a 235-meter (771-foot) wet section that contained 195 hydrophones in 16 groups. A combination of low-frequency hydrophones (Teledyne T-1) and high-frequency hydrophones (Benthos AQ 20) were used (Davis and Fargion 1996).

3.2.4 Tags

Data-logging tags include DTAGs that record acoustic data while being attached to the animal. Funded by the Office of Naval Research (ONR), the Woods Hole Oceanographic Institution developed the DTAG to reduce the size and increase the capabilities of acoustic recording tags in 1999 (Johnson and Tyack 2003). These tags use flash memory to record data and are encased in plastic. The maximum deployment depth is 2,000 meters (6,562 feet), and the audio sampling rate is 48 to 192 kHz.[12] The tags can record sounds, depth, temperature, and orientation (pitch, roll, heading) and can be attached to the animal via a long pole, gun, or crossbow (Johnson and Tyack 2003).

3.2.4.1 The Coastal Alabama Acoustic Monitoring Program, 2009–2017

Additional tagging efforts in the GOM are related to the Coastal Alabama Acoustic Monitoring Program (CAAMP) conducted by Dr. Sean Powers and the University of South Alabama Marine Sciences Department.[13] Although it does not target marine mammals, this program includes an array of 40 hydrophone stations deployed around Mobile Bay and Mississippi Sound to cover the entry and exit points of fish. Sonic devices (tags) are attached to several inshore fish so that the hydrophones will detect the locations of the fish to determine where and how much they travel during a year. Tagged fish include sharks, tarpon (*Megalops* sp.), sturgeon, red drum (redfish), and spotted seatrout (speckled trout; *Cynoscion nebulosus*).

3.2.4.2 The Sperm Whale Seismic Study (SWSS) Program, 2002–2003

As mentioned in **Section 3.2.2**, this three-year study was conducted to establish the baseline behavior of sperm whales in the Northern GOM, characterize sperm whale habitat use in the Northern GOM, and determine possible changes in behavior of sperm whales when subjected to man-made noise, particularly

[12] DTAG: A Digital Acoustic Recording Tag: http://www.whoi.edu/page.do?pid=39337

[13] CAAMP Studies Redfish, Tarpon Movement: http://www.outdooralabama.com/caamp-studies-redfish-tarpon-movement

from seismic airgun arrays (Jochens et al. 2008). The tagging component of this study was part of a controlled experiment to test the responses of sperm whales to exposure to seismic airguns. Two types of DTAGs were used in the study. During 2002, DTAG1 tags were used and recorded audio at a sampling rate of 32 kHz. During 2003, both DTAG1 and DTAG2 tags were used, but only DTAG2 tags were analyzed. These tags recorded audio at a sampling rate of 96 kHz (DeRuiter et al. 2006).

3.2.4.3 The Sperm Whale Acoustic Monitoring Program (SWAMP), 2000–2001

As mentioned in **Section 3.2.2**, this MMS-funded study assessed the behavior of sperm whales in the Northern GOM and their responses to anthropogenic noise (e.g., seismic activity) (Jochens et al. 2006, Lang 2000). As part of this pilot study, suction cup multi-sensor DTAGs were successfully deployed on sperm whales 13 times in 2001. The tags were attached via a 12-meter (40-foot) carbon fiber pole. A total of 26 hours of DTAG data was recorded during NOAA Ship *Gordon Gunter* cruise GU-01-04 (13) from 17 July through 22 August 2001 (Mullin 2001). Additional DTAGs were successfully deployed on sperm whales during other surveys under this program (Thode et al. 2002).

3.2.5 Sonobuoys

Sonobuoys use a transducer and a communication radio transmitter to record and transmit underwater sounds. They can be dropped into the ocean from either an aircraft or a ship to record underwater sounds. There are three types of sonobuoys: (1) passive sonobuoys use a hydrophone to listen for sounds, (2) active sonobuoys use a transducer to send an acoustic signal and then listen for the return echo, and (3) special purpose buoys provide additional information about the environment such as water temperature and wave height.[14] The exact location of a target can be determined by deploying a pattern of sonobuoys.

One type of sonobuoy that has been used in marine mammal studies is the Directional Frequency Analysis and Recording (DIFAR) sonobuoy, which is a passive sonobuoy used by the US Navy to detect underwater submarines. DIFAR generally consists of a directional hydrophone that gives bearings to where the acoustic signal is originated; it can detect acoustic energy from 5 to 2,400 Hz, and can operate for up to 8 hours at depths of up to 305 meters (1,000 feet) (Holler 2014).

3.2.5.1 Bryde's whale sonobuoys, 2011

NMFS shipboard line transect surveys often include the use of sonobuoys to record marine mammal sounds in conjunction with a towed hydrophone array and visual observers. As mentioned previously in **Section 3.2.1**, the 2011 AMAPPS survey deployed sonobuoys as the ship followed the 200-meter (656-foot) isobath from the southeastern edge of the GOM to Pascagoula, Mississippi (NEFSC and SEFSC 2012, Širović et al. 2014). Between 30 July and 1 August 2011, NMFS deployed 13 DIFAR AN/SSQ-53E sonobuoys in arrays to confirm the characteristics of Bryde's whale sounds (Hildebrand 2017, Širović et al. 2014). These sonobuoys consisted of a directional hydrophone with a bandwidth from 10 to 2,400 Hz, and the signals were transmitted to the ship-mounted antenna via a single radio carrier frequency. The sonobuoys automatically scuttled 8 hours after deployment (Širović et al. 2014).[15]

To determine the location of the whale calls, bearings to the same call were compiled from concurrent recordings from multiple sonobuoys in the array, and then the exact location of the call was estimated from the bearing crossings (Širović et al. 2014). During the sightings of three Bryde's whale groups on 31 July 2011 in the Northeastern GOM in De Soto Canyon, three DIFAR sonobuoys were deployed in an array at 0, 11, and 42 minutes after the initial sighting.

[14] Discovery of Sound in the Sea: http://www.dosits.org/galleries/technology/locatingobjectsbylisteningtotheirsounds/directionalfrequencyandrangingdifarsonobuoy/

[15] Sonobuoy deployment locations are available for download at: https://data.gulfresearchinitiative.org/data/R1.x135.120:0005#

3.2.5.2 The Department of the Navy *Empress II* Sonobuoys, 1991–1992

The Mississippi State University Research Center flew aerial surveys approximately 50 kilometers (27 nautical miles) south of Mobile, Alabama from November 1991 to June 1992 to determine the abundance of sea turtles and marine mammals in an area where the Department of the Navy was conducting *Empress II* ship shock trials (Esher et al. 1992). During these surveys, sonobuoys were deployed from the door of the survey aircraft to test the feasibility of using passive acoustics to locate and identify whales and dolphins in shallow coastal waters. A total of 32 AN/SSQ-41B sonobuoys were deployed between 11 November 1991 and 10 June 1992 and consisted of a subsurface hydrophone and preamplifier, a cable assembly, seawater battery pack, and surface electronics such as a VHF transmitter and antenna. The acoustic frequency range was 10 Hz to 10 kHz (Esher et al. 1992).

3.3 Analysis Methods for PAM Data

3.3.1 Using PAM Data for Estimation of Marine Mammal Densities

Density and population estimation is one of the primary techniques used for effective wildlife management and conservation. Reliable estimates of density and abundance are needed to monitor animal movements and population trends and to plan for mitigation of potential impacts from anthropogenic activities. The most common methods of generating density estimates of marine mammal species and populations use visual observation data and include some form of capture-recapture on marked or uniquely identifiable individuals or the use of line transect survey data collected following strict distance sampling protocols (Buckland 2001, Thomas et al. 2010). For example, this method includes shipboard line transect surveys during which the ship travels along randomly generated tracklines, and visual observers record the perpendicular distance between the ship and any marine mammals detected. It is assumed that all animals on the trackline are detected and that the probability of detection decreases with increasing distance from the trackline. The distribution of perpendicular distances between the animals and the trackline is used to estimate the proportion of animals detected within our observer strip which enables a researcher to estimate animal density and abundance (Thomas et al. 2010).

Animal density estimation using PAM data is new and may be the preferred method for species that are often not sighted at sea during shipboard or aerial surveys because they do not surface often and for regions where poor weather conditions limit regular visual survey coverage (Marques et al. 2012). The development of these new methods was initiated through the Density Estimation for Cetaceans from Acoustic Fixed Sensors project funded by the Exploration and Production Sound and Marine Life Joint Industry Program and NOAA under the National Oceanographic Partnership Program. Led by Dr. Len Thomas (St. Andrews University), the Density Estimation for Cetaceans from Acoustic Fixed Sensors team developed and promoted methods for estimating the density of cetacean species from fixed passive acoustic devices during this three-year project (2007–2010). Their methods are applicable to PAM data recorded from arrays of permanent, bottom-mounted sensors and single bottom-mounted or floating sensors (Küsel et al. 2015b, Marques et al. 2013, Thomas et al. 2009).

There are currently several approaches to estimate density from PAM data collected on fixed sensors (Marques et al. 2013). If distances between the detected animal(s) and the acoustic recorder can be obtained from single sensors or clusters of closely spaced sensors, each operating as a single unit, then census and/or strip transect and distance sampling methods are possible.

The census and/or strip transect method requires that all animals within a given area are detected, and the animals outside of that area can be excluded (Marques et al. 2013). For example, Moretti et al. (2010) used this method by counting dives of echolocating beaked whales that dive synchronously. They isolated dive starts using a bottom-mounted hydrophone array and assumed that all dive starts of the target beaked whale species within the study area were detected.

The distance sampling method requires that detected animal distances can be obtained and that the conventional distance sampling assumptions are met so that point transect using detections of animals and/or groups of animals or cue counting can be used (Marques et al. 2013). For example, Marques et al. (2009) used the cue counting method to estimate the density of a population of Blainville's beaked whales. This technique generally involves counting the number of detected acoustic cues for a known period of time and then scaling up this number to estimate animal density. They converted the number of detected cues into density by accounting for the probability of detecting cues, the estimated rate at which animals produce cues, and the proportion of false positive detections (Marques et al. 2011).

Another way to capture detection probability is through spatially explicit capture recapture. This method involves estimating acoustic counts using a subset of data to calculate probability of detection and then combine this probabilty to estimate density and variance (Martin et al. 2013). Similarly, Kyhn et al. (2012) used acoustic data loggers concurrently set up with visual tracking of harbor porpoises. Detection functions were estimated based on probability of detection from a mark-recapture approach using the acoustic data and point transect distance sampling. Density estimates for the Timing Porpoise Detector (T-POD) data were similar to visual densities (Kyhn et al. 2012). Marques et al. (2009) also used passive acoustic monitoring data to develop density estimates for marine mammals. The researchers specifically developed densities for Blainville's beaked whales after accounting for detection function, cue rate, and false positive detections in the US Navy's Atlantic Undersea Test and Evaluation Center range in the Bahamas (Marques et al. 2009).

Both the census and/or strip transect and distance sampling methods are based on estimates of the probability of detecting acoustic mammal sounds (e.g., calls) as functions of distance and require the use of receivers capable of localizing calls or tagging data (Küsel et al. 2011). When distance estimation is not possible, simulations can be used to estimate detection probabilities (Frasier et al. 2016). However, the assumptions used to implement the simulation models are not always met or the potential violation of the assumptions have unforeseen consequences. Therefore, methods based on empirical measurements instead of model-based methods are still preferred when estimating the detection function (Marques et al. 2013).

3.3.2 Habitat Modeling

Estimates of marine mammal density and distribution may be improved through the use of habitat models that can predict spatial distribution of density and/or abundance in relation to environmental variables. For example, density surface modeling is a type of habitat modeling method in which generalized additive models (GAMs) (Wood 2006) are used to estimate the spatial distribution of abundance and/or density or counts (the response variable) as a function of several geographical, physical, and environmental covariates (explanatory variables). Other methods such as species distribution models and density surface models may also be appropriate modeling methods.

For the GAMs example mentioned previously, after fitting GAMs to the survey data, the resulting density surface model (the chosen model) is applied to a prediction grid superimposed upon the area of interest so that animal abundance and/or density can be predicted for any portion of the area and related to specific covariates (Thomas et al. 2010). The covariates may include a variety of static and dynamic variables such as longitude, latitude, water depth, distance from shore, bathymetry, sea surface temperature (SST), and surface chlorophyll concentration. These habitat variables may be derived from in situ oceanographic data, remotely sensed data, or satellite-derived data (Redfern et al. 2006).

Habitat models may be built at finer spatial and temporal resolutions when using in situ data. However, these data are not always available at the required spatial and temporal scales need for a model, and the collection and processing of these data are labor intensive and costly. The ideal habitat models for cetaceans would be based on accurate quantitative measurements of data that characterize habitat variability, prey populations, and predator populations at a wide range of temporal and spatial scales and an understanding of the interactions of these variables and animal density (Redfern et al. 2006).

Roberts et al. (2016) used line transect survey data to develop habitat-based cetacean density models in the GOM for marine mammals based on species where possible. The researchers created models for seventeen species and for two guilds (or family groups), which included beaked whales and *Kogia*. Density was modeled in a two-step process by first determining detectability of each species and guild using data from line transect surveys and by applying this detection function to the survey transects to estimate abundance. Then, Roberts et al. (2016) used GAMs to model the abundance considering the environmental factors that are believed to correspond with distribution of cetaceans in the GOM. These factors included physiographic (i.e., depth, slope, distance to shore, canyons, seamounts, and isobaths), physical oceanographic (i.e., sea surface temperature [SST], distance to SST fronts, wind speed, total and eddy kinetic energies, and distance to geostrophic eddies), and biological (chlorophyll concentration, primary production, potential biomass and production of zooplankton and epipelagic micronekton) covariates (Roberts et al. 2016).

Most cetacean habitat models developed to date have relied on the use of line transect data from shipboard and aerial surveys (e.g., Becker et al. 2014, Forney et al. 2012). However, due to advances in statistical methods and technology, other data types, such as tagging and PAM data, are also now being used for habitat modeling (Redfern et al. 2006). PAM data may improve model accuracy and precision and provide a better representation of cetacean presence due to the increased temporal coverage that PAM can provide when compared to visual survey data (Soldevilla et al. 2011). Of course, using PAM data for cetacean habitat models does have limitations, including the ability to detect and localize mammal calls. As with density estimation, several factors such as sound propagation and acoustic masking can hinder detections. Sound propagation conditions can vary across sites and seasons and lead to variations in detection probability. Weather (wind, waves, rain), anthropogenic activities (sonar, vessels, seismic), and biologic (other marine animals) sounds can mask the marine mammal sounds that are the target of a study, thus minimizing the detections. Therefore, it may be important to develop methods for incorporating ambient noise metrics into future habitat models (Soldevilla et al. 2011). Before performing the habitat modeling, absolute abundance must be computed and this abundance must take into account sources of false negative and positive numbers. Additional advantages and limitations of using PAM for cetacean habitat modeling are discussed in Soldevilla et al. (2011) and Širović and Hildebrand (2015).

3.3.3 Acoustic Propagation Modeling

Underwater acoustic propagation refers to the movement of acoustic waves from one point to another (Lurton 2010). Propagation decreases the amplitude of the acoustic signal via geometrical spreading and absorption, which is based on the chemical propoerties of the seawater. As acoustic waves propagate, they lose their intensity. This propagation loss (also known as transmission loss, TL) is a key factor in PAM studies because it affects the ability of receiver to detect and classify sound source. Therefore, propogation loss must be evaluated when determining the performance of underwater acoustic systems (Lurton 2010).

To estimate TL from absorption and attenuation, acoustic propagation models[16] can be used in addition to direct field measurements. A variety of input parameters are often included in these models to reliably estimate TL. For example, inputs may include source frequency band and configuration, sound speed profile, bathymetry, bottom properties, and source and receiver geometry (Küsel et al. 2009). Acoustic propagation modeling has been applied to military operations, marine seismology, and physical oceanography and is more recently being used to address questions in regards to marine ecology, physics, and conservation (Tennessen and Parks 2016).

Propagation modeling is particularly important in PAM studies to assess marine mammal occurrence and ambient and anthropogenic noise affects on species and populations. For example, knowledge of acoustic propagation of seismic exploration signals is critical when predicting exposure levels and potential impacts to marine wildlife (Jochens et al. 2008). These types of anthropogenic noise propagation studies

[16] The Ocean Acoustics library contains acoustic modeling software and data: http://oalib.hlsresearch.com/

have been conducted in the GOM to assess seismic airgun pulse exposure to cetaceans. As mentioned previously, sperm whales were tagged with acoustic devices during the SWSS Program in 2002 and 2003 (DeRuiter et al. 2006). These tagged whales were exposed to airgun pulses in a controlled experiment. Researchers calculated sound propagation paths of the pulses using ray trace and Fourier models. Results showed that whales near the surface may be exposed to high-frequency sounds (>500 Hz) when surface-ducting conditions are present. Therefore, cetaceans with even poor low-frequency hearing may be affected by airgun noise (DeRuiter et al. 2006).

In addition to examining the characteristics of anthropogenic noise and potential impacts on marine mammals, propagation modeling is used to localize and track individual sound sources. These models are particularly important when assessing the vocalization and/or phonation patterns of different animals and species and trying to discern acoustic sound of a specific individual (Sidorovskaia et al. 2004). For instance, the ability to discern spectral features of whale clicks from single hydrophone recordings based on surface- and bottom-reflected arrivals helps researchers develop algorithms for animal localization and tracking (Sidorovskaia et al. 2004; Tiemann et al. 2006).

Propagation modeling can also be included as part of the density estimation analyses discussed in the previous section. When the location of calling animals is not available and cannot be directly measured, propagation modeling can be used to determine the probability of detection at a single sensor (Marques et al. 2013). A common model used for for high-frequency vocalizations is the Bellhop ray-based propagation model. For example, Küsel et al. (2011) used the Bellhop model to model the high-frequency clicks of beaked whales in order to calculate sound TL values as a function of range and depth. These values are used to predict signal-to-noise ratios of received clicks, which are then used to predict the probability of detection as a function of signal-to-noise ratio. This detection function is combined with call rate and false positive rate to estimate density (Küsel et al. 2011).

Additional studies that include propagation modeling of marine mammal sounds and anthropogenic and/or ambient noise are as follows: Aroyan et al. (2000); DeRuiter et al. (2010); Frasier et al. (2016); Hermannsen et al. (2015); Hildebrand (2006); Küsel et al. (2009); LePage et al. (1996); Malme (1995); McCauley et al. (2000a); Mellinger et al. (2009); Mellinger et al. (2003); Shyu and Hillson (2002); Širović et al. (2007); and Tashmukhambetov et al. (2008). The methods used by these studies include acoustic modeling to further investigate how various species of marine mammals produce sound and use echolocation, as well as the way in which sound travels due to physical characteristics of the marine environment. The studies consider physical characteristics, such as environmental fluctuations, seafloor characteristics, and sound-speed profiles. Some of these studies also look at the characteristics of airgun pulses throughout the marine environment and use propagation loss modeling to explore how marine species respond to seismic survey equipment.

3.3.4 Assessing Behavioral Response and/or Vocal Response to Anthropogenic Sources

There is a growing concern about the effects of underwater anthropogenic sound on marine life. The continuing increase in anthropogenic sounds and sound sources in the marine environment requires a variety of methods to study the behavioral and acoustic responses of marine animals to specific acoustic exposures from sources such as military sonar, seismic exploration, shipping vessels, construction, and others. Tyack (2009) provides a thorough review of the methods to study the effects of these sounds on marine life, particularly marine mammals. These methods are divided into two main types: observational and experimental. Observational studies focus on observing the behavior of animals near the anthropogenic sound source to determine changes in behavior. Experimental studies use a controlled environment to test animal responses under a set of chosen stimuli. These controlled environment experiments (CEEs) provide the best method of proving that a particular sound stimulus causes a response because a specific known dose of sound is broadcast to an animal, and the acoustic exposure and behavioral responses can be directly measured (Tyack 2009).

3.3.5 Detectors and Classifiers

The detection and classification of marine mammal vocalizations is often a time consuming and tedious process when analyzing PAM data, particularly when analyzing data for multiple species. PAM systems are often deployed for long periods of time and can collect large volumes of data. In fact, when multiple recorders are deployed at the same time, years of data can be amassed in just a few months. Manually reviewing all of these data for detections requires excessive labor hours and cost. Researchers have been using several signal processing strategies to automate this process, including supervised and supervised machine learning algorithms. Although no single algorithm can be used to detect and classify all species which may be recorded, algorithms do exist for certain species and groups, and new algorithms are being developed (Bittle and Duncan 2013). For more information, refer to Mellinger et al. (2015), which summarizes detection and classification methods for marine animal sounds.

3.4 Data Availability

The primary databases that are currently used to archive PAM data collected in the GOM are described in the following subsections.

3.4.1 The *Deepwater Horizon*-GOM Research Initiative (GoMRI) and GoMRI Information and Data Cooperative (GRIIDC)

The Gulf of Mexico Research Initiative (GoMRI) was established by a Master Research Agreement between BP and the GOM Alliance. In accordance with this agreement, all data collected or generated under this agreement must be available to the public.[17] To fulfill this requirement, the GoMRI Information and Data Cooperative (GRIIDC) was formed. The GRIIDC is a group of researchers, data specialists, and computer system developers who work together to support the data management system which stores scientific data collected in the GOM. The mission of GRIIDC is to ensure that these data promote continual scientific discovery and public awareness of the GOM ecosystem.

Housed at the Harte Research Institute for Gulf of Mexico Studies at Texas A&M University-Corpus Christi, the GRIIDC database includes over 1,000 datasets which focus primarily on GOM research and which include data from research awarded by the following: GoMRI, BP Gulf Science Data, and Florida RESTORE Act Centers of Excellence Program. The GoMRI research comprises of awards from the Florida Institute of Oceanography, Louisiana State University, the Alabama Marine Environmental Science Consortium, the Northern Gulf Institute, and others. Therefore, the database houses a variety of data types, such as oceanographic and water quality data (e.g., conductivity, temperature, and depth), toxicity data, light detection and ranging, and hyperspectral data, and PAM data (e.g., sonobuoy deployments, marine mammal acoustic detections, ambient noise).

In addition to guiding researchers through data management steps, the GRIIDC provides tools that help researchers manage their data throughout an entire study or project. The one-on-one support provided by GRIIDC is unique in that every data package contributed is reviewed for completeness, and the GRIIDC team works directly with the researchers to improve their data and metadata submissions and teach them about best management practices that they can apply to their current and future studies.

3.4.2 The Ocean Biogeographic Information System Spatial Ecological Analysis of Megavertebrate Populations (OBIS-SEAMAP)

In collaboration with a consortium of international partners, Duke University researchers initiated the Spatial Ecological Analysis of Marine Megavertebrate Animal Populations (SEAMAP) initiative in 2002 to form a taxon-specific geo-informatics facility of the Ocean Biogeographic Information System (OBIS) for global marine mammal, sea turtle, seabird, ray, and shark data (Halpin et al. 2006). This project is a part of the Census of Marine Life. As the project has evolved the team is also working to quantify the

[17] GoMRI and GRIIDC: https://data.gulfresearchinitiative.org/. Census of Marine Life: http://www.coml.org/about-census/ .

goals have expanded to include explaining global patterns of marine species distribution and biodiversity; standardize databases and sampling techniques; provide study status and impacts on threatened species; and support modeling of species distributions in response to environmental change.

Since its beginning, this OBIS-SEAMAP program has amassed a geo-referenced repository that includes 873 datasets (1935–2017) and over 5,550,000 records.[18] This spatially referenced online database is continuously expanding through contributions from data providers (Halpin et al. 2006). OBIS-SEAMAP is not only as a repository of data but it also contains tools for distributing and visualizing data. For instance, the web-based geographic information systems applications make datasets widely accessible to teachers and students, researchers, and other members of the general public, and anyone who may not have access to expensive desktop geographic information systems programs. The mapping interface allows users to map several layers of data. For example, one can map sampling effort (trackline data) along with animal observations to quickly find gaps in survey coverage and concentrations of sightings in a particular area of interest (Halpin et al. 2006).

The OBIS-SEAMAP system accommodates a wide variety of data types, such as sampling effort, telemetry tracking, sightings, strandings, bycatch records, and photo-identification catalogs. Contributors to OBIS-SEAMAP include academic, federal agency, non-governmental, and other private organizations and individuals that span the entire globe. As described in Fujioka et al. (2014), OBIS-SEAMAP has been expanded to accommodate PAM data. These data are distinguished from other data types via classification of a combination of count type and platform where count type is presence (animal was detected) or absence (no animal detected) and platform is stationary (e.g., bottom-mounted recorder) or mobile (e.g., towed array). Advanced features for PAM data include more visualization and analysis tools (e.g., diel plots of detections) and extended metadata. The goal is to provide a common framework to facilitate the wider use and sharing of PAM data (Fujioka et al. 2014).

3.4.3 Tethys

Developed by Scripps Institute of Oceanography, NOAA, and San Diego State University, Tethys is an open source temporal-spatial database for metadata related to acoustic recordings.[19] This acoustic metadata system was designed to enhance meta-analyses over large spatial and temporal scales and to provide a standard for representing detections, classifications, and localizations of biologic, ambient, and anthropogenic signals (Roch et al. 2013). The set of rules for structuring metadata is called Tethys, while the Tethys Metadata Workbench is the implementation of this framework and includes a server program and client libraries (Roch et al. 2016).

Through this workbench, researchers can manipulate their metadata and access additional data sources, such as geophysical, biological, and astronomical data sources (Roch et al. 2016). The Tethys interfaces allows the query and processing of publicly available biological and oceanographic data. However, the client-server framework requires users to work with the data in MATLAB, Java, or Python languages (Roch et al. 2013). The web-services-based server enables exchange of data between research groups. For example, summary data can be exported into OBIS-SEAMAP.

Although Tethys currently focuses on marine mammal, fish, and anthropogenic signals, the framework can be used in a variety of contexts. It has already been used to annotate and derive information from millions of cetacean, pinniped, fish, elephant, and anthropogenic acoustic detections from a decade of deployments across the globe. Tethys is well suited for research involving density and abundance estimates, long-term seasonal and diel patterns, and social network analyses (Roch et al. 2016).

[18] OBIS SEAMAP: http://seamap.env.duke.edu

[19] Tethys: http://tethys.sdsu.edu/

4. The Current State of Knowledge

We identified 32 projects conducted in the Gulf of Mexico (GOM) using passive acoustic monitoring (PAM). **Table 1** provides a summary of the studies including the project title, survey dates, general location, methods used, water depth, sampling rate, data recorded, and literature source. Eight of the studies were designed specifically to gather data on ambient noise in the GOM; the other 24 studies were designed to gather information on marine mammals using PAM. **Figures 11 through 14** show deployment locations for PAM devices and tracklines for surveys involving PAM in the GOM. **Figure 11** provides a map for all three Bureau of Ocean Energy Management (BOEM) Planning Areas. **Figures 12**, **13**, **and 14** give a zoomed-in overview for the Eastern Central, and Western Planning Areas, respectively. The majority of studies occurred in only a portion of the GOM, focusing primarily on the Eastern and Central GOM. PAM surveys have tended to be in waters of the continental shelf and slope up to approximately 1,500 meters (4,921 feet) deep; only a couple of the surveys were in deeper waters extending to approximately 3,200 meters (10,499 feet).

4.1 Ambient and Anthropogenic Underwater Noise Levels in the Gulf of Mexico

Three sources of ambient noise exist—biological and physical (or collectively considered natural ambient noise) and anthropogenic ambient noise. Natural sources of sound include earthquakes, wind and/or waves, rainfall, bio-acoustic sound generation, and thermal agitation of the seawater. Anthropogenic sources include a variety of sounds generated from human activities, including noise related to the following:

- Engines, thrusters, civilian commercial sonar, and other equipment in commercial shipping
- Airguns, oil drilling and other equipment used in oil and gas exploration, development and production
- Sonar, communications, and explosives in military exercises and testing
- Commercial civilian sonars in commercial and recreational fishing and boating
- Acoustic deterrent and harassment devices in the fishing industry
- Airguns, sonar, telemetry, communications, and navigation used during research
- Equipment and vessel operation during construction activities

Noise in the ocean is growing in intensity and expanding across coastal regions, and into deeper habitats (Hildebrand 2009). Noise can be categorized into one of three types: low, medium, and high frequency.

Low-frequency noise generally includes sounds in the bandwidths between 10 and 500 Hz. This category is primarily anthropogenic sources, including commercial shipping followed by seismic sources. However, fish can generate low-frequency sound and make up a large part of this spectrum for natural ambient noise. The most common way fish produce these sounds is by grinding or strumming or by using muscles on or connected to bones around the swim bladder. Fish can chorus together and increase the amount of noise in the low-frequency band by as much as 30 decibels (dB) (Hildebrand 2009). Low-frequency sounds generally travel across ocean basins because they propagate over long ranges. Shipping noise has increased over 12 dB as shipping across the globe has expanded. Over the years, oil exploration and construction has expanded into deeper waters and increased the propagation of seismic sounds.

Medium-frequency noise generally includes sounds from 500 Hz to 25 kHz. This category generally include natural sources of sound, such as sea-surface agitation including break waves, spray, bubble formation and collapse, and rainfall. Heavy precipitation can increase noise levels in this range by as much as 20 dB. Biological sources in the medium-frequency range include snapping shrimp (*Alpheus* spp.). When snapping shrimp are present and actively producing sound, they can also increase the amount of noise by 20 dB. Medium-frequency sounds are more local or regional in nature, as they do not propagate over long distances. Military and mapping sonars and small vessels are in this medium range (see **Section 4.1.3**).

Table 1. Passive Acoustic Monitoring (PAM) Studies for Ambient Noise and Marine Mammals in the Gulf of Mexico

PAM Study	Dates	General Location	PAM Methods	Water Depth m (ft)	Sampling Rate (kHz)	Data Recorded (Marine mammal species; noise types)	Source
Marine Mammal Densities from HARP Studies	16 May 2010–Present	Northern GOM Eastern GOM	Seafloor HARPs	980–1,300 (3,215–4,265)	200	Beaked whales: Gervais' Cuvier's, Blainville's, unknown *Mesoplodon* sp.; *Kogia* spp.; sperm whale; bottlenose dolphin; Atlantic spotted dolphin; Risso's dolphin; pilot whales; oceanic stenellids	Hildebrand et al. 2015b
NMFS SEFSC Bryde's Whale Study	Jun 2016–May 2017	Eastern GOM	ARPs	200 (656)	2000 or 2500 kHz	Recordings in progress	NMFS-SEFSC (unpublished data)
LADC-GEMM Ambient Noise Studies in Mississippi Canyon, 2007–2015	26 Jun–22 Oct 2015; 10–23 Sep 2010; 6–16 Jul 2007;	Northern GOM	EARS, [ASVs with towed arrays, gliders in 2015]	1,000–1,500 (3,281–4,921)	192 kHz	Abiotic, seismic surveys, sperm whale, beaked whales, delphinids, shipping	Sidorovskaia and Li 2017
NMFS SEFSC Shipboard Surveys, 2014	Summer 2014	Eastern GOM	Towed hydrophone array	-	-		NMFS-SEFSC (unpublished data)
Ambient Noise in the GOM, 2010–2013	May 2010-Oct 2013	Northern GOM Eastern GOM	HARPs	90–1,300 (295–4,265)	200	Abiotic (hurricane and wind), anthropogenic (seismic surveys), sperm whale, beaked whales, delphinids	Wiggins et al. 2016
NMFS SEFSC Shipboard Surveys, 2012	Summer 2012	Eastern GOM	Towed hydrophone array	-	-		NMFS-SEFSC (unpublished data)
Assessing Impacts of *Deepwater Horizon* on Large Whale Species, 2010–2012	15 Nov 2011–29 Feb 2012; 16 Jun–15 Oct 2010	Northeastern GOM	MARUSs (22)	231–286 (758–938)	2-20	Potential Bryde's whales; sperm whale; seismic surveys	Rice et al. 2014b
Airborne Mine Neutralization System Monitoring	5–10 Dec 2011	Northeastern GOM	Towed hydrophone array	3.5 (11)	48–192	Bottlenose dolphin, Atlantic spotted dolphin	NSWC PCD 2012
NOAA *Pisces* - Protected Species Monitoring and Mitigation Measures for Mid-Water Trawl Sampling	7–29 Sep 2011; 21 Jun–15 Jul 2011	Northern GOM	Towed hydrophone array	Unknown	Unknown	Sperm whale, delphinids	Geo-Marine, Inc. (unpublished data)
Wave Glider HARPs (WGHs)	Feb–Aug 2011	Northern GOM	Wave Gliders (2) with HARPs	93–980 (305–3,215)	10–100	Sperm whale, delphinids	Hildebrand et al. 2013
HARP Bryde's Whale Study, 2010–2011	29 Jun 2010–14 Nov 2011	Northern and Southeastern GOM	3 HARPs	90–1,320 (295–4,331)	200		Širović et al. 2014

PAM Study	Dates	General Location	PAM Methods	Water Depth m (ft)	Sampling Rate (kHz)	Data Recorded (Marine mammal species; noise types)	Source
Bryde's Whale Sonobuoy	30 Jul–1 Aug 2011	Northeastern GOM	Sonobuoys (13)	NA	0–3.5	Bryde's whale	Hildebrand 2017
Dolphin Distribution on the West Florida Shelf, 2008-2010	Jun 2009–Jun 2010; Jun–Sep 2008	Eastern GOM	DSGs	0–100 (0–328)	37–50	Delphinids	Simard 2012
Measuring Delphinid Whistle Characteristics and Source Levels on West Florida Shelf, 2008-2009	Apr 2008–Apr-May 2009	Eastern GOM	Towed hydrophone array	~10–50 (~33–164)	64	Bottlenose dolphin, Atlantic spotted dolphin	Frankel et al. 2014[1]
Low-frequency Sounds of Bottlenose Dolphins, 2003–2009	2003–2009	Eastern GOM Central GOM	Hydrophones	1–14 (3-46)	48–200	Bottlenose dolphin	Simard et al. 2011[3]
Assessing Echolocation Pulse Rate of Bottlenose Dolphins, 2008	Apr–Sep 2008	Eastern GOM	Towed hydrophone array	1–30 (3–98)	64 and 96	Bottlenose dolphin	Simard et al. 2010[2]
Source Characterization Study, 2007	2–22 Sep 2007	North western GOM	EARS [moored array]	1,000 (3,281)	25 kHz	Seismic survey	Ioup et al. 2009
Ambient Noise Measurements, Gulfport Mississippi Harbor, 2005	Jun–Aug 2005	North central GOM	Stationary hydrophone	10 (33)	N/A	Small vessels, large ships, bottlenose dolphin	Stanic et al. 2007
Long-Term Ambient Noise Statistics in the GOM	3 Apr 2004–23 May 2005	Eastern GOM	EARS	3,200 (10,499)	2.5	Abiotic (weather and/or hurricanes), anthropogenic (shipping vessels)	Snyder 2007[4]
Mississippi Sound Bottlenose Dolphin Whistles	Apr 2004–Mar 2005	North central GOM	Towed hydrophone	-	-	Bottlenose dolphin	Hernandez et al. 2010
SWSS Program	2002–2005	Northern GOM	Towed array & DTAG	800–1,200 (2,625–3,937)	-	Sperm whale, seismic activity	Jochens et al. 2008
NOAA Ship *Gordon Gunter* Cruise GU-04-03 (028) 2004	22 Jun–19 Aug 2004	Eastern GOM	Towed array	-	-		NMFS-SEFSC 2004b
Noise Level Effects on Manatee Habitat Use, 2003–2004	Apr–Sep 2004; Apr–Sep 2003	Eastern GOM	Hydrophone	-	200	Boat noise, snapping shrimp	Miksis-Olds et al. 2007b
NOAA Ship *Gordon Gunter* Cruise GU-04-02 (027) 2004	13 Apr–11 Jun 2004	Northern GOM	Towed array	-	-		NMFS-SEFSC 2004a

PAM Study	Dates	General Location	PAM Methods	Water Depth m (ft)	Sampling Rate (kHz)	Data Recorded (Marine mammal species; noise types)	Source
Source Characterization Study, 2003	Jun 2003	Northern GOM	EARS	990 (3,248)	25 kHz	Seismic surveys	Tashmukhambetov et al. 2008
NOAA Ship *Gordon Gunter* Cruise GU-03-02 (023) 2003	12 Jun–18 Aug 2003	Northern GOM	Towed array	-	-		NMFS-SEFSC 2003
LADC-GEMM Ambient Noise Studies in Mississippi Canyon, 2002	19 Aug–24 Oct 2002	Northern GOM	EARS	645–1,034 (2,116–3,392)	12	Weather (e.g., Tropical Storm Isidore, Hurricane Lili), marine mammals	Newcomb et al. 2007
LADC-GEMM Ambient Noise Studies in Mississippi Canyon, 2001	17 Jul–21 Aug 2001	Northern GOM	EARS	600–1,000 (1,969–3,281)	12	Sperm whale, vessels, seismic airguns, weather (e.g., Tropical Storm Barry)	Newcomb et al. 2002
SWAMP	17 Jul–22 Aug 2001; 16 Mar–3 Apr 2001; 28 Jun–26 Jul 2000;	Northern GOM	Towed array & DTAGs	-	-	Sperm whale, delphinids, seismic activity	Lang 2000; Jochens et al. 2008; Burks et al. 2001
GulfCet II	Late summer 1996; mid-summer 1997	Eastern GOM	Towed array	50–3,000 (164–9,843)	-	Sperm whale, delphinids, seismic activity	Davis et al. 2000
GulfCet I	Apr 1992–May 1994	Northwestern GOM North-central GOM	Towed array	-	-	Sperm whale, delphinids, *Kogia* spp., and a possible sei or Bryde's whale	Davis and Fargion 1996
DoN Empress II	11 Nov 1991–10 Jun 1992	Central GOM	Sonobuoys	-	-	Sperm whale, pilot whale, and *Stenella* spp.	Esher et al. 1992

[1] No tracklines available; georeferenced polygon from figure "Delphinid Whistles."

[2] Georeferenced polygon based on "echolocation."

[3] No tracklines provided; polygons derived based on study area descriptions: Mississippi Sound, Mississippi (30°16' N, 88°31' W); Tampa Bay, Florida (27°40' N, 82°42' W) and Sarasota Bay, Florida (27°30' N, 82°35' W).

[4] Georeferenced locations of EARS from figure "Long-Term Ambient Noise Stats" from Snyder 2007.

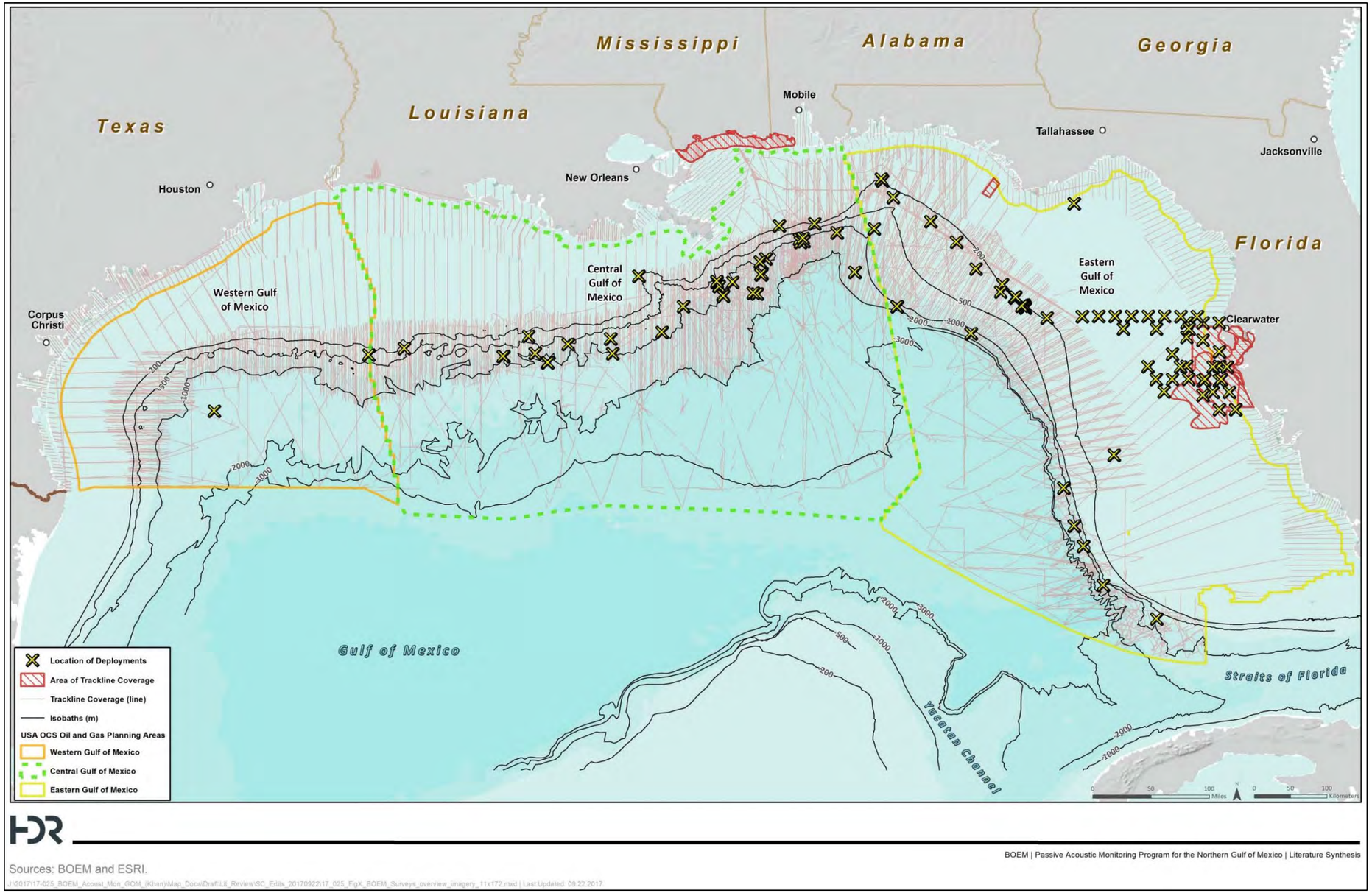

Figure 11. Locations of PAM deployments and trackline coverage in the Gulf of Mexico.

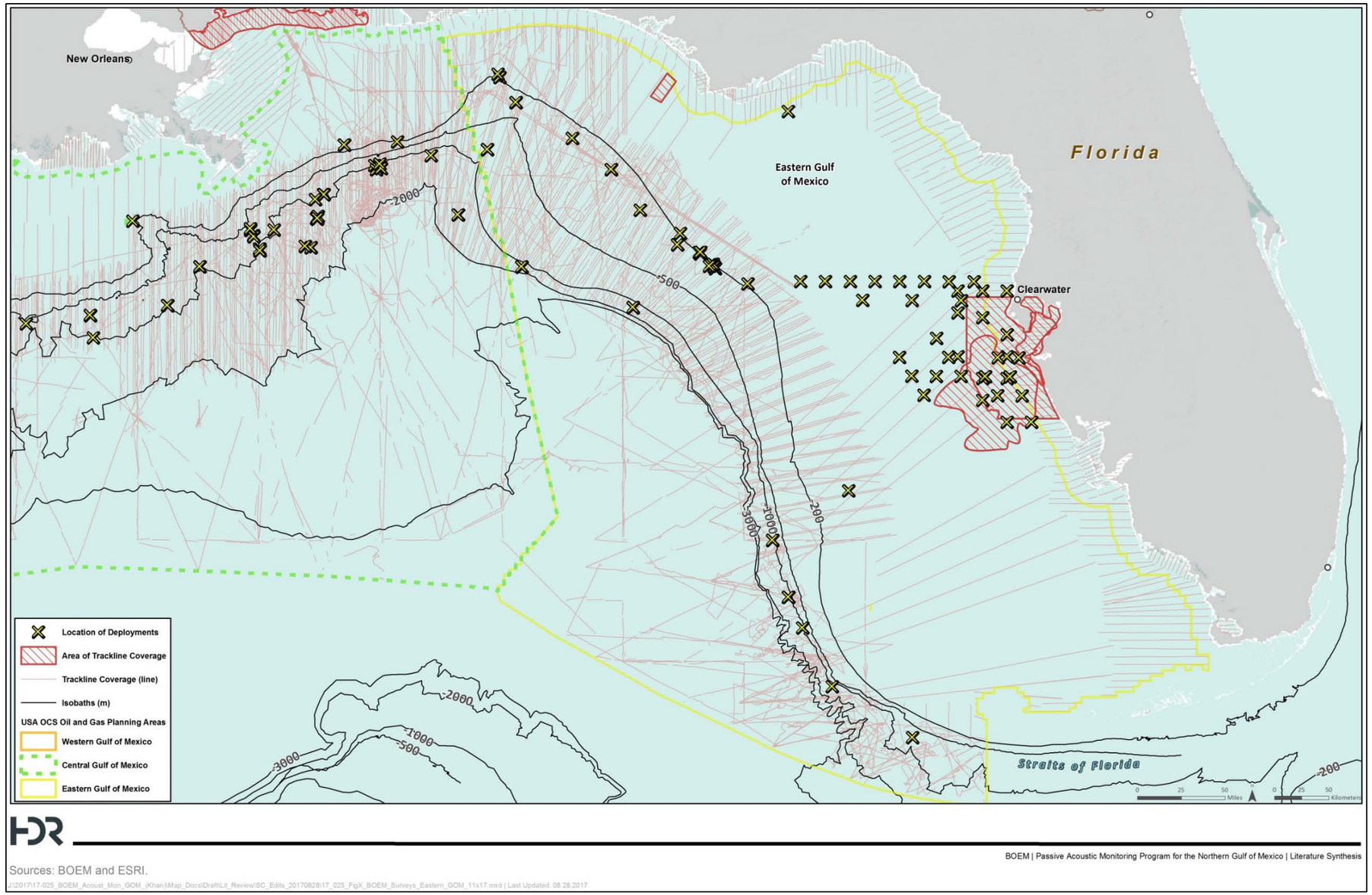

Figure 12. Locations of PAM deployments and trackline coverage in the Gulf of Mexico, Eastern Planning Area.

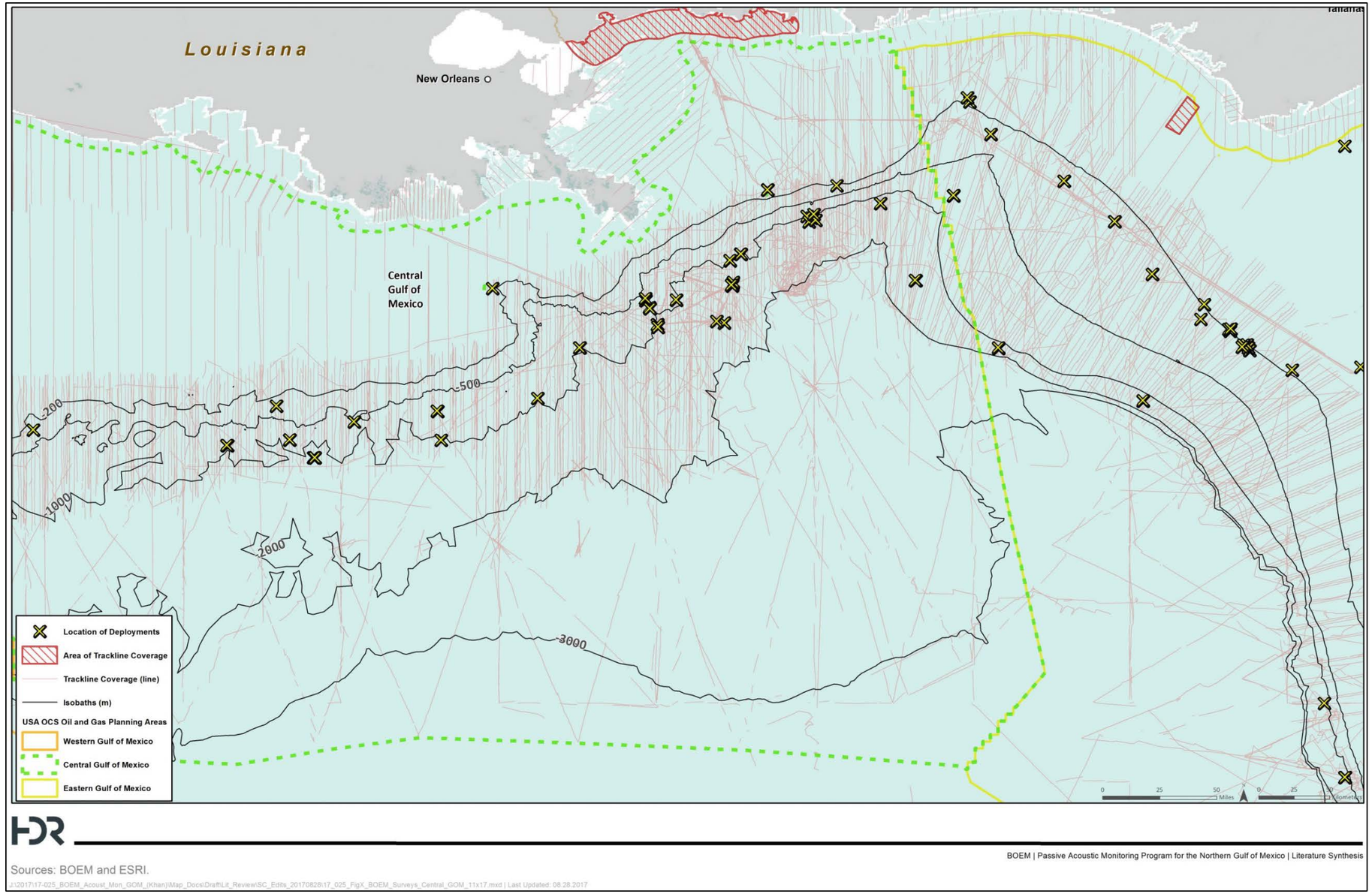

Figure 13. Locations of PAM deployments and trackline coverage in the Gulf of Mexico, Central Planning Area.

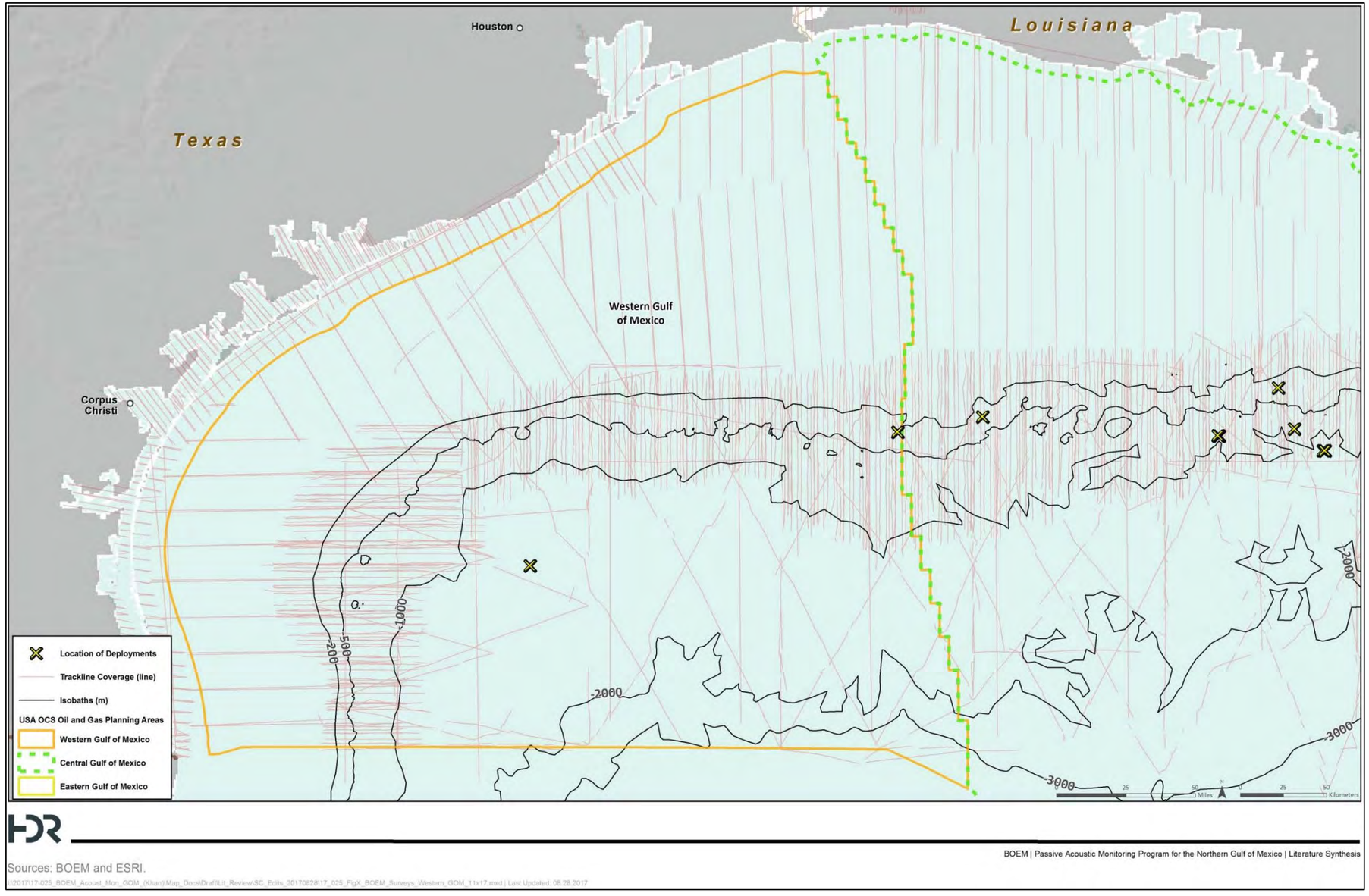

Figure 14. Locations of PAM deployments and trackline coverage in the Gulf of Mexico, Western Planning Area.

High-frequency generally includes sounds above 25 kHz and is generally located close to the receiver. Thermal noise, the result of particles moving close to the hydrophone for instance, is included in this category.

4.1.1 Natural Biological Sound Sources

In the Northern GOM, the Littoral Acoustic Demonstration Center-Gulf Ecological Monitoring and Modeling (LADC-GEMM)[20] research consortium has actively researched the sources of ambient noise and has conducted marine mammal measurement and analysis during the last decade. The consortium is led by the University of Louisiana at Lafayette with academic partners from the University of New Orleans, University of Southern Mississippi, and technical advisers from the Naval Research Laboratory and the Naval Oceanographic Office at Stennis Space Center. The aims of setting up the LADC and of their 2001 study were to measure and characterize the ambient noise baseline within the Northeastern GOM; measure and model noise propagation and examine the associated effects of fronts and eddies; measure and model TL; and determine placements for acoustic sensors and oceanographic equipment considering the incorporation of computer modeling to characterize the littoral environment. Recordings were made using bottom-mounted buoys (previously described as EARS buoys).

In early experiments (2001, 2002) the hydrophones were placed in an area with frequent visual sightings of sperm whales resident to the region. A large portion of the study was relevant to ambient noise, and aimed to achieve the following: detect classify, identify, and track sperm whales, and other marine mammals; coordinate the near-bottom measurements with other researchers conducting visual observation, surface acoustic measurements, and acoustic tag measurements in the region; investigate sperm whale behavior near airguns; and evaluate and modify automatic detection and characterization of marine mammal vocalizations received on near-bottom mounted hydrophones.

The 2001 recordings from three EARS buoys included sound measurements up to 6,000 Hz over 36 days. Recordings contained click and codas vocalizing sperm whales in addition to ships and airgun sounds. The researchers indicated an inverse relationship between the number of vocalizing sperm whales and the amount of geophysical prospecting (i.e., seismic surveys), and shipping activity (Newcomb et al. 2002).

Sidorovskaia and Li (2017) described changes in the baseline noise levels for the Northern GOM (Mississippi Valley-Canyon region) over a short-term seasonal scale and a long-term decadal scale. The field studies focused on the Mississippi Canyon area, where LADC-GEMM continued to deploy bottom-mounted hydrophones in 2007, 2010, and 2015. Recordings were analyzed and bio-sound sources were clearly distinguishable among baseline noise levels for marine mammal activities. Anomalies between 5 and 10 kHz indicate the presence of sperm whales; a 25 to 40 kHz variability indicates the presence of beaked whales and deep-water dolphins.

Sidorovskaia and Li (2017) emphasized that more analysis is required to confirm this hypothesis. The researchers also found high variability in ambient noise between two sites only 28 kilometers (15 nautical miles) apart. This variability in ambient noise could affect the local movement and regional migration patterns for marine mammals in the area. More study is being completed to examine these trends (Sidorovskaia and Li 2017). More information on marine mammal acoustics can be found in **Section 4.2**.

A small number of studies characterize ambient biological noise associated with fish species. Wall et al. (2014) used PAM to map red grouper (*Epinephelus morio*) vocalizations and investigate daily, seasonal, and spatial vocalization patterns on the West Florida Shelf. The University of South Florida researchers collected 11 months of data using fixed recorders and autonomous underwater vehicles (AUVs). The authors concluded that fish calling increased at sunrise and sunset. Although grouper calling was detected throughout the year, calling was highest in the late summer months of July and August and the early winter months of November and December. There was no difference comparing three phases of the lunar cycle. Trends in fish distribution were examined using AUV tracks and researchers found that red grouper

[20] LADC-GEMM: http://www.ladcgemm.org/about/

vocalizations primarily were recorded in waters 15 to 93 meters (49 to 305 feet) deep with the majority occurring between 30 and 50 meters (98 and 164 feet). Vocalizations increased in hard bottom areas and within the Steamboat Lumps Marine Protected Area. These trends corresponded with known spawning habitat for grouper in Steamboat Lumps Marine Protected Area in particular and hard bottom areas in general (Wall et al. 2014). Nelson et al. (2011) found that red grouper vocalizations were dominant in the 50 to 180 Hz range on the West Florida Shelf.

Wall et al. (2012) investigated fish sounds collected from June to September 2008 using 23 autonomous, bottom-mounted acoustic recorders deployed in the Eastern GOM. The aim of the study was to determine the co-occurrence of vocalizations with presence of boats. A peak in sound production by fish was estimated at 500 to 1,500 Hz (Wall et. al 2012).

Finally, the Gulf Coast Research Laboratory has conducted studies using PAM to identify spotted sea trout habitat; however, the location of the study in estuaries and does not extend into BOEM's Planning Areas offshore in the GOM (Gulf Coast Research Laboratory 2017)[21].

4.1.2 Natural Physical Sound Sources

The work by the LADC-GEMM has revealed trends in the ambient noise characteristics for such physical sound sources as wind speed and wave height. For instance, as wind speed increases, associated ambient noise levels also increase (Newcomb et al. 2007). Researchers correlated a Beaufort Sea State 3 to 4 in 200 to 1,000 Hz band with tropical storm events (Newcomb et al. 2002). The studies also indicated a considerable decrease in marine mammal activity during hurricane passes. Sidorovskaia and Li (2017) also identified changes in short –term ambient noise levels with changes in weather conditions. Industrial and natural sources share the range of 200 to 25,000 Hz. In the fall, lower frequency soundscapes are predominantly associated with weather conditions due to low level of exploration activity in the GOM (Sidorovskaia and Li 2017).

In the Eastern Planning Area, the Office of Naval Research deployed EARS to measure ambient noise at approximately 294 kilometers (159 nautical miles) south of Panama City, Florida, in waters with a bottom depth of 3,200 meters (10,498 feet). Data were collected in intervals of 10 to 14 months in the vicinity of a major shipping lane. Sampling occurred at 2,500 Hz with a bandwidth of 10 to 1,000 Hz. The study found that events associated with extremely windy months, which include summer hurricanes and winter storms, have a major impact on ambient noise levels. Sounds from winds peaked at the higher frequencies (400 to 950 Hz) in this portion of the GOM during the summer of 2004, when four hurricanes were recorded. The high-frequency levels were also loud in November through January when wind speed is higher due to winter storms.

On the other hand, low frequencies were loudest in March 2005 and lowest in September 2004. Low-frequency is generally associated with shipping traffic; therefore, more loud noise associated with shipping is heard in periods where conditions are more favorable for ship traffic. The researcher detected a peak in the fluctuation spectrum of 25 Hz at a period of 8 hours, which occurred year round, but was particularly strong from November through February. This could not be attributed to shipping or weather; instead, it was suggested by Snyder (2007) that this is due perhaps to distant drilling operations to the west of the EARS location.

There was no significant difference in noise levels when comparing between daytime and nighttime periods (Snyder 2007). Snyder (2009) found that ambient noise levels also increased during a hurricane. Analysis of recordings made in 2004 during Hurricane Ivan shows an overall increase by 12 dB over the baseline conditions between 200 and 800 Hz (Snyder 2009). Unlike transient anthropogenic sources such as shipping, ambient noise related to weather like wind does not peak in time and tends to exhibit long-term smooth spectral level increase (Snyder and Orlin 2007).

[21] See http://gcrl.usm.edu/research/spotted.seatrout.habitat.php .

4.1.3 Anthropogenic Underwater Noise Levels in the Gulf of Mexico

Whether intentionally or unintentionally introduced, anthropogenic noise in the marine environment is an important component of ocean noise (Richardson et al. 1995; Hildebrand 2009). **Table 2** and **Figure 15** include an overview in general of contributing acoustic sources in each frequency bandwidth.

Table 2. Example Representative Sound Sources by Frequency Level

Frequency Level	Representative Acoustic Sources
1–10 Hz	Ship propellers[1]; explosives
10–100 Hz band	Shipping activities[1]; explosives; seismic surveying sources[1]; construction activities; industrial activities; naval surveillance sonar systems
100–1,000 Hz	Shipping activities[1]; explosives; seismic surveying sources[1]; construction activities; industrial activities; naval surveillance sonar systems
1,000–10,000 Hz	Nearby shipping activities[1]; seismic airguns[1]; underwater communication; naval tactical sonars; seafloor profilers; depth sounders
10,000–100,000 Hz	Underwater communication; naval tactical sonars; seafloor profilers; depth sounders; mine-hunting sonars; fish finders; some oceanographic systems (e.g., acoustic Doppler current profilers)
Above 100,000 Hz	Mine hunting sonar; fish finders; high-resolution seafloor mapping devices (e.g., side-scan sonars, some depth sounders, some oceanographic sonars, and research sonars for small-scale oceanic features)

[1] These sources represent the major noise contributors in the GOM.

Sources: NRC (2003) and Hildebrand (2009).

Northern GOM soundscapes are characterized by a mix of industrial and natural sources across the 200 to 40,000 Hz band, as shown in Figure 15 (Sidorovskaia and Li 2017). Shipping activity and seismic surveys are the major noise contributors in the GOM (Shooter 1982; Newcomb et al. 2002, Snyder 2007; Snyder and Orlin 2007; Estabrook et al. 2016; Wiggins et al. 2016; Sidorovskaia and Li 2017). Analyses of long-term (i.e., multi-year) ambient noise recordings reveal pervasive activity from seismic surveys (Estabrook et al. 2016; Sidorovskaia and Li 2017; Wiggins et al. 2016), often detected across broad expanses of the GOM and ranges extending to at least 700 kilometers (378 nautical miles) (Rice et al. 2015; Estabrook et al. 2016).

Estabrook et al. (2016) noted that sound levels from shipping activity were not nearly as pronounced as those from the seismic surveys, which for the latter, in many cases, persisted for months at a time. In a review of multi-year GOM EARS data, scientists found no indication of an increasing baseline level of ambient noise (Sidorovskaia and Li 2017) below 1,000 Hz. However, Sidorovskaia and Li (2017) noted that high-frequency spectral levels showed an increase in more recent years (2010 and 2015) in the ambient soundscape of the Northern GOM. This increase may be attributed to anthropogenic activities including the increasing use of unmanned devices (sonars, AUVs, etc.) which use high-frequency bands for communication and exploration for seismic exploration.

Airguns and shipping activity are prevailing sources of anthropogenic noise in the GOM, and there were times in this report's focus period with noticeable reductions in noise levels. For example, during hurricane and/or tropical storm passages, low-frequency noise levels decrease. This decrease is attributed to the absence and/or decrease of anthropogenic activity in the interest of human safety (Newcomb et al. 2002; Estabrook et al. 2016; Wiggins et al. 2017). Another time period of reduced anthropogenic baseline noise began on 21 September 2010. During May 2010, the U.S. Department of Interior enacted a moratorium on all deep-water drilling in U.S. waters of the GOM in the wake of the April 2010 explosion of the *Deepwater Horizon* drilling rig and resulting oil spill. The moratorium was lifted in October 2010; however, most oil exploration activity and all exploratory drilling activities in U.S. waters of the GOM

were suspended until 2011. Sidorovskaia and Li (2017) noted that their 2010 EARS data provided a unique dataset of deep-water baseline ambient noise levels in the Northern GOM with reduced industrial operations, particularly for deep-water drilling.

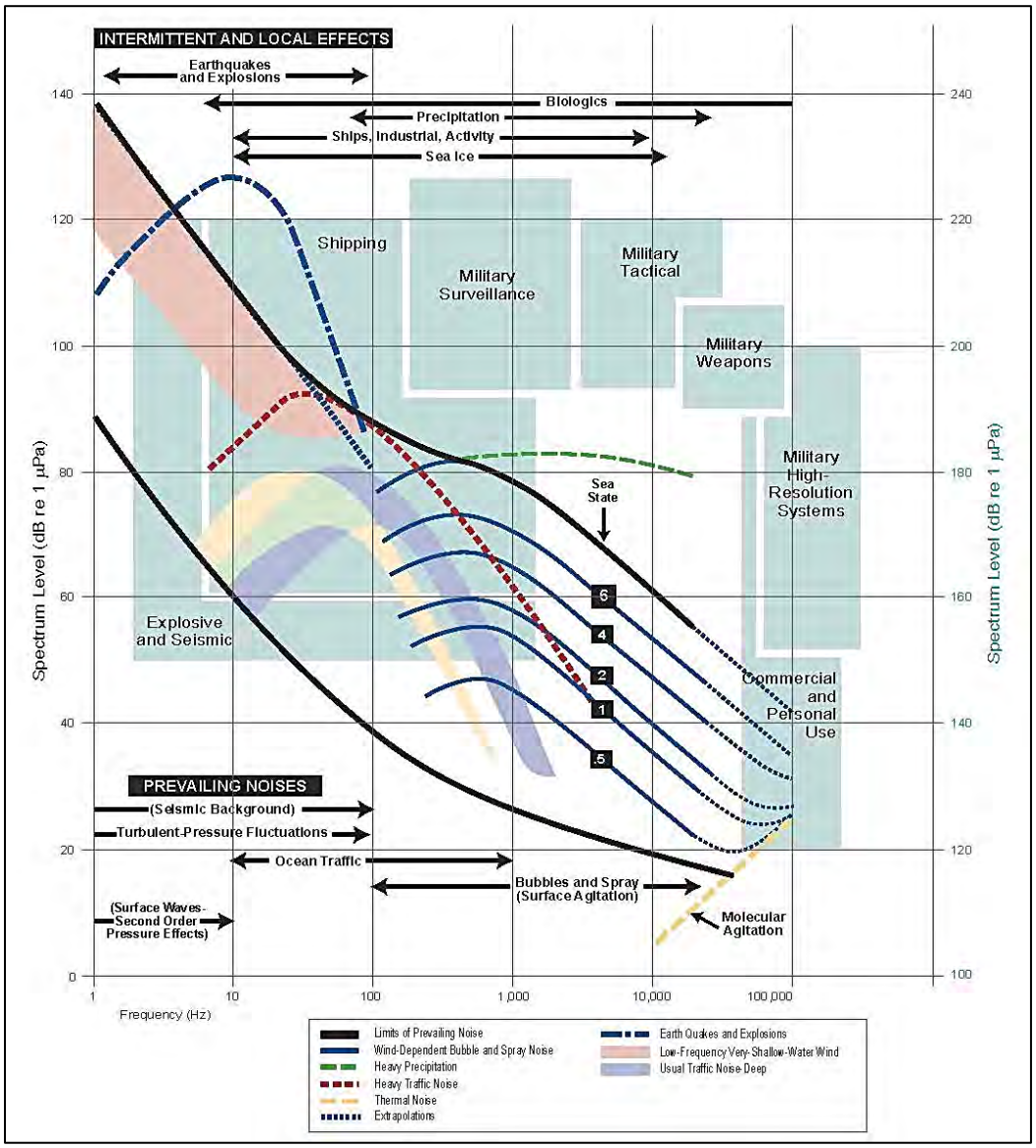

Figure 15. Sources of noise.

Shipping, military, commercial, and personal uses are shown in blue and use the blue spectrum level values on the right axis. These values are 100 dB greater than the values used on the left axis for intermittent, local effects, and prevailing noises (100 dB corresponds to five orders of magnitude). Source: Bradley and Stern 2008 [which was based on Wenz 1962; reprinted with permission, *Journal of the Acoustical Society of America*].

Seasonal variations in ambient noise levels due to industrial exploration are evident in various studies conducted in the GOM (Snyder 2007; Estabrook et al. 2016; Wiggins et al. 2016; Sidorovskaia and Li 2017). Anthropogenic noise sources showed considerable seasonal variability with the highest levels measured during the summer months (Sidorovskaia and Li 2017).

There also is regional variation in anthropogenic noise in the GOM. For example, the two Eastern GOM HARP sites showed high sound pressure spectrum level variability above 200 Hz associated with wind events in contrast to the three north-central GOM sites. (Wiggins et al. 2016). HARP measurements showed high average sound pressure spectrum levels (90 to 95 decibels referenced to 1 microPascal squared [dB re 1 μPa^2]) for deep (approximately 1,000 m) water sites below 50 Hz, caused by a high density of seismic exploration and shipping in the GOM.

Two shallow water HARP sites, one on the shelf and the other on the shelf break, show much different sound pressure spectrum levels compared to the deep water sites and compared to each other. The trends are primarily a function of proximity to anthropogenic activity. In their assessment of the evolution of the GOM soundscape over the past 15 years, Sidorovskaia and Li (2017) noted short-range spatial variability of the soundscapes within the vicinity of the Mississippi Canyon. The scientists noted that the analyses strongly suggest that the noise environment can significantly vary on a daily basis between two sites which are only 28 kilometers (15 nautical miles) apart (Sidorovskaia and Li 2017).

There has been minimal change in the eastern deepwater GOM ambient soundscape recently. Wiggins et al. (2016) compared data collected by HARPs during 2010–2013 to data collected by Snyder et al. (2007) with EARS in 2005. The authors found minimal change in the ambient soundscape of the eastern deepwater GOM over the six to eight years between the two measurements (1/3-octave levels from 2005 were within 1 to 2 dB of those measured in 2010–2013) (Wiggins et al. 2016).

The following subsections address anthropogenic noise contributors to the soundscapes of the Northern GOM.

4.1.3.1 Aircraft

Aircraft support the Outer Continental Shelf (OCS) oil and gas activities, and various research (i.e., aerial surveys) and tourism activities in the GOM. There have been no published measurements of underwater sound transmission and propagation from aircraft flying over the GOM. As noted by Wyatt (2008), little published primary source information is available for underwater noise produced by overflying fixed or rotary-wing aircraft associated with current oil and gas industry activities. Aircraft noise is generally short in duration and transient in nature, although it may ensonify large areas. Dominant tones in noise spectra from helicopters and fixed-wing aircraft are generally below 500 Hz with SPLs around 149 decibels referenced at 1 microPascal root mean square at 1 meter (dB re 1 μPa [rms] m) (Richardson et al. 1995). Underwater sound caused by an overhead airborne source will be highest at the surface and decrease with depth.

Marine mammals can receive both acoustic and visual cues (the aircraft and/or its shadow) from the circling aircraft, if they are located directly under the aircraft and/or well within Snell's predicted sound cone. Marine mammal responses to aircraft were discussed in Richardson et al. (1995) and Smultea et al. (2008). Snell's Law predicts a 26-degree sound cone from the vertical for the transmission of sound from air to smooth-surface water (Urick 1972, Richardson et al. 1995). The angle of the sound cone becomes greater in Beaufort wind force >2. In general, sounds emitted by aircraft are within the hearing range of most cetaceans, particularly those with good low- (<1 kHz) and mid-frequency (1 to 10 kHz) hearing abilities, such as whales and delphinids. The sound emitted from an aircraft varies with aircraft type (e.g., engine number and/or size, helicopter or fixed wing) and maneuvers performed (e.g., straight-line pass, tight or wide circles, speed or engine bursts, etc.) (see Smultea and Lomac-MacNair 2016).

4.1.3.2 Vessels

Shipping activity produces broadband noise as an unintended byproduct that contributes substantially to low-frequency (5 to 300 Hz) noise. Sound produced by motorized vessels contains a set of harmonically related tones caused by the cyclic properties of engine, shaft, and propeller rotation. The fundamental frequency of the tones, and the relative amplitudes at the harmonic frequencies are determined by the boat speed, engine type, propeller movement, and associated characteristics (Ogden 2010). Thus, a boat can be identified by the type of sound it introduces into the water. The noise created by recreational motorized vessels is high amplitude (e.g., typical peak narrowband source levels 150 to 165 dB re 1 µPa) and typically low frequency (e.g., peak frequency at high revolutions per minute approximately 300 to 450 Hz (Barlett and Wilson 2002 as cited in Simard et al. 2016).

Source levels of ships range between 140 and 195 decibels referenced 1 microPascal at 1 meter (dB re 1 µPa @ 1 m) (NRC 2003, Hildebrand 2009), depending upon factors such as ship type, load, and speed, and ship hull and propeller design. McKenna et al. (2012) measured underwater radiated noise for seven types of modern commercial ships during normal operating conditions in the Southern California Bight and found that a 54,000 gross tons container ship had the highest broadband source level at 188 dB re µPa@1m; a 26,000 gross tons chemical tanker had the lowest level at 177 dB re µPa@1m. Bulk carriers had higher source levels near 100 Hz, while container ship and tanker noise was predominantly below 40 Hz. Sound levels typically increase with increasing speed and vessel size (Allen et al. 2012; McKenna et al. 2013). Some energy also is detectable at much higher frequencies (up to 160 kHz) at close ranges (Hermannsen et al. 2014).

Though vessel-specific source levels are generally lower than many other anthropogenic noise sources, the large number of ships makes ship noise a major component of global rising ambient noise levels (e.g., Hatch et al. 2012). The US Department of Transportation Maritime Administration estimates that large vessel traffic (based on number and tonnage of vessels) is higher in the GOM than in other U.S. waters (US Department of Transportation Maritime Administration vessel port call statistics)[22]. A number of studies have been conducted in the GOM on sound associated with shipping and boating activities, including the following:

- Wiggins et al. (2016) collected HARP data that allows to examine contribution of shipping noise into the GOM soundscapes. The authors noted that the noise associated with a particular ship lasted less than 1 hour (due to the ship's movement past detection range of the acoustic recorder) and that shipping sounds were masked by airgun sounds at frequencies below 100 Hz.
- Researchers identified that MARU sites positioned nearest to high-density shipping lanes that lead to the Port of South Louisiana and the Port of Houston recorded the highest levels of 130 and 128 dB, respectively (Estabrook et al. 2016).
- In a study of boat visitation rates at natural and artificial reefs near Tampa Bay, Florida, acoustic data were collected between April 2013 and March 2015 (Simard et al. 2016). In the paper, the authors show a spectrogram of an outboard engine driven boat at high, with harmonics that extended upward to approximately 9,000 Hz. The detected boat sounds were of recreational boats traveling at high speeds based on the presence of higher frequency harmonics, not large commercial vessels which have lower fundamental frequencies.
- During a bottlenose dolphin study conducted on the West Florida Shelf from April to September 2008 and from April 2009 to June 2010, Simard et al. (2015) recorded harmonics from recreational boats extending into ultrasonic frequencies (>20 kHz). The authors also noted that boat noise was noticeably more common in coastal recordings than in offshore recordings; however, lesser variation was observed seasonally.
- From analyses of EARS data collected during 2004 and 2005 (Snyder and Orlin 2007), the average ship noise duration was 1.06 hours with a standard deviation of 1.08 hours. The average inter-arrival

[22] See US Department of Transportation Maritime Administration vessel port call statistics.

time (time between ships) was 3.84 hours with a standard deviation of 3.73 hours. Shipping peaks dominated at levels between 25 and 400 Hz.

- During 2004–2005 in the GOM, Snyder (2007) recorded ambient noise in the 10 to 1,000 Hz band for over 1 year at a site approximately 300 kilometers (162 nautical miles) south of Panama City, Florida at about 3,000 meters (9,843 feet) depth, near local shipping lanes. Spectrum levels were computed in 1/3-octave bands from calibrated hydrophones. Mean sound pressure spectrum levels were approximately 90 decibels referenced 1 microPascal squared per Hz (dB re 1 μPa^2/Hz) at 25 to 50 Hz, approximately 80 dB re 1 μPa^2/ Hz at 100 Hz sloping down to about 60 dB re 1 lμPa^2/Hz near 1,000 Hz with highest variability at 25 Hz and at frequencies above approximately 200 Hz. At the lowest frequencies, these high levels are similar to sites with exposure to heavy commercial shipping, both distant and local (Andrew et al. 2002, Chapman and Price 2011), and at the higher frequencies variability was associated with local wind.

4.1.3.2.1 Echosounders

Commercial and scientific vessels use active sonars for detection, localization, and classification of underwater targets, including the seafloor, plankton, fish, and human divers (Hildebrand 2009). Source frequencies typically range from tens to hundreds of kHz. **Table 3** provides an overview of systems and their associated source levels. Commercial and scientific sonars have lower source levels than military sonars, and many source types are highly directional, such as seafloor mapping and echo-sounding sonars that are directed toward the ocean bottom.

Commercial and scientific sonars are more ubiquitous. For example, most large and small vessels are equipped with commercial sonars for water depth sounding that are operated continuously for aid in navigation (NRC 2003). Acoustic telemetry is becoming more common and is used for underwater communications, remote vehicle command and control, diver communications, underwater monitoring and data logging, trawl net monitoring, and other applications. Acoustic modems operate over distances up to 10 kilometers (5.4 nautical miles) and use signals with frequencies ranging from 7 to 45 kHz and source levels up to 190 dB re 1 µPa @ 1m (Hildebrand 2009).

Table 3. Commercial and Scientific Sonar Sources

Sonar Type (frequency width)	Maximum Source Levels (if known)
Multibeam (seafloor mapping; 12 kHz or 70 to 100 kHz)	245 dB re 1 µPa @ 1m
Sub-bottom profilers (3–7 kHz)	230 dB re 1 µPa @ 1m
Hydroacoustic sonars (20–1,000 kHz)	
Scanning sonars (85–100 kHz)	
Synthetic aperture sonars (85–100 kHz)	
Acoustic modems (7–45 kHz)	190 dB re 1 µPa @ 1m

Source of information: Hildebrand (2009).

Though echosounders may transmit at high source levels, the very short duration of their pulses and their high spatial directivity make them unlikely to cause damage to marine mammal auditory systems, according to current knowledge, based on a review by Lurton and DeRuiter (2011). Behavioral responses are of concern as well. Unlike nonlethal echosounders, effects of various types of sonar on marine mammals were reviewed by Richardson et al. (2010). Richardson et al. (2010) found that there have been few studies conducted on the responses of mysticetes to mid-frequency and high-frequency echosounders. When compared with naval tactical sonar, civilian and commercial echosounders generally produce sound at lower source levels, which translates to lower potential received levels for marine mammals. More information is available in Richardson et al. (2010).

4.1.3.3 Commercial fishing

Commercial fishing vessels radiate broadband noise over a wide range of frequencies. Diesel propulsion engines are typically found on most fishing vessels; these engines radiate energy into the water at low frequencies. These tonals are typically less than 500 Hz and are related to the rotational speed and the number of pistons on the diesel engine. The dominating noise at lower frequencies (below 20 Hz) is generated by sound produced through propeller cavitation (above approximately 1 kHz). Detailed features of the vessel noise spectrum depend on the type of machinery used, vessel speed, and propeller loading (Mitson and Dalen 2007). Much of the machinery on a vessel produces vibration in the frequency range of a few Hz to 1.5 kHz. This acts on the hull and radiates noise into the water.

The major commercial fishery in the Northern GOM is the shrimp fishery, which uses bottom trawl nets. Marine Mammal Organisation (MMO) (2015) reported a frequency range of 40–1,000 Hz with a peak of 100 Hz, and source level of 147 dB re 1 μPa m for an operating trawler. In the case of shrimp trawlers, sound is generated both by the towing vessel and by the fishing gear being dragged across the seabed (Chapman and Hawkins 1969; Normandeau Associates, Inc. 2012). Bottom trawls are fitted with chains, rollers, and metal bobbins that generate irregular sounds as they come into contact with one another and with the seabed. As noted by Normandeau Associates, Inc. (2012), there are also low-frequency (below 100 Hz) sounds from the warps or cables connecting the trawl to the ship, the trawl doors, or spreading devices, and contact with the seabed. Only one published study measuring noise produced by fishing vessels in the GOM was located:

- Newcomb et al. (2008) recorded noise levels at frequencies less than 10 kHz that were generated by a shrimp trawler in Mississippi Sound. The levels due to the shrimp boat were greater than 60 dB at the lowest frequencies. Additional higher frequency spikes were detected at the 30 to 35 kHz and 40 to 50 kHz ranges; these frequencies were attributed to the processing equipment operating on board the trawler. Newcomb et al. (2008) also showed spectrograms with power supply switching transients.

4.1.3.4 The oil and gas industry

Underwater noise associated with offshore petroleum-related operations may be generated by many types of sources and may have a wide variety of acoustic characteristics. The following subsections summarize what is known about noise associated with seismic surveys, operating platforms, and structure removal.

4.1.3.5 The seismic industry (seismic surveys)

Seismic surveys commonly are used not just by the oil and natural gas industry, but also by the US Geological Survey, the National Science Foundation, and in other locales, the offshore wind industry.

Geophysical surveys are conducted to achieve the following goals:

1. Obtain data for hydrocarbon and mineral exploration and production
2. Aid in siting of oil and gas structures, facilities, and pipelines
3. Identify possible seafloor or shallow depth geologic hazards
4. Locate potential archaeological resources and benthic habitats that should be avoided

Geophysical survey types and their purposes are summarized in BOEM (2016b). Noise produced by geophysical seismic surveys includes sounds from airgun pulses, as well as the survey vessel and associated survey boats (Estabrook et al. 2016). In this section, we focus specifically on the contribution of airgun noise to the acoustic environment of the GOM.

Seismic surveys are conducted using an array of airgun releases that introduce compressed air into the water and creates a bubble that generates a pulse of sound sufficiently energetic to penetrate deep beneath the seafloor. A seismic airgun array produces a single downward-directed high-energy impulse that is primarily directed downward to map the composition of the seafloor (Gisiner 2016). Unavoidably, some sound energy is emitted in directions away from vertical (BOEM 2016a). In many instances, the time

between seismic pulse emissions by a seismic array is occupied by a series of multiple arrivals of the same reverberated pulse following or preceding the main pulse arrival at the receiver location (Rankin 1999, Estabrook et al. 2016, Guerra et al. 2016).

Sound energy is reverberated and reflected after propagation over many tens of kilometers or more (Guerra et al. 2016, Estabrook et al. 2016). In fact, Estabrook et al. (2016) determined that seismic airgun noise in the Northern GOM propagated over a large spatial scale of several hundred kilometers. One notable finding from this seismic survey occurred when airgun pulses estimated to originate within the Mississippi Canyon, propagated sound approximately 620 kilometers (335 nautical miles) to the Dry Tortugas, and 165 kilometers (89 nautical miles) southeast, spanning at least 700 kilometers (378 nautical miles) across the Mississippi Fan.

Airguns are broadband acoustic sources that generate energy over a wide range of frequencies, from less than 10 Hz to more than 5 kHz, with industry usable frequencies ranging between 5 and 500 Hz (BOEM 2016a). The acoustic output has its highest energy at relatively low frequencies of 10 to 200 Hz (Goold and Fish 1998). Airgun arrays may also produce significant high-frequency sound energy, up to 22 kHz within a few km of the source (Goold and Fish 1998). Airguns create intense sound impulses with a short rise time and very high peak SPL source levels in the region of 220 to 248 dB re 1 µPa @ 1 m), which are repeated around every 10 to 20 seconds and can travel large distances in the water column. In addition to reporting on airguns, Crocker and Fratantonio (2016) reported on characteristics of radiated sound measured for 18 distinct geophysical survey systems.

Research efforts that have provided information on seismic survey acoustic characterization in the GOM include the following:

- From 2010 to 2017, HARPs deployed by Scripps Institution of Oceanography have monitored the soundscape of three deep and two shallow water sites in the GOM over 10 to 3,300 Hz. Average sound pressure spectrum levels were high, >90 dB re 1 µPa2/Hz at <40 Hz for the deep water sites and were associated with noise from airguns. More moderate SPLs, <55 dB re 1 µPa2/Hz at >700 Hz, were present at a shallow water site in the Northeastern GOM, removed from the zone of industrial development and bathymetrically shielded from deep water anthropogenic sound sources. The study is continuing to date.
- Between July 2010 and February 2012, MARUs deployed by Cornell University collected acoustic data at 7 sites in the Northeastern GOM (Estabrook et al. 2016). Seismic survey and shipping noise dominated the ambient noise environment and chronically elevated noise levels across the Northern GOM ecosystem below 500 Hz throughout the multi-year study (Estabrook et al. 2016). Anthropogenic noise sources significantly contributed to the ambient noise environment; however, seismic survey noise dominated the noise environment and chronically elevated noise levels across several important marine habitats (Estabrook et al. 2016). The 1⁄3-octave band spectrograms illustrated persistent shipping and seismic survey activities throughout the Northern GOM during the study. Seismic and shipping noise appeared to temporarily decrease or stop due to Tropical Storm Lee between 1 and 6 September 2011 (Estabrook et al. 2016). During this time period noise levels above 1 kHz at each site increased and noise below 500 Hz decreased, suggesting a temporary decrease in anthropogenic activity. Seismic surveys occurred persistently during this time period of July 2010 through February 2012 within the De Soto Canyon and Lloyd Ridge areas throughout this study (Estabrook et al. 2016).
- In 2007–2008, two short cruises were conducted to calibrate seismic sources on the R/V *Marcus Langseth* (Diebold et al. 2010). These findings were compared with the 2003 calibration of the seismic sources on the R/V *Maurice Ewing* in the GOM (Tolstoy et al. 2004). The 2007–2008 cruises were moved westward in comparison to the 2003 cruises. This relocation was incorporated to avoid drifting from shallow sites.
- In September 2007, the LADC conducted an experiment in the northwestern GOM to measure the calibrated three-dimensional acoustic field of the primary arrival from a seismic airgun array–the 3D Seismic Source Characterization Project (Newcomb et al. 2009). Twenty paired sensitive and

desensitized hydrophones were deployed at a range of depths on three separate moorings. Special positioning equipment was used to locate these moorings continuously in three dimensions. EARS buoys recorded the wide bandwidth data from the industrial seismic airgun array for a full range of vertical and horizontal arrival angles and broad range of distances between source and receiver. The data were acquired with sufficient shot records to establish a statistically valid sample of SPLs and spectral characteristics in over 1,000 angular bins at frequencies up to 25 kHz.

- In the summer of 2003, the LADC conducted the first GOM acoustic characterization experiment for a 21-element marine seismic exploration airgun array of total volume of 0.0588 cubic meters (3,590 cubic inches). Two EARs buoys, one with a desensitized hydrophone, were deployed at a depth of 758 meters (2,487 feet) in waters with a bottom depth of 990 meters (3,248 feet), near Green Canyon (Tashmukhambetov et al. 2008). The researchers collected data on pressures, which could be used in testing models of the sound propagation from use of seismic equipment. This modeling can be useful in predicting sound exposure levels for marine mammals, which is useful in turn in planning future seismic surveys.
- As part of the Minerals Management Service (MMS, now BOEM)-funded Sperm Whale Seismic Study (SWSS), during 2002 and 2003, tagged sperm whales (*Physeter macrocephalus*) were experimentally exposed to airgun pulses in the GOM, with the multi-sensor, acoustic recording tags (e.g., DTAGs; Johnson and Tyack 2003) providing acoustic recordings at measured ranges and depths (Madsen et al. 2006). Madsen et al. (2006) quantified the sounds exposure levels (SELs) recorded on acoustic tags attached to eight sperm whales at ranges of 1.4 to 12.6 kilometers (0.8 to 6.8 nautical miles) from controlled airgun array sources operated. Madsen et al. (2006) discovered that in the GOM received levels can be as high at a distance of 12 kilometers (6.5 nautical miles) from a seismic survey as they are at 2 kilometers (1.1 nautical miles) (in both cases >160 dB peak-to-peak pressure level). Received levels, as determined from acoustic tags on sperm whales, generally fell at distances of 1.4 to 6 to 8 kilometers (0.8 to 3.2 to 4.3 nautical miles) from the seismic survey, only to increase again at greater distances (Madsen et al. 2006). Due to multi-path propagation, the animals were exposed to multiple sound pulses during each firing of the array with received levels of analyzed pulses falling between 131 to 167 dB re 1 µPa (peak pressure level) [111 to 147 dB re1 µPa (rms pressure level) and 100 to 135 dB re 1 μPa^2 s (SEL) after compensation for hearing sensitivity using the *M*-weighting. Received levels varied widely with range and depth of the exposed animal; when whales were close to the surface, the first arrivals of air-gun pulses contained most energy between 0.3 and 3 kHz, a frequency range well beyond the normal frequencies of interest in seismic exploration. Some arrivals recorded near the surface in 2002 had energy predominantly above 500 Hz; a surface duct in the 2002 sound speed profile helps explain this effect (DeRuiter et al. 2006). Findings indicated that airguns sometimes expose animals to measurable sound energy above 250 Hz, and demonstrated the influences of source and environmental parameters on characteristics of received airgun pulses (DeRuiter et al. 2006).
- In summer 2001, Newcomb et al. (2002) used EARS for approximately one month to record ambient noise. Data clearly revealed seismic airguns. Newcomb et al. (2002) captured similar sound pressure spectrum levels by using similar equipment to Snyder (2007). However, the Newcomb et al. (2002) study was conducted at shallower depths of 600 to 1,000 meters (1,968 to 3,280 feet) on the continental slope as compared with the Snyder (2007) study, which captured data at deeper depths of 3,200 meters (10,499 feet).

Although the following survey falls outside of the 2002–2017 period focused on in this report for the literature review, we have included the following significant and relevant findings for the GOM because the study's emphasis included collection of acoustic information:

- In surveys of the US waters of the Northern GOM, the MMS-sponsored GOM cetacean studies (GulfCet I and II) included using passive acoustical techniques throughout the 1990s (1992–1997) to determine seasonal variability in the occurrence and distribution of marine mammals (Davis and Fargion 1996; Davis et al. 2000). Rankin (1999) studied the potential effects of sounds from seismic exploration on the distribution of cetaceans. She determined that the overall average intensity level

was 8.4 dB re 1 μPa (above ambient), with a maximum of 13. 1 dB at 613.5 Hz and a minimum of 4.3 dB at 26.7 Hz. High-frequencies were measured up to 2,426 Hz for cruise 4 (12 February–27 February 1993) of GulfCet I. The overall average peak was at 81.7 Hz, with a high at 106.9 Hz and low at 35 Hz. Seismic sounds were concentrated in petroleum exploration areas on the upper and middle continental slope.

The airgun pulses recorded within the cold core rings and ring peripheries were generally higher in intensity than those recorded in other hydrographic features. The presence of more intense seismic exploration sounds in these regions appear to be due to the tendency of the cold core ring features to occur in more shallow regions, where oil exploration and production are greater. The confluence zones and the warm core rings were located in deeper waters. Although they contained a large percentage of time with seismic exploration sounds (34 and 31 percent, respectively), the intensities in these habitats were considerably lower.

It is likely that the source of the seismic pulses recorded in the warm core rings were along the continental slope and Rankin's focal study area, where the cold core rings were located. The regions bordering the cold core rings also contained a great deal of time with lower intensity seismic exploration sounds. The Eastern Planning Area was characterized as having little active seismic exploration surveys and, therefore, a low presence of noise from oil and gas exploration.

Summaries of documented behavioral impacts on marine mammals from seismic surveys can be found in a variety of resources including McCauley et al. (2000b), Bain and Williams (2006), Nowacek et al. (2015), BOEM (2016a, 2016b), and Estabrook et al. (2016).Operational Noise from Platforms Drilling and production platforms generate a continuous type sound through the transmission of the vibrations of the machinery and drilling equipment such as pumps, compressors, and generators that are operating on the platform. Noise resulting from the drilling operation may include the following:

1. Machinery noise, such as that from the drill's drive machinery, including drilling noise, engine and exhaust noise, and from the generators and other hotel plant used on the rig;
2. Noise and vibration from the grinding of rock in the seabed, which can either radiate directly from the drill bit through the rock into the water, or can conduct upwards through the drill shaft, radiating into the surrounding water;
3. Noise from communication and positioning systems, such as submarine warning beacons and Doppler type flow meters;
4. In the case of drill ships, noise from dynamic positioning (DP) thrusters (Nedwell and Edwards 2004, Genesis 2011). Drill ships and some types of semi-submersible maintain position using dynamically-positioned thrusters. Where the drilling rig or production platform is reliant on support and supply from other standby and supply vessels, these are often equipped with DP thrusters and powerful engines and therefore contribute to the overall noise level of drilling and production activities.

Noise from conventional metal-legged structures and semisubmersibles is not particularly intense and is strongest at low frequencies, averaging 119 to 127 dB re 1 μPa @1 m levels at 5 Hz and 154 dB re 1 μPa-m in the 10 to 500 Hz band, respectively (Richardson et al. 1995). Noise from drilling is continuous and occurs at low-frequency levels, generally closest to 5 Hz (Nedwell and Edwards 2004) made measurements of the noise radiated during drilling from the *Jack Bates* semi-submersible rig while drilling in deep water northwest of the Shetlands Islands in Scotland, United Kingdom, during September 2000. Measurements were made from the drill rig both during drilling, and when the drill was not in use.

Nedwell and Edwards (2004) noted that tonals could be seen at several unrelated frequencies ranging from approximately 20 to 600 Hz and suggested that they correspond to machinery noise. During drilling, the level of sound in the band from 20 Hz up to 1 kHz was significantly elevated over that for no drilling, and displayed tonal components which were approximately 20 to 30 dB higher than the level with no drilling. These tonals might have corresponded to natural frequencies of the drill shaft, excited by the

drilling machinery on the rig or by the action of cutting at the seabed. Drillships are presumed to be the noisiest way of drilling in water, primarily because the hull has good coupling with the water and thus, facilitates underwater sound radiation (Kyhn et al. 2015). Other types, such as jack-ups and semi-submersible rigs have most machinery well above the water line and therefore, less noise is transmitted to the surrounding water.

Drilling-related noise from semi-submersible platforms in deep waters are between 10 and 40,000 Hz. BOEM estimated sound source levels for semi-submersible platforms at 154 dB re1µPa-m (BOEM 2017). Noise levels on semi-submersibles are typically lower than drillships (BOEM 2017).

As noted by Antunes and Gordon (2008), long periods of monitoring in conjunction with detailed information about rig and platform operations will be required to fully characterize noise output associated with different activities.

Information on drilling noise in the GOM is sparse. However, the following information was found to characterize this type of anthropogenic noise:

- Wiggins et al. (2016) recorded tones in the GOM in the 100–200 Hz band, found that they were common in recordings from deep-water HARP sites, and suggested that they may be related to petroleum extraction or exploration activities.
- During BOEM-funded GOM sperm whale studies in the early- to mid-2000s, 12 recording sessions were conducted in the GOM in the vicinity of drilling rigs and production platforms not drilling at the time in the GOM (Antunes and Gordon 2008). Of particular interest was a recording made at a range of around 9 kilometers (5 nautical miles) from an unidentified drilling rig in 2003; there was a pronounced and constant tonal at 260 Hz that was not pinpointed to a source.
- Antunes and Gordon (2008) noted that they recorded significant noise during two encounters with drilling rigs. On one occasion, during the approach to the *Ocean Lexington* rig on 29 June 2004, noise was heard coming from the drilling rig. A recording was made using the towed hydrophone system. However, the noise ceased before the vessel came within range and the calibrated system could be deployed, so it was not possible to measure absolute SPLs. The noise consisted of pulses lasting for approximately 4 seconds with approximately 1.5 seconds between pulses. Noise was broadband with a band of emphasized frequency at around 8 kHz.

  The drilling rig was contacted by VHF radio, and the research team was informed that it was not drilling, but was engaged in "vibrating cold tubing." During the recording on 2 August 2004 in the vicinity of the *Discovery Enterprise* drill ship, some machinery noise was recorded (Antunes and Gordon 2008). From radio contact with the bridge, scientists found out that the ship was running powerful pumps, and this operation was the likely cause of noise. The noise was continuous with peak levels at approximately 600 Hz and 3 kHz. Many emphasized frequency bands were evident at a spacing of approximately 250 Hz.

Because of the lack of information, we conducted a short review of literature available before the 2002–2017 period that focused on topics relevant to this report. We have included the following findings for the GOM:

- Duggan et al. (1980) reported on two joint-industry research projects conducted in the late 1970s which investigated the feasibility of using ambient surface vibrational measurements to evaluate the structural integrity of three steel template platforms in the GOM. Recordings were taken with signal conditioning filters set at 5, 15, and 30 Hz. The data taken on Gulf South Pass 62B (SP62B) was completely dominated by noise in the region 2.5 to 30 Hz. Scientists attributed the noise to drilling activity. The data from Shell Ship Shoal 274A (SS274A) appeared to be dominated by machinery from 5 to 30 Hz. The gas compressor and diesel generators were responsible for the peaks of greatest amplitude. The data from Conoco Main Pass 296A (MP296A) was, by comparison, relatively free of machinery noise in the region from 0 to 15 Hz.

4.1.3.4.1 Explosives used in rig removal

When oil and gas platforms become obsolete, they go through a decommissioning process. This process may include partial removal (from the surface to 26 meters [85 feet] depth) or complete removal of the platform structure. During the decommissioning of a hydrocarbon production platform in the GOM, all the bottom severance detonations produced a direct shock wave pulse and a pulse from the bubble oscillations; the peak overpressure of the direct shock wave was between 2–10 times greater than the bubble pulse (Connor 1990). The initial wave front contains much of the high-frequency energy of the blast wave, and consequently has a much higher acoustic pressure. The secondary pulses produce a longer duration waveform with significant low-frequency energy components.

Explosions generate low frequencies of 2 to 1,000 Hz with the main energy between 6 and 21 Hz and have very rapid durations <1 ms to 10 ms (Richardson et al. 1995, NRC 2005). The source levels from explosive detonations are some of the largest sounds generated by anthropogenic activities and can produce source levels of 272 to 287 dB re1μPa@1m (0-peak), or greater (Genesis 2011). The objective of the Barkaszi et al. (2016) study was to quantitatively measure the underwater pressure waves and acoustic proprieties generated by the detonation of explosives used for severance during offshore structure removal operations in the GOM. The researchers completed in situ measurements for 8 conductor shots and 11 pile shots and incorporated them into a model that provides a more accurate and conservative prediction of impact criteria.

Potential impacts to marine mammals from the detonation of explosives include lethal and injurious incidental take, as well as physical or acoustic harassment (CSA 2004). Injury to the lungs and intestines and/or auditory system can occur. Harassment of marine mammals as a result of a non-injurious physiological response to the explosion-generated shock wave and to the acoustic signature of the detonation is also possible. Marine mammal injury is not expected from explosive structure removal operations, provided that existing BOEM and BSEE guidelines and conditions of approval requirements are followed.

4.1.3.6 The military

As noted in BOEM (2017), there are multiple US Navy and US Air Force facilities along the US Gulf Coast. Noise sources used during military training and testing activities include aircraft use (including helicopters), live fire air-to-air and air-to-ground missile training, mine warfare training and testing, airborne laser mine detection systems, towed underwater sensors, surface and subsurface training, and shakedown cruises for newly built ships. Military training and exercises use active sonar sources and explosives as part of their operations and each of these sources have the potential to impact marine mammals, which is this the focus of this section.

4.1.3.5.1 Sonar

The US Navy uses mid-frequency active sonars for detecting submarines at ranges less than 10 kilometers (5.4 nautical miles). These systems produce frequency-modulated pulses in the 1 to 5 kHz band (DoN 2018), with signal durations of 1 to 2 seconds, 40-degree vertical beam width, and source levels of 235 dB re 1 μPa @ 1 m or higher (specific to AN/SQS-53C sonar) (Hildebrand 2009). The Atlantic Fleet Training and Testing (AFTT) Environmental Impact Statement (EIS) lists non-impulsive acoustic sources used in the AFTT Study Area, which includes the GOM (Table 2.3-1 in DoN 2018).

4.1.3.5.2 Explosives

The primary military missions involving detonations in the GOM include Naval Explosive Ordnance Disposal School missions. These activities involve underwater detonations of small (e.g., up to 5 kilograms [10 pounds]), live explosive charges adjacent to inert mines. Detonations are conducted on the sea floor, adjacent to an inert mine, at a depth of approximately 18.3 meters (60.0 feet). No acoustic measurements are available for the GOM; however, recent noise measurements were made off Virginia Beach, Virginia and in the Silver Strand Complex near San Diego, California.

Key findings for the California measurements included that measurements of peak (absolute value) acoustic pressure levels ranged from a minimum of 209 dB re 1µPa recorded at 1,651 meters (5,417 feet) to a maximum of 222 dB re 1 µPa recorded at 358 meters (1,175 feet) (Soloway and Dahl 2015). Measurements of (SEL ranged from a minimum of 184 dB re 1 μPa^2s recorded at 1,651 meters (5,417 feet) to a maximum of 191 dB re 1 μPa^2s recorded at 358 meters (1,175 feet). In terms of frequency content, it was found that 90 percent of the underwater-detonation energy is contained in the frequency range from 50 to 2,500 Hz. The AFTT EIS lists explosive sources used in the AFTT Study Area, which includes the GOM (Table 2.3-2 in DoN 2013).

4.1.3.7 Construction

Construction activities involve placing some form of equipment or structure onto the seabed and installing topside equipment, such as platforms. There are many different activities associated with construction. The main types are piling of structures, dredging, and trenching (Genesis 2011). Invariably, offshore construction involves a variety of different types of vessels including heavy lift, barges, pipe lay, anchor handling and support vessels. The study area for this literature review generally excludes coastal waters immediately adjacent to the shoreline where a large part of construction in the marine environment occurs.

However, construction projects have taken place offshore in the GOM and activities beyond the coastal zone primarily include construction of deepwater ports, which is the focus of this discussion of construction. Noise introduced into the water related to this type of construction generally includes pipeline and port construction activities. There are currently five active liquefied natural gas (LNG) terminals in the GOM, located off Texas and Louisiana, with additional terminals approved and applications pending (for locations in the same before-mentioned states).

A marine autonomous recording unit (MARU) array was deployed by Cornell University two months before construction; analyses of the recorded data revealed that construction noise was significant on recorders near the pipeline corridor, but was highly localized, and other areas around the array were much less noisy (see Bingham 2011). The major sources of noise introduced into the water column from LNG terminal construction would be from pile driving and Energy Bridge™ Regasification Vessel (EBRV) thrusters, which are addressed in the following subsections.

4.1.3.7.1 Pile driving

Piling is required to fix subsea structures into the seabed. Offshore pile driving includes impact hammering or in some cases, vibratory driving (i.e., vibro-hammering). Impact pile driving has three subcategories: drop weight, diesel, and hydraulic. Pile driving produces noise at low frequencies and high source levels. The noise generated by impact pile driving ranges from 10 Hz to 120 kHz (Wyatt 2008), with most of the energy in the frequency range of 100 to 500 Hz. Examples of peak underwater SPLs measured from impact pile driving are on the order of 220 dB re 1 µPa at a range of approximately 10 meters (33 feet) from 0.75-meter- (2.5-foot)-diameter and on the order of 200 dB re 1 µPa at a range of 300 meters (984 feet) from piles that are 5 meters (16 feet) in diameter (Dahl et al. 2015). The actual peak SPLs vary substantially and depend on numerous factors such as pile diameter, hammer size, and substrate. A vibratory pile driver is usually hydraulically powered although some electrically driven units are available. The majority of vibrators operate at frequencies between 20 and 40 Hz.

4.1.3.7.2 Vessels (including dynamic thrusters [i.e., barges])

A DP vessel maintains its position (fixed location or predetermined track) by means of active thrusters. Typical DP vessels include survey vessels, drilling ships, work boats, semi-submersible floating rigs, diving support vessels, cable layers, pipe-laying vessels, shuttle tankers, trenching and dredging vessels, supply vessels, and floating, production, storage and offloading vessels. These operations may generate higher levels of sound than drilling from fixed platforms (Hildebrand 2009), with a frequency range of 50 to 3,200 Hz and a source level of 121 to 197 dB re µPa at 1 meter (MMO 2015). The use of the DP

thrusters, and their associated cavitation noise, causes a significant elevation of low-frequency sound from 3 to 30 Hz (Nedwell and Edwards 2004, Genesis 2011).

Measurements collected in the GOM include the following:

- Measurements were collected in August 2006 from the *Excelsior* EBRV while it was moored at the operational Gulf Gateway Deepwater Port located 116 miles offshore of Louisiana (Tetra Tech 2011). The objective of the measurements collected at the Gulf Gateway Deepwater Port was to quantify the underwater noise levels generated by an EBRV as it participated in typical docking maneuvers, onboard closed loop regasification activities, and vessel transiting. The overall purpose of this survey was to verify measurements completed during the first sound survey completed March 2005 when *Excelsior* first visited the Port and to further document sound levels during additional operational and EBRV maneuvering conditions, including the use of stern and bow thrusters required for DP during coupling. Sound levels during closed-loop regasification ranged from 104 to 110 dB re 1 µPA at 1m. Maximum levels during steady state operations were 108 dB re 1 µPA at 1m. Sound levels during coupling operations were dominated by the periodic use of the bow and stern thrusters and ranged from 160 to 170 dB re 1 µPA at 1m.

4.1.3.8 Unoccupied aerial vehicles

The use of unoccupied aerial vehicles (UAVs) is rapidly increasing as technology advances. As noted by Christiansen et al. (2016), UAVs are becoming an increasingly popular tool in wildlife research and monitoring. Christiansen et al. (2016) recorded noise characteristic of two commonly used multi-rotor UAVs, SwellPro Splashdrone and the DJI Inspire 1 Pro. The Splashdrone and Inspire UAVs produced broad-band in-air source levels of 80 dB re 20 µPa and 81 dB re 20 µPa (RMS), with fundamental frequencies centered at 60 and 150 Hz.

The noise of the UAVs coupled poorly into the water, and could be quantified only above background noise of the recording sites at 1 meter (3 feet) depth when flying at altitudes of 5 and 10 meters (16 and 33 feet), resulting in broad-band received levels around 95 dB re µPa rms for the Splashdrone and around 101 dB re µPa rms for the Inspire. The 1/3-octave levels of the underwater UAV noise profiles are close to ambient noise levels in many shallow water habitats. The sound levels are largely below the hearing thresholds at low frequencies of toothed whales, but are likely above the hearing thresholds of baleen whales.

4.1.3.9 Underwater gliders

Underwater gliders are autonomous vehicles that profile vertically by controlling buoyancy and move horizontally on wings. Underwater gliders are being used for a variety of ocean monitoring and/or observation tasks (Meyer 2016). A few types of gliders, including Seagliders, Slocum gliders and Wave Gliders, have been used in the GOM.

Dassatti et al. (2011) reported mean sound levels of 109 dB, with noise peaks (approximately 125 dB re 1µPa) in conjunction with the glider at the surface, due to splashing water or the hydrophone bouncing on the surface, and during engine operation.

A Wave Glider is an autonomous surface vehicle that has a surface float connected by cable to a submerged glider, using wave action for propulsion. The Wave Glider surface float is equipped with real-time communications allowing its track to be controlled remotely. Marine mammal bioacousticians have installed a HARP in the in the Wave Glider surface float, and a hydrophone for sensing underwater sound was connected to the submerged glider, providing a mobile instrument that records cetacean sounds (herein called a WGH).

Wiggins (2009) tested a WGH off the Big Island of Hawaii in October 2009, and as part of the assessment, reported a few observations of self-noise from the WGH that included broad-band pulses lasting two seconds throughout the recording; they presumed these to be glider-related (likely from energized servo motors used to adjust rudder headings) based on the consistent duration of the pulses.

There also were track direction-dependent, broad-band noise (20 to 70 kHz) periods that last around 30 minutes, which Wiggins (2009) speculated may be caused by breaking bubbles from the surface vehicle.

Some acoustic information for self-noise of gliders collected in the Gulf include:

- As noted by Wall et al. (2012) for their study of fish sounds on the West Florida Shelf using a Slocum Glider, the absence of a mechanical propulsion system allows the glider to produce significantly lower noise than a device with a motor. Fish sounds were identified manually because automated detection methods were hampered by the presence of noise from the gliders' altimeter, pump, rudder, and at-surface iridium satellite link.
- The performance of WGHs and seafloor HARPs was studied. Two WGHs were deployed for three sorties (i.e., flights) each for periods of one to two months per sortie in the Northern GOM, with operational periods during 2011 (Hildebrand et al. 2013) (see **Chapter 4** of this report). WGHs noise levels were sometimes, but not always, higher than seafloor HARP noise levels at low frequencies (<400 Hz). This may be due to the shallow depth (~8 meters [26 feet]) of the WGH hydrophone and the need for it to be towed by the Wave Glider. Likewise, the high frequency noise levels of the WGH hydrophone were somewhat higher than those of the seafloor HARP.

4.2 Marine Mammal Acoustics in the Gulf of Mexico

Marine mammals generally detected during the studies included sperm whales, beaked whales, *Kogia* spp., Bryde's whales, killer whales (*Orcinus orca*), and delphinids such as Risso's dolphins (*Grampus griseus*), bottlenose dolphins, Atlantic spotted dolphins, and short-finned pilot whales (*Globicephala macrorhynchus*). Although some study researchers did not report the vocalizing delphinid species, visual observers noted bottlenose dolphins, rough-toothed dolphins, and *Stenella* spp. including Atlantic spotted dolphins as present within the respective survey areas. Noteworthy results from the individual studies are highlighted in the following subsections.

4.2.1 Seagliders™, LADC Noise Studies in Mississippi Canyon, 2015

The Seaglider™ data was lost; therefore, trackline information was not available to be incorporated into this document.

4.2.2 ASV-Towed Arrays, LADC Noise Studies in Mississippi Canyon, 2015

Figures 11 and 13 include the trackline of the Slocum glider where data was collected. Sperm whales were recorded in three regions with some extensive aggregations near the *Deepwater Horizon* site. Additional marine mammal detections included whistles, pulsed calls, and echolocation click trains of delphinids (Dyer et al. 2015, Ziegwied et al. 2016)[23].

4.2.3 EARS Densities, 2007–2015

Figures 11 through 13 include the three EARS deployment locations focused on species in the Mississippi Canyon. Sperm whales, beaked whales, and Risso's dolphins were detected on all three sites. Among beaked whale species, Cuvier's beaked whales (*Ziphius cavirostris*) dominated at deeper sites with Gervais' preferring more shallow waters exhibiting some type of short-range habitat division between two species. Unknown species (signal) of *Mesoplodon* were also detected but less frequently similar to HARP reports (Hildebrand et al. 2015b). The comparison of regional abundance estimates among 2007, 2010, and 2015 deployments shows considerable decrease in sperm whale densities in 2010 (after the spill) as compared to 2007 with trends continued to persist in the 2015 data (Ackhleh et al. 2012). However the beaked whale abundance has increased in the vicinity of the spill site in 2015 as compared to 2007 and 2010 estimates.

[23] The data are available for download: https://data.gulfresearchinitiative.org/data/R4.x261.233:0001

4.2.4 HARP Densities, 2010–2013

Figures 11 through 13 includes the HARP deployment locations for this study. Sperm whales, beaked whales, and *Kogia* spp. were detected at the deep-water sites (Hildebrand et al. 2015b; Merkens 2013). The most frequently detected beaked whale species was Gervais' (*Mesoplodon europaeus*) and Cuvier's (*Ziphius cavirostris*) beaked whales. Blainville's beaked whale (*Mesoplodon densirostris*) and an unknown species of *Mesoplodon* were also detected but less frequently (Hildebrand et al. 2015b). This unknown species could be the True's beaked whale (*Mesoplodon mirus*) based on known habitat associations; however, this species has never been sighted or stranded in the GOM. Therefore, the signals may be from a new species or a known species that produces multiple signal types (Baumann-Pickering et al. 2013).

The PAM data were used to estimate densities of Gervais' and Cuvier's beaked whales based on click and group counting methods (see **Section 4.2.3**) (Hildebrand et al. 2015b). The highest densities of beaked whales were in the Southern GOM in the southeast portion of the Eastern Planning Area near the Dry Tortugas, while the highest rates of sperm whale detections were found in the Northern GOM near the Mississippi Canyon area in the northeastern portion of the Central Planning Area (Hildebrand et al. 2015a). At the two Northern GOM sites, Gervais' beaked whales were detected throughout the project period; Cuvier's beaked whales were detected seasonally with low densities in the summer and higher densities in the winter. Both species had high densities throughout the project period at the Eastern GOM site (Hildebrand et al. 2015b).

Density estimates for delphinids were also generated from the PAM data using group counting and cue counting methods (Frasier 2015, Frasier et al. 2016). Seasonal increases in delphinid densities were evident at most of the deployment sites during the spring and summer (April–August). Since the *Deepwater Horizon* oil spill, the densities of *Stenella* spp. and pilot whales have increased at the site nearest the spill, while Risso's dolphin densities have remained fairly constant. Both stenellids and pilot whales exhibited long-term density increases at the sites east of the spill (Frasier 2015).

4.2.5 MARUs-Assessing Impacts of *Deepwater Horizon* on Large Whale Species, 2010–2012

Figures 11 through 13 include the PAM deployment locations for this study. Potential Bryde's whale detections were recorded on the West Florida Shelf. During the first deployment, researchers recorded three sound types associated with Bryde's whales: "down-sweep-sequences," "long-moans," and "tonal-sequences". The second deployment recorded down-sweep-sequences and long-moans; these sounds were primarily along a northwest to southeast bearing between the 200- and 300-meter (656- and 984-foot) isobaths (Rice et al. 2014a). The highest level of recordings of sperm whales was in the Mississippi Delta region (Clark 2015, Rice et al. 2015). Sperm whale detections decreased immediately after the oil spill but increased several months later. However, this pattern of occurrence was detected 10 more times, suggesting that other factors (e.g., prey availability) besides the oil spill may affect the distribution of this species in this region (Rice et al. 2015).

4.2.6 Wave Glider HARPs, 2011

Figures 11 through 13 include PAM deployment locations and glider tracks for this study. The WGHs recorded both delphinid and sperm whale vocalizations. When compared to the recordings from the seafloor HARPs when the gliders were nearby, the seafloor HARPs had higher detection rates for delphinid and sperm whale vocalizations on the shelf and in deep waters. It was expected that sperm whales would be recorded more often on the seafloor HARPs because they are known to be detected best by deep sensors.

4.2.7 The HARP Bryde's Whale Study, 2010–2011

Figures 11 through 13 includes the HARP deployment locations for this study. Three groups of Bryde's whales were observed by the *Gordon Gunter* visual survey team on 31 July 2011 along the West Florida shelf break; a sonobuoy recorded Bryde's whale Be9 calls on this day. Around the same time and area of

this sighting, the HARP at De Soto Canyon recorded Be9 calls on 8 June 2011 and possible Bryde's whale calls on 24 June 2011. A total of 680 Bryde's whale Be9 calls were recorded from the De Soto Canyon HARP; these calls were consistent between March and July and again in October and January but were absent in November and December. No Bryde's whale vocalizations were recorded from the other two HARPs (Širović et al. 2014).

4.2.8 Dolphin Distribution on the West Florida Shelf, 2008–2010

Figures 11 and 12 include the PAM deployment locations for this study. A total of approximately 270 hours of data were recorded. Acoustic detections confirmed the presence of dolphins on the West Florida Shelf year-round; detection rates were higher in shallow waters and adjacent to Tampa Bay which was consistent with the visual sightings. Although detections were not identified to species, bottlenose dolphins, Atlantic spotted dolphins, and rough-toothed dolphins were sighted during the concurrent visual surveys (Simard et al. 2015).

4.2.9 Arrays Towed from Vessels

4.2.9.1 NMFS-SEFSC Shipboard Surveys, 2012–2016

Figures 11 and **12** include tracklines for this study.

4.2.9.2 The Airborne Mine Neutralization System Monitoring, 2011

Figures 11 and 12 include tracklines for this study. During a total of 29.5 hours of acoustic monitoring effort, three detections were recorded. These were associated with visual sightings and confirmed to be bottlenose dolphins and Atlantic spotted dolphins (NSWC PCD 2012).

4.2.9.3 The NOAA Ship *Pisces*: Protected Species Monitoring and Mitigation Measures during Trawling, 2011

Figures 11, 13, and 14 include tracklines for this study. Sperm whales and delphinids were recorded.

4.2.9.4 Measuring Delphinid Whistle Characteristics and Source Levels on West Florida Shelf, 2008–2009

Tracklines were not available for this study; however, we georeferenced a study area polygon based on figures available in Frankel et al. 2014. Therefore, **Figures 11 and 12** include the area for this study.

Bottlenose and spotted dolphins were observed during the surveys, and analysis of the acoustic recordings resulted in 1,695 bottlenose dolphin whistles and 1,273 spotted dolphin whistles with a high signal-to-noise ratio. In addition, ambient noise levels were recorded; median broadband ambient noise levels (2 to 40 kHz) in Florida were 101.1 dB re 1 µPa (Frankel et al. 2014).

4.2.9.5 Low-frequency Sounds of Bottlenose Dolphins, 2003–2009

Tracklines were not available for this study; however, descriptions of the study area provided in Simard 2012 and Simard et al. 2011 allowed us to create polygons for each study area. Therefore, **Figures 11 through 13** include the area for this study.

4.2.9.6 Assessing Echolocation Pulse Rate of Bottlenose Dolphins, 2008

Tracklines were not available for this study; however, descriptions of the study area provided in Simard et al. 2010 allowed us to create polygons for the study area. Therefore, **Figures 11 and 12** include the area for this study. This study included the first analysis of the echolocation pulse rate of multiple groups of free-ranging delphinids in relation to depth. Results indicate that dolphins alter the timing of their echolocation clicks in relation to depth which may be a function of navigation or foraging (Simard et al. 2010).

4.2.9.7 The Sperm Whale Seismic Study (SWSS) Program, 2002–2005

Tracklines were not available for this study; therefore, this survey is not included in the spatial analysis. Although spatially and seasonally limited, the surveys provided critical information on this sperm whale population and anthropogenic activity in this region (Jochens et al. 2008).

4.2.9.8 NMFS-SEFSC Shipboard Visual Surveys, 2003–2004

Figures 11 through 14 include tracklines for this study.

4.2.9.9 The Sperm Whale Acoustic Monitoring Program (SWAMP), 2000–2001

Figures 11 through 14 include tracklines for this study. Acoustic detections included sperm whales, delphinids, and seismic activity (Mullin et al. 2001).

4.2.9.10 GulfCet II, 1996–1998

Figures 11 and **12** include tracklines for this study. A total of 73 delphinid calls and 20 sperm whale calls were detected along with seismic exploration signals (Davis et al. 2000).

4.2.9.11 GulfCet I, 1992–1994

Figures 11, **13**, and **14** include tracklines for this study. A total of 1,055 hours of acoustic data were recorded, and analyses revealed 487 acoustic contacts from a variety of species including sperm whales, delphinids, *Kogia* spp., and a possible sei (*Balaenoptera borealis*) or Bryde's whale (Davis and Fargion 1996).

4.2.10 Tags

4.2.10.1 The Coastal Alabama Acoustic Monitoring Program (CAAMP), 2009-2017

Data were not available for spatial analysis.

4.2.10.2 Bryde's Whale Sonobuoys, 2011

Figures 11 and 13 include the PAM deployment locations for this study. Using recordings from two sonobuoys, NMFS was able to identify a likely Bryde's whale call consisting of pulse pairs; a total of 14 individual pulses (Be9 calls) were recorded.

4.2.10.3 The Sperm Whale Seismic Study (SWSS) Program, 2002–2003

Data were not available for spatial analysis. Researchers did not find any evidence of horizontal avoidance reactions to airgun sounds of <150 dB re 1 μPa (rms). Researchers did note that sperm whales in this portion of the GOM may be habituated to these anthropogenic noises and that studies are needed to test for avoidance at higher received levels (Jochens et al. 2008, Madsen et al. 2006, Miller et al. 2009).

4.2.10.4 The Sperm Whale Acoustic Monitoring Program (SWAMP), 2000–2001

Data were not available for spatial analysis.

4.2.10.5 The Department of the Navy *Empress II* Sonobuoys, 1991–1992

Figures 11 and 13 include tracklines for this study; sonobuoy locations were not available for spatial analysis. Acoustic detections were confirmed for sperm whales, pilot whales, and *Stenella* spp. (Esher et al. 1992).

4.2.11 Using PAM Data for Estimation of Marine Mammal Densities

As noted previously, the study "Assessing Impacts of *Deepwater Horizon* on Large Whale Species, 2010–2012" included use of MARU arrays to record PAM data for generating density estimates of Bryde's and sperm whales in the Northeastern GOM. Rice et al. (2014b) used distance sampling methods

for both species. For Bryde's whale PAM data, they modified point transect methods to apply conventional distance sampling to estimate Bryde's whale density based on the distance information derived from the location of Bryde's whales calls. The distance of each Bryde's whale call was determined by measuring the distance between the centroid of the low-frequency MARU array and the location of each call.

Using the long-moan calls, researchers estimated 0 to 10 individual Bryde's whales occurring within the detection range of a MARU with a mean daily estimate of 1 to 2 Bryde's whales across all of the low-frequency MARUs. Using the click-counting method, Rice et al. (2014b) generated sperm whale densities from the PAM data recorded from the high-frequency MARU array. The average density of sperm whales between 24 July 2010 and 23 February 2012 was 7.4684 sperm whales per 1,000 square kilometers (292 square nautical miles; coefficient of variation [CV] 58.52%).

Additional examples of studies in which PAM data were used to generate marine mammal density estimates in the GOM and recent studies to refine and further develop PAM density estimation can be found in the following: Ackleh et al. (2012), Frankel et al. (2014), Frasier (2015), Horrocks et al. (2011), Ioup et al. (2016), Kimura et al. (2010), Küsel et al. (2010), Küsel et al. (2015a), Küsel et al. (2015b), Kyhn et al. (2012), Marques et al. (2011), Marques et al. (2012), Martin et al. (2010), Mellinger et al. (2010), Moretti et al. (2010). These studies include a variety of methods to estimate marine mammal density, including the use of both stationary and mobile recording platforms, and the use of propagation modeling and tagging data to derive detection probability and spatial density. The researchers on this BOEM PAM program are considering appropriate study design approaches, including random sensor placement throughout the area of interest to obtain reliable results.

4.2.12 Habitat Modeling

To the best of our knowledge, no habitat models using only PAM data have been developed for marine mammals in the GOM. Most recently, Roberts et al. (2016) developed habitat-based cetacean models for 17 individual species and beaked whales and *Kogia* using line transect survey data. However, habitat models using passive acoustic monitoring data have been used to predict the distribution of vocalizing cetaceans in other regions.

For example, Soldevilla et al. (2011) conducted one of the first studies using PAM data to model delphinid habitat. They used hourly occurrence of Risso's and Pacific white-sided (*Lagenorhynchus obliquidens*) dolphin clicks recorded from HARPs at six sites in the Southern California Bight. GAMs was used to model dolphin acoustic activity as a function of sea surface temperature (SST), SST spatial variability (SST CV [coefficient of variation]), sea surface chlorophyll concentration and CV, upwelling indices, and solar and lunar temporal indices. Model results indicated that mean SST and low SST CV were important predictors of acoustic activity for all dolphins, seasonal variability was an important predictor for Pacific white-sided dolphins, and chlorophyll abundance and variability were important predictors for Risso's dolphins (Soldevilla et al. 2011).

In comparison, several habitat models have investigated the habitat preferences of calling blue whales (*Balaenoptera musculus*) in the Southern Ocean (Širović and Hildebrand 2011) and calling blue and fin whales in the Southern California Bight (Širović and Hildebrand 2015). In the Southern Ocean, visual sightings are rare, so PAM provides insight into blue whale distribution and mesoscale habitat use. In this study, researchers found that blue whale calls were positively correlated with water depth and SST and negatively correlated with mean zooplankton abundance (101 to 300 meters [331 to 984 feet]) and mean krill biomass (<100 meters [328 feet]) although the negative correlation with zooplankton could occur if blue whales do not produce calls when feeding (Širović and Hildebrand 2011).

In the Southern California Bight study, spatially-explicit habitat models for calling blue and fin whales were developed to help the US Navy predict the year-round occurrence of these species. They found that the habitat models built with PAM data provided a much finer and longer temporal resolution than the models derived from visual survey data in this same region (Širović and Hildebrand 2015).

4.2.13 Acoustic Propagation Modeling

The SWSS digital acoustic recording tag (D-TAG) data were used to assess the ability of acoustic propagation models to accurately predict the sound field received by the sperm whales when exposed to airgun noise (Madsen et al. 2006). Researchers were able to quantify the SELs from the D-TAG recordings. These received levels varied greatly with range and depth of the exposed whale. Researchers concluded that the simple geometric spreading propagation models did not obtain accurate predictions of received levels and should not be used to establish impact zones when assessing potential impacts to cetaceans in deep waters. They recommend the use of complex multipath acoustic propagation models (Madsen et al. 2006).

4.2.14 Assessing Behavioral Response and/or Vocal Response to Anthropogenic Sources

Both observation studies and CEEs have been applied to several different marine mammal species to investigate their responses to a variety of sound sources, including seismic exploration, military sonar, and vessels across the globe. For example, studies on responses to seismic exploration have measured the behavioral response of migrating humpback whales (*Megaptera novaeangliae*) to airguns (Dunlop et al. 2015; Dunlop et al. 2016), the effects of airguns on bowhead whale calling rates (Blackwell et al. 2015) and behavior (Ellison et al. 2016), acoustic and behavioral changes of fin whales in response to airgun noise as well as shipping (Castellote et al. 2012), acoustic communication changes of blue whales in response to airguns (Di Iorio and Clark 2010), auditory effects of multiple underwater airgun impulses to the hearing thresholds of bottlenose dolphins (Finneran et al. 2015), and toothed whale reactions to seismic noise (Stone 2003; Tyack et al. 2006).

Many studies have focused on the response of gray whales (*Eschrichtius robustus*) to seismic activity off Sakhalin Island, Russia in the western North Pacific, which is a primary area of seismic exploration (Gailey et al. 2007; Yazvenko et al. 2007). Gordon et al. (2004) provides a summary of observations of behavioral changes in toothed whales, baleen whales, and pinnipeds in response to air guns and seismic surveys.The Department of Fisheries and Oceans Canada (2004) reviews the impacts of seismic sounds on marine mammals, sea turtles, fish, and invertebrates.

A recent long-term study on the behavioral responses of marine mammals to US Navy sonar was initiated in southern California in 2010. The main objective of this behavioral response study was to understand the behavior and responses of different marine mammal species to military sonar signals to inform management decisions about its use (Southall et al. 2012). Researchers used acoustic and/or movement tags on marine mammals, particularly beaked whales, and projected a scaled sound source that simulates military sonar signals. Using this experimental approach, researchers were able to measure calibrated received sound levels and behavioral responses (Southall et al. 2012). Other studies on the response of military activities have been conducted with long-finned pilot whales (*Globicephala melas*) (Antunes et al. 2014) and Blainville's beaked whales (Moretti et al. 2014).

Some of the main anthropogenic sources in the GOM include seismic exploration, shipping, drilling, platform installation, and construction (Azzara 2012, Azzara et al. 2013). Several studies have been conducted in the GOM to assess marine mammal response to anthropogenic noise sources, particularly seismic exploration. The SWSS Program (2002–2005) was an MMS program dedicated to conducting research on GOM sperm whales and their behavioral responses to seismic airguns (DeRuiter et al. 2006, Jochens et al. 2008, Madsen et al. 2006; Miller et al. 2009).

To study sperm whale responses, researchers conducted controlled exposure testing using seismic airgun arrays and tagged sperm whales. The D-TAGs attached to the sperm whales sampled the sounds and behavior of the whales. They were used to measure the acoustic exposures to the whales while also measuring the animal's behavioral responses (e.g., fluke strokes and animal orientation). They did not find any evidence of horizontal avoidance reactions to airgun sound levels of <150 dB re 1 μPa (rms). Also, opportunistic studies of S-tagged sperm whales and seismic activity detected no apparent horizontal avoidance or displacement of whales associated with operational seismic surveys. Researchers did note

that sperm whales in this portion of the GOM may be habituated to these anthropogenic noises and that studies are needed to test for avoidance at higher received levels (DeRuiter et al. 2006, Jochens et al. 2008, Madsen et al. 2006, Miller et al. 2009).

Other examples of studies of marine mammal responses to anthropogenic noise in the GOM include observational studies. For instance, Miksis-Olds et al. (2007b) examined manatee use of foraging habitat in relation to ambient noise in Sarasota Bay, Florida. Ambient noise in the bay is dominated by snapping shrimp and vessels, and researchers found that the presence of vessel noise in the morning may affect manatee use of foraging habitat on a daily time scale. Additional studies on manatee responses to vessel noise have used playback experiments in which prerecorded watercraft sounds were played and manatee swim speed, behavioral state changes, and respiration rates were assessed. The most pronounced manatee responses were in reaction to personal watercraft (Miksis-Olds et al. 2007a). Another study in Sarasota Bay investigated the observed changes in dolphin density and occurrence before, during, and after bridge construction and demolition (Buckstaff et al. 2013). Compared to during construction, dolphin density in the vicinity of the bridge was significantly higher after construction was completed.

4.2.15 Detectors and Classifiers

Bittle and Duncan (2013) provides a fairly recent review of current marine mammal detection and classification algorithms for PAM. Some of these algorithms are actually included in the PAM systems so they are capable of automatically detecting certain marine mammal vocalizations at the source of the recording. These systems are mostly limited to detections of porpoise click trains (e.g., T-POD, C-POD).

Additional real-time automated systems have been developed to detect and classify delphinid vocalizations which typically consist of echolocation clicks, burst pulse sounds, and whistles. Known as Real-time Odontocete Call Classification Algorithm (ROCCA), this MATLAB-based tool (i.e., ROCCA) automatically extracts 10 variables and uses classification and regression tree analysis and discriminant function analysis to identify whistles from spinner, striped, pantropical spotted, long-beaked common, short-beaked common, rough-toothed and bottlenose dolphins, as well as short-finned pilot and killer whales (Oswald et al. 2007). Although the overall percentage of correct classifications is low for some of these species, ROCCA was added to the PAMGUARD software suite in 2011 for improved automated detection and classification (Bittle and Duncan 2013; Oswald et al. 2011).

In addition to ROCCA, other detectors that may be useful for identifying and classifying marine mammal species that occur in the GOM include Listening to the Deep Ocean Environment (LIDO), energy ratio mapping algorithm (ERMA), and Gaussian mixture models (GMMs). LIDO is capable of extracting low-frequency and high-frequency impulses; it uses spectral and temporal features to detect ultrasonic cetacean clicks, such as those from beaked whales and delphinids, sperm whale clicks, and impulsive ship noise (André et al. 2011). ERMA is able to detect clicks of Blainville's beaked whales while rejecting echolocation clicks of Risso's dolphins and pilot whales (Klinck and Mellinger 2011).

GMMs may be used as the second stage of processing to complement ERMA. Compared to other detection methods, GMMs have a high correct detection rate for beaked whales (Bittle and Duncan 2013). GMM development has continued and recent tests resulted in echolocation click detections of bottlenose, short-beaked common, long-beaked common, Pacific white-sided, Risso’s dolphins, and Cuvier’s beaked whales (Roch et al. 2011). General consensus among researchers is that the GOM will require regionally tuned delphinid classifiers which do not currently exist for the region.

4.3 Findings on Data Management

Three databases were identified as containing PAM data from the GOM. Ocean Biogeographic Information System Spatial Ecological Analysis of Megavertebrate Populations (OBIS-SEAMAP), Gulf of Mexico Research Initiative GoMRI Information and Data Cooperative (GoMRI GRIIDC), and Tethys contained some information and data on PAM studies conducted in the GOM. However, all data were not available in the systems and some of the data only were available through requests to and direct communication with the various respective researchers.

5. Recommendations on the Experimental Design for the BOEM Passive Acoustic Monitoring Program for the Northern Gulf of Mexico

The figures and table in Chapter 4 provide a comprehensive review into the trends for data collected using passive acoustic monitoring (PAM) methods in the Gulf of Mexico (GOM). The Eastern and Central Planning Areas within the GOM have been extensively covered by PAM studies, compared with the Western Planning Area. A lack of data and emphasis exist on collecting information from the Western GOM (**Figures 11 through 14**). No stationary deployments have been made in the Western GOM (Western Planning Area) as compared with the 17 distinct sites in the Central Planning Area and over 50 distinct sites in the Eastern Planning Area where stationary PAM devices have been used to collect data. The Bureau of Ocean Energy Management (BOEM) PAM Program for the Northern GOM should consider the need for data collection in the Western Planning Area and include this area as a research emphasis.

Locations of PAM deployments and studies generally have covered the continental shelf and continental slope waters. Researchers have conducted the majority of PAM studies in the GOM in waters between 0 and 1,500 meters (0 and 4,921 feet) (**Table 1**). Only a few studies have focused upon the deep waters of the GOM, which include the abyssal plain. The BOEM PAM Program for the Northern GOM should focus upon this area due to the lack of data collected here, as well as the continuing expansion for a variety of oil and gas exploration activities into deeper waters.

Logistically, we found suggestions within the literature discussed above for PAM data collection methods. Glider use is expanding in marine research, and the types of data gliders can collect continue to be developed by the research community. The variety of information that researchers using gliders can collect includes a wide-spectrum of targeted studies including monitoring marine mammals, collecting ambient noise data, tracking currents and examining hydrographic features, assessing and tracking pollutants, and conducting oceanographic and environmental measurements (Waddell and Olson 2015).

Gliders can survey a large amount of area over a relatively short period of time and at various locations throughout the entire water column, whereas stationary PAM devices can be placed only at a particular location and a particular depth. Gliders can take measurements in the middle of the water column, not just at locations close to the seafloor or water surface. Given the breadth of coverage and types of data that could be collected, the BOEM PAM Program for the Northern GOM should explore the feasibility of mobile platforms fitted with a preferred PAM system to collect data relevant to baseline noise studies at least in selected frequency bands which are not overlapping with ones where the system self-noise is produced.

Gliders are limited to date by the depths at which they can travel; however, the capabilities are expanding. The suggested studies in deep waters may require use of stationary devices given glider limitations, depending on the explorations for the use of gliders as mentioned in the previous paragraph.

The BOEM PAM Program for the Northern GOM could investigate the use of oil and gas facilities such as platforms as locations of opportunistic deployments in deep water, as needed (Waddell and Olson 2015), particularly to address near-field noise levels from such facilities which are not well characterized. Furthermore, when stationary devices may be necessary, Snyder (2007) suggests that EARS should be deployed with weather buoys as possible in order to more accurately determine weather's influence on ambient noise (Snyder 2007). Therefore, researchers using stationary units should consider placing their PAM devices in the proximity of weather buoys[24].

Snyder (2007) concludes that assessing baseline ambient noise levels requires long-term continuous datasets. Longer, continuous monitoring would facilitate a more robust analysis of annual and seasonal variations in the ambient noise environment. Future work should include the continuous, long-term data collection using PAM even beyond the longest intervals in the Snyder (2007: 1 year), marine autonomous

[24] See the website for NOAA's National Data Buoy Center at: http://www.ndbc.noaa.gov/

recording units (MARU) (Estabrook et al. 2016: 1.5 years), and high-frequency recording package (HARP) (Wiggins et al. 2016: 2.5 years) studies. The focus on long-term monitoring would also help track changes in the amount and type of noise being introduced into the GOM and to facilitate a better understanding of the sources contributing to future changes in underwater noise in the GOM (Hildebrand 2009).

There are inherent challenges in examining/comparing the information available on PAM projects. System calibration protocols, processing methods, statistical analysis, and metrics often either differ significantly among studies or are reported in different ways without sufficient details. Therefore, study results may not be comparable across the entire suite of projects available for review. Some PAM projects examining anthropogenic noise trends only include propagation modeling and do not include actual measured noise levels.

For example, studies involving pile-driving activities typically require modeling for "take" estimation of marine mammals; however, actual field measurements during test pile programs or construction periods are either not required or not reported in the literature. Thus, the findings are theoretical and may or may not represent the actual levels of sound introduced into the water column. Calibration is another area that may affect study findings. Some studies include calibration; in others either calibration is not always performed or not reported in the reports. An example of this challenge is often found in monitoring related to construction.

Researchers have identified data gaps concerning differences in sound propagation modeling predictions and field measurements. For instance, academic researchers have theorized that modeling sound propagation from seismic arrays may overestimate propagation losses (Kearns and West 2015). More information is needed to address whether there are discrepancies between modeled and actual propagation losses. As related to this finding, recently, BOEM conducted modeling to develop acoustic zones in the GOM for a Letter of Authorization permit request under the Marine Mammal Protection Act to conduct geological and geophysical exploration activity in the GOM.

In our literature review, we have found no effort to date to ground-truth the modeled acoustic zones with actual PAM data. We suggest that the BOEM PAM Program for the Northern GOM be designed to investigate these identified data gaps. For instance, a program should take into account these acoustic zones and gather information to determine whether the modeling is aligned with actual real-time field measurements.

Recently, BOEM awarded Continental Shelf Associates Inc. a contract to analyze all the visual and acoustic mitigation survey data collected during marine mammal monitoring of seismic operations in the GOM from 2009 through 2015 (CSA Ocean Sciences 2017). Before this effort, there had been no studies in the GOM on the effectiveness of PAM monitoring to assist mitigation efforts. As part of March 2015 webinars on a monitoring plan for marine mammals in the GOM, researchers noted that Arctic research has shown reactions of baleen whales to seismic activity and that the same type of information is needed for species of interest in the GOM, such as sperm whales (Kearns and West 2015).

For instance, research should address at what noise levels sperm whales would cease vocalizing and thereby PAM methods as mitigation and/or monitoring methods would no longer be successful (Kearns and West 2015). The BOEM PAM Program in the Northern GOM should incorporate findings and information available once the reports, publications, and presentations are available on this new contract. Additionally, participants in these 2015 webinars hosted by BOEM noted that there is a lack of information available on detection ranges in the GOM (Kearns and West 2015). Kearns and West (2015) also captured that academic and other researchers suggest the passive acoustic monitoring in the GOM should expand to include the development of a program to include localization capability. The incorporation of such a capability would further allow researchers to investigate population density of marine mammals.

Compared to the literature available on marine mammal species and PAM, there has been less emphasis on non-marine mammal species, such as fish and invertebrates. Kearns and West (2015) captured researchers' concern that the focus on marine mammals is too narrow. The BOEM PAM Program for the Northern GOM should consider a more ecosystem-based approach rather than relying solely on topics centered on marine mammals. Fish and invertebrates are important prey species and information; research should continue to expand upon the knowledge of all ambient biological noise in the GOM.

Similar Kearns and West (2015), we found inconsistencies in the availability of PAM data for the GOM. Some data can be found in the various databases–OBIS-SEAMAP, GoMRI GRIIDC, and/or Tethys–but none of these systems house all of the information available for the GOM. The BOEM PAM Program for the Northern GOM should work with GoMRI GRIIDC and the National Oceanic and Atmospheric Administration (NOAA) to ensure that all noise data from past efforts and from those going forward is available through the system. The data contained from mapping in this report is being consolidated and will be provided to BOEM with the final report deliverable. Future effort in time and funding should be invested to make sure all raw data are housed in single publically available database. Additionally, this future effort should focus on continuing to gather data not acquired under this effort and combine information with the rest of the data.

This report was a preliminary, cursory review of the available literature and data on ambient noise including biological, physical and/or environmental, and anthropogenic noise, particularly focused on the GOM. We were able to broadly characterize the available information and studies conducted. We recommend further effort and time be invested into a comprehensive review of the information available for the GOM. A number of stakeholders could benefit from such a comprehensive review.

Also, the baseline information and PAM data collection would benefit from input by a scientific advisory panel. Kearns and West (2015) captured federal agency comments, during a workshop on GOM research, that a scientific advisory group could help for vetting and managing information and leveraging resources. The US Navy has incorporated a scientific advisory group into its global marine species monitoring program and a similar framework could be used to discuss among stakeholders the current projects, suggested changes and adaptive management, and program goals, and track the evolving science behind the BOEM PAM Program for the Northern GOM.

A preliminary experimental design has been suggested for the proposed acoustic data collection under the BOEM PAM Program for the Northern GOM. This design includes deployment of a carefully selected suite of stationary and mobile data collection platforms at strategically identified locations within Mississippi and De Soto canyons in the Northern GOM. The suggested data collection area will include a 100-kilometer by 200-kilometer (54-nautical mile by 108-nautical mile) box within which data recorders will be placed as shown in **Figure 16**. Data will be collected using this proposed design over a 24-month period.

Based on the literature review findings, the following recommendations are made to improve the preliminary experimental design for the BOEM PAM Program for the Northern GOM:

- Focus the first two-year deployment effort in area of Mississippi Canyon and/or valley where many ambient noise sources are present and majority of previous baseline data collections were conducted. However, expand the sensor deployment to shallow water and abyssal plain.
- If possible, establish at least one stationary monitoring site in the BOEM Western and Eastern planning areas to understand the differences in soundscapes among regions over the first two years of deployment.
- Investigate use of mobile PAM platforms (gliders and autonomous surface vehicles) for ambient noise measurements, where consistent with study goals and objectives.
- Investigate the use of oil and gas facilities as opportunistic platforms for data collection, particularly to characterize near-field anthropogenic noise features of drilling and construction activities.

- Conduct comprehensive oceanographic data collection simultaneously with acoustic measurements to assure proper input into propagation models to study their effectiveness in predicting acoustic energy distribution from different sources.

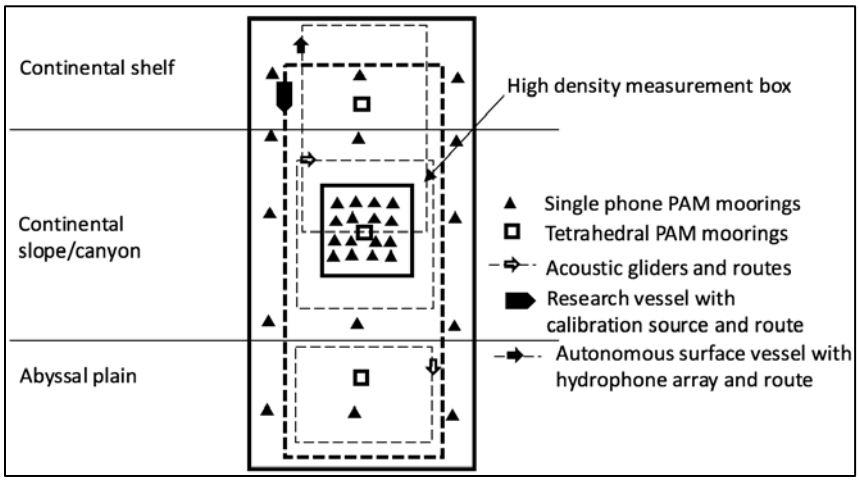

Figure 16. Suggested acoustic data recorder deployment scheme.

Note: The top of the area covers the continental shelf (<200 meters [>656 feet] deep), the middle area covers the continental slope (200 to 1,600 meters [656 to 5,249 feet] deep) and Mississippi Canyon and the bottom area covers the abyssal plain (>1600 meters [> 5,249 feet] deep). The black triangles represent locations of single hydrophone PAM moorings. The squares represent tetrahedral PAM moorings with localization capability. The small arrows represent notional tracks for acoustic gliders and autonomous surface vessel with hydrophone array. Last, a research vessel with a calibration source, denoted by the polygon, is proposed to transit the study area with a known source.

- Focus on long-term multi-year continuous calibrated PAM data collection over broad frequency range with understanding a need for designing special requirements for the systems that will be monitoring different frequency bands (hydrophone sensitivities and dynamic range, system response curves, etc.)
- Implement rigorous unified hydrophone and/or system pre-deployment calibration protocols across different PAM instruments to ensure quantitative data compatibility and comparability across different PAM platforms
- Develop common data processing workflows and reporting metrics across the program in consultation with BOEM.
- Incorporate goals to design experimental data collection in a way that would allow benchmarking modeling results for the GOM against newly collected data through the program for different propagation scenarios (range-independent, range-dependent, canyon propagation, etc.).
- Recommend appropriate PAM methodologies for different GOM regions (e.g., shallow water, continental slope, deep-water, industrially active) and for different study objectives (e.g., baseline noise measurements, anthropogenic soundscapes, species abundance, habitat use, etc.). Consider an ecosystem-based approach to PAM data gathering that would allow biological soundscapes relevant to species that have not been extensively studied in the GOM, such as fish and invertebrates.
- Make all data available to the stakeholders and public through NOAA, the GRIIDC, and other data-sharing databases.
- At a later date, support further effort into the comprehensive review of PAM information available for the GOM to include development and implementation of a scientific advisory group.
- Develop and implement protocols to determine acoustic detection ranges, false positive and negative rates within these ranges.
- Develop and implement protocols to determine acoustic sound production rates for species of interest.

6. References

Ackleh AS, Ioup GE, Ioup JW, Ma B, Newcomb JJ, et al. 2012. Assessing the Deepwater Horizon oil spill impact on marine mammal population through acoustics: endangered sperm whales. J Acoust Soc Am. 131(3): 2306-2314. doi: 10.1121/1.3682042.

Allen JK, Peterson ML, Sharrard GV, Wright DL, Todd SK. 2012. Radiated noise from commercial ships in the Gulf of Maine: implications for whale/vessel collisions. J Acoust Soc Am. 132(3): EL229-EL235. doi: 10.1121/1.4739251.

André M, Van Der Schaar M, Zaugg S, Houégnigan L, Sánchez AM, et al. 2011. Listening to the deep: live monitoring of ocean noise and cetacean acoustic signals. Mar Pollut Bull. 63(1-4): 18-26. doi: 10.1016/j.marpolbul.2011.04.038.

Andrew RK, Howe BM, Mercer JA, Dzieciuch MA. 2002. Ocean ambient sound: comparing the 1960s with the 1990s for a receiver off the California coast. Acoust Res Lett Online. 3:65–70. doi: 10.1121/1.1461915

Antunes R, Kvadsheim PH, Lam FPA, Tyack PL, Thomas L, et al. 2014. High thresholds for avoidance of sonar by free-ranging long-finned pilot whales (*Globicephala melas*). Mar Pollut Bull. 83(1): 165-180. doi: 10.1016/j.marpolbul.2014.03.056

Antunes R, Gordon J. 2008. Acoustic recordings made in the vicinity of deep water drilling rigs and oil platforms in the Gulf of Mexico. In: Jochens A, Biggs D, Benoit-Bird K, Engelhaupt D, Gordon J, et al., editors. Sperm whale seismic study in the Gulf of Mexico: synthesis report. New Orleans (LA): US Department of the Interior Minerals Management Service. 341 p. OCS Study MMS 2008-006. Contract No.: 1435-01-02-CA-85186 (Texas A&M University). p. 60-67.

Aroyan JL, McDonald MA, Webb SC, Hildebrand JA, Clark D, et al. 2000. Acoustic models of sound production and propagation. In: Au WWL, Popper AN, Fay RR, editors. Hearing by whales and dolphins. New York (NY): Springer-Verlag. p. 409-469.

Azzara A. 2012. Impacts of vessel noise perturbations on the resident sperm whale population in the Gulf of Mexico [dissertation]. College Station: Texas A&M University.

Azzara AJ, Van Zharen WM, Newcomb JJ. 2013. Mixed-methods analytic approach for determining potential impacts of vessel noise on sperm whale click behavior. J Acoust Soc Am. 134(6):4566-4574. doi: 10.1121/1.4828819.

Bain DE, Williams R. 2006. Long-range effects of airgun noise on marine mammals: responses as a function of received sound level and distance. Paper SC/58/E35 presented at: Scientific Committee of the International Whaling Commission, June 2006, St. Kitts and Nevis. Report by Sea Mammal Research Unit, University of St. Andrews, and University of Washington. https://tethys.pnnl.gov/sites/default/files/publications/Bain-and-Williams-2006.pdf

Barkaszi MJ, Frankle A, Martin J, Poe W (CSA Ocean Sciences, Stuart, Florida). 2016. Pressure wave and acoustic properties generated by the explosive removal of offshore structures in the Gulf of Mexico. New Orleans (LA): Bureau of Ocean Energy Management, Gulf of Mexico OCS Region. 72 p. OCS Study BOEM 2016-019. Contract No.: M13PX00068. https://www.boem.gov/ESPIS/5/5505.pdf

Barlett ML, Wilson GR. 2002. Characteristics of small boat acoustic signatures. J Acoust Soc Am. 112(5): 2221. doi: http://dx.doi.org/10.1121/1.4778778

Baumann-Pickering S, McDonald MA, Simonis AE, Solsona Berga A, Merkens KP, et al. 2013. Species-specific beaked whale echolocation signals. J Acoust Soc Am. 134(3): 2293-2301. doi: 10.1121/1.4817832.

Becker EA, Forney KA, Foley DG, Smith RC, Moore TJ, et al. 2014. Predicting seasonal density patterns of California cetaceans based on habitat models. Endanger Species Res. 23: 1-22. doi: 10.3354/esr00548.

Bingham G, editor (Resolve, Inc., Washington, DC). 2011. Workshop on the Status and Applications of Acoustic Mitigation and Monitoring Systems for Marine Mammals, November 17–19, 2009, Boston, Massachusetts. New Orleans (LA): US Dept. of the Interior, Bureau of Ocean Energy Management, Regulation, and Enforcement, Gulf of Mexico OCS Region. 384 p. OCS Study BOEMRE 2011-002. Contract No.: M09PC00008

Bishop MJ, Mayer-Pinto M, Airoldi L, Firth LB, Morris RL, et al. 2017. Effects of ocean sprawl on ecological connectivity: impacts and solutions. J Exp Mar Biol Ecol. 492: 7–30. https://doi.org/10.1016/j.jembe.2017.01.021.

Bittle M, Duncan A. 2013. A review of current marine mammal detection and classification algorithms for use in automated passive acoustic monitoring. In: Proceedings of Acoustics 2013 Victor Harbor: Science, Technology, and Amenity. 17–20 November, Victor Harbor, Australia. Canberra, BC (AU): Australian Acoustical Society. p. 17–20. https://www.acoustics.asn.au/conference_proceedings/AAS2013/index.htm

Blackwell SB, Nations CS, McDonald TL, Thode AM, Mathias D, et al. 2015. Effects of airgun sounds on bowhead whale calling rates: evidence for two behavioral thresholds. PLoS ONE 10(6): e0125720. doi:0125710.0121371/journal.pone.0125720

BOEM (Bureau of Ocean Energy Management). 2013. Gulf of Mexico OCS oil and gas lease sales: 2014 and 2016; Eastern Planning Area lease sales 225 and 226—final environmental impact statement. Volume I: chapters 1–8. New Orleans (LA): Bureau of Ocean Energy Management, Gulf of Mexico Region. 710 p. OCS EIS/EA BOEM 2013-200. https://www.boem.gov/sites/default/files/boem-newsroom/Library/Publications/2013/BOEM-2013-200-v1.pdf

BOEM (Bureau of Ocean Energy Management). 2016a. Request to the National Oceanic and Atmospheric Administration for incidental take regulations governing geophysical surveys on the Outer Continental Shelf of the Gulf of Mexico. Submitted to National Marine Fisheries Service, Office of Protected Resources, Silver Spring, (MD) by Bureau of Ocean Energy Management, Sterling (VA). https://www.fisheries.noaa.gov/action/incidental-take-authorization-oil-and-gas-industry-geophysical-survey-activity-gulf-mexico

BOEM (Bureau of Ocean Energy Management). 2016b. Outer Continental Shelf oil and gas leasing program: 2017–2022. Final programmatic environmental impact statement. Volume I: chapters 1–6. Sterling (VA): Bureau of Ocean Energy Management. 359 p. OCS EIS/EA 2016-060. https://www.boem.gov/fpeis-volume1/

Bradley DL, Stern R. 2008. Underwater sound and the marine mammal acoustic environment: a guide to fundamental principles. Bethesda (MD): Marine Mammal Commission. https://www.mmc.gov/wp-content/uploads/sound_bklet.pdf

Buckland ST. 2001. Shipboard sighting surveys: methodological developments to meet practical needs. Bull Int Stat Inst, 53rd Session Proc, Book 1: 315–318.

Buckland, ST, Anderson DR, Burnham KP, Laake JL, Borchers DL, et al. 2001. Introduction to distance sampling: estimating abundance of biological populations. 448 p. Oxford (GB): Oxford University Press.

Buckstaff KC, Wells RS, Gannon JG, Nowacek DP. 2013. Responses of bottlenose dolphins (*Tursiops truncatus*) to construction and demolition of coastal marine structures. Aquat Mamm. 39(2): 174-186. doi: 10.1578/AM.39.2.2013.174

Burks, C, Mullin KD, Swartz, SL, Martinez, A. 2001. Cruise results: NOAA Ship Gordon Gunter cruise GU-OI-Ol (11) 6 February–3 April 2001, Marine mammal survey of Puerto Rico and the Virgin Islands and a study of sperm whales in the Southeastern Gulf of Mexico. Miami (FL): National Marine Fisheries Service, Southeast Fisheries Science Center. NOAA Tech Memo NMFS-SEFSC-462. https://repository.library.noaa.gov/view/noaa/8626

Calupca TA, Fristrup KM, Clark CW. 2000. A compact digital recording system for autonomous bioacoustic monitoring. J Acoust Soc Am. 108(5): 2582. doi: 10.1121/1.474359

Castellote M, Clark CW, Lammers MO. 2012. Acoustic and behavioural changes by fin whales (*Balaenoptera physalus*) in response to shipping and airgun noise. Biol Conserv. 147(1): 115-122. doi: 10.1016/j.biocon.2011.12.021

Chapman CJ, Hawkins AD. 1969. The importance of sound in fish behaviour in relation to capture by trawls. FAO Fish Rep. 621: 717-729.

Chapman NR, Price A. 2011. Low frequency deep ocean ambient noise trend in the Northeast Pacific Ocean. J Acoust Soc Am. 129(5): EL161–EL165.

Christiansen F, Rojano-Doñate L, Madsen PT, Bejder L. 2016. Noise levels of multi-rotor unmanned aerial vehicles with implications for potential underwater impacts on marine mammals. Front Mar Sci. 3: 277. doi: 210.3389/fmars.2016.00277

Clark C. 2015. Variability in the Gulf of Mexico's marine acoustic environment. Slideshow presented at: Gulf of Mexico Marine Mammal Research and Monitoring Meeting, 7–8 April 2015, New Orleans, Louisiana. https://www.mmc.gov/wp-content/uploads/Clark_variability_gom_ma_environment_0415.pdf

Collins MD. 1993. A split-step padé solution for the parabolic equation method. J Acoust Soc Am. 93(4): 1736-1742. doi: 10.1121/1.406739.

CSA (Continental Shelf Associates, Inc., Jupiter, Florida). 2004. Explosive removal of offshore structures: information synthesis report. New Orleans (LA): Minerals Management Service, Gulf of Mexico OCS Region. 236 p. OCS Study MMS 2003-070. Contract No.: 1435-01-02-CT-85237. https://www.boem.gov/ESPIS/2/3042.pdf

CSA Ocean Sciences (Continental Shelf Associates, Inc. Ocean Sciences). 2017. Press release: CSA awarded BOEM contract for analysis of seismic survey mitigation data. https://www.csaocean.com/press-releases/csa-awarded-boem-contract-for-analysis-of-seismic-survey-mitigation-data. March 21.

Crocker SE, Fratantonio FD (US Navy, Sensors and Sonar Systems Department). 2016. Characteristics of sounds emitted during high-resolution marine geophysical surveys. Herndon (VA): Bureau of Ocean Energy Management and Newport (RI): Naval Undersea Warfare Center Division and Washington (DC): US Geological Survey. 266 p. Report No.: OCS Study BOEM 2016-044 and NUWC-NPT Technical Report 12,203. Contract No.: Interagency Agreement No. M15PG00005 and Interagency Agreement No. G16P00011.

Dahl PH, de Jong CAF, Popper AN. 2015. The underwater sound field from impact pile driving and its potential effects on marine life. Acoust Today. 11:18-25.

Dassatti A, Van der Schaar M, Guerrini P, Zaugg S, Houegnigan L, et al. 2011. On-board underwater glider real-time acoustic environment sensing. Oceans 2011 IEEE—Spain. 1 - 8. doi: 10.1109/Oceans-Spain.2011.6003482.

Davis RW, Fargion GS, editors (Texas A&M University at Galveston, Texas). 1996. Distribution and abundance of cetaceans in the north-central and western Gulf of Mexico, final report. [GulfCet Program.] Volume 2: technical report. New Orleans (LA): Minerals Management Service. 380 p. Contract No. 14-35-0001-30619 and Interagency Agreement 16197. OCS Study MMS 96-0027. https://www.boem.gov/ESPIS/3/3297.pdf

Davis RW, Evans WE, Würsig B, editors (Texas A&M University at Galveston; National Marine Fisheries Service). 2000. Cetaceans, sea turtles and seabirds in the northern Gulf of Mexico: distribution, abundance and habitat associations [GulfCet II.] Volume II: technical report. New Orleans (LA) and Galveston (TX): Minerals Management Service and US Geological Survey Biological Resources Division. 383 p. Contract No.: 1445-CTO9-96-0004 and 1445-1A09-96-0009. Report No.: USGS/BRD/CR-1999-0006 and OCS Study MMS 2000-003. https://www.boem.gov/ESPIS/3/3153.pdf

DeRuiter SL, Tyack PL, Lin Y-T, Newhall AE, Lynch JF, et al. 2006. Modeling acoustic propagation of airgun array pulses recorded on tagged sperm whales (*Physeter macrocephalus*). J Acoust Soc Am. 120(6): 4100-4114. doi: 0.1121/1.2359705.

DeRuiter SL, Hansen M, Koopman HN, Westgate AJ, Tyack PL, et al. 2010. Propagation of narrow-band-high-frequency clicks: measured and modeled transmission loss of porpoise-like clicks in porpoise habitats. J Acoust Soc Am. 127(1): 560-567. doi: 10.1121/1.3257203.

DeRuiter SL, Southall BL, Calambokidis J, Zimmer WMX, Sadykova D, et al. 2013. First direct measurements of behavioural responses by Cuvier's beaked whales to mid-frequency active sonar. Biol Lett. 9(4):20130223. https://doi.org/10.1098/rsbl.2013.0223

Department of Fisheries and Oceans Canada. 2004. Review of scientific information on impacts of seismic sound on fish, invertebrates, marine turtles and marine mammals. Ottawa (ON): Department of Fisheries and Oceans. 15 p.

Di Iorio L, Clark CW. 2010. Exposure to seismic survey alters blue whale acoustic communication. Biol Lett. 6:51-54. doi: 10.1098/rsbl.2009.0651

DoN (Department of the Navy), 2018. Atlantic Fleet Training and Testing Final Environmental Impact Statement/Overseas Environmental Impact Statement. Volume 2. https://www.public.navy.mil/usff/environmental/Pages/aftt.aspx

Duggan DM, Wallace ER, Caldwell SR. 1980. Measured and predicted vibrational behavior of Gulf of Mexico platforms. Proceedings of the 12th Annual Offshore Technology Conference, 5–8 May 1980, Houston, Texas. Conference Paper OTC-3864-MS. https://doi.org/10.4043/4137-MS

Dunlop RA, Noad MJ, McCauley RD, Kniest E, Paton D, et al. 2015. The behavioural response of humpback whales (*Megaptera novaeangliae*) to a 20 cubic inch air gun. Aquat Mamm. 41(4): 412–433. doi: 10.1578/AM.41.4.2015.412.

Dunlop RA, Noad MJ, McCauley RD, Kniest E, Slade R, et al. 2016. Response of humpback whales (*Megaptera novaeangliae*) to ramp-up of a small experimental air gun array. Mar Pollut Bull. 103(1–2): 72-83. doi: 10.1016/j.marpolbul.2015.12.044.

Dyer S, Pierpont C, Sidorovskaia N. 2015. ASVs for passive acoustic monitoring: keeping track of marine wildlife in the Gulf post-Deepwater Horizon. Sea Technol. 56(10): 15–18.

Ellison WT, Racca R, Clark CW, Streever B, Frankel AS, et al. 2016. Modeling the aggregated exposure and responses of bowhead whales *Balaena mysticetus* to multiple sources of anthropogenic underwater sound. Endanger Species Res. 30: 95-108. https://doi.org/10.3354/esr00727

Esher RJ, Levenson C, Drummer TD (Mississippi State University Research Center, Waveland, MS). 1992. Aerial surveys of endangered and protected species in the *Empress II* ship trial operating area in the Gulf of Mexico. Stennis Space Center (MS): Naval Research Laboratory. 53 p. Report No. NRL/MR/7174-92-7002. https://apps.dtic.mil/docs/citations/ADA268179

Estabrook BJ, Ponirakis DW, Clark CW, Rice AN. 2016. Widespread spatial and temporal extent of anthropogenic noise across the northeastern Gulf of Mexico shelf ecosystem. Endanger Species Res. 30: 267-282. doi: 10.3354/esr00743

Finneran JJ, Schlundt CE, Branstetter BK, Trickey JS, Bowman V, et al. 2015. Effects of multiple impulses from a seismic air gun on bottlenose dolphin hearing and behavior. J Acoust Soc Am. 137(4): 1634–1646. doi: 10.1121/1.4916591

Forney KA, Ferguson MC, Becker EA, Fiedler PC, Redfern JV, et al. 2012. Habitat-based spatial models of cetacean density in the eastern Pacific Ocean. Endanger Species Res. 16: 113–133. doi: 10.3354/esr00393

Frankel AS, Zeddies D, Simard P, Mann D. 2014. Whistle source levels of free-ranging bottlenose dolphins and Atlantic spotted dolphins in the Gulf of Mexico. J Acoust Soc Am. 135: 1624–1631. doi: 10.1121/1.4863304

Frasier KE. 2015. Density estimation of delphinids using passive acoustics: a case study in the Gulf of Mexico [dissertation]. San Diego (CA): University of California San Diego.

Frasier KE, Wiggins SM, Harris D, Marques TA, Thomas L, et al. 2015. Passive acoustic monitoring of dolphins in the Gulf of Mexico: 2010–2013. Poster presented at: Gulf of Mexico Marine Mammal Research and Monitoring Meeting, New Orleans, Louisiana, 7–8 April 2015.

Frasier KE, Wiggins SM, Harris D, Marques TA, Thomas L, et al. 2016. Delphinid echolocation click detection probability on near-seafloor sensors. J Acoust Soc Am. 140: 1918–1930. doi: 10.1121/1.4962279

Fujioka E, Soldevilla MS, Read AJ, Halpin PN. 2014. Integration of passive acoustic monitoring data into OBIS-SEAMAP, a global biogeographic database, to advance spatially-explicit ecological assessments. Ecol Inform. 21: 59–73. http://doi.org/10.1016/j.ecoinf.2015.12.002

Gailey G, Würsig B, McDonald TL. 2007. Abundance, behavior, and movement patterns of western gray whales in relation to a 3-D seismic survey, northeast Sakhalin Island, Russia. Environ Monit Assess. 134: 75–91. doi 10.1007/s10661-007-9812-1.

Genesis Oil and Gas (Aberdeen, GB). 2011. Review and assessment of underwater sound produced from oil and gas sound activities and potential reporting requirements under the Marine Strategy Framework Directive. London (GB): Department of Energy and Climate Change. 72 p. Report No.: J71656-Final Report –G2. https://pdfs.semanticscholar.org/52b8/08718275e5203637ed083942fff8502adba9.pdf?_ga=2.127125581.1182822865.1571252949-1234317637.1565803837

Gillespie D, Gordon J , McHugh R, McLaren D, Mellinger DK, et al. 2008. PAMGUARD: Semiautomated, open source software for real-time acoustic detection and localisation of cetaceans. Proc Inst Acoust. 30:54–62. 9 p.

Gisiner RC. 2016. Sound and marine seismic surveys. Acoust Today. 12(4):10–18.

Goold JC, Fish PJ. 1998. Broadband spectra of seismic survey air-gun emissions, with reference to dolphin auditory thresholds. J Acoust Soc Am. 103(4): 2177–2184.Gordon J, Gillespie D, Potter J, Frantzis A, Simmonds MP, Swift R, Thompson D. 2004. A review of the effects of seismic surveys on marine mammals. Mar Technol Soc J. 37(4): 16–34.

Halpin PN, Read AJ, Best BD, Hyrenbach KD, Fujioka E, Coyne MS, Crowder LB, Freeman SA, Spoerri C. 2006. OBIS-SEAMAP: developing a biogeographic research data commons for the ecological studies of marine mammals, seabirds, and sea turtles. Mar Ecol Prog Ser. 316: 239–246. doi: 10.3354/meps316239

Hatch LT, Clark CW, Van Parijs SM, Frankel AS, Ponirakis DW. 2012. Quantifying loss of acoustic communication space for right whales in and around a U.S. national marine sanctuary. Conserv Biol. 26(6): 983–994. doi: 10.1111/j.1523-1739.2012.01908.x

Heery EC, Bishop MJ, Critchley LP, Bugnot AB, Airoldi L, et al. 2017. Identifying the consequences of ocean sprawl for sedimentary habitats. J Exp Mar Biol Ecol. https://doi.org/10.1016/j.jembe.2017.01.020.

Hermannsen L, Beedholm K, Tougaard J, Madsen PT. 2014. High frequency components of ship noise in shallow water with a discussion of implications for harbor porpoises (*Phocoena phocoena*). J Acoust Soc Am. 136(4): 1640–1653. doi: 10.1121/1.4893908

Hermannsen L, Tougaard J, Beedholm K, Nabe-Nielsen J, Madsen PT. 2015. Characteristics and propagation of airgun pulses in shallow water with implications for effects on small marine mammals. PLoS ONE. 10(7): e0133436. doi: 10.1371/journal.pone.0133436

Hernandez E, Solangi M. Kuczaj S. 2010. Time and frequency parameters of bottlenose dolphin whistles

as predictors of surface behavior in the Mississippi Sound. J Acoust Soc Am. 127:3232–8. 10.1121/1.3365254.

Hildebrand J. 2006. Physical principles of sound propagation in the marine environment. In: Herata H., editor. International workshop: impacts of seismic survey activities on whales and other marine biota, proceedings, 6–7 September 2006, Dessau, Germany. Dessau (DE): Federal Environment Agency (Umweltbundesamt). p. 22.

Hildebrand JA. 2009. Anthropogenic and natural sources of ambient noise in the ocean. Mar Ecol Progr Ser. 395: 5–20. doi: 10.3354/meps08353

Hildebrand J. 2017. Bryde's whale sonobuoy data in the NE Gulf of Mexico, 2011-07-30 to 2011-08-01. Distributed by: Gulf of Mexico Research Initiative Information and Data Cooperative (GRIIDC), Harte Research Institute, Texas A&M University-Corpus Christi. doi: 10.7266/n7v40s6r

Hildebrand JA, Gentes ZE, Johnson SC, Frasier KE, Merkens K, et al. 2013. Acoustic monitoring of cetaceans in the northern Gulf of Mexico using wave gliders equipped with high frequency acoustic recording packages. La Jolla (CA): Marine Physical Laboratory, Scripps Institution of Oceanography, University of California San Diego. MPL Tech Memo 539.

Hildebrand JA, Baumann-Pickering S, Frasier KE, Trickey JS, Merkens KP, et al. 2015a. Presence of deep-diving cetaceans in the Gulf of Mexico during and following the Deepwater Horizon oil spill. In: Monitoring status and trends of long-lived marine vertebrates as a measurable indicator of restoration and long-term health of the Gulf of Mexico Ecosystem. A special session of the 2015 Gulf of Mexico Oil Spill & Ecosystem Science Conference, 16 February 2015,Houston, Texas. p. 31–32. http://texasseagrant.org/assets/uploads/resources/15-101_Monitoring_Status_program.pdf

Hildebrand JA, Baumann-Pickering S, Frasier KE, Trickey JS, Merkens KP, et al. 2015b. Passive acoustic monitoring of beaked whale densities in the Gulf of Mexico. Sci Rep. 5: 16343. doi: 16310.11038/srep16343

Hildebrand J. 2017. Personal communication between John A. Hildebrand, Scripps Whale Acoustic Lab, and Jennifer N. Latusek-Nabholz, HDR Inc. 06 September 2017.

Holler RA. 2014. The evolution of the sonobuoy from World War II to the Cold War. US Navy J Underwater Acoust. 62: 322–346.

Horrocks J, Hamilton DC, Whitehead H. 2011. A likelihood approach to estimating animal density from binary acoustic transects. Biometrics. 67(3): 681–690. doi: 10.1111/j.1541-0420.2010.01496.x

Ioup GE, Ioup JW, Pflug LA, Tashmukhambetov AM, Sidorovskaia NA, et al. 2009. EARS buoy applications by LADC: I. Marine animal acoustics. In: Proceedings, OCEANS 2009 MTS/IEEE Conference, 26-29 October 2009, Biloxi, Mississippi. doi: 10.23919/OCEANS.2009.5422190.

Ioup GE, Ioup JW, Sidorovskaia NA, Tiemann CO, Kuczaj SA, et al. 2016. Environmental acoustic recording system (EARS) in the Gulf of Mexico. In: Au WWL, Lammers MO, editors. Listening in the ocean: new discoveries and insights on marine life from autonomous passive acoustic recorders. New York (NY): Springer. p. 117–162.

Jochens A, Biggs D, Engelhaupt D, Gordon J, Jaquet N, et al. (Texas A&M University, College Station, Texas). 2006. Sperm whale seismic study in the Gulf of Mexico. Summary report, 2002-2004. New Orleans (LA): Minerals Management Service. 345 p. OCS Study MMS 2006-034. Contract No.: 1435-01-02-CA-85186.

Jochens A, Biggs D, Benoit-Bird K, Engelhardt D, Gordon J, et al. (Texas A&M University, College Station, Texas). 2008. Sperm whale seismic study in the Gulf of Mexico: synthesis report. New Orleans (LA): Minerals Management Service. 341 p. OCS Study MMS 2008-006. Contract No.: 1435-01-02-CA-85186. https://www.boem.gov/ESPIS/4/4444.pdf

Johnson MP, Tyack PL. 2003. A digital acoustic recording tag for measuring the response of wild marine mammals to sound. IEEE J Oceanic Engineer. 28: 3–12. doi: 10.1109/JOE.2002.808212

Kearns & West (Washington, DC). 2015. Synthesis report: stakeholder webinars to inform development of a monitoring plan for marine mammals in the Gulf of Mexico. Prepared by Kearns and West for the Bureau of Ocean Energy Management. 24 p. https://www.boem.gov/Synthesis-Report-Stakeholder-Webinars/

Kimura S, Akamatsu T, Li S, Dong S, Dong L, et al. 2010. Density estimation of Yangtze finless porpoises using passive acoustic sensors and automated click train detection. J Acoust Soc Am. 128(3): 1435-1445. doi: 10.1121/1.3442574

Kirkpatrick, B. 2015. GCOOS [Gulf of Mexico Coastal Ocean Observing System] build-out plan and marine mammals. In: Cornish V, editor. Gulf of Mexico marine mammal research and monitoring meeting: summary report. Bethesda (MD): Marine Mammal Commission. p. 31–32.

Klinck H, Mellinger DK. 2011. The energy ratio mapping algorithm: A tool to improve the energy-based detection of odontocete echolocation clicks. J Acoust Soc Am. 129(4):1807–1812. doi: 10.1121/1.3531924

Küsel ET, Mellinger DK, Thomas L, Marques TA, Moretti DJ, Ward J. 2009. Beaked whale density estimation from single hydrophones by means of propagation modeling. J Acoust Soc Am. 125(4): 2589. doi: http://dx.doi.org/10.1121/1.4783840

Küsel ET, Mellinger DK, Thomas L, Marques TA, Moretti DJ, et al. 2010. Estimating beaked whale density from single hydrophones by means of propagation modeling. J Acoust Soc Am. 127(3): 1824. doi: http://dx.doi.org/10.1121/1.3384225

Küsel ET, Mellinger DK, Thomas L, Marques TA, Moretti D, et al. 2011. Cetacean population density estimation from single fixed sensors using passive acoustics. J Acoust Soc Am. 129(6): 3610–3622. http://dx.doi.org/10.1121/1.3583504.

Küsel ET, Siderius M, Mellinger DK, Heimlich SL (Portland State University, Portland, Oregon). 2015a. Application of density estimation methods to datasets collected from a glider. Arlington (VA): Office of Naval Research. 12 p. Accession No.: AD1014307. Contract No.: N00014-13-1-0769. https://apps.dtic.mil/docs/citations/AD1014307

Küsel ET, Siderius M, Mellinger DK, Heimlich SL. 2015b. Application of density estimation methods to datasets collected from a glider. J Acoust Soc Am. 138(3):1760–1761. doi: http://dx.doi.org/10.1121/1.4933563.

Kyhn LA, Tougaard J, Thomas L, Duve LR, Stenback J, et al. 2012. From echolocation clicks to animal density - acoustic sampling of harbor porpoises with static dataloggers. J Acoust Soc Am. 131(1): 550–560. doi: 10.1121/1.3662070

Kyhn LA, Jørgensen PB, Carstensen J, Bechl NI, Tougaard J, et al. 2015. Pingers cause temporary habitat displacement in the harbour porpoise *Phocoena phocoen*a. Mar Ecol Prog Ser. 526:253–265. doi: https://doi.org/10.3354/meps11181

LaBrecque E, Curtice C, Harrison J, Van Parijs SM, Halpin PN. 2015. 3. Biologically Important Areas for cetaceans within U.S. waters–Gulf of Mexico region. Aquat Mammals 41(1): 30–38. http://dx.doi.org/10.1578/AM.41.1.2015.1

Lang W. 2000. MMS acoustic studies in the Gulf of Mexico, FY 2000. The Leading Edge. 19(8): 907–909.

LePage K, Malme C, Mlawski R, Krumhansel P. 1996. Mississippi Canyon sound propagation study. Cambridge (MA): BBN Acoustic Technologies. BBN Report No. 8139.

Love M, Baldera A, Robbins C, Spies RB, Allen JR. 2015. Charting the Gulf: analyzing the gaps in long-term monitoring of the Gulf of Mexico. New Orleans (LA): Ocean Conservancy. 102 p. https://oceanconservancy.org/wp-content/uploads/2017/06/Charting-the-Gulf.pdf

Lurton X. 2010. An introduction to underwater acoustics: principles and applications. New York (NY): Springer. 680 p.

Lurton X, DeRuiter SL. 2011. Sound radiation of seafloor-mapping echosounders in the water column, in relation to the risks posed to marine mammals. Int Hydrograph Rev. 6: 7–17.

Madsen PT, Johnson M, Miller PJ, Aguilar Soto N, Lynch J, et al. 2006. Quantitative measures of air-gun pulses recorded on sperm whales (*Physeter macrocephalus*) using acoustic tags during controlled exposure experiments. J Acoust Soc Am. 120(4): 2366–2379.

Malme CI. 1995. Sound propagation. In: Richardson WJ, Greene CR Jr, Malme CI, Thomson DH, editors. Marine mammals and noise. San Diego (CA): Academic Press. p. 59–86.

Manley J, Willcox S. 2010. The Wave Glider: A persistent platform for ocean science. In: Proceedings, OCEANS ‘10 MTS/IEEE [Marine Technology Society/Institute of Electrical and Electronic Engineers] Conference, 24–27 May 2010, Sydney, Australia. doi: 10.1109/OCEANSSYD.2010.5603614

Marques TA, Thomas L, Ward J, DiMarzio N, Tyack PL. 2009. Estimating cetacean population density using fixed passive acoustic sensors: an example with Blainville’s beaked whales. J Acoust Soc Am. 125(4): 1982–1994. doi: 10.1121/1.3089590.

Marques TA, Thomas L, Munger L, Wiggins S, Hildebrand JA. 2011. Estimating North Pacific right whale *Eubalaena japonica* density using passive acoustic cue counting. Endang Species Res. 13:163–172. doi: 10.3354/esr00325.

Marques TA, Thomas L, Martin SW, Mellinger DK, Jarvis S, et al. 2012. Spatially explicit capture recapture methods to estimate minke whale abundance from data collected at bottom mounted hydrophones. J Ornithol. 152: 445–455. doi: https://doi.org/10.1007/s10336-010-0535-7

Marques TA, Thomas L, Martin SW, Mellinger DK, Ward JA, et al. 2013. Estimating animal population density using passive acoustics. Biol Rev. 88(2): 287–309. doi:10.1111/brv.12001

Martin SW, Marques TA, Thomas L, Morrissey RP, Jarvis S, et al. 2013. Estimating minke whale (*Balenoptera acutorostrata*) boing sound density using passive acoustic sensors. Marine Mammal Science 29 (1): 142–158. http://lenthomas.org/papers/MartinMMS2013.pdf

Martin SW, Thomas L, Marques TA, Morrissey RP, Jarvis S, et al. 2010. Minke whale boing vocalization density estimation at the Pacific Missile Range Facility, Hawaii. J Acoust Soc Am. 127(3): 1824. doi: http://dx.doi.org/10.1121/1.3384224

McCauley RD, Fewtrell J, Duncan AJ, Jenner C, Jenner M-N, et al. 2000a. Marine seismic surveys: analysis and propagation of air-gun signals; and effects of air-gun exposure on humpback whales, sea turtles, fishes and squid. Prepared for Australian Petroleum Production and Exploration Association. Bentley (AU): Curtin University of Technology, Centre for Marine Science and Technology. 203 p. Project: CMST 163. Report No.: R99-15.

McCauley RD, Fewtrell J, Duncan AJ, Jenner C, Jenner M-N, et al. 2000b. Marine seismic surveys: A study of environmental implications. APPEA J. 38: 692–707. https://doi.org/10.1071/AJ99048

McKenna MF, Ross D, Wiggins SM, Hildebrand JA. 2012. Underwater radiated noise from modern commercial ships. J Acoust Soc Am. 131(1): 92-103. doi: 10.1121/1.3664100

McKenna MF, Wiggins SM, Hildebrand JA. 2013. Relationship between container ship underwater noise levels and ship design, operational and oceanographic conditions. Sci Rep. 3: 1760. doi: 1710.1038/srep01760

Mellberg LE, Robinson AR, Botseas G. 1990. Modeled time variability of acoustic propagation through a Gulf Stream meander and eddies. J Acoust Soc Am. 87(3): 1044–1054. doi: http://dx.doi.org/10.1121/1.398831

Mellberg LE, Robinson AR, Botseas G. 1991. Azimuthal variation of low-frequency acoustic propagation through asymmetrical Gulf Stream eddies. J Acoust Soc Am. 89(5): 2157–2167. doi: http://dx.doi.org/10.1121/1.400909

Mellinger DK (Oregon State University, Newport, Oregon). 2015. Acoustically-equipped ocean gliders for environmental and oceanographic research. Arlington (VA): Office of Naval Research. 6 p. Contract No.: 00014-13-1-0682. Accession No.: ADA618007. https://apps.dtic.mil/docs/citations/ADA618007

Mellinger DK, Küsel ET, Thomas L, Marques T. 2009. Taming the jez monster: estimating fin whale spatial density using acoustic propagation modeling. J Acoust Soc Am. 126(4): 2229. doi: http://dx.doi.org/10.1121/1.3248985

Mellinger DK, Thode A, Martinez A. 2003. Passive acoustic monitoring of sperm whales in the Gulf of Mexico, with a model of acoustic detection distance. In: McKay M, Nides J, editors (University of New Orleans). Proceedings: Twenty-first Annual Gulf of Mexico Information Transfer Meeting, January 2002. New Orleans (LA): Minerals Management Service, Gulf of Mexico OCS Region. 748 p. OCS Study MMS 2003-005. Contract No.: 1435-00-01-CA-31060. p. 493–501.

Mellinger, DK, Roch MA, Nosal EM, Klinck H. 2015. Signal processing. In: Au WWL, Lammers MO, editors. Listening and the ocean: new discoveries and insights on marine life from autonomous passive acoustic recorders. New York (NY): Springer Science+Business Media LLC. p. 359–409.

Mellinger DK, Küsel ET, Thomas L, Marques T, Moretti D, et al. 2010. Population density of sperm whales in the Bahamas estimated using propagation modeling. J Acoust Soc Am. 127(3):1824. doi: http://dx.doi.org/10.1121/1.3384226

Merkens K. 2013. Deep-diving cetaceans of the Gulf of Mexico: acoustic ecology and response to natural and anthropogenic forces including the Deepwater Horizon oil spill [dissertation]. University of California-San Diego.

Meyer D. 2016. Glider technology for ocean observations: a review. 2016. Ocean Sci Discuss. doi: 10.5194/os-2016-40

Miksis-Olds JL, Donaghay PL, Miller JH, Tyack PL, Reynolds JE III. 2007a. Simulated vessel approaches elicit differential responses from manatees. Mar Mammal Sci. 23(3): 629–649. doi: 10.1111/j.1748-7692.2007.00133.x

Miksis-Olds JL, Donaghay PL, Miller JH, Tyack PL, Nystuen JA. 2007b. Noise level correlates with manatee use of foraging habitats. J Acoust Soc Am. 121(5): 3011–3020.

Miller PJO, Johnson MP, Madsen PT, Biassoni N, Quero M, et al. 2009. Using at-sea experiments to study the effects of airguns on the foraging behaviour of sperm whales in the Gulf of Mexico. Deep-Sea Res I. 56(7): 1168–1181. doi: 10.1016/j.dsr.2009.02.008

Mitson R, Dalen J. 2007. Fishing vessels as sampling platforms. In: Karp WA, editor. Collection of acoustic data from fishing vessels. Copenhagen (DK): International Council for the Exploration of the Sea [ICES]. ICES Res Coop Rep. No. 287. p 19–29.

MMO (Marine Management Organisation). 2015. Modelled mapping of continuous underwater noise generated by activities. A report produced for the Marine Management Organisation, Technical Annex. MMO Project No: 1097. https://www.gov.uk/government/publications/underwater-noise-1097

Moretti D, Marques TA, Thomas L, DiMarzio N, Dilley A, et al. 2010. A dive counting density estimation method for Blainville's beaked whale (*Mesoplodon densirostris*) using a bottom-mounted hydrophone field as applied to a Mid-Frequency Active (MFA) sonar operation. Appl Acoust. 71: 1036–1042. doi: 10.1016/j.apacoust.2010.04.011

Moretti D, Thomas L, Marques T, Harwood J, Dilley A, et al. 2014. A risk function for behavioral disruption of Blainville's beaked whales (*Mesoplodon densirostris*) from mid-frequency active sonar. PLoS ONE. 9(1): e85064. doi: 85010.81371/journal.pone.0085064

Mullin KD. 2001. NOAA Ship *Gordon Gunter* cruise GU-01-04 (13), 17 July–2 August 2001: a study of sperm whales in the north-central Gulf of Mexico. Unpublished cruise report. Pascagoula (MS): National Marine Fisheries Service.

Mullin K, Hoggard W, Roden C, Lohoefener R, Rogers C, et al (National Marine Fisheries Service, Pascagoula, Mississippi). 1991. Cetaceans on the upper continental slope in the north-central Gulf of Mexico. New Orleans (LA): Minerals Management Service. 118 p. OCS Study MMS 91-0027. Interagency Agreement No.: 14-12-0001-30398. https://espis.boem.gov/final%20reports/3641.pdf

NEFSC (Northeast Fisheries Science Center, Woods Hole, Massachusetts)), SEFSC (Southeast Fisheries Science Center, Miami, Florida). 2012. A comprehensive assessment of marine mammal, marine turtle, and seabird abundance and spatial distribution in US waters of the western North Atlantic Ocean [AMAPPS]. Annual report to Bureau of Ocean Energy Management, Sterling, Virginia. Woods Hole (MA): National Marine Fisheries Service, Northeast Fisheries Science Center; Miami (FL): National Marine Fisheries Service, Southeast Fisheries Science Center. 121 p. Inter-Agency Agreement No.: M10PG00075 and NEC-11-009.

Nedwell JR, Edward B. 2004. A review of measurements of underwater man-made [sic] noise carried out by Subacoustech Ltd, 1993–2003. Subacoustech Report ref: 534R0109. Report submitted to Chevron Texaco Ltd. https://pebbleprojecteis.com/files/e4016575-7325-44d7-b7de-12b271076f4a

Nelson MD, Koenig CC, Coleman FC, Mann DA. 2011. Sound production of red grouper *Epinephelus morio* on the West Florida Shelf. Aquat Biol. 12: 97–108. doi: 10.3354/ab00325

Newcomb J, Fisher R, Field R, Rayborn G, Kuczaj S, et al. 2002. Measurements of ambient noise and sperm whale vocalizations in the northern Gulf of Mexico using near bottom hydrophones. IEEE J Oceanic Eng. 3: 1365–1371. doi: 10.1109/OCEANS.2002.1191837

Newcomb JJ, Snyder MA, Hillstrom WR, Goodman R. 2007. Measurements of ambient noise during extreme wind conditions in the Gulf of Mexico. In: Proceedings, OCEANS 2007 MTS [Marine Technology Society]/IEEE [Institute of Electrical and Electronic Engineers] Conference, 8–21 June 2007, Aberdeen, Scotland. doi: 10.1109/OCEANS.2007.4449256.

Newcomb JJ, Stanic S, Cranford A, Vanderpool D, Solangi M. 2008. Ambient noise measurements in the Mississippi Sound. Stennis Space Center (MS): Naval Research Laboratory; Gulfport (MS): Institute for Marine Mammal Studies. 23 p. Report No.: NRL/MR/7185-08-9117.

Newcomb JJ, Tashmukhambetov AM, Ioup GE, Ioup JW, Sidorovskaia NA, et al. 2009. EARS buoy applications by LADC: II. 3-D seismic airgun array characterization. In: Proceedings, OCEANS 2009 MTS [Marine Technology Society]/IEEE [Institute of Electrical and Electronic Engineers] Conference, 26–29 October 2009, Biloxi, Mississippi. https://ieeexplore.ieee.org/document/5422198

NMFS (National Marine Fisheries Service). 2016. Technical guidance for assessing the effects of anthropogenic sound on marine mammal hearing: underwater acoustic thresholds for onset of permanent and temporary threshold shifts. Silver Spring (MD): National Marine Fisheries Service, Office of Protected Resources. 189 p. NOAA Tech Memo NMFS-OPR-55.

National Marine Fisheries Service (NMFS). 2018. 2018 Revisions to: Technical guidance for assessing the effects of anthropogenic sound on marine mammal hearing (version 2.0): underwater thresholds for onset of permanent and temporary threshold shifts. U.S. Dept. of Commerce, NOAA Technical Memorandum NMFS-OPR-59. 167 p.

NMFS SEFSC (National Marine Fisheries Service-Southeast Fisheries Science Center). 2003. Cruise results, NOAA Ship *Gordon Gunter* cruise GU-03-02, 12 June–18 August 2003: a study of oceanic cetaceans in the northern Gulf of Mexico. Unpublished cruise report. Pascagoula (MS): National Marine Fisheries Service.

NMFS SEFSC (National Marine Fisheries Service-Southeast Fisheries Science Center). 2004a. Cruise results, NOAA Ship *Gordon Gunter* cruise GU-04-03 (028), 22 June–19 August: a survey for abundance and distribution of cetaceans in the U.S. mid-Atlantic with an emphasis on pilot whales. Unpublished cruise report. Pascagoula (MS): National Marine Fisheries Service.

NMFS SEFSC (National Marine Fisheries Service, Southeast Fisheries Science Center). 2004b. Cruise results, NOAA Ship *Gordon Gunter* cruise GU-04-02 (027), 13 April–11 June 2004: a study of sperm whales and other oceanic cetaceans in the Northern Gulf of Mexico. Unpublished cruise report. Pascagoula (MS): National Marine Fisheries Service.

Normandeau Associates, Inc. (Bedford, New Hampshire). 2012. Effects of noise on fish, fisheries, and invertebrates in the U.S. Atlantic and Arctic from energy industry sound-generating activities: workshop report. Washington, DC: Bureau of Ocean Energy Management. 361 p. Report No.: BOEM 2013-300. Contract No.: M11PC00031. https://marinecadastre.gov/espis/#/search/study/23174

Norris T, Jacobsen J. 2015. Passive listening, active mitigation: passive acoustic monitoring and mitigation of oceanic delphinids during mid-water net trawl sampling on NOAA's R/V *Pisces*. Poster presented at: Gulf of Mexico Marine Mammal Research and Monitoring Meeting, 7–8 April 2015, New Orleans, Louisiana. https://www.mmc.gov/wp-content/uploads/Norris_passive_listening_active_mitigation_0415.pdf

NOAA (National Oceanic and Atmospheric Administration). n.d. Phase 1 – CetSound. https:// https://cetsound.noaa.gov/cetsound

NRC (National Research Council). 2003. Ocean noise and marine mammals. Washington, DC: National Academies Press. 204 p.

NRC (National Research Council). 2005. Marine mammal populations and ocean noise: Determining when noise causes biologically significant effects. Washington, DC: National Academies Press. 142 p.

NSWC PCD (Naval Surface Warfare Center Panama City Division). 2012. Airborne mine neutralization system RDT&E event marine species monitoring, vessel monitoring surveys, 5–10 December 2011: trip report. Submitted to Naval Surface Warfare Center Panama City Division, Panama City (FL), under Contract No. CON0053537, Delivery Order H18, issued to HDR Inc., Niceville (FL).

Ogden G. 2010. Extraction of small boat harmonic signatures from passive sonar [thesis]. Portland (OR): Portland State University.

Oswald, M, Oswald, JN, Lammers, MO, Rankin, S, Au, WWL. 2011. Integration of real-time odontocete call classification algorithm into PAMGUARD signal processing software. J Acoust Soc Am. 129(4): 2639. doi: 10.1121/1.3588787

Oswald JN, Rankin S, Barlow J, Lammers MO. 2007. A tool for real-time acoustic species identification of delphinid whistles. J Acoust Soc Am. 122(1): 587–595. doi: 10.1121/1.2743157

Parks SE, Clark CW, Tyack PL. 2007. Short- and long-term changes in right whale calling behavior: the potential effects of noise on acoustic communication. J Acoust Soc Am. 122(6): 3725–3731. doi:10.1121/1.2799904

Paulos RLD. 2007. Sperm whale (*Physeter macrocephalus*) codas and creaks in the northern Gulf of Mexico: classification, comparison, and co-occurrence [dissertation]. Hattiesburg (MS): University of Southern Mississippi.

Popper AN, Hawkins AD, Fay RR, Mann DA, Bartol S, et al. 2014. Sound exposure guidelines for fishes and sea turtles: a technical report prepared by ANSI-Accredited Standards Committee S3/SC1 and registered with ANSI. ASA S3/SC1.4 TR-2014. New York (NY): Acoustical Society of America and Springer. 73 p.

Rankin S. 1999. The potential effects of sounds from seismic exploration on the distribution of cetaceans in the northern Gulf of Mexico [master's thesis]. College Station (TX): Texas A&M University.

Redfern JV, Ferguson MC, Becker EA, Hyrenbach KD, Good C, et al. 2006. Techniques for cetacean-habitat modeling. Mar Ecol Progr Ser. 310: 271–295. https://doi.org/10.3354/meps310271

Rice AN, Palmer KJ, Tielens JT, Muirhead CA, Clark CW. 2014a. Potential Bryde's whale (*Balaenoptera edeni*) calls recorded in the northern Gulf of Mexico. J Acoust Soc Am. 135:3066–3076. doi: 10.1121/1.4870057

Rice AN, Tielens JT, Morano JL, Estabrook BJ, Shiu Y, et al. 2014b. Passive acoustic monitoring of marine mammals in the northern Gulf of Mexico: June 2010–March 2012. Prepared for BP Production & Exploration, Inc., Houston (TX) and the National Oceanic and Atmospheric Administration, Silver Spring (MD) by Ithaca (NY): Bioacoustics Research Program, Cornell Lab of Ornithology, Cornell University. BRP Technical Report 14-07.

Rice AN, Tielens JT, Morano JL, Estabrook BJ, Shiu Y, Clark CW. 2015. Using passive acoustic monitoring to evaluate acute impacts and chronic influences of the Deepwater Horizon oil spill on large whale species. In: Monitoring status and trends of long-lived marine vertebrates as a measurable indicator of restoration and long-term health of the Gulf of Mexico ecosystem. A special session of the 2015 Gulf of Mexico Oil Spill & Ecosystem Science Conference, 16 February 2015, Houston, Texas. p. 34–35.

Richardson WJ, Greene CR, Jr, Malme CI, Thomson DH. 1995. Marine mammals and noise. San Diego (CA): Academic Press. 576 p.

Richardson WJ, Moulton VD, Abgrall P, Cross WE, Holst M, et al. (LGL Ecological Research Associates Inc., Bryan, Texas). 2010. Appendix E: review of the effects of seismic and oceanographic sonar effects on marine mammals. In: 2011. Final programmatic environmental impact statement/overseas environmental impact statement for marine seismic research funded by the National Science foundation or conducted by the U.S. Geological Survey. 981 p. Arlington (VA): National Science Foundation. p. E-13–E-60. https://www.nsf.gov/geo/oce/envcomp/peis_marine_seismic_research/appendix_e-effects_of_seismic_%2B_sonar_on_marmam.pdf

Roberts JJ, Best BD, Mannocci L, Fujioka E, Halpin PN, et al. 2016. Habitat-based cetacean density models for the U.S. Atlantic and Gulf of Mexico. Sci Rep 6: 22615. doi: 10.1038/srep22615

Roch MA, Batchelor H, Baumann-Pickering S, Berchok CL, Cholewiak D, et al. 2016. Management of acoustic metadata for bioacoustics. Ecol Inform. 31: 122–136. http://doi.org/10.1016/j.ecoinf.2015.12.002

Roch MA, Brandes TS, Patel B, Barkley Y, Baumann-Pickering S, et al. 2011. Automated extraction of odontocete whistle contours. J Acoust Soc Am. 130(4): 2212–2223. doi: 10.1121/1.3624821

Roch MA, Baumann-Pickering S, Batchelor H, Hwang D, Širović A, et al. 2013. Tethys: A workbench and database for passive acoustic metadata. In: Proceedings of OCEANS 2013 MTS/IEEE Conference, 23–26 September 2013, San Diego, CA. doi: 10.23919/OCEANS.2013.6741361

Rosel PE, Corkeron P, Engleby L, Epperson D, Mullin KD, et al. 2016. Status review of Bryde's whales (*Balaenoptera edeni*) in the Gulf of Mexico under the Endangered Species Act. Lafayette (LA): National Marine Fisheries Service. NOAA Tech Memo NMFS-SEFSC-692. 149 p.

Shooter JA, DeMary TE, Koch RA. 1982. Ambient noise in the western Gulf of Mexico. Austin (TX): Applied Research Laboratories, University of Texas. Report No. ARL-TR-82-15.

Shyu H-J, Hillson R. 2002. Integrating ocean acoustic propagation models and marine mammal auditory models. In: Proceedings, Oceans 2002 MTS/IEEE Conference, 29–31 October 2002, Biloxi, Mississippi. doi: 10.1109/OCEANS.2002.1192117

Sidorovskaia N, Ames A, Fuselier J, Greenhow D, Griffin S, et al. 2015a. Proceedings of the LADC-GEMM 2015 Gulf of Mexico experiment, part II: recovery cruise, LADC-GEMM Gulf ecological monitoring and modeling, October 26–October 30, 2015, R/*V Pelican* Cruise PE16-10, Cocodrie to Cocodrie. Cruise Report.

Sidorovskaia N, Griffin S, Küsel E, Lee K, Lingsch B, et al. 2015b. Proceedings of the LADC-GEMM 2015 Gulf of Mexico experiment, LADC-GEMM Gulf ecological monitoring and modeling, June 23–July 2, 2015, *R/V Pelican* Cruise PE15-28, Cocodrie to Cocodrie. Cruise Report.

Sidorovskaia NA, Li K. 2017. Decadal evolution of the northern Gulf of Mexico soundscapes. Proc Mtg Acoust. 27: 040014. doi: 040010.041121/040012.0000382

Sidorovskaia NA, Ioup GE, Ioup JW, Caruthers JW. 2004. Acoustic propagation studies for sperm whale phonation analysis during LADC experiments. In: Porter MB, Siderius M, Kuperman WA, editors. High frequency ocean acoustics: High Frequency Ocean Acoustics Conference, La Jolla, California, 1–5 March 2004. Melville (NY): American Institute of Physics. p. 285–295.

Simard P. 2012. Dolphin sound production and distribution on the West Florida Shelf [dissertation]. Tampa (FL): University of South Florida.

Simard P, Hibbard AL, McCallister KA, Frankel AS, Zeddies DG, et al. 2010. Depth dependent variation of the echolocation pulse rate of bottlenose dolphins (*Tursiops truncatus*). J Acoust Soc Am. 127(1): 568–578. doi: 10.1121/1.3257202

Simard P, Lace N, Gowans S, Quintana-Rizzo E, Kuczaj SA, et al. 2011. Low frequency narrow-band calls in bottlenose dolphins (*Tursiops truncatus*): signal properties, function, and conservation implications. J Acoust Soc Am. 130(5): 3068–3076. doi: 10.1121/1.3641442

Simard P, Wall CC, Allen JB, Wells RS, Gowans S, et al. 2015. Dolphin distribution on the West Florida Shelf using visual surveys and passive acoustic monitoring. Aquat Mamm. 41: 167–187. doi: 10.1578/AM.41.2.2015.167

Simard P, Wall KR, Mann DA, Wall CC, Stallings CD. 2016. Quantification of boat visitation rates at artificial and natural reefs in the eastern Gulf of Mexico using acoustic recorders. PLoS ONE. 11(8): e0160695. doi:10.1371/journal.pone.0160695

Širović A, Hildebrand JA. 2011. Using passive acoustics to model blue whale habitat off the western Antarctic Peninsula. Deep-Sea Res II. 58: 1719–1728. doi:10.1016/j.dsr2.2010.08.019

Širović A, Hildebrand JA (Scripps Institution of Oceanography, La Jolla, CA). 2015. Blue and fin whale habitat modeling from long-term year-round passive acoustic data from the Southern California Bight. 11 p. Award No.: N000141210904. https://www.onr.navy.mil/reports/FY12/mbhilde2.pdf

Širović A, Hildebrand JA, Wiggins SM. 2007. Blue and fin whale call source levels and propagation range in the Southern Ocean. J Acoust Soc Am. 122(2): 1208–1215. doi: 10.1121/1.2749452

Širović A, Bassett HR, Johnson SC, Wiggins SM, Hildebrand JA. 2014. Bryde's whale calls recorded in the Gulf of Mexico. Mar Mammal Sci. 30: 399–409. doi: 10.1111/mms.12036

Smultea MA, Lomac-MacNair K. 2016. Assessing "observer effects" from a research aircraft on behavior of three Delphinidae species (*Grampus griseus*, *Delphinus delphis*, and *Orcinus orca*). Wildl Biol Pract. 12: 75–90. doi: 10.2461/wbp.2016.12.8

Smultea MA, Mobley JR Jr., Fertl D, Fulling GL. 2008. An unusual reaction and other observations of sperm whales near fixed-wing aircraft. Gulf Caribb Res. 20: 75–80. https://doi.org/10.18785/gcr.2001.10

Snyder MA. 2007. Long-term ambient noise statistics in the Gulf of Mexico [dissertation]. New Orleans (LA): University of New Orleans.

Snyder MA. 2009. Effects of hurricanes on ambient noise in the Gulf of Mexico. In: Proceedings, OCEANS 2009 MTS/IEEE Conference, 26–29 October 2009, Biloxi, Mississippi. doi: 10.23919/OCEANS.2009.5422087

Snyder MA, Orlin PA. 2007. Ambient noise classification in the Gulf of Mexico. In: Proceedings, OCEANS 2007 MTS/IEEE Conference, 8–21 June 2007, Aberdeen, Scotland. doi: 10.1109/OCEANS.2007.4449320

Soldevilla MS, Wiggins SM, Hildebrand JA, Oleson EM, Ferguson MC. 2011. Risso's and Pacific white-sided dolphin habitat modeling from passive acoustic monitoring. Mar Ecol Progr Ser. 423: 247–260. doi: 10.3354/meps08927

Soloway AG, Dahl PH (University of Washington, Seattle, WA; HDR, San Diego, CA). 2015. Noise source level and propagation measurement of underwater detonation training at the Silver Strand Training Complex, Naval Base Coronado, Coronado, CA. Pearl Harbor (HI): US Pacific Fleet. 40 p. Contract No.: N62470-10-3011. Project No.: CTO OE31.

Sousa-Lima RS, Norris TF, Oswald JN, Fernandes DP. 2013. A review and inventory of fixed autonomous recorders for passive acoustic monitoring of marine mammals. Aquat Mamm. 39(1): 23–53. doi: 10.1578/AM.39.1.2013.23

Southall BL, Moretti D, Abraham B, Calambokidis J, DeRuiter SL, et al. 2012. Marine mammal behavioral response studies in southern California: advances in technology and experimental methods. Mar Technol Soc J. 46(4): 48–59.

Stanic S., Brown RA, Kennedy ET, Malley DA, Solangi MA. 2007. Ambient noise measurements in and around the Gulfport Mississippi Harbor and its potential influence on marine mammals. Stennis Space Center (MS): Naval Research Laboratory. 21 p. Report No.: NRL/MR/7184-07-9049. Project No.: 71-M297-X4.

Stone JC. 2003. The effects of seismic activity on marine mammals in UK waters, 1998–2000. Aberdeen (GB): Joint Nature Conservation Committee. 74 p. JNCC Report No. 323.

Tashmukhambetov AM, Ioup GE, Ioup JW, Sidorovskaia NA, Newcomb JJ. 2008. 3-Dimensional seismic array calibration study: experiment and modeling. J Acoust Soc Am. 123(6):4094–4108. doi: 10.1121/1.2902185

Tennessen JB, Parks SE. 2016. Acoustic propagation modeling indicates vocal compensation in noise improves communication range for North Atlantic right whales. Endang Species Res. 30: 225–237. https://doi.org/10.3354/esr00738

Thode, A., Mellinger, D.K., Stienessen, S., Martinez, A., Mullin, K., 2002. Depth-dependent acoustic features of diving sperm whales (*Physeter macrocephalus*) in the Gulf of Mexico. Journal of the Acoustical Society of America 112, 308-321.

Thomas L, Marques T, Borchers D, Harris C, Moretti D, et al. (CREEM, University of St. Andrews FIFE, Scotland, UK). 2009. DECAF–density estimation for cetaceans from passive acoustic fixed sensors. 7 p. National Oceanographic Partnership Program (NOPP).

Thomas L, Buckland ST, Rexstad EA, Laake JL, Strindberg S, et al. 2010. Distance software: design and analysis of distance sampling surveys for estimating population size. J Appl Ecol. 47: 5–14. doi: 10.1111/j.1365-2664.2009.01737.x

Tiemann CO, Thode AM, Straley J, O'Connell V, Folkert K. 2006. Three-dimensional localization of sperm whales using a single hydrophone. J Acoust Soc Am. 120(4): 2355–2365.

Tolstoy M, Diebold JB, Webb SC, Bohnenstiehl DR, Chapp, E, et al. 2004. Broadband calibration of R/V *Ewing* seismic sources. Geophys Res Lett, 31, L14310. doi: 10.1029/2004GL020234.

Tyack P. 2009. Acoustic playback experiments to study behavioral responses of free-ranging marine animals to anthropogenic sound. Mar Ecol Progr Ser. 395: 187–200. https://doi.org/10.3354/meps08363

Tyack PL, Johnson MP, Madsen PT, Miller PJ, Lynch J. 2006. Biological significance of acoustic impacts on marine mammals: examples using an acoustic recording tag to define acoustic exposure of sperm whales, *Physeter catodon*, exposed to airgun sounds in controlled exposure experiments. Eos, Transactions of the American Geophysical Union 87(36), Joint Assembly Supplement, Abstract OS42A-02. 23–26 May, Baltimore, MD.

Urick RJ (Catholic University, Washington, DC). 1984. Ambient noise in the sea. Washington (DC): Naval Sea Systems Command. 194 p.

Urick RJ. 1972. Noise signature of an aircraft in level flight over a hydrophone in the sea. J Acoust Soc Am. 52(3, Part 2): 993–999.

Van Parijs S, Southall B, editor. 2007. Report of the 2006 NOAA National Passive Acoustics Workshop: Developing a strategic program plan for NOAA's Passive Acoustics Ocean Observing System (PAOOS), Woods Hole, Massachusetts, 11–13 April 2006. Seattle (WA): National Marine Fisheries Service. NOAA Tech Memo NMFS-F/SPO-81. https://repository.library.noaa.gov/view/noaa/4056

Waddell K, Olson S. 2015. Opportunities for the Gulf Research Program. Monitoring ecosystem restoration and deep water environments. Summary of a workshop. Washington (DC): National Academies Press. 52 p.

Wall C, Simard P, Lindemuth M, Lembke C, Naar DF, et al. 2014. Temporal and spatial mapping of red grouper *Epinephelus morio* sound production. J Fish Biol. 85(5): 1470–1488. doi: https://doi.org/10.1111/jfb.12500

Wall CC, Lembke C, Mann DA. 2012. Shelf-scale mapping of sound production by fishes in the eastern Gulf of Mexico using autonomous glider technology. Mar Ecol Progr Ser. 449: 55–64. doi: https://doi.org/10.3354/meps09549

Wiggins SM (Scripps Institution of Oceanography, Sand Diego, CA). 2009. Integration and Use of a High Frequency Acoustic Recording Package (HARP) on a Wave Glider. Sunnyvale (CA): Liquid Robotics, Inc. (Boeing). 15 p. Report No.: MPL TM-528.

Wiggins SM, Hildebrand JA. 2007. High-frequency Acoustic Recording Package (HARP) for broad-band, long-term marine mammal monitoring. In: International Workshop on Scientific Use of Submarine Cables & Related Technologies 2007. Tokyo (JP): Institute of Electrical and Electronics Engineers. p. 551–557. doi: 10.1109/UT.2007.370760

Wiggins SM, Hall JM, Thayre BJ, Hildebrand JA. 2016. Gulf of Mexico low-frequency ocean soundscape impacted by airguns. J Acoust Soc Am. 140(1):176–183. doi: 10.1121/1.4955300

Wood SN. 2006. Generalized additive models: an introduction with R. Boca Raton (FL): Chapman & Hall/CRC. 410 p.

Würsig B, Jefferson TA, Schmidly DJ. 2000. The marine mammals of the Gulf of Mexico. College Station (TX): Texas A&M University Press. 256 p. Wyatt R. 2008. Joint Industry Programme on Sound and Marine Life: review of existing data on underwater sounds produced by the oil and gas industry, Issue 1. Prepared by Seiche Measurements Ltd. for Joint Industry Programme on Sound and Marine Life. Seiche Measurements Limited Ref – S186. https://gisserver.intertek.com/JIP/DMS/ProjectReports/Cat1/JIP-Proj1.4_Soundsinventory_Seiche_2008.pdf

Yazvenko SB, McDonald TL, Blokhin SA, Johnson SR, Meier SK, et al. 2007. Distribution and abundance of western gray whales during a seismic survey near Sakhalin Island, Russia. Environ Monitor Assess. 134(1-3): 45-73. doi 10.1007/s10661-10007-19809-10669

Zeddies DG, Zykov M, Yurk H, Deveau T, Bailey L, et al. (JASCO Applied Sciences, Dartmouth, Nova Scotia, CAN). 2015. Acoustic propagation and marine mammal exposure modeling of geological and geophysical sources in the Gulf of Mexico: 2016–2025 annual acoustic exposure estimates for marine mammals. Sterling (VA): Bureau of Ocean Energy Management. JASCO Document 00976, Version 3.0. https://www.boem.gov/2015-July15-BOEM-Phase-2-Acoustic-Exposure-Report/

Ziegwied AT, Dobbin V, Dyer S, Pierpont C, Sidorovskaia N. 2016. Using autonomous surface vehicles for passive acoustic monitoring (PAM). In: Proceedings of OCEANS 2016 MTS/IEEE Conference, 19–23 September 2016, Monterey, CA. doi: 10.1109/OCEANS.2016.7761380

Appendix 1. Keywords for Literature Search

Monitoring and/or Research Keywords

Monitoring and/or Research
acoustic dataset
acoustic mapping
acoustic modeling
acoustic propagation
acoustic tag
aircraft noise
airgun (sound)
algorithm
ambient noise/sound
anthropogenic noise
ASVs
autonomous acoustic instrument
AUVs
Baseline noise
biological sound sources (ex. fish, invertebrates)
construction noise sources
Classification
Datalogging tag (DTAG)
DECAF (Density Estimation for Cetaceans from Passive Acoustic Fixed Sensors)
Density modeling
Detection
EARS
electronic tag data
explosives (platform removal)
explosives (military)
Gliders
HARPs
hydrophones
marine mammal observations
MARUs
natural sound sources (storm and/or hurricane; rain, rainfall, precipitation)
noise exposure criteria
noise level
noise statistics
ocean noise

Monitoring and/or Research
oceanographic
operational noise (oil and gas platforms)
passive acoustic monitoring
passive acoustic monitoring during seismic survey
pile driving
satellite-tracked radio tag (S-TAG)
signal processing
seismic sound
seismic airgun array
shipping noise
sonar
Song Meter SM3 acoustic recorder
Song Meter SM2 acoustic recorder
sound mapping
sound propagation
sound propagation, canyon
towed acoustic array
towed hydrophone array
UUVs
vessel (sound)
wave noise
weather noise
Wenz curves
wind noise

Regions and/or Events Keywords

Regions and/or Events
Biologically Important Areas (BIAs)
Central Planning Area
Desoto Canyon
Deepwater Horizon
Eastern Planning Area
Gulf of Mexico
Mississippi Canyon
Mississippi Valley
Outer Continental Shelf
Panama City

Regions and/or Events
Shelf
Shelf break
Slope
Western Planning Area

Focus Animals Keywords

Focus Animals
beaked whales
Bryde's whales
cetaceans
dolphins
marine mammals
Risso's dolphins
sperm whales
whales

Researchers, Funding Sources, Monitoring Programs Keywords

Researchers, Funding Sources, Monitoring Programs
Abadi
Ackleh
Benoit-Bird
Berchok
Biggs, Douglas
Bingham
Bio-Waves
BOEM
Center for the Integrated Modeling and Analysis of the Gulf Ecosystem (C-IMAGE) C-IMAGE Institutions: University of South Florida; Eckerd College; Florida State; Institute of Technology; Mote Marine Laboratory; Scripps; Pennsylvania State University; Hamburg University of Technology; Texas A&M University; Texas A&M University-Corpus Christi; University of Calgary; University of Miami; Universidad Nacional Autónoma de México; University of Florida; University of West Florida; Virginia Institute of Marine Sciences; University of Western Australia; NHL Stenden University of Applied Sciences, Terschelling [the Netherlands]; Woods Hole Oceanigraphic Institution; Mind Open Media; Florida Institute of Oceanography
CetSound (Researchers: Gedamke, Ferguson, Harrison, Hatch, Henderson, Porter, Southall, Van Parijs)
Cornell University
Cornish
Gordon
CREEM

Researchers, Funding Sources, Monitoring Programs
Dauphin Island
Dudzinski
Frasier
Gulf of Mexico Research Initiative
Howard, Matt
Hildebrand
Ioup
Industry Research Funding Coalition
Joint Industry Programme
Jochens, Ann
Johnson, Mark
Littoral Acoustic Demonstration Center-Gulf Ecological Monitoring and Modeling (LADC GEMM) Institutions: University of Louisiana at Lafayette; University of New Orleans; University of Southern Mississippi; Oregon State University; Proteus Technologies, LLC; R2Sonic, LLC; ASV Global; and Seiche Measurements Limited
Lang, Bill
Littoral Acoustic Demonstration Center
Mate
Mellinger
Merkens
MMS
Mullin, Keith
Naval Oceanographic office
NSF
Natural Resource Damage Assessment partners
Navy
Newcomb, Joal
NMFS
NOAA
Office of Naval Research
Olson
Pierpoint
Rice
Scripps
Sidorovskaia
Simard
Snyder, Mark
Southall

Researchers, Funding Sources, Monitoring Programs
SWAMP (Sperm Whale Acoustic Monitoring Program)
SWSS (Sperm Whale Seismic Study)
Texas A&M University
The Nature Conservancy
Tiemann
Thode
Tyack
University of Louisiana
University of St. Andrews, UK
USGS
Waddell
WHOI
Wiggins
Wildlife Acoustics
Wursig

The Department of the Interior Mission

As the Nation's principal conservation agency, the Department of the Interior has responsibility for most of our nationally owned public lands and natural resources. This includes fostering sound use of our land and water resources; protecting our fish, wildlife, and biological diversity; preserving the environmental and cultural values of our national parks and historical places; and providing for the enjoyment of life through outdoor recreation. The Department assesses our energy and mineral resources and works to ensure that their development is in the best interests of all our people by encouraging stewardship and citizen participation in their care. The Department also has a major responsibility for American Indian reservation communities and for people who live in island territories under US administration.

BOEM
Bureau of Ocean Energy Management

The Bureau of Ocean Energy Management

As a bureau of the Department of the Interior, the Bureau of Ocean Energy (BOEM) primary responsibilities are to manage the mineral resources located on the Nation's Outer Continental Shelf (OCS) in an environmentally sound and safe manner.

The BOEM Environmental Studies Program

The mission of the Environmental Studies Program (ESP) is to provide the information needed to predict, assess, and manage impacts from offshore energy and marine mineral exploration, development, and production activities on human, marine, and coastal environments.

Appendix B: Monitoring Instrument Specifications

Three different types of stationary moorings equipped with sensors (hydrophones) and recording systems were used for data collection, namely RHs, EARS, and SHRU VLAs. Additionally, two separate mobile autonomous platforms (Seaglider™) were also deployed within selected portions of the study area to collect data in between the stationary moorings. The different data recording systems differed in detail such as depth rating, battery capability, data storage capability, sampling rates and type of data stored. Between the different systems there is a trade-off between the schedule, power, and storage under similar conditions. There is also a trade-off between using stationary and mobile data collection platforms. Additional specifications for each instrument type are presented below.

B.1 Rockhoppers

RHs are a newer version of the bottom-mounted marine autonomous recording buoys developed in the late 1990s by the Center for Conservation Bioacoustics at the Cornell Laboratory of Ornithology (Calupca et al. 2000) (**Figure B-1**). The RHs deployed under the GOM PAM MPs are small and compact versions that are encased in a 17-inch glass sphere. They are capable of recording with a sampling rate as high as 384 kHz with 24-bit resolution, are depth rated to 3,500 m, and can be deployed from a research vessel with only a few people to handle equipment for each deployment.

The RHs had an effective recording bandwidth of 10 Hz to 75 kHz; the bandwidth was optimized for recording cetacean species that occur in the survey area. They were programmed to collect data continuously at a 197-kHz sampling rate and 24-bit resolution. The lower sampling rate also reduced battery power demand, therefore extending the deployment duration. The true dynamic range of the system at the 197-kHz sampling rate is approximately 17.5 bits (107 dB). The analog system sensitivity is shown in **Figure B-2** . The clipping level of the analog-to-digital converter is ± 5 Volts.

The electronic noise floor is illustrated in **Figure B-2**. All units were fully characterized prior to deployment. One representative RH hydrophone was sent to the Naval Undersea Warfare Center (NUWC), Rhode Island, for characterization at 3 degrees Celsius and 1,000 pounds per square inch (psi) pressure. The sensitivity curve provided by NUWC for this hydrophone was universally applied to all units (see **Section 2.6** for additional details on the calibration process).

The RHs were deployed on a short (approximately 10-m) mooring, which makes deployment and recovery easy. The hydrophone sits approximately 11 m above the seafloor and is separated from the glass sphere by approximately 20 centimeters to minimize acoustic interference. The overall buoyancy of the system is approximately +5 kilograms, which results (depending on oceanographic conditions) in ascent rates of approximately 1 m/second during recovery. Each RH is equipped with a pressure switch-enabled recovery system featuring a GPS/Iridium transmitter, a VHF radio transmitter, and a LED-flasher.

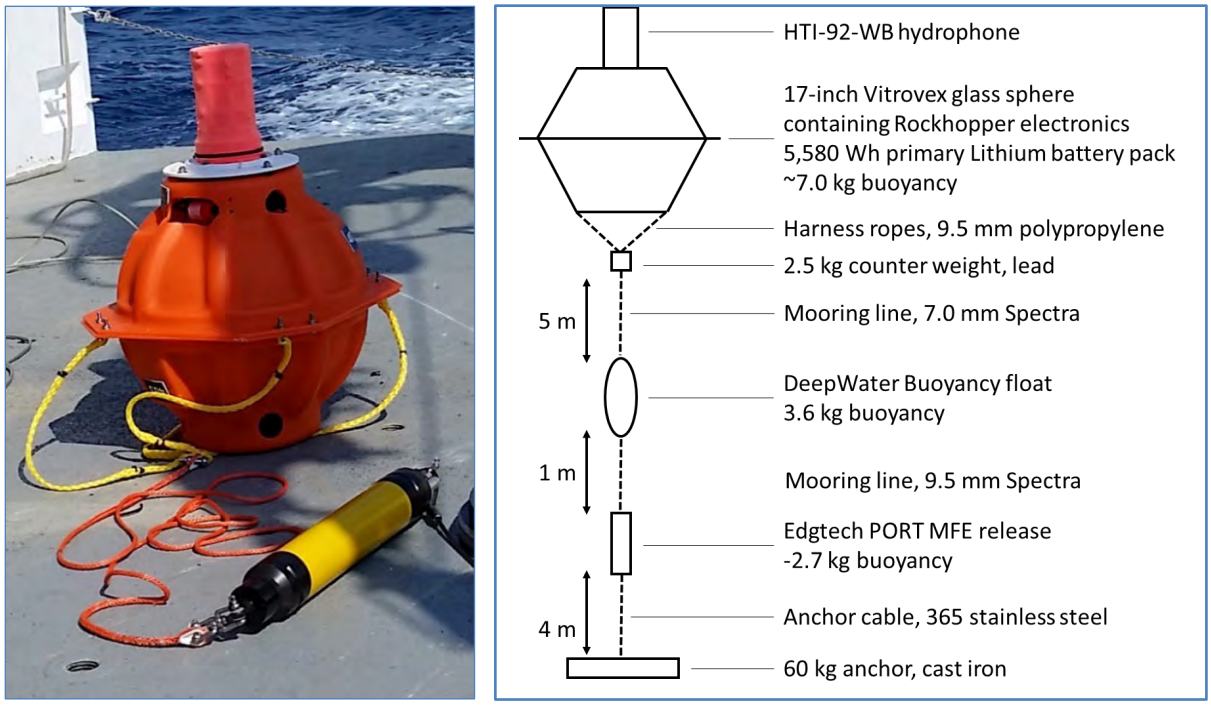

Figure B-1. RH mooring design and system components

Note: Not to scale; all components are rated to 3,500 depth.

Key: kg=kilogram(s); mm=millimeter(s)

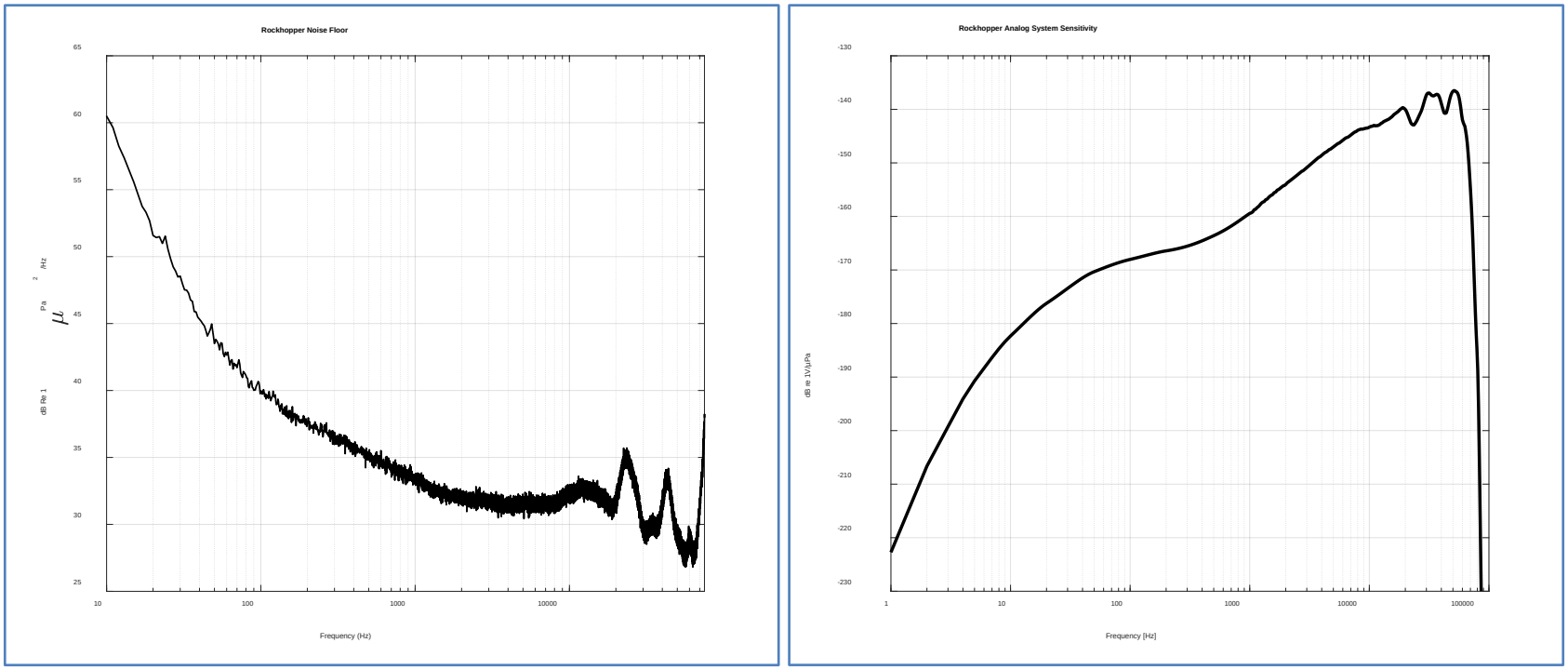

Figure B-2. Rockhopper (A) system noise floor (left) and (B) analog system sensitivity (right)

Note: At a sampling rate of 197 kHz, the corner frequency of the anti-aliasing filter is approximately 65 kHz resulting in a practical system sensitivity up to approximately 75 kHz.

B.2 EARS

EARS were developed by the U.S. Naval Oceanographic Office for ambient water column noise measurements. Past EARS deployments in the GOM (2001, 2002, 2007, 2010, 2015, and 2017) targeted monitoring of ambient noise soundscapes and deep-diving marine mammals (sperm whales, beaked whales, and deep-water dolphins) (Ackleh et al. 2012). They have also been used extensively by the Gulf Ecological Monitoring and Modeling Project, which the LADC has been implementing in the northern GOM between the Mississippi and DeSoto Canyons since 2015. The LADC is a consortium of research faculties that includes GOM PAM Program Team member University of Louisiana at Lafayette.

EARS are bottom-moored, recording systems (**Figure B-3**) and are depth-rated for use up to 6,000 m. All electronics and batteries are contained in an 8-inch-diameter by 24-inch-long pressure vessel. The battery pack consists of 124 alkaline D cells, which are preferred because of transportation safety issues and ease of disposal. The electronics are a low-power design (average power under 70 megawatts), providing extended recording durations with minimal battery requirements. Four 2.5-inch disk drives provide the recording capacity for the EARS. Recording is continuous, and all data are stored to magnetic disks for post-mission analysis. Use of four 2-terabyte disks allows continuous recording for up to 8 months. Similar to the RHs, the EARS also have an effective recording bandwidth of 10 Hz to 96 kHz (192 kHz, 16-bit sampling) in a one-channel configuration.

The versions deployed under the 2018 MP consist of electronics and hydrophones mounted between a 500-kilogram anchor and 10 to 12 glass ball floats (**Figure B-3**). This configuration allows for the positioning of the recording system in free field to minimize unwanted interference from acoustic signals scattered from the mooring parts and bottom. An additional battery pack ensures 6 months of uninterrupted data recordings. Data are continuously recorded at a 192-kHz sampling rate. The data are stored as 16-bit integers in proprietary binary format. The recovery uses acoustic releases that detach from the anchor weight when a special acoustic message is received from a release communication transducer. The recording package then floats to the surface for recovery.

Before deployment, each EARS buoy was subjected to electronics and hard drive tests and internal clock synchronization with the GPS onboard the deployment vessel. The frequency response function of each EARS buoy was measured prior to deployment by inputting the set of sinusoidal signals of pre-defined frequencies (**Figure B-4**) into the recording system. The frequency response function is interpolated to a resolution of 1 Hz and used to calibrate the recorded signals during the data processing stage. As with RHs, one representative hydrophone was calibrated at the NUWC Rhode Island at 3 degrees Celsius and 1,000 psi pressure. The sensitivity curve provided by NUWC for this hydrophone was universally applied to all units. The calibration adjustments were made, and selective datasets were reprocessed (see **Section 2.6** for additional details on the calibration process).

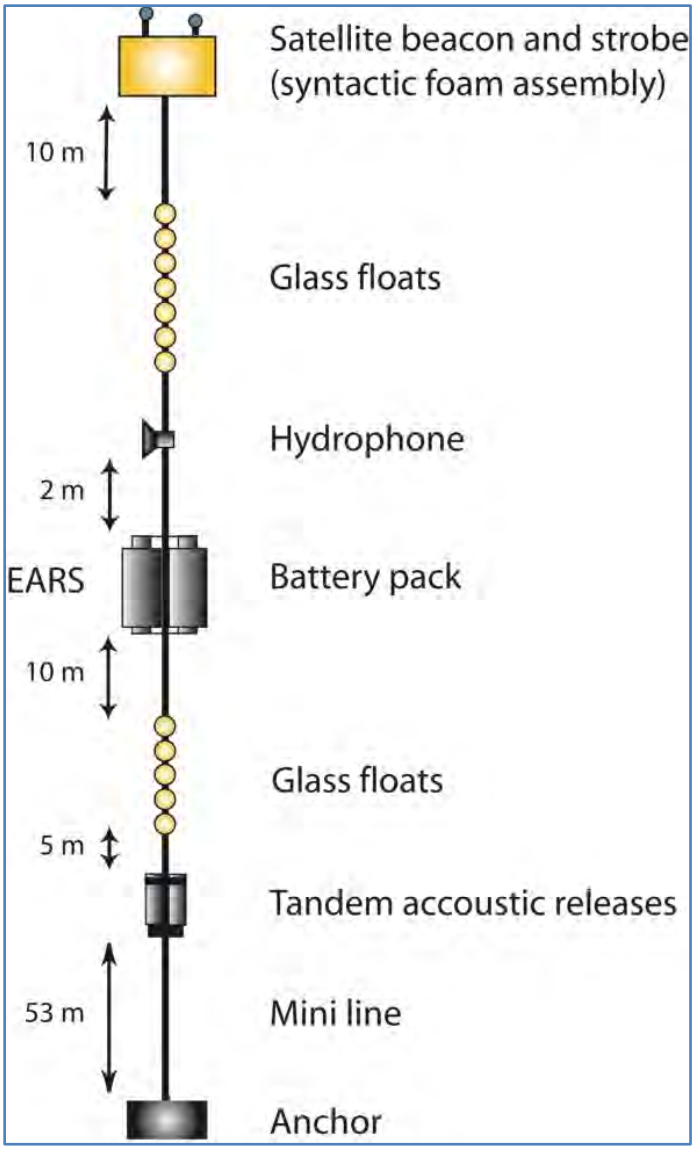

Figure B-3. EARS mooring design and system components

50

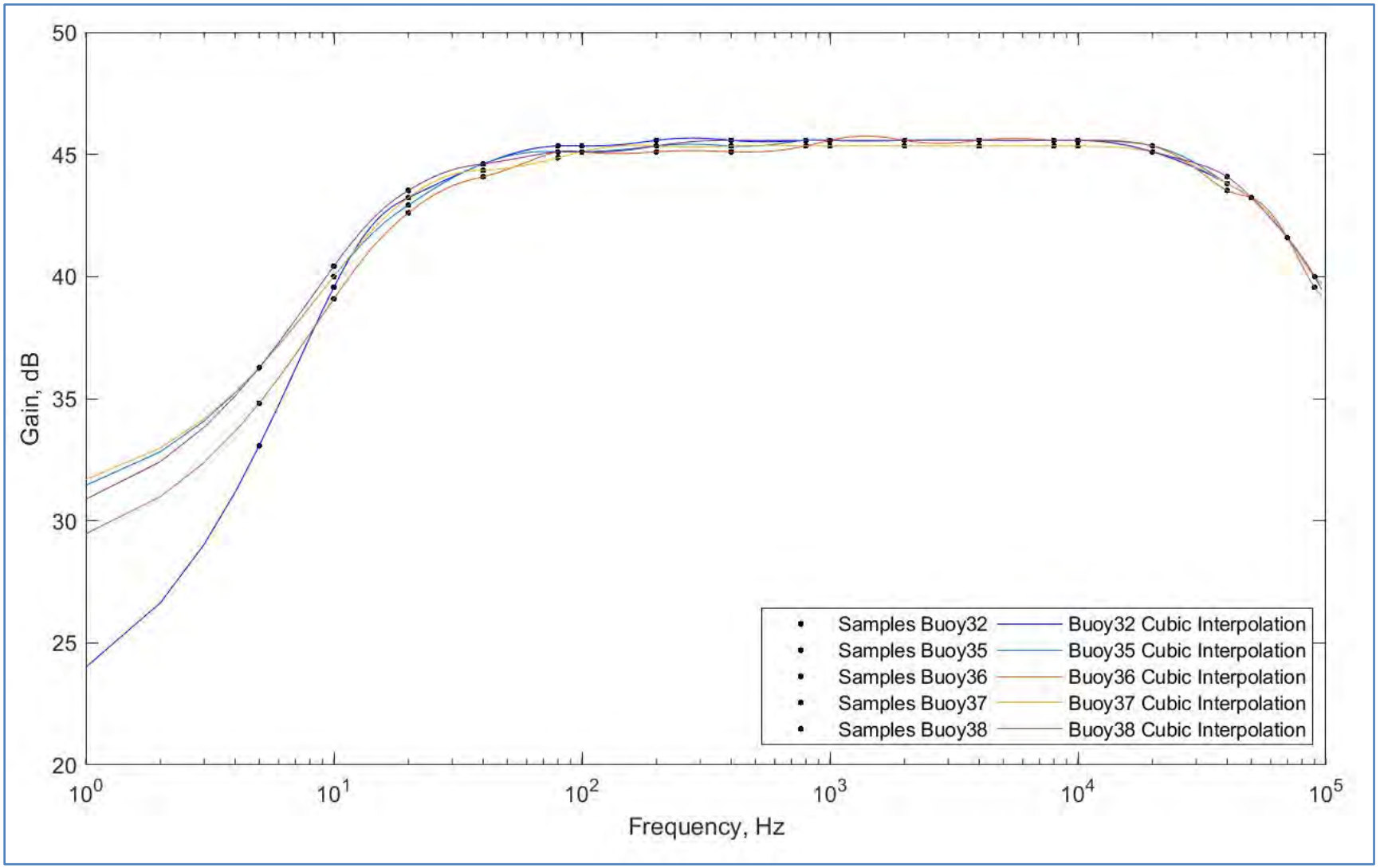

Figure B-4. The EARS transfer functions for five EARS used for the fall 2018 deployment

Note: Black dots are measured data; the five curves are interpolated to 1-Hz resolution.

B.3 SHRU VLAs

SHRU VLAs have been developed by the Woods Hole Oceanographic Institution and have been successfully used for PAM at many different locations. These systems have unique, state-of-the-art technologic features to ensure the most robust and accurate passive acoustic measurements. First, the electronics utilize a CSAC for extreme timing precision, and the hydrophone mount uses a robust aluminum cage with flow shield and hairy fairing wire to minimize flow and strumming noise (**Figure B 5**).

For the 2018 MP, each SHRU VLA was equipped with four hydrophones, had a continuous duty cycle, and had a sampling rate of 9.8 kHz with 24-bit resolution. The monitoring band width was 10 Hz to 4.5 kHz. The four-element hydrophone array provided directional passive acoustic data as a function of arrival angles in vertical dimension. Two slightly differing mooring configurations were deployed: one on the Mississippi Canyon floor and the other on the slope (**Figures B-6 and B-7**). To improve the mooring stability within the canyon due to anticipated strong currents, the SHRU mooring was equipped with a large fluid-dynamic design buoy (StableMoor® Buoy) (**Figure B-8**). The hydrophone mounting design for both SHRUs was intended to minimize flow and strumming noise. Besides hydrophones, the SHRUs also recorded data from water temperature and pressure sensors.

After deployment, the SHRU VLA positions were surveyed to improve position accuracy using an acoustic triangulation method based on in-situ sound speed profile measurements and sound propagation modeling (**Figure B-9**). An acoustic transducer was deployed off the ship with a known position derived from the ship's GPS position. The transducer transmitted 12-kHz signals to communicate with the acoustic release at the bottom of the hydrophone moorings.

Figure B-5. A) CSAC-SHRU electronic board(A) and (B) Hydrophone cage with flow shield and hairy fairing wire (B)

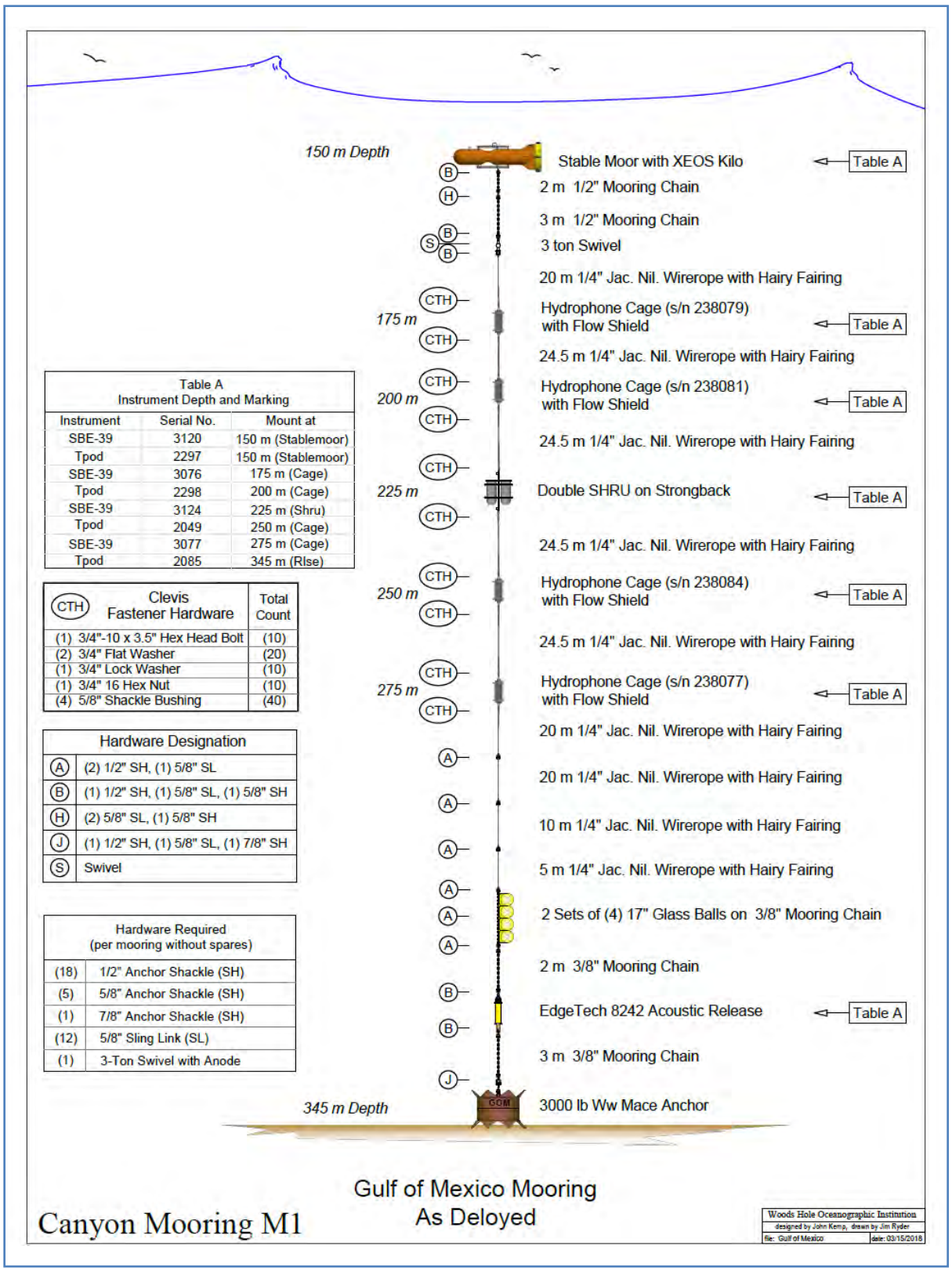

Figure B-6. Canyon SHRU mooring design (with StableMoor® buoy)

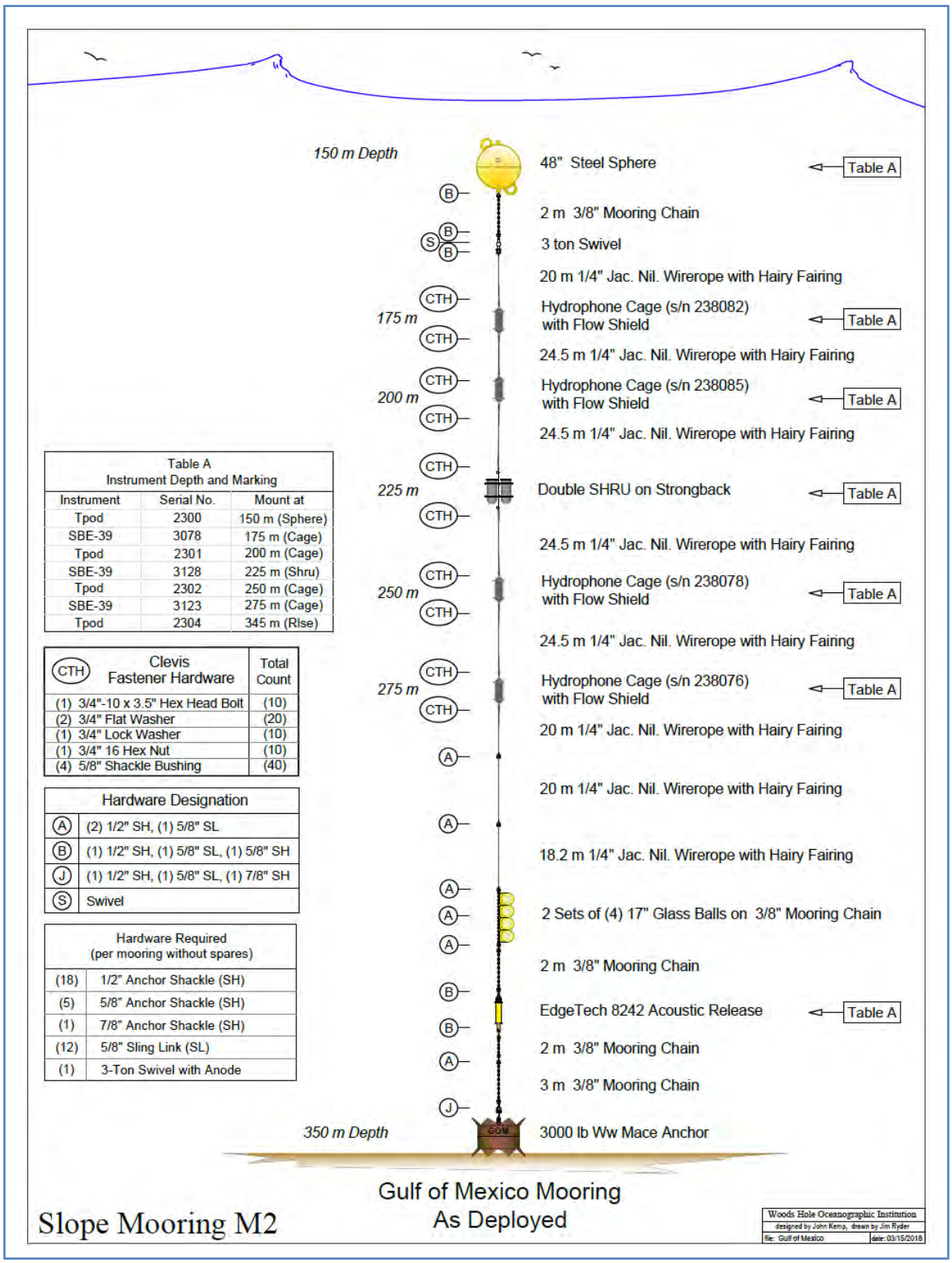

Figure B-7. Slope SHRU mooring design

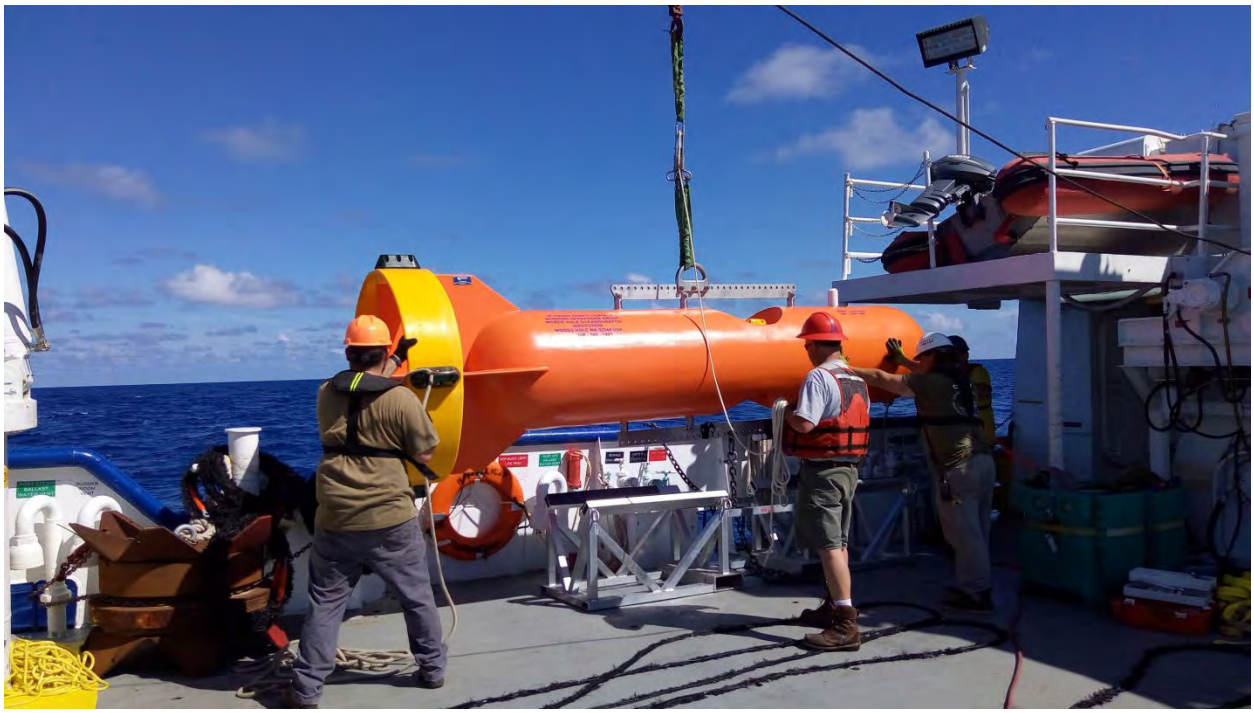

Figure B-8. Canyon SHRU StableMoor® buoy

73

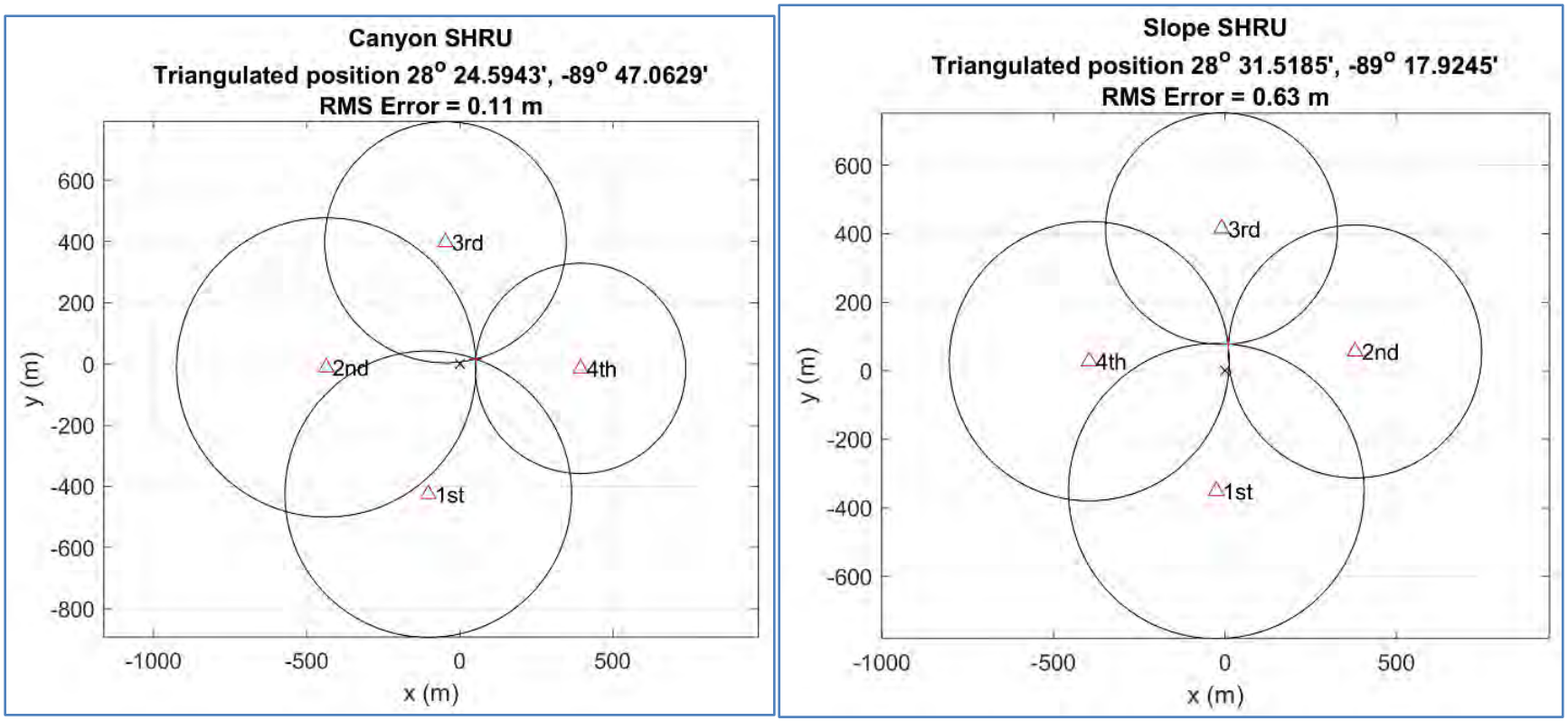

Figure B-9. Surveyed (triangulated) Canyon (left) and Slope (right) SHRU mooring positions

B.4 Seaglider

The Seaglider is a mobile Autonomous Underwater Vehicle (**Figure B-10**) that moves through the water in a saw-tooth like pattern and surfaces every few hours. Navigation is accomplished using a combination of GPS fixes while on the surface, and internal sensors that monitor the vehicle heading, depth, and attitude during dives. Rather than an electrically driven propeller, the vehicle uses small changes in buoyancy and wings to achieve forward motion. The glider can travel approximately 20 km/day, and dive to 1,000 m. The unit also collects physical oceanographic data throughout the water column during each dive.

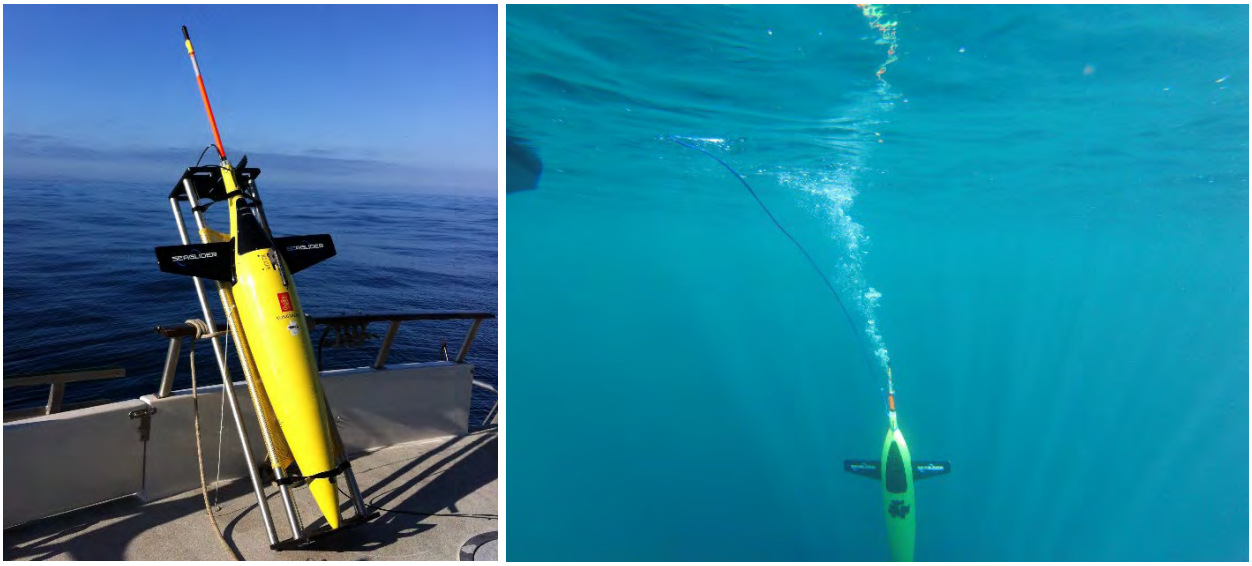

Figure B-10. Seaglider Autonomous Underwater Vehicle

B.4.1 2018 MP Seaglider

For the 2018 MP, a glider (SG639) was deployed in selected portions of the study area by the Cooperative Institute for Marine Resources Studies, Oregon State University. The unit is commercially available from Huntington Ingalls Industries/Technical Solutions, Lynnwood, Washington. It was outfitted with an acoustic recording system (Wideband Intelligent Signal Processor and Recorder available from Embedded Ocean Systems, Seattle, Washington), which was programmed to record sound continuously at all depths below 25 m, at a sampling rate of 125 kHz and a resolution of 16 bits, with sounds compressed for storage using the FLAC.

The recording system includes a “pre-whitening” filter to effectively capture ocean sounds without either clipping or hitting the noise floor (Christensen and Jakobsson 2009). Self-noise from glider operations that may be caused by pumping of the buoyancy bladder, movement of the ballast to steer and orient the glider, and so on, was removed using a table of all glider roll, pitch, and buoyancy operations. Recordings that occurred within 10 seconds of any of these actions were removed before further processing of the acoustic data.

The system's pitch and roll are controlled using an adjustable ballast (the vehicle battery). Because the glider travels slowly, it does not generate much flow noise. This is especially important at low frequencies, where this noise is most prevalent and can be problematic.

B.4.2 2019 MP Seaglider

For the 2019 MP, another Seaglider was deployed in selected portions of the study area by the Ocean Engineering Department of the University of Rhode Island. The unit is commercially available from Huntington Ingalls Industries/Technical Solutions, Lynnwood, Washington. In addition to the standard conductivity, temperature and pressure sensors, it was equipped with the PAM MK II Observer System. The Observer is a mature stand-alone acoustic recording package developed by JASCO Applied Sciences and was adapted to integrate with the Seaglider platform. The Observer was programed to record sound continuously at a sampling rate of 128 kHz and resolution of 24 bits. The system boasts 4 terabytes of data storage, and data were stored at full resolution in 30-minute .WAV files onboard. Files were also later converted to FLAC.

B.5 Instrument Calibration

B.5.1 RHs and EARS Hydrophones

Using representative calibration data for testing and verifying functionality of hydrophones to be deployed in the field is a standard approach for underwater PAM projects. This approach also was adopted for the 2018 MP. It was assumed that all hydrophones acquired for data collection using the RH and EARS moorings would have the same or similar sensitivity curves. Therefore, one representative RH hydrophone (HTI-92WB) and one representative EARS hydrophone (HTI 97) were selected for calibration at NUWC in Newport, Rhode Island. The NUWC's Underwater Sound Reference Division serves as the equivalent to the National Institute of Standards and Technology in underwater acoustics. It provides the U.S. with a wide variety of underwater transducer standards just as the National Institute of Standards and Technology provides for other types of measurements.

Typical curves of receive sensitivity up to the first resonance and a beam pattern at a lower frequency for one plane for the HTI-92WB as well as beam patterns for both planes up to 23 kHz for the HTI-97 were provided by the hydrophone manufacturer. A few additional calibration steps were taken to ensure data quality. The rationale for these additional steps is described below.

Since the Program measures sound in three dimensions and requires accurate sensitivity measurements for the class of hydrophones being used over a wider range of frequencies (much wider than specified by the manufacturer), the Program Team needed to do a representative calibration supply for the unknown information. The manufacturer provides a sensitivity measurement (free field voltage sensitivity [FFVS]) that defines the sensitivity along the hydrophone's primary axis at a frequency below the first resonance peak. Hydrophone sensitivity is nearly flat over frequencies below the first resonance point. Generally, the hydrophone variation is less than +/- 1 dB from the manufacturer's listed sensitivity and is better.

Additionally, there are no hydrophones that are highly sensitive, omni-directional, and flat across the bandwidths desired and used recorded by RHs and EARS. The FFVS curves also provide information regarding how the hydrophone sensitivity rolls off at and well above resonance. Without knowledge of the direction from which sound arrives, the sensitivity of the hydrophone is only accurate up to the frequency where the beam pattern is omni-directional in three dimensions.

Calibration methods typically make measurements in two planes (X-Y and X-Z) to provide a general description of the beam patterns. Each planar measurement is done at a single frequency. Multiple beam pattern measurements are made at different frequencies to gain a better understanding of where omni-directionality begins to degrade. Hydrophone beam patterns are a function of geometry and construction. Theoretically, only the geometry matters but realistically, the construction degrades the performance. Typically, where the wires enter the hydrophone mold will be the first place the beam pattern starts to

degrade from omni-directional. Beam pattern measurements are limited by costs since they take significant time to make.

Additionally, hydrophones are affected as pressure is increased. Well-designed hydrophones like the HTI 92WB and HTI-97DA minimize these effects up to their rated pressures. As part of the additional calibration steps, EARS and RH hydrophones were also tested down to 1,000 psi to determine if there are any significant changes in sensitivity for these designs.

The following steps were undertaken as part of the calibration process:

1. Hydrophone sensitivity (FFVS) typically ranges from 3 Hz to 90 kHz (unamplified version of the hydrophone) at ambient pressure and 20 degrees Celsius. The hydrophone manufacturer had provided NUWC FFVS runs from 2 Hz to 25 kHz. During the calibration process, additional FFVS runs were conducted from 3 Hz to 90 kHz and up to 1,000 psi pressure (approximately 675-m depth).
2. For the HTI-97, X-Z and X-Y plane beam patterns—which included frequencies of 4 kHz, 8 kHz, 10 kHz, 15 kHz, and 23 kHz—were provided by the hydrophone manufacturer based on NUWC testing. Similar testing for the 40-, 60-, and 80-kHz frequencies were performed at the Naval Surface Warfare Center's Panama City calibration facility.
3. No beam pattern measurements were provided by the manufacturer for the HTI-92WB, and that testing could not be performed for all frequencies due to resource limitations. Therefore, X-Z plane measurements were performed at NUWC for the 5-, 10-, and 50-kHz frequencies, and X-Y beam pattern measurements were conducted for the 5- and 10-kHz frequencies.

Except for some military applications, it is standard practice in acoustic monitoring to use representative calibration data to calibrate sensors to be deployed in the field. Representative calibration curves were used to calibrate the hydrophone mounted on the deployed RHs and EARS moorings. Prior to each deployment of RHs, air tests were conducted in the laboratory to compare the outputs of hydrophones intended for deployment against the calibrated reference hydrophones to ensure that the sensitivities were close. For EARS, a tap test was performed in air to validate that the hydrophone and wiring were functional.

The EARS hydrophones also undergo a more elaborate QA/QC procedure that is performed every 3 to 5 years. Key steps in this process are summarized below:

1. Electronic noise analysis

a. A spectral noise analysis is performed in the laboratory using the standard EARS Graphic User Interface (GUI) program. The EARS assembly is powered on the bench using a battery, and the front-end of EARS is terminated with an equivalent impedance to the transducer. The EARS GUI provides the PSD of the resultant data sampled by the EARS electronics (**Figure B-11**).

b. The front-end preamp is terminated with an equivalent capacitance and sample data for approximately 10 to 20 minutes. The amplitude per square Hz is determined as the square root of the calculated PSD.

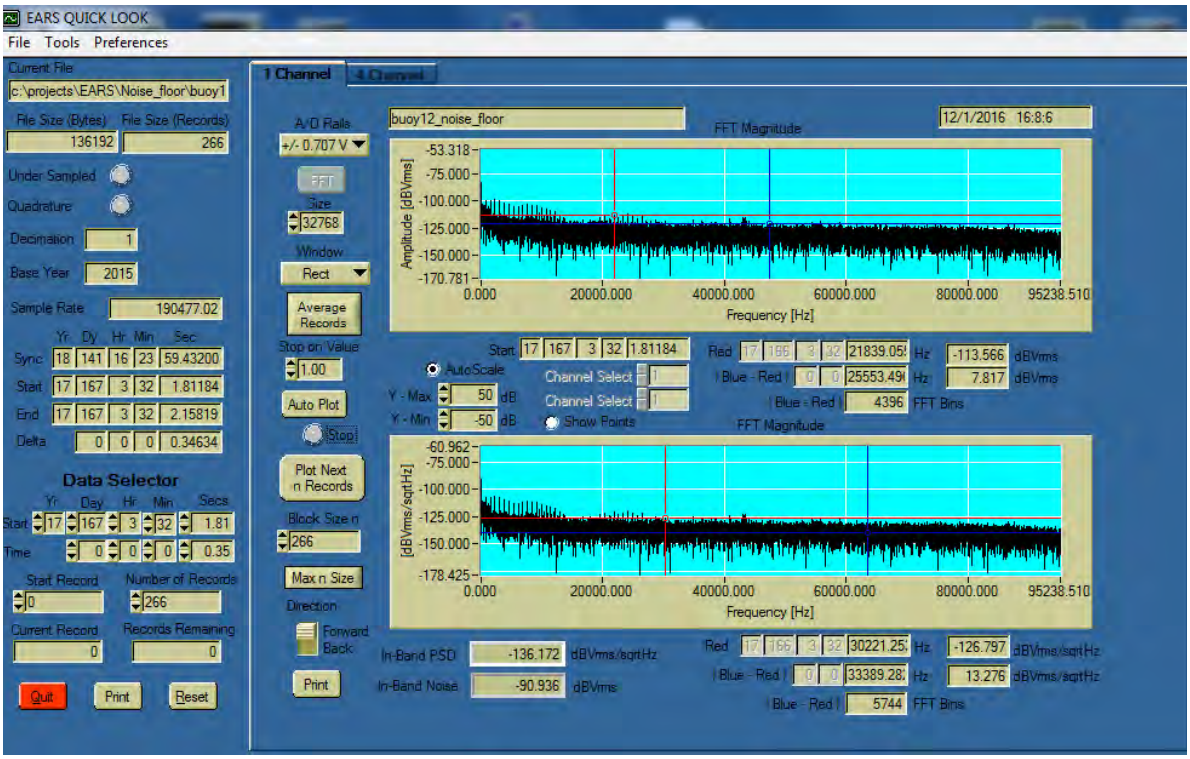

Figure B-11. EARS PSD plot from Bench Noise Test Buoy 12

2. EARS Electronic Gain Measurement

A function generator is used to output a known amplitude tone (20 millivolts peak to peakmVp-p) at various frequencies (**Table B-1**). The EARS sampled amplitude is obtained using the EARS GUI program. The gain is computed from the ratio of the output to the input signal levels. Gain spot checks are run at select frequencies on all units prior to deployment to ensure gains are reasonable.

Table B-1. Amplitude tones and frequencies used for EARS electronic gain measurement

Frequency (Hz)	Output (mVp-p)	dB
5	800	32.04
10	1,800	39.08
20	2,800	42.92
40	3,500	44.86
80	3,700	45.34
100	3,700	45.34
200	3,800	45.34
400	3,800	45.58
800	3,800	45.58
1,000	3,800	45.58
2,000	3,800	45.58
4,000	3,800	45.58
8,000	3,700	45.34

Frequency (Hz)	Output (mVp-p)	dB
10,000	3,700	45.34
20,000	3,600	45.11
40,000	3,100	43.81
50,000	2,800	42.92
70,000	2,400	41.58
90,000	2,000	40.00

Key: dB = decibel(s); Hz = Hertz; mVp-p = millivolts peak to peak

3. EARS Electronic Gain Measurement

Hydrophone sensitivity is an important factor in the accuracy of SPLs. A hydrophone's sensitivity curve relates the measured SPL to the output voltage across the hydrophone's leads. The hydrophone's manufacturer will provide these measurements for the rated bandwidth of the hydrophone, which is generally the sensitivity of the hydrophone up to the maximum frequency that the hydrophone is omni-directional (near equal sensitivity from sound received from any direction).

The omni-directionality of a hydrophone is a function of the hydrophone's geometry (e.g., cylindrical, spherical, circular), source wavelength (1/frequency) and to some extent the hydrophone construction. Manufacturers provide a hydrophone's sensitivity when purchased and generally have at least a sensitivity curve of a representative hydrophone. The single value of sensitivity provided by the manufacturer is the sensitivity of that hydrophone in the LF region (left side of the sensitivity curve).

Hydrophones typically have flat sensitivity curves in this region. As the wavelength of a sound wave approaches the geometric size (e.g., length, diameter, ceramic thickness) of the hydrophone's shape, the hydrophone beam pattern will begin to degrade from omni-directional. Once this happens, to report accurate sensitivities, the direction sound is received in relation to the hydrophone's orientation must be known. This requires a 3D array of hydrophones. A very small hydrophone will maintain omni-directionality over a broad bandwidth but will have very low sensitivity.

Selection of a hydrophone for an application is a tradeoff between bandwidth and sensitivity. The HTI-97DA was used for EARS for the soundscape work as it has reasonably good bandwidth and sensitivity. It was also rated for depths up to the required field measurements. It is omni-directional up to approximately 20 kHz (**Figure B-12**).

A calibration of sensitivity and beam pattern over a wide range of frequencies was performed to understand the hydrophone's performance. The manufacturer's measured sensitivities for each hydrophone used in the soundscape work all fell within a +/- 0.5 dB range of the manufacturer's quoted sensitivity (-193 dB re 1V/uPa). The sensitivity curve shown in **Figure B-12** (upper left corner) was the result of a representative HTI-97DA calibration at high (1,000 psi) and low pressure (50 psi). A 40-dB gain preamp was used in the calibration work.

The sensitivity of some hydrophones will change with pressure, and this sensitivity measurement was performed to ensure that the sensitivities of the HTI-97DA design did not change significantly with pressure since the field measurements were made up to approximately 1,200 m. The Program's calibration measurement was limited to 1,000 psi due to financial constraints. EARS uses the performance of the representative hydrophone for its performance measurements since it is too costly to perform detailed calibrations on all hydrophones used during the soundscape work.

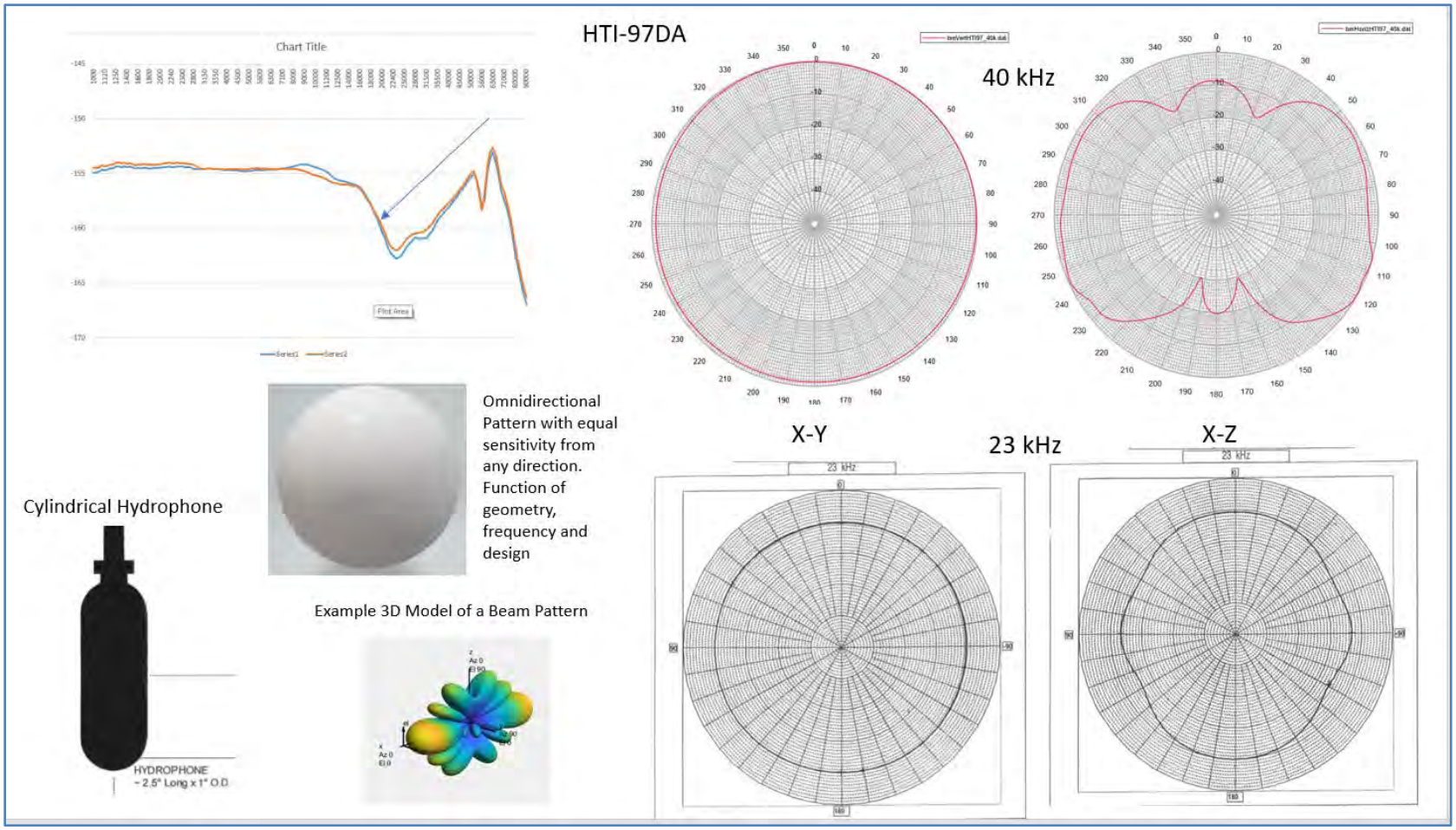

Figure B-12. HTI-97A sensitivity and beam pattern

B.5.2 SHRUs

New hydrophones were acquired for SHRU VLAs from High Tech Inc.[8] Calibration specifications were provided by the manufacturer for the listening frequency range from 10 to 5,000 Hz for these sensors.

B.5.3 Seagliders

Calibration data for the hydrophone used on the Seagliders were also provided by the hydrophone manufacturer, High Tech Inc. Data were provided on hydrophone sensitivity (-164.5 dB re 1 V/µPa) and included a spectral sensitivity curve. Calibration data for the recorder system were provided by the manufacturer EOS, Inc. These data included specified pre-amplifier gain and spectrum and analong-to-digital sensitivity.

[8] http://www.hightechincusa.com/products/hydrophones/hti92wb.html

Appendix C: Monitoring Platform Deployment and Recovery Protocols

C.1 Field Deployment and Retrieval Protocols for Stationary Moorings

C.1.1 RHs and EARS Deployment

A similar process was followed for deployment of RHs and EARS. The EARS moorings are preassembled on deck (**Figure C-1**), which is staged with gear and sensors deployed from starboard to port, or right to left. All loads are secured and orderly handled over the side as they are deployed. No personnel are allowed to position themselves in the bight (anywhere inside the starboard glass balls and the anchor attached to the crane) as the potential exists to be snagged and pulled overboard.

Figure C-1. Shipboard deck set up for deployment of EARs

The first "load" sent over the side is a series of glass balls, which are part of the top flotation device, until the tag point on the last yellow strap of the top set of glass balls. The top float is pushed over manually by a technician, and the remaining floats are helped along while one person operates the tag line. As the floats are deployed, the vessel is instructed to move forward at 2 knots via radio communications with the bridge. Note, on the R/V Pelican, the captain has the capability to steer the ship from the aft deck controls.

Once the top floats are in the water, the mooring's recording package is sent over the side, while a third person operates a second tag line on it. Once the mooring is tagged, the first tag line is released, and the assembly is allowed to slide (pulled by drag from the top floats in the water) into the water and is controlled by the second tag line.

The technician responsible for the first tag line moves to the third tag line at the rear end of the bottom float chain, and once secured, the second tag line is released. A fourth tag line is attached to the acoustic

releases, and the bottom floats are allowed to slide slowly into the water. Once tension is applied to the fourth tag line, the third tag line is released. The technician responsible for the fourth tag line then allows the releases to slide into the water.

A smaller line is wound onto the sea winch, and the load on the fourth tag line is transferred to the ship's sea winch. Once the sea winch has the tension, the ship is instructed to increase speed to 4 to 5 knots, and the ship's crew pays out line using the winch. It is critical to maintain tension on the mini line since slack may be sucked into the ship's propeller.

Once all the mini line is deployed, the load is transferred to the anchor, which is secured to the crane. The anchor chain is shackled to the mini line. The load from the sea winch is transferred to the crane (via the quick release), and the sea winch's wire line shackle is removed as tension is released. The crane then moves the weight overboard, and the quick release is used to drop the anchor.

C.1.2 RHs Retrieval

The RH unit, as retrieved, is composed of a glass sphere instrument housing and tether attached to an Edgetech acoustic release (Figure C-2). The total mass of the package is approximately 50 kilograms. The general process is as follows: arrive at station, interrogate, wait for signal/sighting, locate, and retrieve. The following stepwise process will be followed at each station:

- Upon reaching the station, the field technician is informed by the captain that the ship is on station and over the gear; permission to deploy transducer is obtained by the field technician.
- The Edgetech transducer is lowered into the water, and the captain is informed that gear is in the water.
- The RH mooring is interrogated by the Edgetech deck-box, confirming its presence and functionality.
- The Edgetech acoustic release command is sent, and time of response is recorded.
- The Edgetech transducer is removed from the water, and the captain is informed that all gear is out of the water.
- The ship remains on station while the requisite time is spent awaiting surfacing of the RH. Early estimates for time to surface at the deployed depth is 45 minutes.
- A visual, radio, and satellite/GPS watch is maintained during the recovery period.
- When the RH unit surfaces, a VHF radio signal at 154.585 megahertz is sent, a strobe is activated, and notification of its GPS location is transmitted via satellite.
- When a valid location, VHF signal, or visual sighting of the RH is obtained, the captain is informed and is directed by the field technician to the location of the surfaced equipment.
- The RH position is approached, and the ship is positioned alongside the unit, which is secured by a gaff and lifted aboard by the crew.
- The RH is then powered down for shipment back to Ithaca.
- No data manipulation, collection, or analysis is performed in situ.

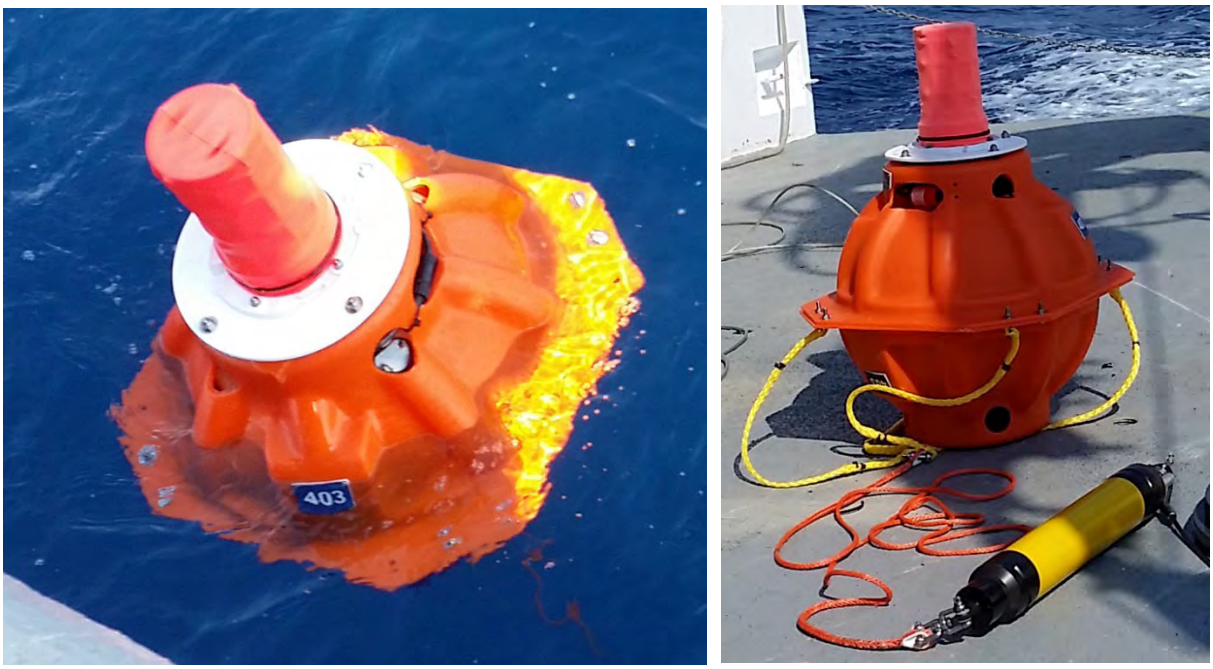

Figure C-2. Left panel: RH in water (left) and. Right panel: RH on deck (right)

C.1.3 EARS Retrieval

Recovery of the EARS moorings begins with establishing an initial vessel position based on wind and currents in the area to ensure the mooring does not rise up under the vessel. The Team generally stays up current of the mooring. In 2,000 m of water, the EARS mooring requires approximately 10 minutes to break the surface and can move hundreds of meters during its ascent after release from the bottom. Once in position, communication is established with the mooring releases.

Prior to a release command, all hands will be on deck for visual location of the mooring when it surfaces. The release is only performed during daylight hours to ensure the mooring can be visually located even though there is a satellite location beacon and a strobe on the mooring. In addition, the Team maintains acoustic release ranging to monitor the mooring ascent to obtain an approximate range as the mooring nears the surface. Once the mooring is located, the ship transits close to the mooring from the downwind side (the ship moves faster than the mooring in wind) and backs towards the mooring.

The captain uses the aft vessel controls to easily and safely position the vessel close to the mooring. When close, a grapple is used to snag the mooring and pull it close to the vessel while the vessel secures the aft propellers. A line is then attached to one of the float straps, allowing the crane to lift the mooring onto the aft deck. This usually requires three lifts with the crane per mooring due to the length of the mooring. Once on-board, the EARS data recorder is removed from the mooring and safely secured for transportation. Typically, no data manipulation, collection, or analysis is performed *in-situ*. A refurbished recorder (tested and repowered) will then be inserted into the recovered mooring. The mooring is inspected, and all suspect components replaced to prepare the mooring for redeployment.

C.1.4 SHRU VLA Deployment

The SHRU mooring design includes vertical array moorings with a 3,000-pound anchor, acoustic release, and subsurface StableMoor® buoy (for the Canyon SHRU) or a 41-ft steel sphere (for the Slope SHRU) for flotation. The deployment protocol for the Canyon and Slope SHRU VLAs are similar with the subsurface steel ball first deployed off the aft of the research vessel as the vessel moves ahead at 1–2 knots.

The mooring is slowly paid out and various mooring attachments such as temperature sensors are strapped on. When the research vessel reaches the specified location for the mooring, the 3,000-pound anchor is lifted by the A-frame over the fantail. The anchor is held by the winch and a quick release. The captain notifies the deck that the position has been reached, the anchor is lowered until reaching the water surface, and the lead mooring technician activates the quick release. The anchor falls to the bottom and pulls the mooring to the bottom upright.

C.1.5 SHRU VLA Recovery

Upon arriving at the site, the team interrogates the acoustic release on the mooring, then maneuvers the vessel 300 m away from the mooring location and releases the mooring. The StableMoor® buoy on the Canyon SHRU or the 48-inch steel sphere on the Slope SHRU rises to the sea surface first, and the team waits until the bottom 4 glass ball floats come up to the sea surface before retrieving the mooring and all components (except the 3,000-pound anchor).

For the Canyon SHRU mooring, the StableMoor® buoy is recovered first using the ship's crane from the port side. For the Slope SHRU, the 48-inch steel sphere is recovered with the A-frame. After the StableMoor® or steel sphere is placed in the cradle and secured, the mooring load is transferred to the ship's small deck winch to recover the mooring in segments. Each SHRU VLA mooring consists of a total of five segments, which are necessary to recover the hydrophone cages and the electronic packages. During the recovery, the ship is held stationary.

After each mooring is recovered, the team checks the SHRU clocks against the GPS time to record the total clock drift during the deployment. The data disks are recovered, and the data files are immediately copied to a backup disk. Data processing typically begins after the units are returned to the laboratory.

Appendix D: Field Cruise Photograph Log

Photo D-1. *R/V* Pelican docked at Cocodrie, Louisiana

Photo D-2. The 2018 MP field deployment team with the *R/V* Pelican crew

From left to right: Derek Jaskula (Cornell University), Brad Lingsch (Proteus Technologies LLC), Kenny (R/V Pelican intern), Matthew Firneno (University of New Orleans graduate student), Natalia Sidorovskaia (University of Louisiana at Lafayette), Evan Wellmeyer (University of New Orleans graduate student), Jerome Hamilton (cook), John Lacross (R/V Pelican marine technician), Fred Channell (Cornell University), Tad Berkey (R/V Pelican captain), Sean Griffin (Proteus Technologies LLC, Chief Scientist), Dirk Wacker (R/V Pelican deckhand), Elliot (R/V Pelican crew))

Photo D-3. RHs ready for deployment

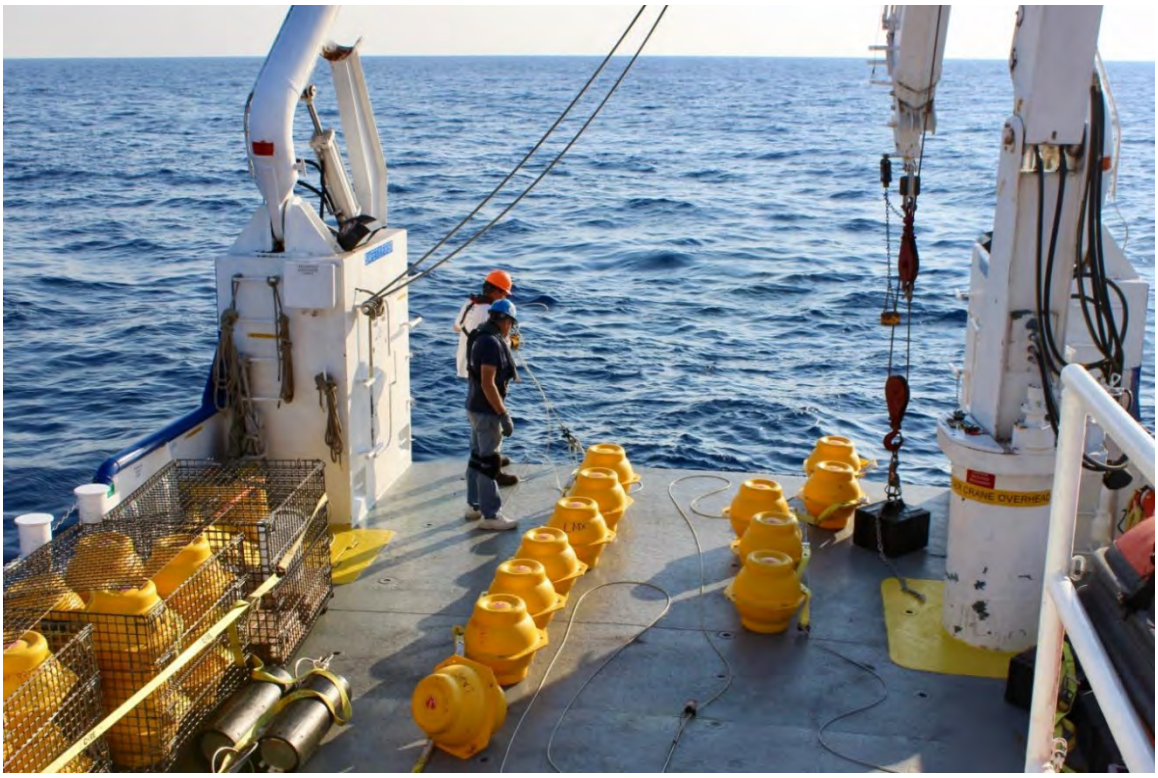

Photo D-4. EARS mooring ready for deployment

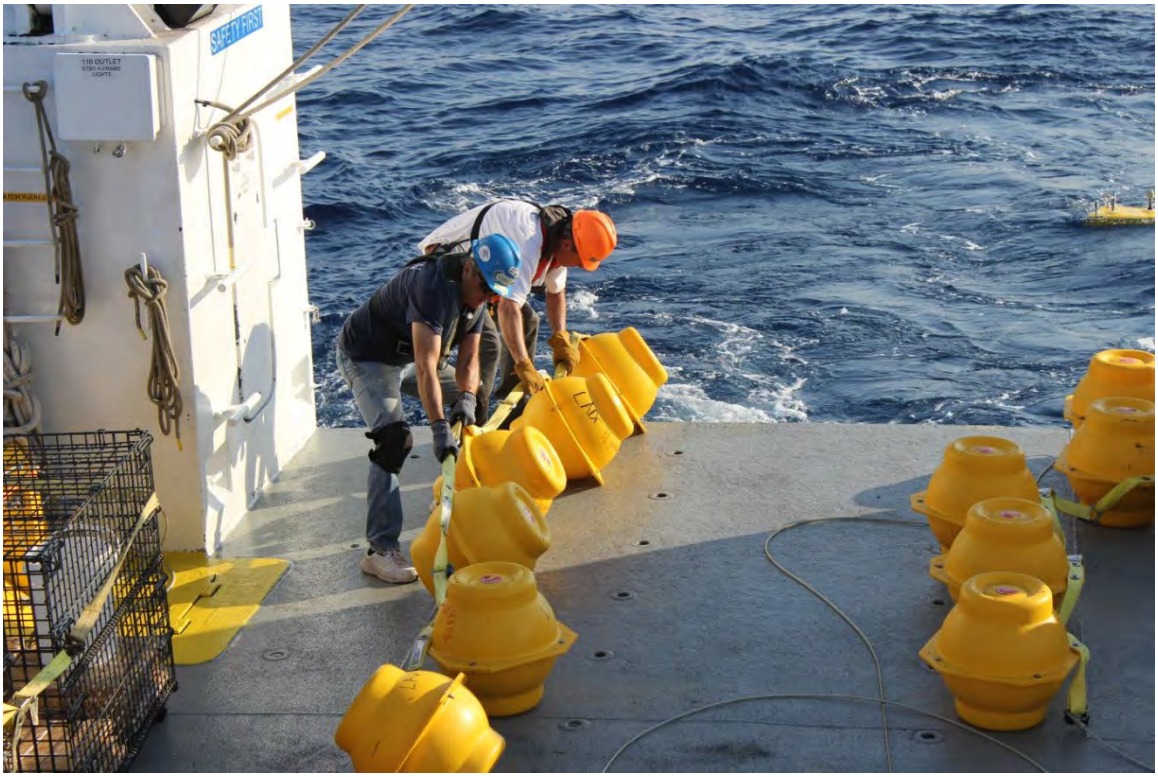

Photo D-5. EARS mooring deployment, satellite beacon in the water

Photo D-6. EARS mooring deployment, top floats in the water

Photo D-7. EARS mooring deployment, final stage (anchor release preparation)

Photo D-8. Preparing the RH mooring for deployment

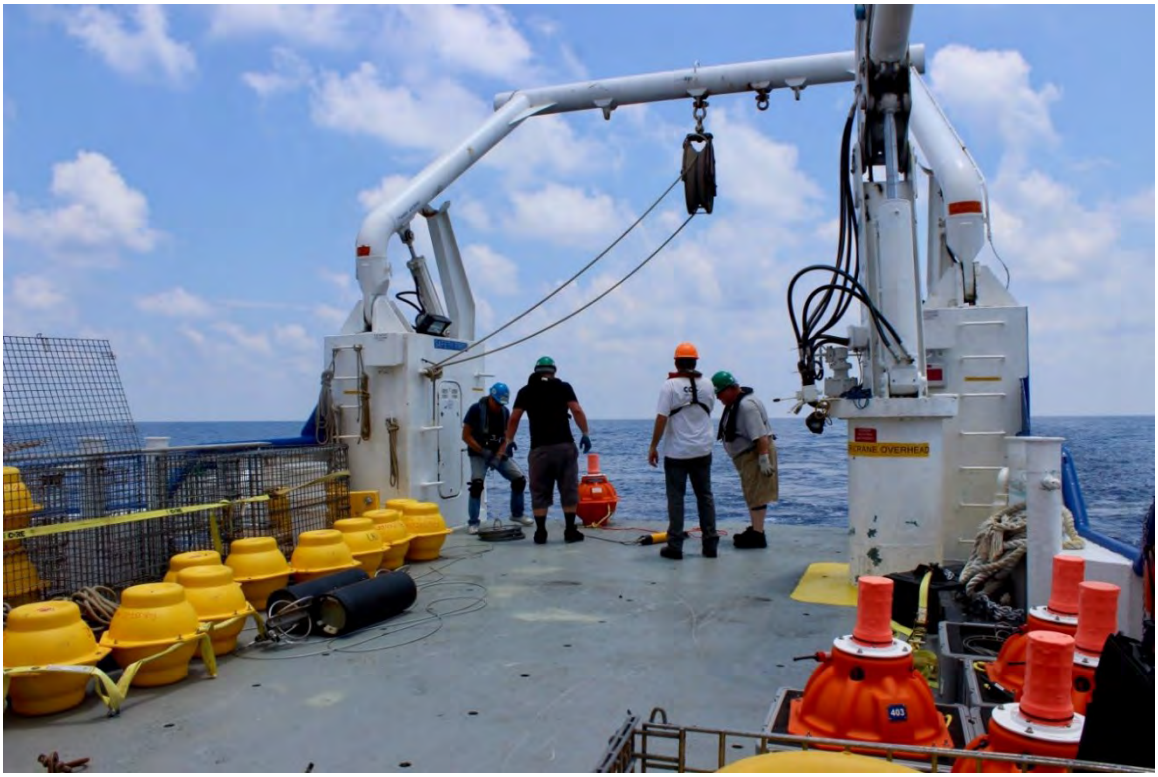

Photo D-9. RH mooring deployment

Photo D-10. CTD unit deployment for collection of oceanographic data

Photo D-11. Deployment of the CTD unit

Photo D-12. StableMoor® buoy for the Canyon SHRU VLA

Photo D-13. SHRU VLA hydrophone cage

Photo D-14. Principal Investigator Dave Mellinger setting up the glider, dockside at Venice, Louisiana

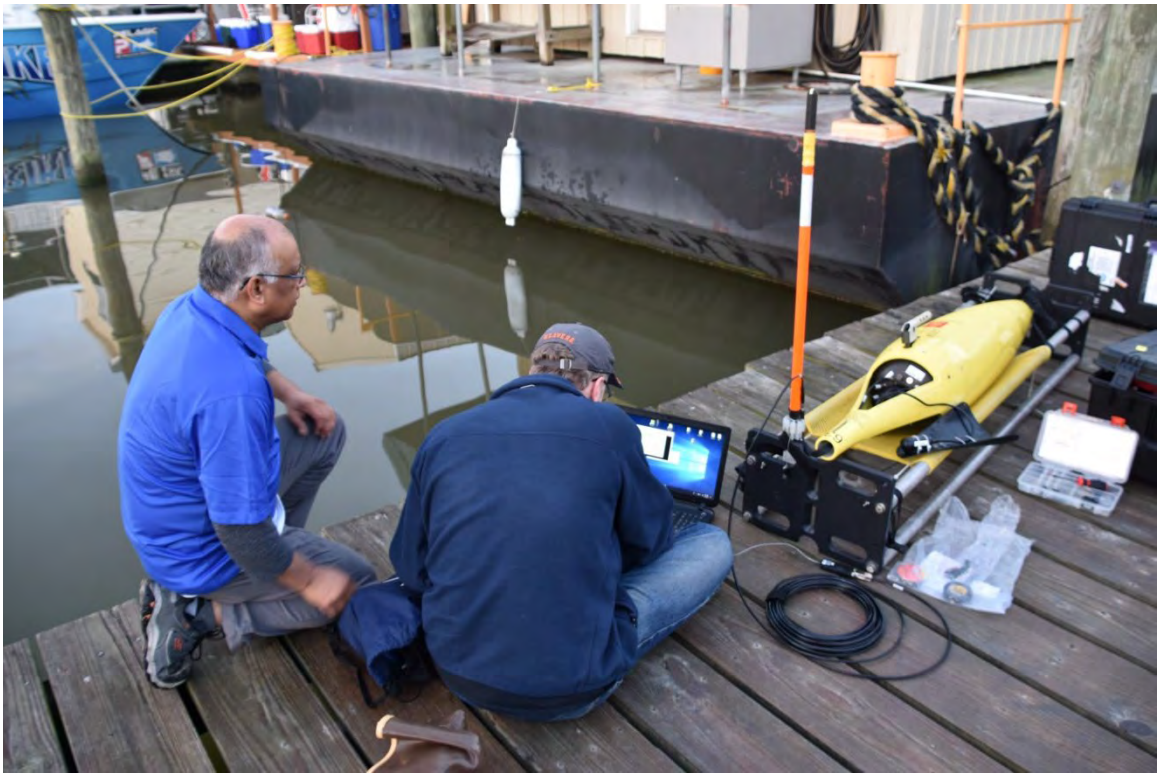

Photo D-15. Seaglider system check

Photo D-16. Glider hydrophone check

Photo D-17. Turning the Seaglider using a magnetic key

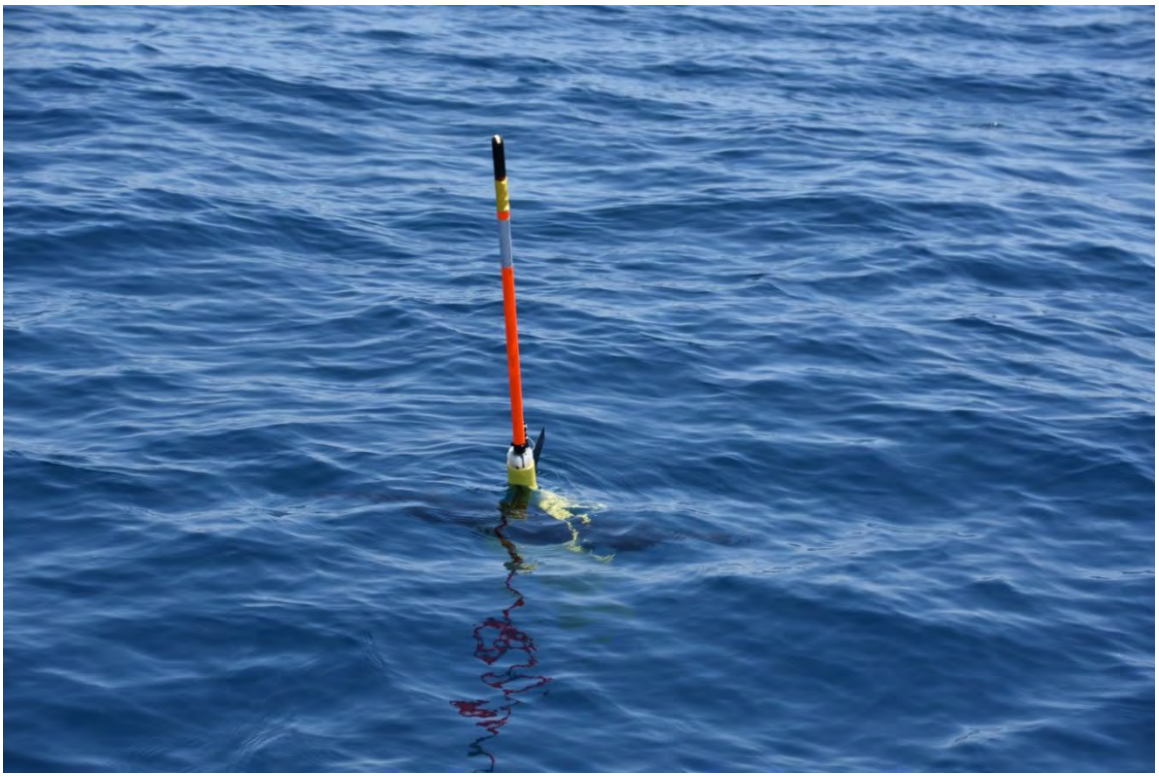

Photo D-18. Seaglider in the water, immediately prior to making its first dive

Appendix E: GOM PAM Program Advanced Data Synthesis and Analysis Report

Prepared Under:
BOEM IDIQ Contract No. M17PC00001, Task Order No. 140M0119F0001, Task 7 (Data Analysis, Synthesis, and Annual and Final Reports)

by:

Marine Acoustics, Inc.

MAI
MARINE ACOUSTICS, INC.

In Collaboration with:

HDR
300 N. Madison Street
Athens, AL 35611

Table of Contents

List of Figures

List of Tables

List of Acronyms and Abbreviations

ACF	autocorrelation function plots
AR	autoregressive
ADEON	Atlantic Deepwater Ecosystem Observatory Network
AIS	Automatic Identification System
AUV	autonomous underwater vehicle(s)
BB	broadband
BIAS	Baltic Sea Information on the Acoustic Soundscape
BOEM	Bureau of Ocean Energy Management
BSEE	Bureau of Safety and Environmental Enforcement
CCB	Cornell Conservation Bioacoustics program
COVID	corona virus disease
CPA	closest point of approach
CSAC-SHRU	Chip Scale Atomic Clock-Several Hydrophone Recording Unit
dB	decibel(s)
dB re 1µPa2	decibel(s) referenced to 1 microPascal squared
EARS	Environmental Acoustic Recording System
edf	empirical distribution function (statistics)
ESA	Endangered Species Act
F-value	value on the F distribution calculated by dividing two mean squares
GAMs	generalized additive model(s)
GAMMs	generalized additive mixed model(s)
GDEM	Global Digital Elevation Model
GOM	Gulf of Mexico
HF	high frequency
HP	hydrophone(s)
Hz	Hertz
ID	identification
kHz	kiloHertz
km	kilometer(s)
LF	low frequency
m	meter(s)
MF	mid frequency
MAI	Marine Acoustics, Inc.
MATLAB®	MATrix LABoratory
MMPA	Marine Mammal Protection Act
MMSI	Maritime Mobile Service Identity
MP	Monitoring Project
N/A	not applicable
NASA	National Aeronautics and Space Administration
NEPA	National Environmental Policy Act
NOAA	National Oceanic and Atmospheric Administration
OSCAR	Ocean Surface Current Analysis Real-time

OSU	Oregon State University
P-value	level of marginal significance within a statistical hypothesis test, representing the probability of the occurrence of a given event
PAM	Passive Acoustic Monitoring
Program	Gulf of Mexico Passive Acoustic Monitoring Program
Ref.df	reference degrees of freedom (statistics)
RH	Rockhopper(s)
RL	received level
R-squared	measure of how much of the variance is in the dependent variable (statistics)
s	scaled
SA2	simple or second statistical approach
SHRU	Several Hydrophone Recording Units
SL	source level
SLBB	broadband source level
SNR	signal-to-noise ratio
SOG	speed over ground
SPL	sound pressure level
Std. Error	Standard Error
STW	speed through the water
SVP	sound velocity profile(s)
TL	transmission loss
TOB	third-octave band
VLA	vertical line array(s)
WHOI	Woods Hole Oceanographic Institution

Glossary of Acoustic Terminology

Amplitude. The magnitude of the signal. Amplitude is perceived as loudness and typically reported using a decibel unit.

Decibel (dB): Defined as 10 x log10(Io/Iref), where Io is the measured intensity and Iref is the reference intensity. In underwater acoustics, the reference intensity is typically 1 µPa.

Frequency: Frequency is defined as the number of cycles of sound occur within a second. Frequency is perceived as pitch and typically reported with units of Hertz (Hz) or kilohertz (kHz).

Hertz (Hz): The number of cycles per second of a sound wave.

Received Level (RL): This refers to the amplitude at any receiver at any arbitrary distance. It is also known as Sound Pressure Level (SPL). The unit for continuous sources are dB re 1µPa2.

Signal To Noise Ratio (SNR): Literally the comparison of the amplitude of a sound signal and the (typically background) noise level. In intensity terms, it is signal intensity divided by noise level intensity. Alternatively, it can be derived as subtracting the noise level in dB from the signal level in dB.

Source Level (SL): This value describes the amplitude of a source. It is traditionally presented as the value that occurs at a distance 1 meter from the source. The proper unit for a SL is dB re 1µPa2-m2. Historically, it was often used with a unit of dB re 1µPa at 1m.

Spectral Level: The amount of sound intensity in a 1-Hz-wide frequency band. The proper unit is dB re 1µPa2/Hz.

Third-Octave band: The amount of sound intensity in a one-third octave wide frequency band. The proper unit is dB re 1µPa2.

Transmission (Propagation) Loss (TL or PL): The amount of sound intensity lost between the sound source and the sound receiver.

E.1 Introduction

E.1.1 Background

The northern Gulf of Mexico (GOM) is a highly industrialized environment with multiple anthropogenic sound sources, including shipping, oil and gas activities, and military operations. Noise impacts to protected species (e.g., cetaceans) may occur as a result of activities associated with oil and gas exploration licensed by Bureau of Ocean Energy Management (BOEM) and the Bureau of Safety and Environmental Enforcement (BSEE). These activities may include seismic surveys, platform decommissioning, drilling, and resulting increases in vessel traffic. However, characterizing the acoustic impacts and trends associated with such activities is difficult without comprehensive baseline data on the ambient noise environment in the GOM.

Also, BOEM and BSEE are required to assess potential impacts on protected species, specifically under the Marine Mammal Protection Act (MMPA), Endangered Species Act (ESA), and the National Environmental Policy Act (NEPA) to assist and guide their decision making. Future BOEM MMPA rulemaking for seismic activities in the GOM will have a monitoring requirement associated with it, including collection of ambient noise data and noise data associated with seismic activities. In short, there was an urgent need to implement a systematic and comprehensive acoustic data collection effort in the GOM. BOEM's Passive Acoustic Monitoring (PAM) Program in the northern GOM was intended to collect and analyze data to meet this need.

Prior to developing an experimental design for the data collection program, a comprehensive literature review was conducted to identify and evaluate available relevant data from previous GOM underwater soundscape characterization efforts (Latusek-Nabholz et al. 2020).

E.1.1.1 Key Literature Findings

Low-frequency (LF) noise generally includes sounds in the bandwidths between 10 and 500 Hertz (Hz). This frequency range of underwater sound is primarily produced by anthropogenic sound sources, including commercial shipping and seismic surveys. Medium-frequency (MF) noise includes sounds from 500 Hz to 25 kiloHertz (kHz), and this range is dominated by natural sources of sound, such as sea-surface agitation, including break waves, spray, bubble formation and collapse, and rainfall. Heavy precipitation can increase noise levels in this range by as much as 20 decibels (dB). Sound generated by military and small vessels are also included in the medium-frequency range. Overall, medium-frequency sounds are more local or regional in nature, as they do not propagate over long distances. High-frequency (HF) sound generally ranges above 25 kHz and is generally located close to the receiver. Thermal noise, the result of particles moving close to the hydrophone for example, as well as mapping sonars, are included in this category.

The literature review conducted for the Gulf of Mexico Passive Acoustic Monitoring Program (Program) showed that the northern GOM soundscapes are characterized by a mix of industrial and natural sound sources across the 200 to 40,000 Hz band (Sidorovskaia and Li 2016). Shipping activity and seismic surveys are the major noise contributors in the GOM (Estabrook et al. 2016; Wiggins et al. 2016; Sidorovskaia and Li 2017). Analysis of long-term (i.e., multi-year) sound recordings reveal pervasive activity from seismic surveys (Estabrook et al. 2016; Sidorovskaia and Li 2017; Wiggins et al. 2016), often detected across broad expanses of the GOM and ranges extending to at least 700 kilometers (km) (378 nautical miles) (Rice et al. 2015; Estabrook et al. 2016). Estabrook et al. (2016) noted that sound levels from shipping activity were not nearly as pronounced as those from seismic surveys, which for the latter, in many cases, persisted for months at a time.

In a review of multi-year GOM Environmental Acoustic Recording Systems (EARS) data, scientists found no indication of an increasing baseline level of ambient noise (Sidorovskaia and Li 2017) below 1,000 Hz. However, Sidorovskaia and Li (2017) noted that high-frequency spectral levels showed an increase in more recent years (2010 and 2015) in the ambient soundscape of the northern GOM. This increase in the ambient soundscape may be attributed to anthropogenic activities, including the increasing use of unmanned devices (e.g., sonars, autonomous underwater vehicles [AUV]), which use high-frequency bands for communication and exploration for seismic exploration.

Seasonal variations in ambient noise levels due to industrial exploration are evident in various studies conducted in the GOM (Snyder 2007; Estabrook et al. 2016; Wiggins et al. 2016; Sidorovskaia and Li 2017). Anthropogenic noise sources showed considerable seasonal variability, with the highest levels measured during the summer months (Sidorovskaia and Li 2017). There is also documented evidence of regional variations in anthropogenic noise in the GOM (Wiggins et al. 2016).

E.1.2 Advanced Data Synthesis and Analysis

The primary objective of the Program was to design and field test implementation of a large-scale, multi-year, passive underwater acoustic monitoring effort in the northern GOM. Data collected under the first 2 years of the Program (2018 and 2019) were analyzed in two separate phases to generate outputs for characterization of the existing underwater soundscape (including sounds contributed by both natural and anthropogenic sources) in the northern GOM. Under Phase 1, *basic* data analyses were separately performed on data collected in each year. *Advanced* data analyses were performed on the combined 2-year data set under Phase 2. Results and recommendations from these advanced analyses are presented in this report.

The Program was initiated and implemented as two distinct 12-month Monitoring Projects (MP):

- 2018 MP (**Figure E-1**): Acoustic monitoring was conducted within a 100- by 200-km study area box located in the northern GOM for the 12-month period from May 2018 to April 2019. Two separate deployments were conducted, the first from May to October 2018 (designated as Deployment 1) and the second from November 2018 to April 2019 (Deployment 2).
- 2019 MP (**Figure E-1**): Monitoring initiated under the 2018 MP was continued for an additional 12 months (May 2019 to April 2020). Lessons learned from the 2018 MP were used to guide delineation of the study area boundaries and placement of sensors for the 2019 MP. The 2019 MP study area box measured approximately 100 by 140 km. Two separate deployments were conducted, the first from May to October 2019 (designated as Deployment 3) and the second from November 2019 to April 2020 (Deployment 4).

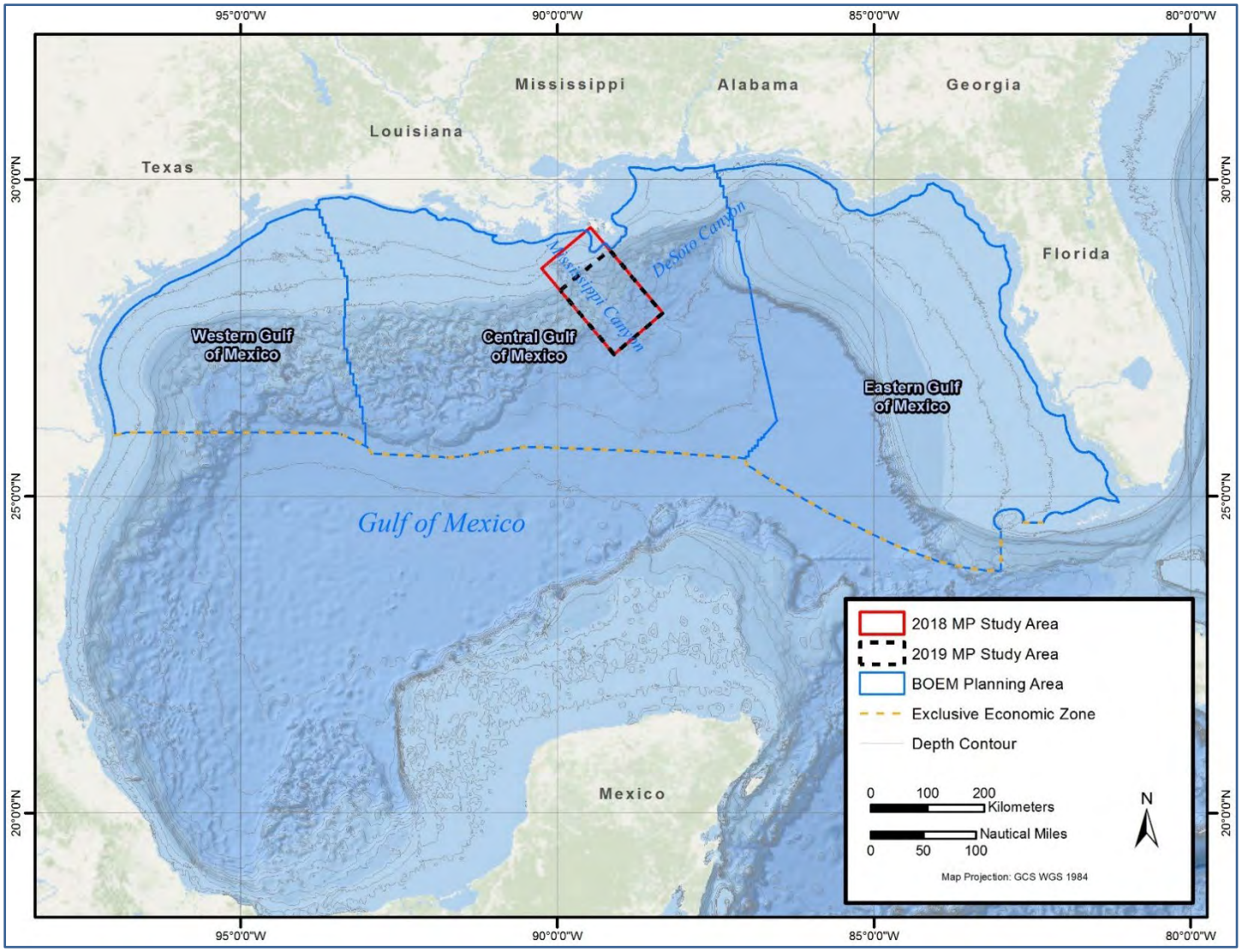

Figure E-1. Northern GOM BOEM planning areas and GOM Program 2018 and 2019 MP study areas

E.1.3 Monitoring Instrumentation

During both MPs, underwater acoustic data were collected using a mix of stationary and mobile platforms that were deployed at selected locations within the respective study areas (**Figures E-2** and **E-3**). Data were collected at depths ranging from 53 to 2,148 meters (m) within the main habitat types in the region, including the continental shelf (less than 200 m deep), continental slope (200 to 1,600 m deep), and the abyssal plain (more than 1,600 m deep).

Three different types of stationary moorings equipped with sensors (hydrophones) and recording systems were used, namely Rockhoppers (RH) and EARS, both with effective recording bandwidth ranging from 10 Hz to 96 kHz; and Chip Scale Atomic Clock-Several Hydrophone Recording Unit (CSAC-SHRU) vertical line arrays (VLA), with effective recording bandwidth of 10 Hz to 4.5 kHz. Additionally, two separate mobile autonomous underwater platforms (Seagliders), with an effective recording bandwidth of 10 Hz to 62.5 kHz, were also deployed within selected portions of the study area to collect data from the areas between the stationary moorings within the Mississippi Canyon and to cover selected areas in the DeSoto Canyon.

E.1.4 Monitoring Locations

Under both the 2018 and 2019 MPs, 12 stationary moorings (5 RH, 5 EARS, and 2 CSAC-SHRUs) were deployed (**Table E-1** and **Figure E-2,** and **Table E-2** and **Figure E-3**, respectively). Between the 12 moorings, the 2018 MP covered a depth range of 53 to 1,672 m. In the 2019 MP, for placement of EARS and RH, five locations were retained from the 2018 MP and five new locations were added within the delineated study area. The CSAC-SHRU locations remain unchanged from 2018. Between the 12 moorings, the 2019 MP covered a depth range of 356 to 2,170 m.

E.1.4.1 Seaglider Flight Paths

For the 2018 MP, the Seaglider path consisted of three contiguous segments to cover approximately 2 weeks of data collection in the DeSoto Canyon and 2 weeks in the Mississippi Canyon (**Table E-3** and **Figure E-2**). For the 2019 MP, very limited underwater acoustic and environmental data were collected with the Seaglider due to operational and weather constraints (**Table E-4** and **Figure E-3**).

E.1.5 Data Analysis Approach

A two-step data analysis approach was adopted:

- **Phase 1 (Basic Data Analyses):** Data collected under the 2018 MP by each instrument type were separately processed, analyzed, and reported. RH and Seaglider data were analyzed using the noise analysis tools within the Raven-X toolbox for MATrix LABoratory (MATLAB®) developed by the Cornell University Center for Conservation Bioacoustics. EARS data were analyzed using the EARS MATLAB noise analysis software; as a quality control check both analyses toolboxes were tested on the same data subset to ensure identical outputs. SHRU VLA data were analyzed using standardized acoustic data analyses protocols.

  Phase 1 data analyses outputs included long-term spectral average plots, equivalent sound levels, cumulative percentage distribution, temporal trends, power spectral density levels, and spectral probability density plots. The data standards for the analyses generally were consistent with guidelines adopted by the Baltic Sea Information on the Acoustic Soundscape (BIAS) project as well as the Atlantic Deepwater Ecosystem Observatory Network (ADEON) project (Ainslie et al. 2017).

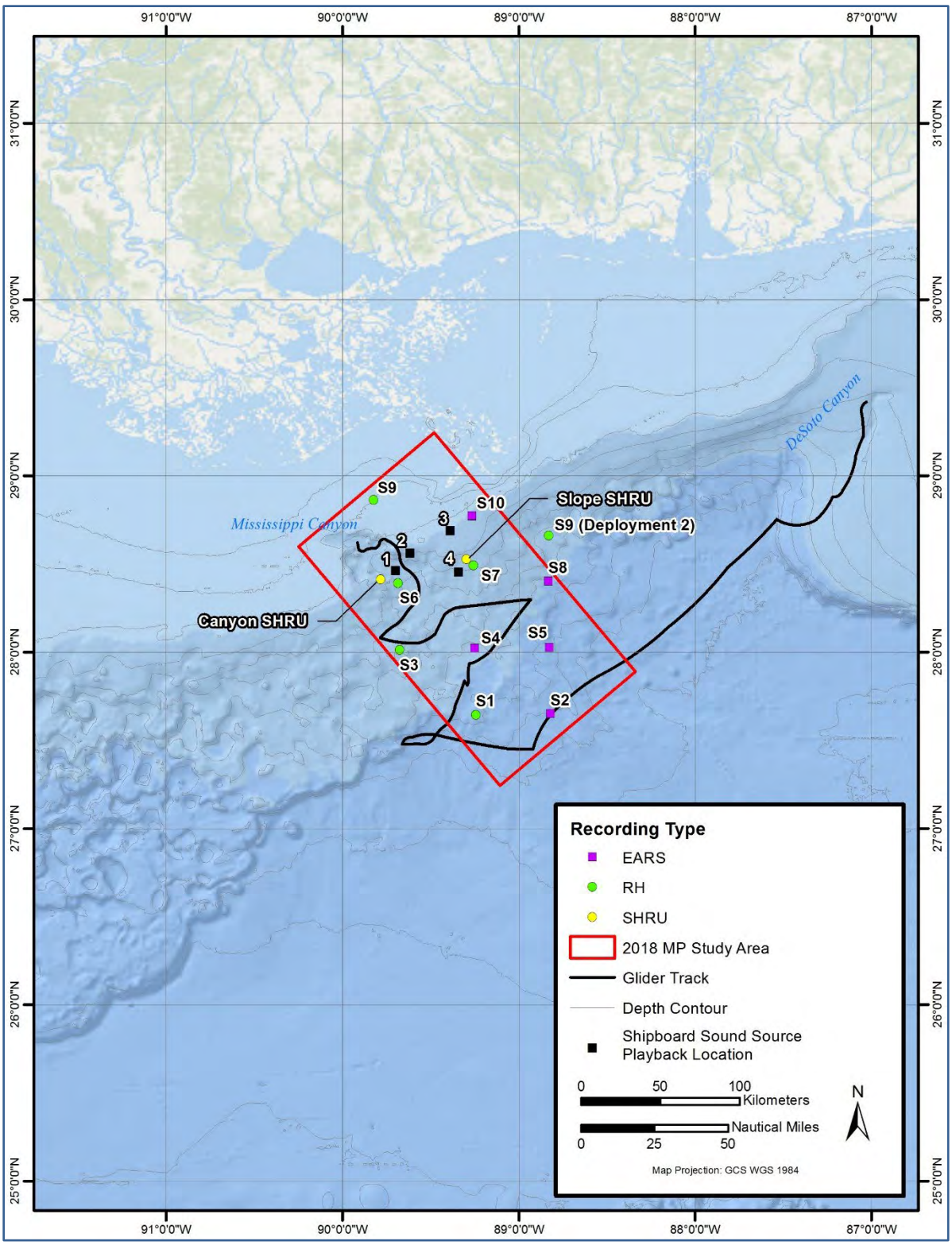

Figure E-2. Locations of stationary and mobile platform deployments (Deployments 1 and 2) under the 2018 MP

119

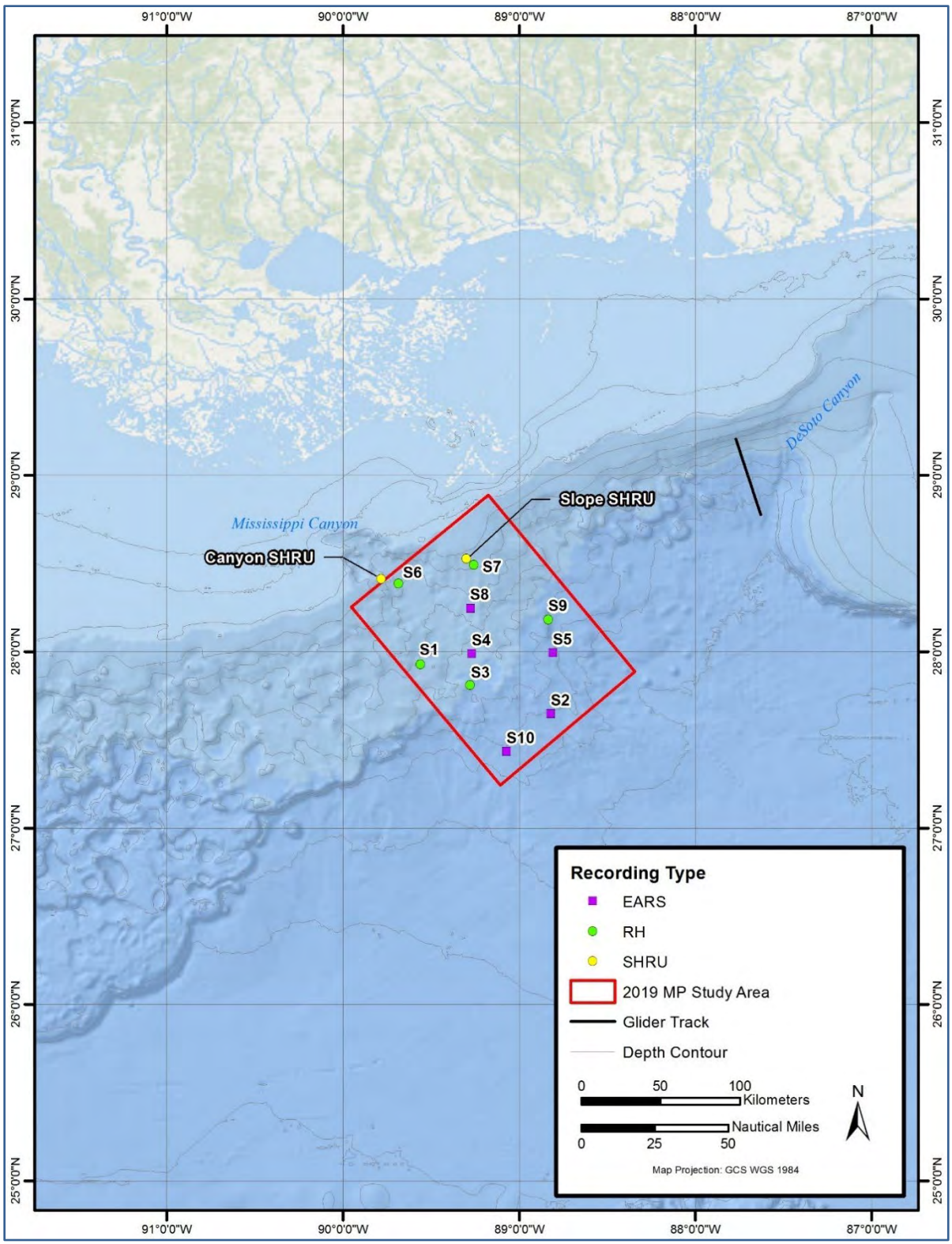

Figure E-3. Locations of stationary and mobile platform deployments (Deployments 3 and 4) under the 2019 MP

120

Table E-1. Stationary mooring locations under the 2018 MP

Monitoring Station No.	Data Recording System	Monitoring Bandwidth	Deployment 1 (May to October 2018)				Deployment 2 (November 2018 to April 2019)			
			Latitude (°)	Longitude (°)	Water Depth (m)#	Duration Data Recorded (hours)	Latitude (°)	Longitude (°)	Water Depth (m)	Duration Data Recorded (hours)
S1	RH	10 Hz – 96 kHz	27.64300	-89.24300	1,413	3,141	same as Deployment 1			4,368
S2	EARS	10 Hz – 96 kHz	27.65000	-88.82000	1,772	4,179	same as Deployment 1			3,745
S3	RH	10 Hz – 96 kHz	28.01100	-89.67500	712	3,106	same as Deployment 1			4,359
S4	EARS	10 Hz – 96 kHz	28.02000	-89.25100	1,280	1,678	27.98713	-89.27067	1,280	3,820
S5	EARS	10 Hz – 96 kHz	28.02600	-88.82700	1,672	4,227	27.99418	-88.80950	1,672	3,703
S6	RH	10 Hz – 96 kHz	28.38900	-89.68500	685	3,065	same as Deployment 1			3,052
S7	RH	10 Hz – 96 kHz	28.49000	-89.25800	440	3,030	same as Deployment 1			4,415
S8	EARS	10 Hz – 96 kHz	28.40200	-88.83200	1,262	1,332	same as Deployment 1			3,960
S9	RH	10 Hz – 96 kHz	28.86100	-89.82400	53	1,108	28.66000	-88.83000	1,067	4,491
S10	EARS	10 Hz – 96 kHz	28.77100	-89.26600	131	4,128	28.77180	-89.26640	131	3,808
Canyon SHRU	SHRU	10 Hz – 4.5 kHz	28.40991	-89.78438	4 HP[a]: 175, 200, 250, 275	3,648	N/A			
Slope SHRU	SHRU	10 Hz – 4.5 kHz	28.52531	-89.29874	4 HP[a]: 175, 200, 250, 275	624	N/A			

Key: RH=Rockhopper; EARS=Environmental Acoustic Recording Systems; N/A=not applicable; SHRU=Several Hydrophone Recording Units

[a] # HP=hydrophones

Notes:

1. RHs and EARS were deployed for a total of 24 months (4 separate deployments each lasting 6 months).
2. SHRU data collection period was only 6 months during each deployment, for a total of 12 months over 2 years.
3. During Deployment 1, the RH at Site 9 was dragged up by a fishing trawler; as a result, the Site 9 location was moved to deeper waters during Deployment 2.
4. During Deployment 1, the Slope SHRU had an electrical malfunction due to seepage of salt water into the sensor housing, resulting in the recording systems failing after 26 days of data collection.
5. Approximately 2 weeks into the second deployment, the RH at Site 3 developed an issue with one of the two 4-terabyte hard drives. The unit successfully switched over to the second hard drive. However, the capacity of the second solid state drive (hard drive) alone was not quite sufficient to store recordings for the entire deployment period. The data storage limit was reached approximately 4 months after the start of the deployment.

Table E-2. Stationary mooring locations under 2019 MP

Monitoring Station No.	Data Recording System	Monitoring Bandwidth	Deployment 3 (May 2019 to October 2019)				Deployment 4 (November 2019 to June 2020)			
			Latitude (°)	Longitude (°)	Water Depth (m)#	Duration Data Recorded (hours)	Latitude (°)	Longitude (°)	Water Depth (m)	Duration Data Recorded (hours)
S1	RH	10 Hz – 96 kHz	27.92710	-88.56040	2,148	4,390	same as Deployment 3			Unit lost
S2	EARS	10 Hz – 96 kHz	27.64837	-88.82111	1,777	1,048	same as Deployment 3			5,077
S3	RH	10 Hz – 96 kHz	27.80900	-89.27890	1,375	4,396	same as Deployment 3			5,096
S4	EARS	10 Hz – 96 kHz	27.98871	-89.26963	1,332	5,057	same as Deployment 3			4,682
S5	EARS	10 Hz – 96 kHz	27.99373	-88.80897	1,671	5,160	same as Deployment 3			4,371
S6	RH	10 Hz – 96 kHz	28.38520	-89.68530	685	4,375	same as Deployment 3			5,276
S7	RH	10 Hz – 96 kHz	28.49160	-89.25810	440	3,973	same as Deployment 3			2,881
S8	EARS	10 Hz – 96 kHz	28.24345	-89.27747	830	5,223	same as Deployment 3			5,071
S9	RH	10 Hz – 96 kHz	28.17980	-88.83490	1,526	4,388	same as Deployment 3			5,171
S10	EARS	10 Hz – 96 kHz	27.43412	-89.07278	1,797	5,159	same as Deployment 3			4,680
Canyon SHRU	SHRU	10 Hz – 4.5 kHz	28.77150	-89.78500	4 HP[a] at 175, 200, 250, 275	3,480	N/A			
Slope SHRU	SHRU	10 Hz – 4.5 kHz	28.4124	-89.29920	4 HP[a] at 175, 200, 250, 275	3,480	N/A			

Key: RH=Rockhopper; EARS=Environmental Acoustic Recording Systems; N/A=not applicable; SHRU=Several Hydrophone Recording Units

[a] # HP=hydrophones

Notes:

1. RH and EARS were deployed for a total of 24 months (4 separate deployments each lasting 6 months).
2. SHRU data collection period was only 6 months during each deployment, for a total of 12 months over 2 years.
3. During Deployment 4, the RH at Site 1 was lost and could not be recovered due to a communication system failure.

Table E-3. Segment and coordinates of 2018 MP Seaglider flight path

Flight Path Segment Number	Flight Path Segment ID	Data Collection Dates	To		From	
			Latitude (°)	Longitude (°)	Latitude (°)	Longitude (°)
1	DeSoto Canyon	05/10/2018 – 5/19/2018	29.419722	-86.995378	28.705587	-87.574675
2	Deep Slope	05/19/2018 – 05/30/2018	28.676265	-87.601155	27.518300	-89.415167
3	Mississippi Canyon	05/30/2018 – 06/20/2018	27.519063	-89.415153	28.640717	-89.894550

Table E-4. Segment and coordinates of 2019 MP Seaglider flight path

Flight Path Segment Number	Flight Path Segment ID	Data Collection Dates	From		To	
			Latitude (°)	Longitude (°)	Latitude (°)	Longitude (°)
1	DeSoto Canyon	09/24/2019 – 10/05/2019	29.2043882	-87.769433	28.776567	-87.630433

- **Phase 2 (Advanced Data Analyses):** In Phase 2, acoustic data collected under the two MPs were combined to create a 24-month dataset for detailed analyses and soundscape characterization. Based on guidance provided by BOEM, Phase 2 analyses were to include anthropogenic noise source identification and characterization (e.g., received level, spectrum, duration, and, if possible, localization, tracking, and estimation of source levels). *Due to schedule, resources, or logistical constraints, representative datasets were used for some of the analyses.* The results of the data analyses also were used to identify data and information gaps. Key steps in Phase 2 analyses included the following:
    - **Raw Data Power Spectral Density Analysis**: Raw data were collected using different instruments, each of which uses a different data format. A project-customized module of Raven-X was used to generate summary statistics for the raw acoustic data in 1-Hz, 1-second resolution. The Raven-X outputs, which served as inputs for the Phase 2 analyses, are compliant with ADEON-guidelines. Therefore, by extension, the Phase 2 outputs are also ADEON-guidelines compliant.
    - **Detector Band Creation**: Known acoustic sources have specific frequency characteristics. Candidate frequency bands that are likely to be able to indicate the presence of different sources were identified. Some of these frequency bands were determined from the literature, while the remaining bands (defined as empirical bands) were identified through a review of the data. While these frequency bands were observed, they were not associated *a priori* with any particular source(s).
    - **Detection of Acoustic Events in Candidate Bands**: The hourly mean received level (RL) in each band was calculated and subtracted from each "candidate" band to produce a "normalized" band. The detection threshold is taken as the sum of standard deviation of the normalized band plus 3 dB. A subset of the data was hand scored for vessel and airgun presence. The 3 dB threshold was established based on comparison of detection rates at different thresholds and hand-scored values. Any level exceeding this threshold was taken as a detection.

- **Automatic Identification System (AIS) Data**: AIS data for 2018 and 2019 were obtained from BOEM and the National Oceanic and Atmospheric Administration (NOAA)-sponsored website (https://marinecadastre.gov/) and incorporated into the analyses to identify specific acoustic sources.
- **Statistical Analysis**: The "bandstats" output, the cumulative acoustic power in a 1-hour band in each of the source candidate frequency bands, were analyzed with a suite of predictor variables. These variables include the AIS metrics and the windspeed values. The resulting analyses clarifies the relative power of these metrics to predict acoustic levels. Graphical representations of the candidate frequency bands were used to identify spatiotemporal patterns.

In Phase 2, data collected by the mobile platforms were evaluated independently of data collected by stationary platforms because of the differences in spatial and temporal extent and coverage of different areas with potentially different species assemblages and soundscape drivers. To the extent practicable, data analysis protocols for stationary and mobile platforms were made consistent to ensure compatibility of results. As appropriate and relevant, meteorological/oceanographic data collected during the MPs or acquired from external sources were also incorporated into the analyses to support data interpretation.

E.2 Data Analysis Challenges

COVID-19 pandemic related lockdowns at various team partner institutions created serious challenges for completing the field work safely and on time and consequently led to a significant delay in conducting data analyses and reporting. Another significant challenge was the delay in acquisition of the AIS data, which is the backbone of the vessel soundscape analysis. The 2018 AIS data were not available until 2020, and the last part of the 2019 AIS data were not available until mid-2021.

E.3 Methods

Phase 2 analysis were conducted in accordance with a BOEM-approved Advanced Data Analyses Plan and the primary objective of these analysis was to advance basic soundscape characterization conducted under Phase 1. In both phases, stationary and mobile platform data were evaluated separately since they were collected in somewhat different areas and therefore likely to consist of different species mix. To the extent practicable, the analysis protocols for stationary and mobile platforms were made consistent to ensure compatibility of results.

Since the overall objective of the Phase 2 analysis was to support underwater soundscape characterization, the following specific types of assessments were performed:

a) Define and create source-specific frequency bands for 10 EARS/RHs. These bands were based on published reports of the characteristics of sources known to occur in the study area, including some biological sources.
b) Perform detection operations on the EARS/RH frequency bands. The detections of signals in these bands would reflect the presence of the sources nominally associated with each band.
c) Perform vessel and airgun detection operations. This discrimination detection effort focused on the presence of vessels and airgun activity, using an approach derived to create additional frequency bands that represented the presence of airguns and vessel passings.
d) Statistical analyses of the vessel noise band RLs. This effort determined how much of the variability in sound RLs at each buoy can be explained by independent predictors of windspeed, wave height, and vessel presence (i.e., AIS data).
e) Consideration of the "extrapability" of results. Initial analysis was based upon a comparison of the glider that overflew a static receiver. The expectation was that during the close approach, the

two receivers would record similar data and the similarity would decrease with increasing distance.

E.3.1 Comparison of RH and EARS datasets

Prior to combining the RH and EARS datasets for use in the statistical analyses, a comparison of the spectral properties of the five RH and five EARS recorders was performed using data from all four deployments. The same instrument type was deployed at each site regardless of the deployment number. For example, for Deployments 1 through 4, a RH recorder was always deployed at site S1 (**Table E-5**).

Table E-5. Recorder type deployed at each site for all deployments

Site	Recorder Type
S1	RH
S2	EARS
S3	RH
S4	EARS
S5	EARS
S6	RH
S7	RH
S8	EARS
S9	RH
S10	EARS
Key: RH=Rockhopper; EARS= Environmental Acoustic Recording Systems	

E.3.2 Frequency Band Detection Analyses

E.2.2.1 Creation of Defined Frequency Bands

Predefined sound frequency bands were compiled to identify the sources of sound in the data recordings as they were assessed. The underlying assumption of this process is that the presence of sound in a defined frequency band indicates the potential presence of that sound source in the Program environment. For example, sounds in the frequency band from 2,000 to 4,000 Hz may be indicative of the presence of sperm whales (**Table E-6**).

These predefined frequency bands were derived from published descriptions of biological and anthropogenic sounds or from collected data (**Table E-6**). The "Empirical" frequency bands were defined after manual examination of the recorded acoustic data. However, several of the identified frequency bands have overlapping frequency ranges.

The selection of the frequency bands for the biological sources was based on the species of marine mammals and other sound-producing marine taxa potentially occurring in the Program area. Similarly, the selection of the possible sound-producing anthropogenic sources was based on the types of human activities that occur in the Program study area and the types of sound sources employed during the execution of those activities. For example, various sonar and subsea imaging sources (**Table E-6**, rows 13 to 18) may be used during scientific research, fishing, or geophysical exploration in the GOM.

Table E-6. Sound sources, frequency ranges, and references for the pre-defined frequency bands

Band Number	Band Name	Frequency Range (Hz)		Reference
		Low	High	
1	Bottlenose Dolphin Whistles	2,000	12,500	Frankel et al. 2014
2	Bryde's Whale	70	160	Rice et al. 2014
3	Cuvier's Beaked Whale	29,000	43,000	Erbe et al. 2017
4	Short-finned Pilot Whale	3,000	6,000	Baron et al. 2008
5	Sperm Whale	2,000	4,000	Thode et al. 2002
6	Fish	25	2,000	Staaterman et al. 2014
7	Snapping Shrimp	2,000	10,000	Staaterman et al. 2014
8	Vessels, Airgun, Piles	10	40	McPherson et al. 2016
9	Vessels	200	2,500	Sidorovskaia and Li 2016
10	Airguns, Piles	200	1,000	Hildebrand 2009; Sidorovskaia and Li 2016
11	Weather	200	10,000	Sidorovskaia and Li 2016
12	Chirp Sonar	1,000	15,000	Schock 2004
13	Deep Side Scan	11,500	12,500	Hildebrand 2009
14	Sub-bottom profiler	3,000	7,000	Hildebrand 2009
15	Edgetech 424	8,000	15,000	Crocker and Fratantonio 2016
16	Knudsen TR-1075	3,500	5,500	Crocker and Fratantonio 2016
17	Edgetech 4200 EMI	60,000	70,000	Crocker and Fratantonio 2016
18	Empirical Band 2	10,000	20,000	Observed in Data
19	Empirical Band 3	20,000	30,000	Observed in Data
20	Empirical Band 5	40,000	50,000	Observed in Data
21	Empirical Band 6	50,000	60,000	Observed in Data
22	Empirical Dolphins	5,000	15,000	Observed in Data
23	Empirical Chirp Sonar	49,000	51,000	Observed in Data
24	Empirical 500–1000 pulses	500	1,000	Observed in Data

E.2.2.2 Anthropogenic Sound (Vessel and Airgun) Detection Analysis

Band-limited energy detectors were developed for vessel and airgun signals, the two most prominent sources of anthropogenic sound in the northern GOM. The airgun detector calculated the energy in the 10 to 100 Hz band on an hourly basis and then subtracted the value from the 25 to 63 kHz reference band to produce the airgun detection index. Detections occurred when this index was greater 12 dB above the 10th percentile level of the index.

The vessel detection algorithm was similar. It was based on a vessel detection index calculated as the hourly signal to noise ratio of the 250 to 2,500 Hz band relative to the same 25 to 63 kHz reference band. This detector was tuned for the broadband Lloyd mirror interference patterns that accompany a close passage of a vessel moving past the recorder. A daily moving mean of the vessel detection index was calculated, and detections occurred when the index was 3 dB greater than the moving mean.

The acoustic record of the 2018 MP Seaglider was also examined for the presence of vessels and airgun activity. The noise characteristics of the glider acoustic record were different from that of the moored autonomous recorders. Therefore, the glider recordings were “hand scored” for the presence of vessels and airguns rather than tuned to a detection algorithm.

E.2.2.3 Biological Sound Detection Analysis

To attempt to document or investigate the presence of marine animals in the Program area, several frequency band metrics were added to the analysis suite. These included frequency bands for the known vocalizations of the following marine mammal species and groups: Rice's whale (*Balaenoptera ricei)*, beaked whales, and dolphins. Detection efforts for *Kogia* species were not attempted due to bandwidth limitations caused by the anti-aliasing filters on the recorders (Klinck, pers. comm.).

Since the data provided was for only summary energy metrics and did not include the waveforms, only simple energy detectors could be used for nominal marine mammal species assessed. As such, these results should be considered preliminary at best. It would be desirable for future dedicated biological analyses to be conducted using the waveform data and more sophisticated detection methods.

The energy detection method used was based on Clark et al. (in prep.). This method computes the signal-to-noise ratio (SNR) of a frequency band of the signal of interest with a frequency band in which the signal does not occur. When an animal vocalizes, there is energy in the signal band but no additional energy in the reference band. Therefore, the ratio of the two (i.e., the SNR) increases. For beaked whales, the possibility of adjacent frequency bands both above and below the beaked whale band existed (**Figure E-4**). A SNR for the beaked whale band was generated that spanned 29 to 43 kHz, relative to the 20 to 30 kHz and 40 to 50 kHz bands. In this case, the two SNR metrics were multiplied in an element-wise fashion, and the product of the two was taken as the beaked whale index (**Figure E-5**). Strong positive values of this index (greater than 10 dB) were taken as potential indicators of beaked whale presence.

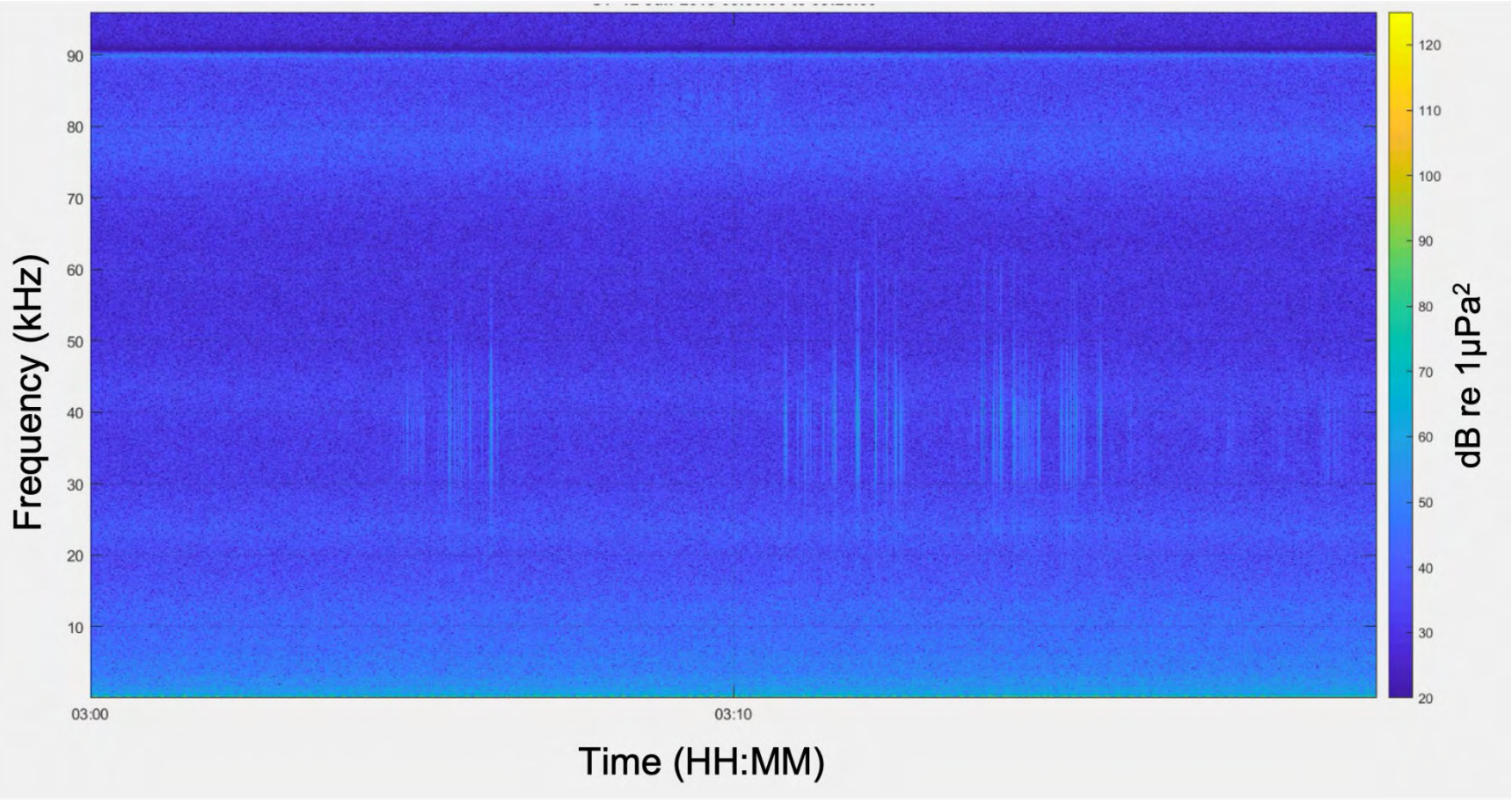

Figure E-4. Sample nominal beaked whale band (mid-frequency clicks) spectrogram

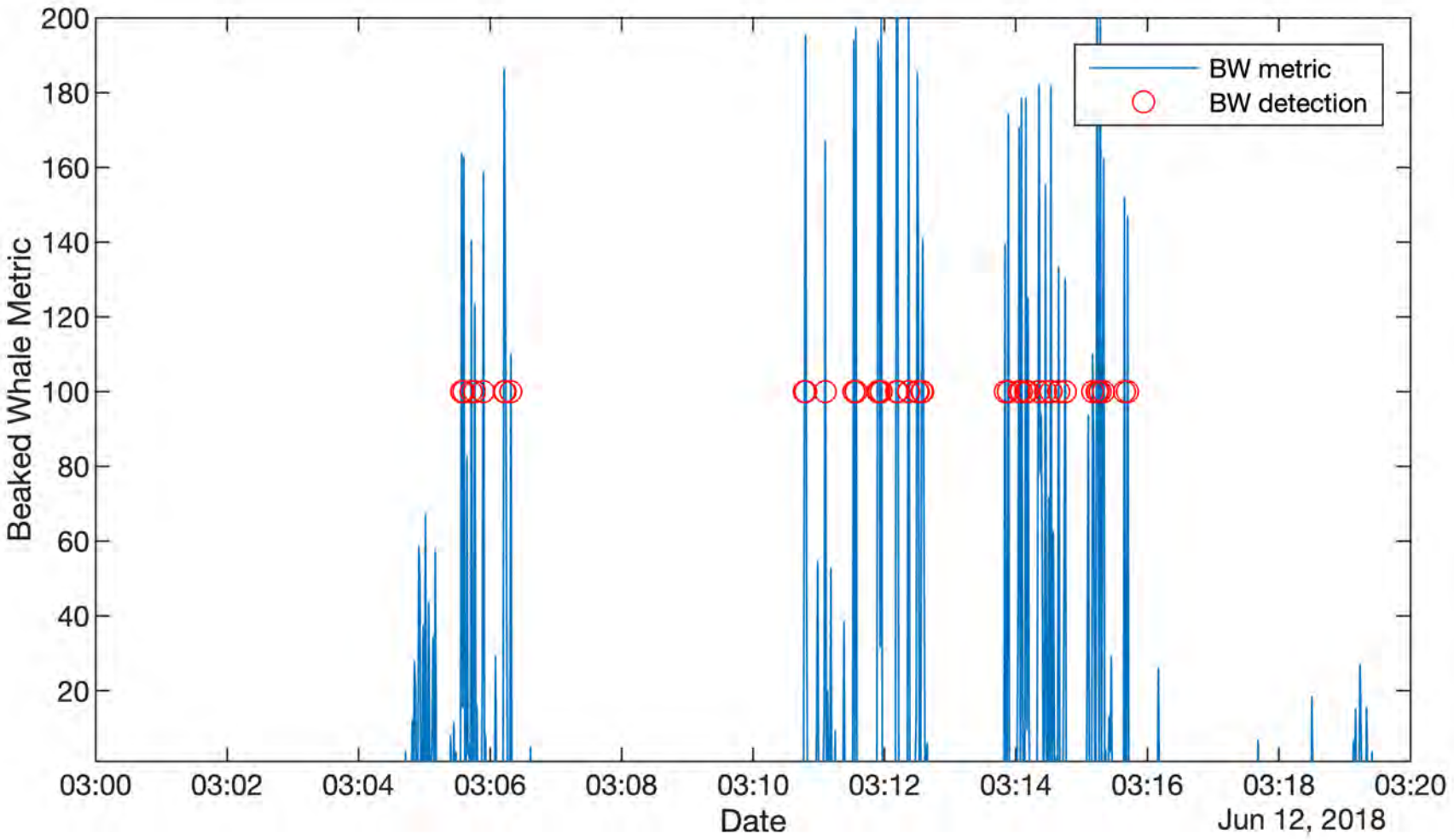

Figure E-5. Sample nominal beaked whale band (mid-frequency click) detection, with the blue lines representing the second-by-second beaked whale index, while the red circles represent signal exceedances or potential detections of beaked whales

E.3.3 Statistical Analysis of Measured Vessel Received Levels

One approach to characterizing the sources of ambient noise was to predict how much of the variability in the recorded sound levels at each receiver could be explained by environmental conditions and independently available vessel descriptors.

E.2.3.1 Automatic Identification System Data

The AIS was developed with the intent to increase vessel safety (Tetreault 2005). An AIS-equipped ship continuously broadcasts its location, speed, course, identity, and additional information. Other vessels use this information to increase their situational awareness of surrounding vessel traffic. Shore-based receivers began archiving AIS data for management and research purposes. Among the AIS data fields transmitted are the Maritime Mobile Service Identity (MMSI) number, which provides a unique identification for each vessel. The MMSI number can be used to extract descriptive characteristics from a vessel database (e.g., IHS4 Markit). Processed AIS data (MarineCadestre.gov n.d.) were downloaded as datasets became available over time.

E.2.3.2 Source Level Models

A shipping noise model that can produce dynamic and static noise maps of broadband (BB) vessel noise was created (Frankel et al. 2017). The overall model is based on vessel speed and other descriptors as provided in the AIS tracks and IHS Markit database. These empirical data were viewed as an excellent complement to existing vessel source level models (e.g., Ross 1976). Additional vessel source-level information was discovered in the publications of McKenna et al. (2013) and Veirs et al. (2016). The authors of these two studies were contacted and agreed to provide copies of their measurements to be used as inputs into modeling and analyses for this project.

McKenna et al. (2013) collected and published 944 source level (SL) estimates for 570 different vessels transiting the Santa Barbara Channel. Some vessels were measured more than once. They used a simple $20 \log_{10}(\text{range})$ transmission loss (TL) model to calculate SLs. This simple spherical spreading approach presents a possible source of bias in their published values. Nevertheless, these data are the first large modern measurement set of vessel SLs. The authors also reported the speed through the water (STW) for the vessels. STW was obtained by subtracting the effect of surface currents from the measured speed over ground (SOG).

Veirs et al. (2016) also reported 2,182 SL estimates of 1,582 different vessels that passed by a calibrated hydrophone. The authors used both spherical spreading and an empirical TL measurement to produce multiple SL estimates. This dataset also included AIS-derived SOG. MAI converted their SOG speeds to STW.

The need to calculate STW from SOG values requires a surface current measurement or estimate. Regional current models were used for the vessels in the source level measurements. However, for the creation of the larger AIS-based noise model, a single worldwide current speed database was preferred. The Ocean Surface Current Analysis Real-time (OSCAR) database funded by the National Aeronautics and Space Administration (NASA) (ESR 2009) was selected for this purpose. OSCAR has monthly temporal and 1/3° latitude and longitude spatial resolutions.

The details of the SL measurements from McKenna et al. (2013) and Veirs et al. (2016) can be found in their respective papers; both papers used a similar methodology. Acoustic recordings were made of vessels as they passed by calibrated hydrophones, which allowed for measurement of the absolute received sound pressure level (SPL). The range from the receiver to the vessels was determined using AIS data. TL was estimated and added to the RL to produce the estimated vessel SLs.

Veirs et al. (2016) reported SLs in four forms representing two TL models, both with and without frequency absorption terms. The first model was based on simple spherical spreading, which was also used by McKenna et al (2013). The second model was empirically based on a single TL experiment conducted in March 2014 that produced a TL estimate of 18.6 x $\log_{10}$(range).

McKenna et al. (2013) provided SL data for 570 vessels, and their data set included both broadband (20 to 1,000 Hz) and one-third octave band SLs. The mean and standard deviation for each of these band levels were calculated **(Figure E-6**).

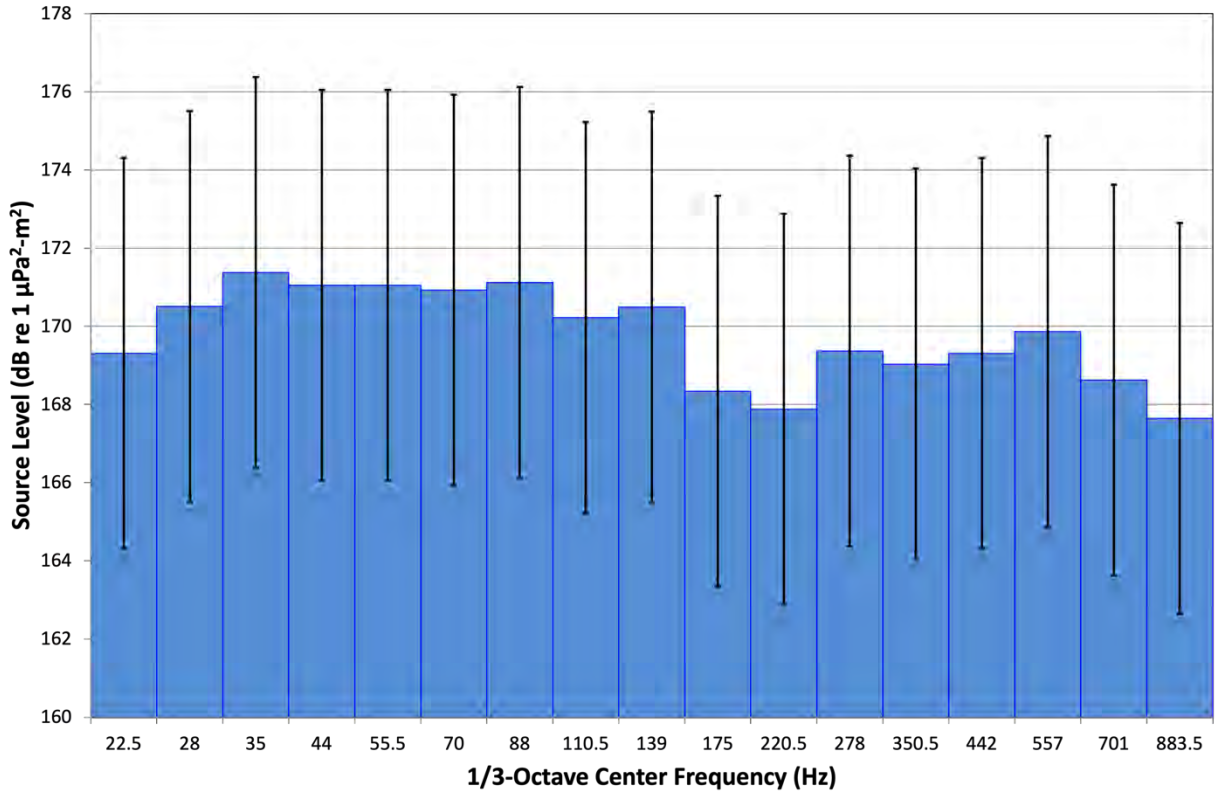

Figure E-6. Mean vessel spectrum as reported in McKenna et al. (2013)

Veirs et al. (2016) provided broadband source level data for 1,595 separate vessels that were measured between 1 and 23 times during their study. A total of 2,182 measurements were made. The broadband source level (SLBB) values provided by both Veirs et al. (2016) and McKenna et al. (2013) were used as inputs to the SL model.

The identity and speed of the vessel during the measurement was determined from AIS data. McKenna et al. (2013) adjusted the AIS SOG to STW using a local current model for Southern California (Interdisciplinary Oceanography Group 2017). Veirs et al. (2016) reported the AIS SOG value. Part of the analysis for this project was converting the McKenna et al. (2013) and Veirs et al. (2016) speed values to STW values using the Haro Strait model (NOAA 2016). Simard et al. (2016) also produced a vessel SL model that reports one-third-octave band levels. SLs for each vessel were calculated for the bands centered on 50 and 200 Hz.

E.2.3.3 Transmission Loss Model

The three-dimensional (3d) underwater sound propagation model, which was developed under the GOM Program (Lin 2019, 2021), was used to predict the TL between vessels and the stationary recorders. The principle of reciprocity was used as the models were run from each recorder location. Seasonal sound velocity profiles (SVP) were selected to reduce computational load and were extracted from the Global Digital Elevation Model (GDEM) database (Carnes 2009), which has a spatial resolution of 0.25° in latitude and longitude. The nearest node (location) in the database to each actual recorder position was selected. A grid of nine positions, spanning 0.5° by 0.5° and centered on the selected position, was averaged over space. The resulting monthly mean SVP profiles were plotted and grouped by season (**Figure E-7**). Winter included January, February, and March; spring consisted of April, May, and June; summer included July, August, and September; and fall consisted of October, November, and December. The mean SVP profile of each 3-month period for each site were exported and used to calculate the TL fields.

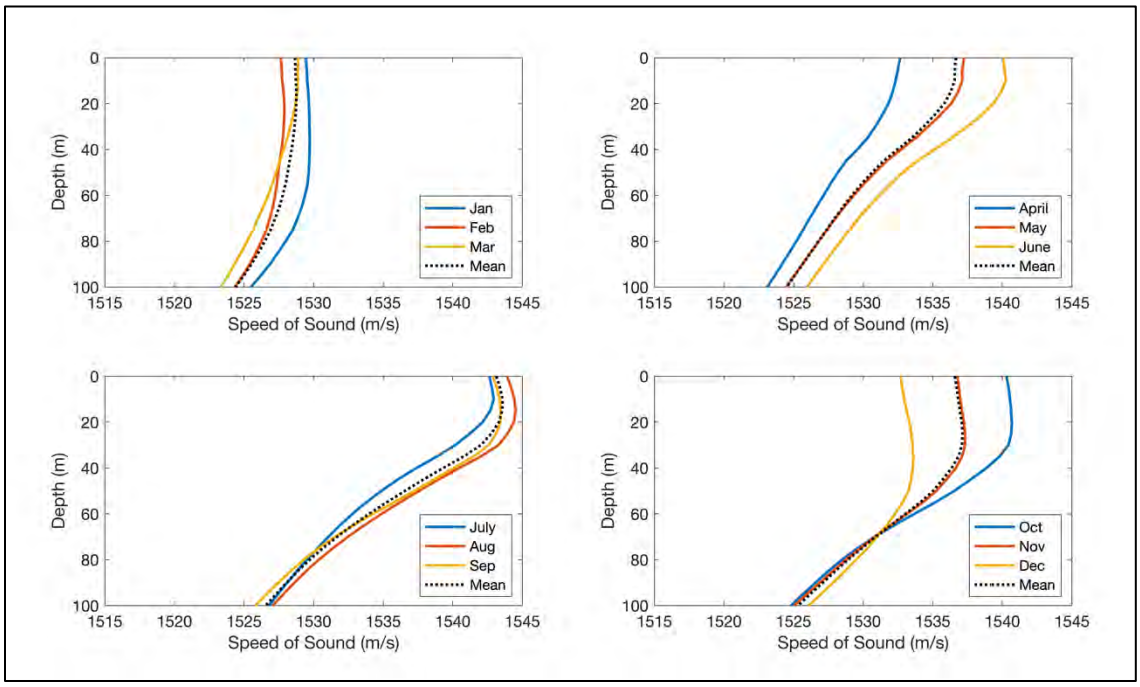

Figure E-7. Seasonal mean sound velocity profiles extracted from the GDEM database (Carnes 2009) for Site 10 during Deployment 1

The propagation models were run for 50 and 200 Hz, as these frequencies are found within the main energy distribution of vessel and airgun noise. TLs were reported for three water depths (5, 10, and 20 m), which covered the nominal depth range of vessel propellers.

E.2.3.4 Received Sound Pressure Levels

Predicted received SPLs at each recorder were calculated by subtracting the TL from the broadband SL estimates and the one-third-octave estimates. Two broadband estimates were produced using the 50 Hz TL predictions (BB1) and the 200 Hz TL predictions (BB2). The one-third-octave SLs used their respective TL predictions to generate the predicted the third-octave band (TOB) RLs (Hz50 and Hz200).

E.2.3.5 Statistical Modeling

The goal of the statistical modeling was the prediction of the variance amount in the measured SPLs with independently derived predictor variables. These variables include the distance of the vessel from the recorder as well as the predicted received sound level at the recorder. Additional metrics of windspeed and wave height were included since these environmental conditions are known to influence the level of LF sound.

Statistical analyses were run using generalized additive mixed models (GAMMs), although the initial analyses used simple generalized additive models (GAMs). GAMs and GAMMs both fit smoothed weighting curves to the dependent and predictor variables. These curve fits are then tested to see whether they are statistically significant. The values of the dependent variables may be adjusted during the modeling process by the additional predictor variables. Therefore, these curve fits show the general form of the relationship (e.g., **Figures E-8** and **E-9**). In these examples, the y-axis values of these smoothed plots differ from the original data because these curves are fit to adjusted modeled values that include the influence of the other predictor variables. The shape of the curve is the important component in illustrating the relationship between two variables.

GAM analyses were used to explore the relationship between the variables and determine the appropriate statistical distribution and link function. A gamma distribution with a log link function was used. These initial analyses also examined evidence of autocorrelation in the data. The existence of autocorrelation was anticipated given that the SLs at time 't' are very much related to the final SLs at time 't +10'.

Autocorrelation function plots (ACF) showed strong evidence of autocorrelation within the data. The method chosen to address this issue was to move to a GAMM model using autoregressive (AR) 1 correlation structure. The GAMM was first run without the AR1 correlation structure, and the value of the first lag of the autocorrelation function was used as the predicted value for the AR1 correction factor in the subsequent GAMM.

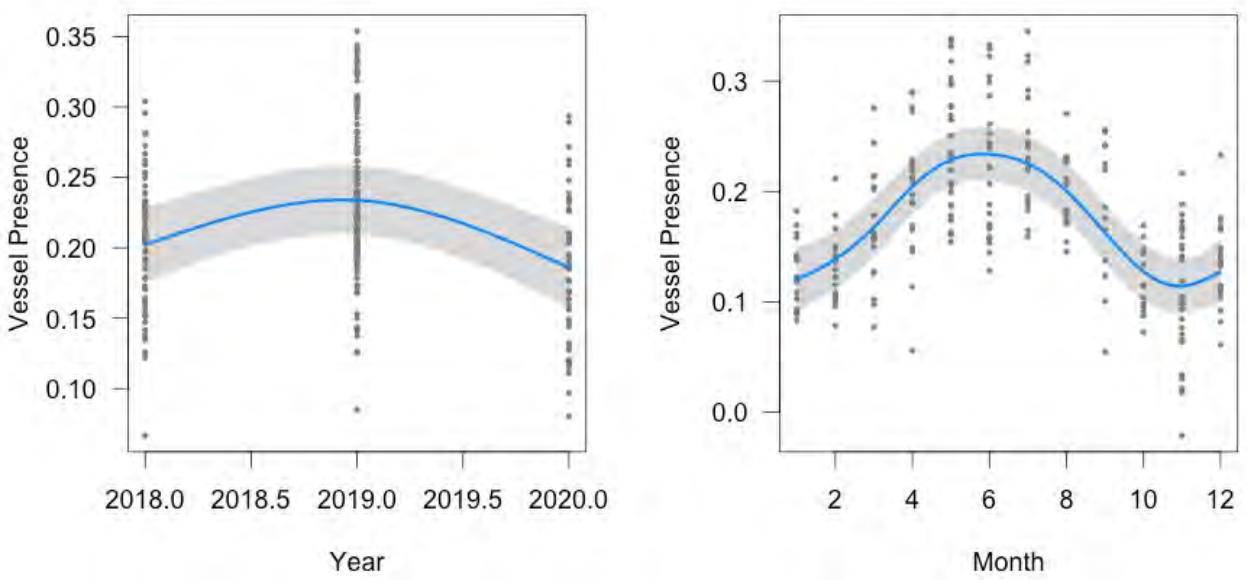

Figure E-8: GAM smoothing functions for Year and Month effects on vessel detections

Note: The Vessel Presence metric represents the monthly mean of hourly detections. The temporal patterns of vessel detection rates are explored as a function of year and month.

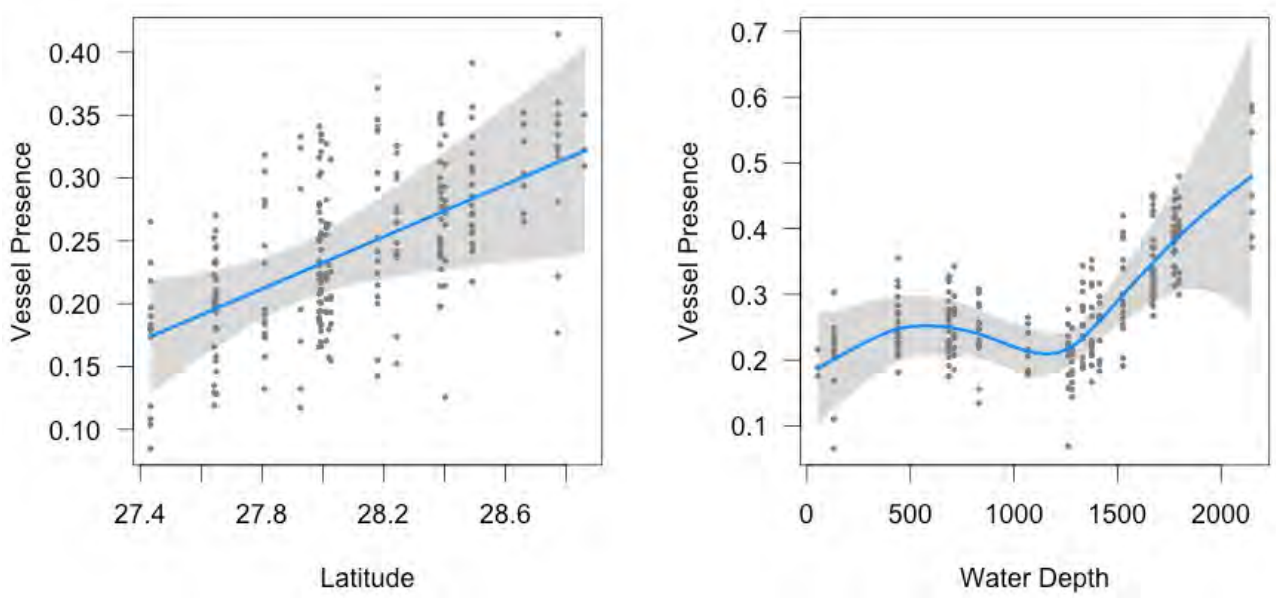

Figure E-9: GAM smoothing functions for Latitude and Water Depth effects on vessel detections

Note: The Vessel Presence metric represents the monthly mean of hourly detections. The temporal patterns of vessel detection rates are explored as a function of year and month.

E.2.3.6 Revised Simplified Statistical Analysis of Measured Vessel Received Levels

Deployment 1 RL data were assessed using the full predicted RL model statistical approach previously outlined herein. However, based on the Deployment 1 results, it was apparent that a different statistical approach was needed. The predicted RL variables in the original GAMM analysis did not result in a strong predictive power and were frequently outperformed by the weather and AIS-derived statistical variables.

Therefore, a second, more simple statistical approach was implemented to characterize the sources of ambient noise from vessel RLs and predict or identify the sources of variability at each of the 10 EARS and RH receivers. The simplified statistical analysis approach was based on the 1-hour, 1-Hz resolution data and used only weather and AIS-derived predictor variables for the GAMM analysis. The same Vessel Band acoustic measure was calculated for each hour, and the minimum closest point of approach (CPA) for each vessel in that hour was determined. The minimum CPA and the number of vessels passing from 0 to 2 km, 2 to 4 km, and 4 to 10 km were tabulated and input into the statistical model. The simplified model used the form: Gamma Family with the log Link Function. The following is the formula for the simplified model:

VesselBand ~ s(sDate, k = 50, bs = "ts") + s(WaveHeight) + s(Windspeed) + s(CPAmin) + (km2) + (km4) + (km10)

Where:

VesselBand is measured SPL in the band from AA to BB Hz.

sDate is the "normalized date", which spans from -365 to 365 representing the date range of the project. This transformation of date values is done to improve the performance of the statistical model.

WaveHeight is the wave height in meters reported by the weather buoys.

Windspeed is the wind speed reported by the weather buoys in (check units).

CPAmin is the minimum CPA of any vessel in the 1-hour time period determined by analysis of the AIS data.

Km2 represents the number of vessels that approached within 2 km of the recording buoys during the hour.

Km4 represents the number of vessels than approached between 2 and 4 km of the recorder.

Km10 represents the number of vessels that approached between 4 and 10 km of the recorder.

E.4 Results

E.4.1 Comparison of Data from EARS and RH Recorders

A comparison of data from each deployment of the RH and EARS recorders was conducted to obtain the median spectra for each recorder and deployment (**Figures E-10** to **E-13**). There appears to be a consistent difference between the two recording systems below 100 Hz, which is also evident in the monthly temporal and spatial spectral data.

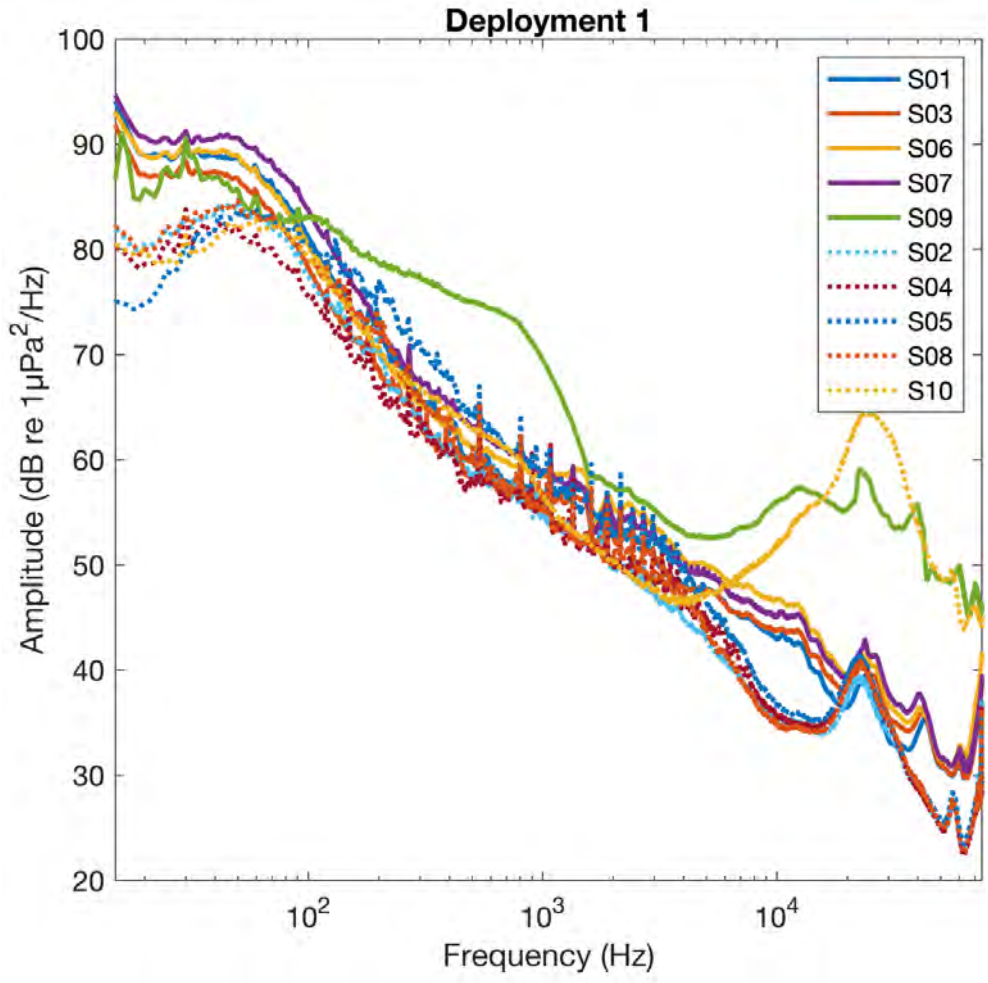

Figure E-10. Median spectra for all 10 EARS and RH recorders during Deployment 1

Note: Data recorded by the RHs are shown as solid lines, and data from EARS are shown as dotted lines. Stations 9 and 10, which were the shallowest water recorder locations, show an elevation in high frequency noise.

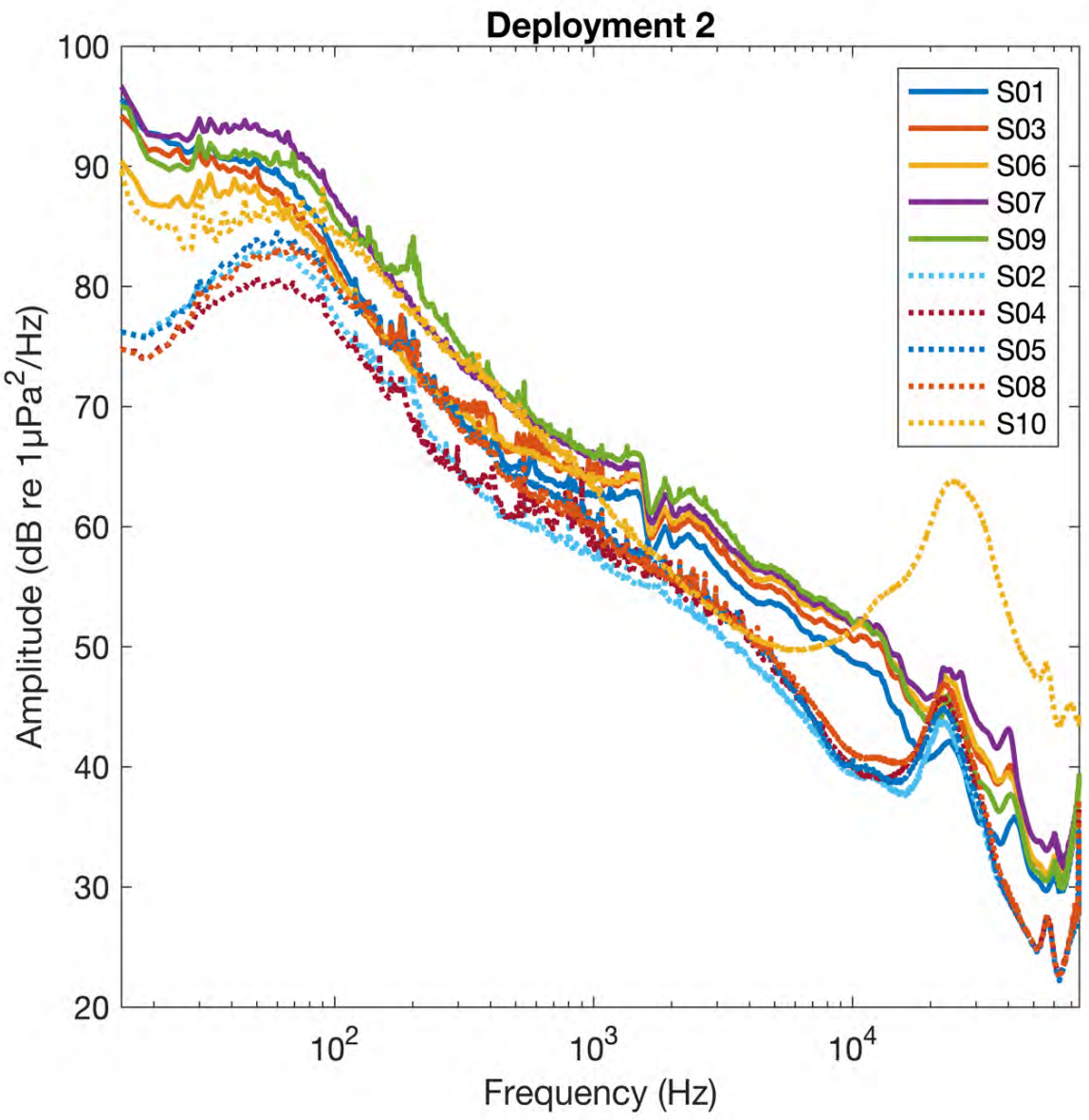

Figure E-11. Median spectra for all 10 EARS and RH recorders during Deployment 2

404 Note: Data recorded by the RHs are shown as solid lines, while data from EARS are shown as dotted lines.

405

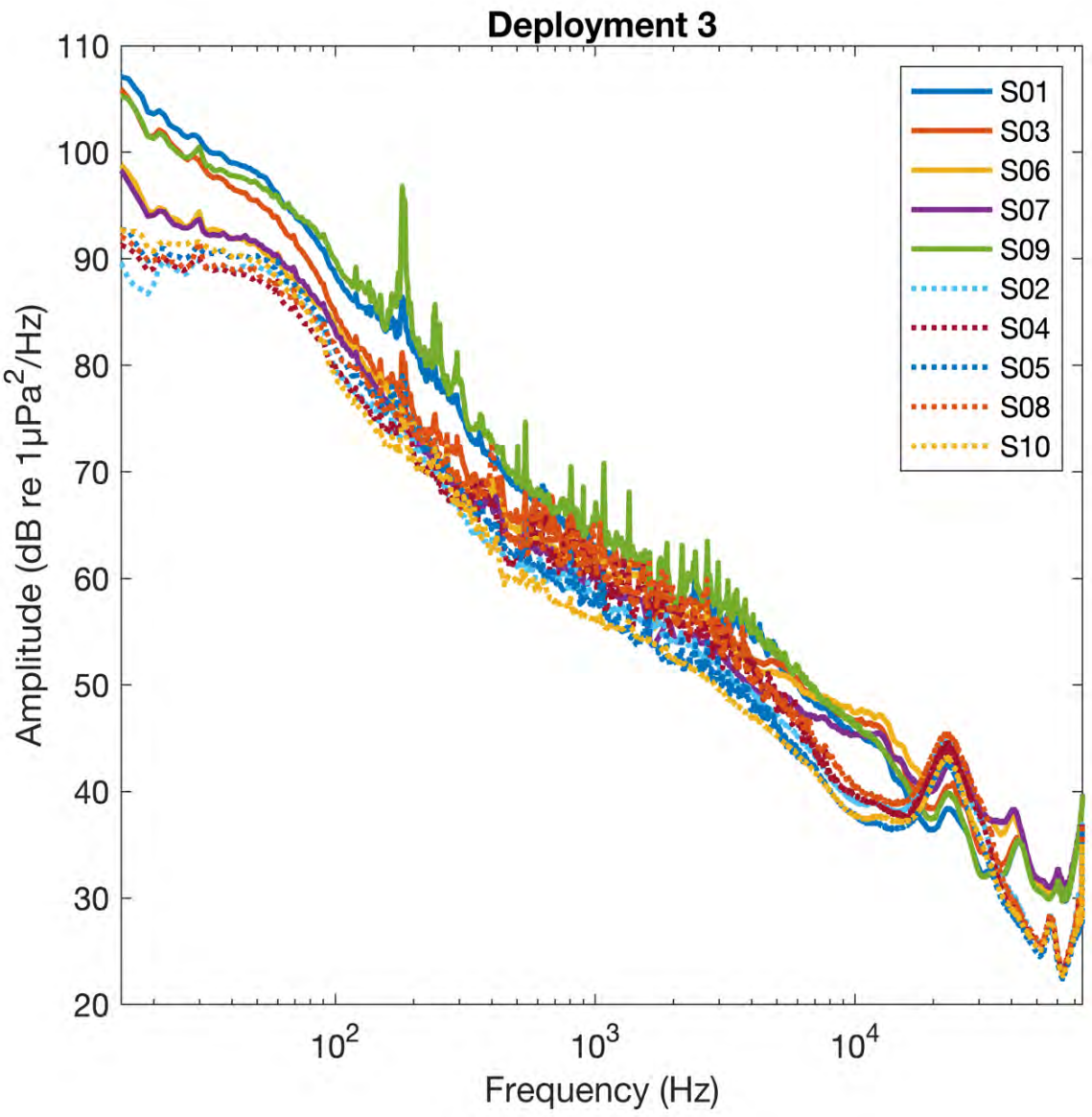

Figure E-12. Median spectra for all 10 EARS and RH recorders during Deployment 3

406 Note: Data recorded by the RHs are shown as solid lines, while data from EARS are shown as dotted lines.

407

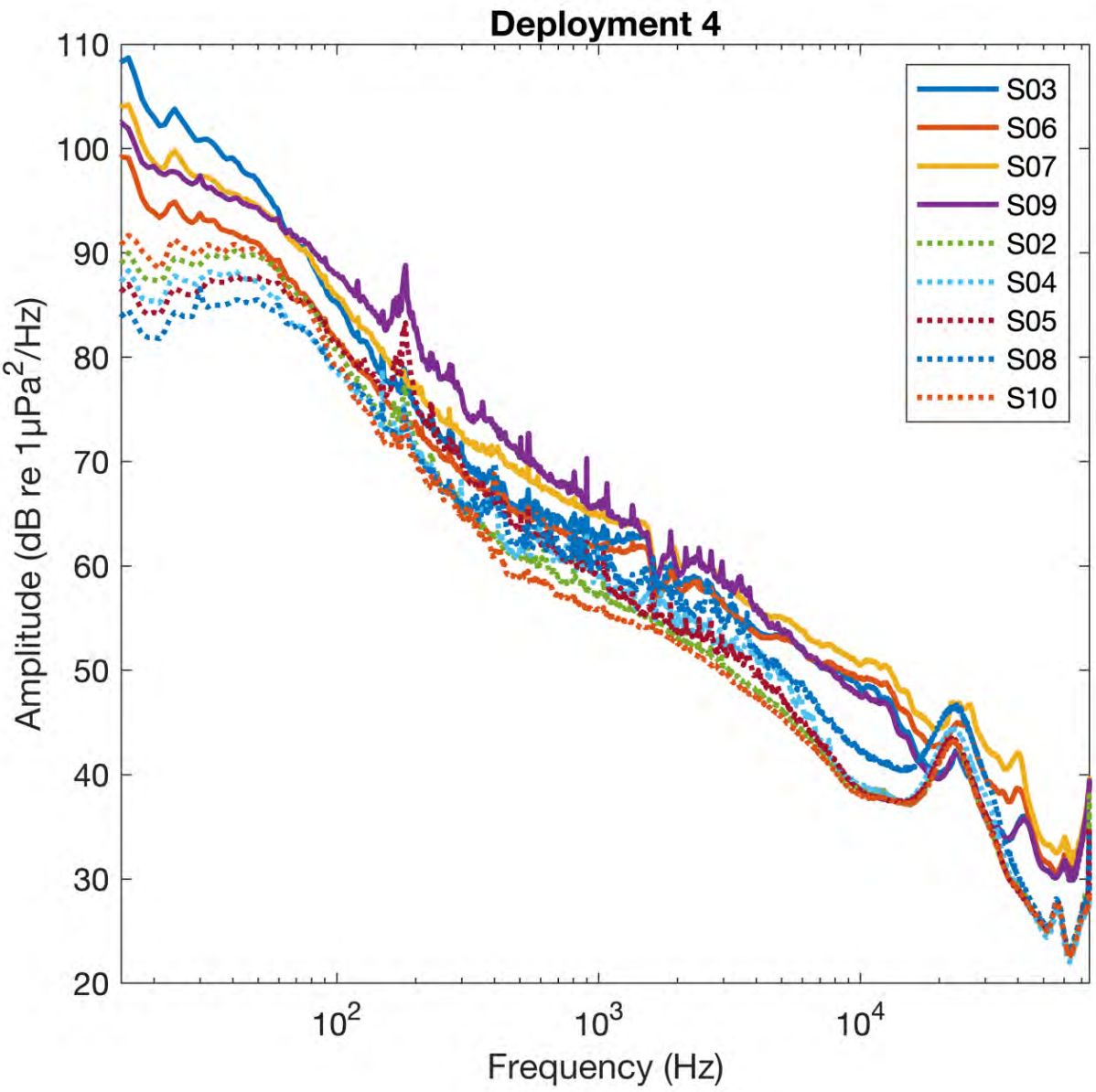

Figure E-13. Median spectra for all 10 EARS and RH recorders during Deployment 4

Note: Data recorded by the RHs are shown as solid lines, while data from EARS are shown as dotted lines.

E.4.2 Anthropogenic (Vessel and Seismic Airgun) Sound Detection Analysis

The primary goal of this analysis was to characterize the anthropogenic input into the soundscape of the northern GOM (**Figure E-1**), an area characterized by a large amount of vessel traffic. Furthermore, seismic exploration using airguns is a common input into the northern GOM soundscape.

Exploratory detection analyses investigated the performance of band limited energy detectors over a variety of integration times using data from Deployment 1. The best detection performance was found to occur with a 1-hour integration time. This allowed the use of the summarized 1-hour, third octave band (TOB) datasets, which accelerated the detection analysis process.

E.3.2.1 Vessel Detection Analysis

Vessel detections were made on an hourly basis, which were then converted to daily estimates of vessel presence. If a vessel was detected for at least 1 hour, a vessel was associated with that day. Finally, monthly values were taken as the mean of hourly and daily estimates of vessel presence (**Figure E-14**). The metric based on hourly inputs ranges from 0 to 0.4 and has a quasi-normal distribution. The metric based on daily input ranges from 0 to 1.0 and is highly skewed to the maximum value; this shows that vessels were present almost every day at every receiver location. The difference in the hourly and daily based airgun metrics was less since airgun operations tend to be more persistent in time than transitory vessel passages.

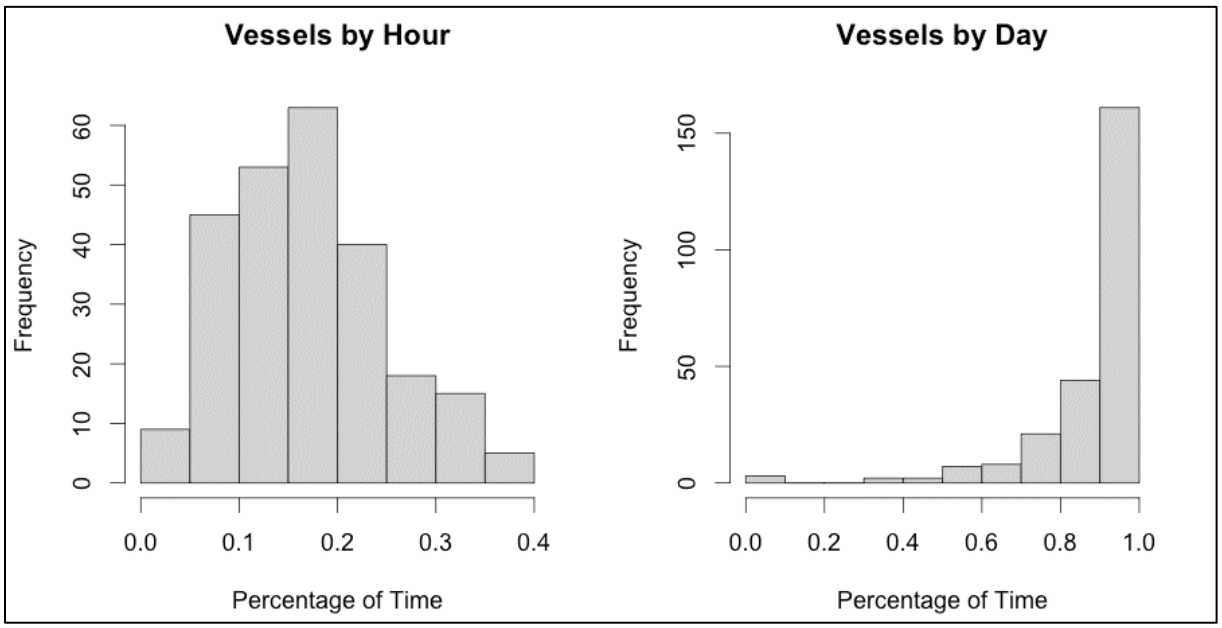

Figure E-14. Comparison of monthly values for vessel detection based on hourly inputs (left) and daily inputs (right)

The effects of spatial and temporal variables on vessel detection rates were explored with a GAM. Significant patterns by year and month were observed. Numbers of vessel detection increased from 2018 to 2019 but decreased again in 2020. This may be a side effect of the sampling period and the markedly strong monthly pattern, where the number of vessels was highest in summer and lower in winter months (**Table E-7** and **Figure E-8**). The patterns seen for latitude and water depth were also significant and indicated more contradictory patterns of increased vessel detection rates as latitude and water depth increased (**Figure E-9**).

Table E-7. GAM details for vessel detections

A. Parametric Coefficients	Estimate	Std. Error	t-value	p-value
(Intercept)	0.1687	0.0034	49.9252	< 0.0001
B. Smoothing Terms	**edf**	**Ref.df**	**F-value**	**p-value**
s(Year)	1.9697	1.9988	16.3144	< 0.0001
s(Month)	5.5831	6.7431	27.1694	< 0.0001
s(Lat)	1.0000	1.0000	6.0799	0.0144
s(Lon)	5.4112	5.9740	5.8301	< 0.0001
s(WaterDepth)	4.7717	5.4302	9.4967	< 0.0001
Key: edf=empirical distribution function; F-value=value on the F distribution calculated by dividing two mean				

A. Parametric Coefficients	Estimate	Std. Error	t-value	p-value
squares; Lat=latitude; Lon=longitude; p-value= level of marginal significance within a statistical hypothesis test, representing the probability of the occurrence of a given event; Ref.df=reference degrees of freedom; s=scaled; Std. Error=Standard Error				

The number of vessel detection was greatest in the middle longitudes and decreased strongly to the east, probably related to the location of port facilities (**Figure E-15**).

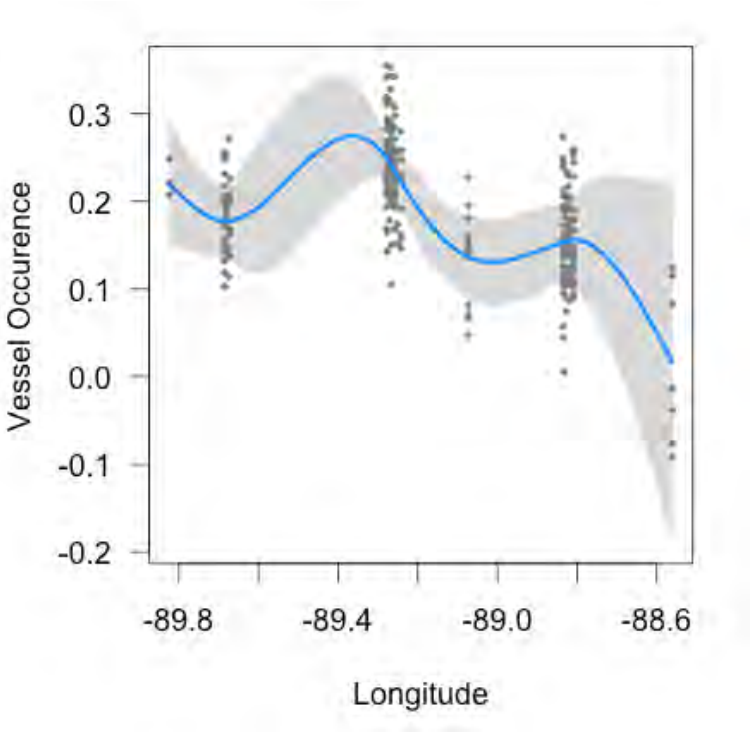

Figure E-15. GAM smoothing functions for Longitude effects on vessel detections

E.3.2.2 Airgun Detection Analysis

A similar detection analysis was conducted for airgun signal detections (**Table E-8**). Month and year for airgun signal detections had similar patterns to that of vessel detections (**Figure E-16**). Latitude and longitude effects for airgun signals were borderline statistically significant, with a dip in the frequency of airgun detections in the middle latitudes and, again, a higher frequency of signal detection in the middle longitudes (**Figure E-17**).

Table E-8. GAM details for airgun detections

A. Parametric Coefficients	Estimate	Std. Error	t-value	p-value
(Intercept)	0.3668	0.0144	25.5239	< 0.0001
B. Smooth Terms	**edf**	**Ref.df**	**F-value**	**p-value**
s(Year)	1.9816	1.9995	39.2143	< 0.0001
s(Month)	7.0302	8.0963	13.5408	< 0.0001
s(Lat)	2.7219	3.2705	2.9462	0.0428
s(Lon)	6.4339	6.9885	2.0527	0.0436
s(WaterDepth)	1.0000	1.0000	0.0878	0.7673

A. Parametric Coefficients	Estimate	Std. Error	t-value	p-value
Key: edf=empirical distribution function; F-value=value on the F distribution calculated by dividing two mean squares; Lat=latitude; Lon=longitude; p-value= level of marginal significance within a statistical hypothesis test, representing the probability of the occurrence of a given event; Ref.df=reference degrees of freedom; s=scaled; Std. Error=Standard Error				

443

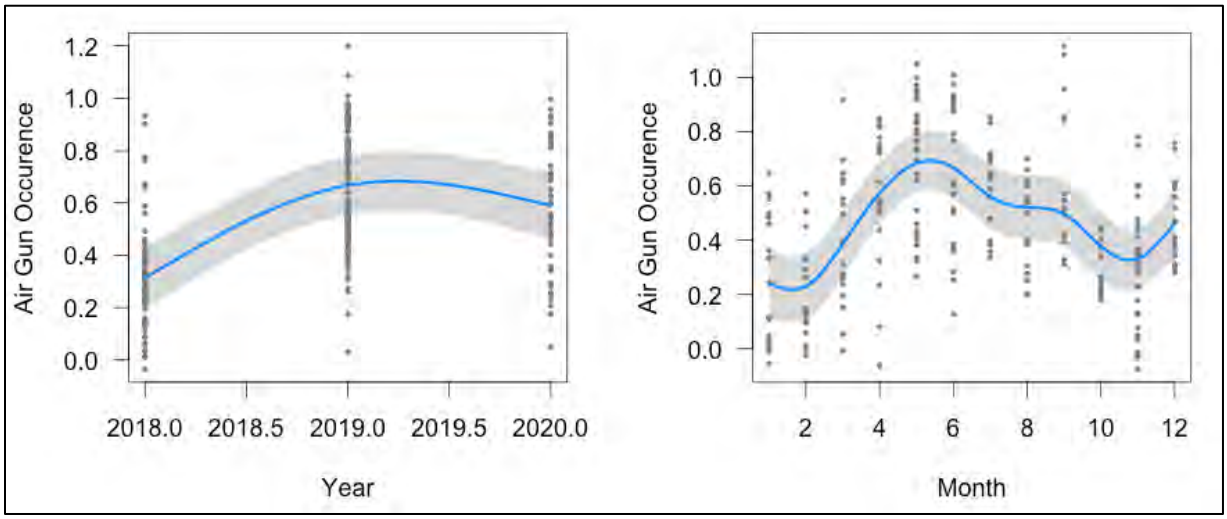

Figure E-16. GAM smoothing functions for Year and Month effects on air gun signal detections

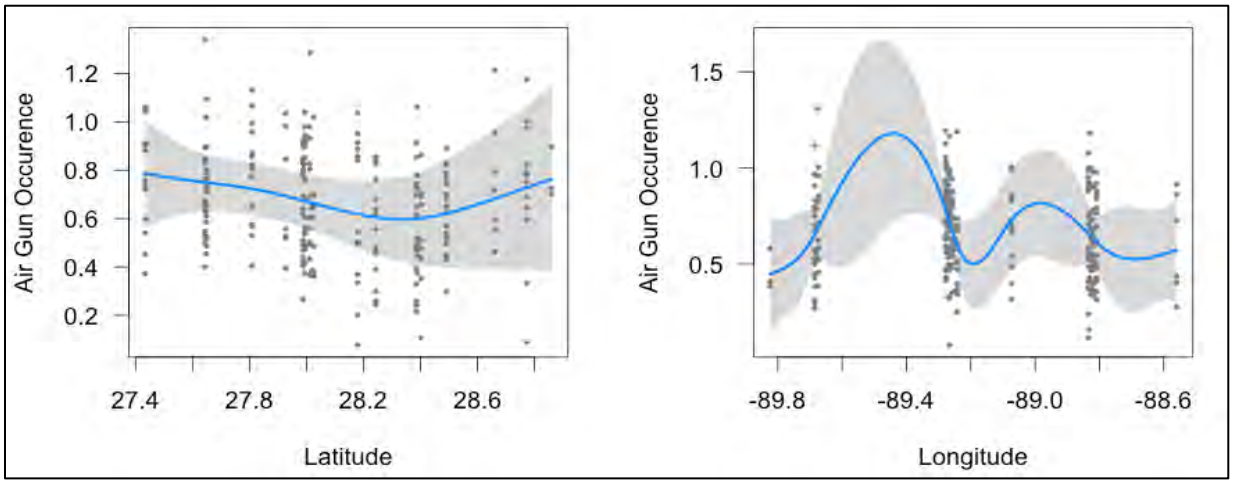

Figure E-17. GAM smoothing functions for Latitude and Longitude effects on air gun signal detections

444 ### E.3.2.3 Vessel and Airgun Detection Patterns

445 The spatial and temporal patterns of the vessel and airgun detections can be found in **Appendix E-A**. For
446 each month and buoy location, the percentage of vessel and airgun detections is shown as the pie charts
447 (**Appendix E-A, Figures E-A1 to E-A26**). At a given time, it is possible for both an airgun and a vessel
448 to be detected. Therefore, a pie chart filled to 50 percent with green would indicate continuous airgun
449 presence. Airguns were detected operating continuously during some months (e.g., May and June 2019
450 and April and May 2020).

E.3.2.4 Seaglider Vessel and Airgun Detection Analysis

The hand-scored glider acoustic records produced 65 hours with vessel detections and only 8 hours with airgun detections. The distribution of vessel detections was examined as a function of latitude, longitude, and glider depth using a GAMM with an autocorrelation correction (**Table E-9**). The model was significant with an adjusted R-square of 0.26 (N=750). The curve fit functions show an increased number of vessel detections at higher latitudes and western longitudes (**Figure E-18**).

Table E-9. GAMM details for Seaglider vessel detections

A. Parametric Coefficients	Estimate	Std. Error	t-value	p-value
(Intercept)	-3.0497	0.2133	-14.2976	< 0.0001
B. Smooth Terms	**edf**	**Ref.df**	**F-value**	**p-value**
s(Lat)	1.0000	1.0000	40.4632	< 0.0001
s(abs(Lon))	3.8768	3.8768	25.1599	< 0.0001
s(Depth)	1.0000	1.0000	0.5670	0.4517

Key: edf=empirical distribution function; F-value=value on the F distribution calculated by dividing two mean squares; Lat=latitude; Lon=longitude; p-value= level of marginal significance within a statistical hypothesis test, representing the probability of the occurrence of a given event; Ref.df=reference degrees of freedom; s=scaled; Std. Error=Standard Error

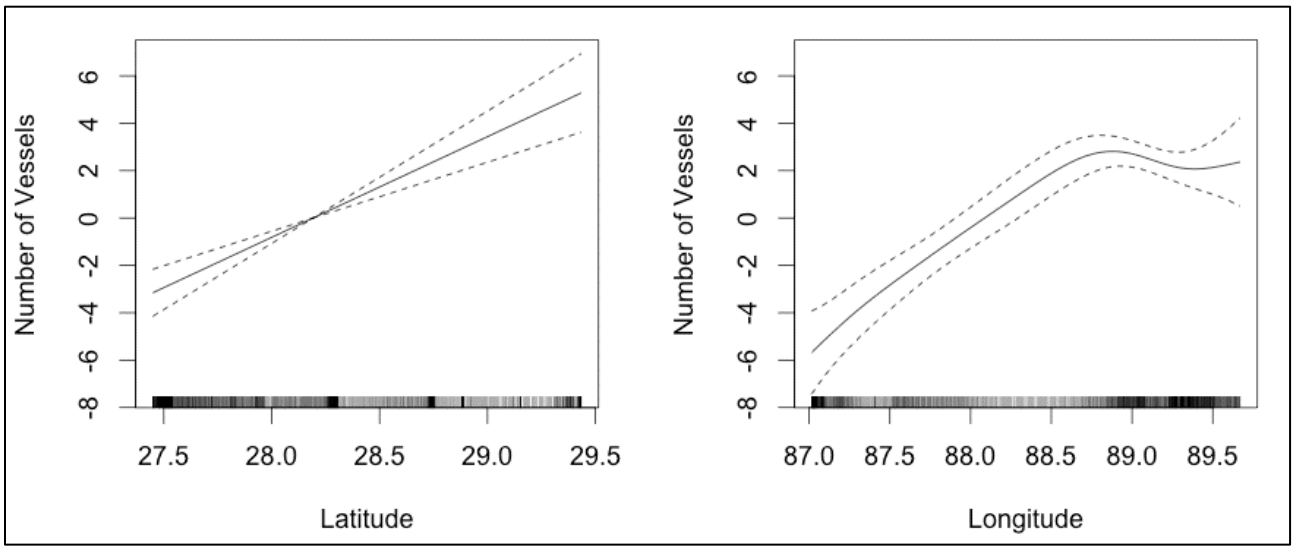

Figure E-18. GAM smoothing functions for Latitude and Longitude effects on vessel detections from the Seaglider

E.4.3 Biological Detection Analysis

E.3.3.1 Rice's Whale (*Balaenoptera ricei*) Detections

The frequency overlap between the signals of Rice's whales and the prevalent anthropogenic noise made it difficult to reliably detect the calls of Rice's whales using only the spectrally analyzed data. A better approach would be to use a matched-filter detection process that operates on the waveform data.

E.3.3.2 Dolphin Band Detections: Low-frequency Clicks

Hourly detection rates were converted to binary yes/no values. The daily mean of these values was calculated and analyzed as a function of month, latitude, longitude, and water depth to examine for spatial

and temporal patterns. All predictors for the dolphin band detections were statistically significant (**Table E-10**). The overall model had an adjusted R-square of 0.257. Throughout the first deployment, dolphin band detections rose from May until September and then fell precipitously, both in rate and number of detections, in November (**Figure E-19**). Detection rates peaked in nearshore shallow waters as well as in offshore water deeper than 1,000 m. This may be due to the detection function being triggered by multiple species. Detection rates appeared to increase with latitude. Peak rates were seen in the middle longitudes and decreased to the east and west (**Figure E-20**).

Table E-10. GAM output of dolphin band detection rates

A. Parametric Coefficients	Estimate	Std. Error	t-value	p-value
(Intercept)	-1.1931	0.0244	-48.9009	< 0.0001
B. Smooth Terms	**edf**	**Ref.df**	**F-value**	**p-value**
s(Month)	2.9484	2.9979	30.0646	< 0.0001
te(Lat)	1.0003	1.0004	4.4688	0.0347
te(Lon)	2.7912	2.8335	4.9775	0.0017
s(WaterDepth)	4.2630	4.6721	7.7719	< 0.0001

Key: edf=empirical distribution function; F-value=value on the F distribution calculated by dividing two mean squares; Lat=latitude; Lon=longitude; p-value= level of marginal significance within a statistical hypothesis test, representing the probability of the occurrence of a given event; Ref.df=reference degrees of freedom; s=scaled; Std. Error=Standard Error

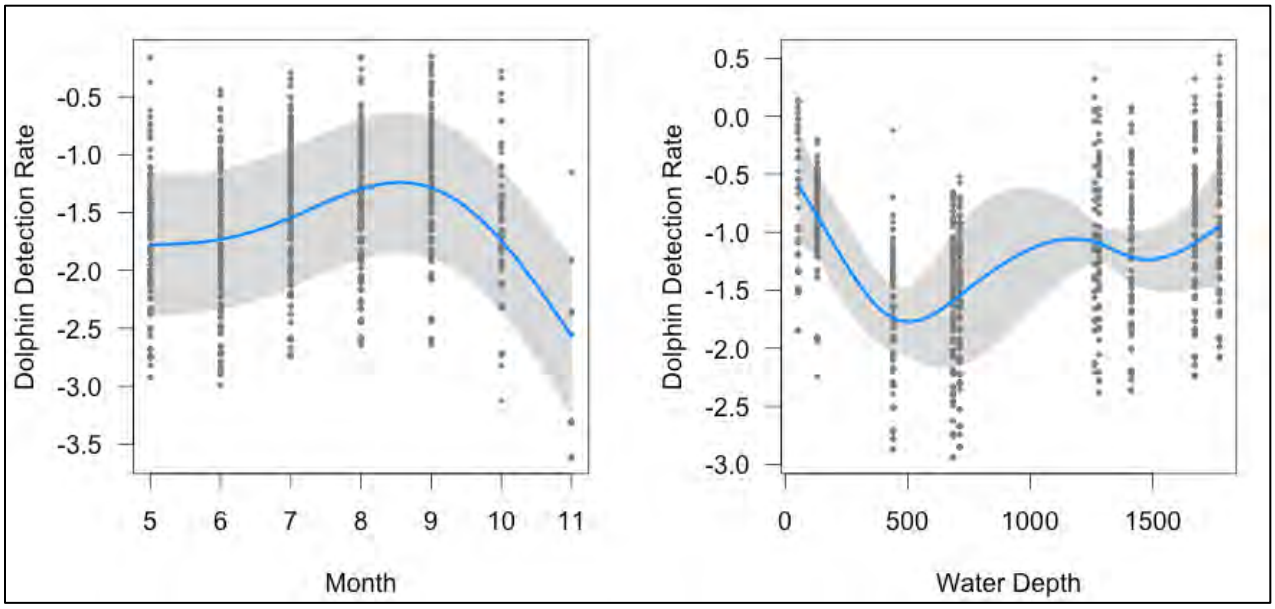

Figure E-19. Month and Water Depth prediction functions for dolphin band detection rates

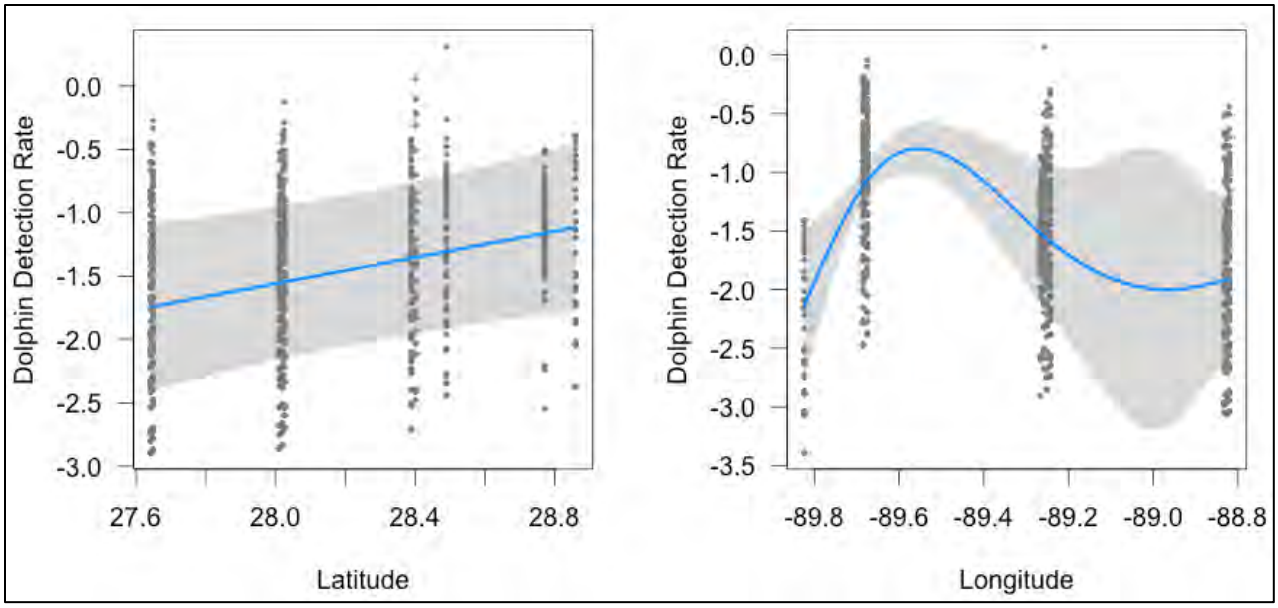

Figure E-20. Latitude and Longitude prediction functions for dolphin band detection rates

E.3.3.3. Beaked Whale Band Detections: Mid-frequency Clicks

Hourly "beaked whale band" detection rates were converted to binary yes/no values. The daily means of these values were calculated and analyzed as a function of month, latitude, longitude, and water depth to examine for spatial and temporal patterns (**Table E-11**). All predictors for the beaked whale band detections were statistically significant. The overall model had a remarkably high adjusted R-square value of 0.594. Detection rates appear to increase from May through September and then begin to decline in October (**Figure E-21**). The peak of beaked whale detections appeared to occur at intermediate water depths of 500 to 1,000 m and decline in the very shallow and very deep depths, which may indicate a habitat preference for slope environments.

Table E-11. GAM output for Beaked Whale band detection rates.

A. Parametric Coefficients	Estimate	Std. Error	t-value	p-value
(Intercept)	-2.9421	0.0646	-45.5107	< 0.0001
B. Smooth Terms	**edf**	**Ref.df**	**F-value**	**p-value**
s(Month)	2.9527	2.9982	35.2393	< 0.0001
te(Lat)	2.0576	2.0690	24.2420	< 0.0001
te(Lon)	2.9340	2.9506	27.4816	< 0.0001
s(WaterDepth)	3.9361	3.9784	10.3034	< 0.0001

Key: edf=empirical distribution function; F-value=value on the F distribution calculated by dividing two mean squares; Lat=latitude; Lon=longitude; p-value= level of marginal significance within a statistical hypothesis test, representing the probability of the occurrence of a given event; Ref.df=reference degrees of freedom; s=scaled; Std. Error=Standard Error

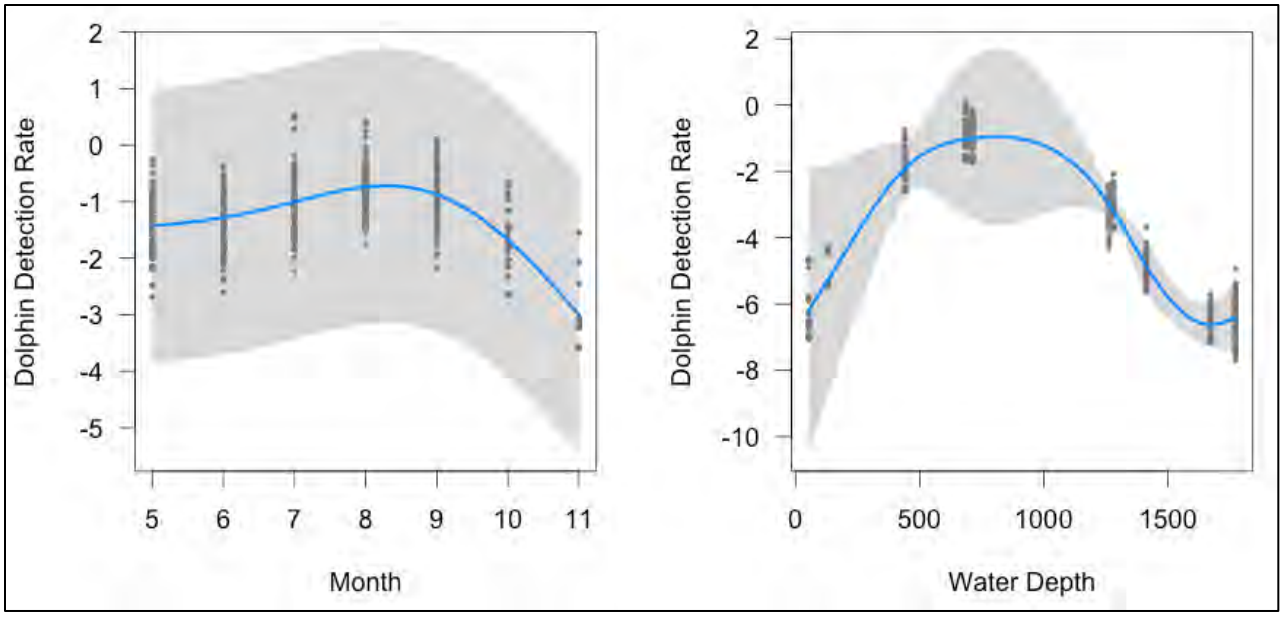

Figure E-21. Month and Water Depth prediction functions for beaked whale band detection rates

Detection rates appear to be highest in lowest latitudes and decrease as latitude increases. The effect of longitude here appears to be the opposite of that for the dolphin band results, with highest values to the west and east (**Figure E-22**).

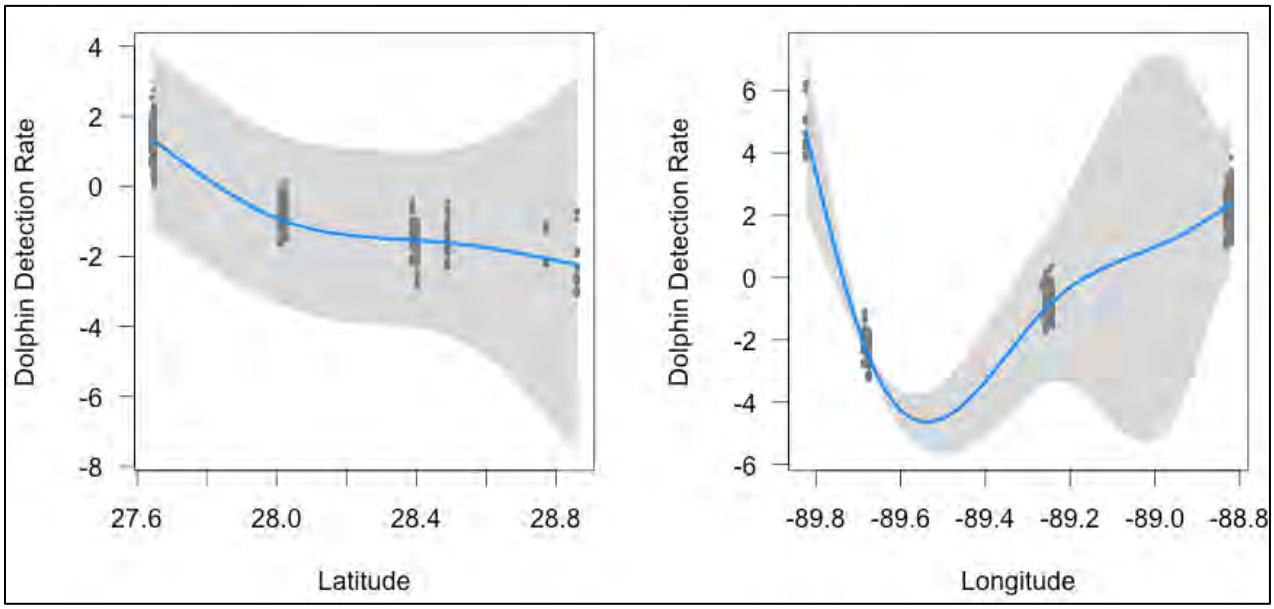

Figure E-22. Latitude and Longitude prediction functions for beaked whale band detection rates

E.4.4 Statistical Analysis of Vessel Received Levels

This analysis was undertaken to determine the contribution of vessel noise to the overall soundscape. An added benefit is that it offers a method to predict or model vessel noise contributions in unmonitored areas. The northern GOM is a highly industrialized area, and noise from vessels and airgun operations are the major anthropogenic contribution to the ambient soundscape (Estabrook et al. 2016; Wiggins et

al. 2016). Accordingly, the predicted contribution of vessels to the measured RLs in the 200 to 2,500 Hz band at each receiver was analyzed. Additional predictive variables include the windspeed, wave height, CPA between each vessel, and receiver.

The AIS-based modeling to predict vessel RLs was conducted in several bands. Hz50 and Hz200 represent the predicted spectral levels at 50 Hz and 200 Hz. Note that in each of these analyses, the date values were "scaled" so the "sDate" values only spanned the 2-year period of the experiment (from -1 to 1). The R-squared (i.e., measure of how much of the variance is in the dependent variable) for each analysis is also reported. R-squared is a measure of how much of the variance is in the dependent variable (i.e., the 200 to 2,500 Hz vessel band sound level is explained by the independent or predictor variables).

Results from statistical analyses of vessel received levels using Deployment 1 data are presented and discussed below

E.3.4.1 Deployment 1, Receiver 1

The significant predictors for Receiver 1 included scaled date, windspeed, CPA, and predicted BB level (**Table E-12**; **Figures E-23** and **E-24**). The R-squared value was 0.483. The date function is complex and may reflect the contribution of airgun signals to the measured levels.

The windspeed function shows a simple increase in LF noise as windspeed increases. The CPA function shows a clean and marked increase in Vessel Band noise level as vessels approach closer to the receiver. The predicted BB function was borderline significant, and its curve fit shows little relationship between the two variables.

Table E-12. GAM output for Deployment 1, Receiver 1

A. Parametric Coefficients	Estimate	Std. Error	t-value	p-value
(Intercept)	4.5799	0.0007	6428.4166	< 0.0001
B. Smooth Terms	**edf**	**Ref.df**	**F-value**	**p-value**
s(sDate)	36.7457	49.0000	25.3114	< 0.0001
s(WaveHeight)	1.0001	1.0001	2.9124	0.0879
s(Windspeed)	1.0000	1.0000	49.2164	< 0.0001
s(CPA)	8.9311	8.9311	166.1668	< 0.0001
s(Hz200) -200 Hz TOB RL	1.0000	1.0000	0.0528	0.8182
s(BB1) BB RL (w 50 Hz TL)	3.9427	3.9427	3.0960	0.0220
s(BB2) BB RL (w/200 Hz TL)	1.0000	1.0000	0.0538	0.8166

Key: BB=broadband; CPA= closest point of approach; edf=empirical distribution function; F-value=value on the F distribution calculated by dividing two mean squares; Hz=Hertz; Lat=latitude; Lon=longitude; p-value= level of marginal significance within a statistical hypothesis test, representing the probability of the occurrence of a given event; Ref.df=reference degrees of freedom; RL=received level; s=scaled; Std. Error=Standard Error; TL=transmission loss; TOB=third-octave band

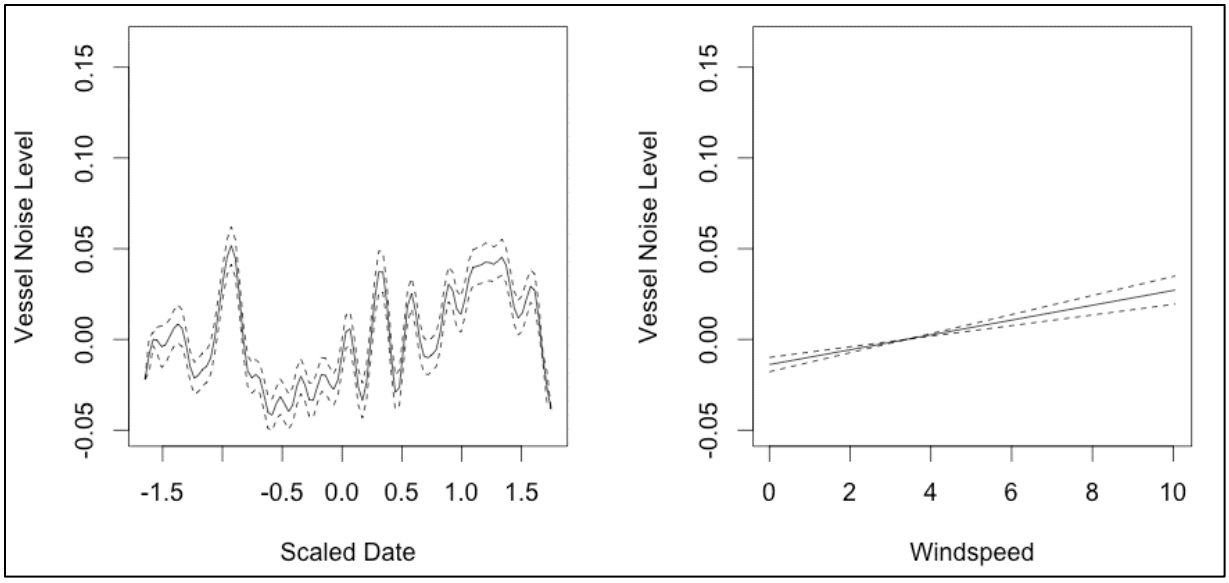

Figure E-23. Smoothing functions for Measured Vessel Band Noise as a function of Scaled Date and Windspeed for Receiver 1

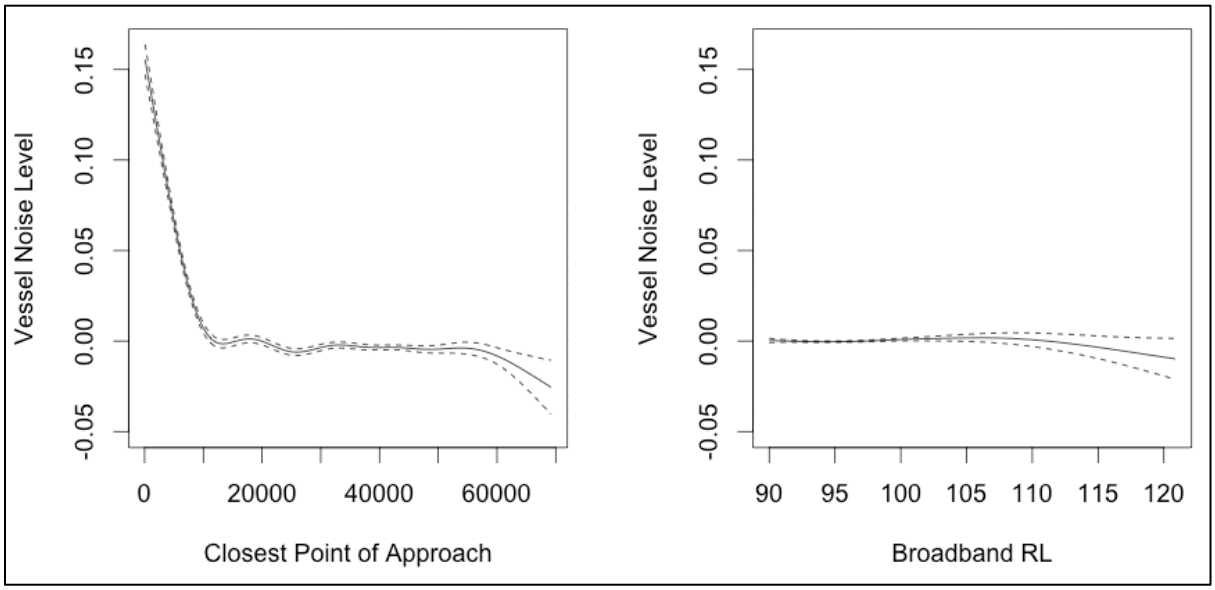

Figure E-24. Smoothing functions for Measured Vessel Band Noise as a function of CPA and predicted RL for Receiver 1, Deployment 1

E.3.4.2 Deployment 1, Receiver 2

The significant predictors for Receiver 2 included scaled date, CPA, and predicted BB level (**Table E-13**; **Figure E-25**). The R-squared value was 0.500. The date function is complex and may reflect the contribution of airgun signals to the measured levels. The CPA function shows a clear increase in Vessel band noise level as vessels approach the receiver. This effect becomes apparent at a range of approximately 10 km.

Table E-13. GAM output for Deployment 1, Receiver 2

A. Parametric Coefficients	Estimate	Std. Error	t-value	p-value
(Intercept)	4.4876	0.0008	5299.3872	< 0.0001
B. Smooth Terms	**edf**	**Ref.df**	**F-value**	**p-value**
s(sDate)	40.1935	49.0000	29.5363	< 0.0001
s(WaveHeight)	1.0000	1.0000	2.5937	0.1073
s(Windspeed)	1.6665	1.6665	1.1491	0.1999
s(CPA)	8.8453	8.8453	289.9161	< 0.0001
s(Hz200) -200 Hz TOB RL	3.0302	3.0302	2.0410	0.0949
s(BB1) BB RL (w 50 Hz TL)	1.0000	1.0000	0.1162	0.7332
s(BB2) BB RL (w/200 Hz TL)	1.0006	1.0006	2.5905	0.1075

Key: BB=broadband; CPA= closest point of approach; edf=empirical distribution function; F-value=value on the F distribution calculated by dividing two mean squares; Hz=Hertz; Lat=latitude; Lon=longitude; p-value= level of marginal significance within a statistical hypothesis test, representing the probability of the occurrence of a given event; Ref.df=reference degrees of freedom; RL=received level; s=scaled; Std. Error=Standard Error; TL=transmission loss; TOB=third-octave band

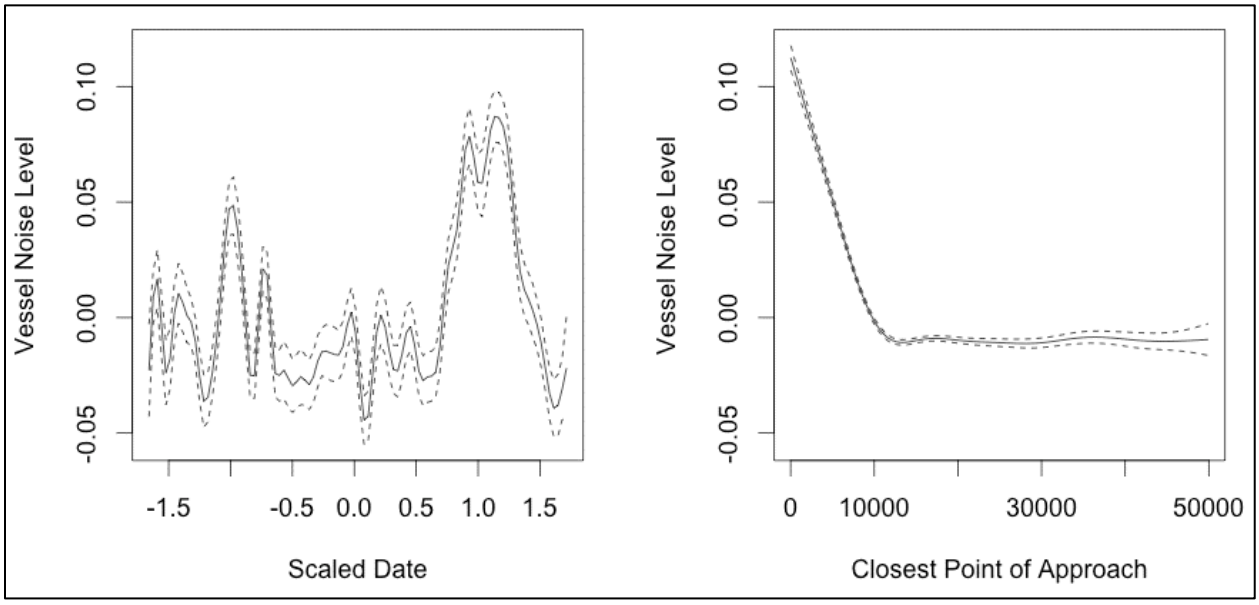

Figure E-25. Smoothing functions for Measured Vessel Band Noise as a function of Wave Height and Windspeed for Receiver 2, Deployment 1

E.3.4.3 Deployment 1, Receiver 3

The significant predictors for Receiver 3 included scaled date, windspeed, wave height, CPA, and predicted BB level (**Table E-14**; **Figures E-26**, **E-27**, and **E-28**). The R-squared value was 0.283.

The scaled date function for this receiver is simple and shows a slight increase in LF noise across the entire recording period. The wave height function shows a simple increase in LF noise as wave height increases up to approximately 2 m. There are a few measurements of wave height more than 6 m that complicate the shape of the smoothing function. The windspeed function shows a simple increase in LF noise as windspeed increases. The CPA function shows increases in measured LF noise as vessels

approach within 10 km of the recorder. As the predicted RLs increased above 100 decibels referenced to 1 microPascal squared (dB re 1µPa^2), the predicted RL shows an increase in the measured RL.

Table E-14. GAM output for Deployment 1, Receiver 3

A. Parametric Coefficients	Estimate	Std. Error	t-value	p-value
(Intercept)	4.5639	0.0012	3727.8837	< 0.0001
B. Smooth Terms	**edf**	**Ref.df**	**F-value**	**p-value**
s(sDate)	0.9175	49.0000	0.1689	0.0023
s(WaveHeight)	3.9106	3.9106	17.3975	< 0.0001
s(Windspeed)	1.0000	1.0000	33.0425	< 0.0001
s(CPA)	8.8051	8.8051	99.7800	< 0.0001
s(Hz200) -200 Hz TOB RL	1.0000	1.0000	0.4744	0.4910
s(BB1) BB RL (w 50 Hz TL)	1.0000	1.0000	1.5468	0.2137
s(BB2) BB RL (w/200 Hz TL)	3.0172	3.0172	4.0763	0.0067

Key: BB=broadband; CPA= closest point of approach; edf=empirical distribution function; F-value=value on the F distribution calculated by dividing two mean squares; Hz=Hertz; Lat=latitude; Lon=longitude; p-value= level of marginal significance within a statistical hypothesis test, representing the probability of the occurrence of a given event; Ref.df=reference degrees of freedom; RL=received level; s=scaled; Std. Error=Standard Error; TL=transmission loss; TOB=third-octave band

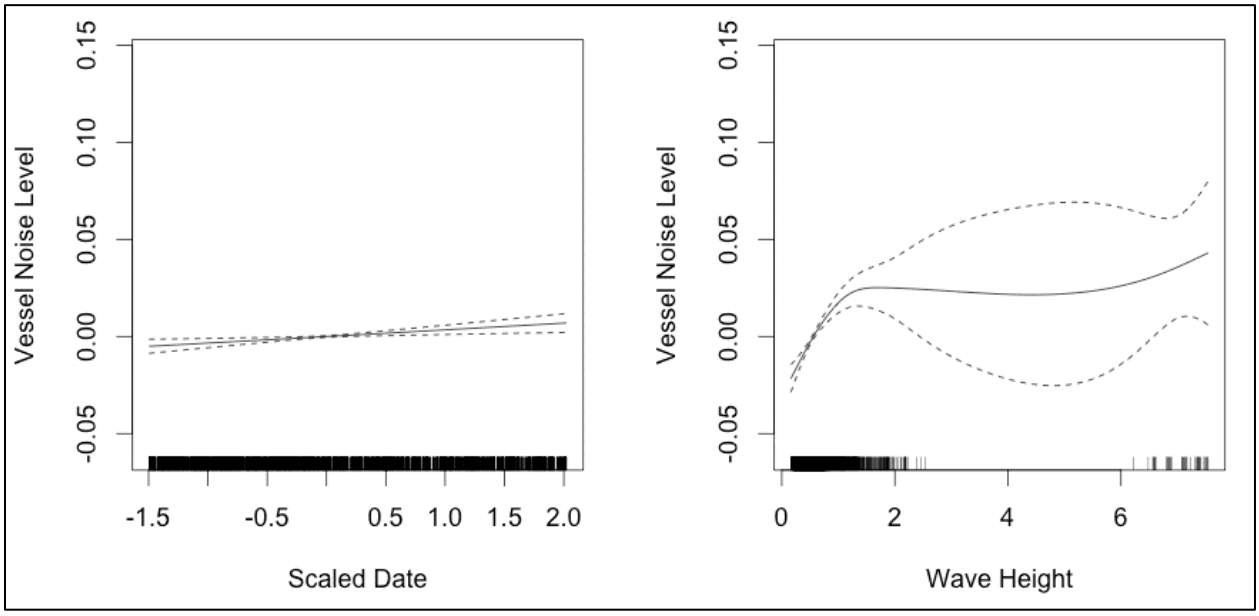

Figure E-26. Smoothing functions for Measured Vessel Band Noise as a function of Scaled Date and Wave Height for Receiver 3, Deployment 1

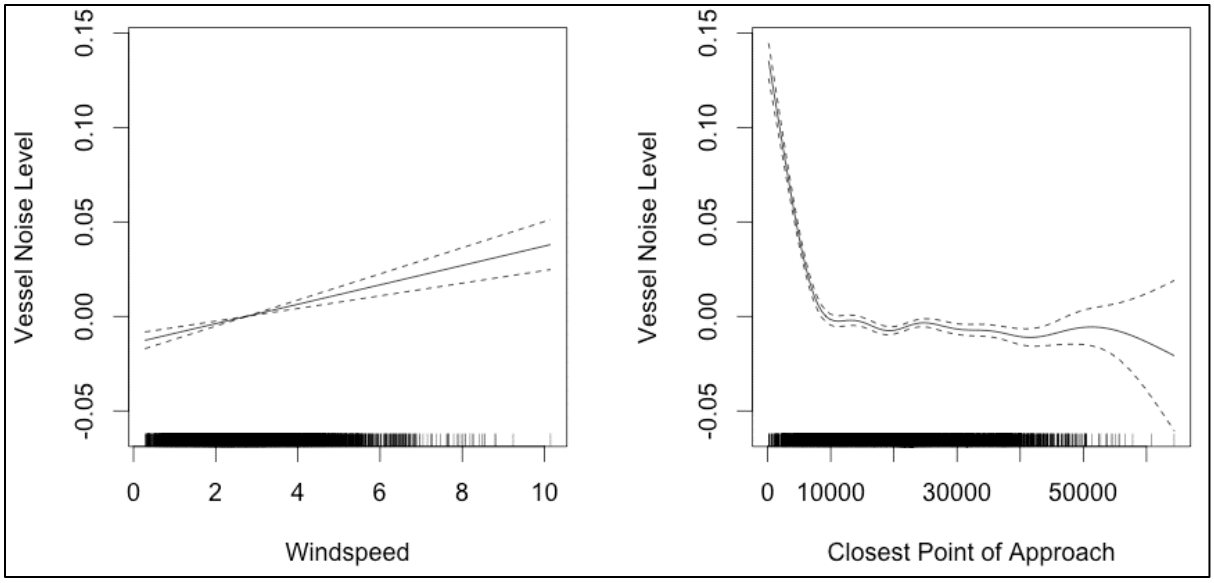

Figure E-27. Smoothing functions for Measured Vessel Band Noise as a function of Windspeed and CPA for Receiver 3

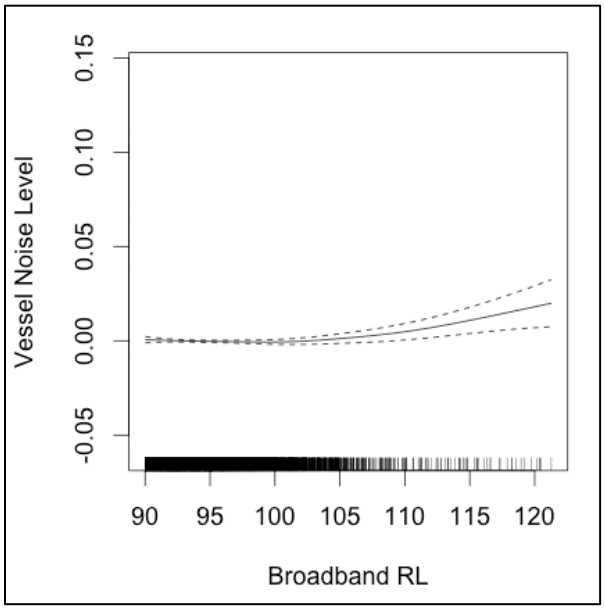

Figure E-28. Smoothing functions for Measured Vessel Band Noise as a function of predicted BB RL for Receiver 3, Deployment 1

E.3.4.4 Deployment 1, Receiver 4

The significant predictors for Receiver 4 included scaled date, wave height, windspeed, and CPA (**Table E-15**; **Figures E-29**, and **E-30**). The R-squared value was 0.516. The data function is complex and likely reflects the contribution of airgun signals to the measured data. The wave height function reflects an increase in measured LF noise as wave height increases to 2.5 m. The windspeed function shows a simple increase in LF noise as windspeed increases. The CPA function shows that LF noise increases as vessels approach within 10 km of the recorder (**Figure E-30**).

539 **Table E-15. GAM output for Deployment 1, Receiver 4**

A. Parametric Coefficients	Estimate	Std. Error	t-value	p-value
(Intercept)	4.4781	0.0009	5070.0197	< 0.0001
B. Smooth Terms	**edf**	**Ref.df**	**F-value**	**p-value**
s(sDate)	43.7241	49.0000	24.4023	< 0.0001
s(WaveHeight)	1.0000	1.0000	5.1574	0.0232
s(Windspeed)	1.0000	1.0000	17.3588	< 0.0001
s(CPA)	8.6951	8.6951	128.5288	< 0.0001
s(Hz200) -200 Hz TOB RL	1.0000	1.0000	0.2316	0.6303
s(BB1) BB RL (w 50 Hz TL)	1.0000	1.0000	0.9053	0.3414
s(BB2) BB RL (w/200 Hz TL)	1.0000	1.0000	3.5316	0.0602

Key: BB=broadband; CPA= closest point of approach; edf=empirical distribution function; F-value=value on the F distribution calculated by dividing two mean squares; Hz=Hertz; Lat=latitude; Lon=longitude; p-value= level of marginal significance within a statistical hypothesis test, representing the probability of the occurrence of a given event; Ref.df=reference degrees of freedom; RL=received level; s=scaled; Std. Error=Standard Error; TL=transmission loss; TOB=third-octave band

540

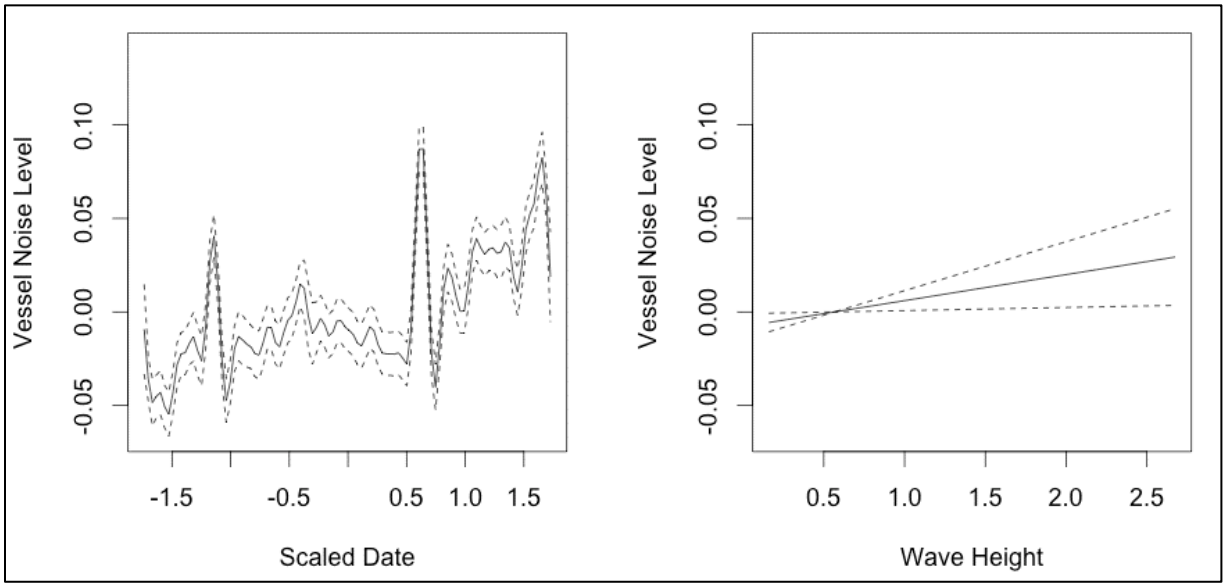

Figure E-29. Smoothing functions for Measured Vessel Band Noise as a function of Scaled Date and Wave Height for Receiver 4, Deployment 1

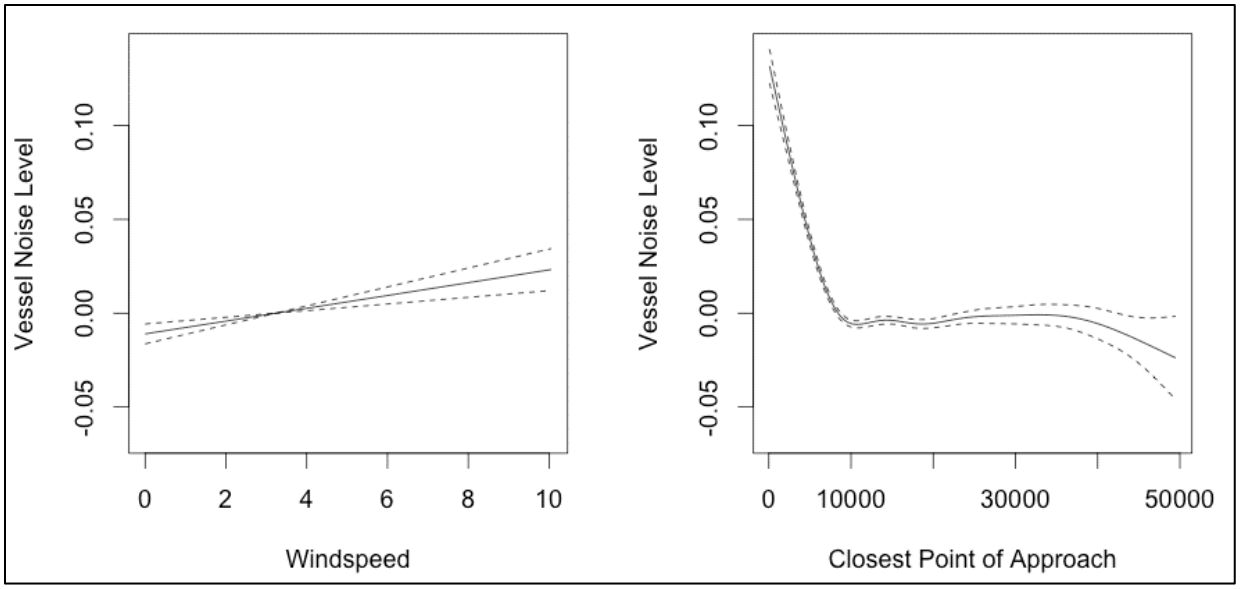

Figure E-30. Smoothing functions for Measured Vessel Band Noise as a function of Windspeed and CPA for Receiver 4, Deployment 1

E.3.4.5 Deployment 1, Receiver 5

The significant predictors for Receiver 5 included scaled date, wave height, windspeed, and CPA (**Table E-16; Figures E-31 and E-32**). The R-squared value was 0.612. The data function is complex and likely reflects the contribution of airgun signals to the measured data. The wave height function paradoxically predicts a decrease in measured LF noise as wave height increases to 6 m. This may be the result of inclusion of a handful of very high measured wave heights. The windspeed function shows a simple increase in LF noise as windspeed increases. The CPA function shows that LF noise increases as vessels approach within 10 km of the recorder.

Table E-16. GAM output for Deployment 1, Receiver 5

A. Parametric Coefficients	Estimate	Std. Error	t-value	p-value
(Intercept)	4.5578	0.0008	5603.2702	< 0.0001
B. Smooth Terms	**edf**	**Ref.df**	**F-value**	**p-value**
s(sDate)	40.7308	49.0000	56.8832	< 0.0001
s(WaveHeight)	1.0000	1.0000	4.5267	0.0334
s(Windspeed)	1.0000	1.0000	11.5082	0.0007
s(CPA)	8.5924	8.5924	216.3535	< 0.0001
s(Hz200) -200 Hz TOB RL	1.0000	1.0000	0.1717	0.6786
s(BB1) BB RL (w 50 Hz TL)	1.0000	1.0000	2.7581	0.0968
s(BB2) BB RL (w/200 Hz TL)	1.0000	1.0000	0.0012	0.9723

Key: BB=broadband; CPA= closest point of approach; edf=empirical distribution function; F-value=value on the F distribution calculated by dividing two mean squares; Hz=Hertz; Lat=latitude; Lon=longitude; p-value= level of marginal significance within a statistical hypothesis test, representing the probability of the occurrence of a given event; Ref.df=reference degrees of freedom; RL=received level; s=scaled; Std. Error=Standard Error; TL=transmission loss; TOB=third-octave band

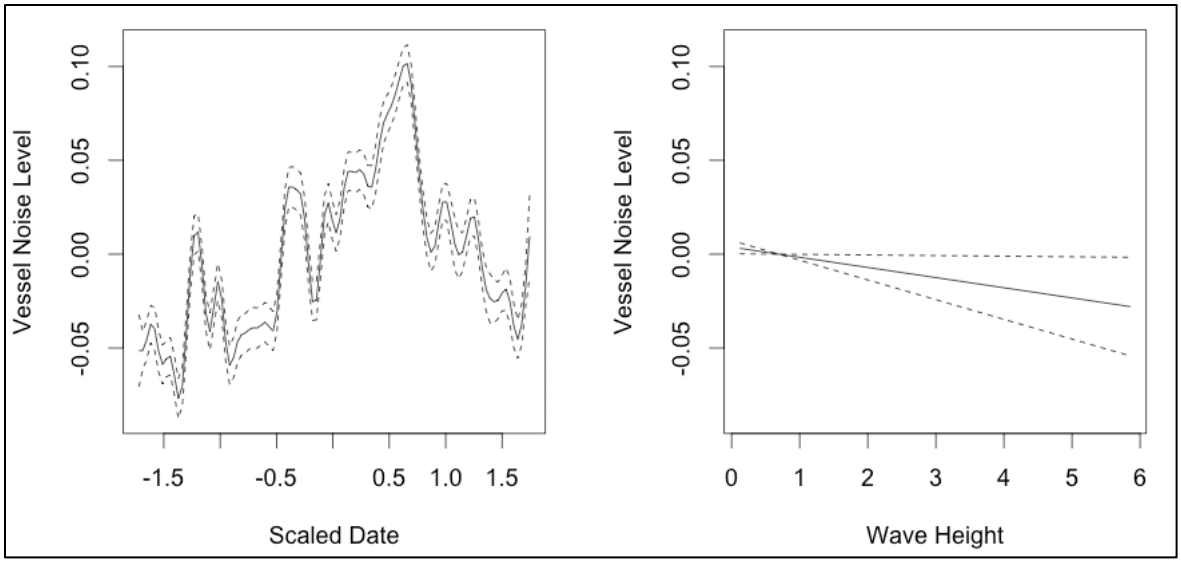

Figure E-31. Smoothing functions for Measured Vessel Band Noise as a function of Wave Height and Windspeed for Receiver 5, Deployment 1

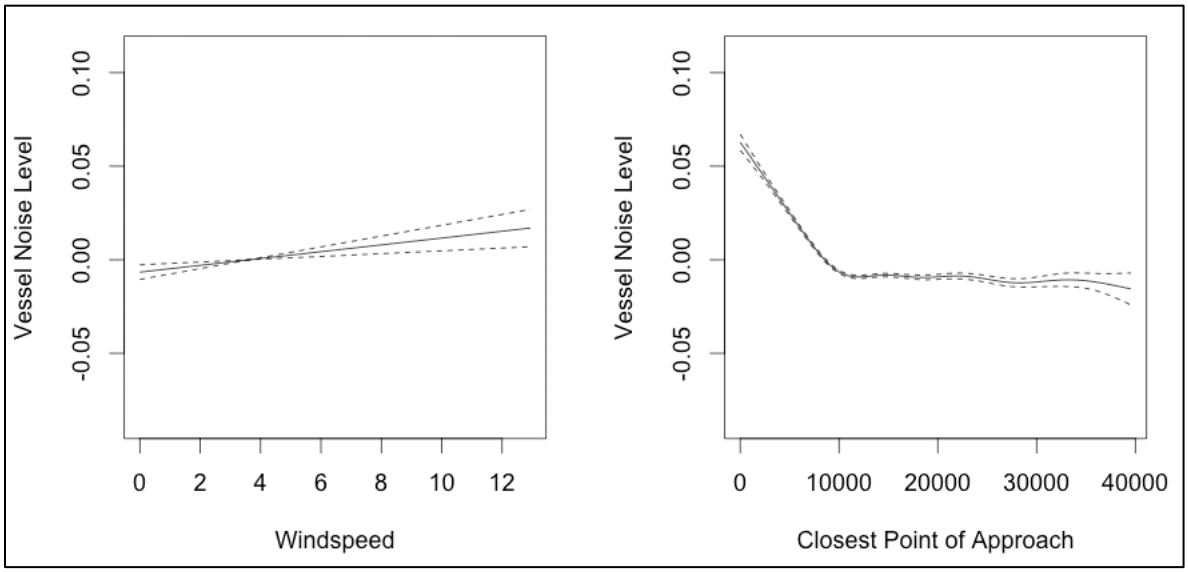

Figure E-32. Smoothing functions for Measured Vessel Band Noise as a function of Wave Height and Windspeed for Receiver 5, Deployment 1

E.3.4.6 Deployment 1, Receiver 6

The significant predictors for Receiver 6 included scaled date, windspeed, and CPA (**Table E-17; Figures E-33 and E-34**). The R-squared value was 0.349. The scaled Date function is complex and hard to interpret. The windspeed functions shows a clear increase in LF noise as windspeed increases. The function clearly shows the increase in received levels as vessel approach the receiver within 10 km.

555 **Table E-17. GAM output for Deployment 1, Receiver 6.**

A. Parametric Coefficients	Estimate	Std. Error	t-value	p-value
(Intercept)	4.5834	0.0012	3669.6195	< 0.0001
B. Smooth Terms	**edf**	**Ref.df**	**F-value**	**p-value**
s(sDate)	28.1260	49.0000	8.6928	< 0.0001
s(WaveHeight)	0.9999	0.9999	1.2730	0.2592
s(Windspeed)	1.0000	1.0000	48.0183	< 0.0001
s(CPA)	8.9244	8.9244	189.6414	< 0.0001
s(Hz200) -200 Hz TOB RL	1.0000	1.0000	0.0234	0.8785
s(BB1) BB RL (w 50 Hz TL)	1.0000	1.0000	1.7653	0.1840
s(BB2) BB RL (w/200 Hz TL)	1.0000	1.0000	0.4031	0.5255

Key: BB=broadband; CPA= closest point of approach; edf=empirical distribution function; F-value=value on the F distribution calculated by dividing two mean squares; Hz=Hertz; Lat=latitude; Lon=longitude; p-value= level of marginal significance within a statistical hypothesis test, representing the probability of the occurrence of a given event; Ref.df=reference degrees of freedom; RL=received level; s=scaled; Std. Error=Standard Error; TL=transmission loss; TOB=third-octave band

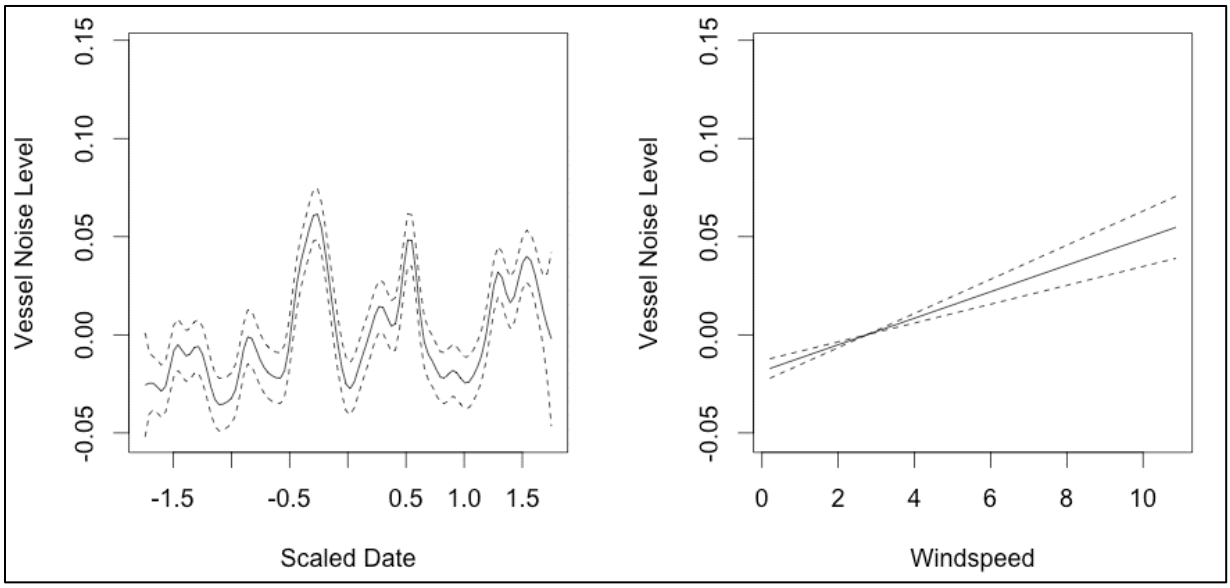

Figure E-33. Smoothing functions for Measured Vessel Band Noise as a function of Scaled Date and Windspeed for Receiver 6, Deployment 1

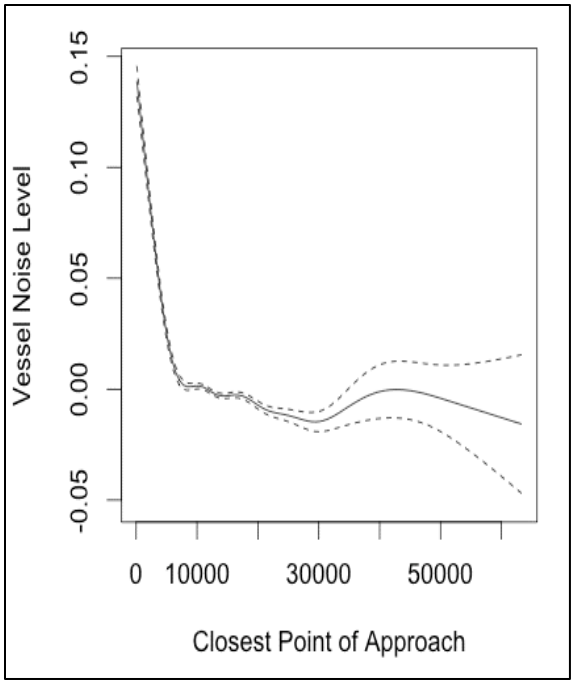

Figure E-34. Smoothing functions for Measured Vessel Band Noise as a function of CPA for Receiver 6, Deployment 1

E.3.4.7 Deployment 1, Receiver 7

The significant predictors for Receiver 7 included scaled date, wave height, windspeed, CPA, and predicted BB RL (**Table E-18**; **Figures E-35**, **E-36**, and **E-37**). The R-squared value was 0.486. The Scaled Date function shows a slight increase in RL throughout the first deployment. The wave height function oscillates at higher wave heights but shows the increase in received noise level from 0 to 2 m as seen in other receivers. The most consistent trends are seen with increased Vessel band noise level as windspeed increases and CPA decreases. These functions curiously show a negative relationship with measured noise levels, which may be due to overprediction of noise levels at this location.

Table E-18. GAM output for Deployment 1, Receiver 7

A. Parametric Coefficients	Estimate	Std. Error	t-value	p-value
(Intercept)	4.5900	0.0009	5331.6673	< 0.0001
B. Smooth Terms	**edf**	**Ref.df**	**F-value**	**p-value**
s(sDate)	0.9997	49.0000	0.3482	< 0.0001
s(WaveHeight)	6.9005	6.9005	7.2718	< 0.0001
s(Windspeed)	1.9177	1.9177	51.6145	< 0.0001
s(CPA)	8.9762	8.9762	868.9379	< 0.0001
s(Hz200) -200 Hz TOB RL	3.8095	3.8095	1.1637	0.2073
s(BB1) BB RL (w 50 Hz TL)	6.3829	6.3829	25.1998	< 0.0001
s(BB2) BB RL (w/200 Hz TL)	3.4084	3.4084	2.8563	0.0195

Key: BB=broadband; CPA= closest point of approach; edf=empirical distribution function; F-value=value on the F distribution calculated by dividing two mean squares; Hz=Hertz; Lat=latitude; Lon=longitude; p-value= level of marginal significance within a statistical hypothesis test, representing the probability of the occurrence of a given event; Ref.df=reference degrees of freedom; RL=received level; s=scaled; Std. Error=Standard Error; TL=transmission loss; TOB=third-octave band

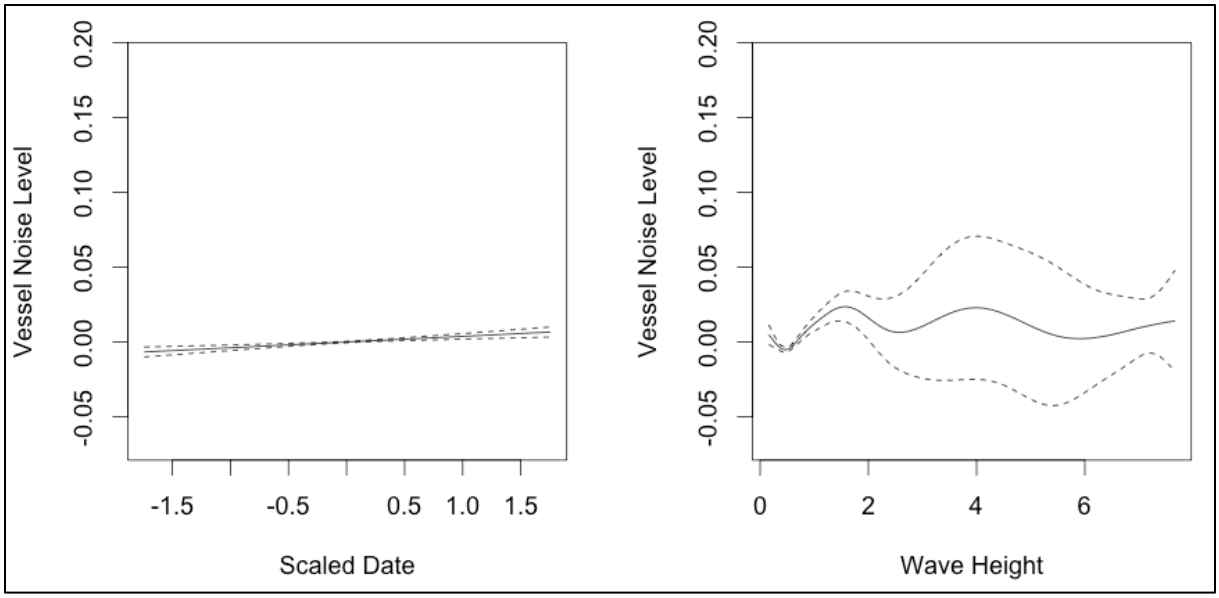

Figure E-35. Smoothing functions for Measured Vessel Band Noise as a function of Scaled Date and Wave Height for Receiver 7, Deployment 1

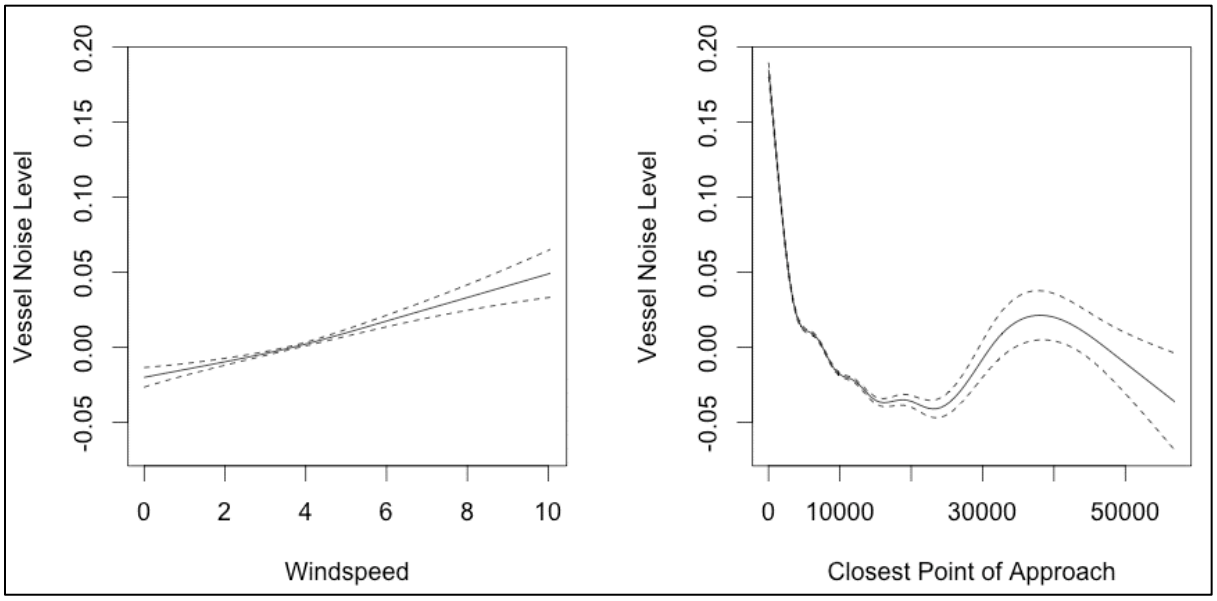

Figure E-36. Smoothing functions for Measured Vessel Band Noise as a function of Windspeed and CPA for Receiver 7, Deployment 1

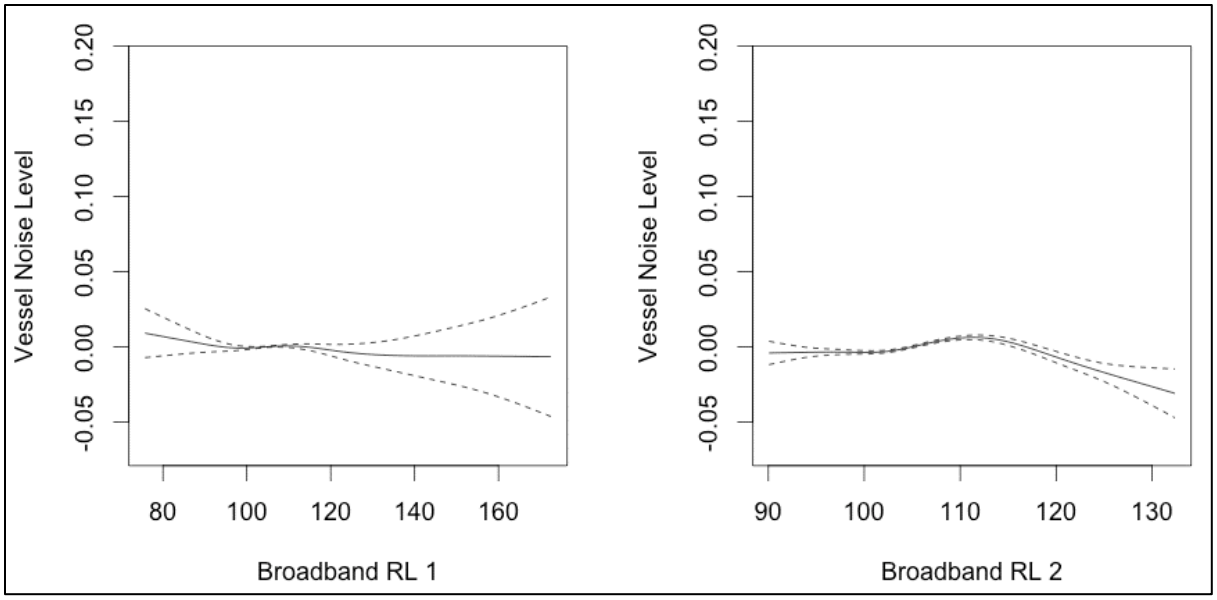

Figure E-37. Smoothing functions for Measured Vessel Band Noise as a function of Predicted BB Levels for Receiver 7, Deployment 1

E.3.4.8 Deployment 1, Receiver 8

The significant predictors for Receiver 8 included windspeed, CPA, and predicted BB RL (**Table E-19**; **Figures E-38** and **E-39**). The R-squared value was only 0.115. The windspeed functions show a clear increase in LF noise as windspeed increases. The CPA function shows a clear increase in measured LF noise as vessels approach within approximately 7 km of the receiver. Paradoxically, the modeled BB RL predicts a decrease in measured LF noise at higher noise levels. This could be the result of an error in source level estimation or TL predictions for this location.

Table E-19. GAM output for Deployment 1, Receiver 8

A. Parametric Coefficients	Estimate	Std. Error	t-value	p-value
(Intercept)	4.5067	0.0027	1650.9840	< 0.0001
B. Smooth Terms	**edf**	**Ref.df**	**F-value**	**p-value**
s(sDate)	0.5701	49.0000	0.0259	0.1347
s(WaveHeight)	1.0000	1.0000	0.1520	0.6966
s(Windspeed)	3.3137	3.3137	4.1362	0.0054
s(CPA)	8.6430	8.6430	129.7145	< 0.0001
s(Hz200) -200 Hz TOB RL	1.0000	1.0000	2.6352	0.1046
s(BB1) BB RL (w 50 Hz TL)	3.7221	3.7221	4.9365	0.0016
s(BB2) BB RL (w/200 Hz TL)	2.3834	2.3834	1.5937	0.1242

Key: BB=broadband; CPA= closest point of approach; edf=empirical distribution function; F-value=value on the F distribution calculated by dividing two mean squares; Hz=Hertz; Lat=latitude; Lon=longitude; p-value= level of marginal significance within a statistical hypothesis test, representing the probability of the occurrence of a given event; Ref.df=reference degrees of freedom; RL=received level; s=scaled; Std. Error=Standard Error; TL=transmission loss; TOB=third-octave band

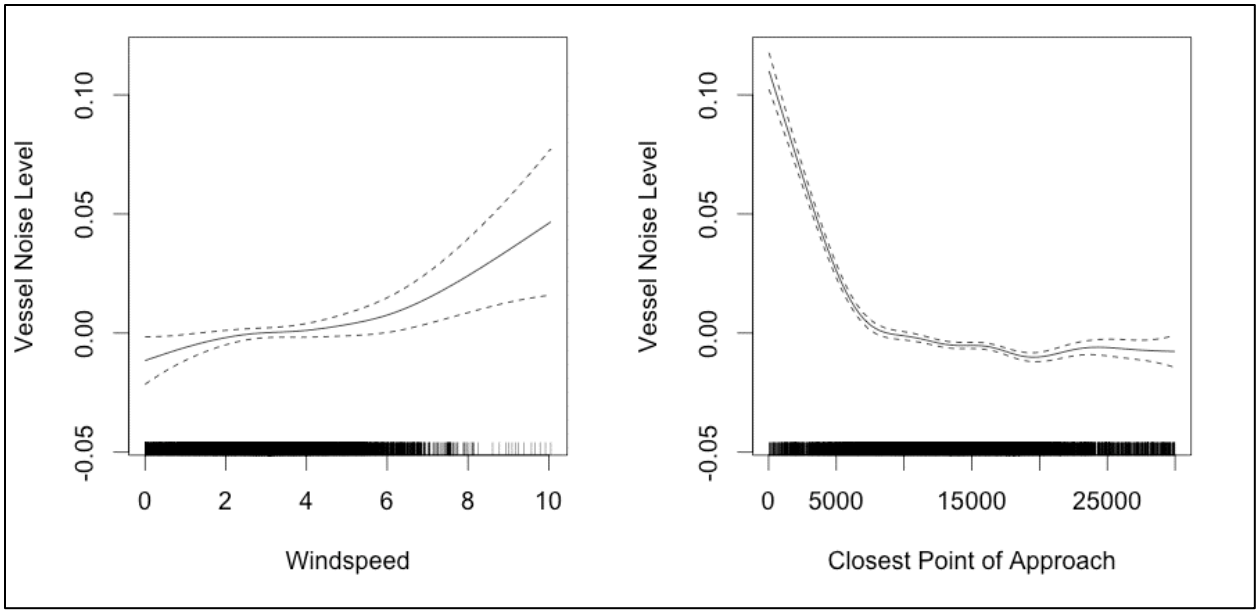

Figure E-38. Smoothing functions for Measured Vessel Band Noise as a function of Wave Height and Windspeed for Receiver 8, Deployment 1

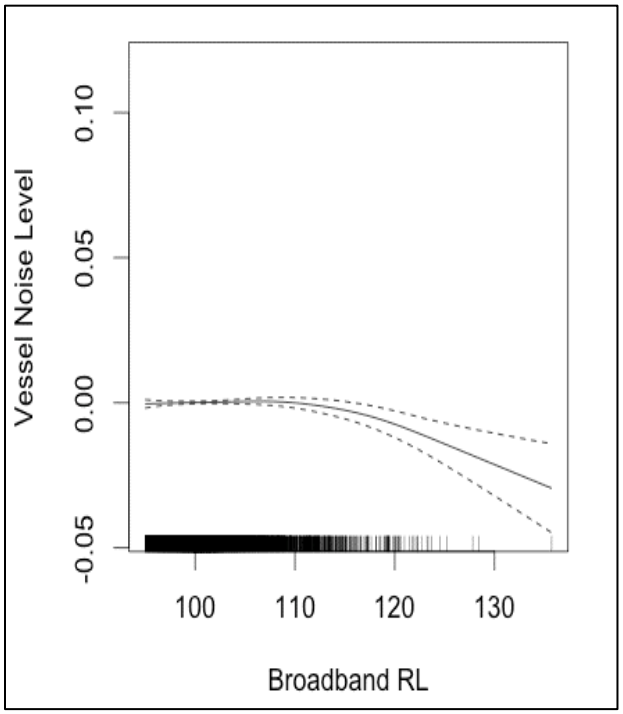

Figure E-39. Smoothing Functions for Measured Vessel Band Noise as a function of CPA for Receiver 8, Deployment 1

E.3.4.9 Deployment 1, Receiver 9

The significant predictors for Receiver 9 included wave height, windspeed, and CPA (**Table E-20**; **Figures E-40** and **E-41**). The R-squared value was only 0.100. Paradoxically, the wave height function shows a decrease in LF noise as wave height increases to 2.5 m, while increases in windspeed predicted

increased Vessel band noise levels. CPAs within approximately 5 km predicted strong increases in received vessel band noise levels.

Table E-20. GAM output for Deployment 1, Receiver 9

A. Parametric Coefficients	Estimate	Std. Error	t-value	p-value
(Intercept)	4.7060	0.0031	1511.0153	< 0.0001
B. Smooth Terms	**edf**	**Ref.df**	**F-value**	**p-value**
s(sDate)	0.0000	49.0000	0.0000	0.7788
s(WaveHeight)	1.0000	1.0000	7.6108	0.0058
s(Windspeed)	1.0000	1.0000	5.2447	0.0220
s(CPA)	8.8484	8.8484	209.0272	< 0.0001
s(Hz200) -200 Hz TOB RL	1.0000	1.0000	2.1859	0.1393
s(BB1) BB RL (w 50 Hz TL)	1.0000	1.0000	0.4827	0.4872
s(BB2) BB RL (w/200 Hz TL)	1.0000	1.0000	0.0926	0.7609

Key: BB=broadband; CPA= closest point of approach; edf=empirical distribution function; F-value=value on the F distribution calculated by dividing two mean squares; Hz=Hertz; Lat=latitude; Lon=longitude; p-value= level of marginal significance within a statistical hypothesis test, representing the probability of the occurrence of a given event; Ref.df=reference degrees of freedom; RL=received level; s=scaled; Std. Error=Standard Error; TL=transmission loss; TOB=third-octave band

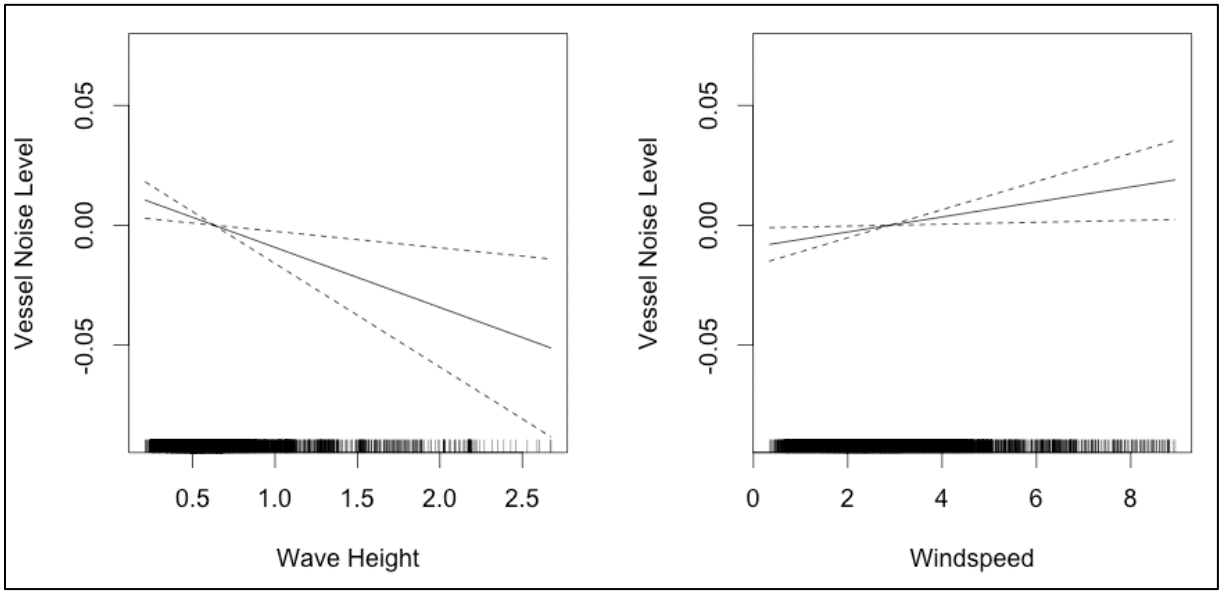

Figure E-40. Smoothing functions for Measured Vessel Band Noise as a function of Wave Height and Windspeed for Receiver 9, Deployment 1

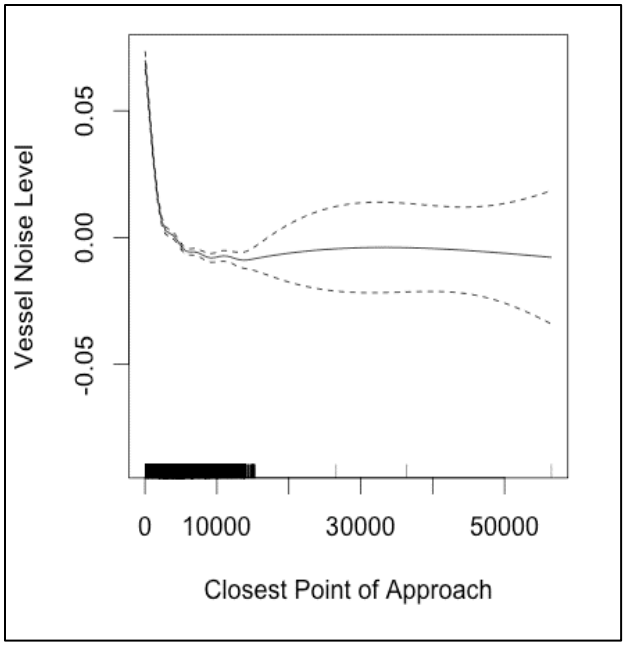

Figure E-41. Smoothing functions for Measured Vessel Band Noise as a function of CPA for Receiver 9, Deployment 1

E.3.4.10 Deployment 1, Receiver 10

The significant predictors for Receiver 10 included scaled date, wave height, windspeed, CPA, and all three predicted RL metrics (**Table E-21**; **Figures E-42**, **E-43**, and **E-44**). The R-squared value was 0.421. The scaled Date function is complex and likely reflects the airgun activity late in the recording period. The wave height function for Receiver 10 is complex, unusual, and hard to interpret. The windspeed functions shows a clear increase in LF noise as windspeed increases. The CPA function shows an increase in measured LF noise as vessels approached within 10 km of the recorder. The 200 Hz RL function and the BB RL function both show a positive near-linear relationship between predicted and measured RL. However, the 200 Hz function shows a stronger relationship.

Table E-21. GAM output for Deployment 1, Receiver 10

A. Parametric Coefficients	Estimate	Std. Error	t-value	p-value
(Intercept)	4.5273	0.0012	3752.5849	< 0.0001
B. Smooth Terms	**edf**	**Ref.df**	**F-value**	**p-value**
s(sDate)	36.4854	49.0000	18.3865	< 0.0001
s(WaveHeight)	6.8869	6.8869	7.4095	< 0.0001
s(Windspeed)	4.2631	4.2631	6.3593	< 0.0001
s(CPA)	8.9509	8.9509	665.2577	< 0.0001
s(Hz200) -200 Hz TOB RL	1.0000	1.0000	18.6362	< 0.0001
s(BB1) BB RL (w 50 Hz TL)	5.2608	5.2608	12.7145	< 0.0001
s(BB2) BB RL (w/200 Hz TL)	5.0689	5.0689	5.8241	< 0.0001

Key: BB=broadband; CPA= closest point of approach; edf=empirical distribution function; F-value=value on the F distribution calculated by dividing two mean squares; Hz=Hertz; Lat=latitude; Lon=longitude; p-value= level of marginal significance within a statistical hypothesis test, representing the probability of the occurrence of a given event; Ref.df=reference degrees of freedom; RL=received level; s=scaled; Std. Error=Standard Error; TL=transmission loss; TOB=third-octave band

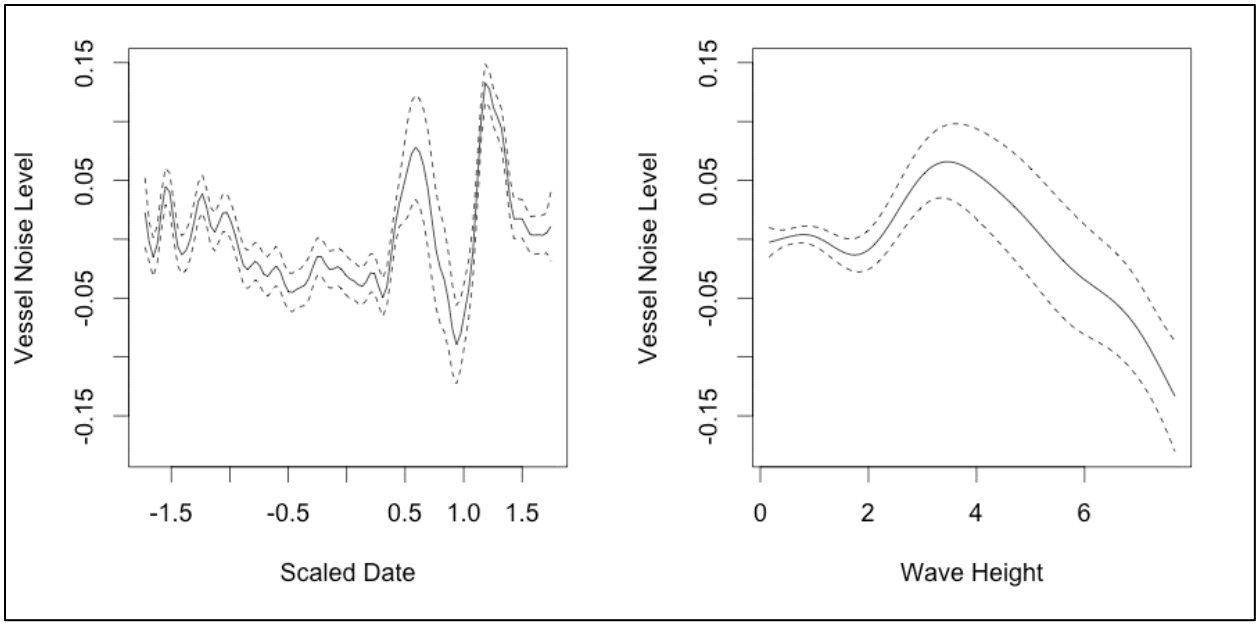

Figure E-42. Smoothing functions for Measured Vessel Band Noise as a function of Scaled Date and Wave Height for Receiver 10, Deployment 1

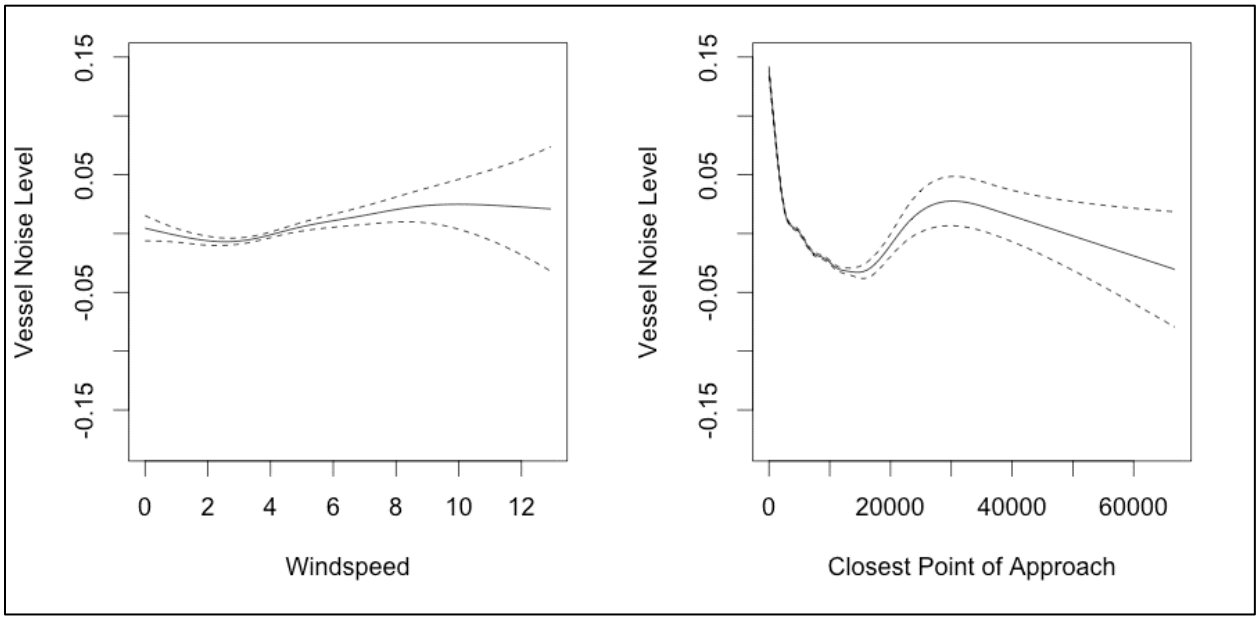

Figure E-43. Smoothing functions for Measured Vessel Band Noise as a function of Windspeed and CPA for Receiver 10, Deployment 1

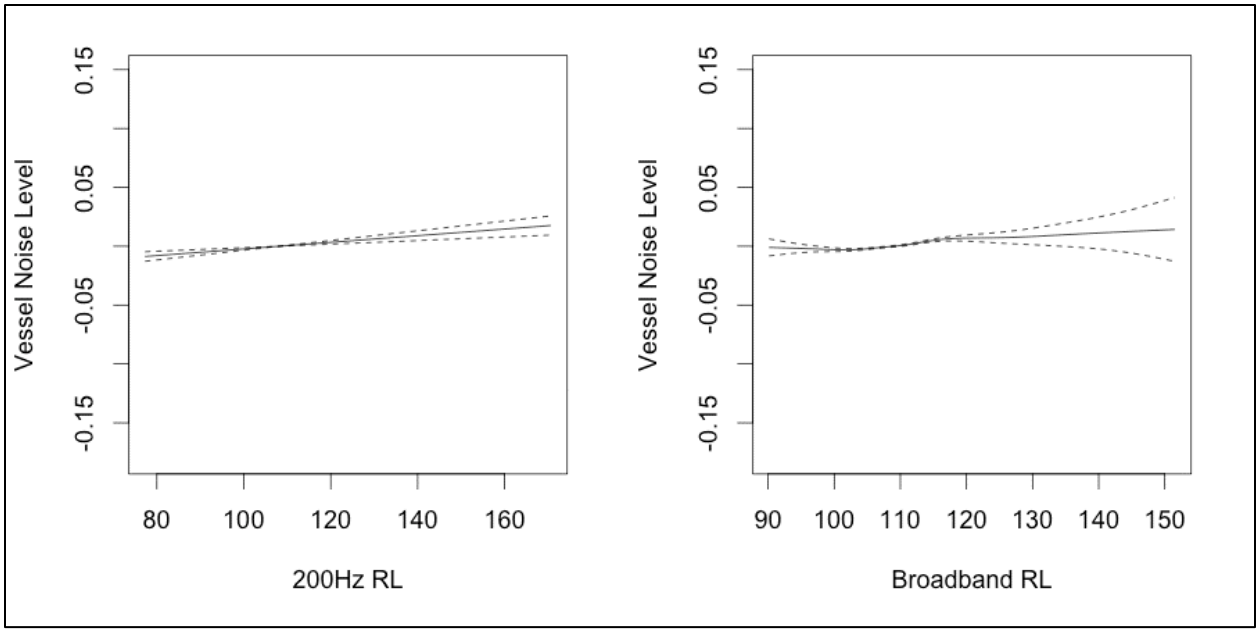

Figure E-44. Smoothing functions for Measured Vessel Band Noise as a function of 200 Hz RL and BB RL for Receiver 10, Deployment 1

E.4.5 Revised Simplified Statistical Modeling Results of Vessel Received Levels

The model and analysis results of a second, simpler statistical approach that was implemented to assess vessel RLs for all 10 EAR and RH sensors for all 4 deployments resulted in higher R-square values (i.e., or a better model fit) for the vessel data. Accordingly, all sensor data for all four deployments was assessed using the simpler statistical approach. To provide a comparison for the data presented and discussed in **Section E.4.4**, results from the simplified statistical modeling for the 10 sensors for Deployment 1 are presented and discussed below. Similar results for Deployments 2 through 4 are presented in **Appendix E-B**. To differentiate the figure and table modeling results resulting from the Simple Statistical Analysis from those of the full statistical modeling, the designation SA2 is given in the caption.

E.3.5.1 Deployment 1, Receiver 1 (Statistical Approach 2)

The simplified statistical analysis resulted in a greater R-square (0.671) than resulted from the full statistical predicted RL analysis (**Table E-22**). Both approaches resulted in a significant and complex smooth fit to the scaled date, and both results reported increased vessel band noise levels with increasing windspeed (**Figure E-45**). The smooth fit to minimum CPA had a similar shape, with the inflection point at approximately 10 km in both analyses.

Table E-22. GAM SA2 output for Deployment 1, Receiver 1

A. Parametric Coefficients	Estimate	Std. Error	t-value	p-value
(Intercept)	4.7106	0.0008	5583.3855	< 0.0001
km2	0.0392	0.0051	7.6588	< 0.0001
km4	0.0203	0.0036	5.6526	< 0.0001
km10	0.0205	0.0023	8.7221	< 0.0001

B. Smooth Terms	edf	Ref.df	F-value	p-value
s(sDate)	44.0524	49.0000	147.6610	< 0.0001
s(WaveHeight)	6.2418	6.2418	9.3809	< 0.0001
s(Windspeed)	1.0000	1.0000	10.5758	0.0012
s(CPAmin)	1.0000	1.0000	36.7337	< 0.0001
Key: CPA= closest point of approach; edf=empirical distribution function; F-value=value on the F distribution calculated by dividing two mean squares; km=kilometer; min=minimum; p-value= level of marginal significance within a statistical hypothesis test, representing the probability of the occurrence of a given event; Ref.df=reference degrees of freedom; s=scaled; Std. Error=Standard Error				

609

610 E.3.5.2 Deployment 1, Receiver 2 (Statistical Approach 2)

611 The simplified analysis had a larger R-square (0.515 [vice 0.500 for statistical approach 1) than the
612 predicted RL analysis (**Table E-23**). Scaled date and minimum CPA were significant in both models.
613 However, windspeed was significant in the simplified analysis and was not in the predicted RL analysis
614 (**Figure E-46**).

615 **Table E-23. GAM SA2 output for Deployment 1, Receiver 2**

A. Parametric Coefficients	Estimate	Std. Error	t-value	p-value
(Intercept)	4.4932	0.0012	3625.2581	< 0.0001
km2	-0.0059	0.0085	-0.6876	0.4917
km4	-0.0063	0.0049	-1.2989	0.1941
km10	0.0039	0.0019	2.0298	0.0425
B. Smooth Terms	**edf**	**Ref.df**	**F-value**	**p-value**
s(sDate)	43.7402	49.0000	52.5753	< 0.0001
s(WaveHeight)	1.0000	1.0000	0.0027	0.9583
s(Windspeed)	1.0000	1.0000	6.2093	0.0128
s(CPAmin)	7.7553	7.7553	19.5051	< 0.0001
Key: CPA= closest point of approach; edf=empirical distribution function; F-value=value on the F distribution calculated by dividing two mean squares; km=kilometer; min=minimum; p-value= level of marginal significance within a statistical hypothesis test, representing the probability of the occurrence of a given event; Ref.df=reference degrees of freedom; s=scaled; Std. Error=Standard Error				

616

617 E.3.5.3 Deployment 1, Receiver 3 (Statistical Approach 2)

618 For Receiver 3, both statistical analyses showed that scaled date, wave height, wind speed, and minimum
619 CPA were all significant predictors (**Table E-24**), with an R-square value of 0.491. The shape of the
620 smooth fits for these variables in both analyses were similar (**Figure E-47**).

621 **Table E-24. GAM SA2 output for Deployment 1, Receiver 3**

A. Parametric Coefficients	Estimate	Std. Error	t-value	p-value
(Intercept)	4.5561	0.0010	4566.3883	< 0.0001
km2	0.0151	0.0120	1.2571	0.2088
km4	-0.0021	0.0080	-0.2560	0.7979
km10	-0.0127	0.0042	-2.9962	0.0028

B. Smooth Terms	edf	Ref.df	F-value	p-value
s(sDate)	39.8317	49.0000	34.9559	< 0.0001
s(WaveHeight)	6.4432	6.4432	8.6504	< 0.0001
s(Windspeed)	1.0000	1.0000	85.4003	< 0.0001
s(CPAmin)	6.2801	6.2801	12.4484	< 0.0001
Key: CPA= closest point of approach; edf=empirical distribution function; F-value=value on the F distribution calculated by dividing two mean squares; km=kilometer; min=minimum; p-value= level of marginal significance within a statistical hypothesis test, representing the probability of the occurrence of a given event; Ref.df=reference degrees of freedom; s=scaled; Std. Error=Standard Error				

622

623

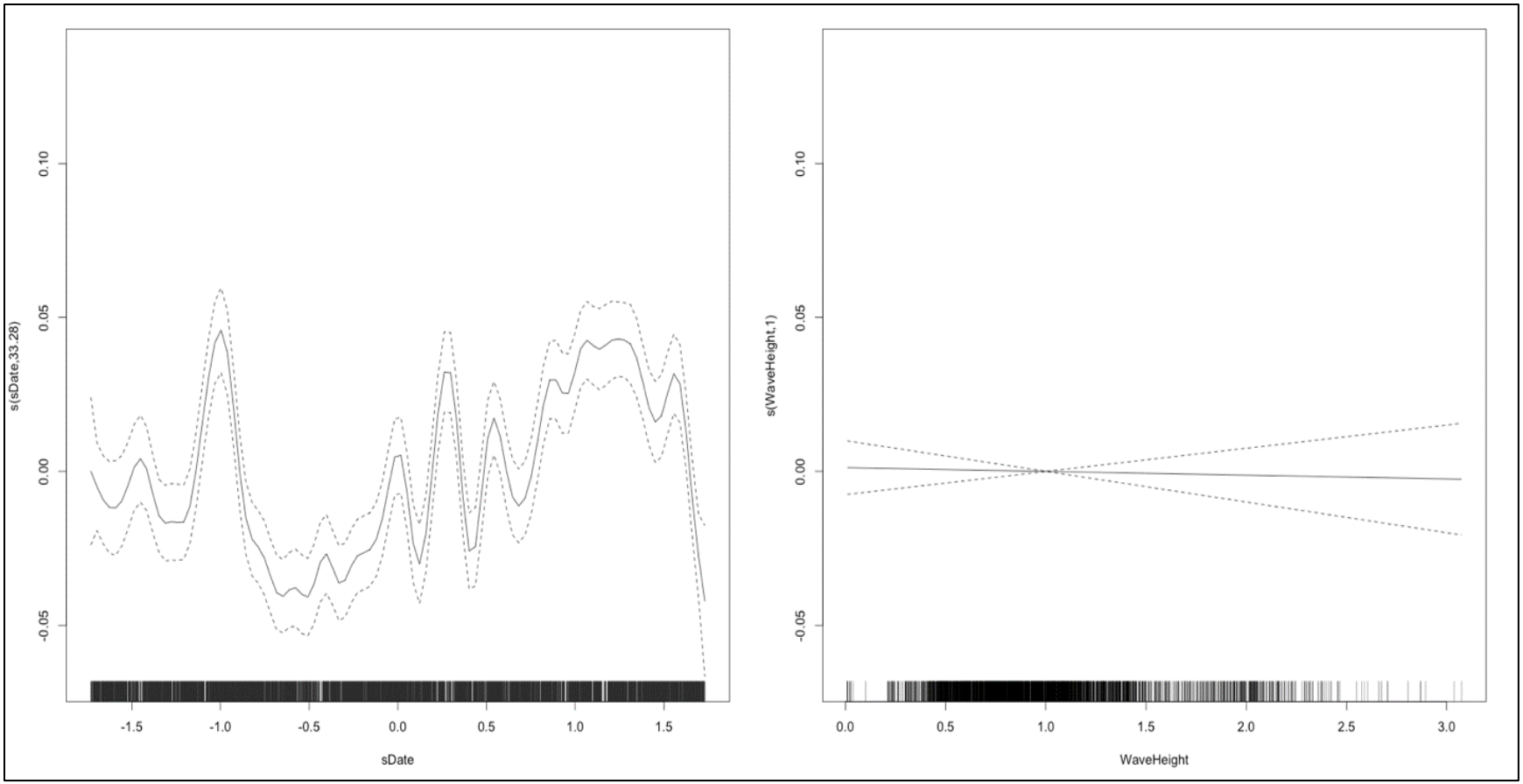

Figure E-45a. SA2 smoothing functions for Measured Vessel Band Noise as a function of Date, Wave Height, Windspeed, and CPA for Receiver 1, Deployment 1

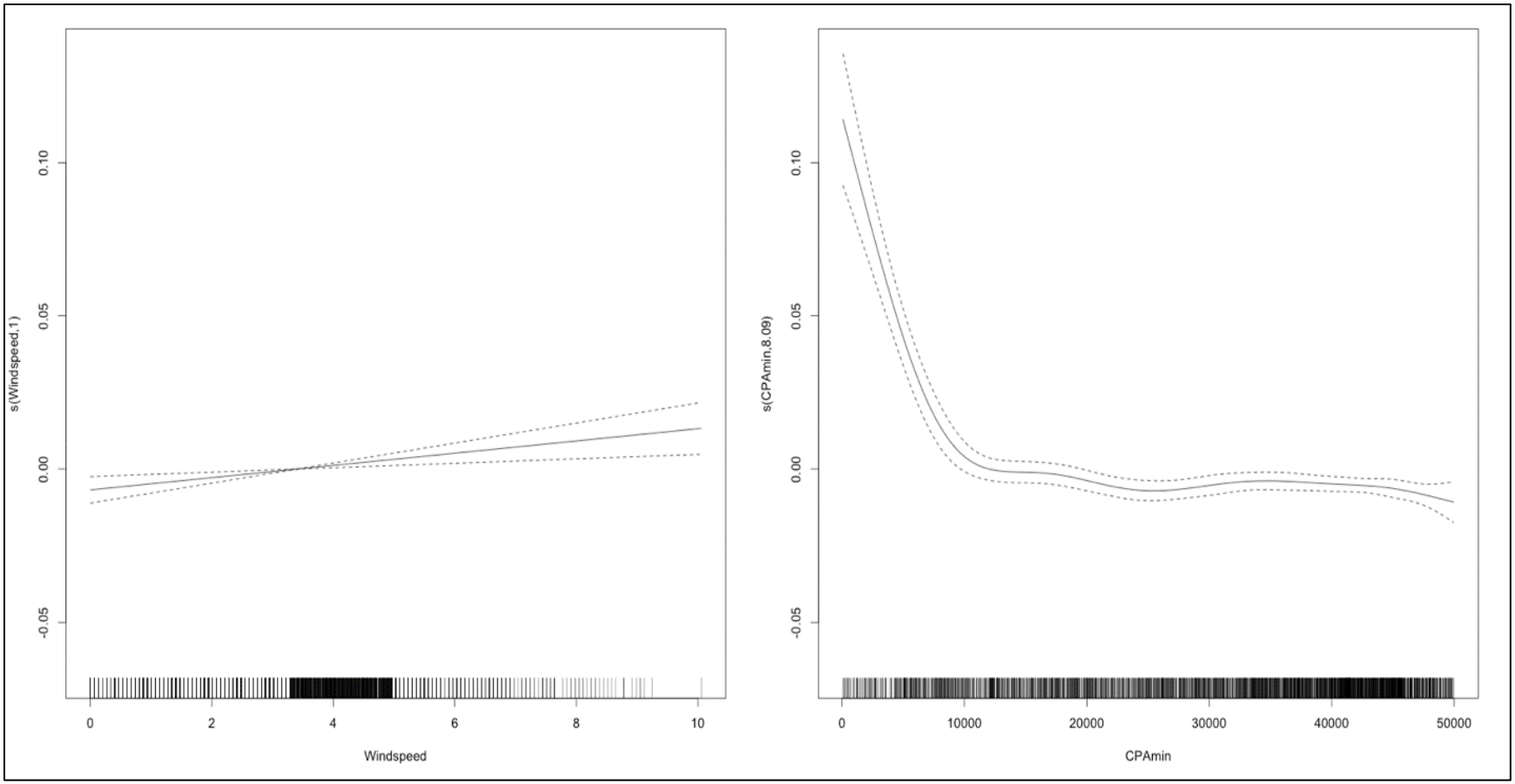

Figure E-45b. SA2 smoothing functions for Measured Vessel Band Noise as a function of Date, Wave Height, Windspeed, and CPA for Receiver 1, Deployment 1

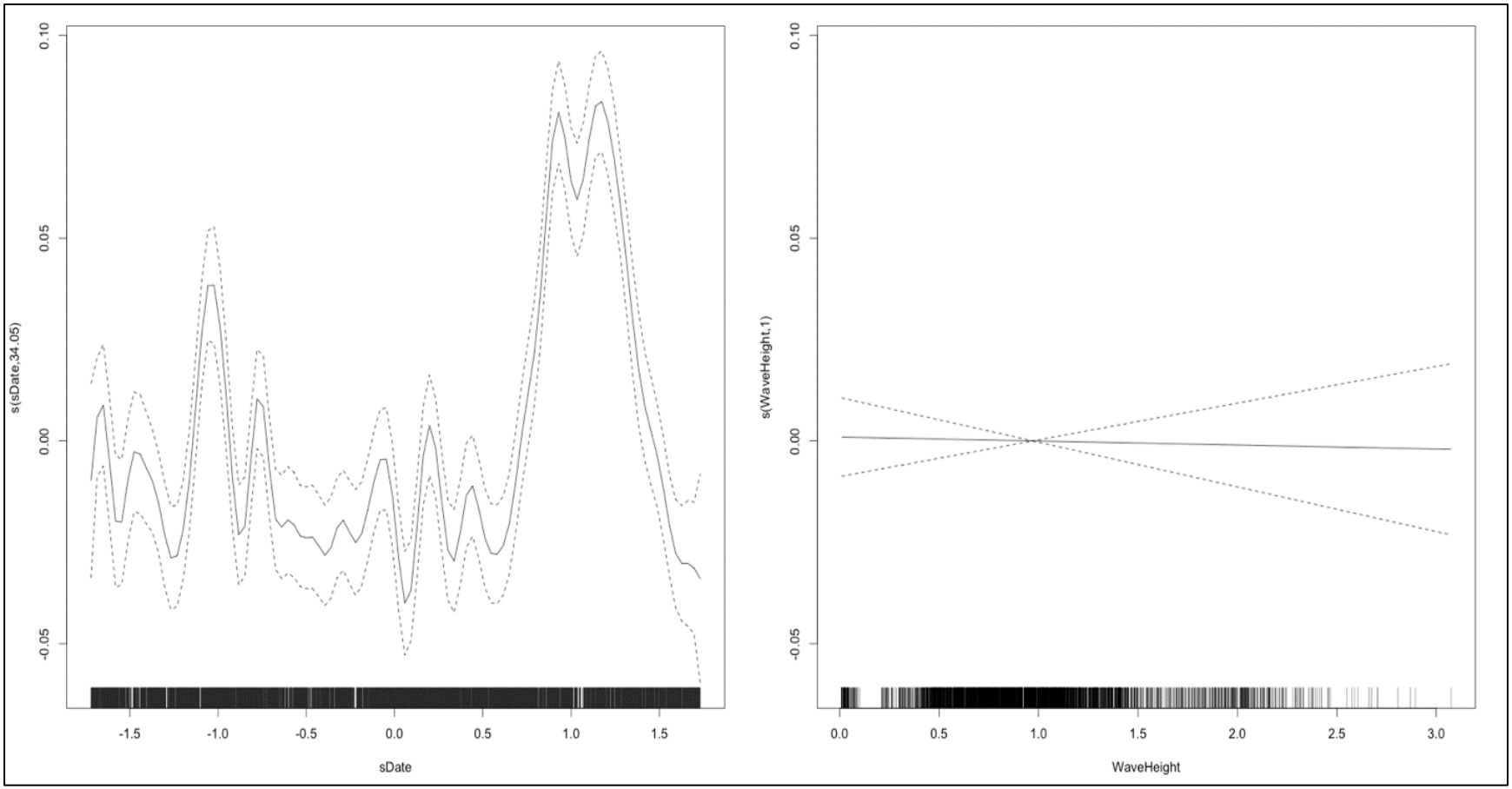

Figure E-46a. SA2 smoothing functions for Measured Vessel Band Noise as a function of Date, Wave Height, Windspeed, and CPA for Receiver 2, Deployment 1

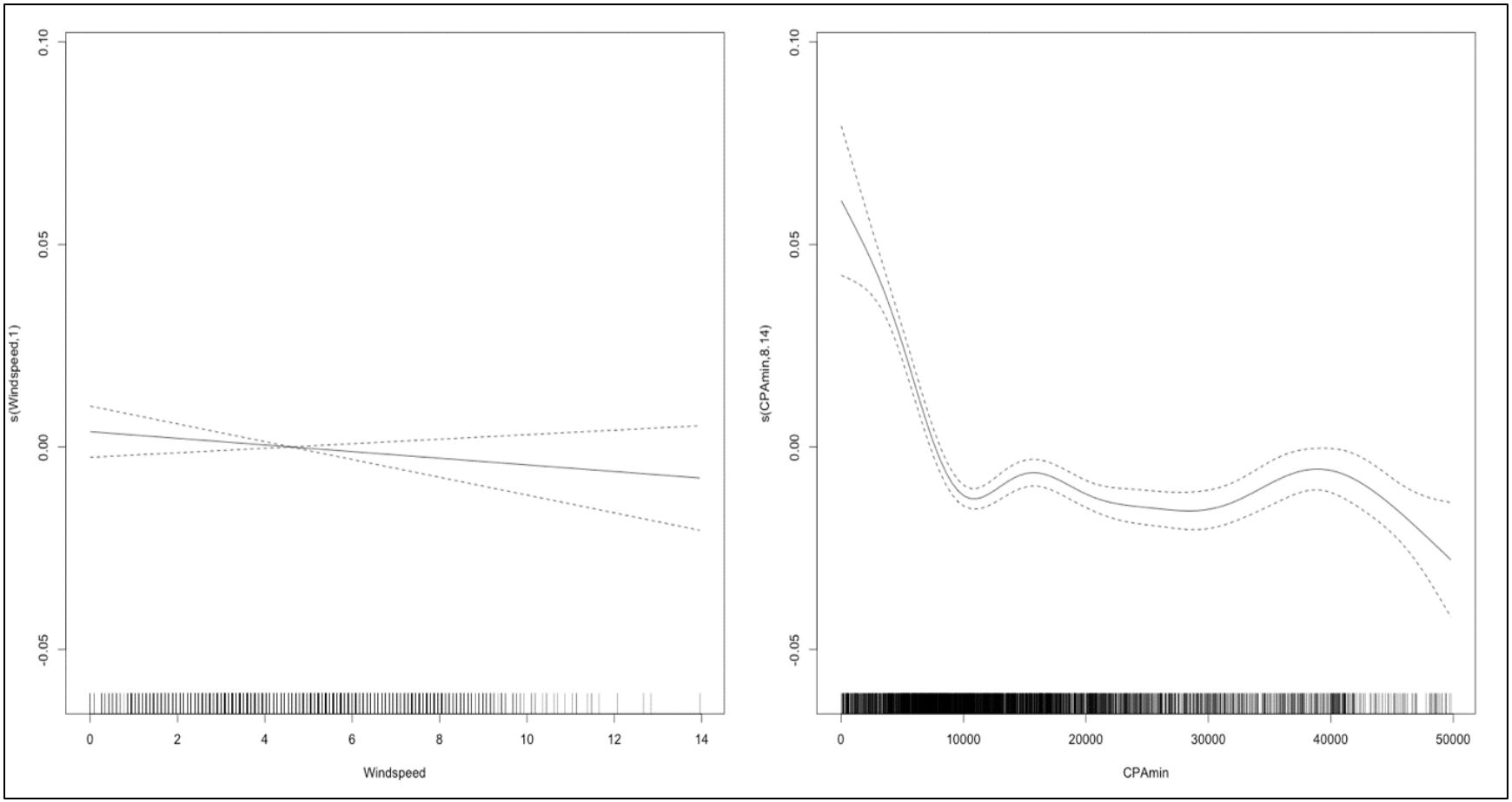

Figure E-46b. SA2 smoothing functions for Measured Vessel Band Noise as a function of Date, Wave Height, Windspeed, and CPA for Receiver 2, Deployment 1

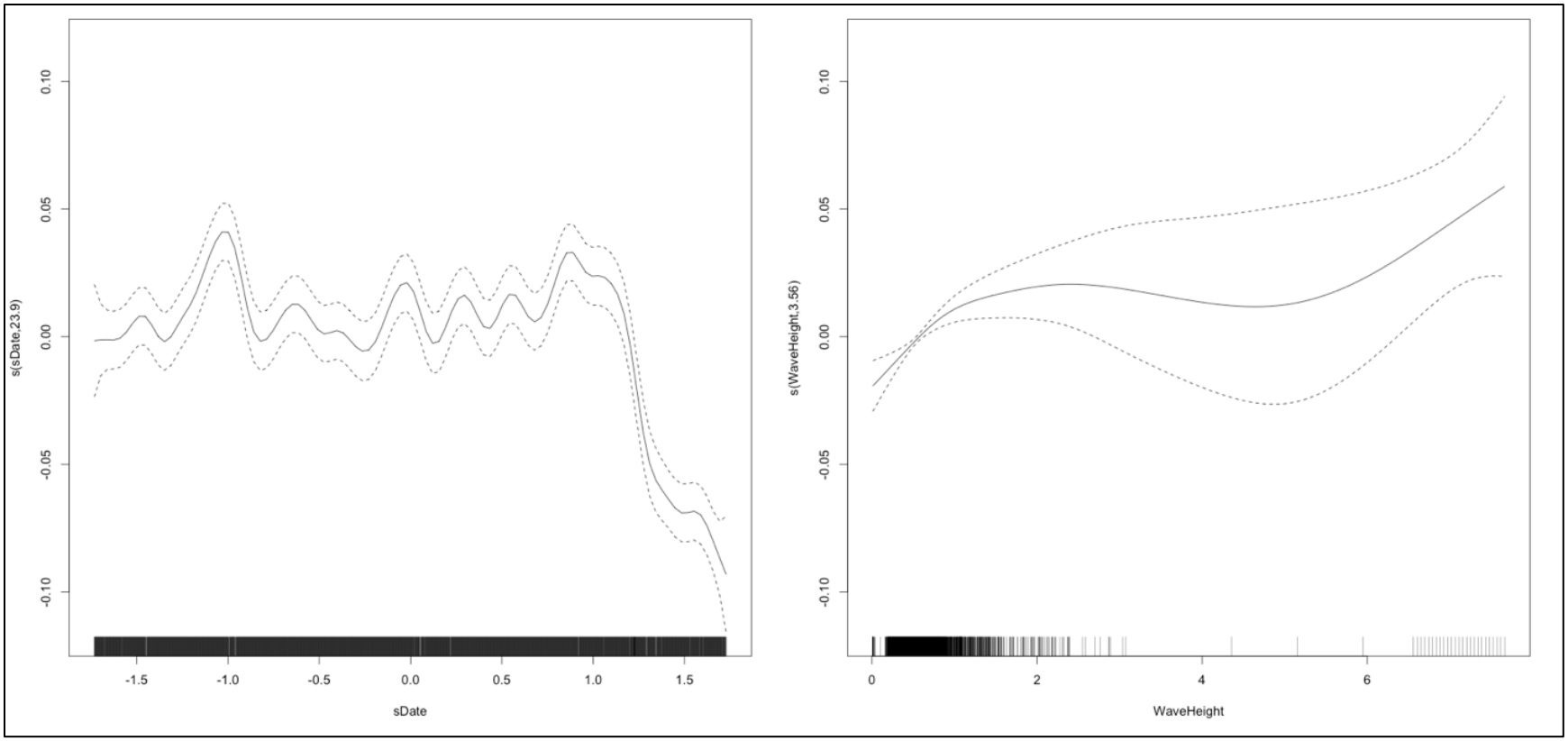

Figure E-47a. SA2 smoothing functions for Measured Vessel Band Noise as a function of Date, Wave Height, Windspeed, and CPA for Receiver 3, Deployment 1

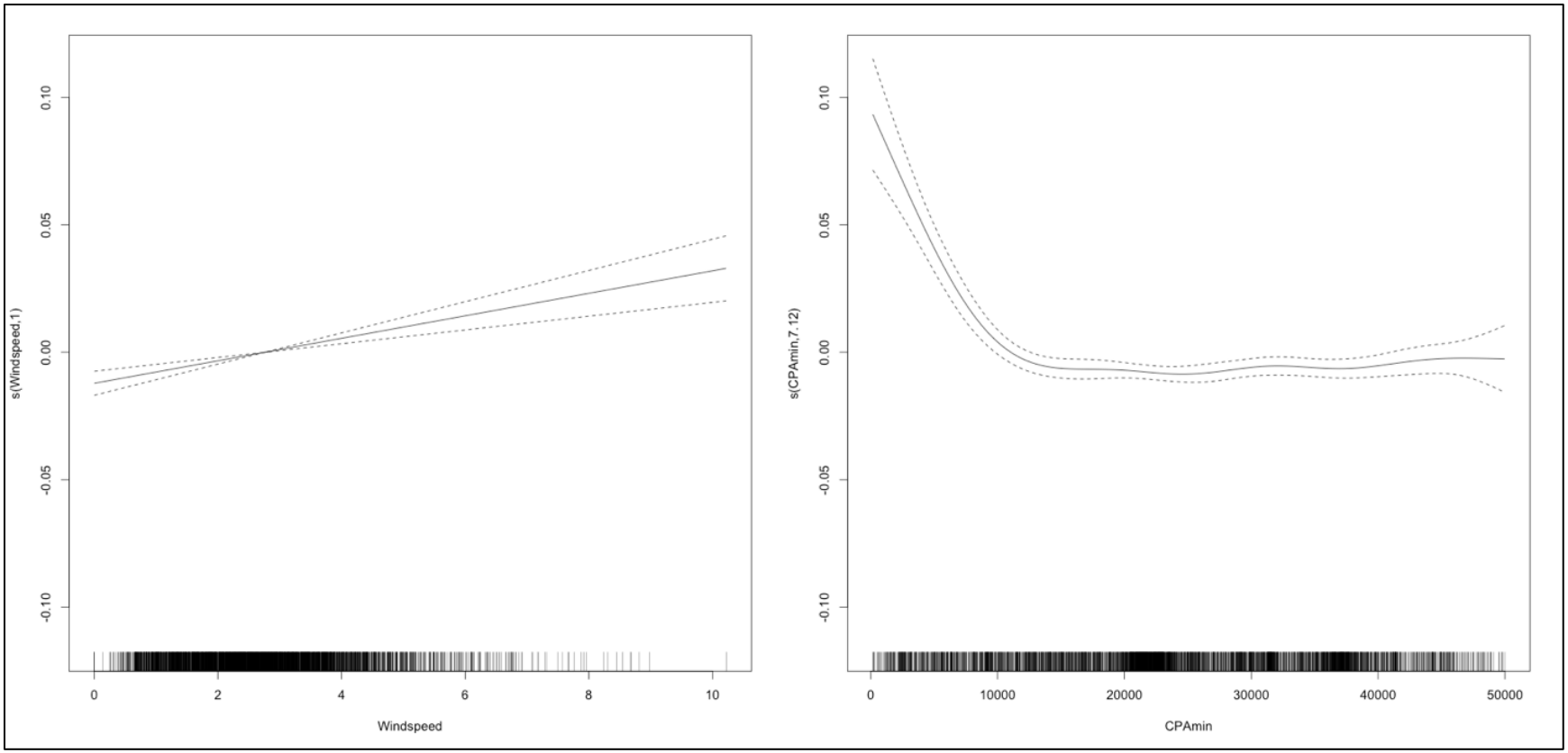

Figure E-47b. SA2 smoothing functions for Measured Vessel Band Noise as a function of Date, Wave Height, Windspeed, and CPA for Receiver 3, Deployment 1

E.3.5.4 Deployment 1, Receiver 4 (Statistical Approach 2)

Both statistical analyses for Receiver 4, Deployment 1 resulted in scaled date, wave height, wind speed, and minimum CPA as all significant predictors (**Table E-25**). The R-square for the shape of the smooth fits for these variables in both analyses were similar (**Figure E-48**).

Table E-25. GAM SA2 output for Deployment 1, Receiver 4

A. Parametric Coefficients	Estimate	Std. Error	t-value	p-value
(Intercept)	4.4815	0.0016	2785.4192	< 0.0001
km2	0.0280	0.0109	2.5765	0.0101
km4	0.0184	0.0075	2.4420	0.0147
km10	0.0009	0.0025	0.3719	0.7100
B. Smooth Terms	**edf**	**Ref.df**	**F-value**	**p-value**
s(sDate)	44.0743	49.0000	29.0284	< 0.0001
s(WaveHeight)	1.0000	1.0000	5.6692	0.0174
s(Windspeed)	1.0000	1.0000	17.5270	< 0.0001
s(CPAmin)	5.3380	5.3380	5.4207	< 0.0001

Key: CPA= closest point of approach; edf=empirical distribution function; F-value=value on the F distribution calculated by dividing two mean squares; km=kilometer; min=minimum; p-value= level of marginal significance within a statistical hypothesis test, representing the probability of the occurrence of a given event; Ref.df=reference degrees of freedom; s=scaled; Std. Error=Standard Error

E.3.5.5 Deployment 1, Receiver 5 (Statistical Approach 2)

For Receiver 5, both statistical analyses resulted in the scaled date, wave height, wind speed, and minimum CPA all being significant predictors (**Table E-26**). The R-square value is 0.674. The shape of the smooth fits for these variables in both analyses were similar (**Figure E-49**).

Table E-26. GAM SA2 output for Deployment 1, Receiver 5

A. Parametric Coefficients	Estimate	Std. Error	t-value	p-value
(Intercept)	4.5559	0.0010	4626.2543	< 0.0001
km2	0.0093	0.0052	1.7946	0.0728
km4	0.0022	0.0028	0.7945	0.4269
km10	0.0029	0.0009	3.2223	0.0013
B. Smooth Terms	**edf**	**Ref.df**	**F-value**	**p-value**
s(sDate)	45.8967	49.0000	149.1195	< 0.0001
s(WaveHeight)	5.9244	5.9244	8.5030	< 0.0001
s(Windspeed)	1.0000	1.0000	24.3613	< 0.0001
s(CPAmin)	5.9998	5.9998	19.1413	< 0.0001

Key: CPA= closest point of approach; edf=empirical distribution function; F-value=value on the F distribution calculated by dividing two mean squares; km=kilometer; min=minimum; p-value= level of marginal significance within a statistical hypothesis test, representing the probability of the occurrence of a given event; Ref.df=reference degrees of freedom; s=scaled; Std. Error=Standard Error

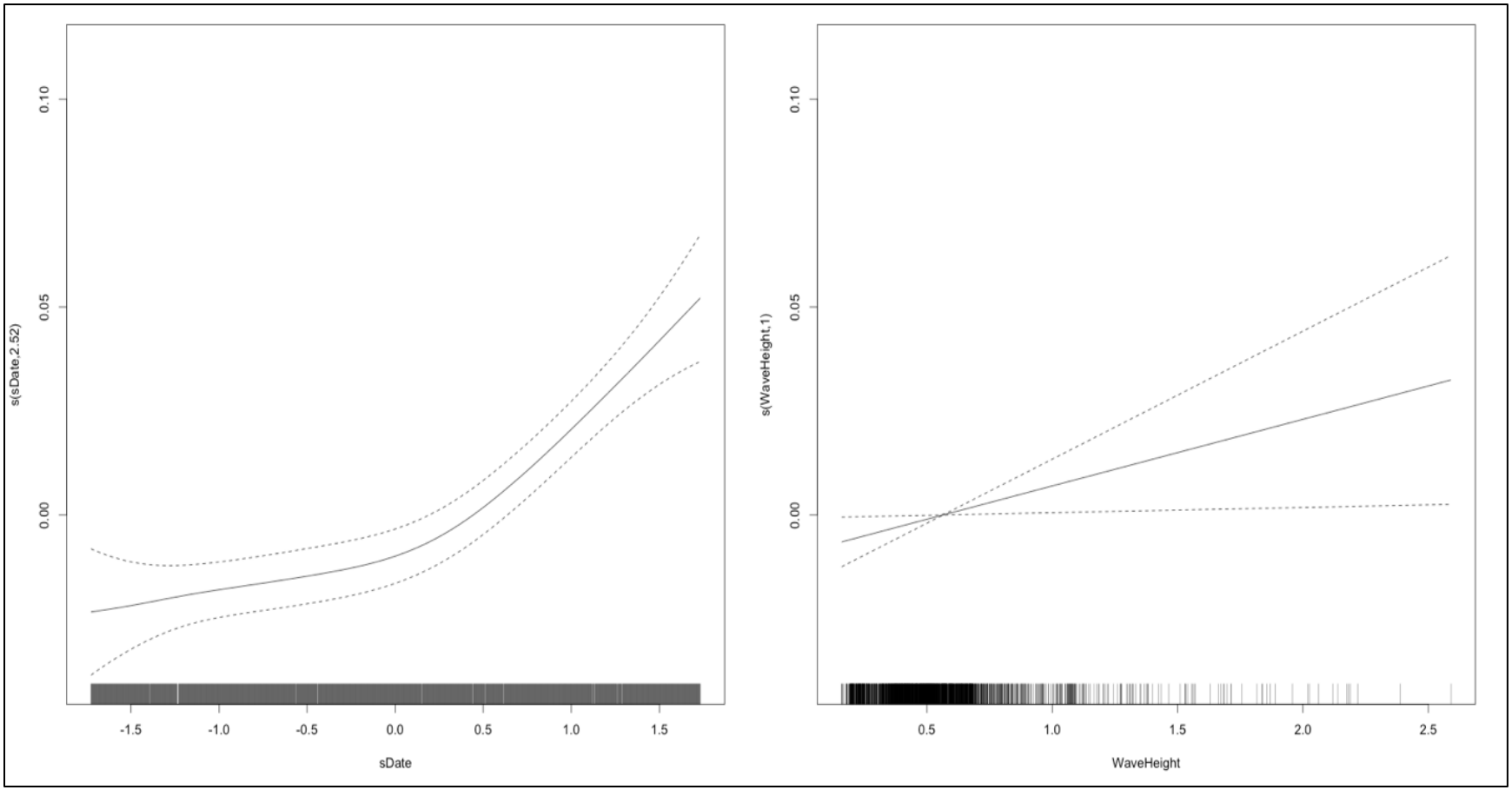

Figure E-48a. SA2 smoothing functions for Measured Vessel Band Noise as a function of Date, Wave Height, Windspeed, and CPA for Receiver 4, Deployment 1

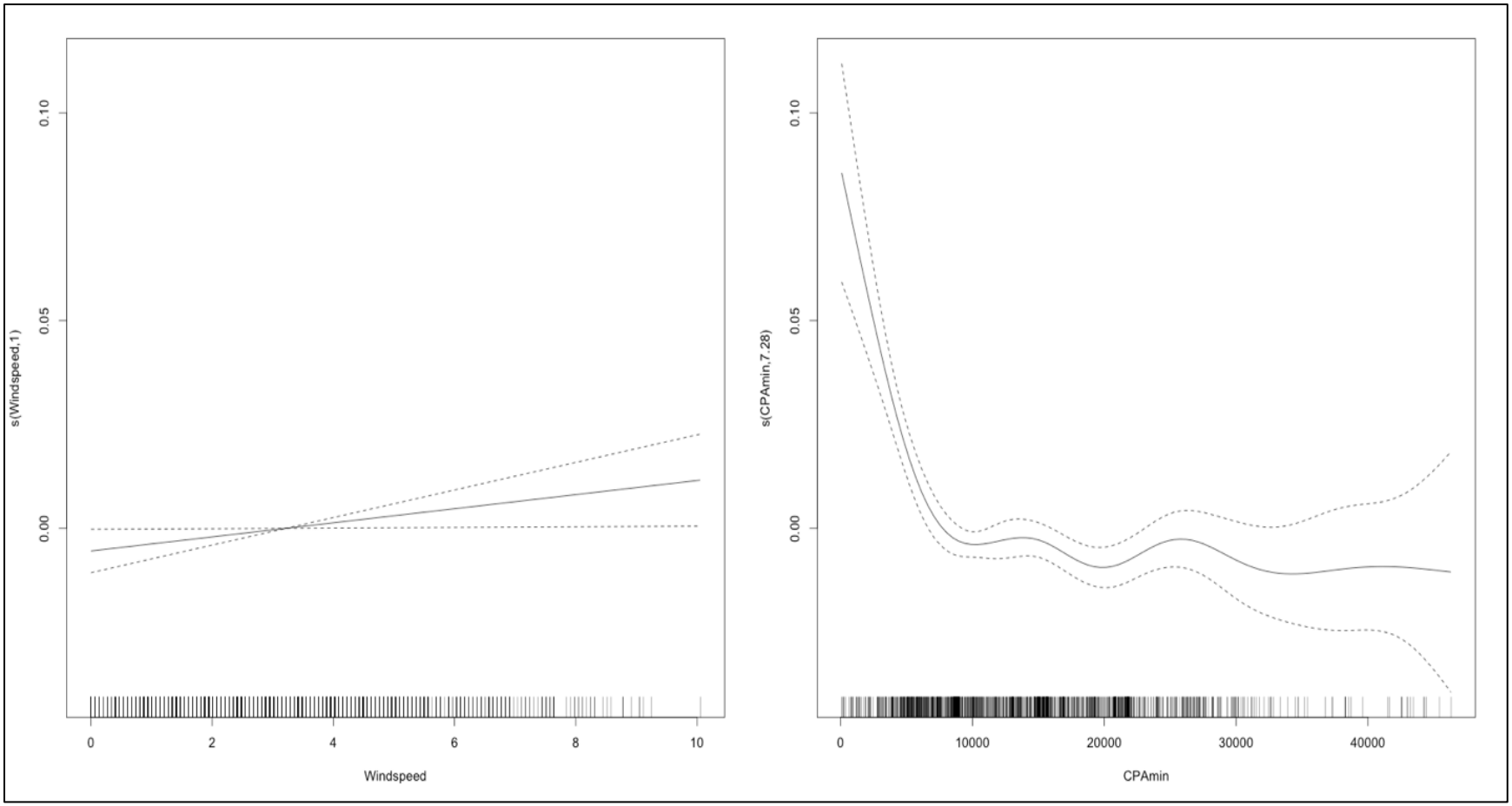

Figure E-48b. SA2 smoothing functions for Measured Vessel Band Noise as a function of Date, Wave Height, Windspeed, and CPA for Receiver 4, Deployment 1

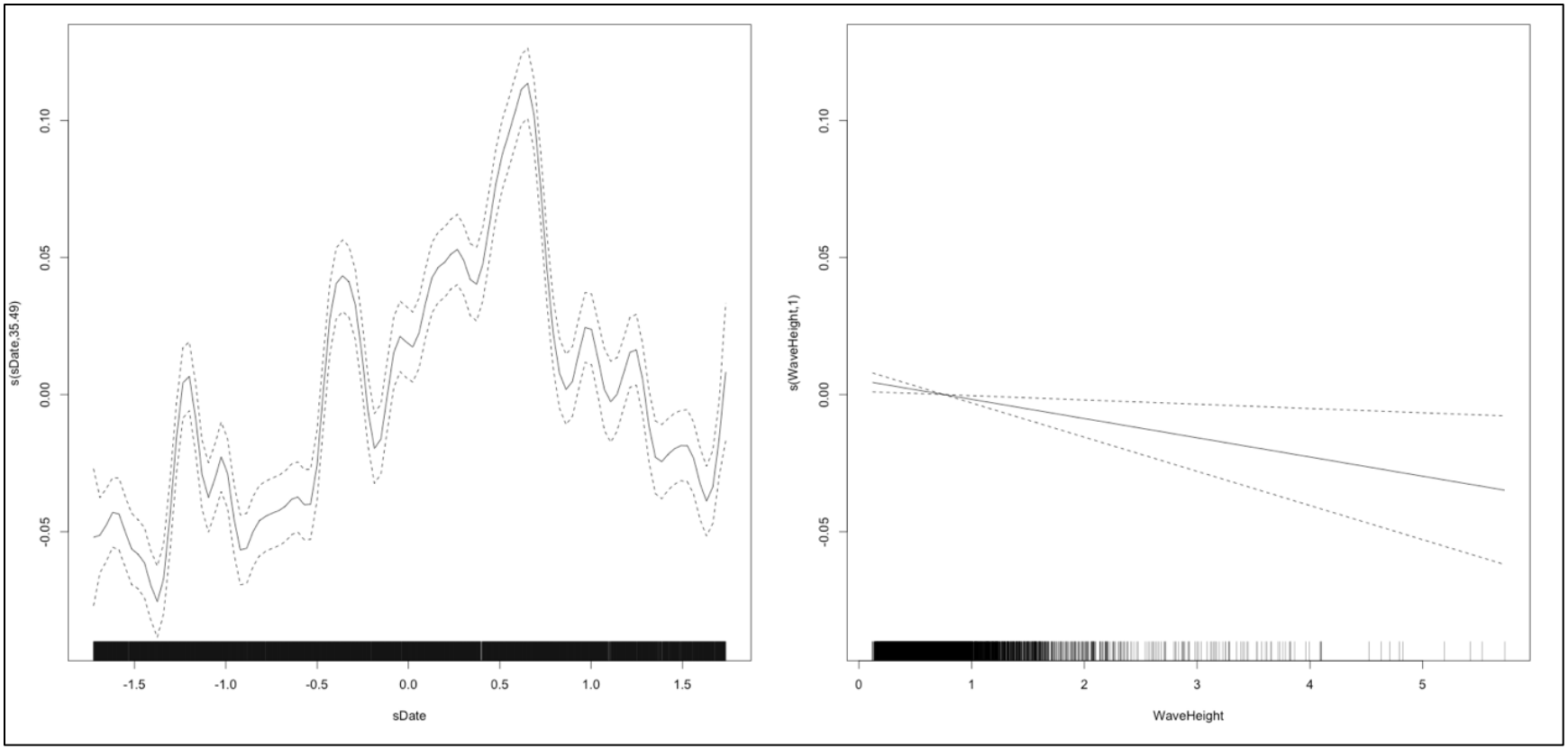

Figure E-49a. SA2 smoothing functions for Measured Vessel Band Noise as a function of Date, Wave Height, Windspeed, and CPA for Receiver 5, Deployment 1

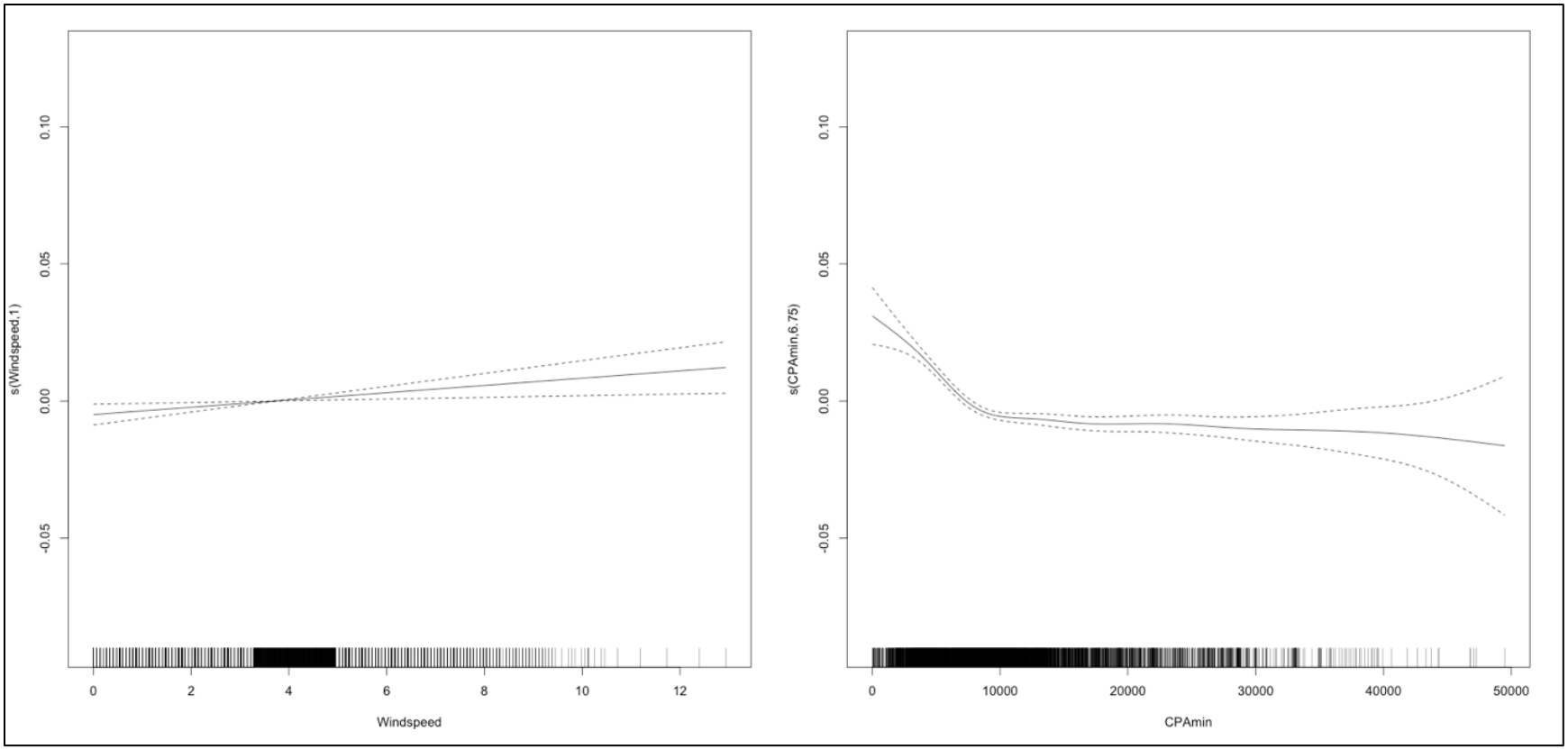

Figure E-49b. SA2 smoothing functions for Measured Vessel Band Noise as a function of Date, Wave Height, Windspeed, and CPA for Receiver 5, Deployment 1

E.3.5.6 Deployment 1, Receiver 6 (Statistical Approach 2)

Both statistical analyses for Receiver 6 showed that scaled date, wind speed, and minimum CPA were all significant predictors (**Table E-27**). The R-square was 0.407. The simplified analysis also found that wave height predicted increased LF noise levels (**Figure E-50**). The shape of the smooth fit to the scaled date, wind speed, wave height, and minimum CPA variables in both analyses were similar, except for minimum CPA. The simplified analysis curve showed increased LF noise as the minimum CPA decreased, but the shape of the curve did not have the notable inflection point seen in all previous sensors.

Table E-27. GAM SA2 output for Deployment 1, Receiver 6

A. Parametric Coefficients	Estimate	Std. Error	t-value	p-value
(Intercept)	4.5861	0.0012	3935.9757	< 0.0001
km2	0.0800	0.0056	14.2991	< 0.0001
km4	0.0313	0.0044	7.0286	< 0.0001
km10	0.0043	0.0016	2.6848	0.0073
B. Smooth Terms	**edf**	**Ref.df**	**F-value**	**p-value**
s(sDate)	40.7142	49.0000	19.2240	< 0.0001
s(WaveHeight)	4.6228	4.6228	2.8579	0.0265
s(Windspeed)	1.0000	1.0000	66.8009	< 0.0001
s(CPAmin)	1.0000	1.0000	37.4071	< 0.0001

Key: CPA= closest point of approach; edf=empirical distribution function; F-value=value on the F distribution calculated by dividing two mean squares; km=kilometer; min=minimum; p-value= level of marginal significance within a statistical hypothesis test, representing the probability of the occurrence of a given event; Ref.df=reference degrees of freedom; s=scaled; Std. Error=Standard Error

E.3.5.7 Deployment 1, Receiver 7 (Statistical Approach 2)

Both analyses resulted in the scaled date, wave height, wind speed, and minimum CPA variables being all significant predictors for Receiver 7 in Deployment 1 (**Table E-28**). The shape of the smooth fits for these variables in both analyses were similar (**Figure E-51**). The adjusted R-square value for the simplified analysis was also higher, 0.552 versus 0.486 resulting from statistical approach 1.

Table E-28. GAM SA2 output for Deployment 1, Receiver 7

A. Parametric Coefficients	Estimate	Std. Error	t-value	p-value
(Intercept)	4.5957	0.0019	2421.2043	< 0.0001
km2	0.0094	0.0049	1.9053	0.0568
km4	0.0059	0.0018	3.1865	0.0015
km10	0.0062	0.0008	7.8988	< 0.0001
B. Smooth Terms	**edf**	**Ref.df**	**F-value**	**p-value**
s(sDate)	1.0091	49.0000	0.3969	< 0.0001
s(WaveHeight)	1.8954	1.8954	4.2832	0.0118
s(Windspeed)	3.9156	3.9156	26.8821	< 0.0001
s(CPAmin)	7.7710	7.7710	51.1244	< 0.0001

Key: CPA= closest point of approach; edf=empirical distribution function; F-value=value on the F distribution calculated by dividing two mean squares; km=kilometer; min=minimum; p-value= level of marginal significance within a statistical hypothesis test, representing the probability of the occurrence of a given event; Ref.df=reference degrees of freedom; s=scaled; Std. Error=Standard Error

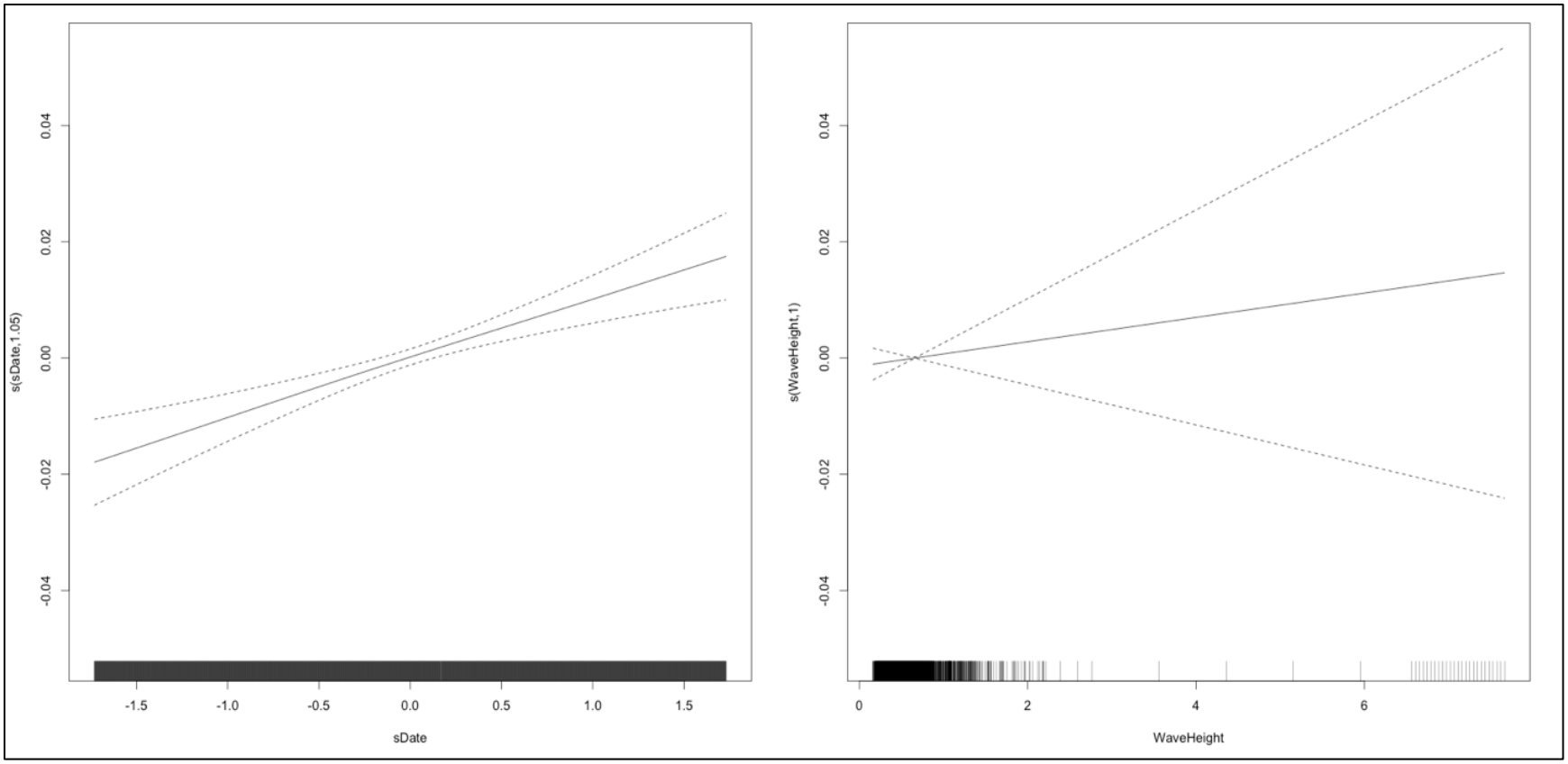

Figure E-50a. SA2 smoothing functions for Measured Vessel Band Noise as a function of Date, Wave Height, Windspeed, and CPA for Receiver 6, Deployment 1

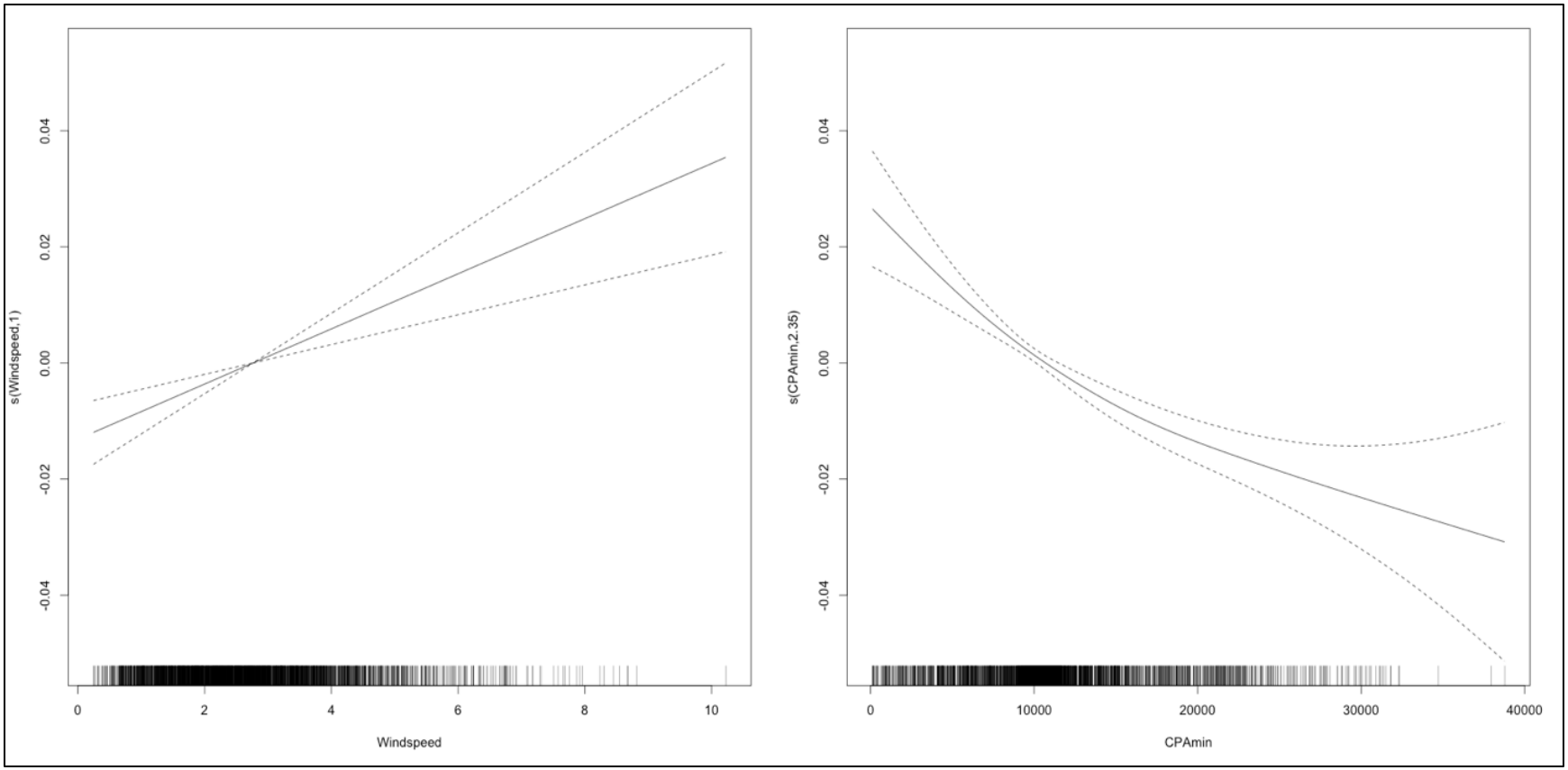

Figure E-50b. SA2 smoothing functions for Measured Vessel Band Noise as a function of Date, Wave Height, Windspeed, and CPA for Receiver 6, Deployment 1

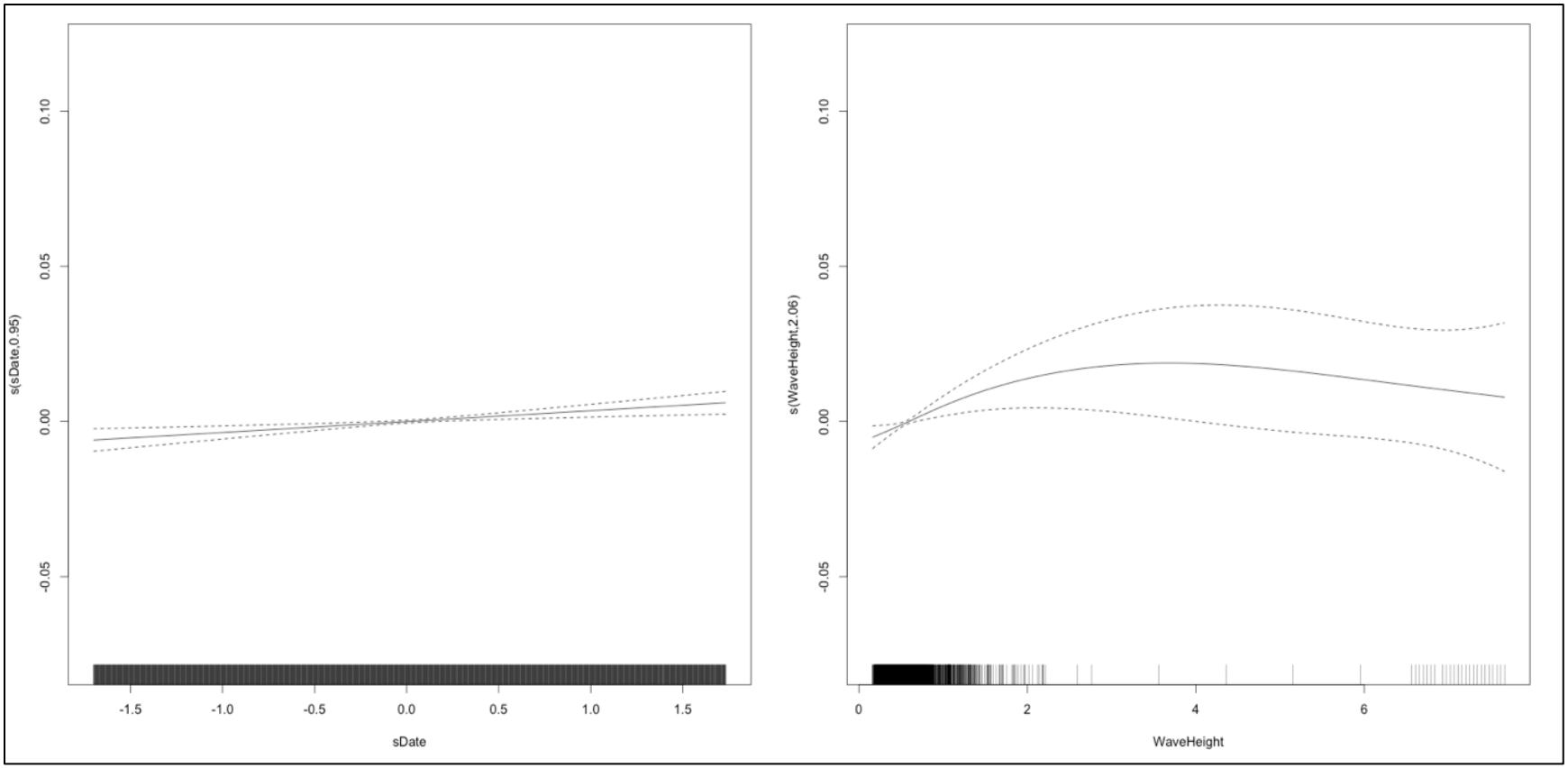

Figure E-51a. SA2 smoothing functions for Measured Vessel Band Noise as a function of Date, Wave Height, Windspeed, and CPA for Receiver 7, Deployment 1

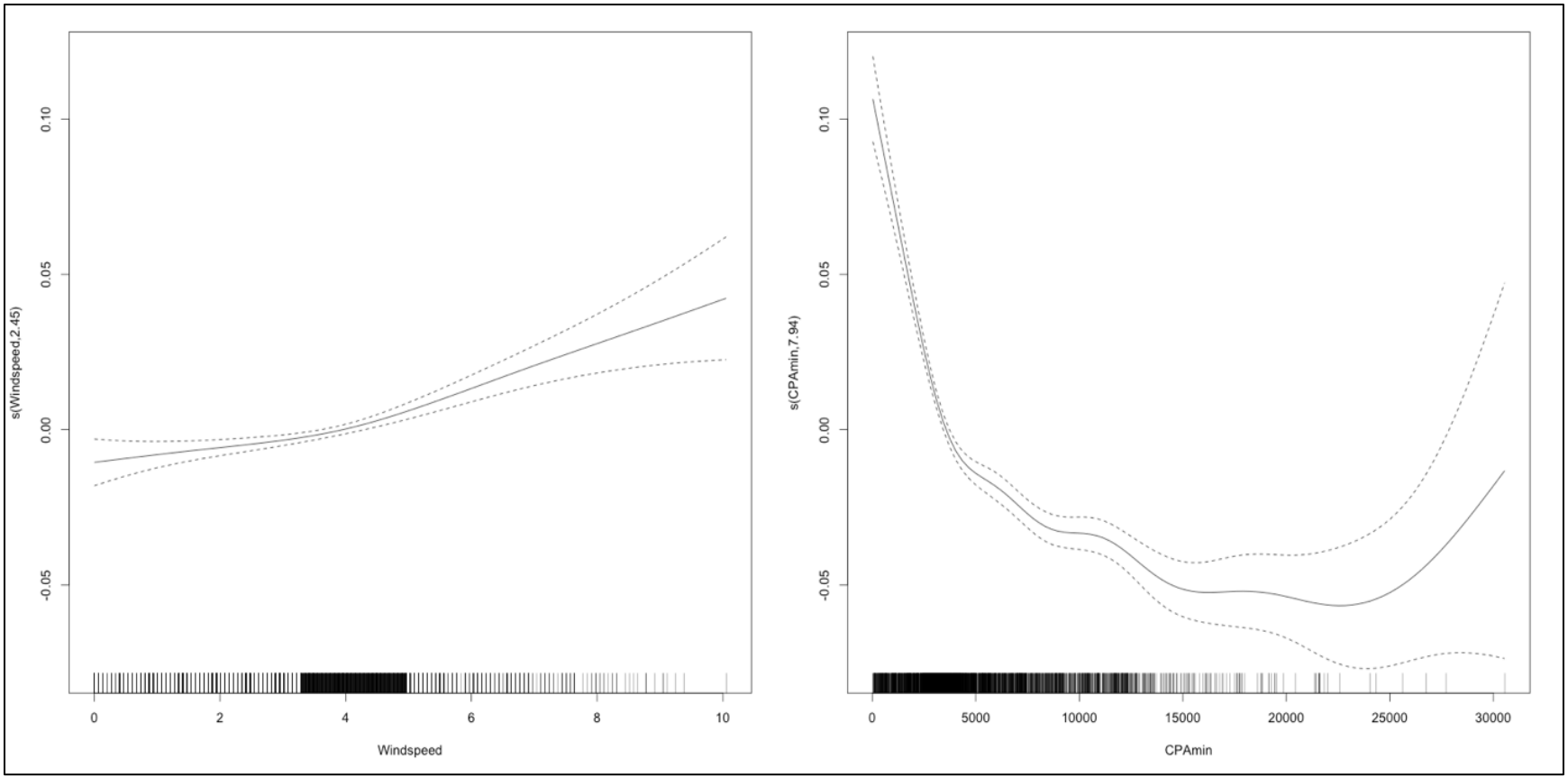

Figure E-51b. SA2 smoothing functions for Measured Vessel Band Noise as a function of Date, Wave Height, Windspeed, and CPA for Receiver 7, Deployment 1

E.3.5.8 Deployment 1, Receiver 8 (Statistical Approach 2)

The result of the original statistical predicted RL analysis for Receiver 8 was that only windspeed and minimum CPA were significant predictors. However, only date and minimum CPA were significant predictors as the result of the simplified statistical analysis (**Table E-29**). The R-square value for the SA2 was 0.633. The shape of the minimum CPA curve fit was similar in both analyses (**Figure E-52**). The relatively small sample size for this Receiver during Deployment 1 may be partially responsible for the uncertainty in predictor variables other than minimum CPA.

Table E-29. GAM SA2 output for Deployment 1, Receiver 8

A. Parametric Coefficients	Estimate	Std. Error	t-value	p-value
(Intercept)	4.5051	0.0015	3010.2755	< 0.0001
km2	0.0286	0.0108	2.6514	0.0081
km4	0.0125	0.0062	2.0138	0.0442
km10	0.0069	0.0025	2.7816	0.0055
B. Smooth Terms	**edf**	**Ref.df**	**F-value**	**p-value**
s(sDate)	40.6895	49.0000	35.9378	< 0.0001
s(WaveHeight)	1.7724	1.7724	1.4944	0.2996
s(Windspeed)	1.0000	1.0000	1.6056	0.2053
s(CPAmin)	6.3320	6.3320	4.5896	0.0001

Key: CPA= closest point of approach; edf=empirical distribution function; F-value=value on the F distribution calculated by dividing two mean squares; km=kilometer; min=minimum; p-value= level of marginal significance within a statistical hypothesis test, representing the probability of the occurrence of a given event; Ref.df=reference degrees of freedom; s=scaled; Std. Error=Standard Error

E.3.5.9 Deployment 1, Receiver 9 (Statistical Approach 2)

The smallest sample size (N=1108) and lowest R-square value compared to all other sensors were the result of the SA2 (**Table E-30**) for Receiver 9. The Receiver 9 R-square value was 0.100 for the original predicted RL analysis, while the SA2 resulted in a R-square value of 0.253. The shapes of the smooth fit curves for all variables were similar from both analyses (**Figure E-53**).

Table E-30. GAM SA2 output for Deployment 1, Receiver 9

A. Parametric Coefficients	Estimate	Std. Error	t-value	p-value
(Intercept)	4.7045	0.0035	1344.1693	< 0.0001
km2	0.0043	0.0043	1.0030	0.3161
km4	0.0033	0.0020	1.6111	0.1074
km10	0.0006	0.0008	0.7182	0.4728
B. Smooth Terms	**edf**	**Ref.df**	**F-value**	**p-value**
s(sDate)	17.8830	49.0000	3.0201	< 0.0001
s(WaveHeight)	4.2038	4.2038	5.2304	0.0003
s(Windspeed)	1.0000	1.0000	5.0738	0.0245
s(CPAmin)	5.7121	5.7121	5.1273	0.0001

Key: CPA= closest point of approach; edf=empirical distribution function; F-value=value on the F distribution calculated by dividing two mean squares; km=kilometer; min=minimum; p-value= level of marginal significance within a statistical hypothesis test, representing the probability of the occurrence of a given event; Ref.df=reference degrees of freedom; s=scaled; Std. Error=Standard Error

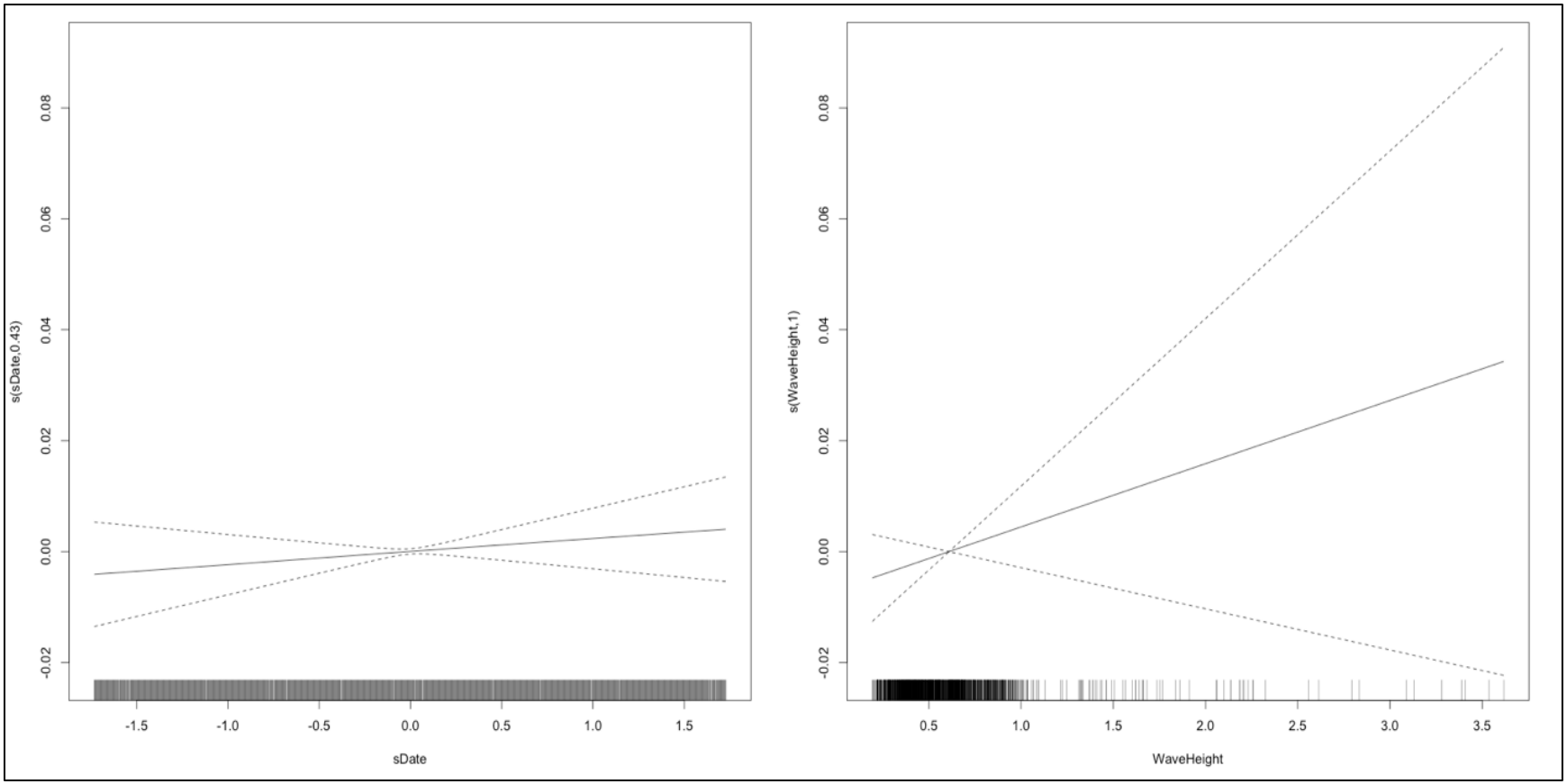

Figure E-52a. SA2 smoothing functions for Measured Vessel Band Noise as a function of Date, Wave Height, Windspeed, and CPA for Receiver 8, Deployment 1

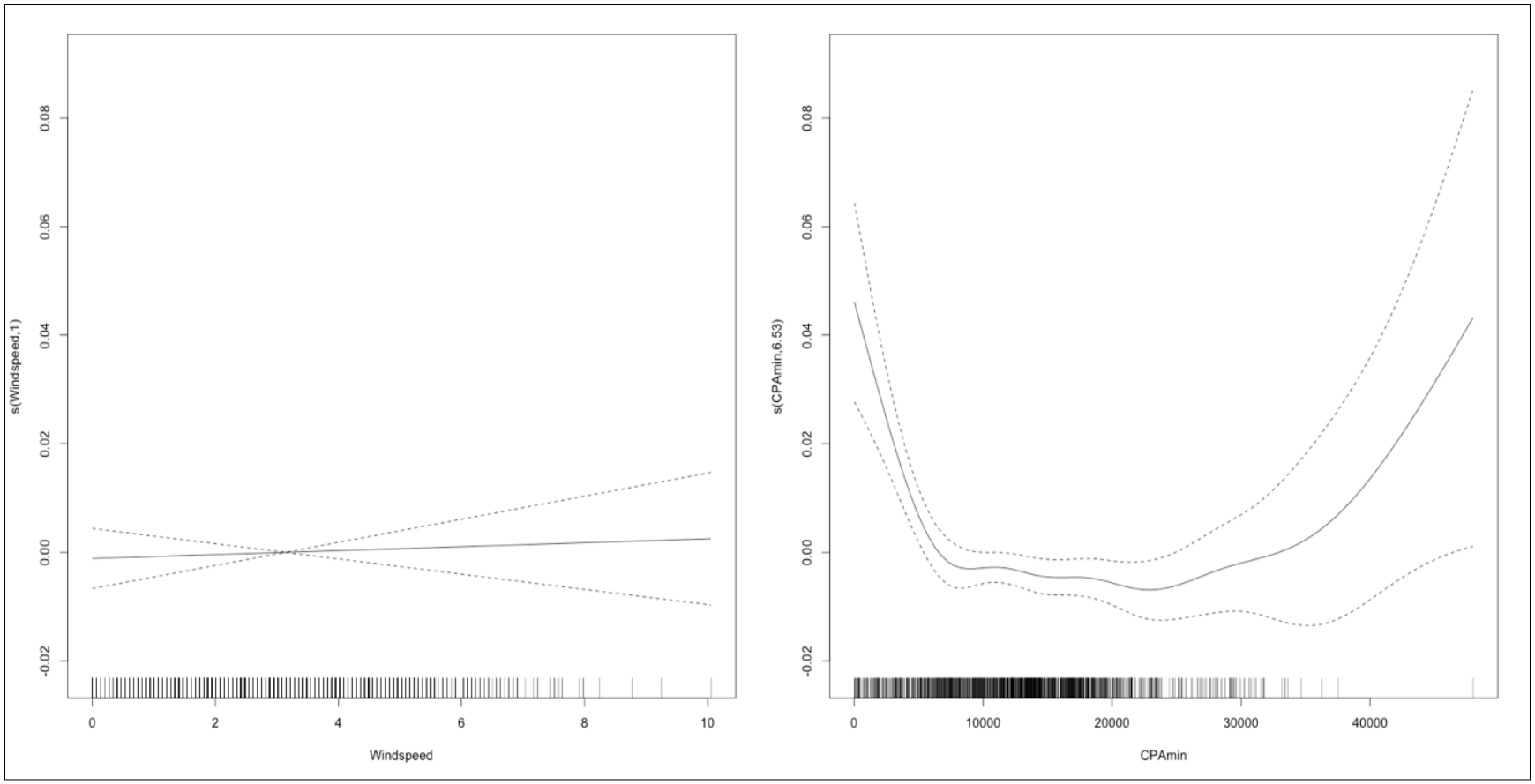

Figure E-52b. SA2 smoothing functions for Measured Vessel Band Noise as a function of Date, Wave Height, Windspeed, and CPA for Receiver 8, Deployment 1

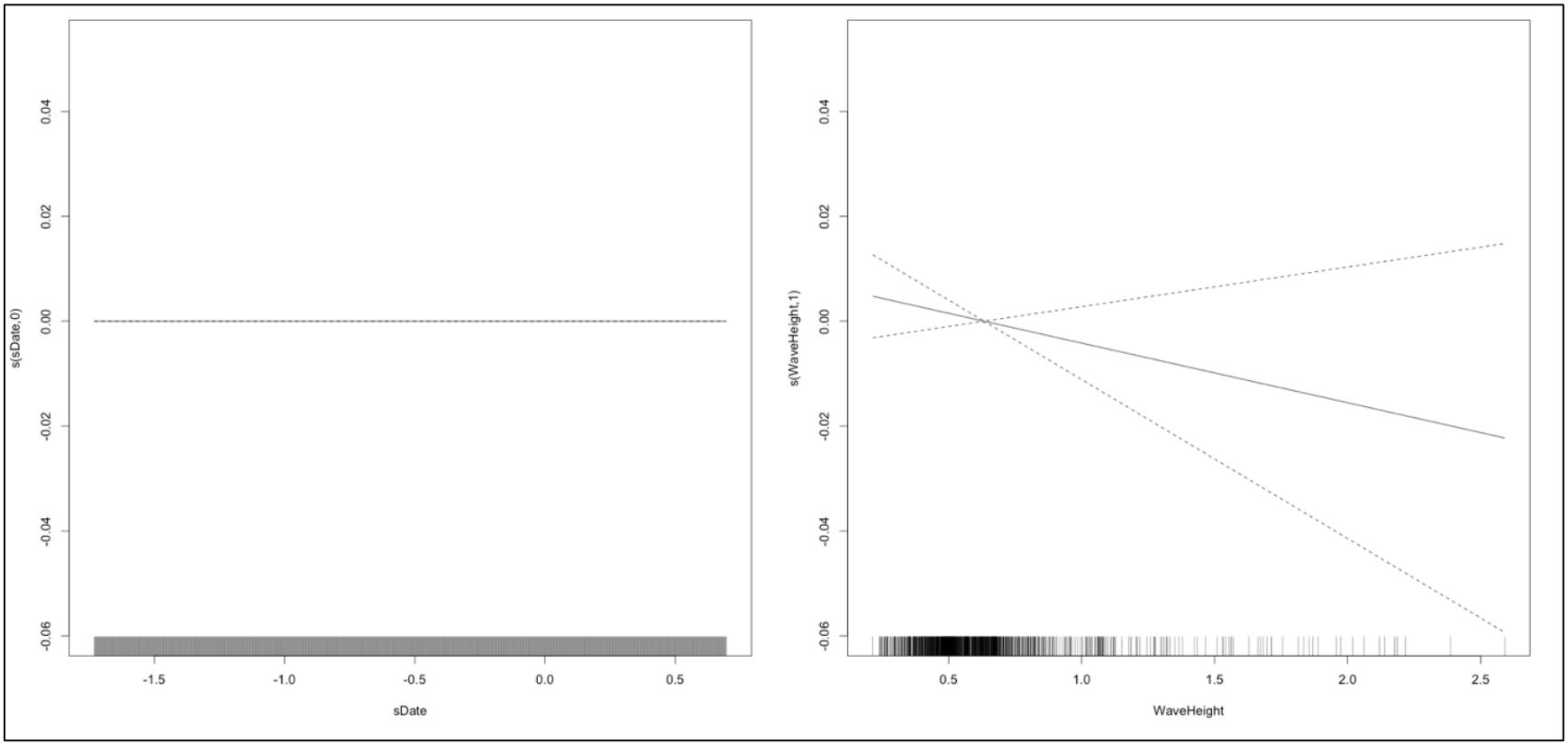

Figure E-53a. SA2 smoothing functions for Measured Vessel Band Noise as a function of Date, Wave Height, Windspeed, and CPA for Receiver 9, Deployment 1

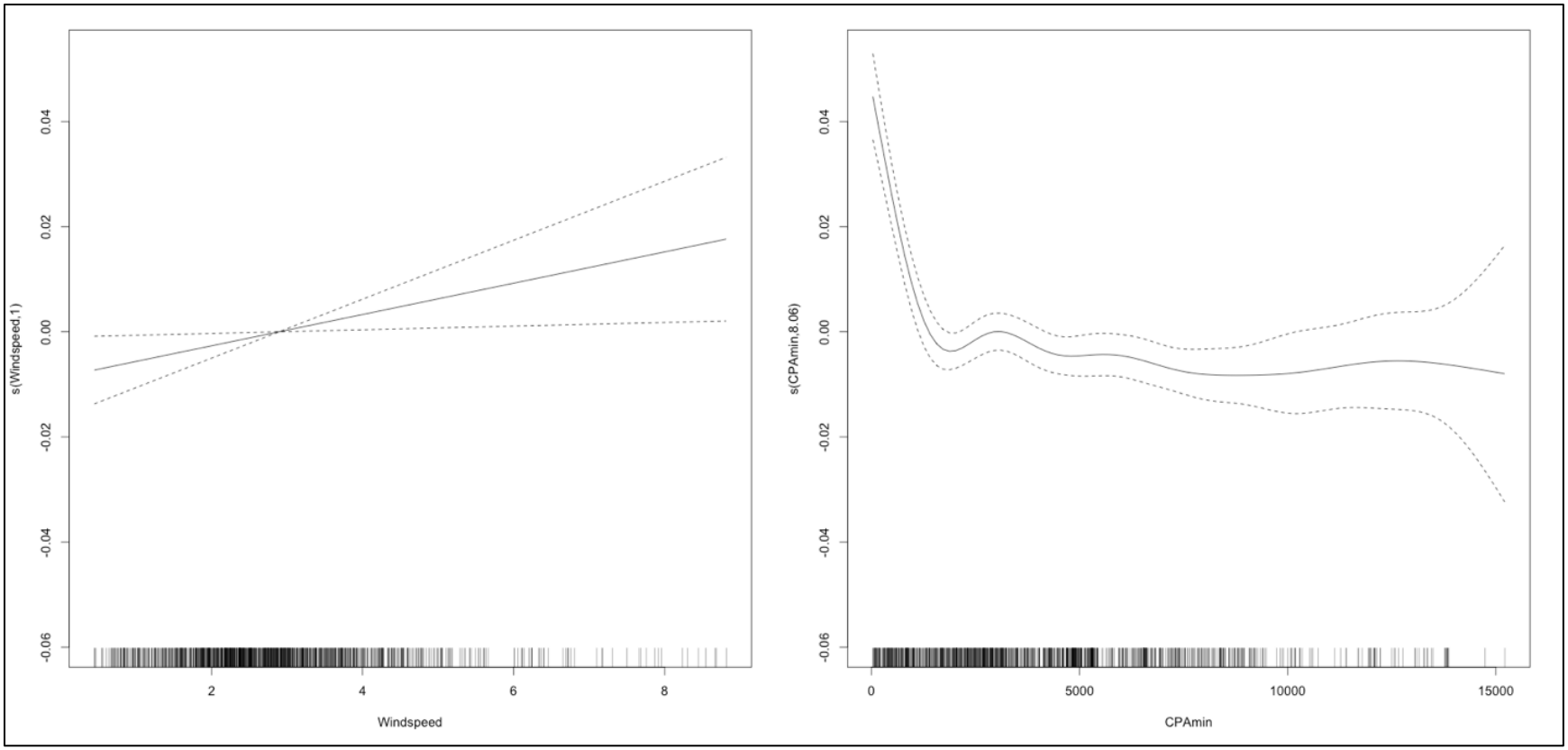

Figure E-53b. SA2 smoothing functions for Measured Vessel Band Noise as a function of Date, Wave Height, Windspeed, and CPA for Receiver 9, Deployment 1

E.3.5.10 Deployment 1, Receiver 10 (Statistical Approach 2)

Both statistical analyses for Receiver 10, Deployment 1 resulted in significant predictors of scaled date, wave height, windspeed, and minimum CPA (**Table E-31**). The shapes of the smoothed fitted curves were similar in both analyses (**Figure E-54**). The R-squared value was somewhat higher in the simplified analysis versus the original statistical analysis (0.492 versus 0.421).

Table E-31. GAM SA2 output for Deployment 1, Receiver 10

A. Parametric Coefficients	Estimate	Std. Error	t-value	p-value
(Intercept)	4.5200	0.0020	2280.8793	< 0.0001
km2	0.0182	0.0039	4.7058	< 0.0001
km4	0.0150	0.0017	8.9266	< 0.0001
km10	0.0045	0.0007	6.5022	< 0.0001
B. Smooth Terms	**edf**	**Ref.df**	**F-value**	**p-value**
s(sDate)	43.4332	49.0000	38.4445	< 0.0001
s(WaveHeight)	8.0524	8.0524	14.7354	< 0.0001
s(Windspeed)	5.7822	5.7822	8.2390	< 0.0001
s(CPAmin)	8.2372	8.2372	33.4353	< 0.0001

Key: CPA= closest point of approach; edf=empirical distribution function; F-value=value on the F distribution calculated by dividing two mean squares; km=kilometer; min=minimum; p-value= level of marginal significance within a statistical hypothesis test, representing the probability of the occurrence of a given event; Ref.df=reference degrees of freedom; s=scaled; Std. Error=Standard Error

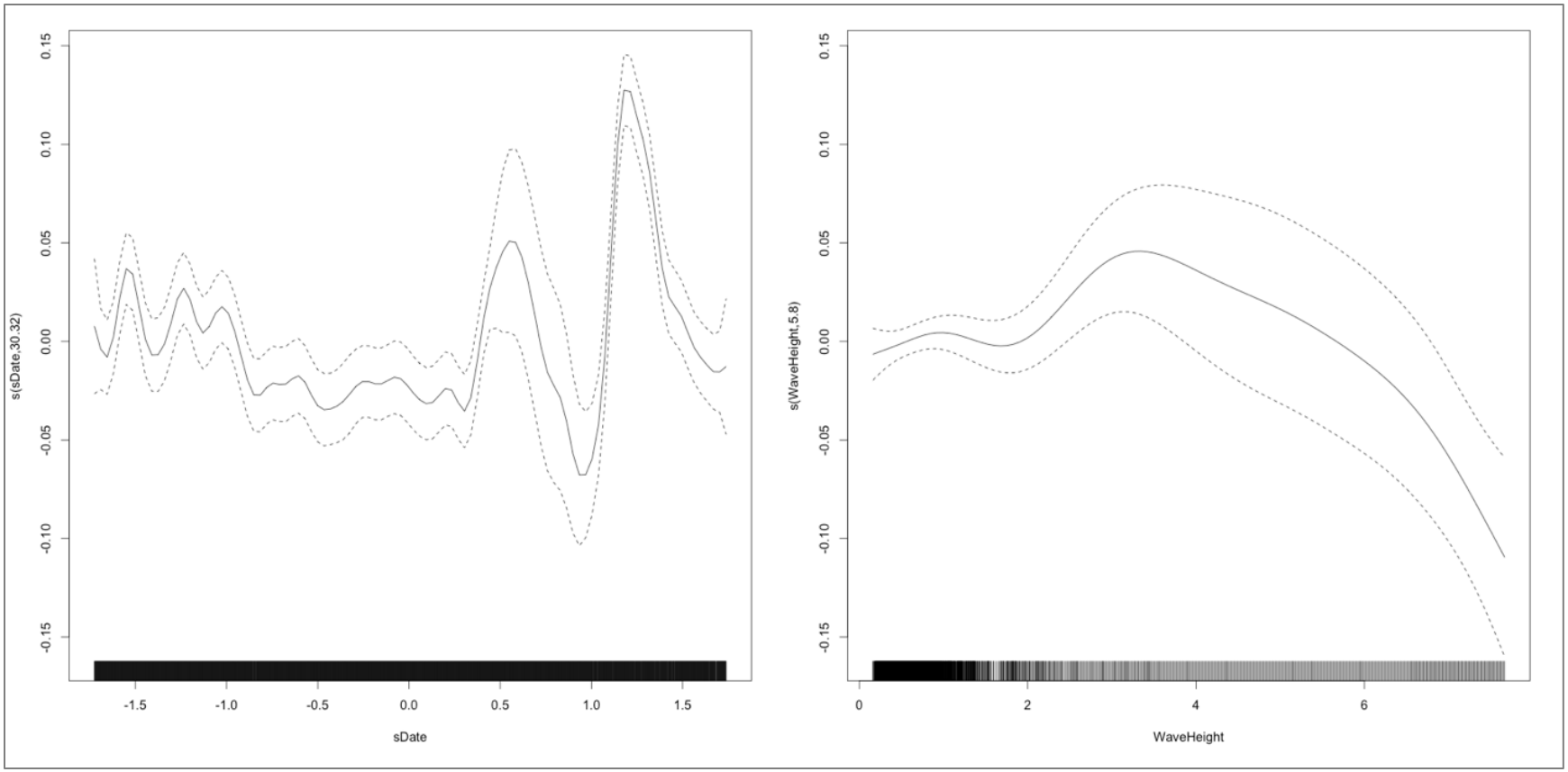

Figure E-54a. SA2 smoothing functions for Measured Vessel Band Noise as a function of Date, Wave Height, Windspeed, and CPA for Receiver 10, Deployment 1

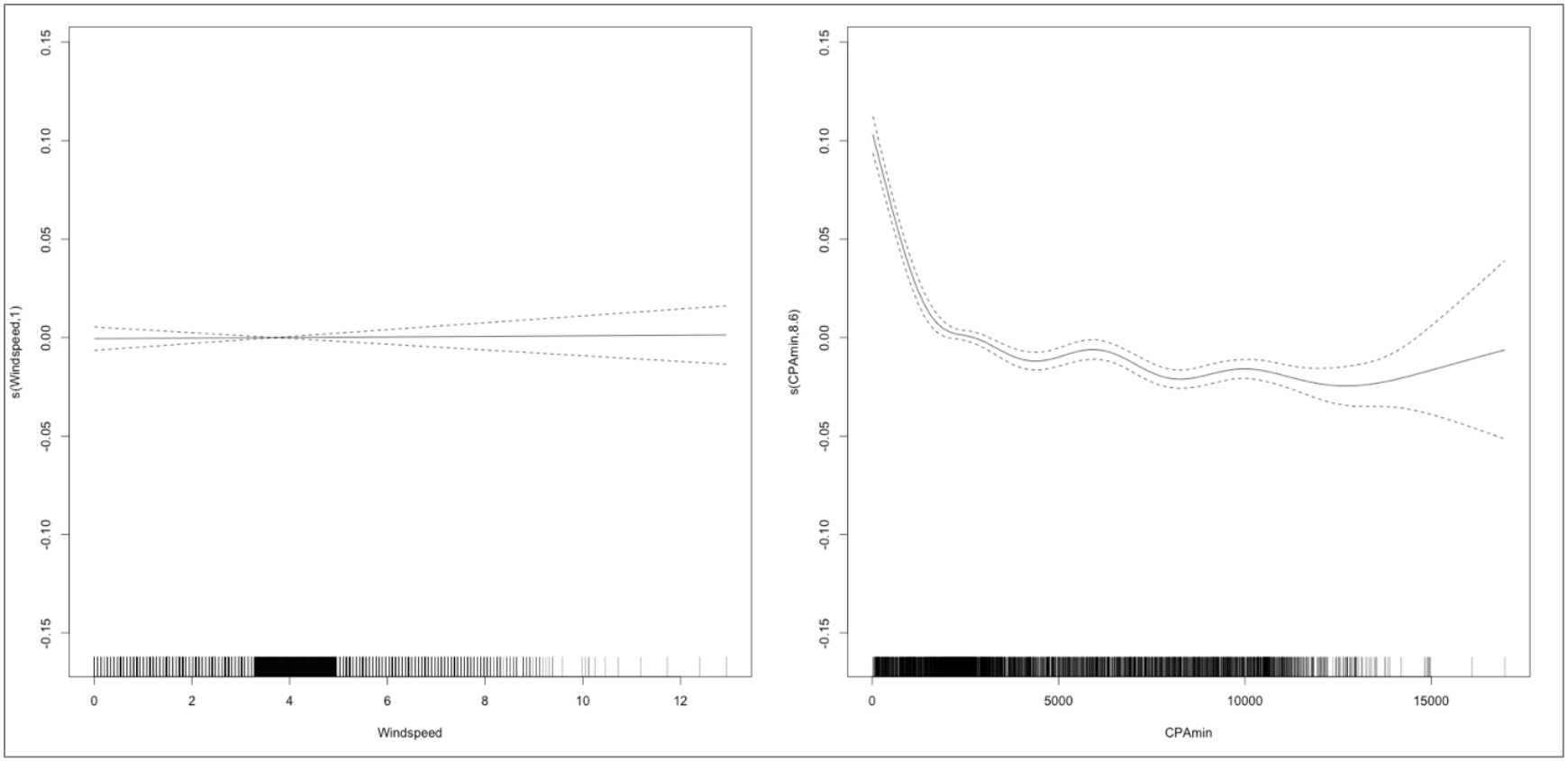

Figure E-54b. SA2 smoothing functions for Measured Vessel Band Noise as a function of Date, Wave Height, Windspeed, and CPA for Receiver 10, Deployment 1

E.4.6 Summary of Statistical Modeling of Vessel Received Levels

The individual analyses of the 10 receivers produced several common patterns. First the R-squared for most of the analyses was quite high, exceeding 0.5 in some cases. This indicates that a goodly amount, if not most, of the variance in the measured RL could be explained by the statistical models. One of the most common patterns in the data was a strong relationship between CPA distance and measured LF sound level. In almost all analyses, this relationship was very similar, with a near linear increase in RL as vessels approached within 10 km. This relationship was much stronger than any of the predicted RL values. Based on this finding, it is recommended that future efforts to predict LF noise in the GOM should rely directly upon AIS data as predictor variables. In most of the receivers, there was also the expected positive relationship between windspeed and wave height with increased measured LF noise.

E.4.7 Temporal/Spatial Trends of Recorder Data

The monthly spectral levels of the 10 RH and EARS recorders were assessed to determine whether any spatial or temporal trends were evident in the data. The monthly median spectral levels of the 10 RH and EARS recorders over the duration of the Program are presented in **Appendix E-C**. In each monthly figure, the top spectrum represents the entire frequency range, while the bottom panel presents the LF band (10 to 1,000 Hz) in more detail. These figures illustrate the temporal variability at each recorder sensor. In all **Appendix E-C** figures, there is an apparent difference in the data recorded by the RH and EARS recorders.

E.4.8 Extrapolation Capability of Acoustic Data: Glider/Fixed Sensor Comparison

This analysis was intended to answer the question: How far can data from a single buoy be extrapolated? To answer this question acoustic data from the 2018 MP Deployment 1 Seaglider flight as it approached, nearly flew over, and then departed from one of the stationary recorders (EARS buoy at Site 2) were compared. The Seaglider approached within 1,500 m of the EARS buoy at this site (**Table E-1**) during Deployment 1 (**Figure E-55**).

In evaluating the spectrograms of the 24 hours of data before and after the CPA of the OSU glider to the Site 2 EARS recorder, the expectation was that the acoustic characteristics of the collected data would be similar at CPA but would diverge as the range between the recorders increased (**Figure E-56**). However, the spectrograms from the Seaglider and Site 2 EARS data show minimal similarity at any point. Furthermore, the monthly spectra (**Appendix E-B, Figures E-B1 to E-B6**) show that in some months, the spectral profiles for individual recorders in deep water are almost identical. However, in other months, the spectral differences can exceed 20 dB. This indicates that the glider-static receiver comparison is not generalizable to the full range and temporal scale of the project. Instead, a statistical analysis of RL as a function of latitude, longitude, and water depth would be a more promising avenue to pursue, similar to the analysis results in **Section E.3.4** of this report.

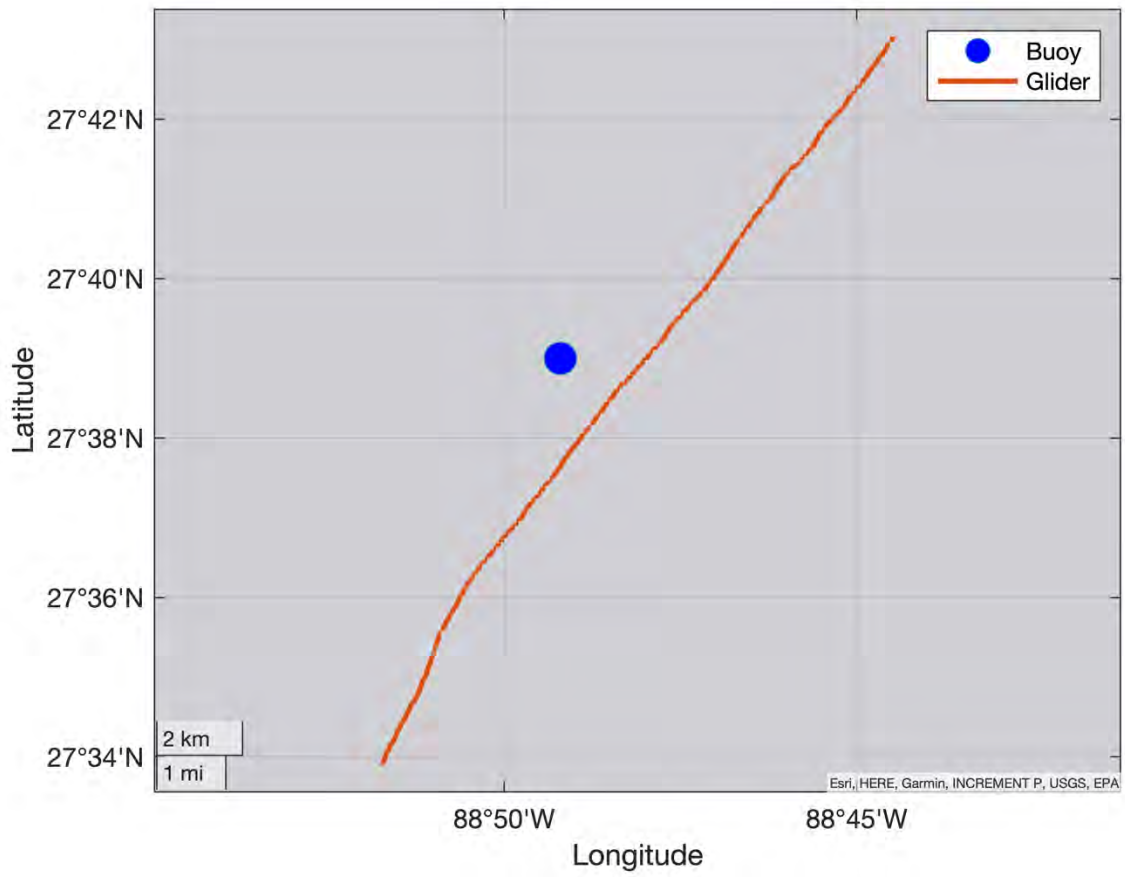

Figure E-55. Path of the 2018 MP Seaglider past the Site 2 EARS recorder during Deployment 1

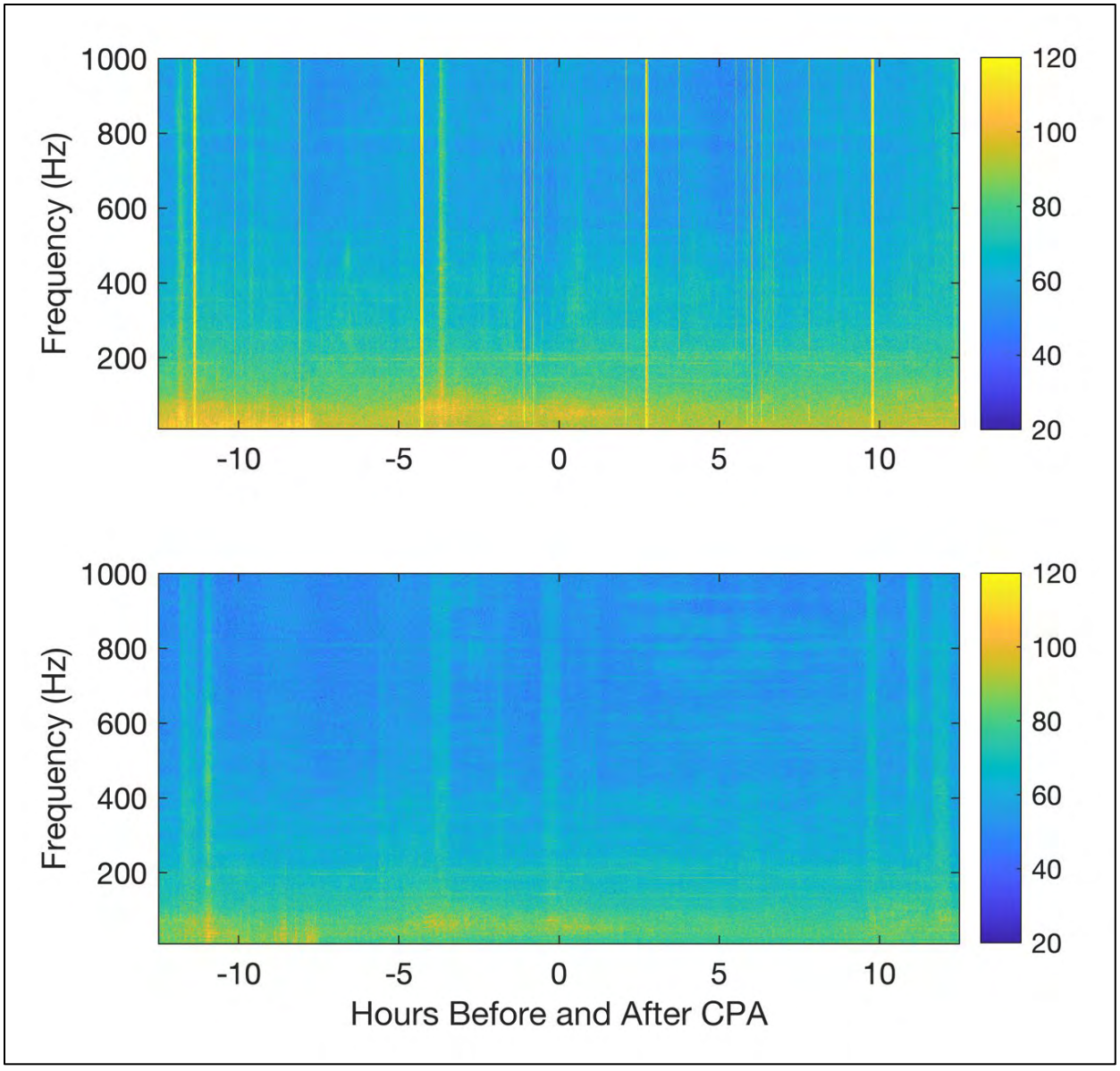

Figure E-56. Comparison of spectrograms from the 2018 MP Seaglider (top panel) and the Site 2 EARS recorder (bottom panel) for the 12 hours before and after the CPA (color bar units are dB re 1µPa^2)

706

E.5 Discussion

The marine environment of the northern GOM is highly industrialized with anthropogenic sound sources such as shipping, oil and gas activities, military operations, and scientific research contributing to the GOM's ambient soundscape. Noise impacts to protected marine species (e.g., marine mammals) may occur in association with oil and gas exploration and development activities, which include seismic surveys, platform decommissioning, drilling, construction, and the resulting increases in vessel traffic. The purpose of the GOM PAM Program was to establish a baseline of the ambient soundscape in the northern GOM and characterize one of the dominant noise inputs from vessel traffic.

A substantial portion of the work in this Program has been in the development of new analysis tools that are based on the spectral analysis output provided by the Cornell Conservation Bioacoustics program (CCB). These tools are available for continued analysis of additional data as well as providing a springboard for derivative analytical procedures.

E.5.1 Anthropogenic Detection

Daily detections of vessel activity, reported for close passbys to the receivers (i.e., close enough to create a Lloyd mirror interference pattern), varied from below 10 percent to near constant or daily occurrences. There was a strong seasonal pattern, with most vessel detections occurring in summer months (May to June). The annual pattern indicated an increase in vessel traffic from 2018 to 2019 and a subsequent decrease in 2020. However, the sampling within the first and last year only covered a portion of the years 2018 and 2020. Monitoring in 2018 began in late May, and most recording was completed by May 2020. Therefore, these partial years may have missed a portion of the peak in vessel traffic. Another possibility is that the decline in vessel numbers in 2020 may reflect reduced vessel traffic due to the corona virus disease (COVID)-19 pandemic.

The effects of latitude and longitude on the distribution of vessel detections were both statistically significant, but the patterns were not particularly informative. Vessel detection rates increased with both water depth and latitude. However, the magnitudes of these effects were not equivalent (**Table E-7; Figure E-14**). Water depth appears to be the stronger predictor, and this may reflect better acoustic propagation in deeper waters, or all these effects could reflect the prominent shipping routes into the Port of New Orleans.

Airgun occurrence had similar strong annual and monthly patterns. Latitude and longitude predictors were both borderline significant, and water depth had no significant effect. This likely reflects the greater distance over which airgun operations could be detected. The same temporal pattern of airgun activity was seen on many of the recorders.

E.5.2 Biological Detection

More than 20 species of marine mammals occur in the waters of the northern GOM, with species of dolphins, including the bottlenose dolphin, predominantly populating continental shelf waters, and deeper diving species such as beaked whales and the sperm whale inhabiting offshore waters (Fulling et al. 2003). One baleen whale, the newly named Rice's whale (formerly GOM Bryde's whale), is a year-round resident of northeastern GOM waters, with a very small population (50 to 100 whales) that is listed as endangered under the ESA (Hayes et al. 2021; SMM 2021).

To differentiate some of the most common sound-producing marine mammals in the northern GOM that may contribute to the ambient soundscape, frequency bands for the known vocalizations of five marine mammal species or species groups (Rice's whale, beaked whales, and dolphins) were identified. The

recorded acoustic data were assessed to determine which characteristics informed the spatial and temporal patterns of these marine mammal species or groups.

The frequency overlap between the signals of Rice's whales and the prevalent anthropogenic noise environment made reliably detecting the calls of Rice's whales difficult using only the spectrally analyzed data. A better approach would be to use a matched-filter detection process that operates on the waveform data.

The detection rate results from the "dolphin" and "beaked whale" frequency bands had similar temporal patterns. Detection rates increased from May to September and began to decline in October. November rates were lower still, but the data from November 2018 were sparse, as some recorders stopped recording early due to internal faults in the recorders, severed moorings, trawled recorders, and data compression issues (Klinck et al. 2019; Sidorovskaia and Bhattarai 2019). All these issues were addressed in subsequent deployments.

The effect of water depth on detection rates had opposite effects for these two bands. In the dolphin band, peaks were seen in both shallow and deep waters, while the values from approximately 400 to 700 m were lower. This pattern is perhaps most easily explained by multiple species being detected. The peak of beaked whale band detections appeared to occur at intermediate water depths of 500 to 1,000 m and then declined in the very shallow and very deep depths. This may indicate a habitat preference for slope environments.

Latitude also had opposite effects between the two detection band results. For the dolphin band, the detection rates were lowest in the southernmost waters and increased over the more northerly recorders. For beaked whale band detections, the rates were highest in the south and decreased to the north. Finally, longitude also had opposite trends for these two bands. The highest dolphin band detection rates were found in the central longitudes, while the highest beaked whale band detection rates were found to the far west and east of the Program area.

E.5.3 Statistical Analysis of Measured Vessel Noise Levels

The statistical analysis of Received Vessel Band noise focused on predicting the actual RL at the receivers. This involved 1) measurement of distance from each vessel to the receiver, 2) estimation of the SL of the vessel, and 3) prediction of the TL between the two. Modeled vessel noise level was most often a good predictor of measured levels. However, on occasion these functions curiously showed a negative relationship with measured noise levels. Such an occurrence may be due to overprediction of noise levels at this location.

However, the analyses shown in **Section E.3.4** show that the most important vessel predictor for measured sound level was CPA. This variable is relatively easy and quick to calculate. Future analyses should consider focusing on the AIS metrics and omit the time-consuming three-dimensional propagation modeling. Furthermore, if propagation predictions are needed, then three-dimensional modeling should be conducted along with a comparison of simpler propagation models.

E.6 Recommendations

The analysis effort completed required compilation and understanding of numerous different datasets collected by multiple institutions. The quality and duration of the data allowed for different types of analyses that yielded valuable insight into the soundscape of the Program study area. Lessons learned from this analysis effort resulted in the following recommendations for future efforts:

1. Approximately 250 terabytes of raw data were collected during the Program by six different types of recorders, each one of which stored raw data in a different format. Using six differently

formatted, very large raw datasets for Phase 2 analyses would therefore have been extremely time consuming and involve an inordinate amount of manual labor. In consultation with BOEM, it was therefore decided to pre-process the raw data prior to using it as an input for Phase 2 analyses. In future Program phases, if time and resource constraints are not a significant issue, then it is recommended that advanced data analyses be conducted using raw data as this would allow for use of standard analytical tools and outputs (instead of instead of development and application of custom analysis tools).

2. Also, for future analysis, if pre-processed data are used, it is recommended that hybrid millidecade data representations (Martin et al. 2021) be considered. This is because use of one second, one Hz resolution data, while appealing, result in very large data files, which are difficult to exchange, manipulate, and analyze.
3. It is recommended that future efforts that involve detection and classification of signals begin with actual waveforms. Without waveform data it is much more difficult to correctly assign sources to received signals and to ground-truth automated detection efforts.
4. Based on the results of the statistical analysis, it is recommended that future analyses of vessel noise levels should consider focusing on the AIS metrics and omit the time-consuming three-dimensional propagation modeling. If propagation predictions are needed, then 3D modeling should be conducted along with a comparison of simpler propagation models to determine if simpler models can be used instead to save time.
5. Also based on the statistical analysis results, it is recommended that future efforts to predict LF noise in the GOM should rely directly upon AIS data as predictor variables.
6. The cause of the differences in LF data reported by EARS and RH should be investigated further.
7. A better approach for detecting the frequency bands of the Rice's whale would be to use a matched-filter detection process that operates on the waveform data.

E.7 Acknowledgements

Dr. Stacy DeRuiter of Calvin College provided invaluable assistance with the statistical analysis, notably the treatment of the autocorrelation in the data.

E.8 Literature Cited

(GOM PAM interim deliverables highlighted in bold font)

Ainslie MA, de Jong CAF, Martin B, Miksis-Olds JL, Warren JD, Heaney KD. 2017. Project Dictionary (Terminology Standard). DRAFT. Technical report by TNO for ADEON Prime Contract No. M16PC00003. Available from https://adeon.unh.edu/standards (last accessed March 29, 2018).

Baron SC, Martinez A, Garrison LP, and Keith EO. 2008. Differences in acoustic signals from Delphinids in the western North Atlantic and northern Gulf of Mexico. Marine Mammal Science 24, 4256.

Carnes MR. 2009. Description and Evaluation of GDEM-V 3.0. Naval Research Laboratory, p. 24.

Clark CW, Gagnon GC, Stevenson D, Frankel AS, and Vigness-Raposa K. (in prep.). Demonstration of Ocean Basin Scale Passive Acoustic Tracking of Marine Mammals and Response to Anthropogenic Noise Sources.

Crocker SE, Fratantonio FD. 2016. Characteristics of Sounds Emitted During High-Resolution Marine Geophysical Surveys.

[ESR] Earth and Space Research. 2009. ESR. 2009. OSCAR third degree resolution ocean surface currents. Ver. 1.

Erbe C, Dunlop R, Jenner KCS, Jenner MNM, McCauley RD, Parnum I, Parsons M, Rogers T, Salgado-Kent C. 2017. Review of Underwater and In-Air Sounds Emitted by Australian and Antarctic Marine Mammals. Acoustics Australia.

Estabrook BJ, Ponirakis DW, Clark CW, and Rice AN. 2016. Widespread spatial and temporal extent of anthropogenic noise across the northeastern Gulf of Mexico shelf ecosystem. Endangered Species Research 30, 267–282.

Frankel AS, Amaral JL, Ellison WT. 2017. NOAA Shipping Noise Mapping Pilot Project Final Report. Marine Acoustics, Inc., TN-17-017. pp.

Frankel AS, Zeddies D, Simard P, Mann D. 2014. Whistle source levels of free-ranging bottlenose dolphins and Atlantic spotted dolphins in the Gulf of Mexico. The Journal of the Acoustical Society of America 135, 1624–1631.

Fulling GL, Mullin KD, Hubard CW. 2003. Abundance and distribution of cetaceans in outer continental shelf waters of the U.S. Gulf of Mexico. Fishery Bulletin, 101, 923–932.

Hayes SA, Josephson E, Maze-Foley K, Rosel PE, Turek J. (Eds.). 2021. US Atlantic and Gulf of Mexico marine mammal stock assessments 2020 (NOAA Technical Memorandum NMFS-NE-271). Woods Hole, MA: Northeast Fisheries Science Center, National Marine Fisheries Service. 403 pages.

Hildebrand JA. 2009. Anthropogenic and natural sources of ambient noise in the ocean. Marine Ecology Progress Series 395, 5–20.

Interdisciplinary Oceanography Group. 2017. UCSB Ocean Surface Currents Mapping Project – Real Time Data.

Klinck H, Ponirakis DW, Dugan PJ, and Rice AN. 2019. Assessment of ocean ambient sound levels in the northern Gulf of Mexico, May - October 2018. Preliminary Report. Prepared for the Bureau of Ocean Energy Management (BOEM), United States Department of the Interior under Contract No. M17PC00001, Task Order M17PD00011, issued to HDR Inc., Vienna, VA, USA. Prepared by Cornell University, Ithaca, NY, USA. January 2019.

Klinck H, Ponirakis DW, Dugan PJ, Rice AN. 2020. Assessment of ocean ambient sound levels in the northern GOM, May 2019 – June 2020. Preliminary report. Washington DC: Bureau of Ocean Energy Management (BOEM). Contract No. M17PC00001, Task Order 140M0119F0001.

Latusek-Nabholz JN, Whitt AD, Fertl D, Gallien DR, Ampela K, Khan AA, Sidorovskaia N. 2020. Literature synthesis on passive acoustic monitoring projects and sound sources in the GOM. Washington DC: Bureau of Ocean Energy Management (BOEM). 104 p. OCS Study BOEM 2020-009. Contract No. M17PC00001.

Lin YT. 2021. Three-dimensional propagation of seismic airgun signals in the Mississippi Canyon area of the Gulf of Mexico. JASA Express Letters 1.

Lin YT. 2019. GOM PAM 2018 program monitoring project SHRU report. Washington DC: Bureau of Ocean Energy Management (BOEM). Contract No. M17PC00001, Task Order M17PD00011.

Lin YT. 2021. GOM PAM program 2019 monitoring project SHRU report. Washington DC: Bureau of Ocean Energy Management (BOEM). Contract No. M17PC00001, Task Order No. 140M0119F0001.

MarineCadestre.gov. No Date. Vessel Traffic Data.

Martin SB, Gaudet BJ, Klinck H, Dugan PJ, Miksis-Olds JL, Mellinger DK, Mann DA, Boebel O, Wilson CC, Ponirakis DW, and Moors-Murphy H. 2021. Hybrid millidecade spectra: A practical format for exchange of long-term ambient sound data. JASA Express Letters 1.

McKenna MF, Wiggins SM, Hildebrand JA. 2013. Relationship between container ship underwater noise levels and ship design, operational and oceanographic conditions. Scientific Reports 3, 1–10.

McPherson C, Martin B, MacDonnell J, Whitt C. 2016. Examining the value of the Acoustic Variability Index in the characterisation of Australian marine soundscapes. in Proceedings of ACOUSTICS 2016 (Brisbane, Australia).

Mellinger DK, Fregosi S. Assessment of ocean ambient sound levels in the northern GOM, May - June 2018. Final Report. Washington DC: Bureau of Ocean Energy Management (BOEM). Contract No. M17PC00001, Task Order M17PD00011.

[NOAA] National Oceanic and Atmospheric Administration. 2016. Tides and Currents Model.

Rice AN, Palmer KJ, Tielens JT, Muirhead CA, and Clark CW. 2014. Potential Bryde's whale (*Balaenoptera edeni*) calls recorded in the northern Gulf of Mexico. The Journal of the Acoustical Society of America 135, 3066–3076.

Ross D. 1976. *Mechanics of Underwater Noise* (Pergamon, New York).

Schock SG. 2004. A Method for Estimating the Physical and Acoustic Properties of the Sea Bed Using Chirp Sonar Data. IEEE Journal of Oceanic Engineering 29.

Sidorovskaia N, Bhattarai K. 2019a. Assessment of ocean ambient sound levels in the northern GOM, May - October 2018: autonomous Environmental Acoustic Recording System (EARS) buoys. Preliminary data processing report. Washington DC: Bureau of Ocean Energy Management (BOEM). Contract No. M17PC00001, Task Order M17PD00011.

Sidorovskaia N, Bhattarai K. 2019b. Assessment of ocean ambient sound levels in the northern GOM, October 2018 – April 2019: autonomous Environmental Acoustic Recording System (EARS) buoys. Preliminary data processing report. Washington DC: Bureau of Ocean Energy Management (BOEM). Contract No. M17PC00001, Task Order M17PD00011.

Sidorovskaia N, Bhattarai K. 2020. Assessment of ocean ambient sound levels in the northern GOM, April - November 2019: autonomous Environmental Acoustic Recording System (EARS) buoys. Preliminary data processing report. Washington DC: Bureau of Ocean Energy Management (BOEM). Contract No. M17PC00001, Task Order 140M0119F0001.

Sidorovskaia N, Griffin S. 2020. Assessment of ocean ambient sound levels in the northern GOM, November 2019-June 2020: autonomous Environmental Acoustic Recording System (EARS) buoys. Preliminary data processing report. Washington DC: Bureau of Ocean Energy Management (BOEM). Contract No. M17PC00001, Task Order 140M0119F0001.

Sidorovskaia NA, Li K. 2016. Decadal evolution of the northern Gulf of Mexico soundscapes. Proceedings of Meetings on Acoustics 27, 040014.

Simard, YR, Nathalie & Gervaise, Cédric & Giard, Samuel. 2016. Analysis and modeling of 255 source levels of merchant ships from an acoustic observatory along St. Lawrence Seaway. The Journal of the Acoustical Society of America. 140. 2002-2018. 10.1121/1.4962557.

[SMM] Society for Marine Mammalogy. 2021. List of marine mammal species and subspecies. Committee on Taxonomy, Society for Marine Mammalogy. https://marinemammalscience.org/science-and-publications/list-marine-mammal-species-subspecies/ (accessed November 2021).

Staaterman E, Paris CB, DeFerrari HA, Mann DA, Rice AN, and D'Alessandro EK. 2014. Celestial patterns in marine soundscapes. Marine Ecology Progress Series 508, 17–32.

Tetreault BJ. 2005. Use of the Automatic Identification System (AIS) for Maritime Domain Awareness (MDA). IEEE Oceans 2005 2, 1590-1594.

Thode A, Mellinger DK, Stienessen S, Martinez A, Mullin K. 2002. Depth-dependent acoustic features of diving sperm whales (*Physeter macrocephalus*) in the Gulf of Mexico. The Journal of the Acoustical Society of America 112, 308–321.

Veirs S, Veirs V, Wood JD. 2016. Ship noise extends to frequencies used for echolocation by endangered killer whales. PeeerJ 4:e1657.

Wiggins SM, Hall JM, Thayre BJ, Hildebrand JA. 2016. Gulf of Mexico low-frequency ocean soundscape impacted by airguns. The Journal of the Acoustical Society of America 140, 176–183.

Appendix E-A: Spatial and Temporal Patterns of the Detection of Vessels and Airguns

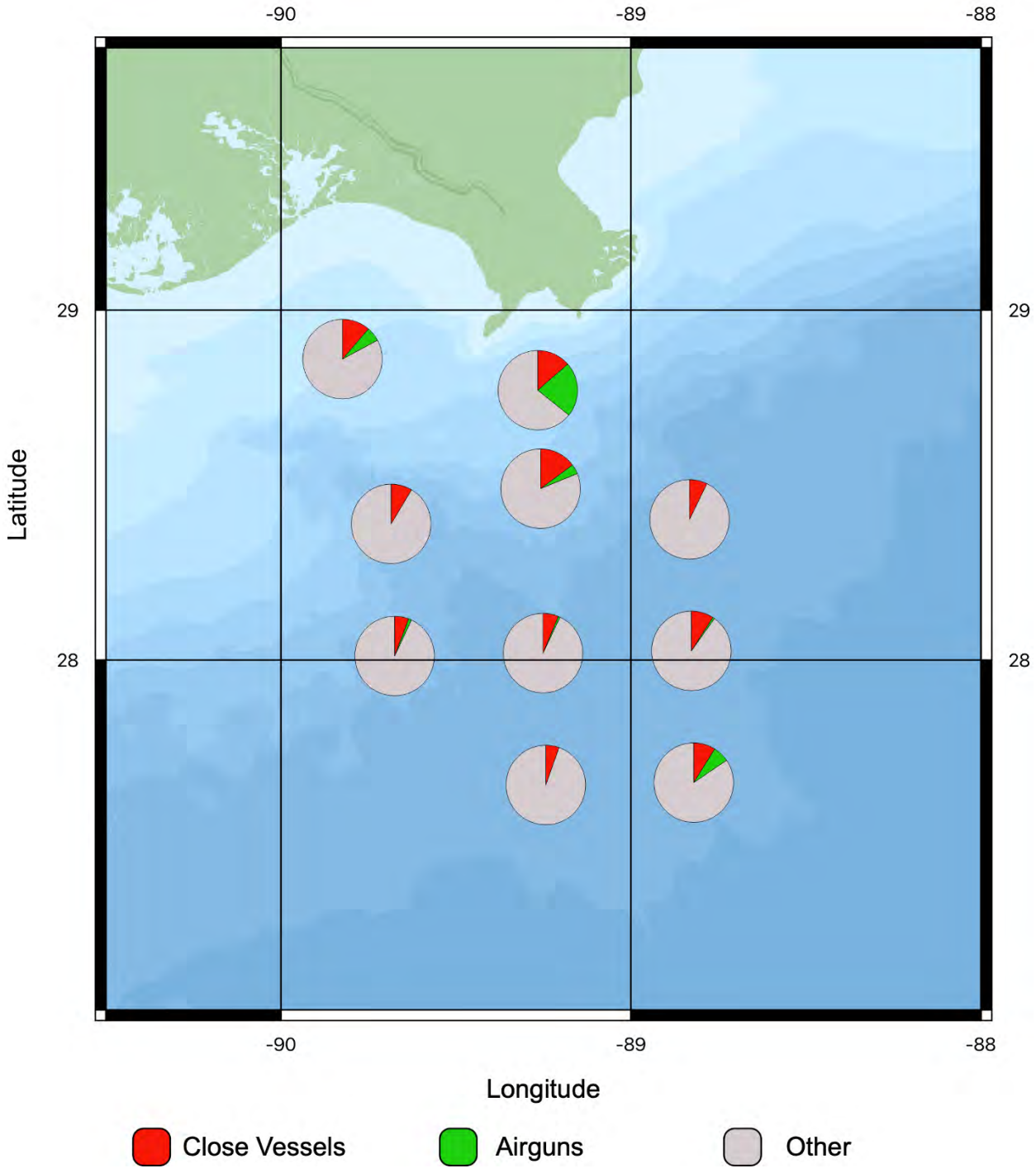

Figure E-A1. Vessel and airgun detections for May 2018

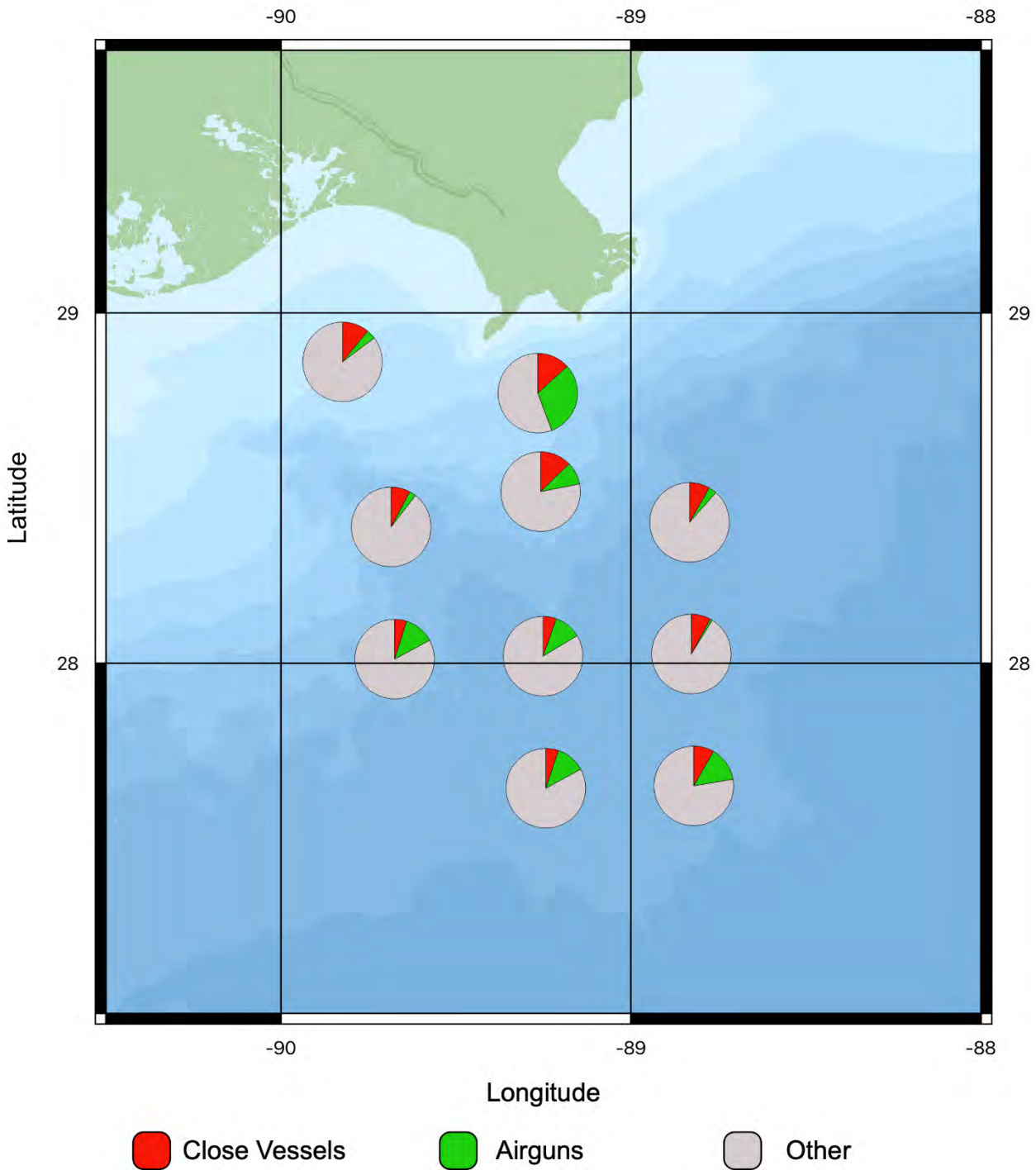

Figure E-A2. Vessel and airgun detections for June 2018

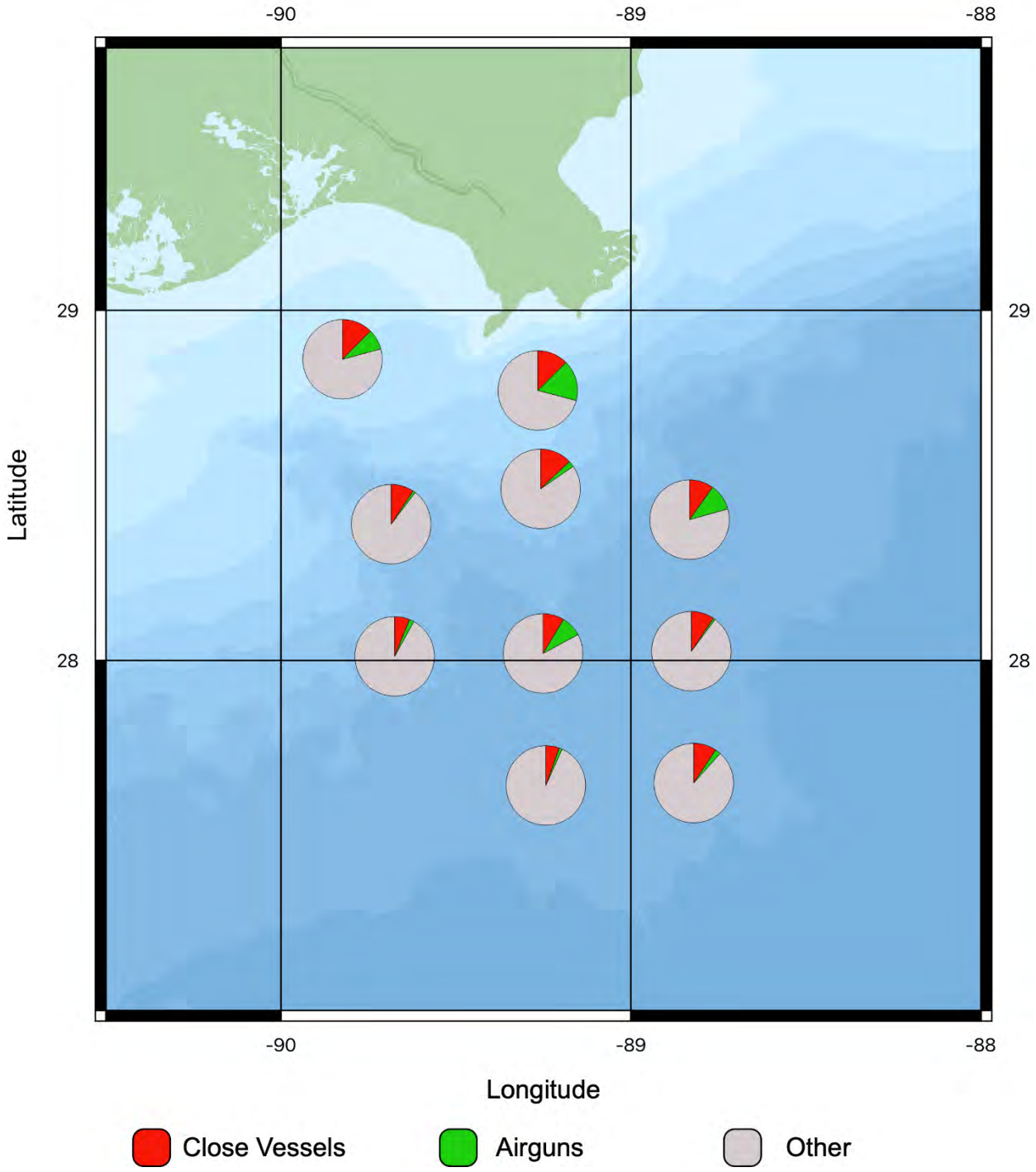

Figure E-A3. Vessel and airgun detections for July 2018

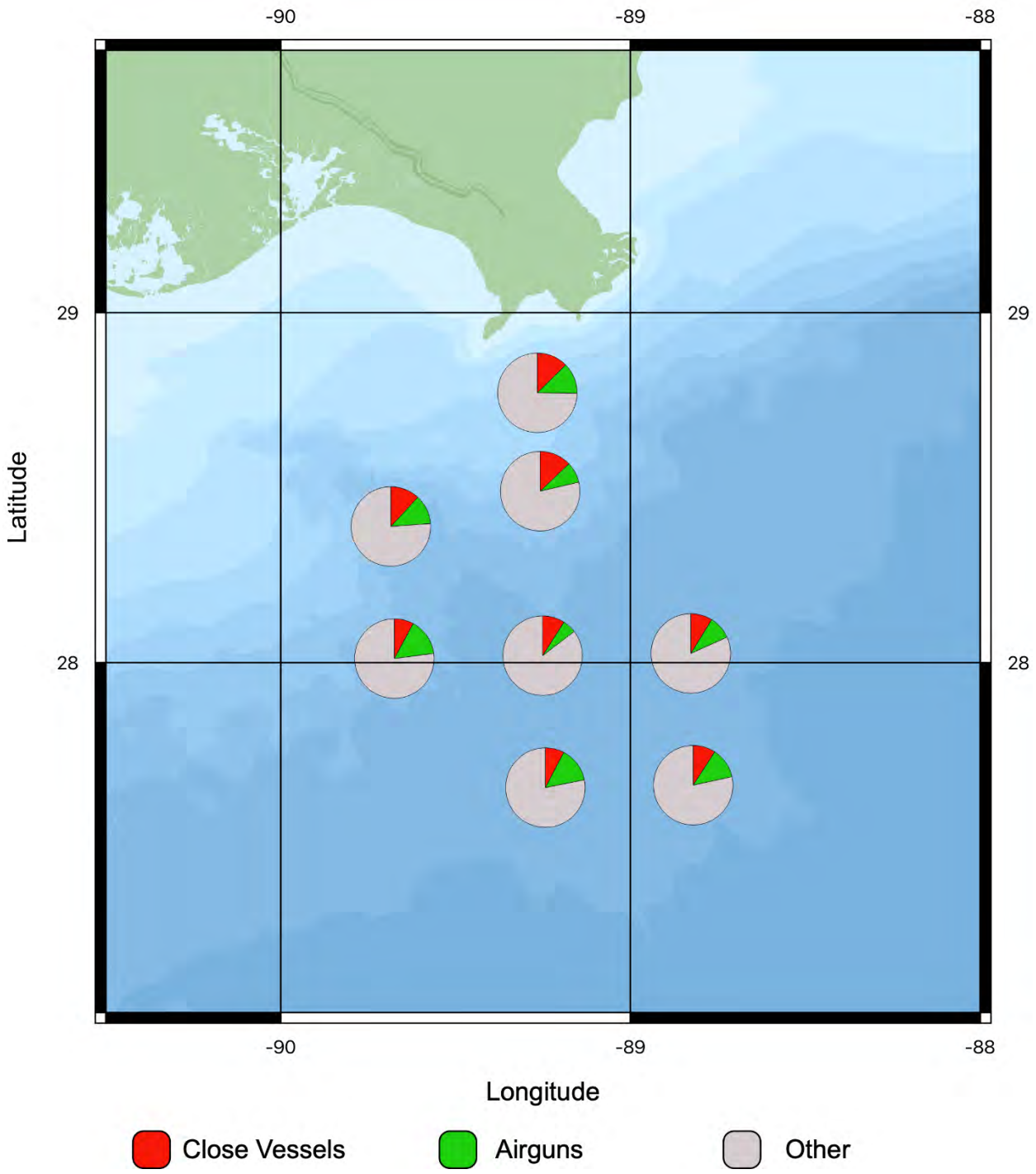

Figure E-A4. Vessel and airgun detections for August 2018

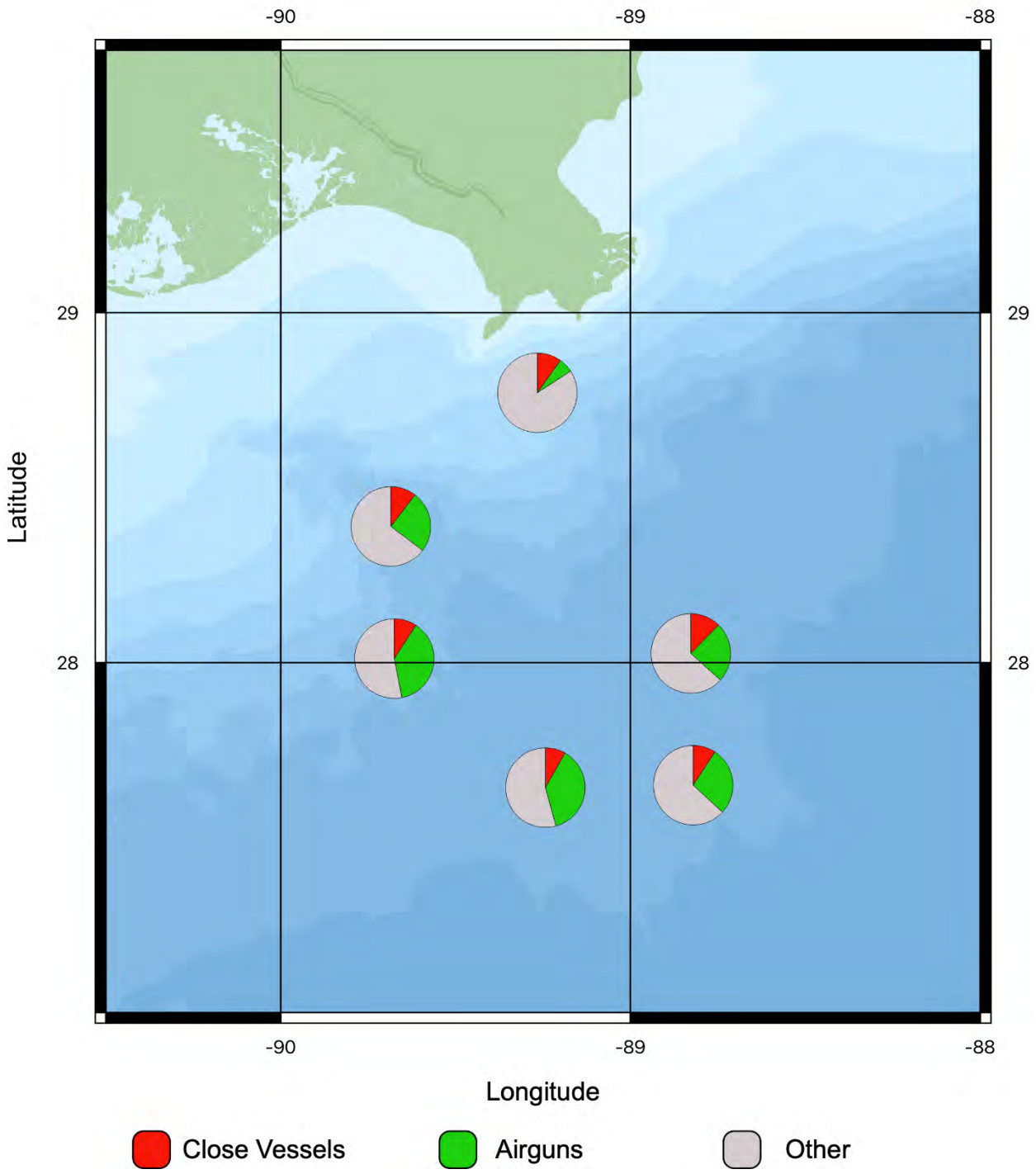

Figure E-A5. Vessel and airgun detections for September 2018

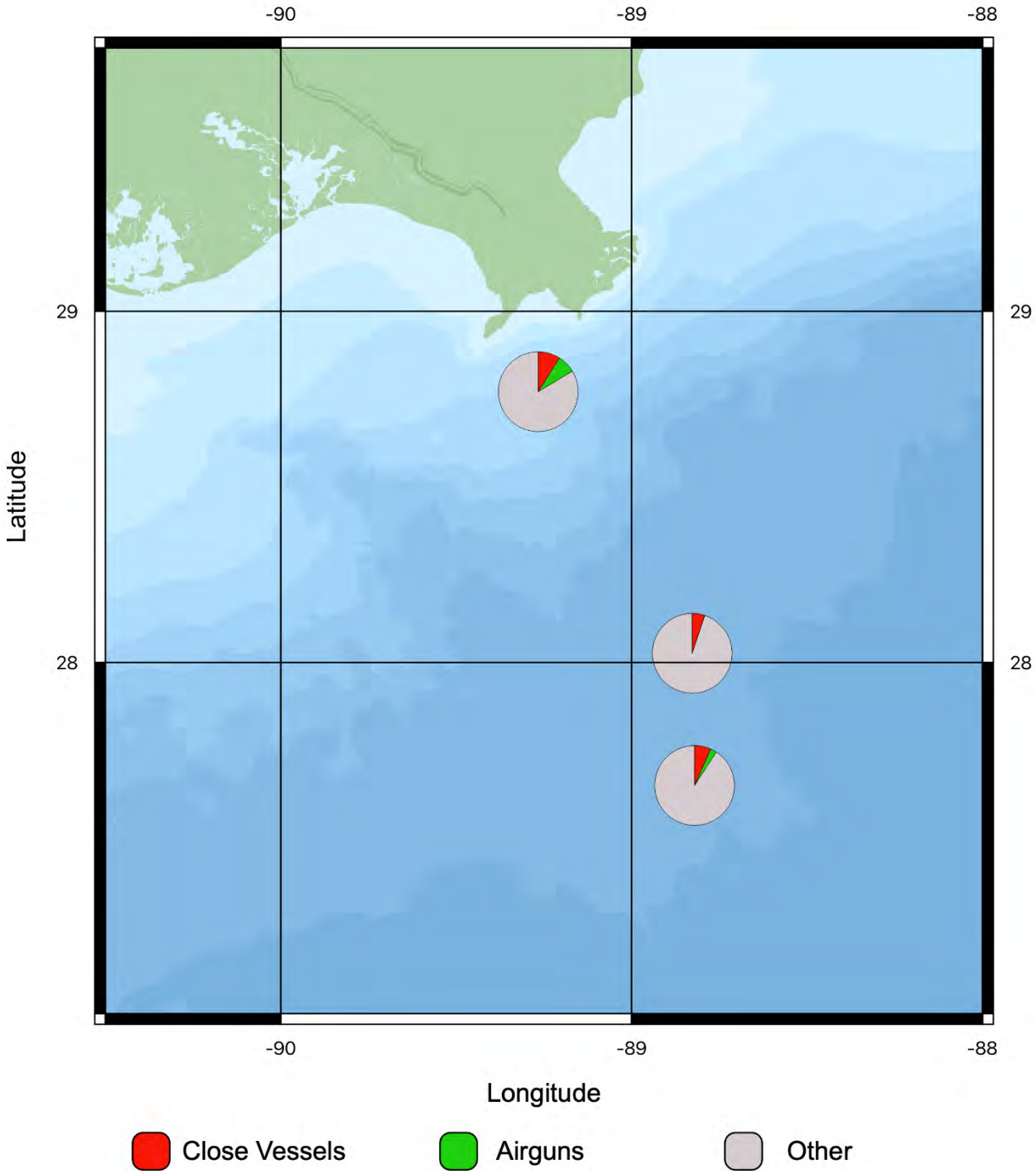

Figure E-A6. Vessel and airgun detections for October 2018

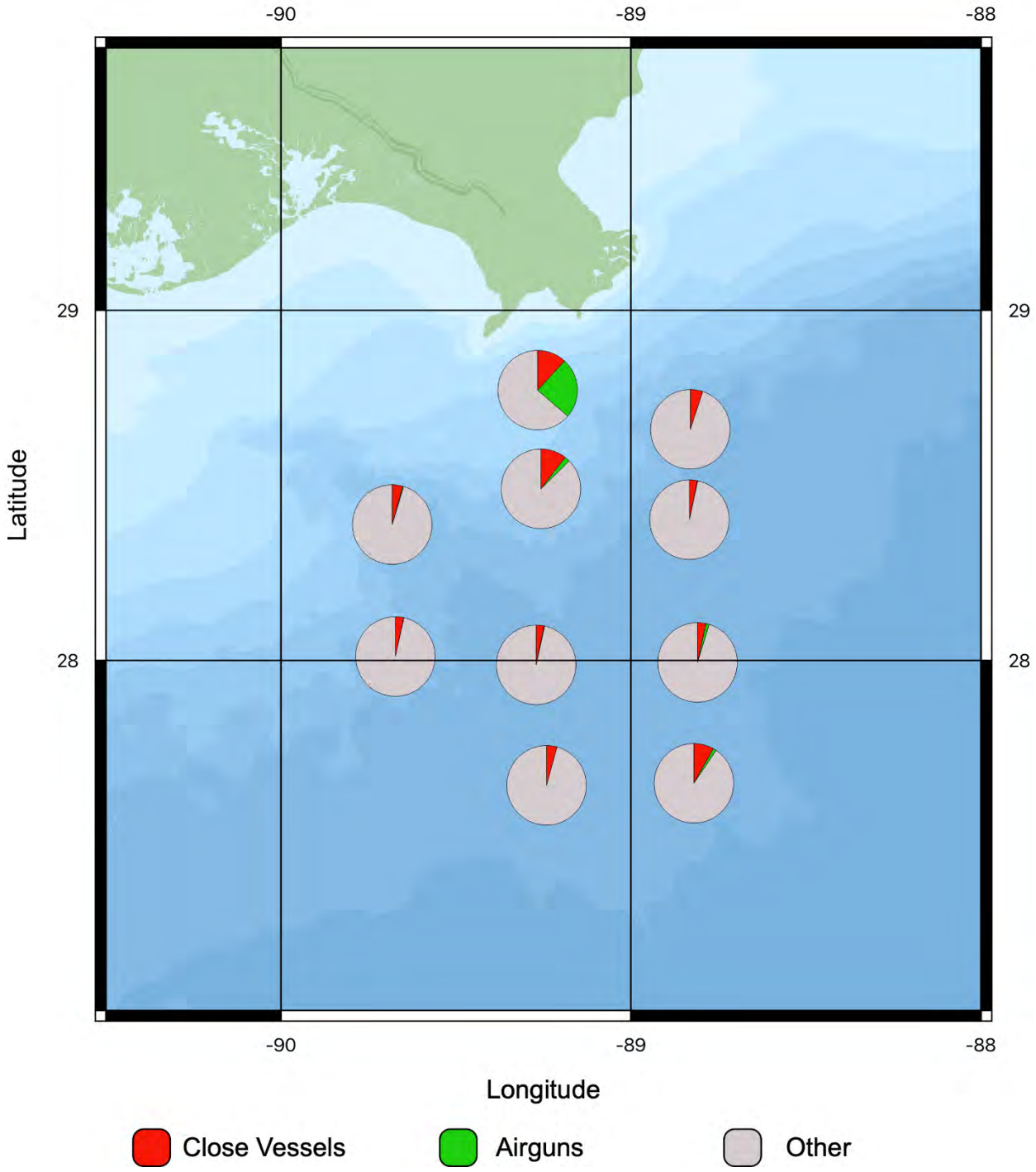

Figure E-A7. Vessel and airgun detections for November 2018

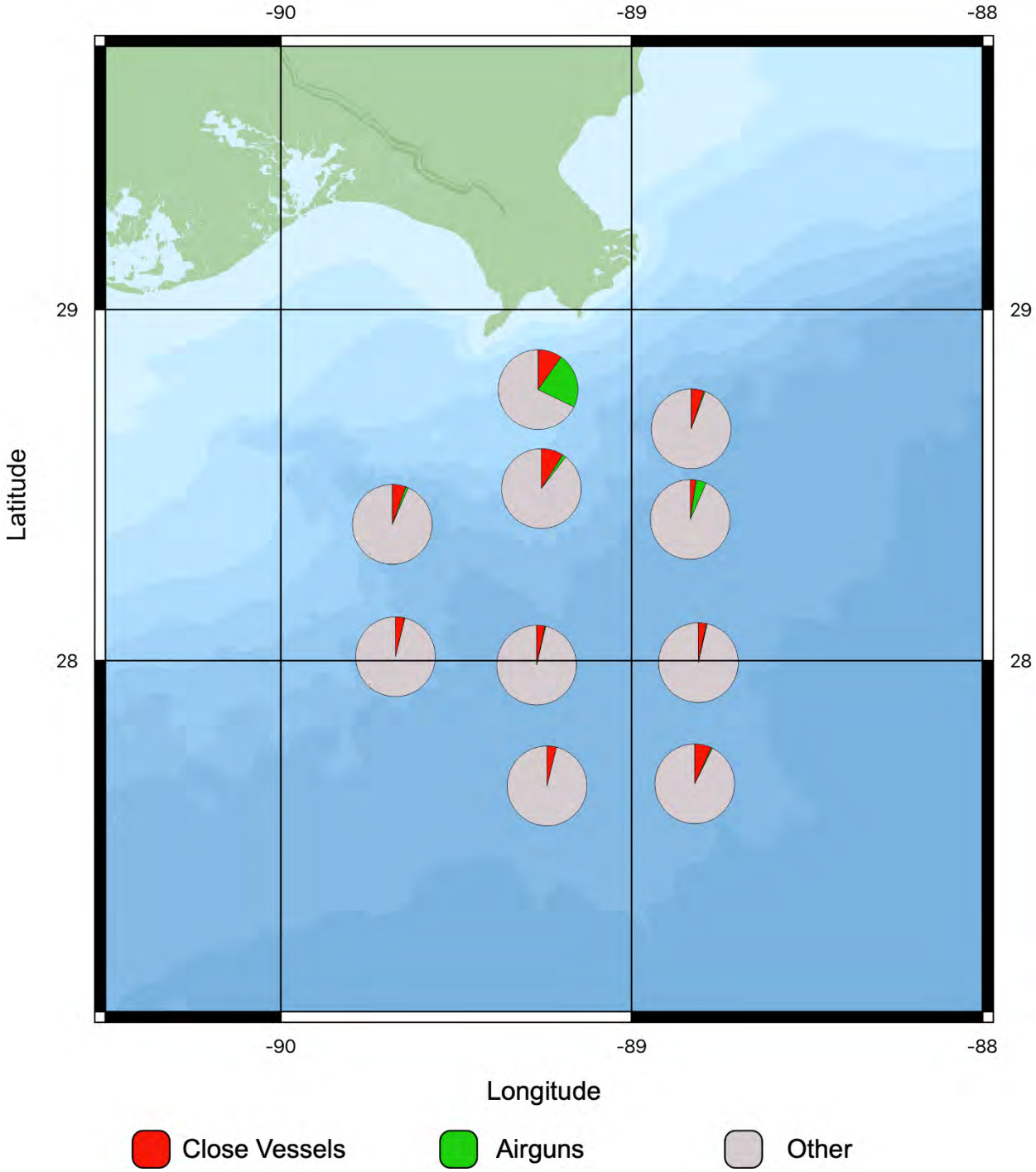

Figure E-A8. Vessel and airgun detections for December 2018

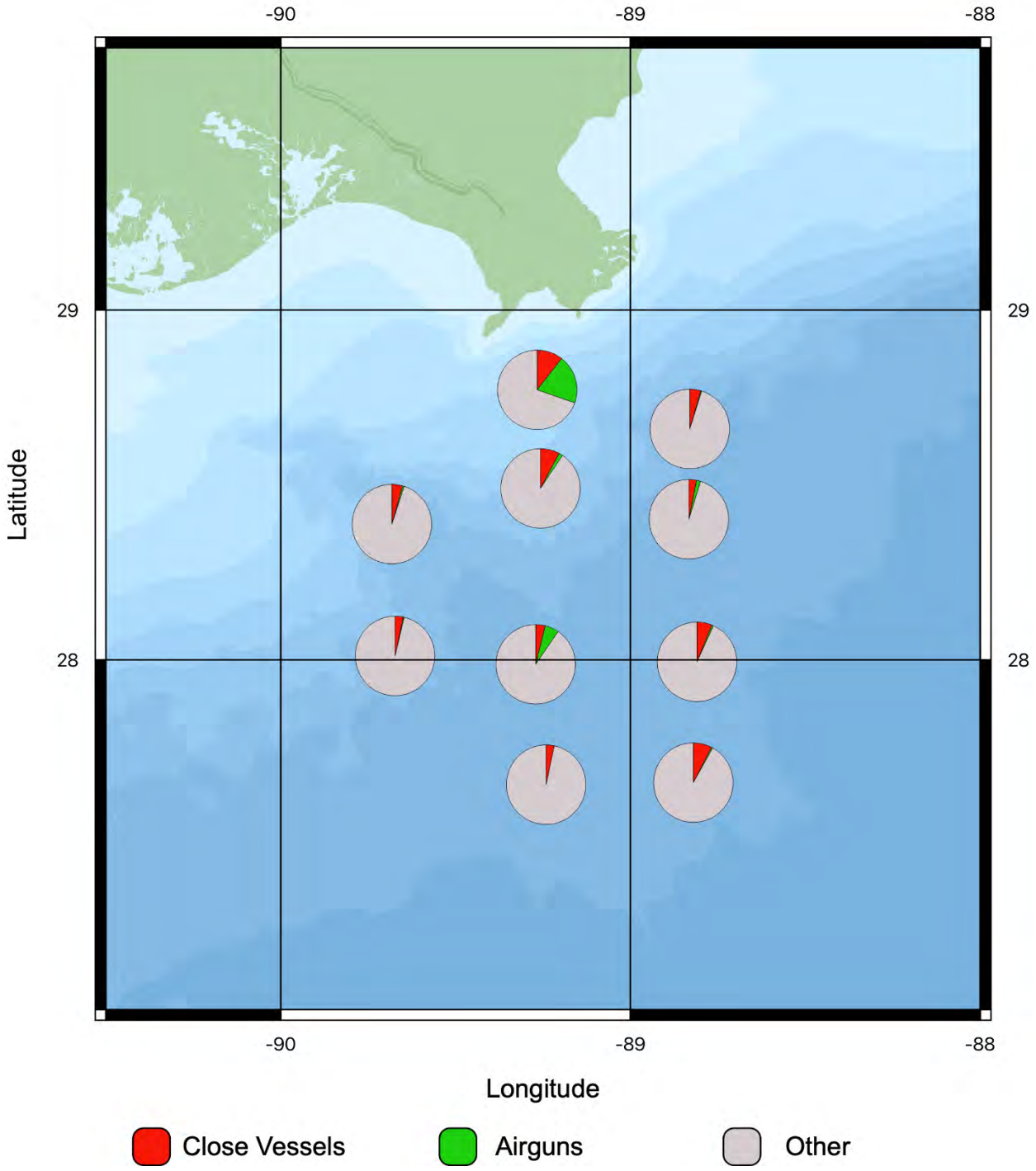

Figure E-A9. Vessel and airgun detections for January 2019

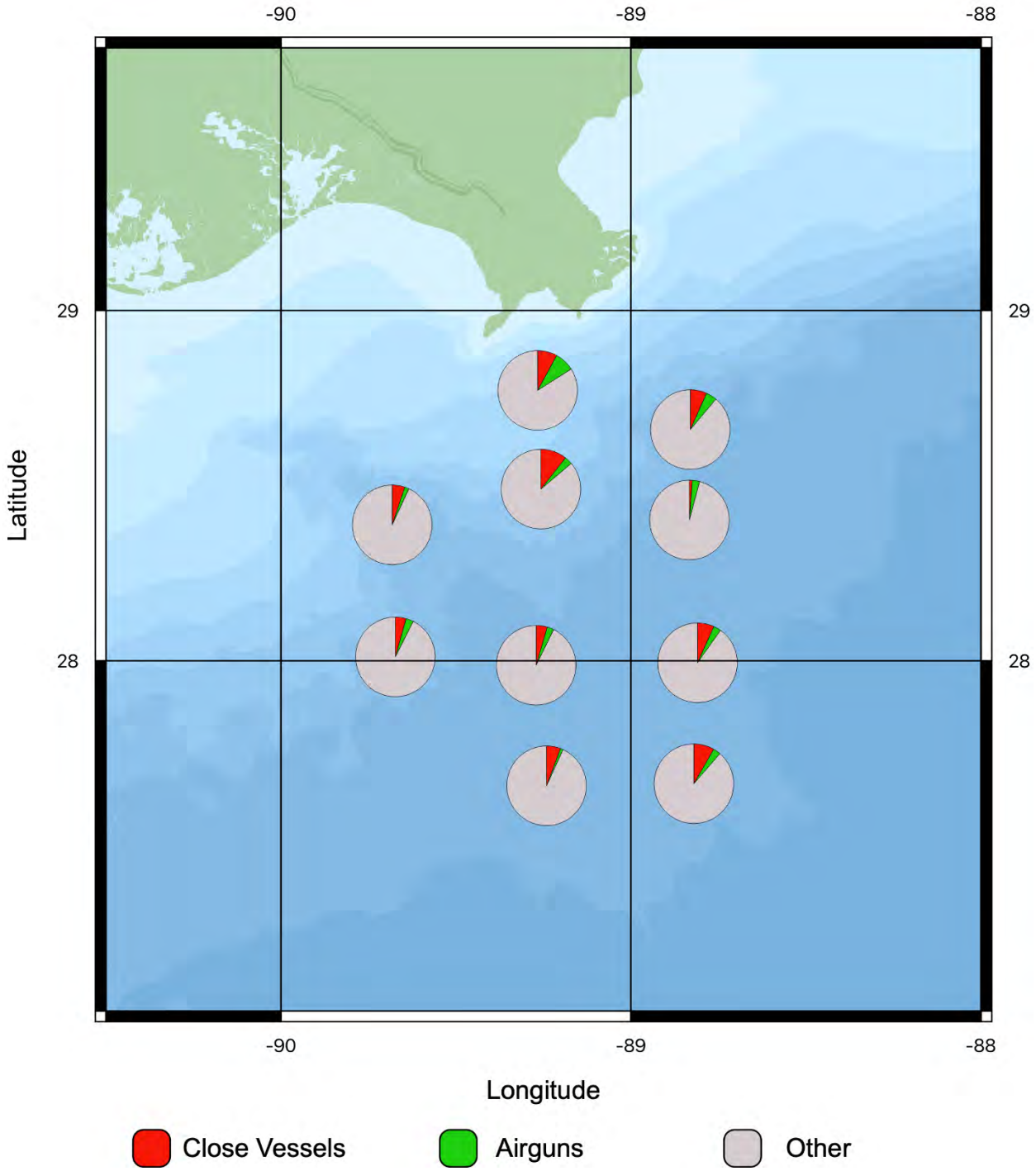

Figure E-A10. Vessel and airgun detections for February 2019

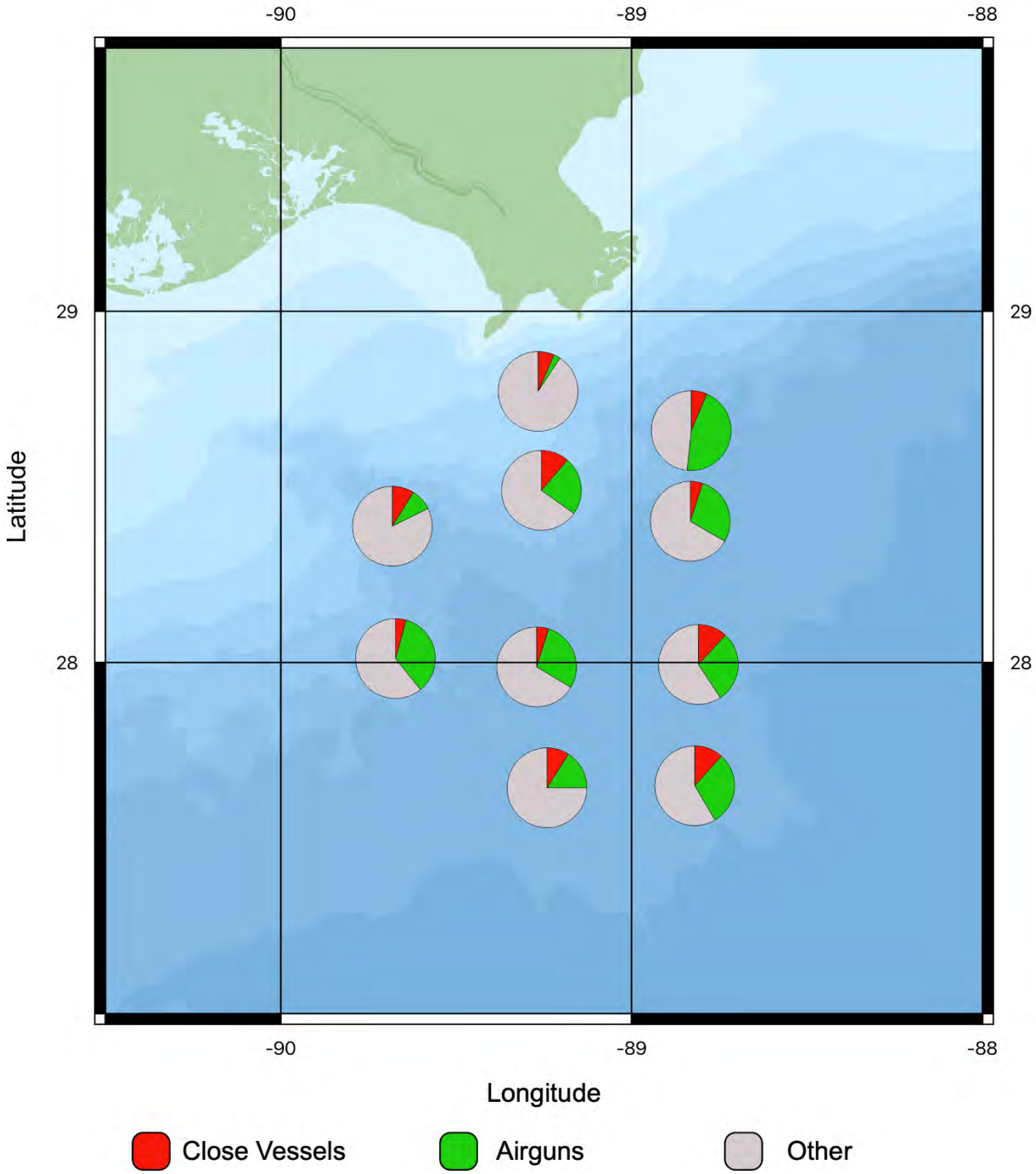

Figure E-A11. Vessel and airgun detections for March 2019

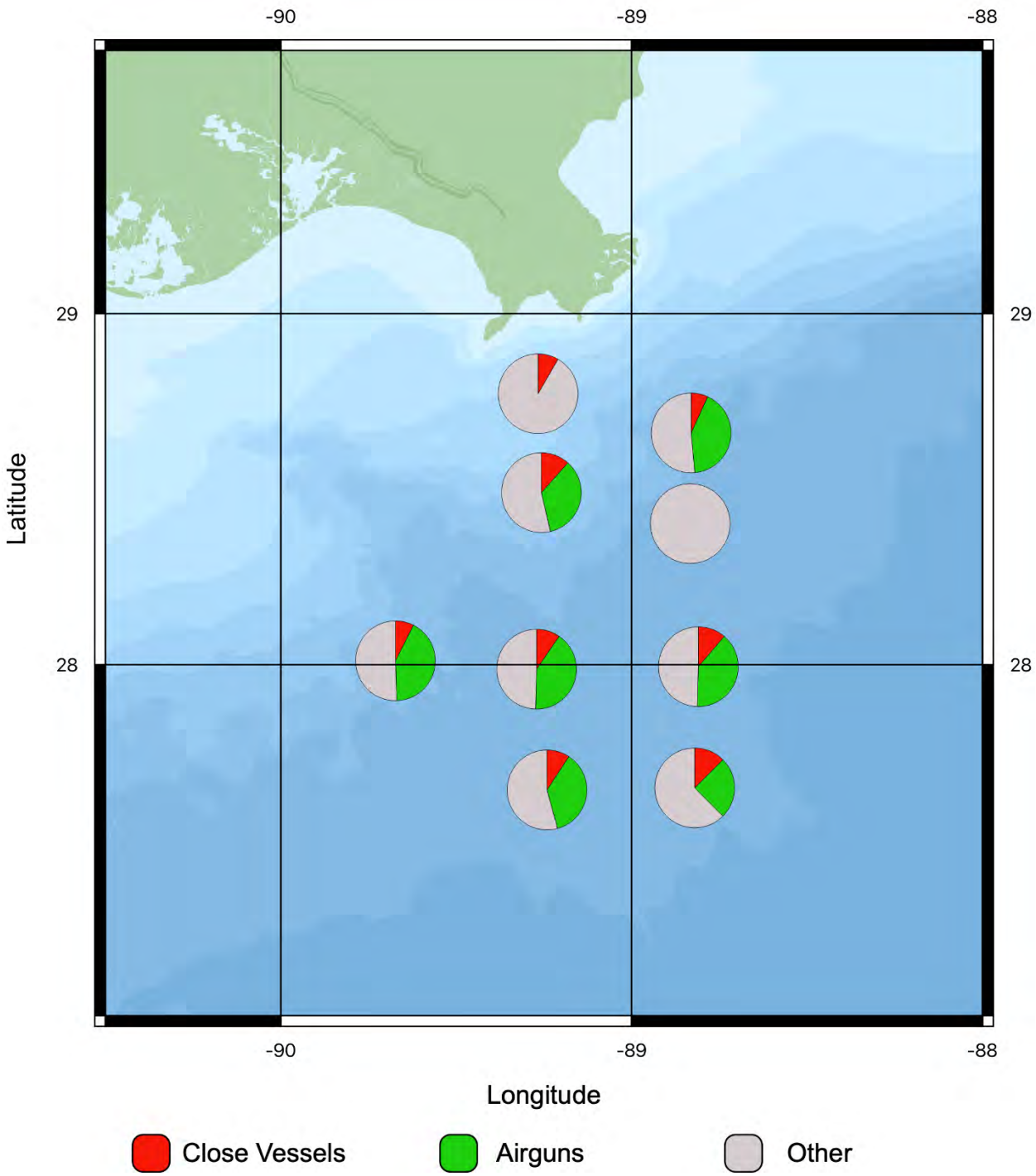

Figure E-A12. Vessel and airgun detections for April 2019

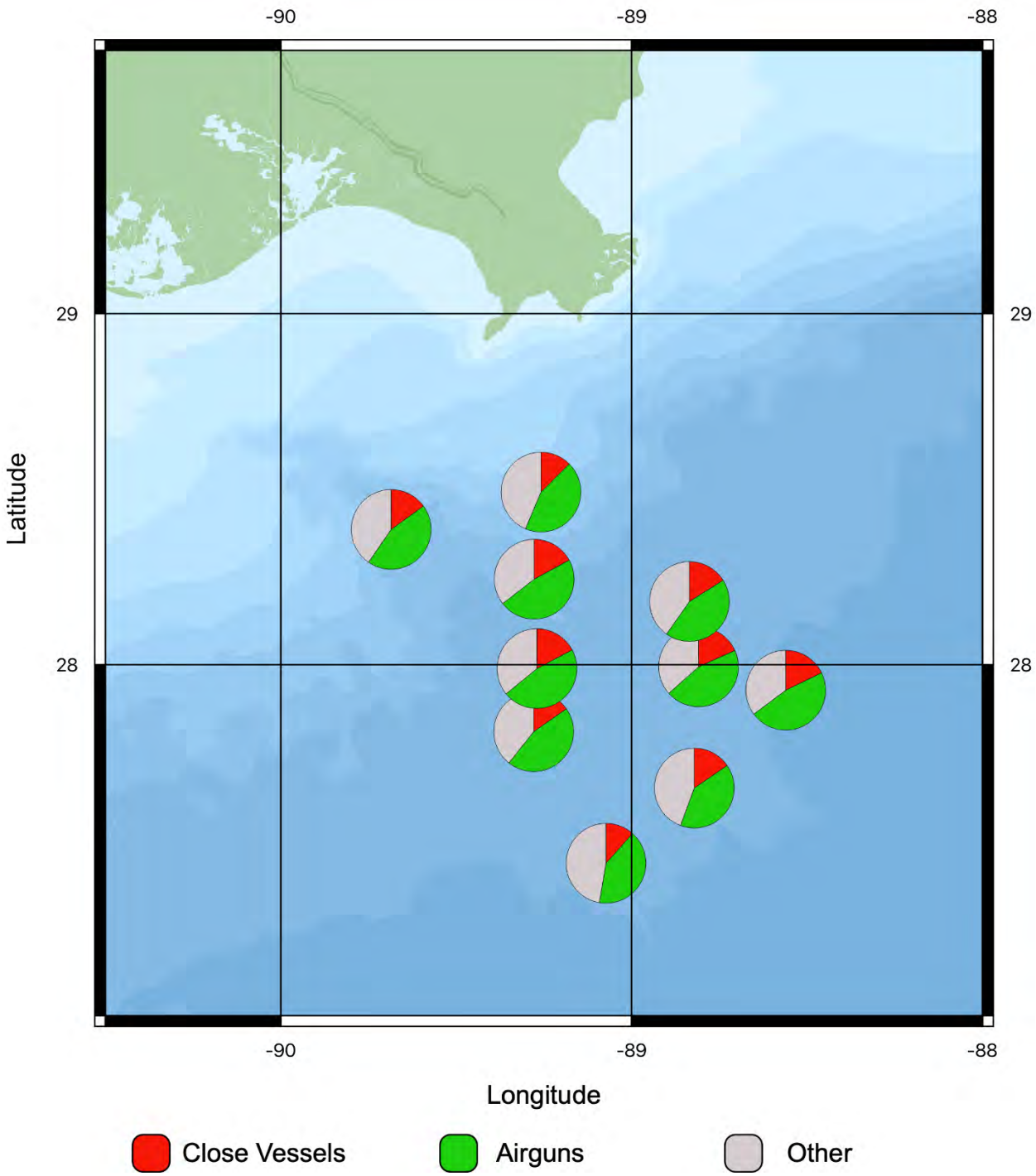

Figure E-A13. Vessel and airgun detections for May 2019

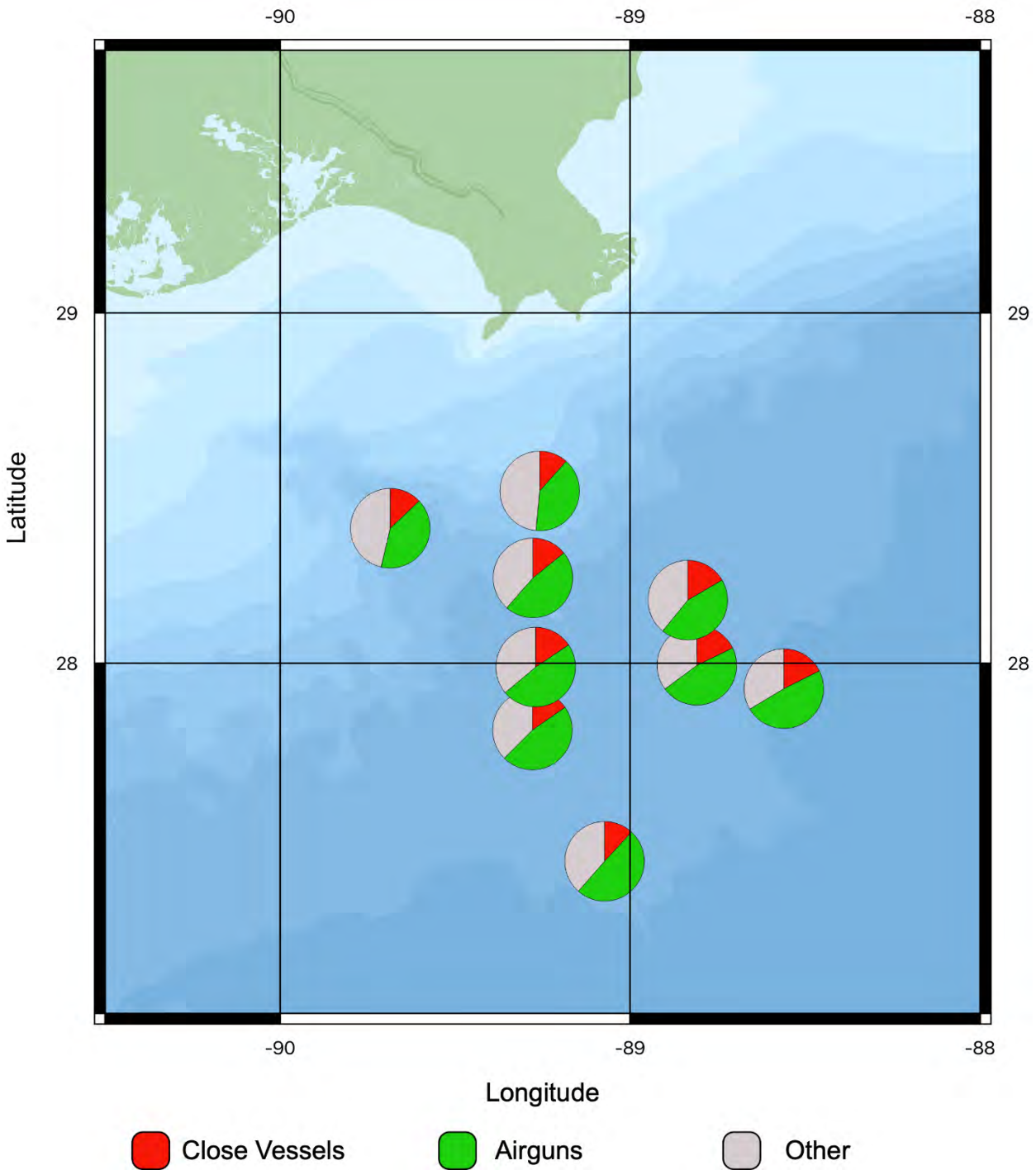

Figure E-A14. Vessel and airgun detections for June 2019

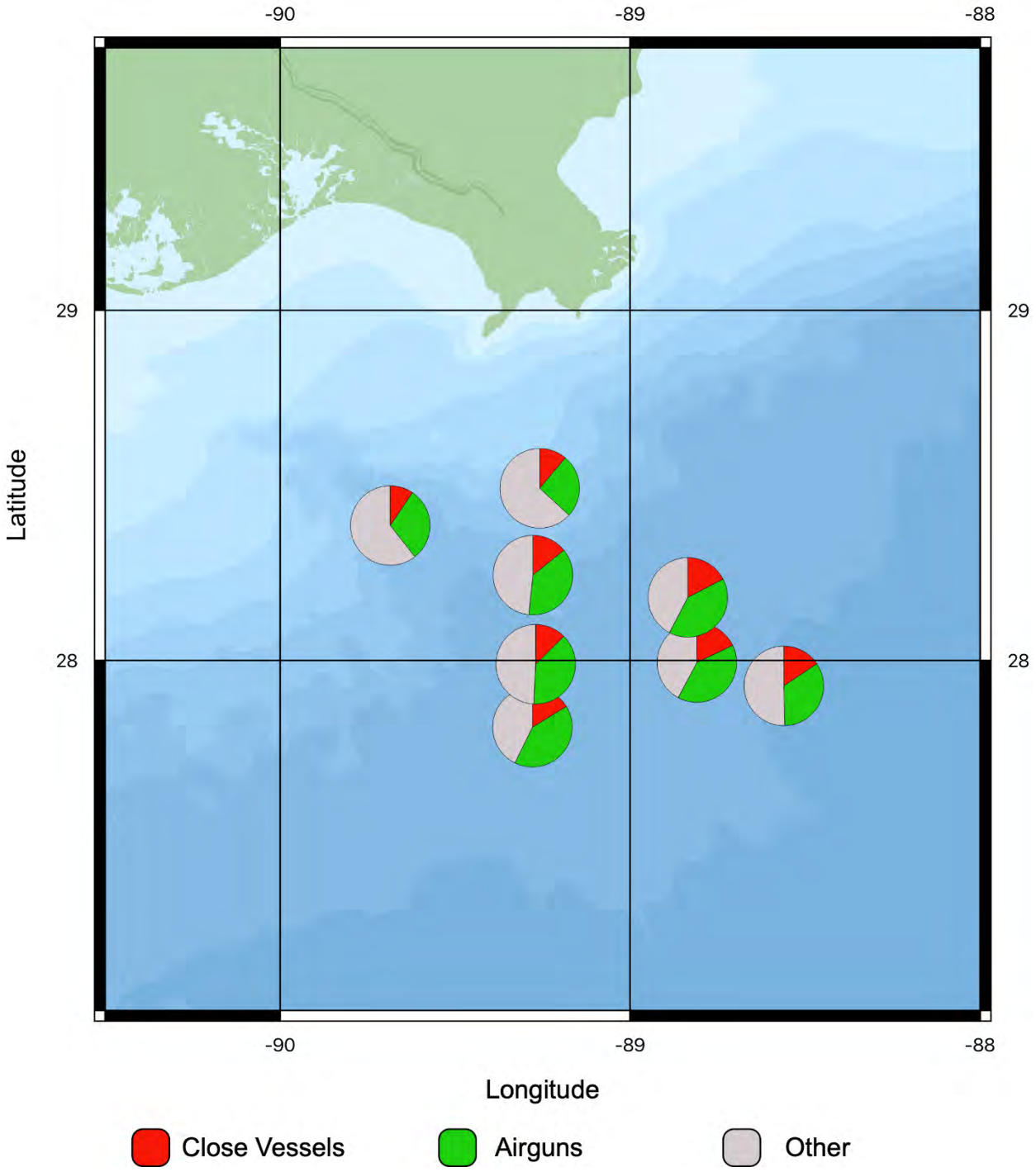

Figure E-A15. Vessel and airgun detections for July 2019

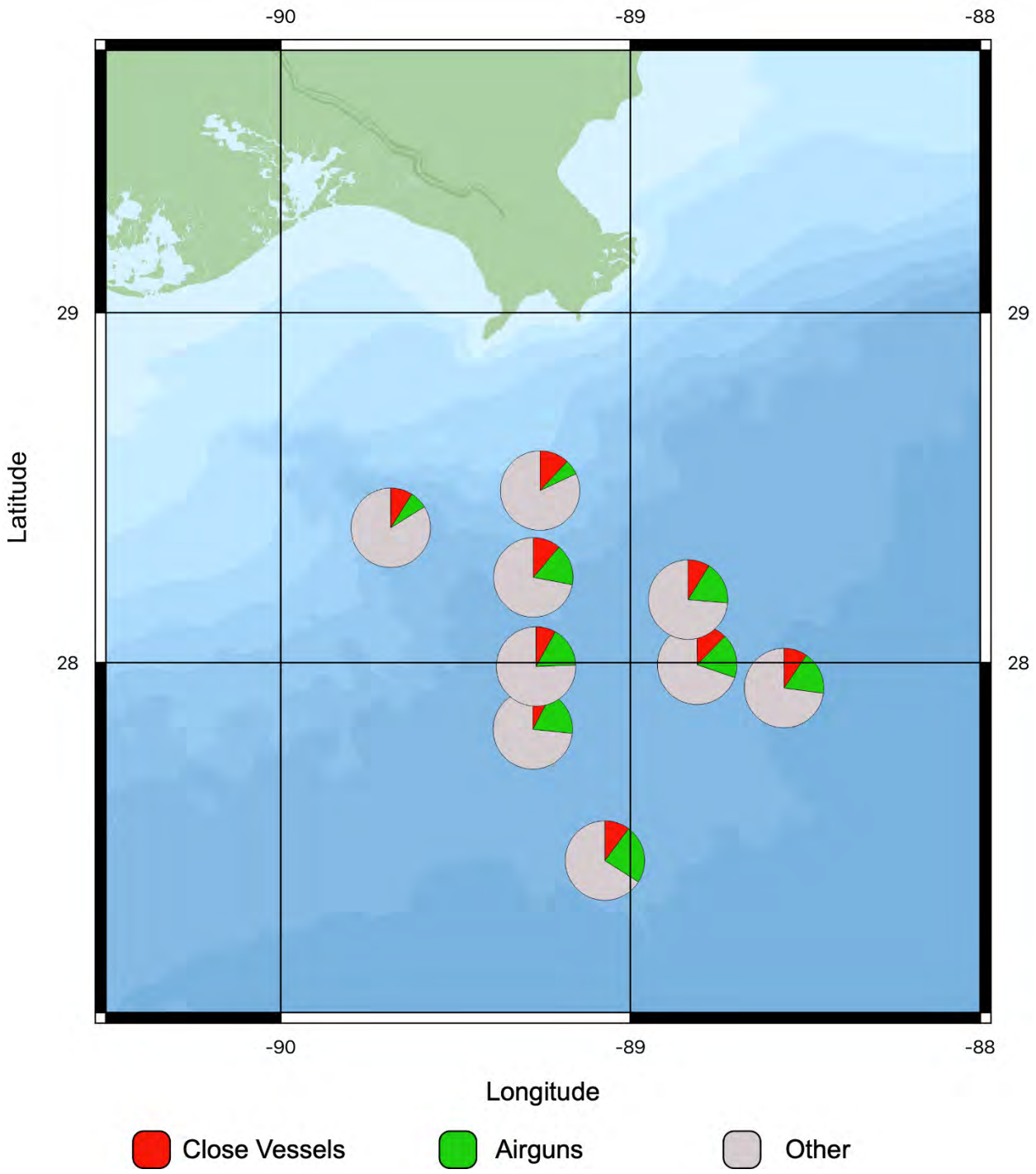

Figure E-A16. Vessel and airgun detections for August 2019

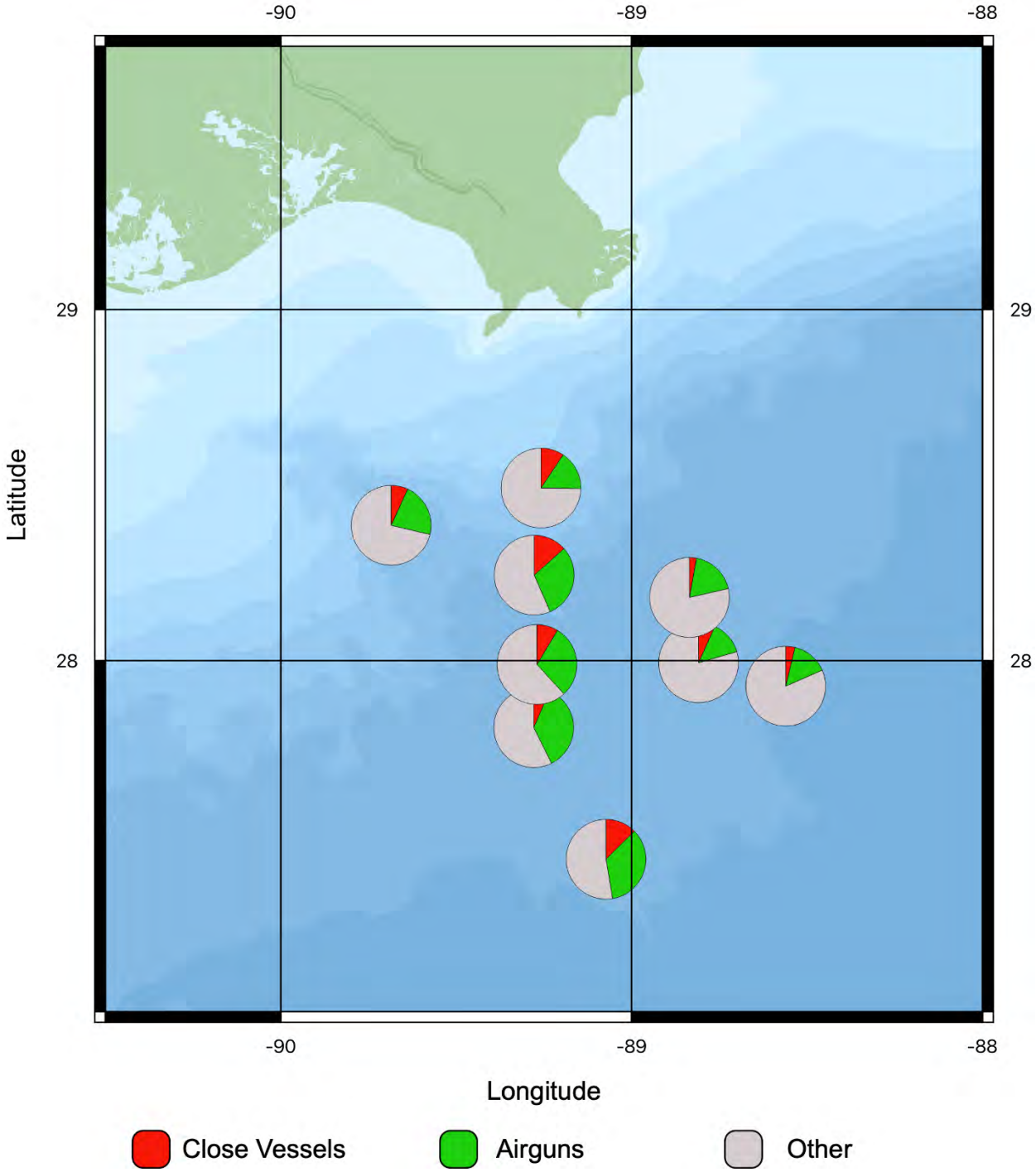

Figure E-A17. Vessel and airgun detections for September 2019

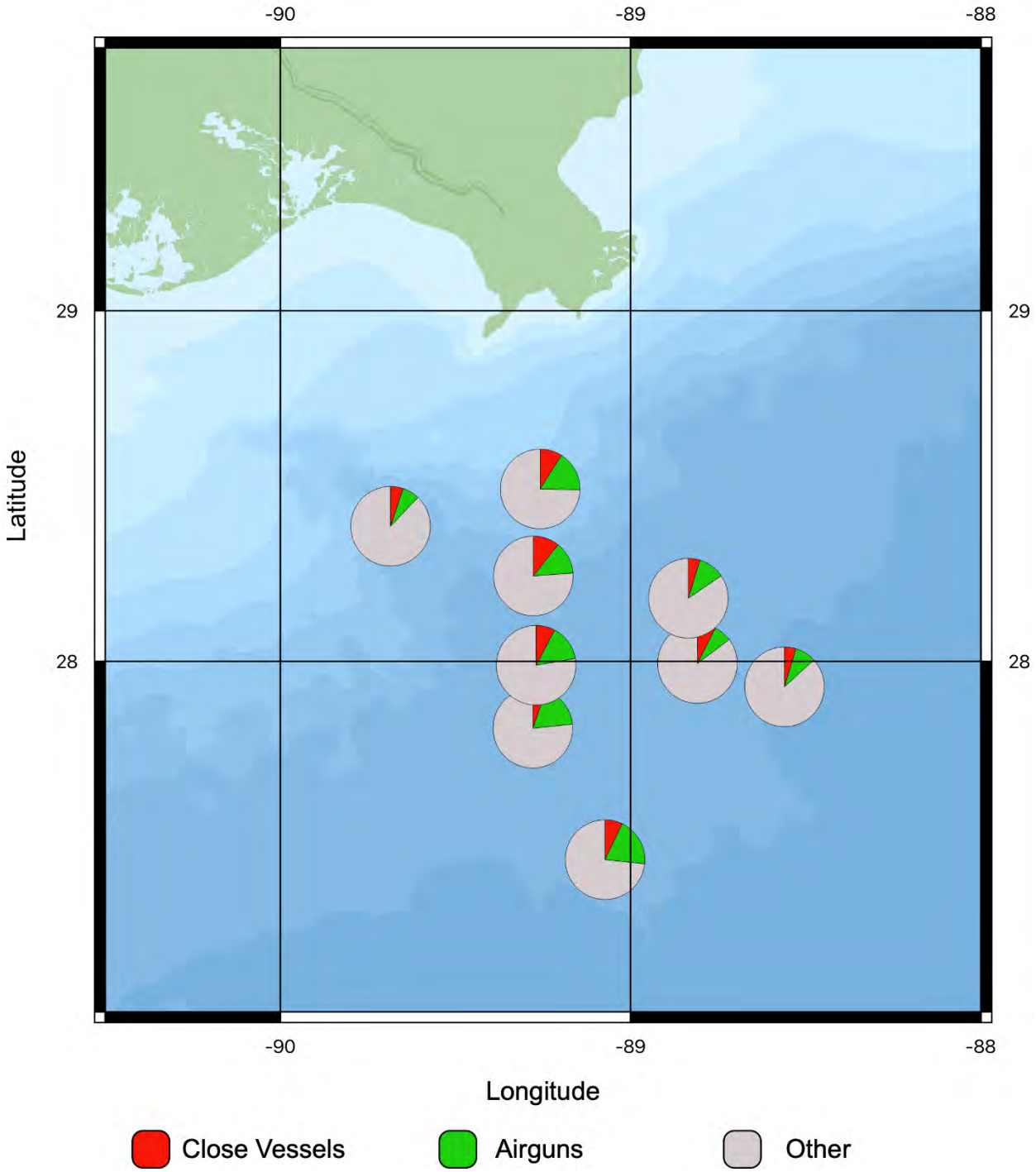

Figure E-A18. Vessel and airgun detections for October 2019

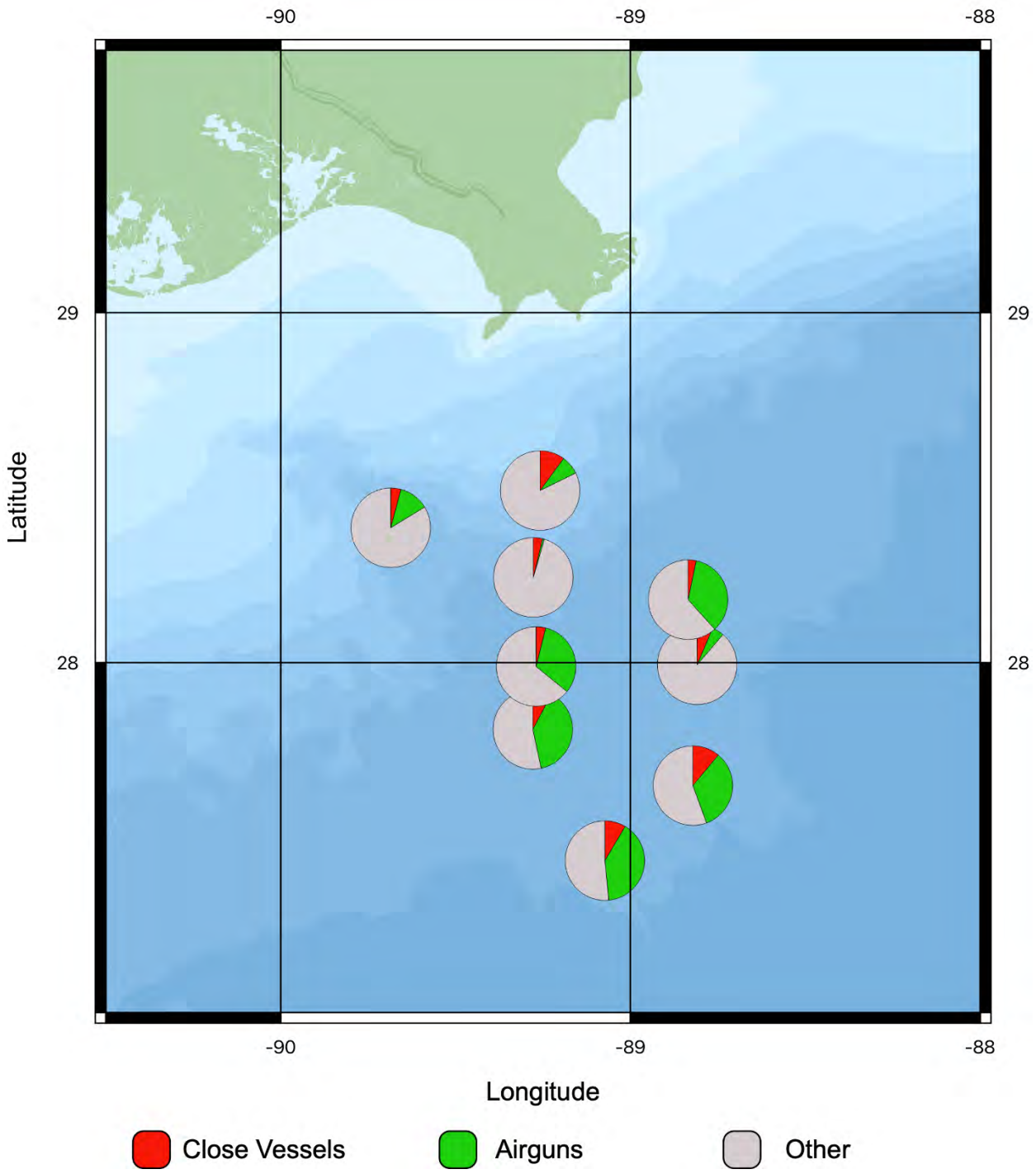

Figure E-A19. Vessel and airgun detections for November 2019

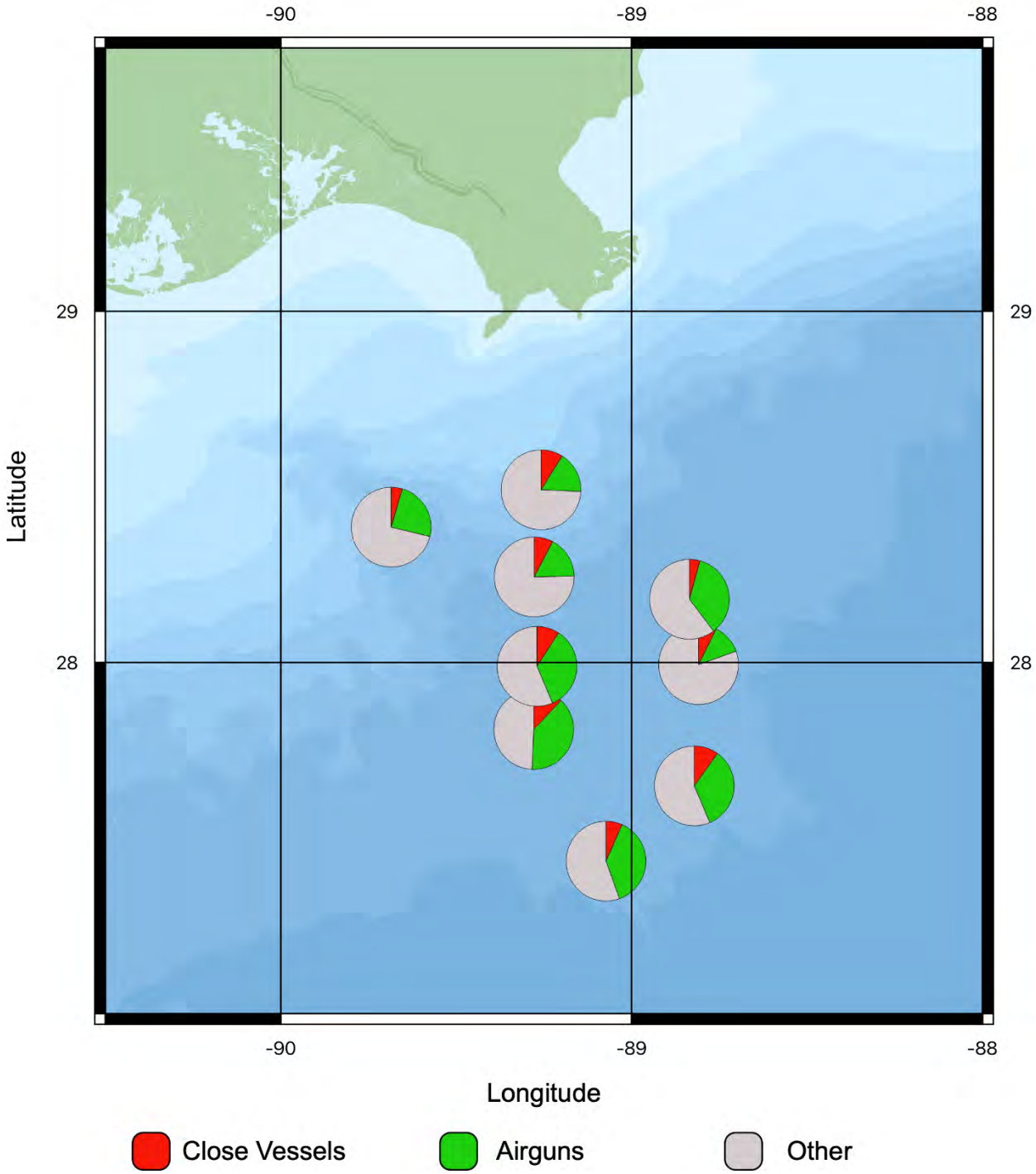

Figure E-A20. Vessel and airgun detections for December 2019

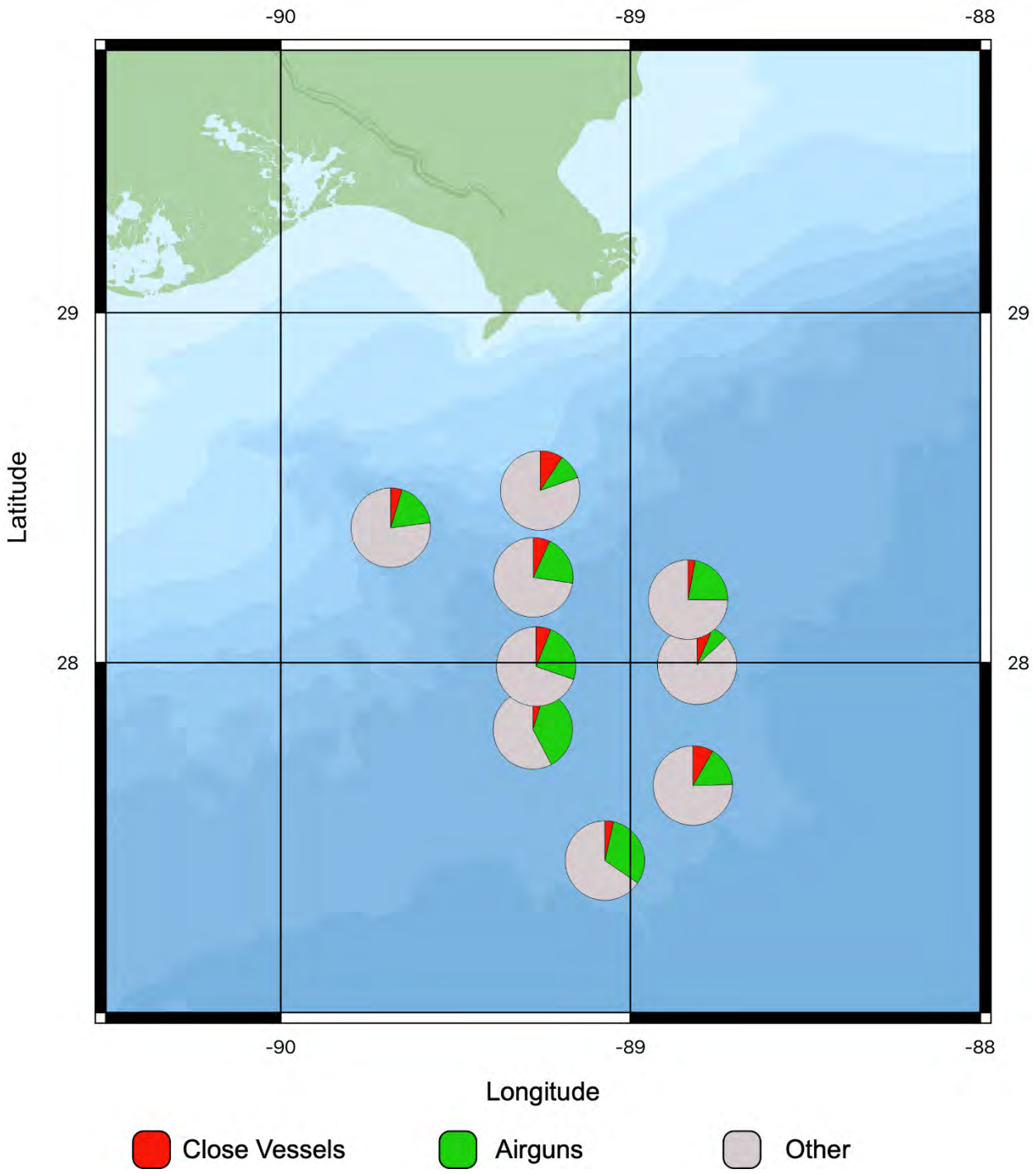

Figure E-A21. Vessel and airgun detections for January 2020

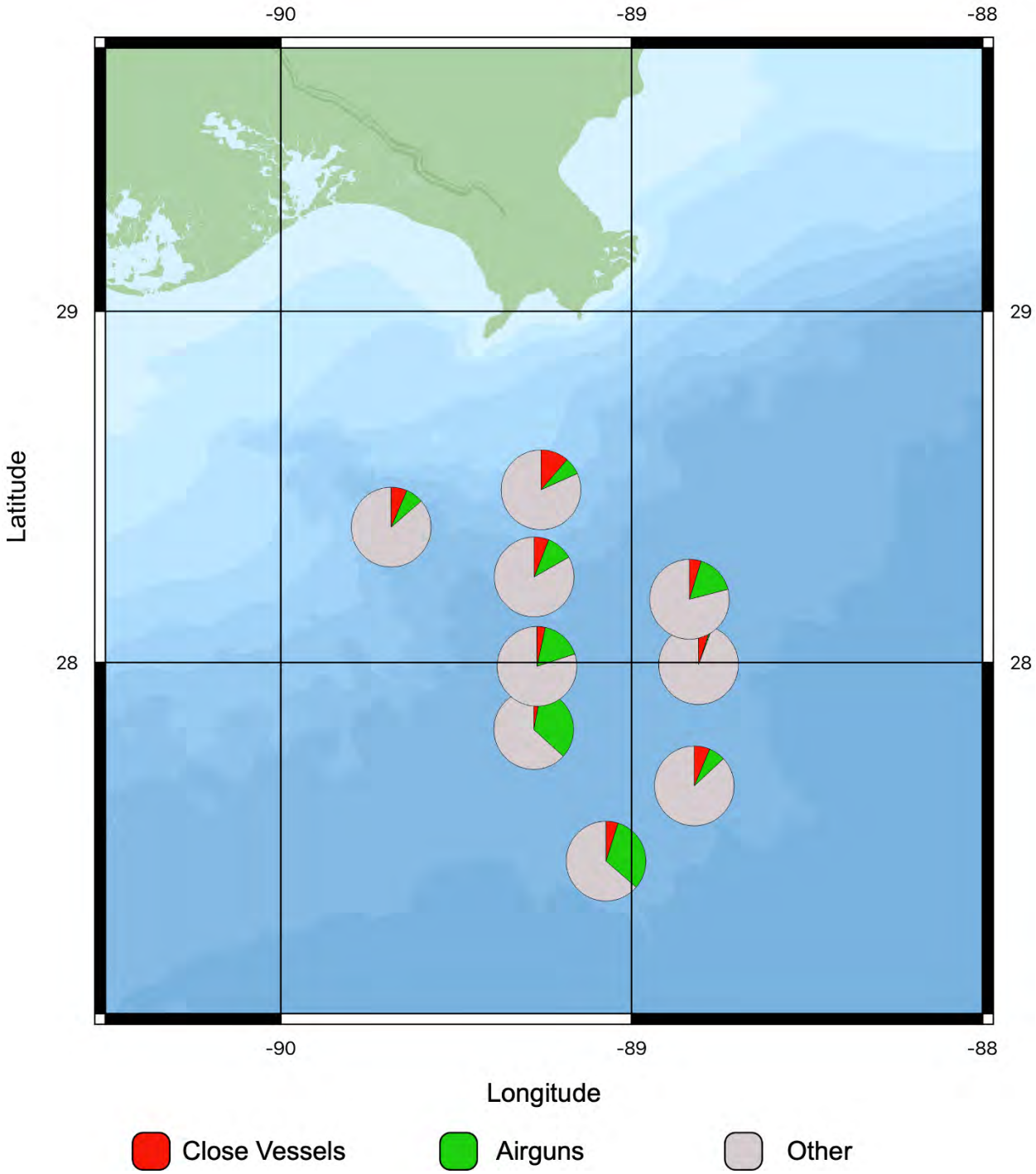

Figure E-A22. Vessel and airgun detections for February 2020

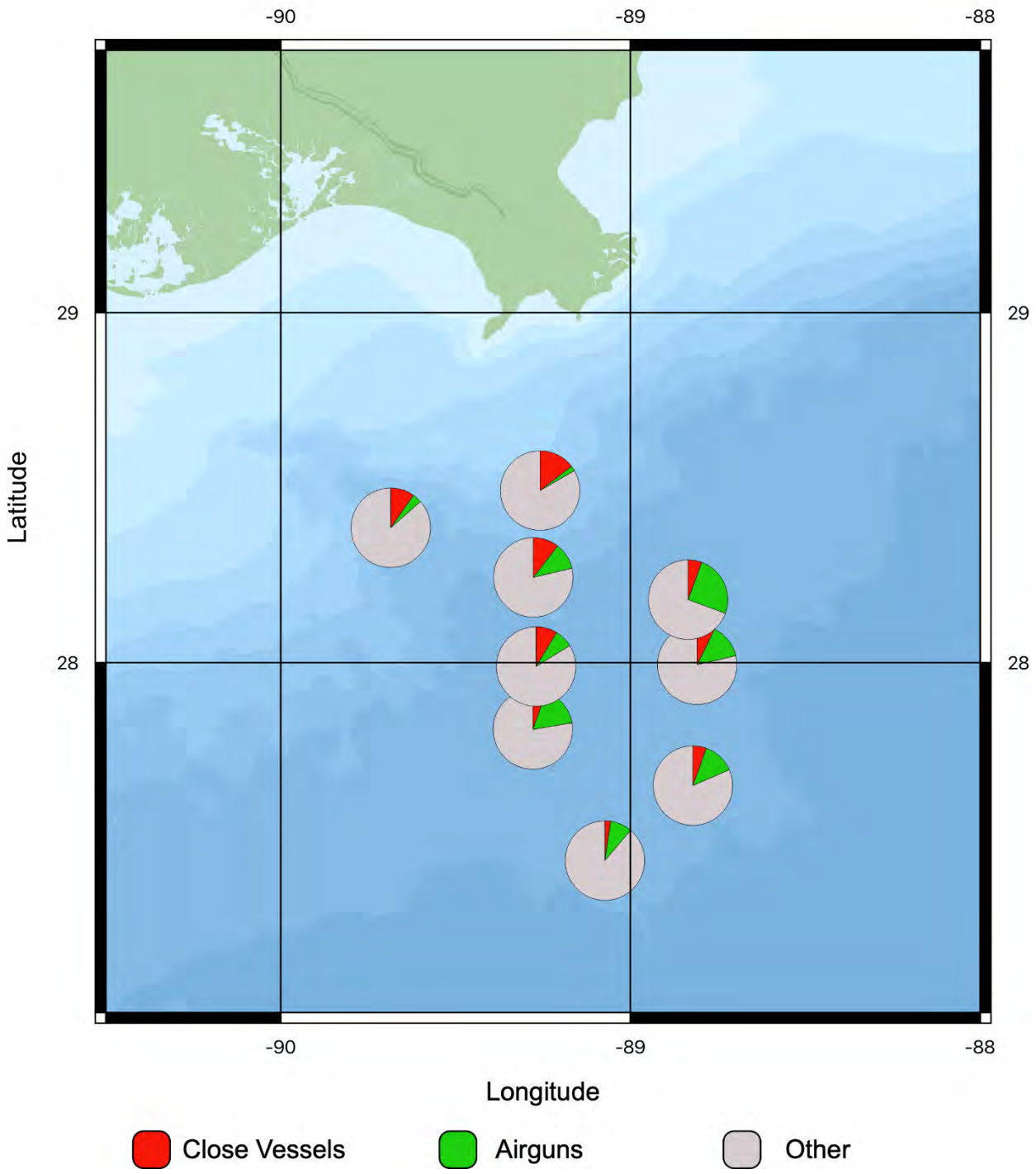

Figure E-A23. Vessel and airgun detections for March 2020

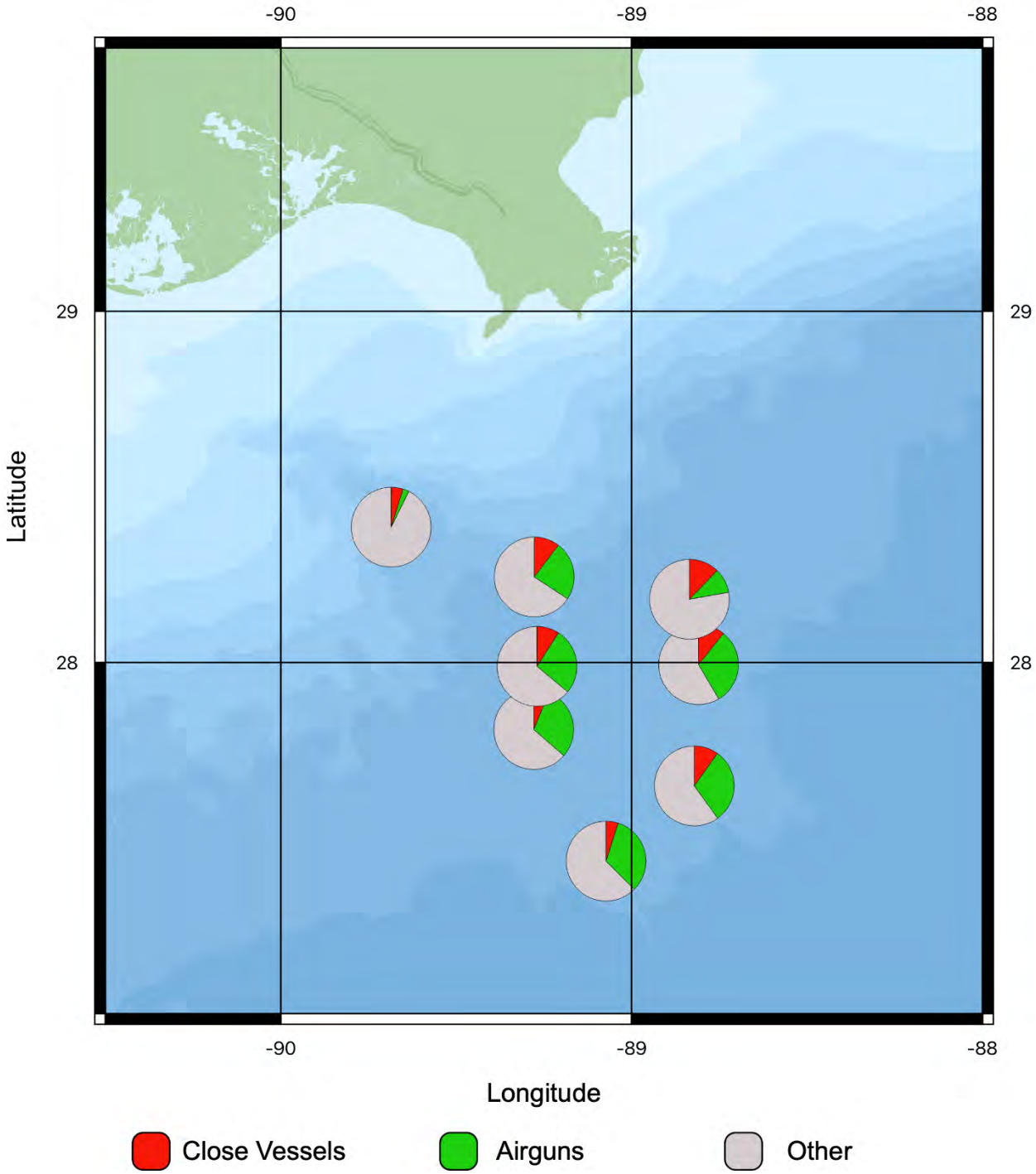

Figure E-A24. Vessel and airgun detections for April 2020

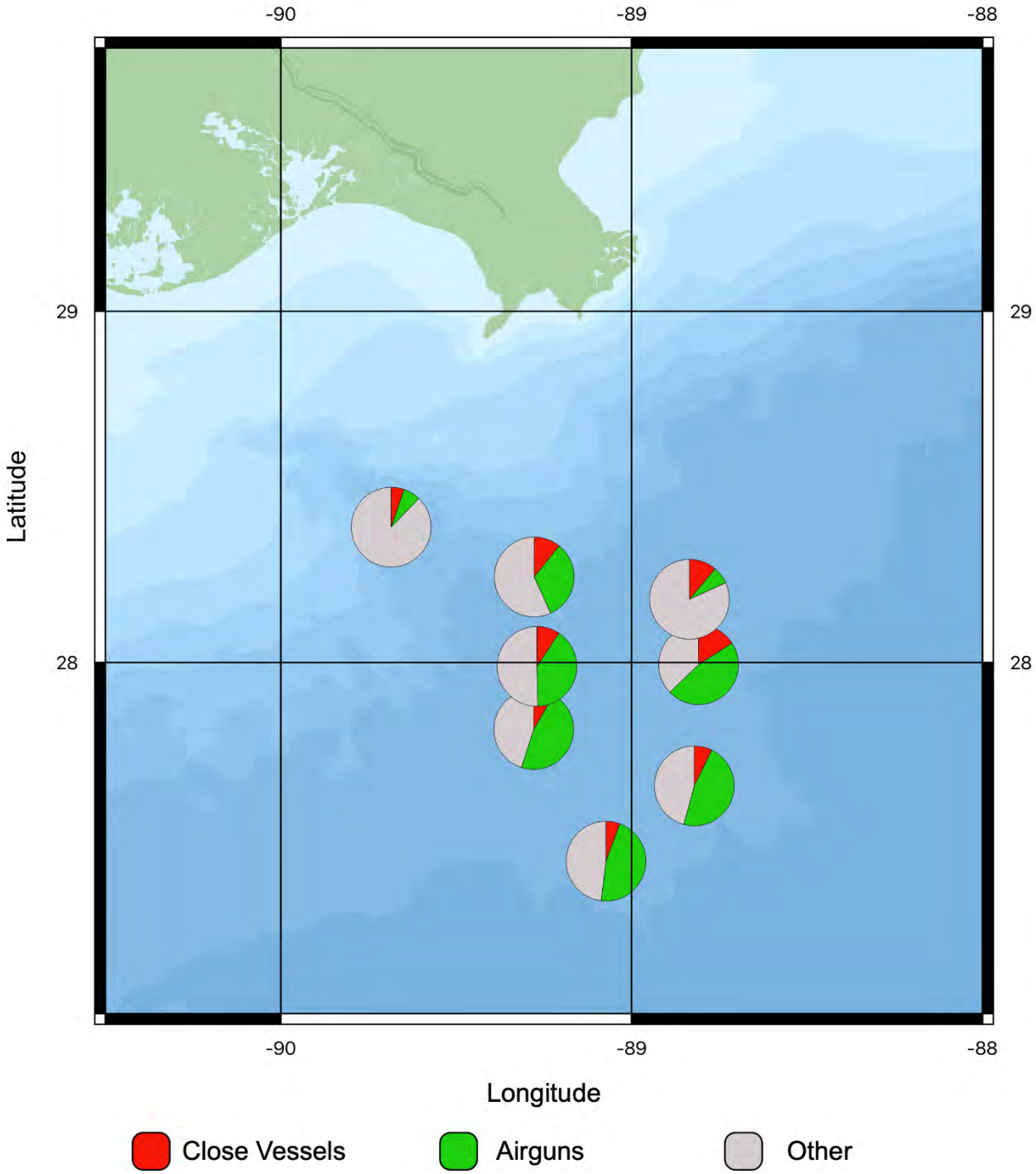

Figure E-A25. Vessel and airgun detections for May 2020

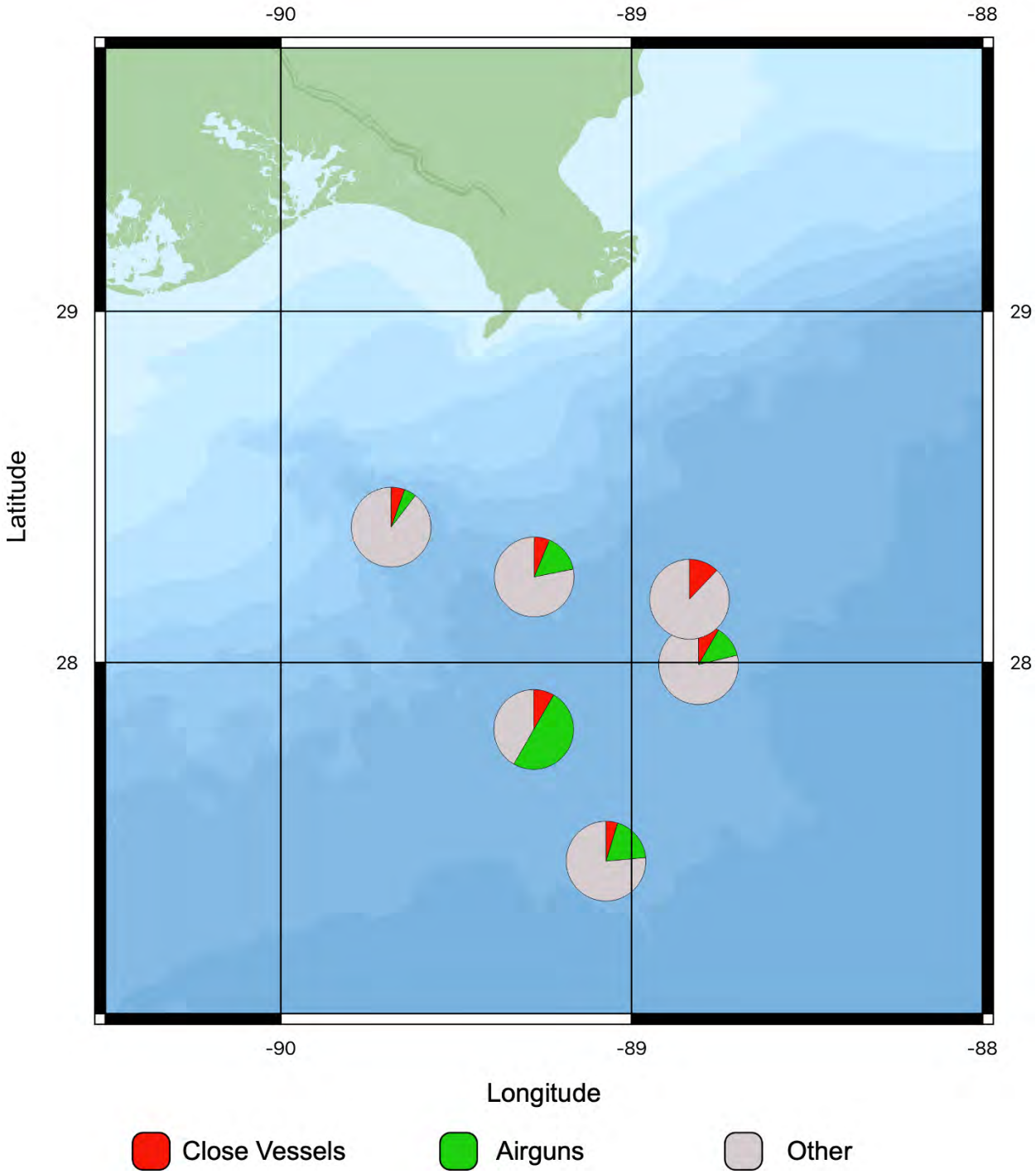

Figure E-A26. Vessel and airgun detections for June 2020

Appendix E-B: Simplified Statistical Approach Results of Deployments 2 through 4 Vessel Received Levels

DEPLOYMENT 2

Table E-B1. GAM output for Deployment 2, Receiver 1

A. parametric coefficients	Estimate	Std. Error	t-value	p-value
(Intercept)	4.6169	0.0007	6385.6556	< 0.0001
km2	0.0097	0.0107	0.9098	0.3630
km4	-0.0023	0.0078	-0.2989	0.7650
km10	-0.0007	0.0038	-0.1840	0.8540
B. smooth terms	**edf**	**Ref.df**	**F-value**	**p-value**
s(sDate)	42.7750	49.0000	71.5179	< 0.0001
s(WaveHeight)	3.9348	3.9348	20.5096	< 0.0001
s(Windspeed)	3.6754	3.6754	29.6019	< 0.0001
s(CPAmin)	6.7332	6.7332	7.8383	< 0.0001

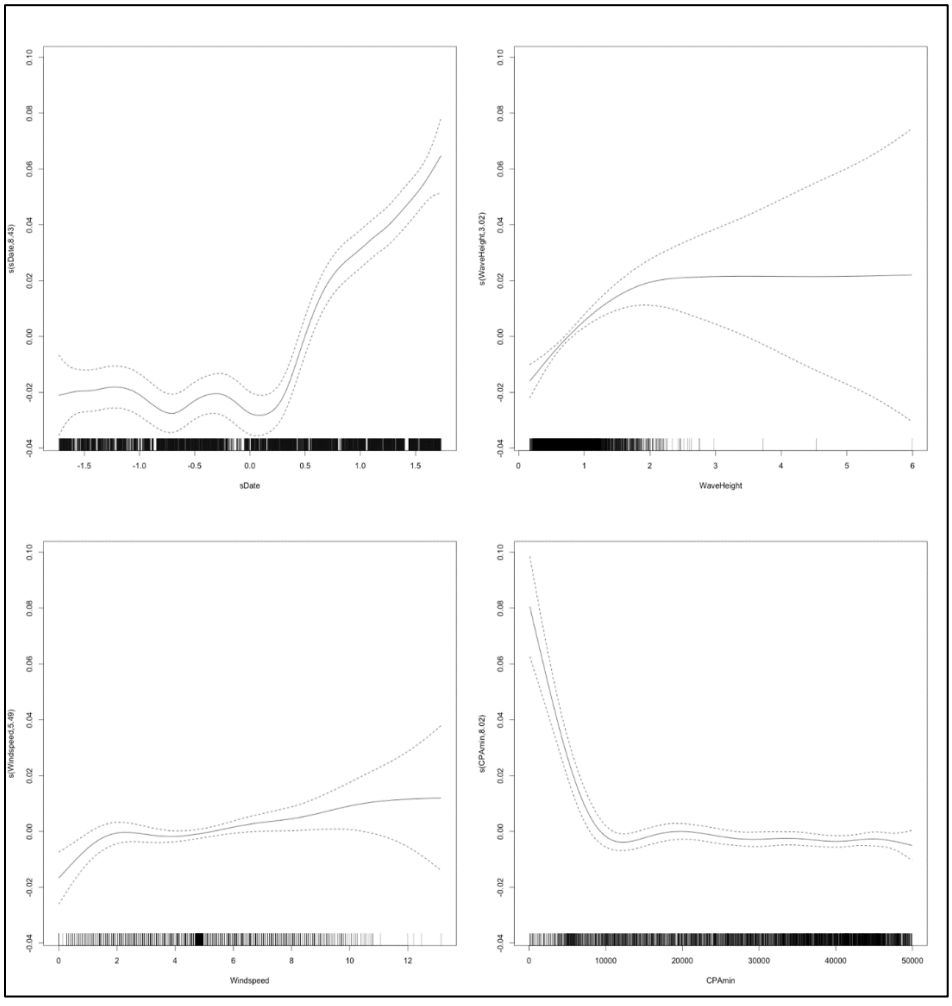

Figure E-B1. SA2 smoothing functions for Measured Vessel Band Noise as a function of Date, Wave Height, Windspeed, and CPA for Receiver 1, Deployment 2

Table E-B2. GAM output for Deployment 2, Receiver 2

A. parametric coefficients	Estimate	Std. Error	t-value	p-value
(Intercept)	4.5136	0.0012	3899.8731	< 0.0001
km2	0.0293	0.0048	6.0980	< 0.0001
km4	0.0201	0.0037	5.3839	< 0.0001
km10	0.0085	0.0017	5.0327	< 0.0001
B. smooth terms	**edf**	**Ref.df**	**F-value**	**p-value**
s(sDate)	38.8337	49.0000	117.6090	< 0.0001
s(WaveHeight)	1.0000	1.0000	24.6496	< 0.0001
s(Windspeed)	1.0000	1.0000	17.8622	< 0.0001
s(CPAmin)	3.2779	3.2779	9.3601	< 0.0001

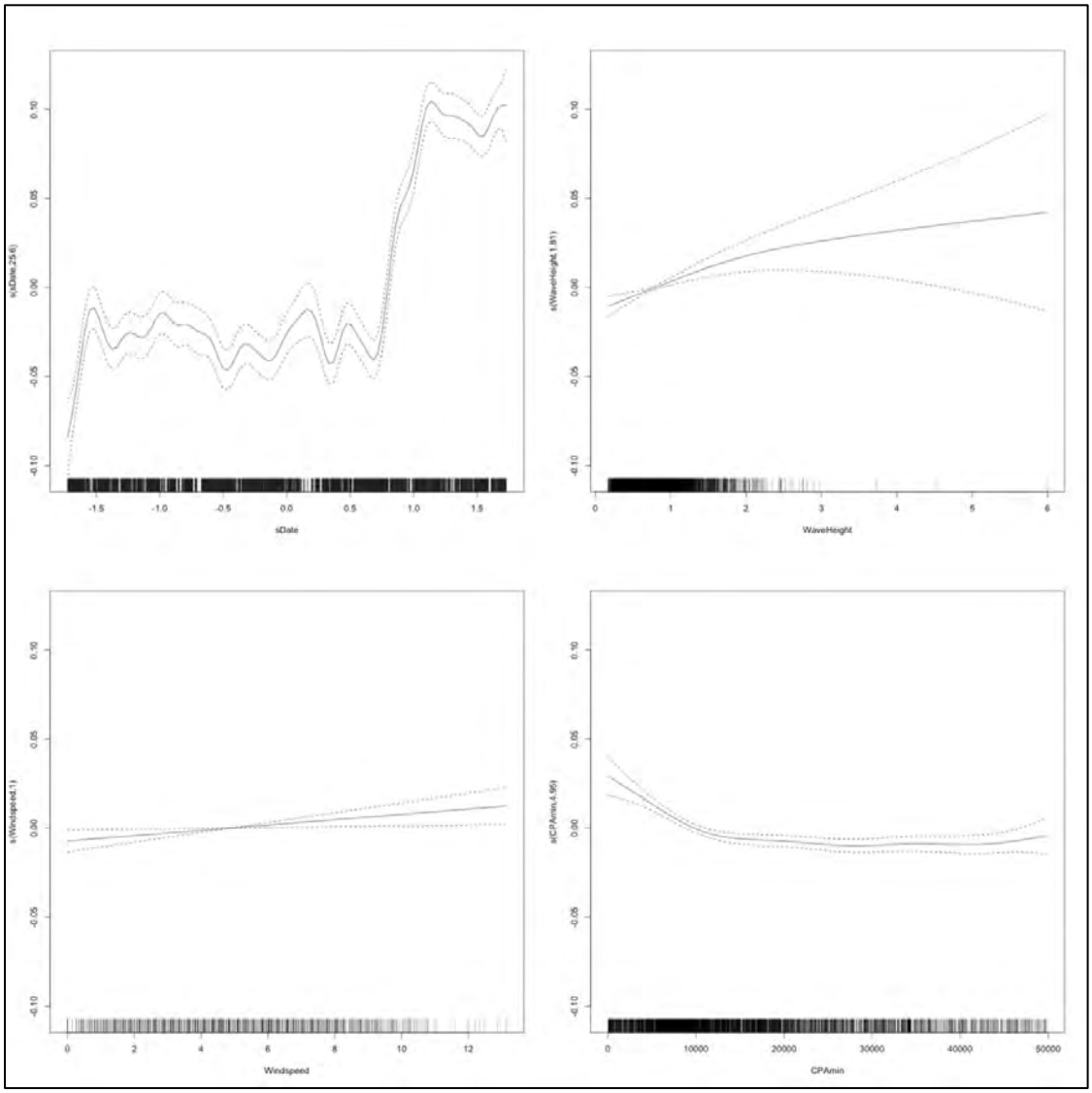

Figure E-B2. SA2 smoothing functions for Measured Vessel Band Noise as a function of Date, Wave Height, Windspeed, and CPA for Receiver 2, Deployment 2

Table E-B3. GAM output for Deployment 2, Receiver 3

A. parametric coefficients	Estimate	Std. Error	t-value	p-value
(Intercept)	4.6174	0.0006	8156.1005	< 0.0001
km2	0.0530	0.0066	8.0384	< 0.0001
km4	0.0346	0.0045	7.7606	< 0.0001
km10	0.0110	0.0020	5.4315	< 0.0001
B. smooth terms	**edf**	**Ref.df**	**F-value**	**p-value**
s(sDate)	43.1319	49.0000	58.0407	< 0.0001
s(WaveHeight)	3.4464	3.4464	71.1011	< 0.0001
s(Windspeed)	1.0000	1.0000	163.6694	< 0.0001
s(CPAmin)	3.2739	3.2739	4.8104	0.0013

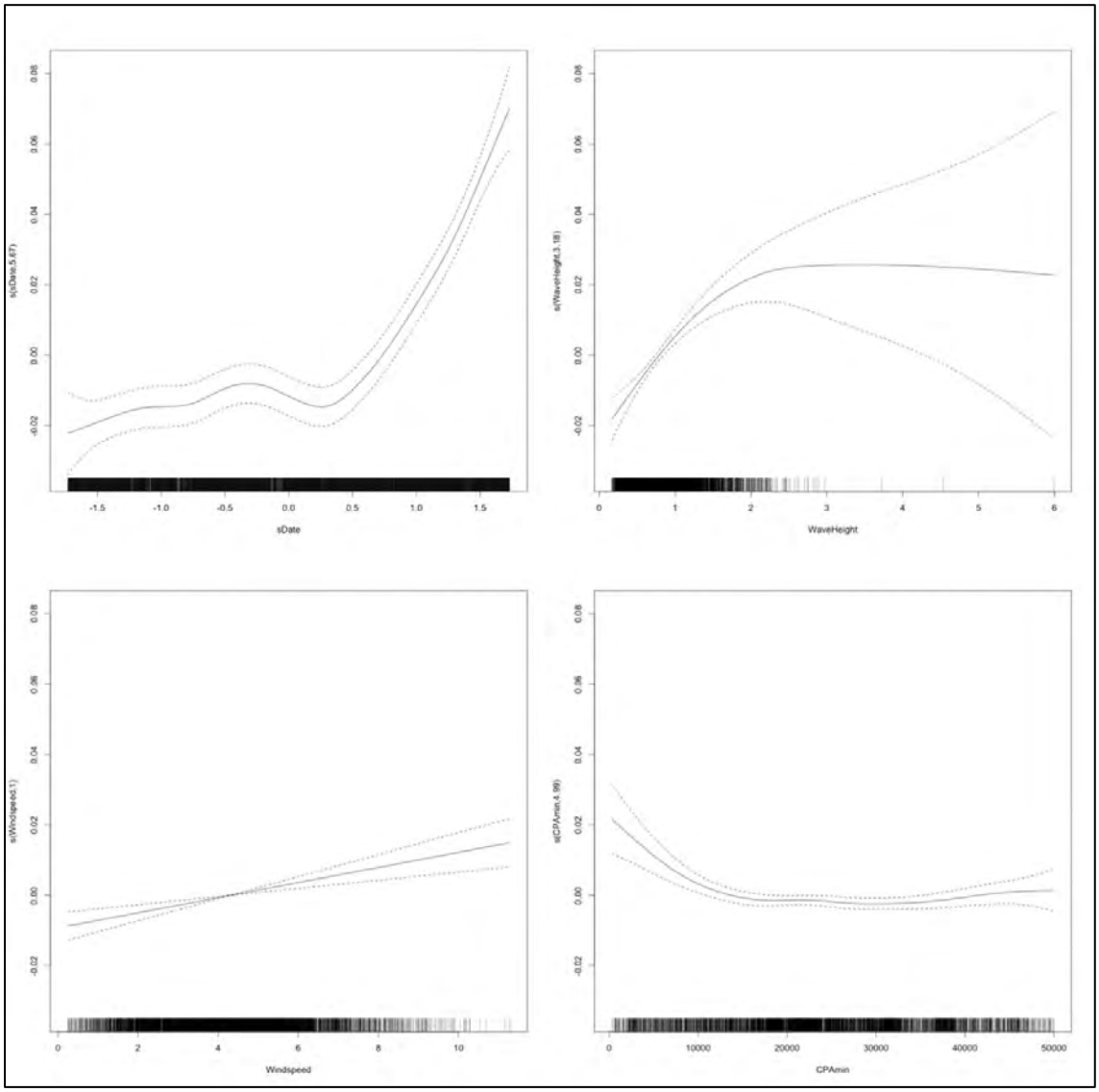

Figure E-B3. SA2 smoothing functions for Measured Vessel Band Noise as a function of Date, Wave Height, Windspeed, and CPA for Receiver 3, Deployment 2

Table E-B4. GAM output for Deployment 2, Receiver 4

A. parametric coefficients	Estimate	Std. Error	t-value	p-value
(Intercept)	4.5015	0.0006	7062.4300	< 0.0001
km2	0.0044	0.0086	0.5146	0.6068
km4	0.0165	0.0059	2.8079	0.0050
km10	0.0026	0.0023	1.1468	0.2515
B. smooth terms	edf	Ref.df	F-value	p-value
s(sDate)	41.7865	49.0000	60.9431	< 0.0001
s(WaveHeight)	4.9438	4.9438	29.6807	< 0.0001
s(Windspeed)	3.9395	3.9395	31.6058	< 0.0001
s(CPAmin)	7.3711	7.3711	9.2162	< 0.0001

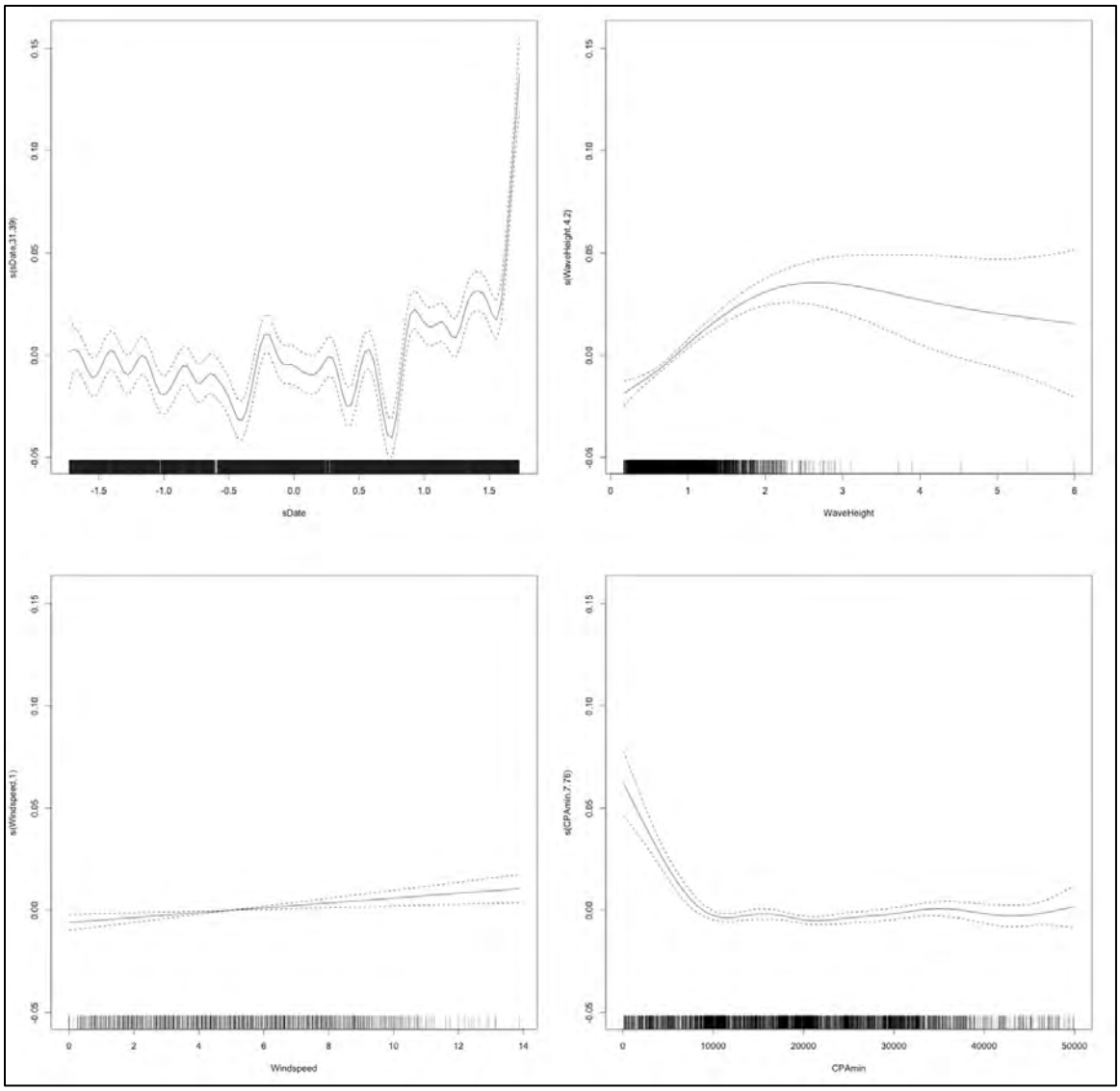

Figure E-B4. SA2 smoothing functions for Measured Vessel Band Noise as a function of Date, Wave Height, Windspeed, and CPA for Receiver 4, Deployment 2

Table E-B5. GAM output for Deployment 2, Receiver 5

A. parametric coefficients	Estimate	Std. Error	t-value	p-value
(Intercept)	4.5500	0.0007	6105.8569	< 0.0001
km2	0.0328	0.0029	11.2034	< 0.0001
km4	0.0146	0.0021	6.8469	< 0.0001
km10	0.0076	0.0008	9.1069	< 0.0001
B. smooth terms	**edf**	**Ref.df**	**F-value**	**p-value**
s(sDate)	39.5263	49.0000	108.5052	< 0.0001
s(WaveHeight)	1.0000	1.0000	29.2715	< 0.0001
s(Windspeed)	3.3844	3.3844	20.2612	< 0.0001
s(CPAmin)	1.0000	1.0000	0.0776	0.7806

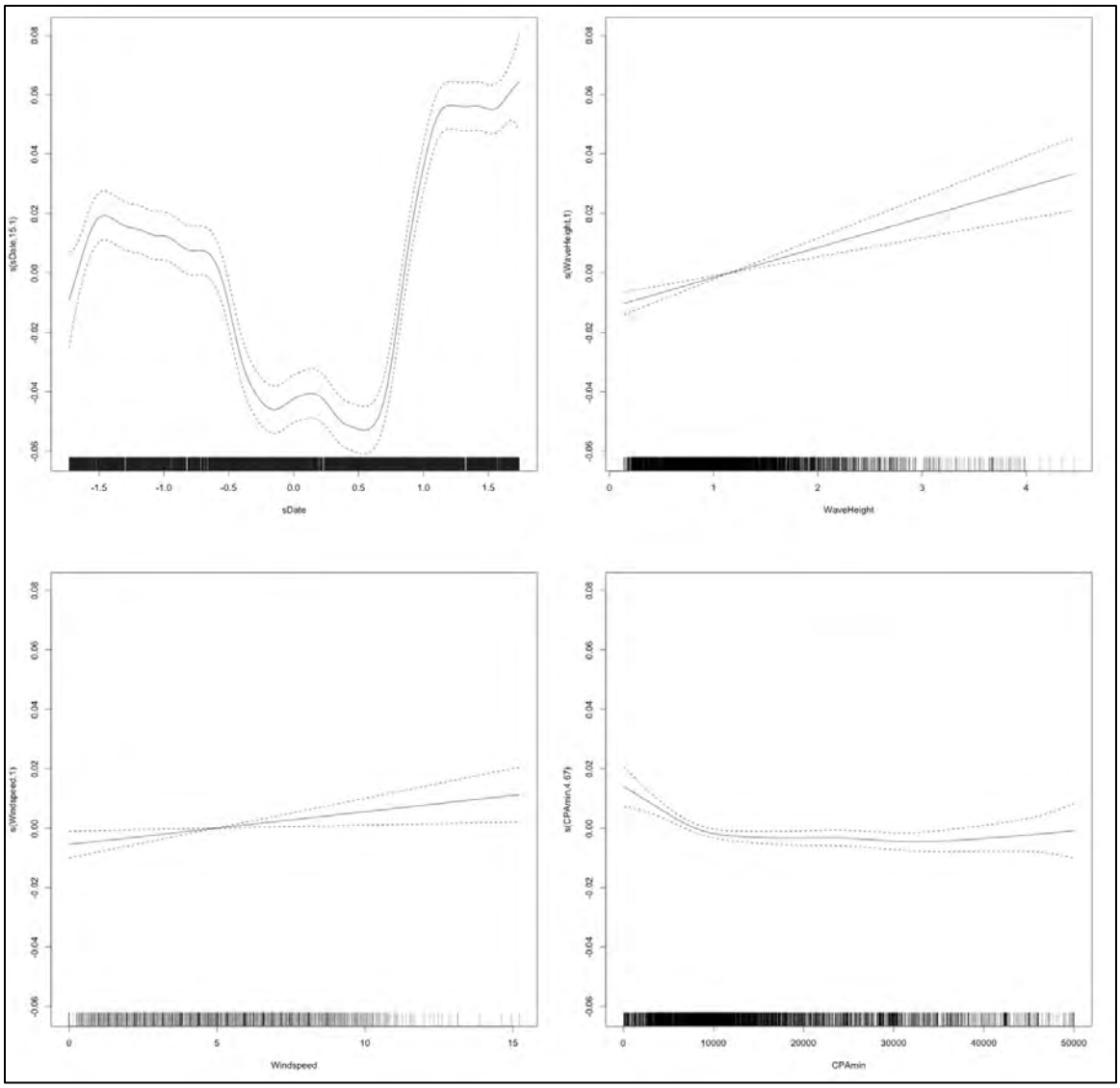

Figure E-B5. SA2 smoothing functions for Measured Vessel Band Noise as a function of Date, Wave Height, Windspeed, and CPA for Receiver 5, Deployment 2

Table E-B6. GAM output for Deployment 2, Receiver 6

A. parametric coefficients	Estimate	Std. Error	t-value	p-value
(Intercept)	4.6034	0.0008	5967.1622	< 0.0001
km2	0.0523	0.0046	11.3207	< 0.0001
km4	0.0120	0.0032	3.7479	0.0002
km10	0.0034	0.0013	2.6437	0.0082
B. smooth terms	**edf**	**Ref.df**	**F-value**	**p-value**
s(sDate)	42.6212	49.0000	44.2084	< 0.0001
s(WaveHeight)	3.8132	3.8132	36.4942	< 0.0001
s(Windspeed)	4.4370	4.4370	57.6110	< 0.0001
s(CPAmin)	3.0912	3.0912	20.6640	< 0.0001

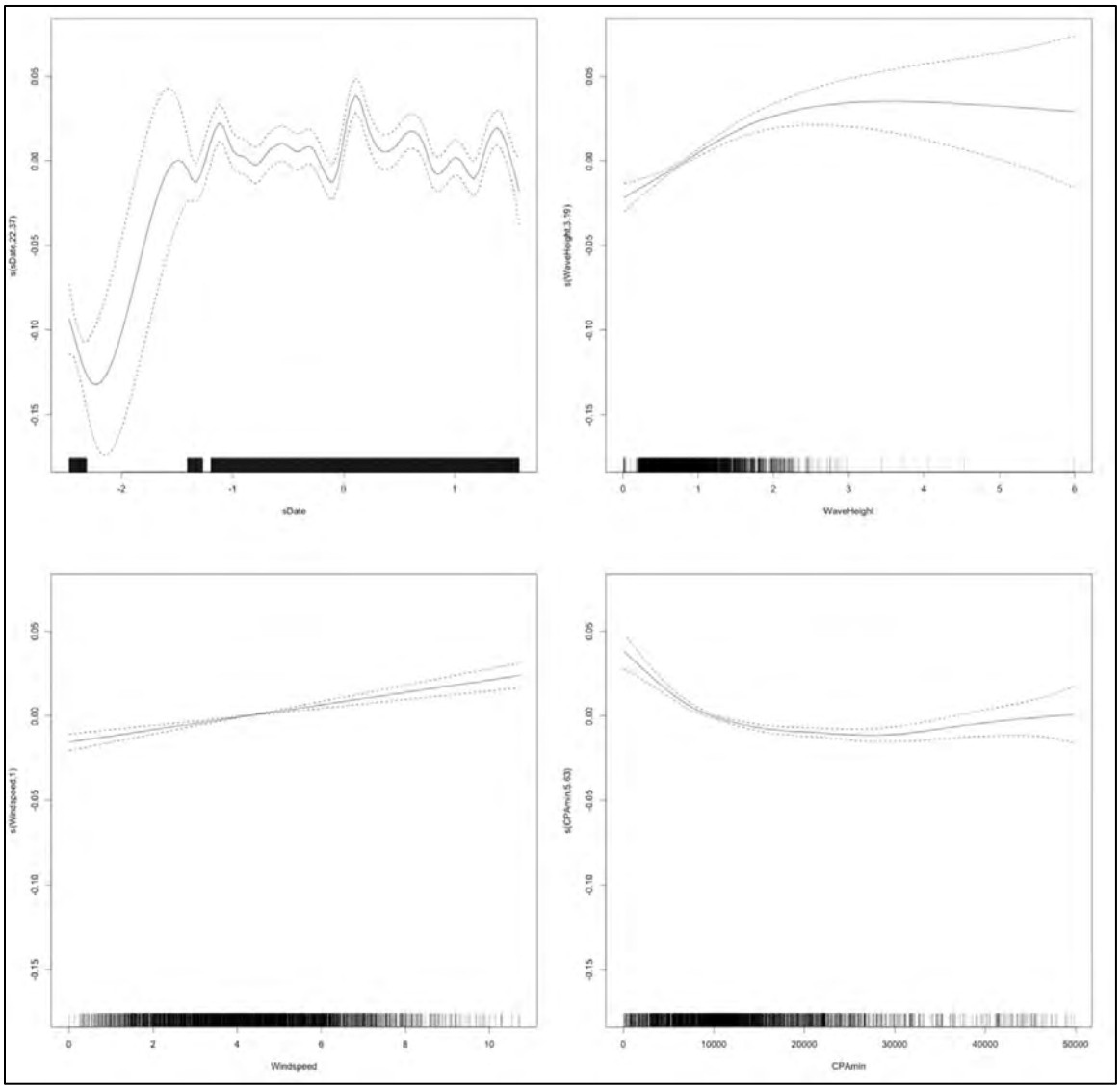

Figure E-B6. SA2 smoothing functions for Measured Vessel Band Noise as a function of Date, Wave Height, Windspeed, and CPA for Receiver 6, Deployment 2

Table E-B7. GAM output for Deployment 2, Receiver 7

A. parametric coefficients	Estimate	Std. Error	t-value	p-value
(Intercept)	4.6444	0.0012	3772.6038	< 0.0001
km2	0.0090	0.0031	2.9288	0.0034
km4	0.0098	0.0011	8.7537	< 0.0001
km10	0.0081	0.0005	15.2436	< 0.0001
B. smooth terms	**edf**	**Ref.df**	**F-value**	**p-value**
s(sDate)	33.4126	49.0000	29.6004	< 0.0001
s(WaveHeight)	1.0000	1.0000	14.4946	0.0001
s(Windspeed)	1.0000	1.0000	113.9104	< 0.0001
s(CPAmin)	7.8582	7.8582	32.9471	< 0.0001

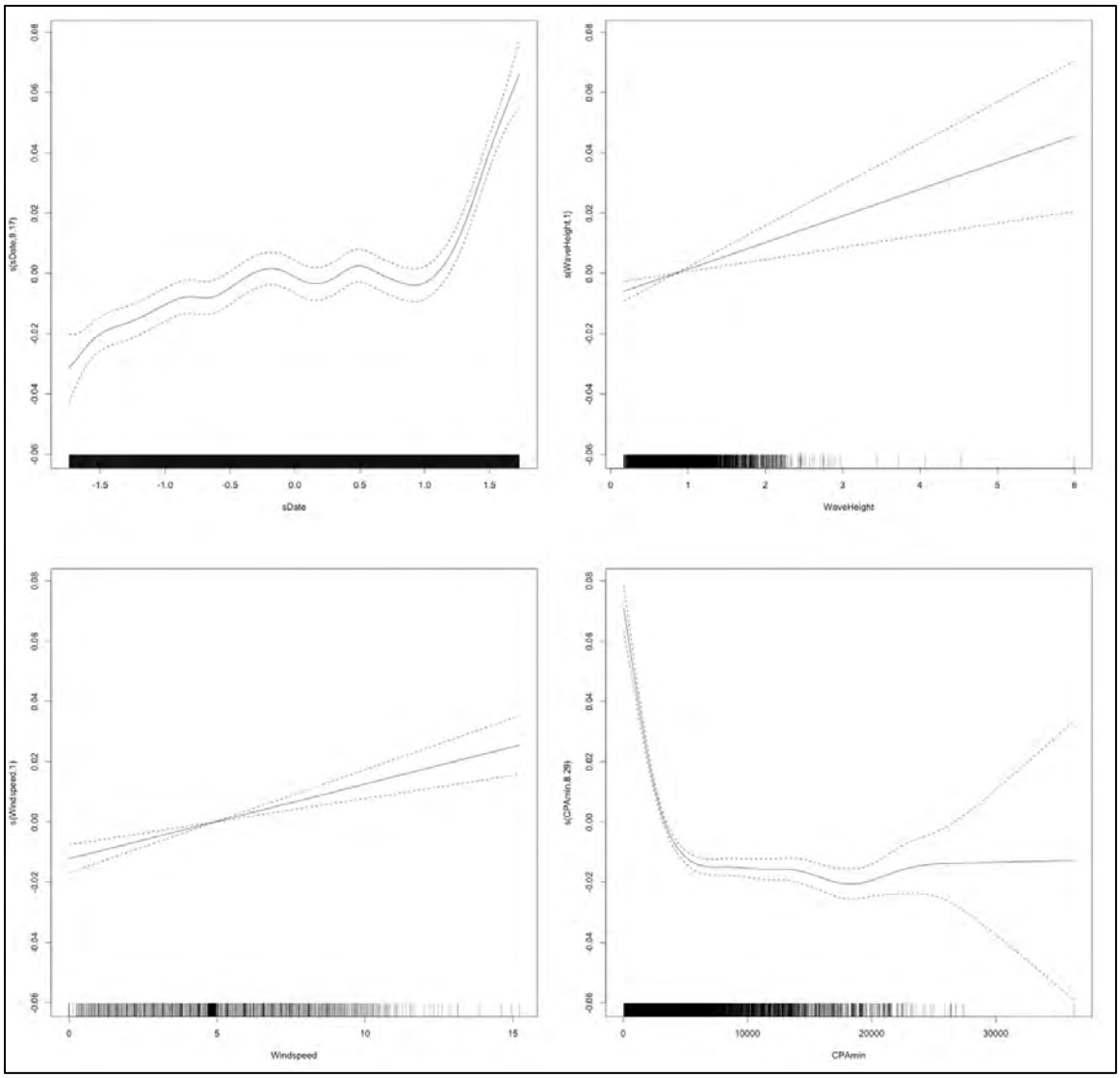

Figure E-B7. SA2 smoothing functions for Measured Vessel Band Noise as a function of Date, Wave Height, Windspeed, and CPA for Receiver 7, Deployment 2

Table E-B8. GAM output for Deployment 2, Receiver 8

A. parametric coefficients	Estimate	Std. Error	t-value	p-value
(Intercept)	4.5371	0.0011	4005.3062	< 0.0001
km2	0.0181	0.0059	3.0607	0.0022
km4	0.0033	0.0040	0.8269	0.4084
km10	0.0028	0.0015	1.8543	0.0639
B. smooth terms	**edf**	**Ref.df**	**F-value**	**p-value**
s(sDate)	43.8914	49.0000	41.1393	< 0.0001
s(WaveHeight)	1.0000	1.0000	14.9270	0.0001
s(Windspeed)	1.0000	1.0000	29.0399	< 0.0001
s(CPAmin)	4.2942	4.2942	3.3612	0.0076

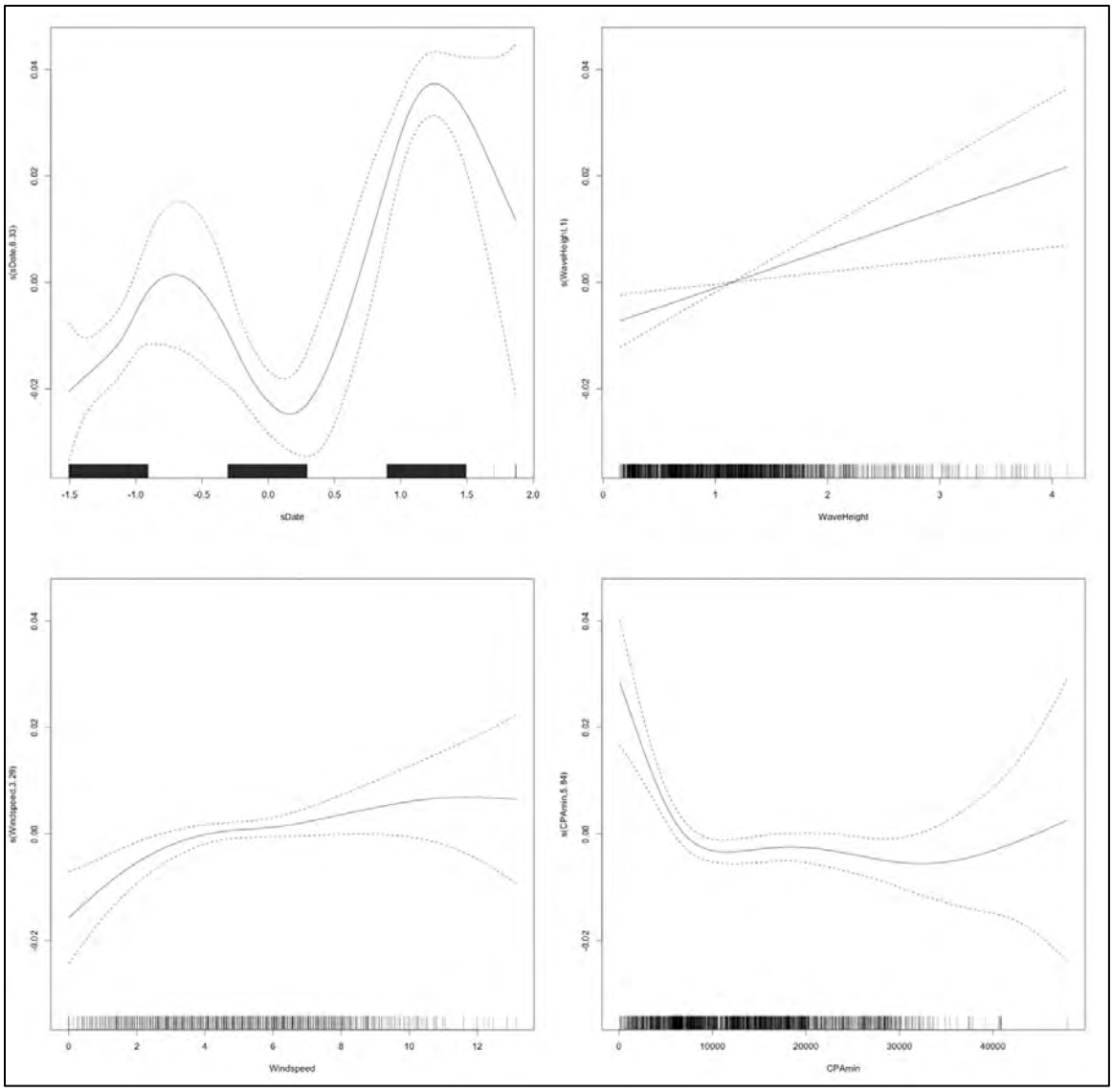

Figure E-B8. SA2 smoothing functions for Measured Vessel Band Noise as a function of Date, Wave Height, Windspeed, and CPA for Receiver 8, Deployment 2

Table E-B9. GAM output for Deployment 2, Receiver 9

A. parametric coefficients	Estimate	Std. Error	t-value	p-value
(Intercept)	4.6645	0.0007	6926.7316	< 0.0001
km2	0.0184	0.0044	4.2264	< 0.0001
km4	0.0089	0.0023	3.9112	0.0001
km10	0.0021	0.0009	2.3536	0.0186
B. smooth terms	**edf**	**Ref.df**	**F-value**	**p-value**
s(sDate)	44.6442	49.0000	74.4437	< 0.0001
s(WaveHeight)	1.0000	1.0000	3.9165	0.0479
s(Windspeed)	3.8640	3.8640	58.4151	< 0.0001
s(CPAmin)	7.9599	7.9599	21.8303	< 0.0001

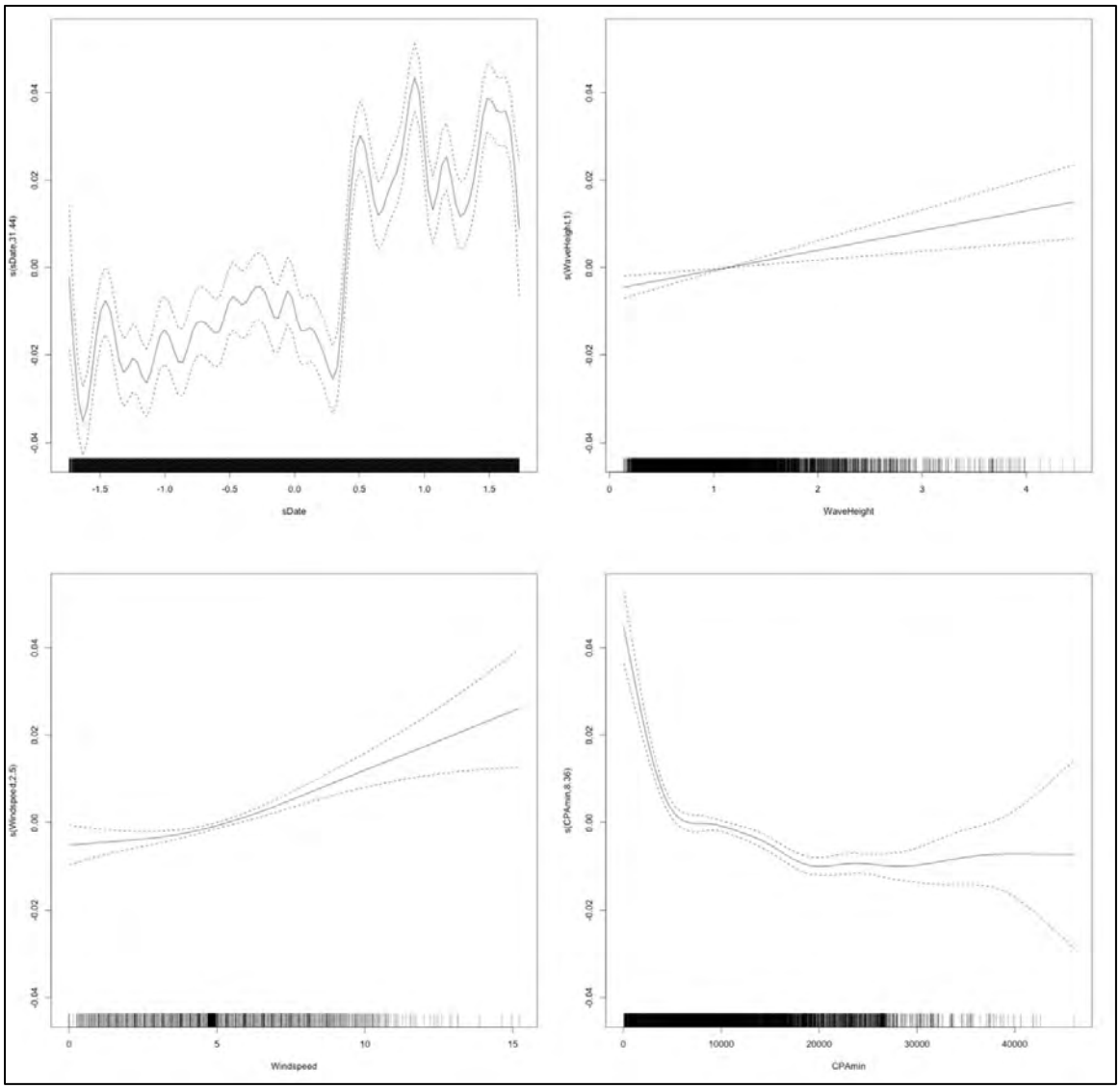

Figure E-B9. SA2 smoothing functions for Measured Vessel Band Noise as a function of Date, Wave Height, Windspeed, and CPA for Receiver 9, Deployment 2

Table E-B10. GAM output for Deployment 2, Receiver 10

A. parametric coefficients	Estimate	Std. Error	t-value	p-value
(Intercept)	4.5866	0.0022	2131.0235	< 0.0001
km2	0.0093	0.0040	2.3409	0.0193
km4	0.0068	0.0020	3.4809	0.0005
km10	0.0006	0.0005	1.1033	0.2700
B. smooth terms	**edf**	**Ref.df**	**F-value**	**p-value**
s(sDate)	45.3898	49.0000	24.7921	< 0.0001
s(WaveHeight)	7.4772	7.4772	7.8193	< 0.0001
s(Windspeed)	4.3854	4.3854	8.6116	< 0.0001
s(CPAmin)	7.9034	7.9034	23.5431	< 0.0001

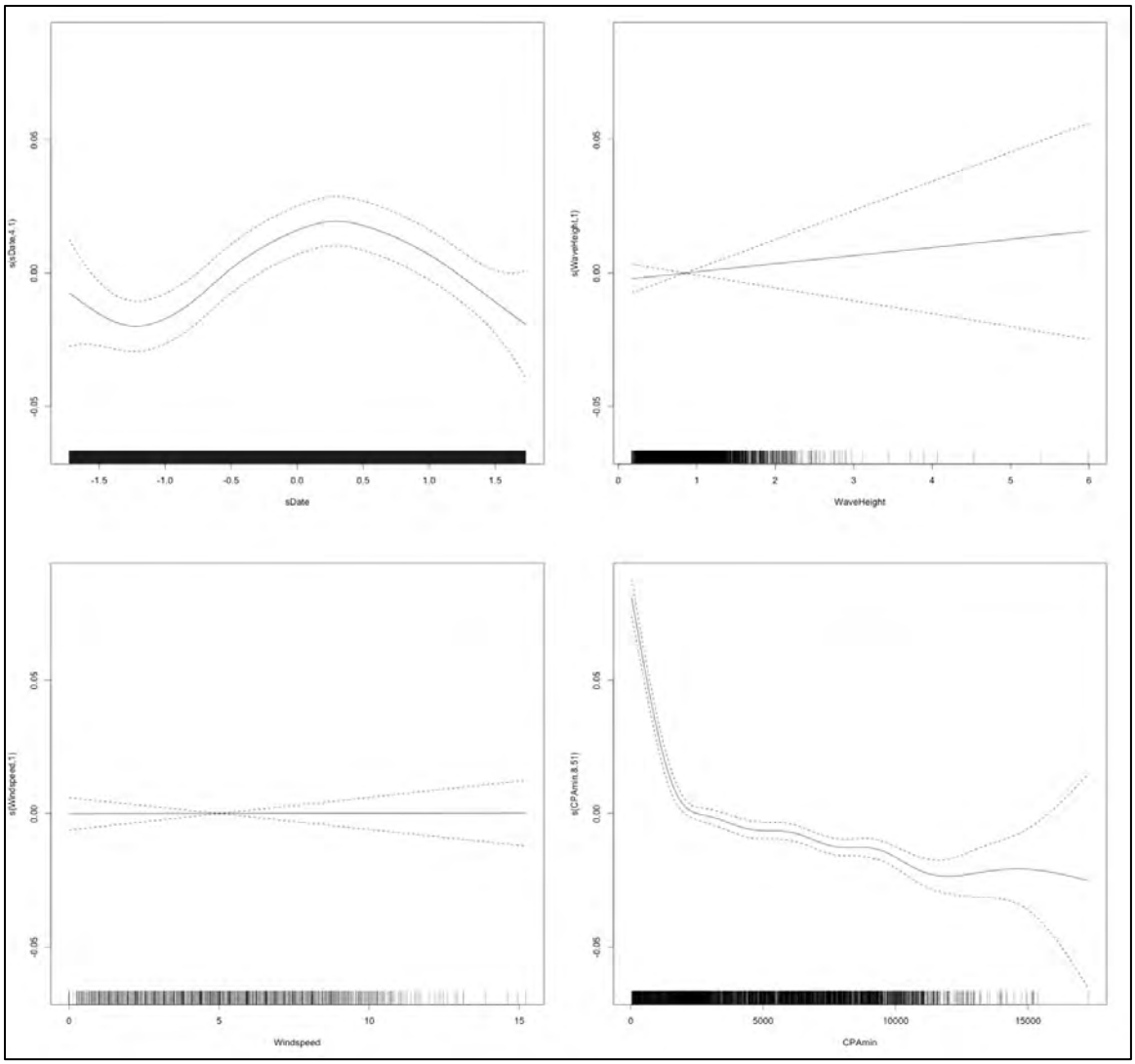

Figure E-B10. SA2 smoothing functions for Measured Vessel Band Noise as a function of Date, Wave Height, Windspeed, and CPA for Receiver 10, Deployment 2

DEPLOYMENT 3

Table E-B11. GAM output for Deployment 3, Receiver 1

A. parametric coefficients	Estimate	Std. Error	t-value	p-value
(Intercept)	4.7106	0.0008	5583.3855	< 0.0001
km2	0.0392	0.0051	7.6588	< 0.0001
km4	0.0203	0.0036	5.6526	< 0.0001
km10	0.0205	0.0023	8.7221	< 0.0001
B. smooth terms	**edf**	**Ref.df**	**F-value**	**p-value**
s(sDate)	44.0524	49.0000	147.6610	< 0.0001
s(WaveHeight)	6.2418	6.2418	9.3809	< 0.0001
s(Windspeed)	1.0000	1.0000	10.5758	0.0012
s(CPAmin)	1.0000	1.0000	36.7337	< 0.0001

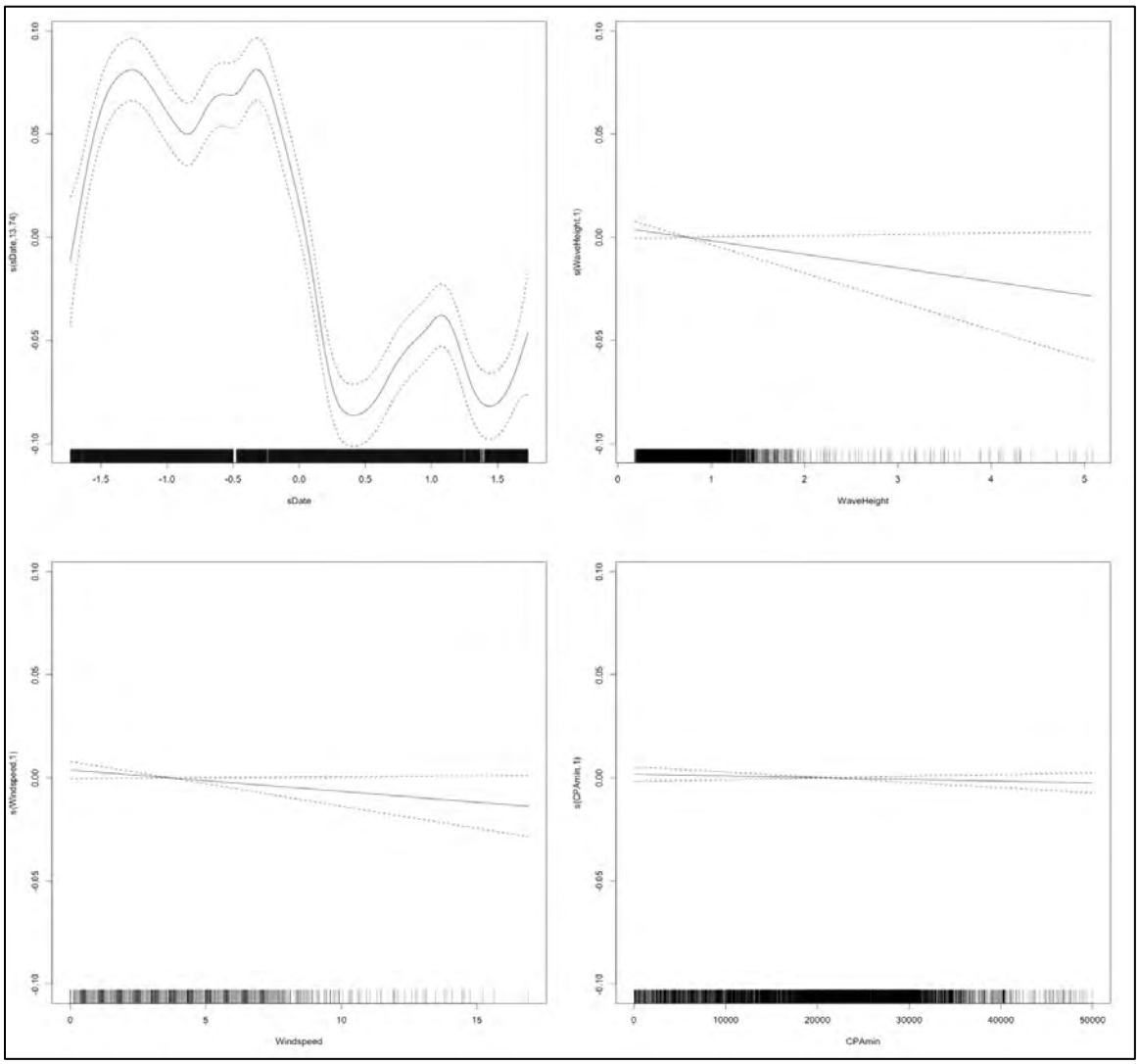

Figure E-B11. SA2 smoothing functions for Measured Vessel Band Noise as a function of Date, Wave Height, Windspeed, and CPA for Receiver 1, Deployment 3

Table E-B12. GAM output for Deployment 3, Receiver 2

A. parametric coefficients	Estimate	Std. Error	t-value	p-value
(Intercept)	4.5523	0.0011	4004.1760	< 0.0001
km2	-0.0112	0.0103	-1.0841	0.2784
km4	-0.0312	0.0068	-4.5934	< 0.0001
km10	-0.0137	0.0028	-4.9573	< 0.0001
B. smooth terms	**edf**	**Ref.df**	**F-value**	**p-value**
s(sDate)	42.6704	49.0000	144.4241	< 0.0001
s(WaveHeight)	1.0000	1.0000	3.1564	0.0757
s(Windspeed)	1.0000	1.0000	32.8006	< 0.0001
s(CPAmin)	5.4551	5.4551	25.9581	< 0.0001

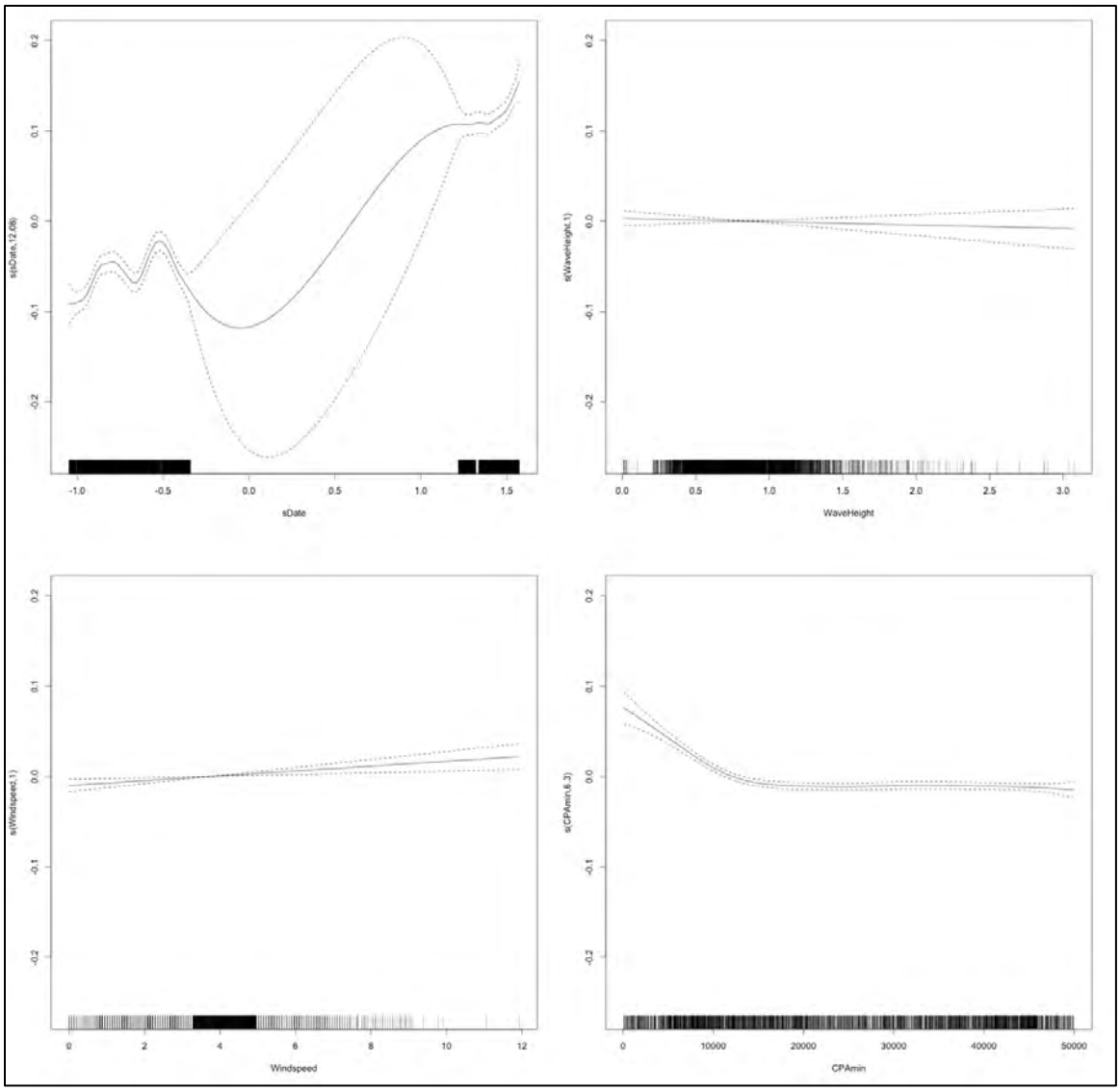

Figure E-B12. SA2 smoothing functions for Measured Vessel Band Noise as a function of Date, Wave Height, Windspeed, and CPA for Receiver 2, Deployment 3

Table E-B13. GAM output for Deployment 3, Receiver 3

A. parametric coefficients	Estimate	Std. Error	t-value	p-value
(Intercept)	4.6716	0.0012	4015.3891	< 0.0001
km2	0.0253	0.0120	2.1138	0.0346
km4	0.0303	0.0083	3.6505	0.0003
km10	0.0209	0.0039	5.4245	< 0.0001
B. smooth terms	**edf**	**Ref.df**	**F-value**	**p-value**
s(sDate)	43.0388	49.0000	86.1402	< 0.0001
s(WaveHeight)	1.8306	1.8306	1.4331	0.1646
s(Windspeed)	2.3699	2.3699	5.2449	0.0090
s(CPAmin)	7.0365	7.0365	23.1367	< 0.0001

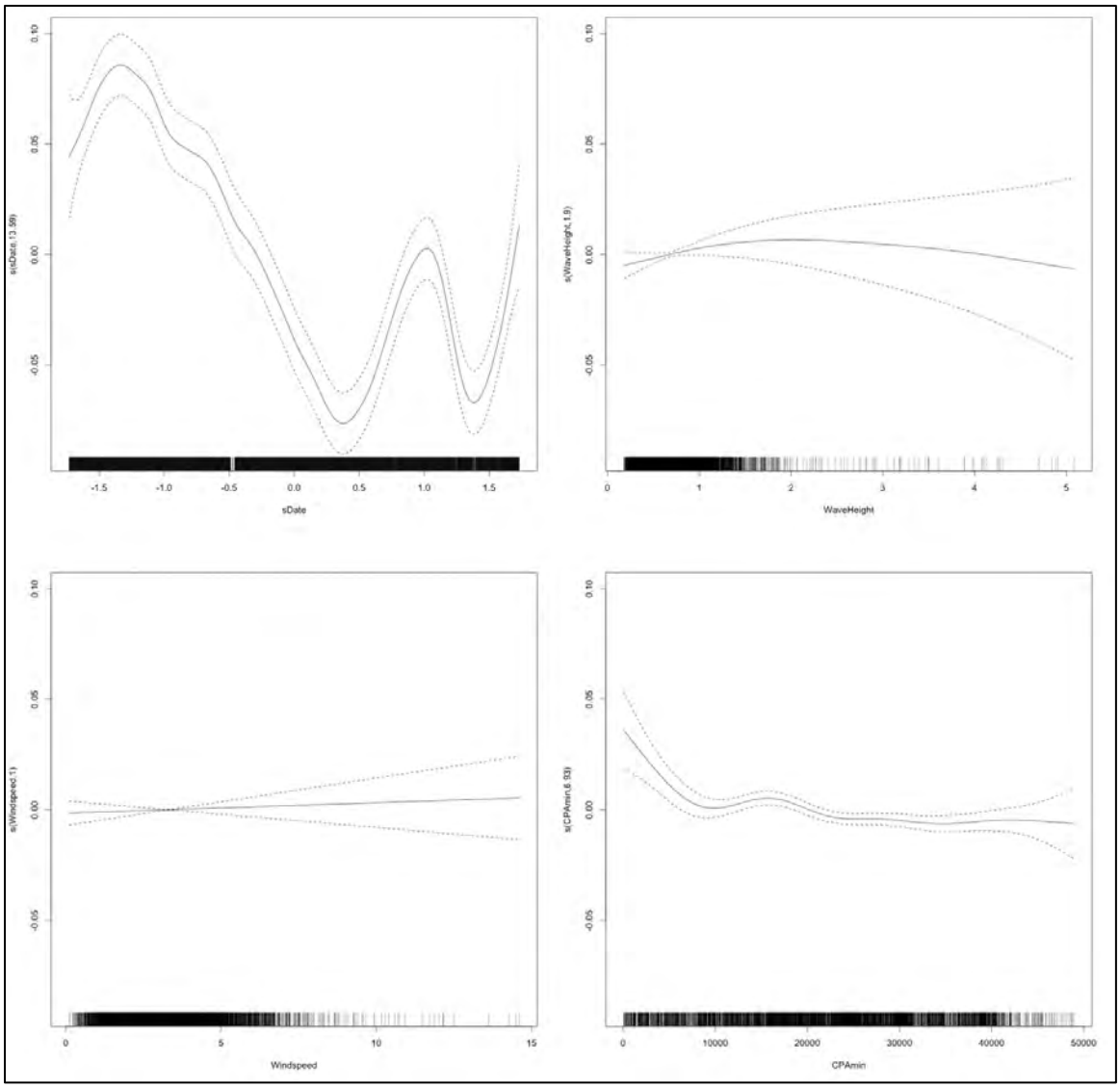

Figure E-B13. SA2 smoothing functions for Measured Vessel Band Noise as a function of Date, Wave Height, Windspeed, and CPA for Receiver 3, Deployment 3

Table E-B14. GAM output for Deployment 3, Receiver 4

A. parametric coefficients	Estimate	Std. Error	t-value	p-value
(Intercept)	4.6399	0.0010	4692.0769	< 0.0001
km2	0.0271	0.0089	3.0515	0.0023
km4	0.0076	0.0044	1.7342	0.0830
km10	0.0078	0.0018	4.3025	< 0.0001
B. smooth terms	**edf**	**Ref.df**	**F-value**	**p-value**
s(sDate)	45.8327	49.0000	138.4059	< 0.0001
s(WaveHeight)	1.0000	1.0000	0.0533	0.8175
s(Windspeed)	1.9841	1.9841	4.1933	0.0216
s(CPAmin)	8.3865	8.3865	15.2919	< 0.0001

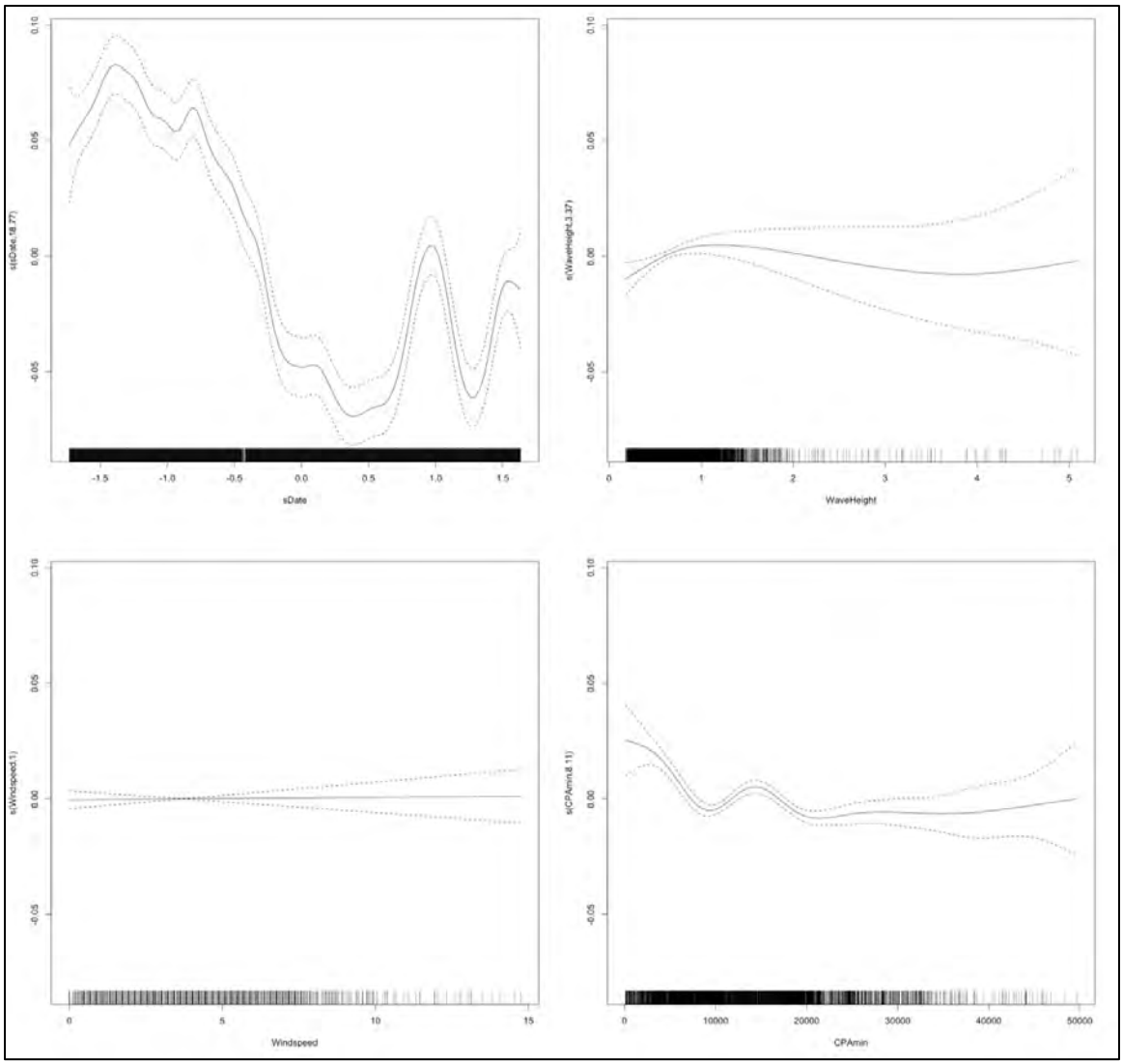

Figure E-B14. SA2 smoothing functions for Measured Vessel Band Noise as a function of Date, Wave Height, Windspeed, and CPA for Receiver 4, Deployment 3

Table E-B15. GAM output for Deployment 3, Receiver 5

A. parametric coefficients	Estimate	Std. Error	t-value	p-value
(Intercept)	4.6514	0.0012	3788.2411	< 0.0001
km2	0.0149	0.0064	2.3187	0.0205
km4	0.0115	0.0041	2.7675	0.0057
km10	0.0059	0.0015	3.9861	0.0001
B. smooth terms	**edf**	**Ref.df**	**F-value**	**p-value**
s(sDate)	44.6340	49.0000	176.4041	< 0.0001
s(WaveHeight)	4.6557	4.6557	3.2043	0.0116
s(Windspeed)	1.0000	1.0000	0.0003	0.9874
s(CPAmin)	4.7100	4.7100	9.8872	< 0.0001

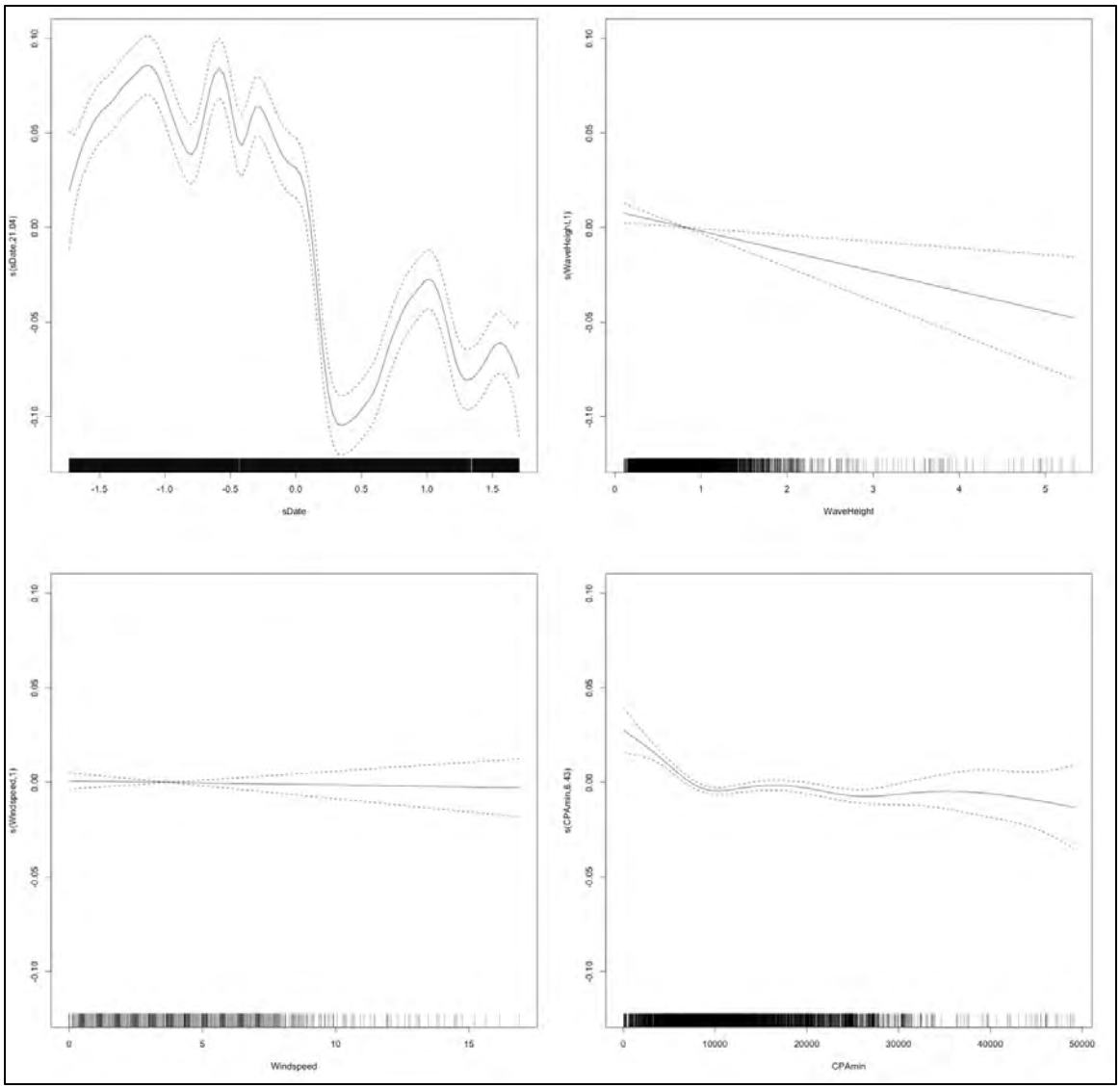

Figure E-B15. SA2 smoothing functions for Measured Vessel Band Noise as a function of Date, Wave Height, Windspeed, and CPA for Receiver 5, Deployment 3

Table E-B16. GAM output for Deployment 3, Receiver 6

A. parametric coefficients	Estimate	Std. Error	t-value	p-value
(Intercept)	4.6818	0.0081	579.0495	< 0.0001
km2	-0.0034	0.0250	-0.1365	0.8917
km4	-0.0080	0.0187	-0.4276	0.6699
km10	-0.0000	0.0085	-0.0003	0.9997
B. smooth terms	**edf**	**Ref.df**	**F-value**	**p-value**
s(sDate)	0.0000	49.0000	0.0000	0.1608
s(WaveHeight)	1.0000	1.0000	4.6772	0.0331
s(Windspeed)	1.0000	1.0000	4.0072	0.0481
s(CPAmin)	1.0001	1.0001	0.7616	0.3850

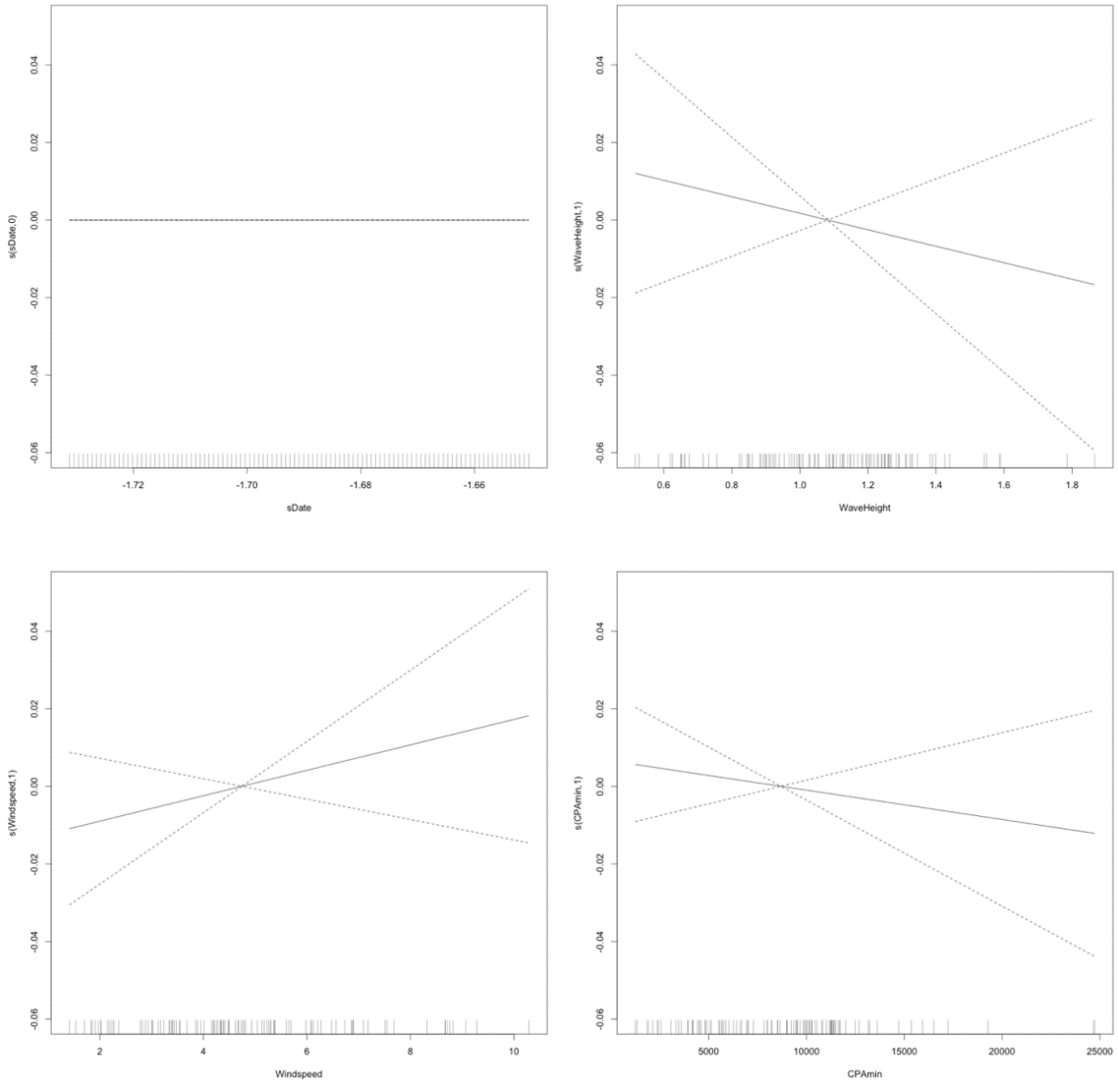

Figure E-B16. SA2 smoothing functions for Measured Vessel Band Noise as a function of Date, Wave Height, Windspeed, and CPA for Receiver 6, Deployment 3

Table E-B17. GAM output for Deployment 3, Receiver 7

A. parametric coefficients	Estimate	Std. Error	t-value	p-value
(Intercept)	4.6113	0.0013	3561.7373	< 0.0001
km2	0.0051	0.0031	1.6183	0.1057
km4	0.0078	0.0013	6.0980	< 0.0001
km10	0.0048	0.0006	8.3078	< 0.0001
B. smooth terms	**edf**	**Ref.df**	**F-value**	**p-value**
s(sDate)	20.5795	49.0000	16.8289	< 0.0001
s(WaveHeight)	2.4064	2.4064	11.1277	< 0.0001
s(Windspeed)	4.0557	4.0557	22.8863	< 0.0001
s(CPAmin)	8.6301	8.6301	62.8541	< 0.0001

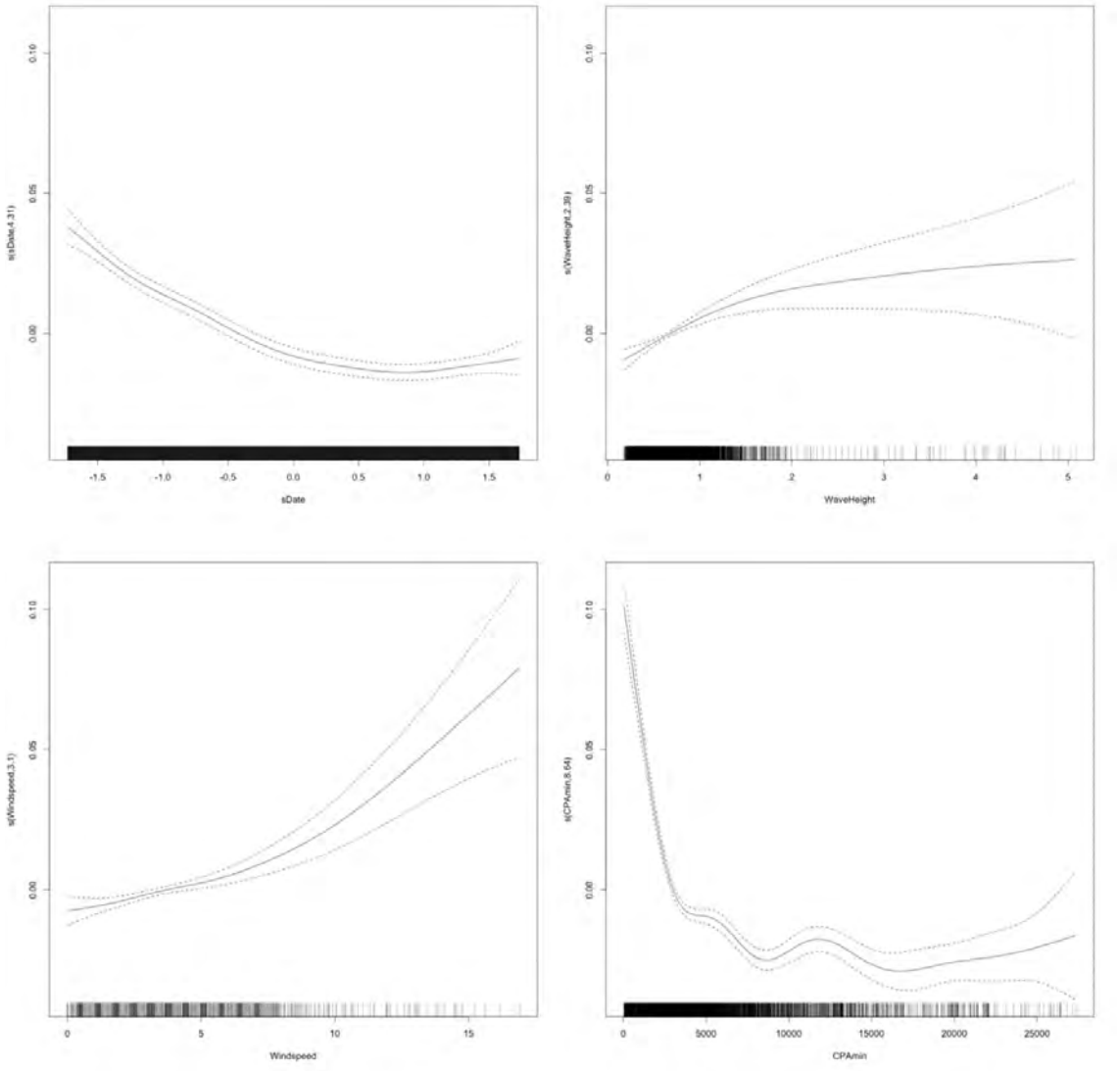

Figure E-B17. SA2 smoothing functions for Measured Vessel Band Noise as a function of Date, Wave Height, Windspeed, and CPA for Receiver 7, Deployment 3

Table E-B18. GAM output for Deployment 3, Receiver 8

A. parametric coefficients	Estimate	Std. Error	t-value	p-value
(Intercept)	4.6536	0.0015	3025.7303	< 0.0001
km2	0.0241	0.0033	7.3836	< 0.0001
km4	0.0191	0.0026	7.3730	< 0.0001
km10	0.0081	0.0011	7.6352	< 0.0001
B. smooth terms	**edf**	**Ref.df**	**F-value**	**p-value**
s(sDate)	46.5480	49.0000	66.2399	< 0.0001
s(WaveHeight)	4.9890	4.9890	4.8216	0.0003
s(Windspeed)	3.4829	3.4829	10.4949	< 0.0001
s(CPAmin)	1.0000	1.0000	1.8984	0.1683

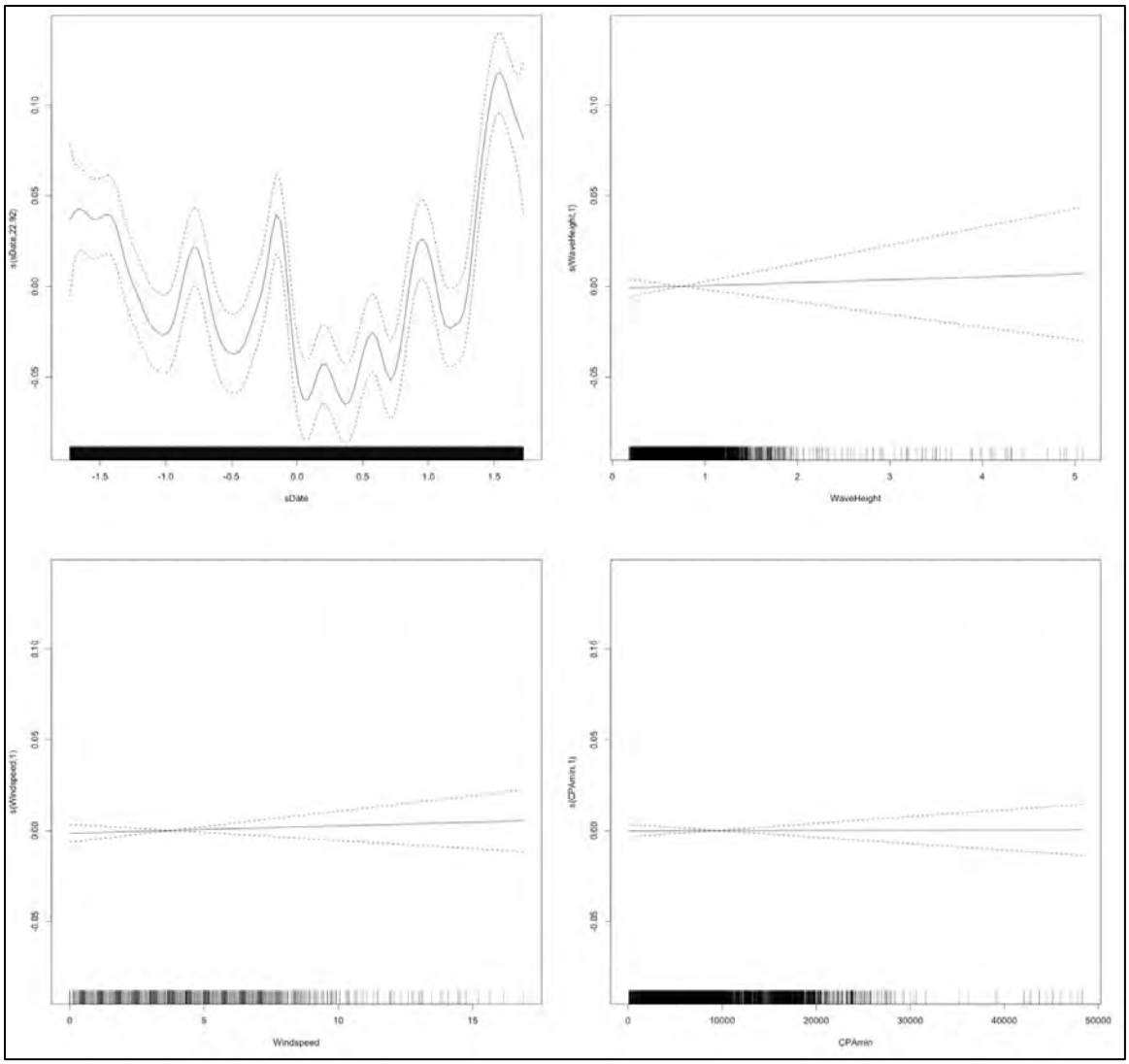

Figure E-B18. SA2 smoothing functions for Measured Vessel Band Noise as a function of Date, Wave Height, Windspeed, and CPA for Receiver 8, Deployment 3

Table E-B19. GAM output for Deployment 3, Receiver 9

A. parametric coefficients	Estimate	Std. Error	t-value	p-value
(Intercept)	4.7204	0.0013	3536.0458	< 0.0001
km2	0.0090	0.0059	1.5319	0.1256
km4	0.0150	0.0042	3.5468	0.0004
km10	0.0043	0.0011	3.9506	0.0001
B. smooth terms	**edf**	**Ref.df**	**F-value**	**p-value**
s(sDate)	43.2615	49.0000	147.6671	< 0.0001
s(WaveHeight)	4.8635	4.8635	4.1541	0.0019
s(Windspeed)	1.0000	1.0000	5.5435	0.0186
s(CPAmin)	4.3039	4.3039	2.8746	0.0155

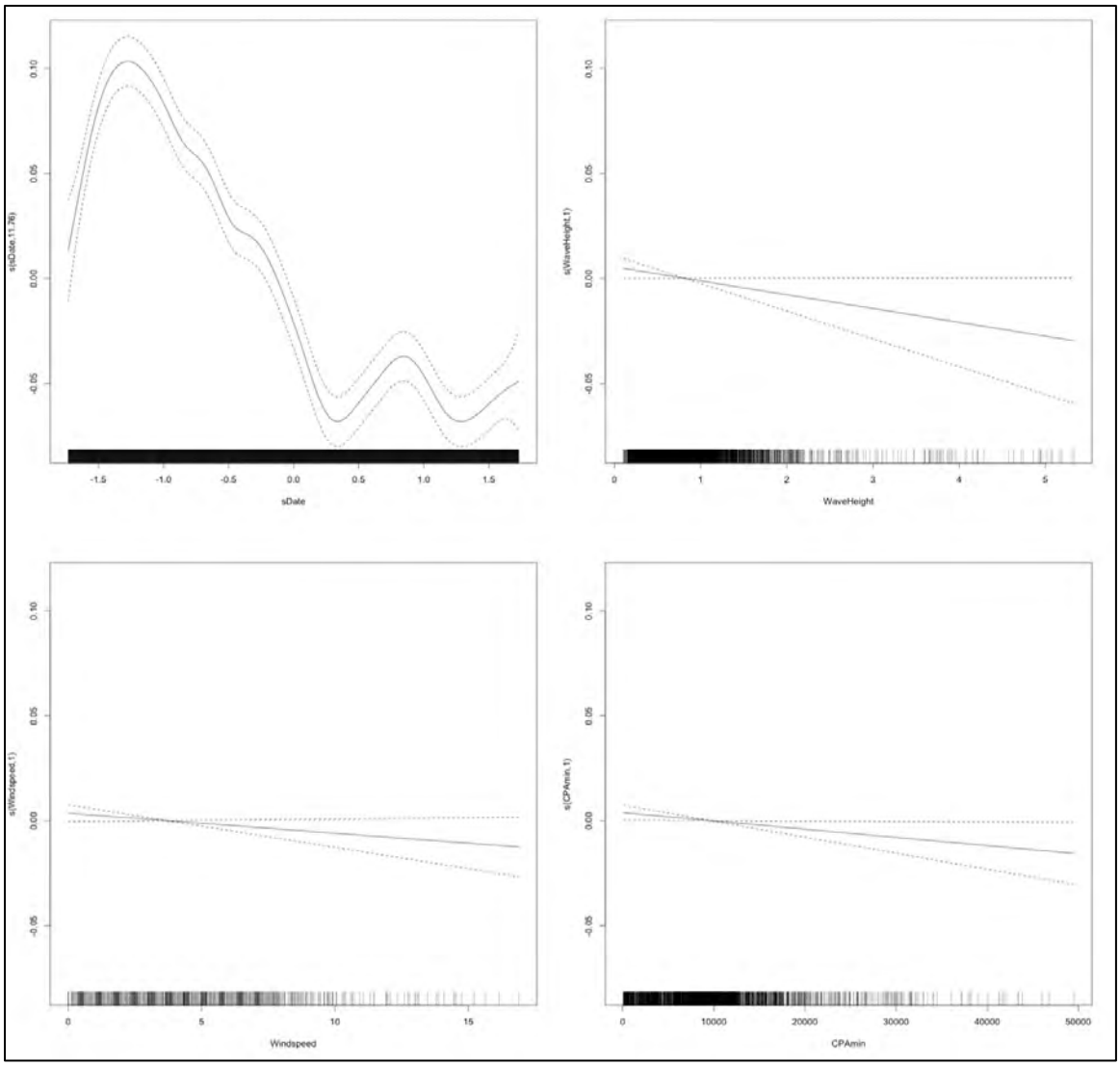

Figure E-B19. SA2 smoothing functions for Measured Vessel Band Noise as a function of Date, Wave Height, Windspeed, and CPA for Receiver 9, Deployment 3

Table E-B20. GAM output for Deployment 3, Receiver 10

A. parametric coefficients	Estimate	Std. Error	t-value	p-value
(Intercept)	4.5806	0.0008	5402.7881	< 0.0001
km2	-0.0836	0.0221	-3.7799	0.0002
km4	-0.0666	0.0135	-4.9520	< 0.0001
km10	-0.0351	0.0069	-5.1095	< 0.0001
B. smooth terms	**edf**	**Ref.df**	**F-value**	**p-value**
s(sDate)	46.2455	49.0000	333.3361	< 0.0001
s(WaveHeight)	1.0000	1.0000	0.0866	0.7685
s(Windspeed)	1.0000	1.0000	18.6115	< 0.0001
s(CPAmin)	7.5534	7.5534	14.9459	< 0.0001

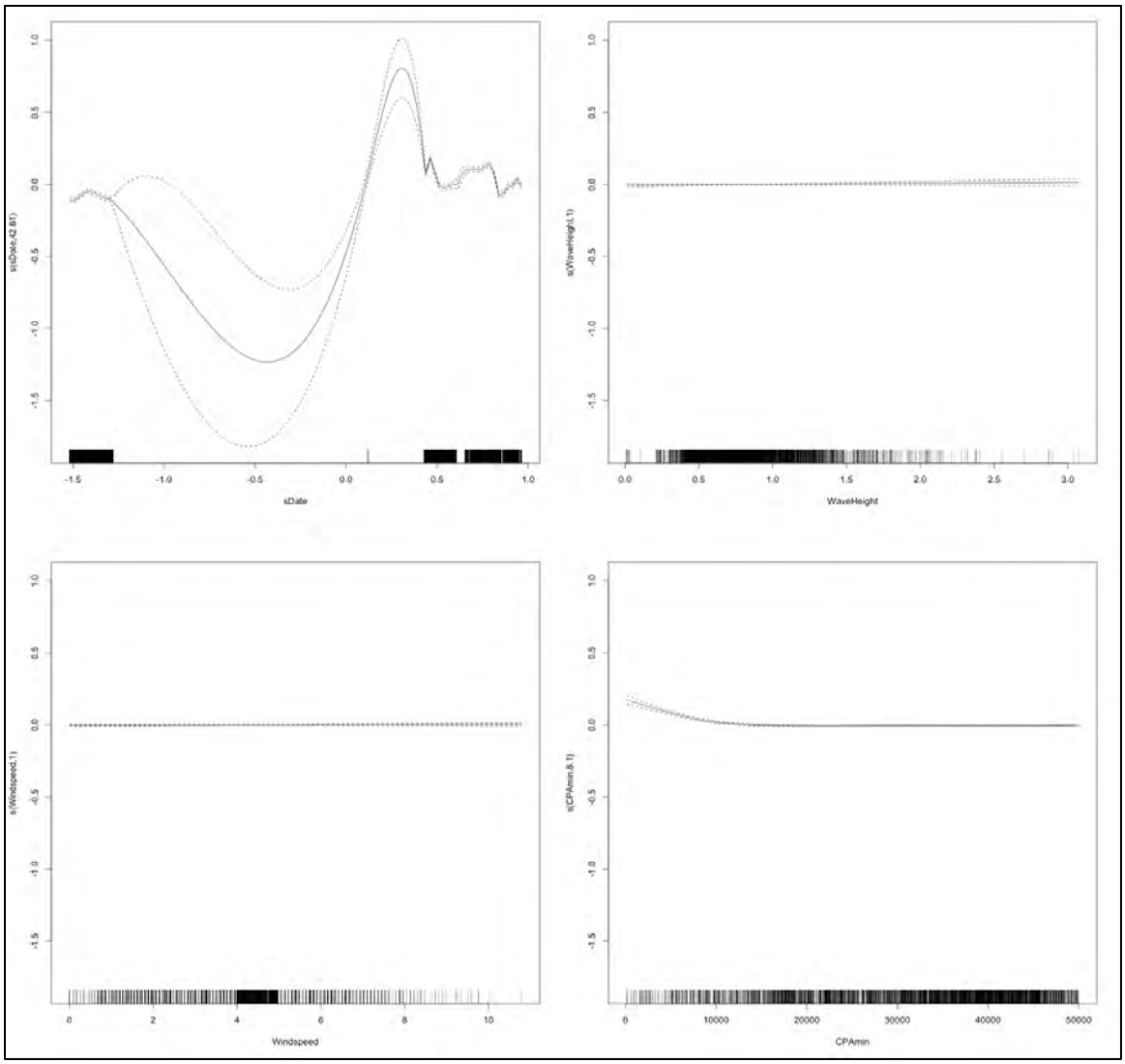

Figure E-B20. SA2 smoothing functions for Measured Vessel Band Noise as a function of Date, Wave Height, Windspeed, and CPA for Receiver 10, Deployment 3

Table E-B21. GAM output for Deployment 4, Receiver 1

A. parametric coefficients	Estimate	Std. Error	t-value	p-value
(Intercept)	4.5883	0.0008	5444.7796	< 0.0001
km2	0.0072	0.0057	1.2568	0.2089
km4	0.0113	0.0033	3.4648	0.0005
km10	0.0076	0.0011	6.7575	< 0.0001
B. smooth terms	**edf**	**Ref.df**	**F-value**	**p-value**
s(sDate)	47.5477	49.0000	114.2021	< 0.0001
s(WaveHeight)	1.0000	1.0000	1.5406	0.2146
s(Windspeed)	4.2631	4.2631	25.2727	< 0.0001
s(CPAmin)	6.8045	6.8045	8.0060	< 0.0001

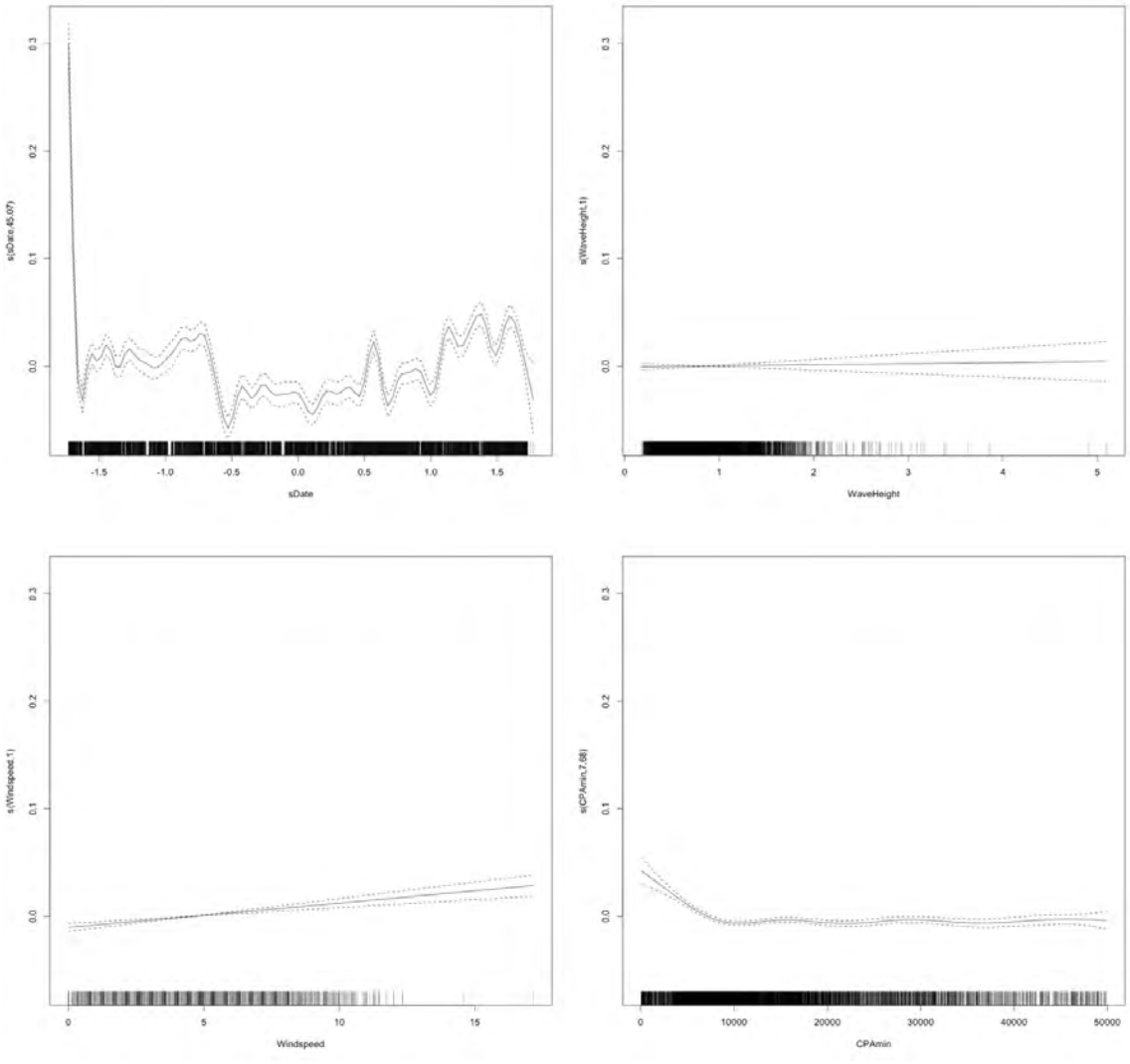

Figure E-B21. SA2 smoothing functions for Measured Vessel Band Noise as a function of Date, Wave Height, Windspeed, and CPA for Receiver 1, Deployment 4

Table E-B22. GAM output for Deployment 4, Receiver 2

A. parametric coefficients	Estimate	Std. Error	t-value	p-value
(Intercept)	4.5883	0.0008	5444.7796	< 0.0001
km2	0.0072	0.0057	1.2568	0.2089
km4	0.0113	0.0033	3.4648	0.0005
km10	0.0076	0.0011	6.7575	< 0.0001
B. smooth terms	**edf**	**Ref.df**	**F-value**	**p-value**
s(sDate)	47.5477	49.0000	114.2021	< 0.0001
s(WaveHeight)	1.0000	1.0000	1.5406	0.2146
s(Windspeed)	4.2631	4.2631	25.2727	< 0.0001
s(CPAmin)	6.8045	6.8045	8.0060	< 0.0001

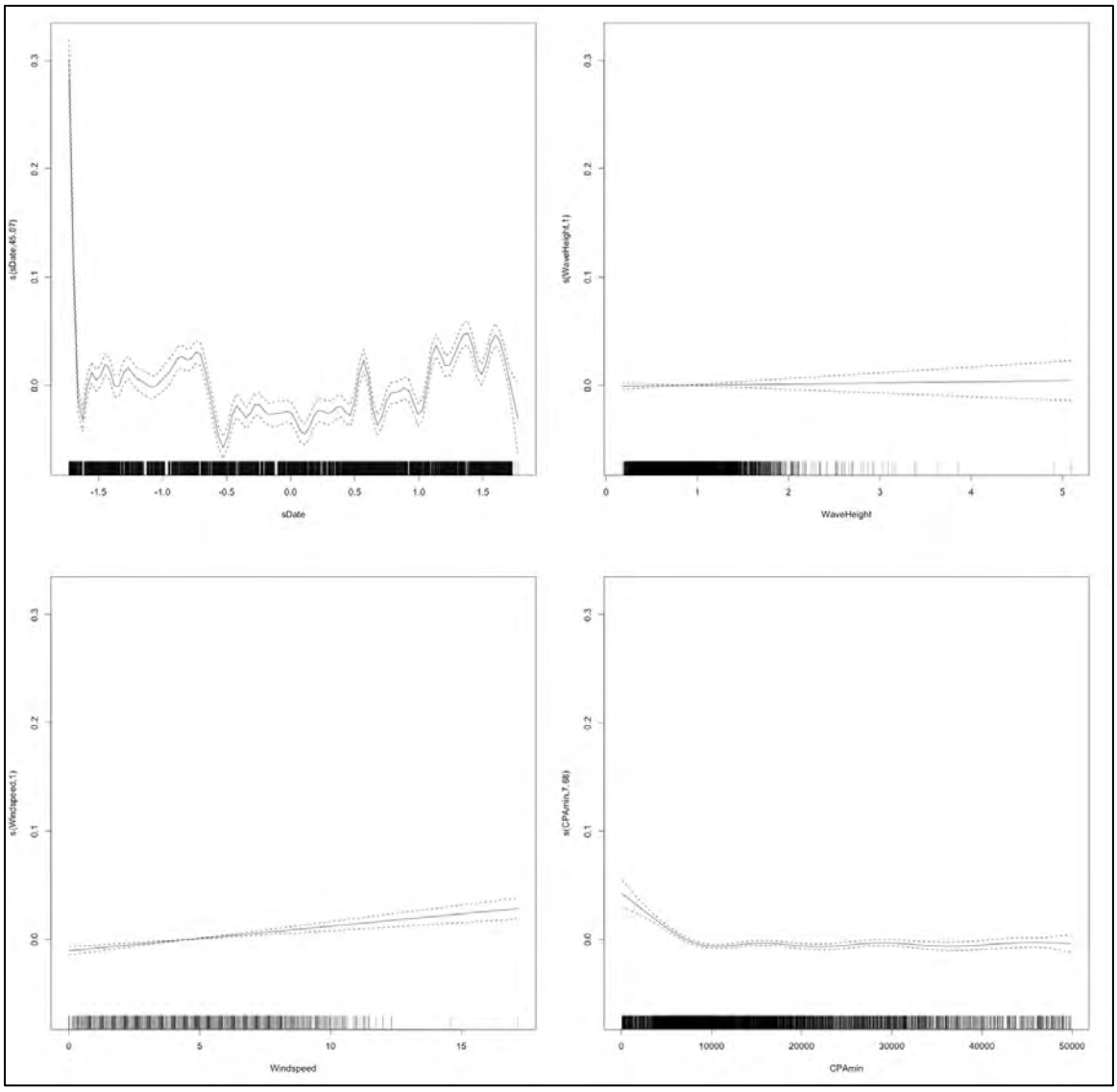

Figure E-B22. SA2 smoothing functions for Measured Vessel Band Noise as a function of Date, Wave Height, Windspeed, and CPA for Receiver 2, Deployment 4

Table E-B23. GAM output for Deployment 4, Receiver 3

A. parametric coefficients	Estimate	Std. Error	t-value	p-value
(Intercept)	4.6453	0.0005	10197.2121	< 0.0001
km2	0.0536	0.0034	15.7011	< 0.0001
km4	0.0282	0.0034	8.2993	< 0.0001
km10	0.0071	0.0020	3.4685	0.0005
B. smooth terms	**edf**	**Ref.df**	**F-value**	**p-value**
s(sDate)	46.6381	49.0000	168.6880	< 0.0001
s(WaveHeight)	7.4054	7.4054	5.9423	< 0.0001
s(Windspeed)	7.2849	7.2849	28.8772	< 0.0001
s(CPAmin)	1.0000	1.0000	0.0007	0.9788

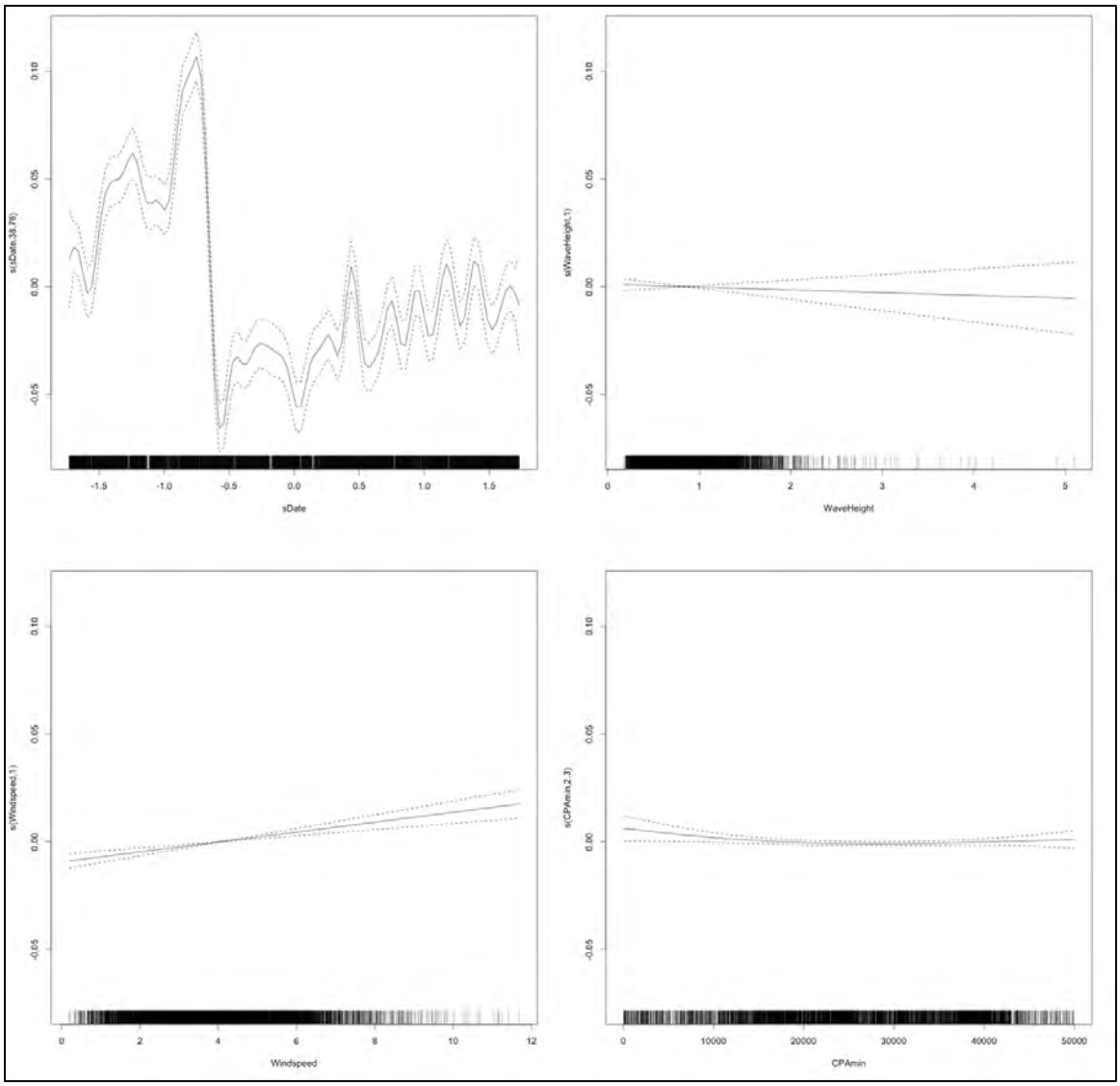

Figure E-B23. SA2 smoothing functions for Measured Vessel Band Noise as a function of Date, Wave Height, Windspeed, and CPA for Receiver 3, Deployment 4

Table E-B24. GAM output for Deployment 4, Receiver 4

A. parametric coefficients	Estimate	Std. Error	t-value	p-value
(Intercept)	4.6076	0.0005	8797.6343	< 0.0001
km2	-0.0005	0.0047	-0.1152	0.9083
km4	-0.0036	0.0030	-1.2038	0.2287
km10	0.0024	0.0015	1.5669	0.1172
B. smooth terms	**edf**	**Ref.df**	**F-value**	**p-value**
s(sDate)	47.2705	49.0000	212.8172	< 0.0001
s(WaveHeight)	3.1221	3.1221	7.1035	0.0001
s(Windspeed)	7.3690	7.3690	12.5711	< 0.0001
s(CPAmin)	7.3001	7.3001	8.8686	< 0.0001

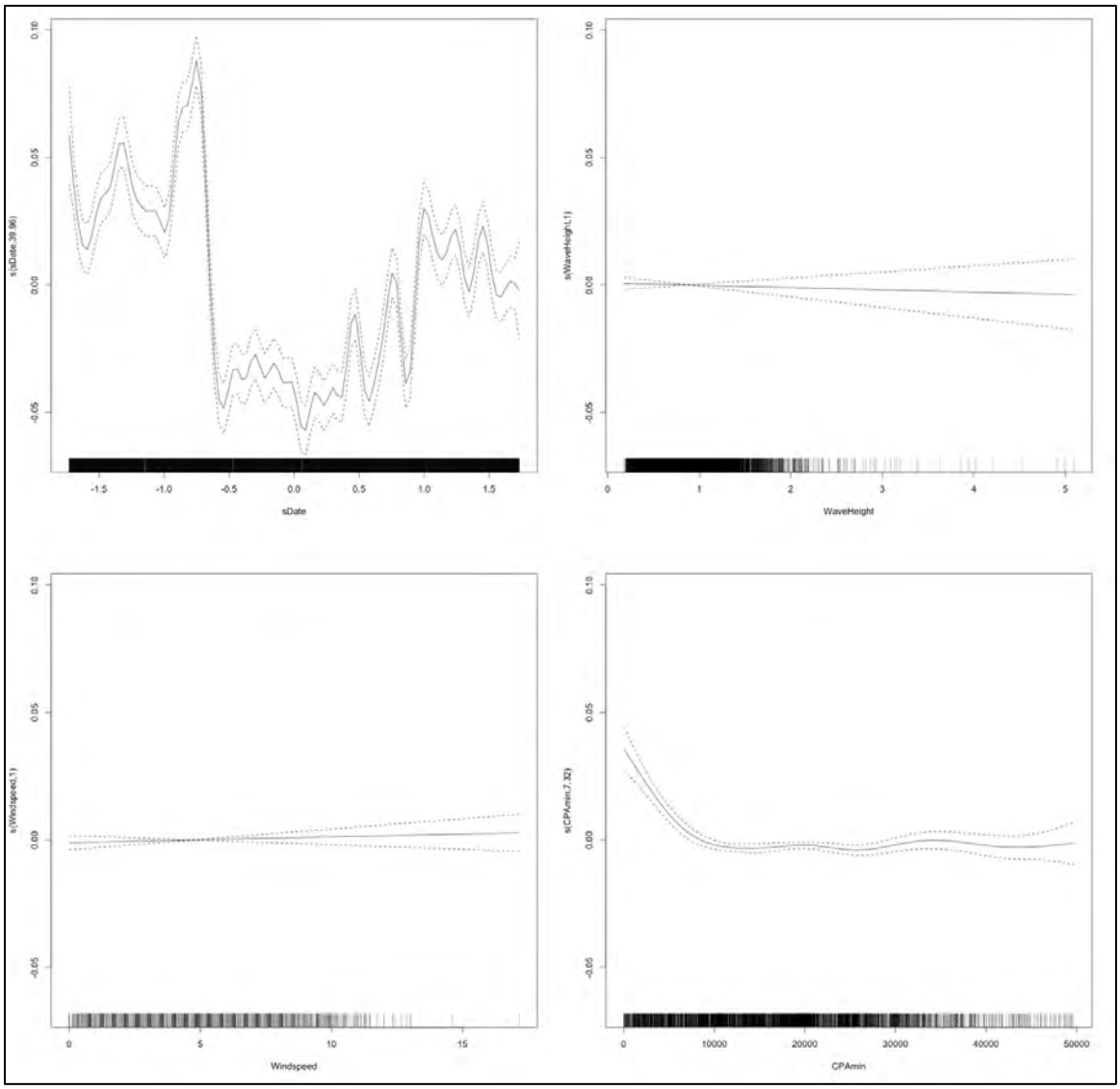

Figure E-B24. SA2 smoothing functions for Measured Vessel Band Noise as a function of Date, Wave Height, Windspeed, and CPA for Receiver 4, Deployment 4

Table E-B25. GAM output for Deployment 4, Receiver 5

A. parametric coefficients	Estimate	Std. Error	t-value	p-value
(Intercept)	4.6397	0.0008	6059.5104	< 0.0001
km2	0.0037	0.0048	0.7645	0.4446
km4	0.0031	0.0032	0.9704	0.3319
km10	0.0034	0.0010	3.3206	0.0009
B. smooth terms	**edf**	**Ref.df**	**F-value**	**p-value**
s(sDate)	47.9023	49.0000	271.6773	< 0.0001
s(WaveHeight)	3.0305	3.0305	12.5542	< 0.0001
s(Windspeed)	2.7783	2.7783	12.3704	< 0.0001
s(CPAmin)	5.1568	5.1568	4.8082	0.0002

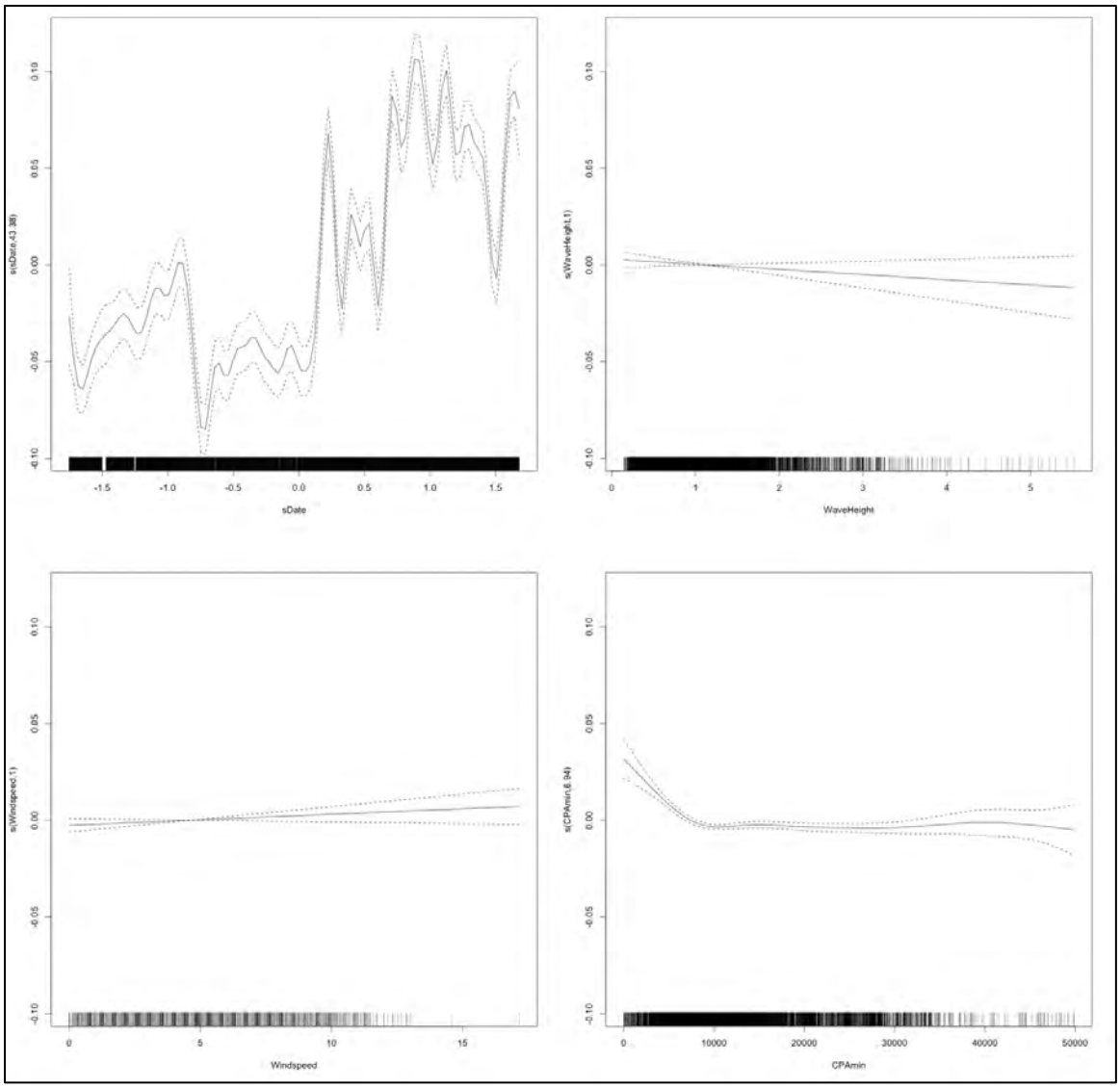

Figure E-B25. SA2 smoothing functions for Measured Vessel Band Noise as a function of Date, Wave Height, Windspeed, and CPA for Receiver 5, Deployment 4

Table E-B26. GAM output for Deployment 4, Receiver 6

A. parametric coefficients	Estimate	Std. Error	t-value	p-value
(Intercept)	4.6020	0.0006	7347.5126	< 0.0001
km2	0.0220	0.0071	3.0808	0.0021
km4	0.0119	0.0032	3.7137	0.0002
km10	0.0032	0.0012	2.6970	0.0070
B. smooth terms	**edf**	**Ref.df**	**F-value**	**p-value**
s(sDate)	46.0139	49.0000	24.7882	< 0.0001
s(WaveHeight)	2.4235	2.4235	30.6503	< 0.0001
s(Windspeed)	2.5259	2.5259	300.8994	< 0.0001
s(CPAmin)	8.5607	8.5607	26.0196	< 0.0001

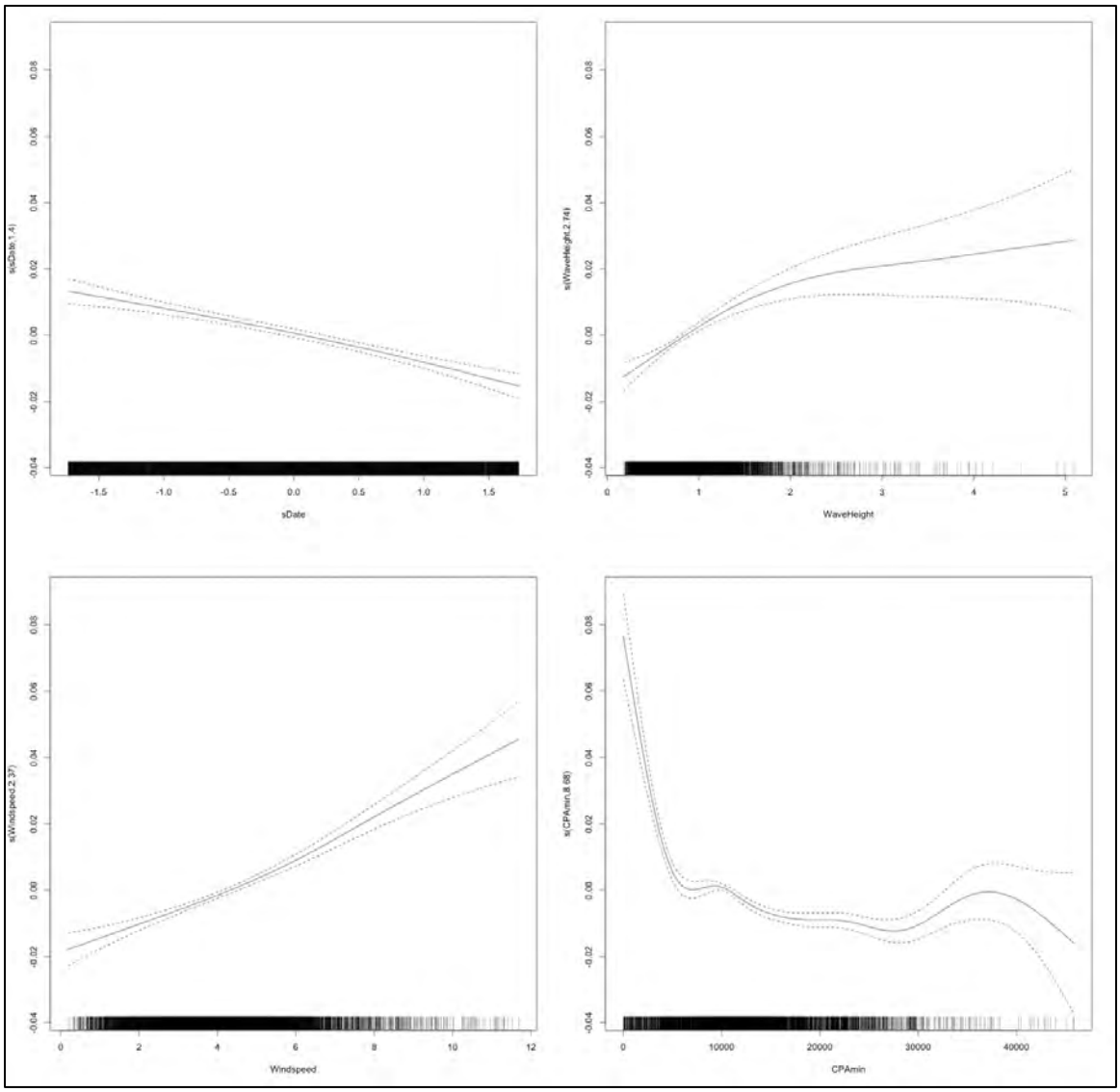

Figure E-B26. SA2 smoothing functions for Measured Vessel Band Noise as a function of Date, Wave Height, Windspeed, and CPA for Receiver 6, Deployment 4

Table E-B27. GAM output for Deployment 4, Receiver 7

A. parametric coefficients	Estimate	Std. Error	t-value	p-value
(Intercept)	4.6381	0.0012	3768.9476	< 0.0001
km2	0.0031	0.0029	1.0720	0.2838
km4	0.0084	0.0012	7.1174	< 0.0001
km10	0.0051	0.0006	9.1537	< 0.0001
B. smooth terms	**edf**	**Ref.df**	**F-value**	**p-value**
s(sDate)	37.6492	49.0000	7.4021	< 0.0001
s(WaveHeight)	7.2361	7.2361	10.7915	< 0.0001
s(Windspeed)	1.0000	1.0000	166.2904	< 0.0001
s(CPAmin)	8.2418	8.2418	57.0747	< 0.0001

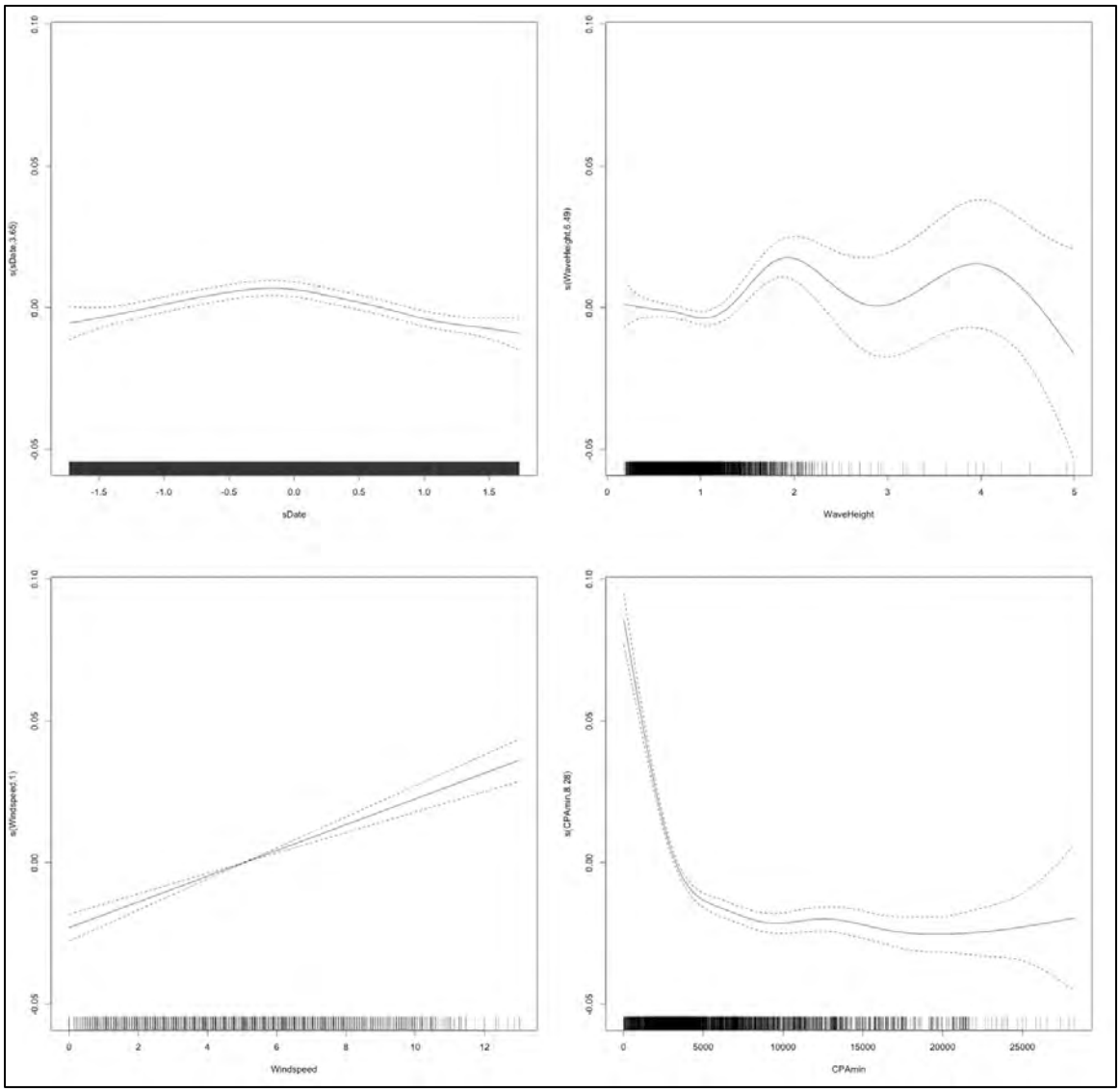

Figure E-B27. SA2 smoothing functions for Measured Vessel Band Noise as a function of Date, Wave Height, Windspeed, and CPA for Receiver 7, Deployment 4

Table E-B28. GAM output for Deployment 4, Receiver 8

A. parametric coefficients	Estimate	Std. Error	t-value	p-value
(Intercept)	4.6186	0.0008	5639.2788	< 0.0001
km2	0.0018	0.0024	0.7633	0.4453
km4	0.0085	0.0017	4.8952	< 0.0001
km10	-0.0014	0.0006	-2.2015	0.0277
B. smooth terms	**edf**	**Ref.df**	**F-value**	**p-value**
s(sDate)	47.0673	49.0000	251.8503	< 0.0001
s(WaveHeight)	1.0000	1.0000	1.1667	0.2801
s(Windspeed)	5.2050	5.2050	16.3722	< 0.0001
s(CPAmin)	5.9901	5.9901	35.8062	< 0.0001

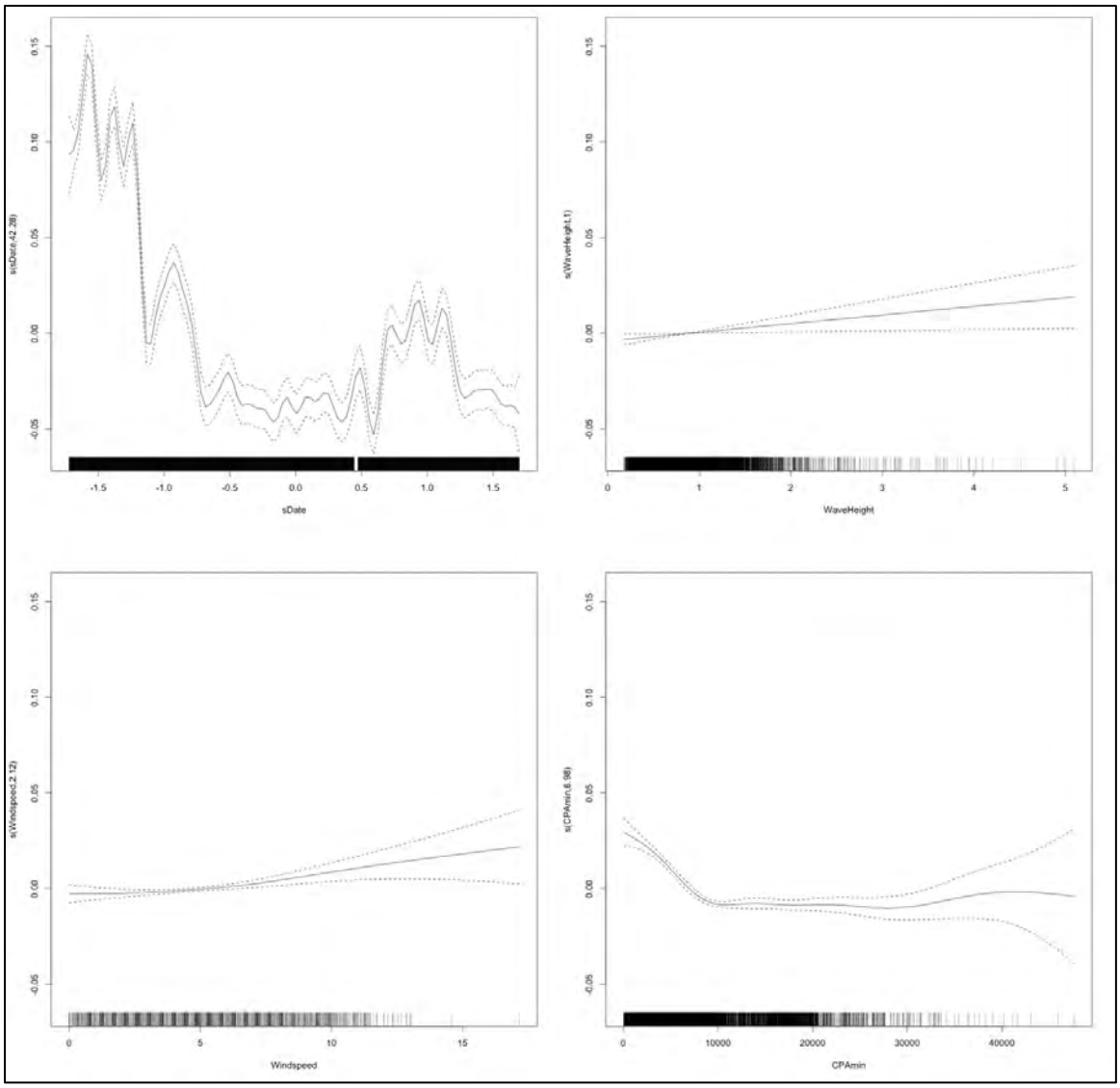

Figure E-B28. SA2 smoothing functions for Measured Vessel Band Noise as a function of Date, Wave Height, Windspeed, and CPA for Receiver 8, Deployment 4

Table E-B29. GAM output for Deployment 4, Receiver 9

A. parametric coefficients	Estimate	Std. Error	t-value	p-value
(Intercept)	4.6668	0.0007	6413.5372	< 0.0001
km2	0.0138	0.0025	5.5763	< 0.0001
km4	0.0078	0.0023	3.3444	0.0008
km10	0.0011	0.0008	1.4499	0.1471
B. smooth terms	**edf**	**Ref.df**	**F-value**	**p-value**
s(sDate)	45.0765	49.0000	137.3508	< 0.0001
s(WaveHeight)	5.2936	5.2936	10.9832	< 0.0001
s(Windspeed)	1.0000	1.0000	7.0446	0.0080
s(CPAmin)	1.0000	1.0000	8.9335	0.0028

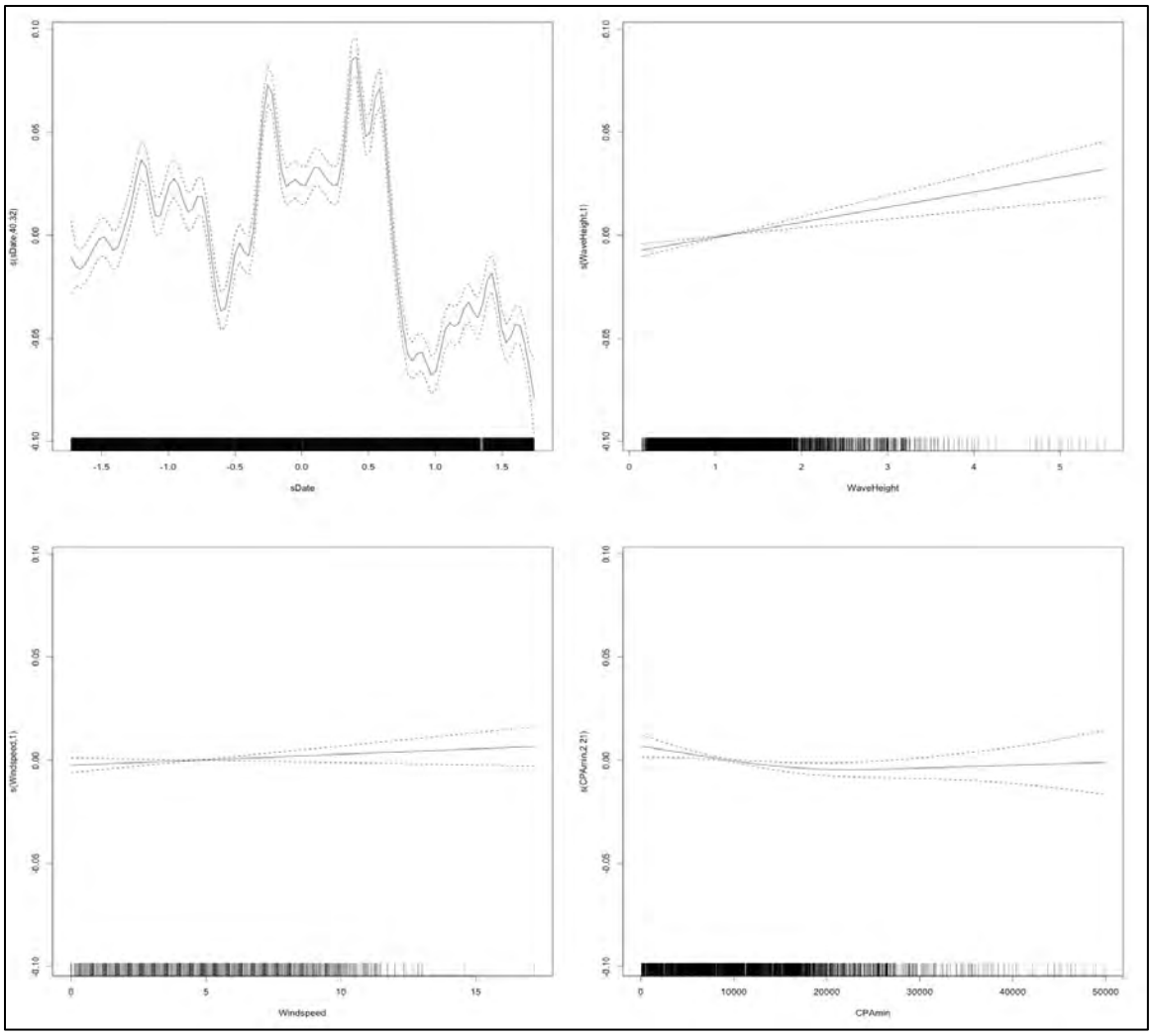

Figure E-B29. SA2 smoothing functions for Measured Vessel Band Noise as a function of Date, Wave Height, Windspeed, and CPA for Receiver 9, Deployment 4

Table E-B30. GAM output for Deployment 4, Receiver 10

A. parametric coefficients	Estimate	Std. Error	t-value	p-value
(Intercept)	4.5756	0.0007	6719.7106	< 0.0001
km2	0.0333	0.0078	4.2686	< 0.0001
km4	0.0381	0.0074	5.1250	< 0.0001
km10	0.0143	0.0040	3.6062	0.0003
B. smooth terms	**edf**	**Ref.df**	**F-value**	**p-value**
s(sDate)	45.9727	49.0000	46.9735	< 0.0001
s(WaveHeight)	1.0000	1.0000	0.9119	0.3397
s(Windspeed)	1.6279	1.6279	1.9398	0.1033
s(CPAmin)	1.0000	1.0000	3.0621	0.0802

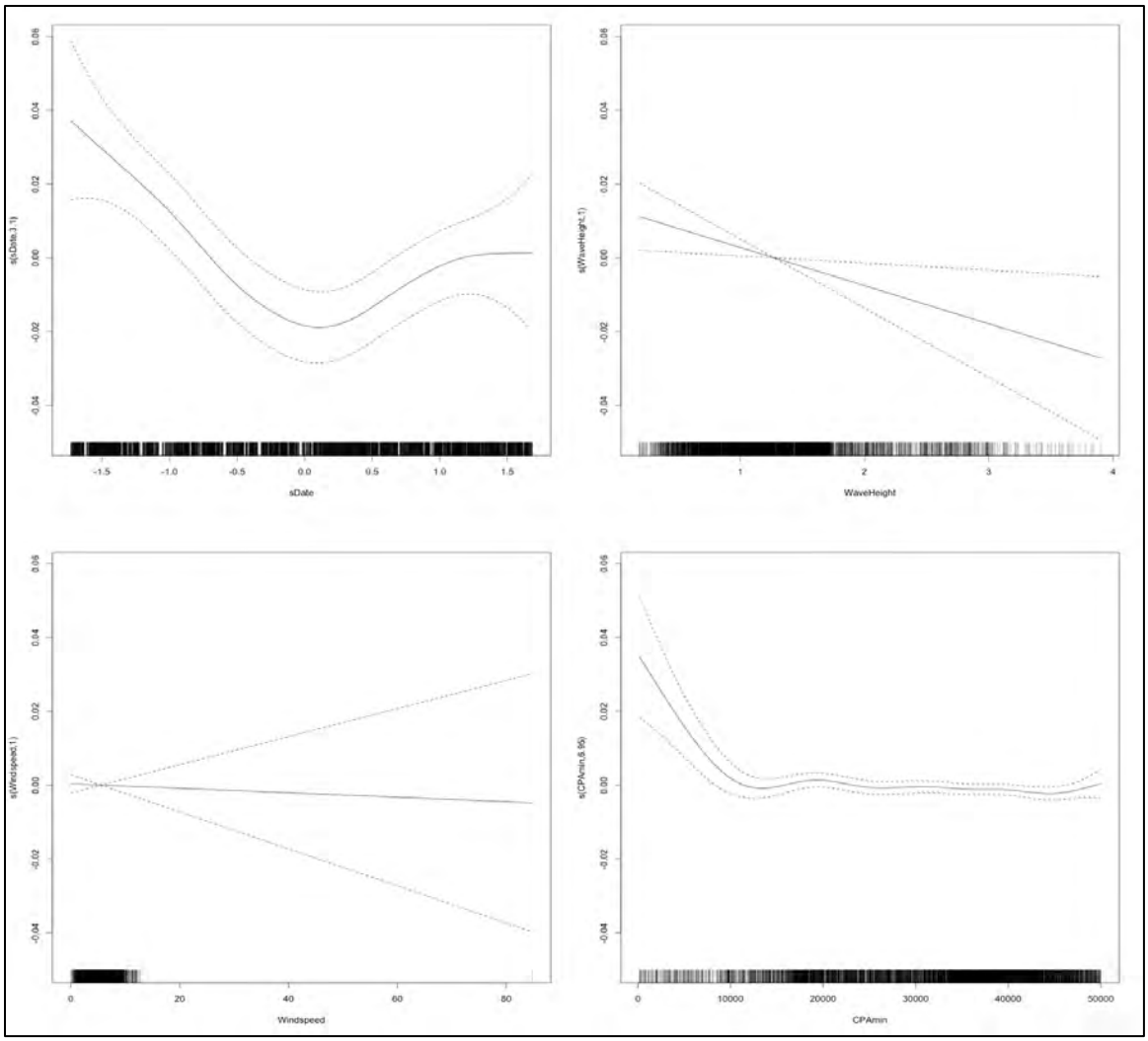

Figure E-B30. SA2 smoothing functions for Measured Vessel Band Noise as a function of Date, Wave Height, Windspeed, and CPA for Receiver 10, Deployment 4

Appendix E-C: Spatial and Temporal Spectral Trends in RH and EARS Recorded Data

These **Appendix E-C** figures depict the temporal and spatial spectral levels recorded at the RH and EARS Sites 1 through 10 during the deployments that occurred from 2018 through early 2020. In each monthly figure, the solid lines represent the sites where RH recorders were deployed (Sites 1, 3, 6, 7, and 9), while the dashed lines represent the sites where EARS recorders were deployed (Sites 2, 4, 5, 8, and 10). The top spectrum in each of these **Appendix E-C** figures represents the entire frequency range, while the bottom panel presents the LF band (10 to 1,000 Hz) in more detail.

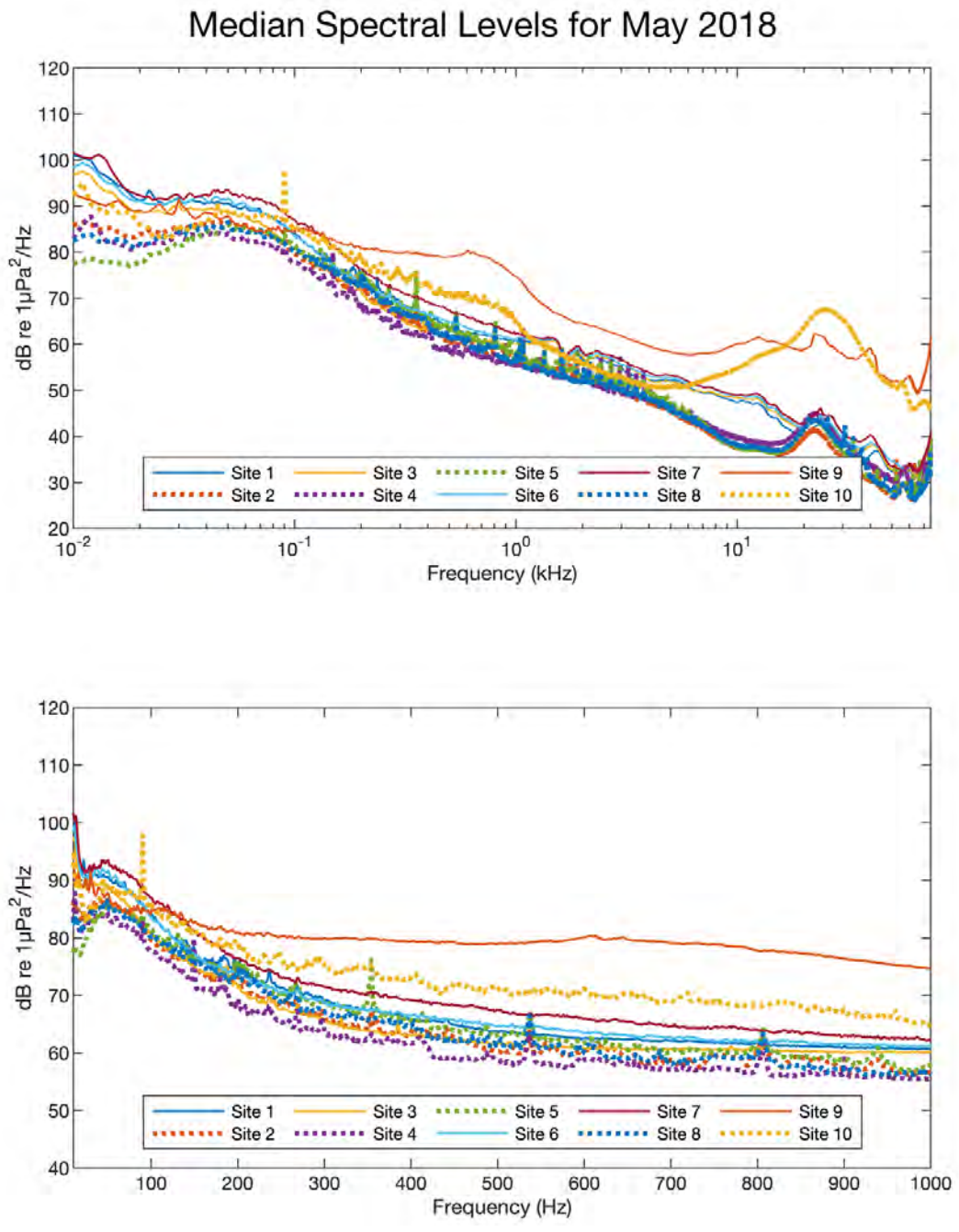

Figure E-C1. Median spectral values for May 2018

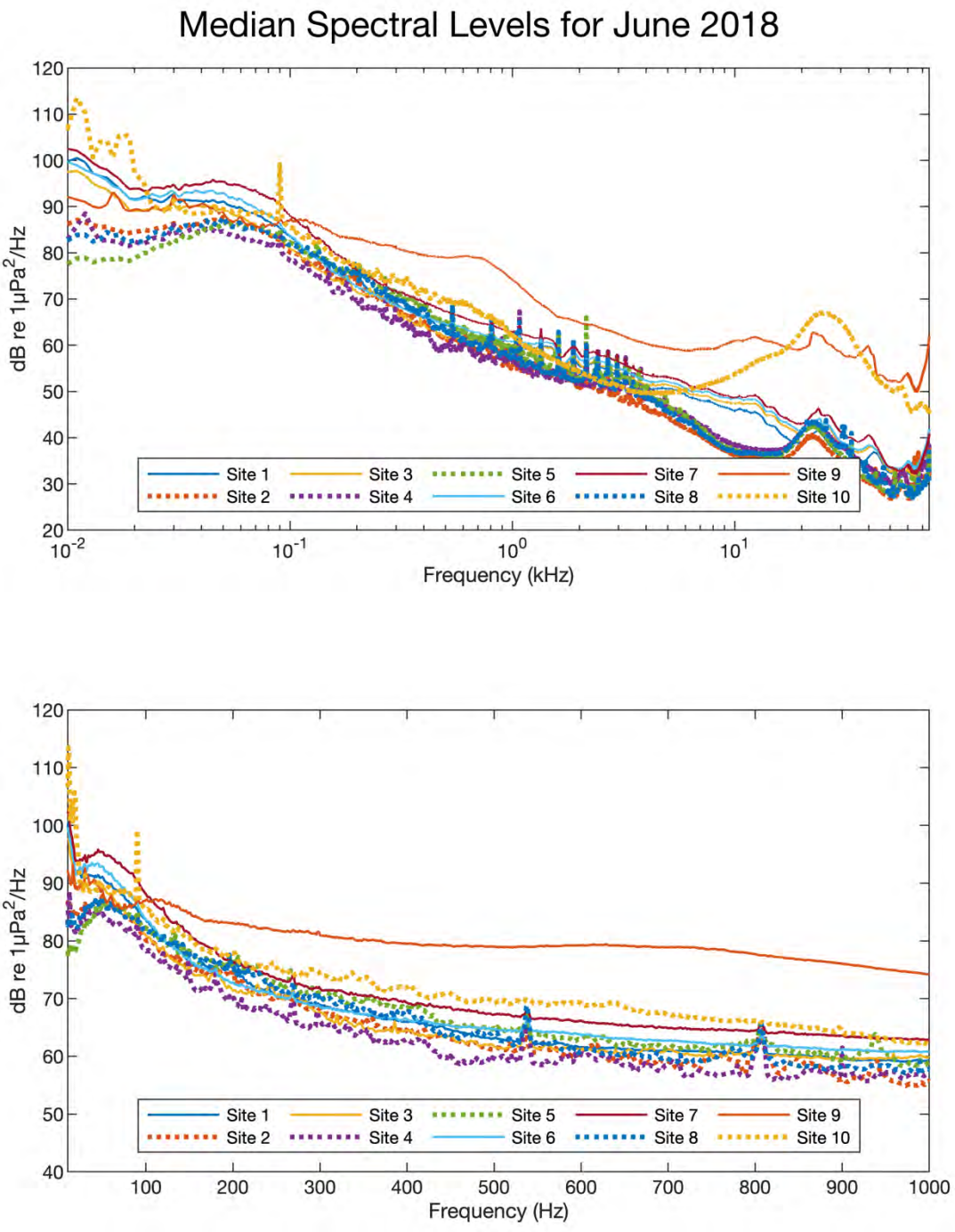

Figure E-C2. Median spectral values for June 2018

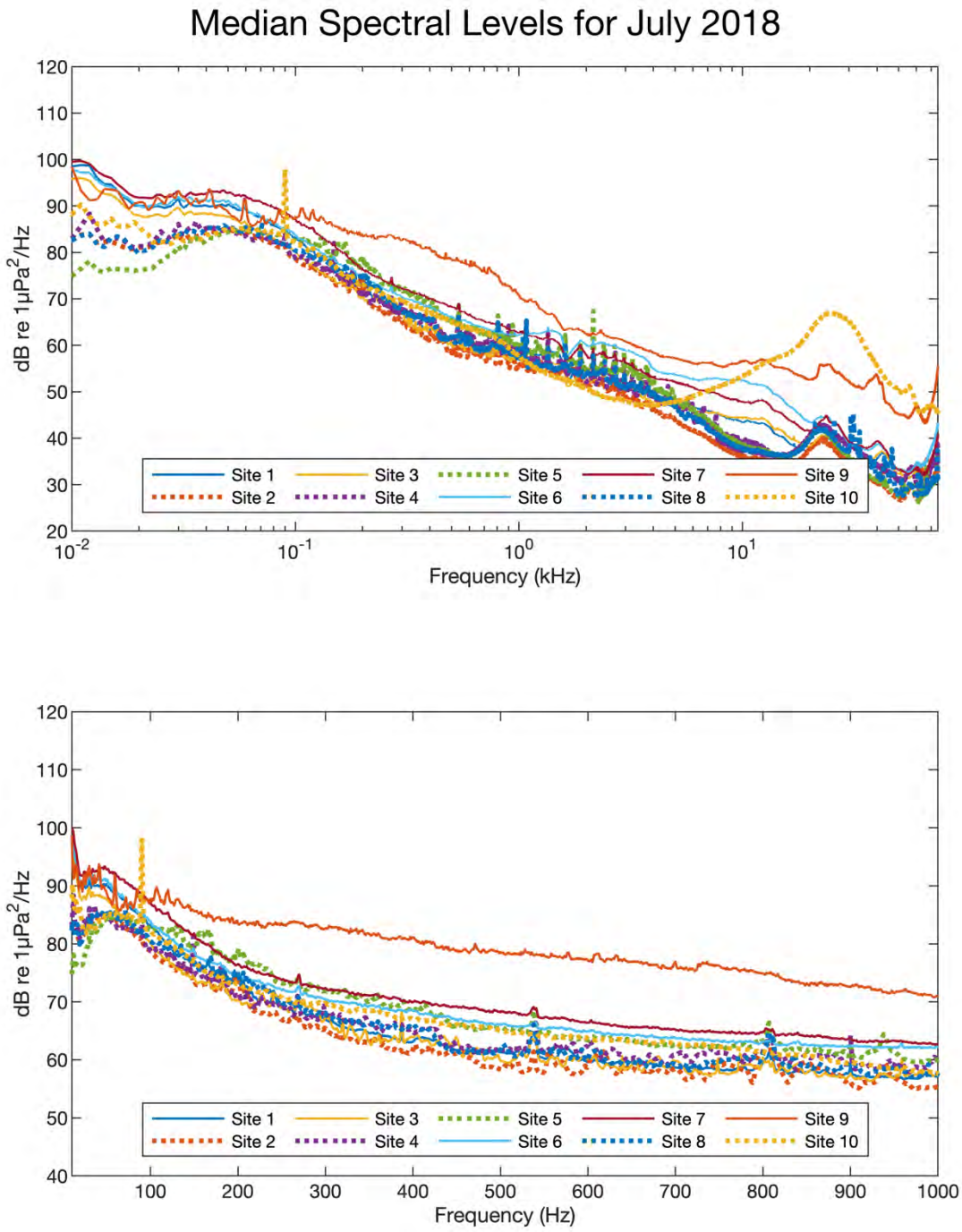

Figure E-C3. Median spectral values for July 2018

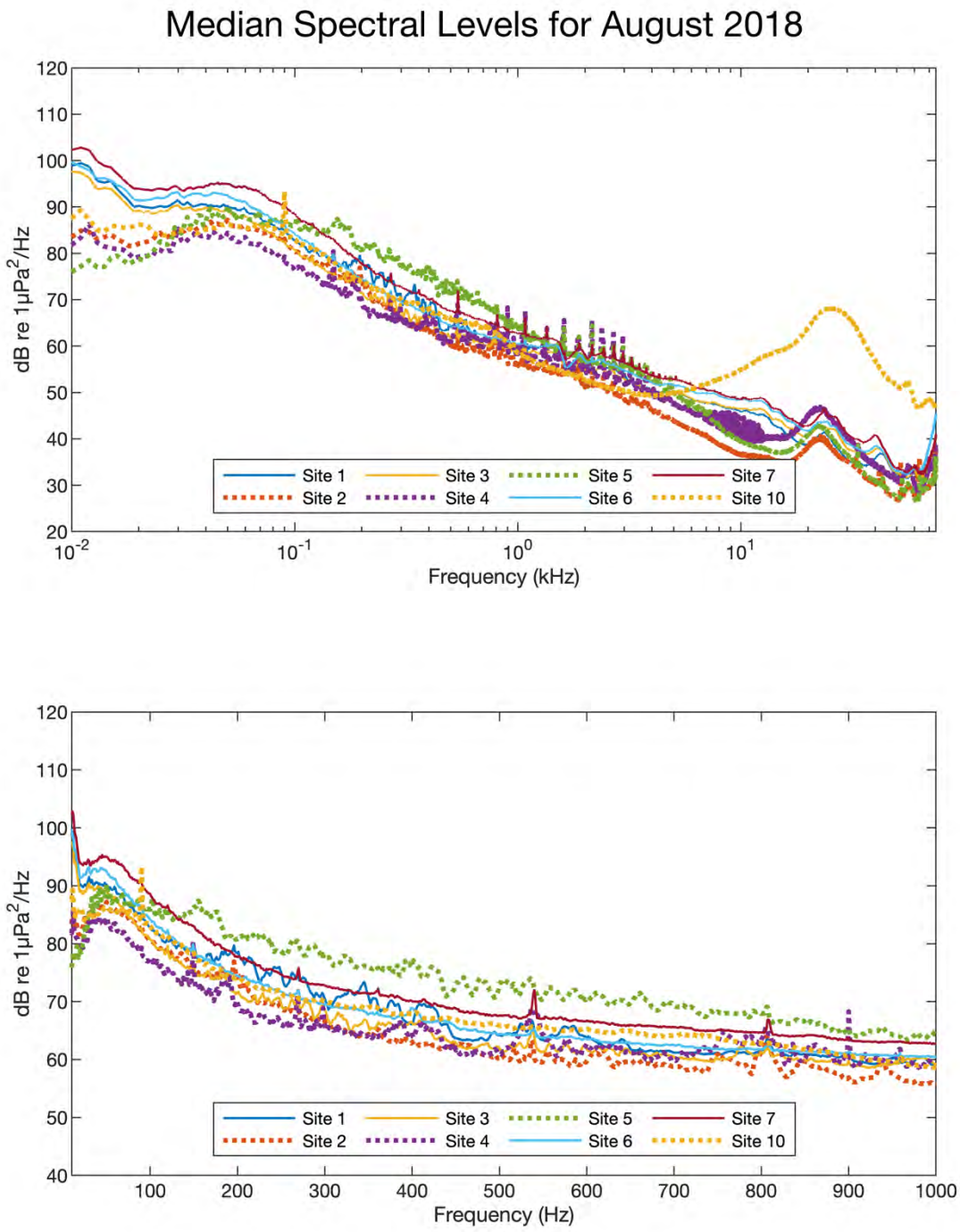

Figure E-C4. Median spectral values for August 2018

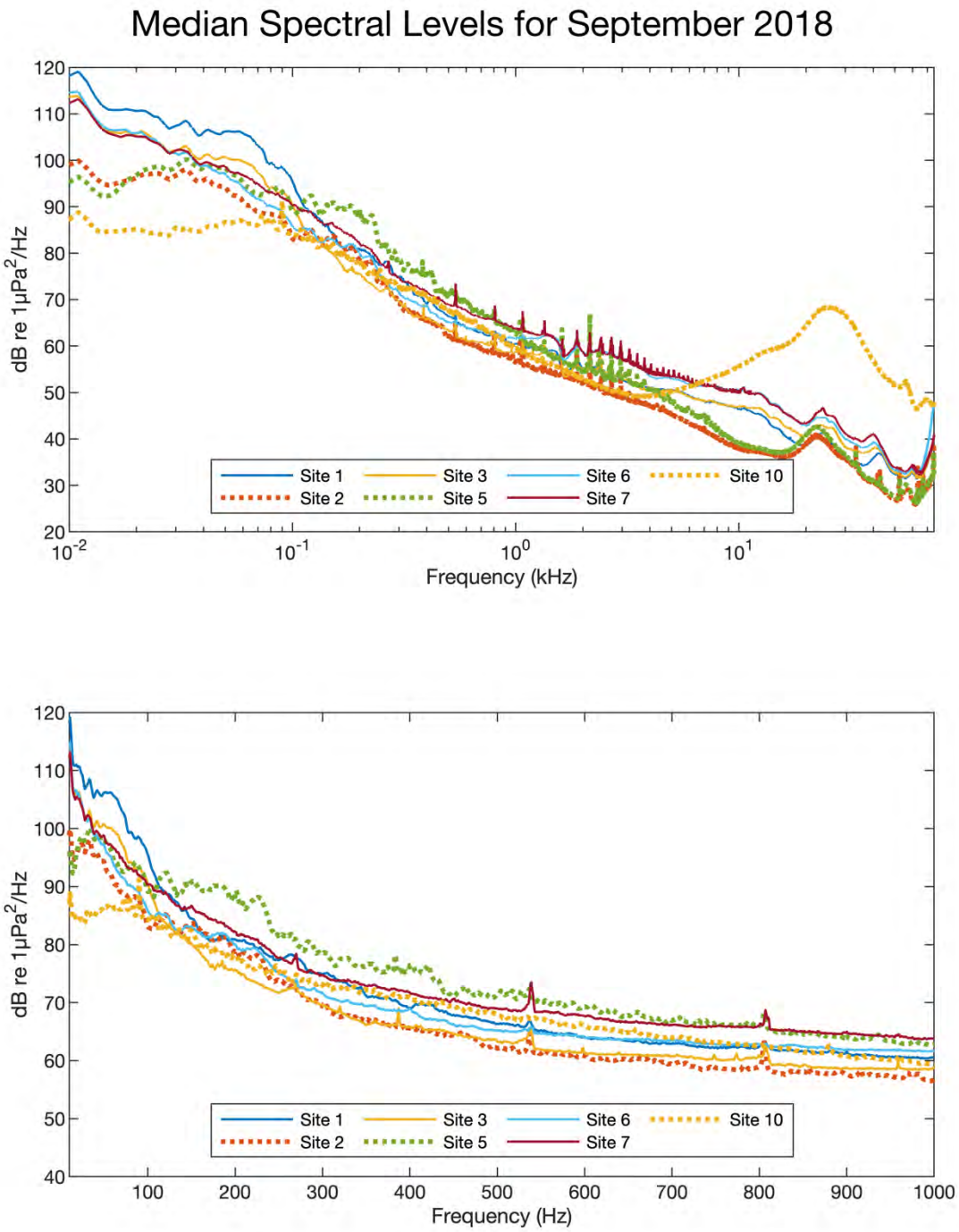

Figure E-C5. Median spectral values for September 2018

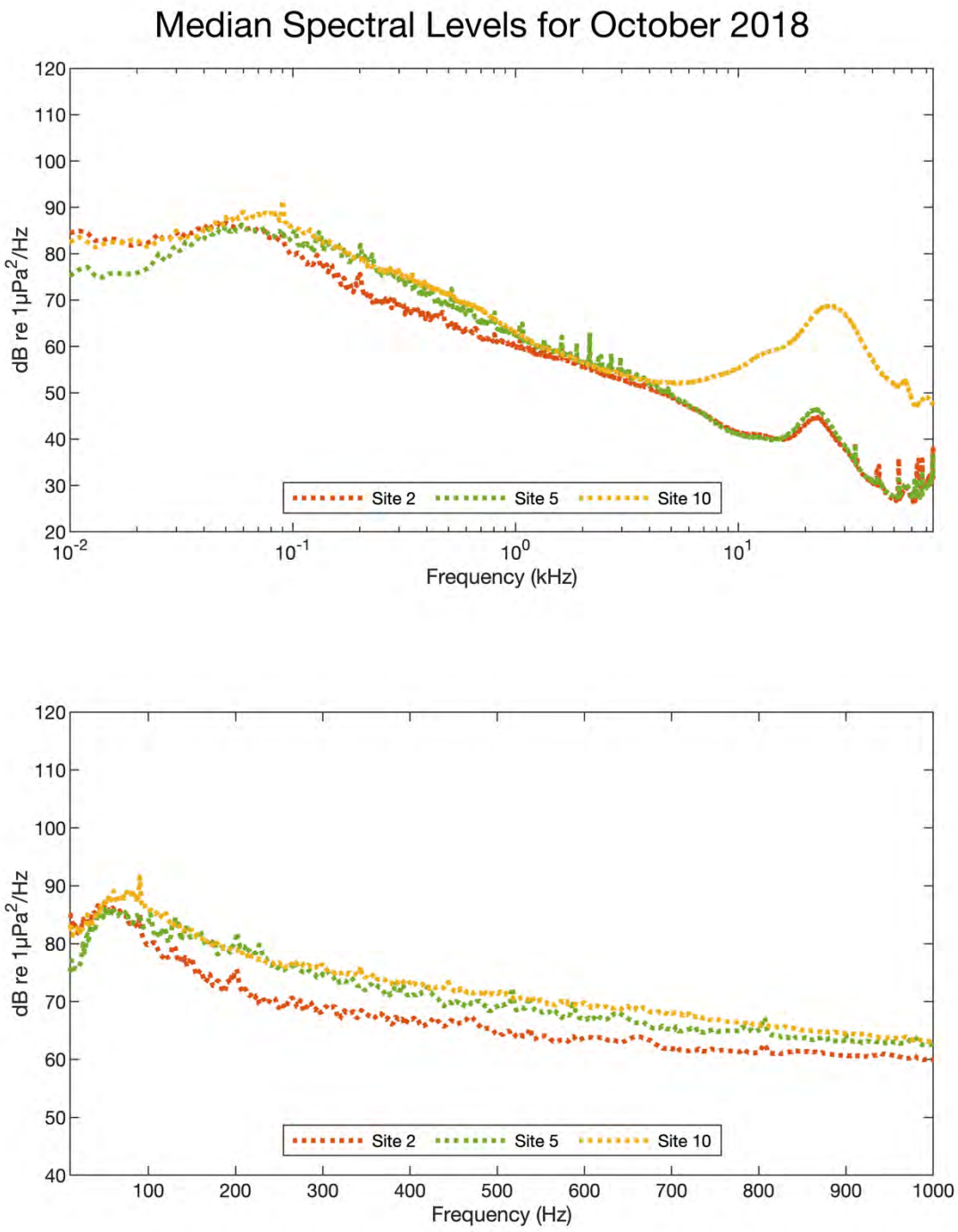

Figure E-C6. Median spectral values for October 2018

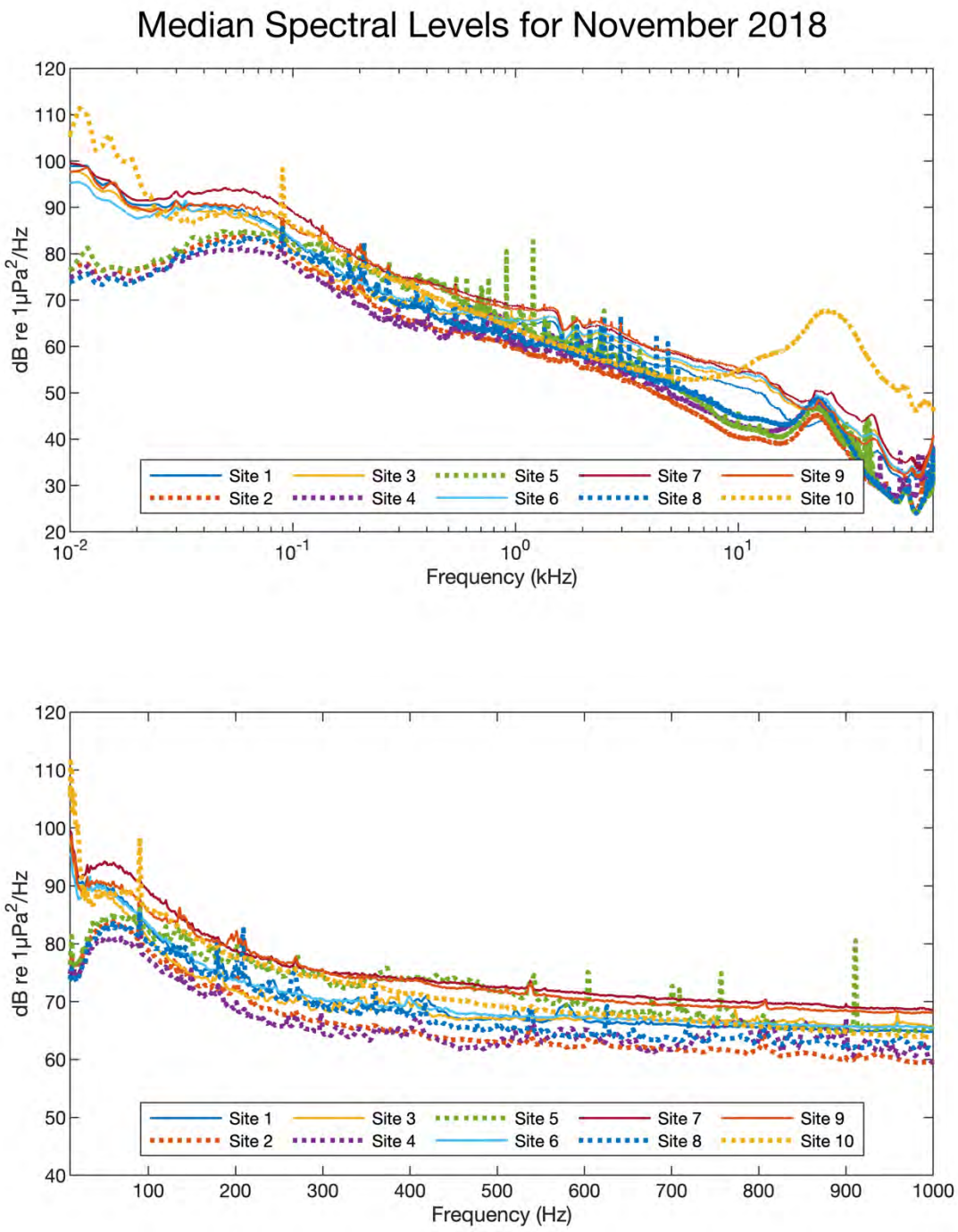

Figure E-C7. Median spectral values for November 2018

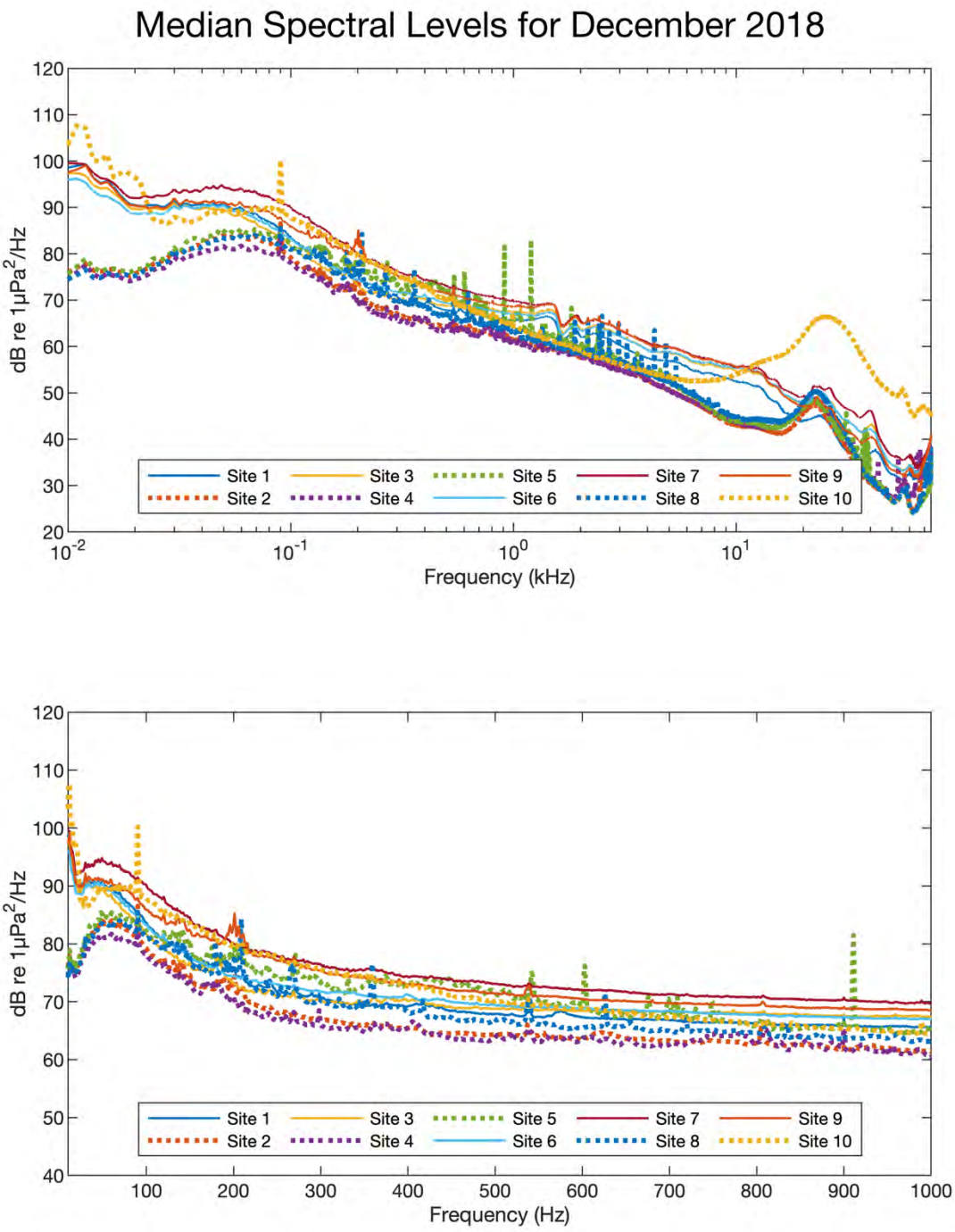

Figure E-C8. Median spectral values for December 2018

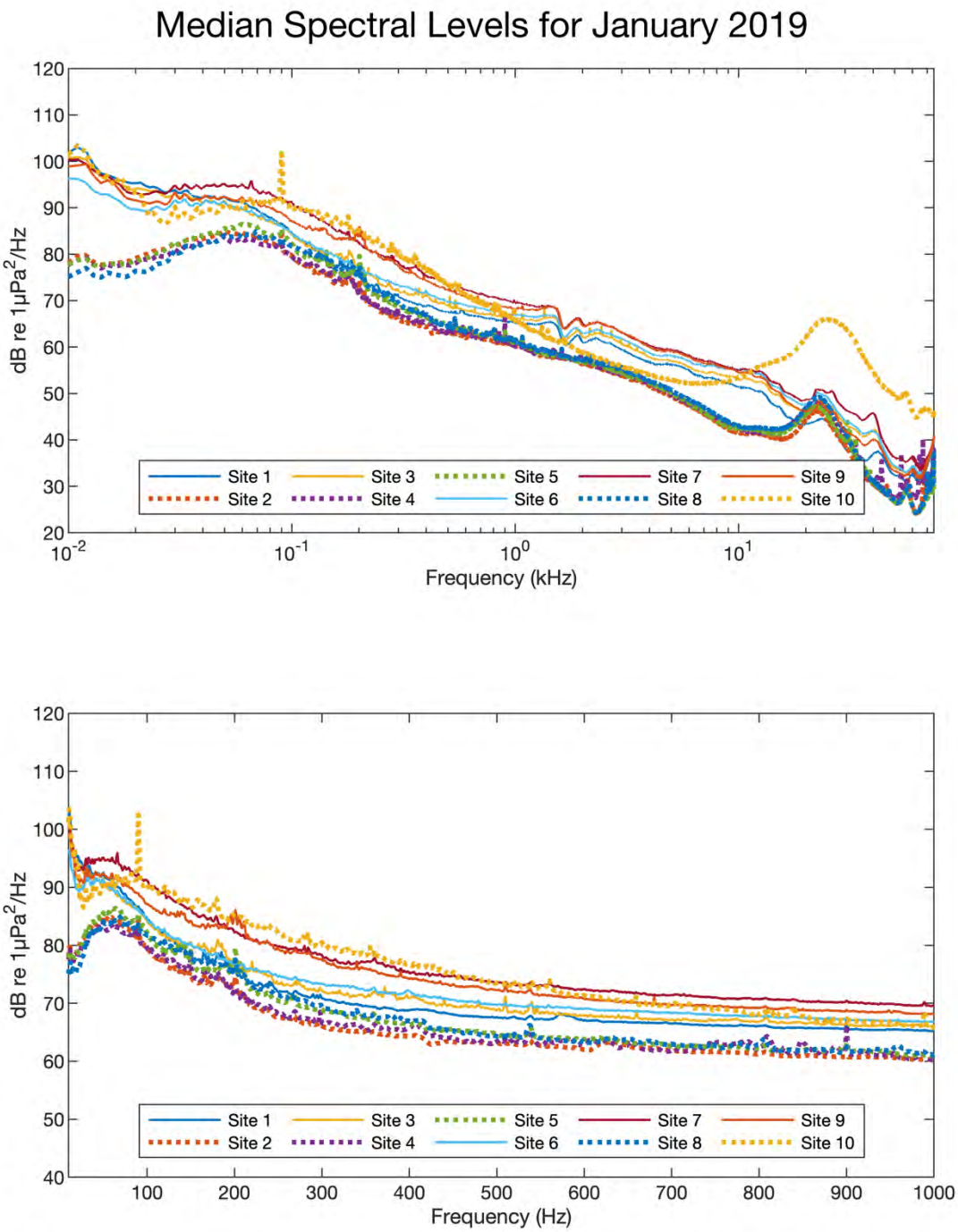

Figure E-C9. Median spectral values for January 2019

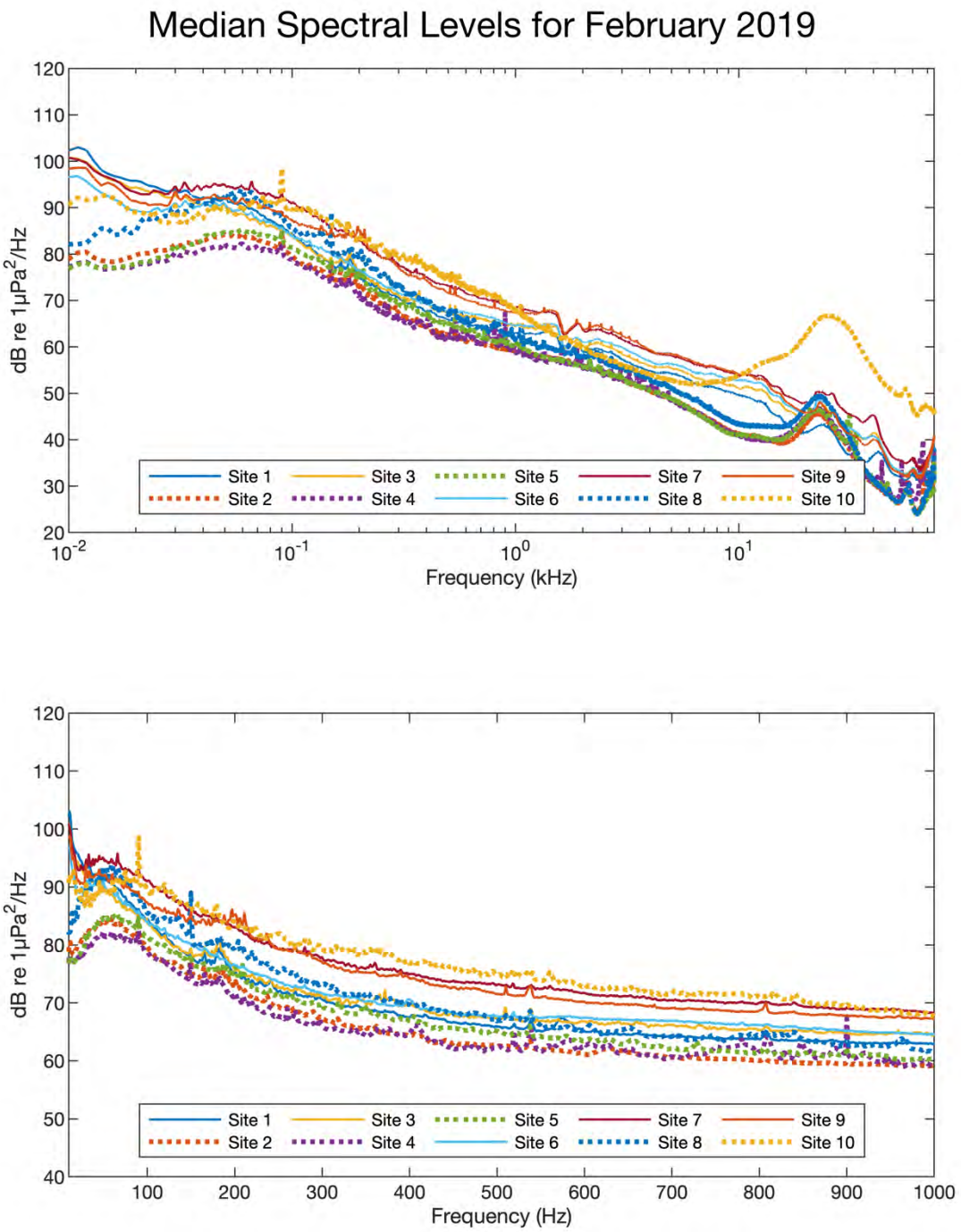

Figure E-C10. Median spectral values for February 2019

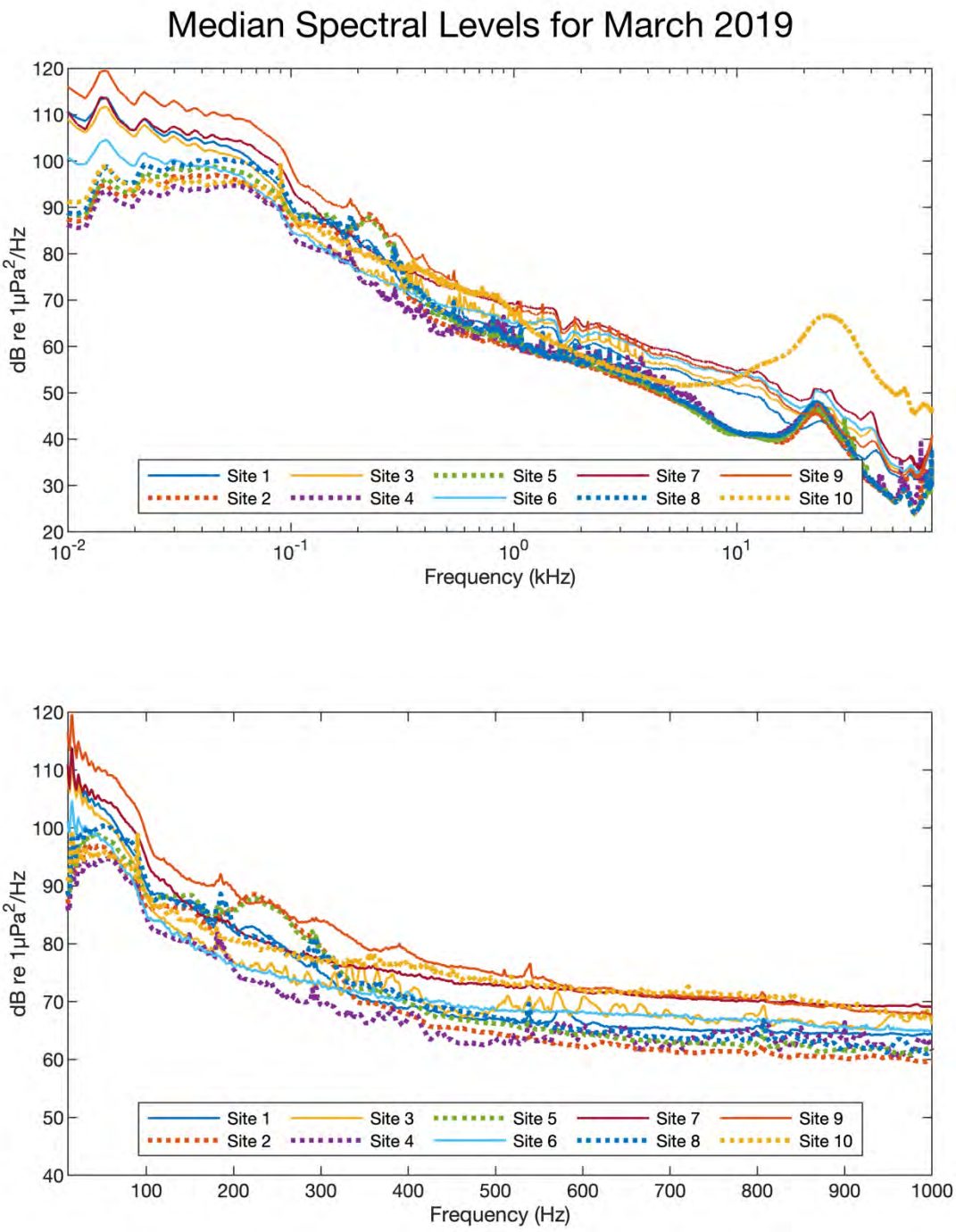

Figure E-C11. Median spectral values for March 2019

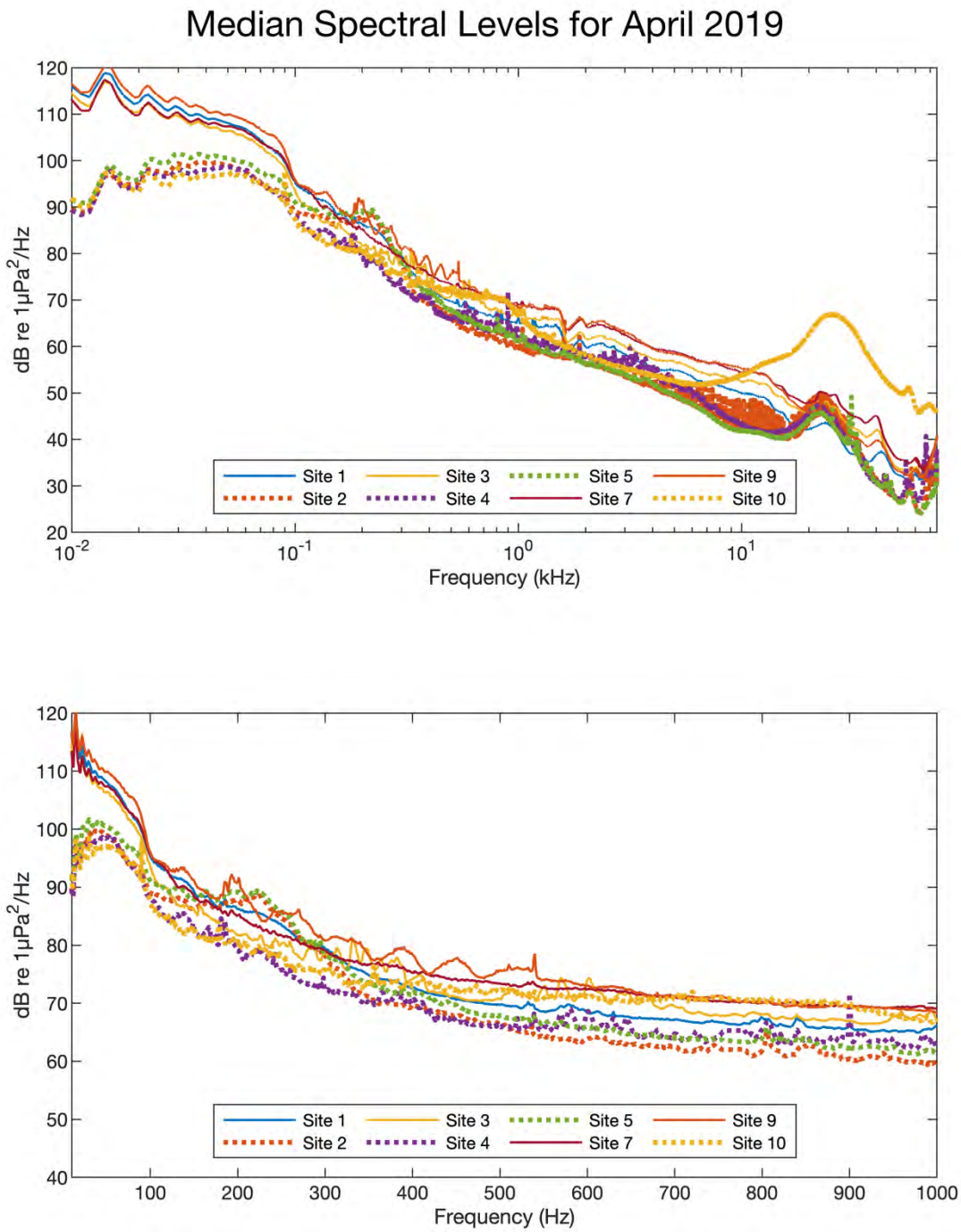

Figure E-C12. Median spectral values for April 2019

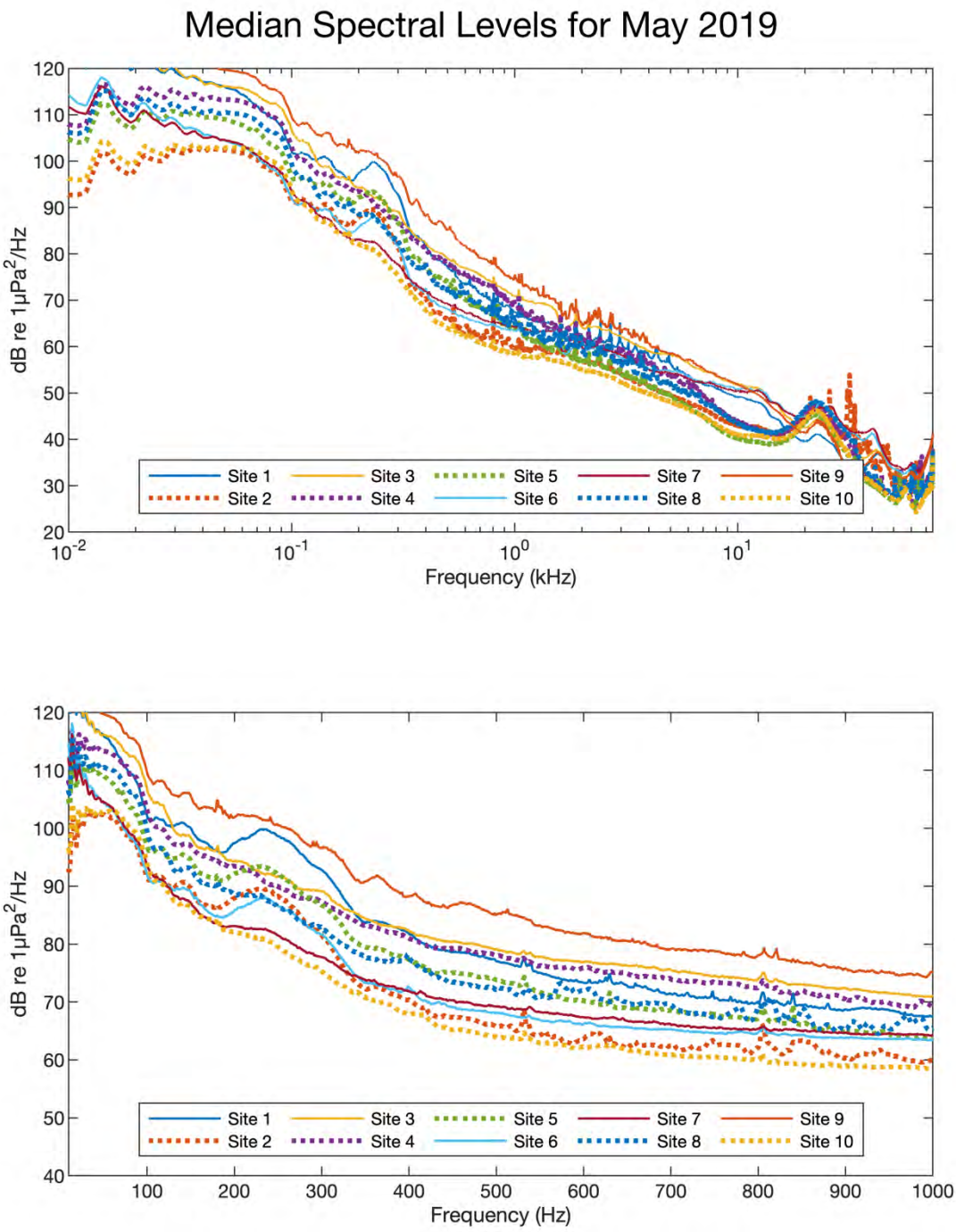

Figure E-C13. Median spectral values for May 2019

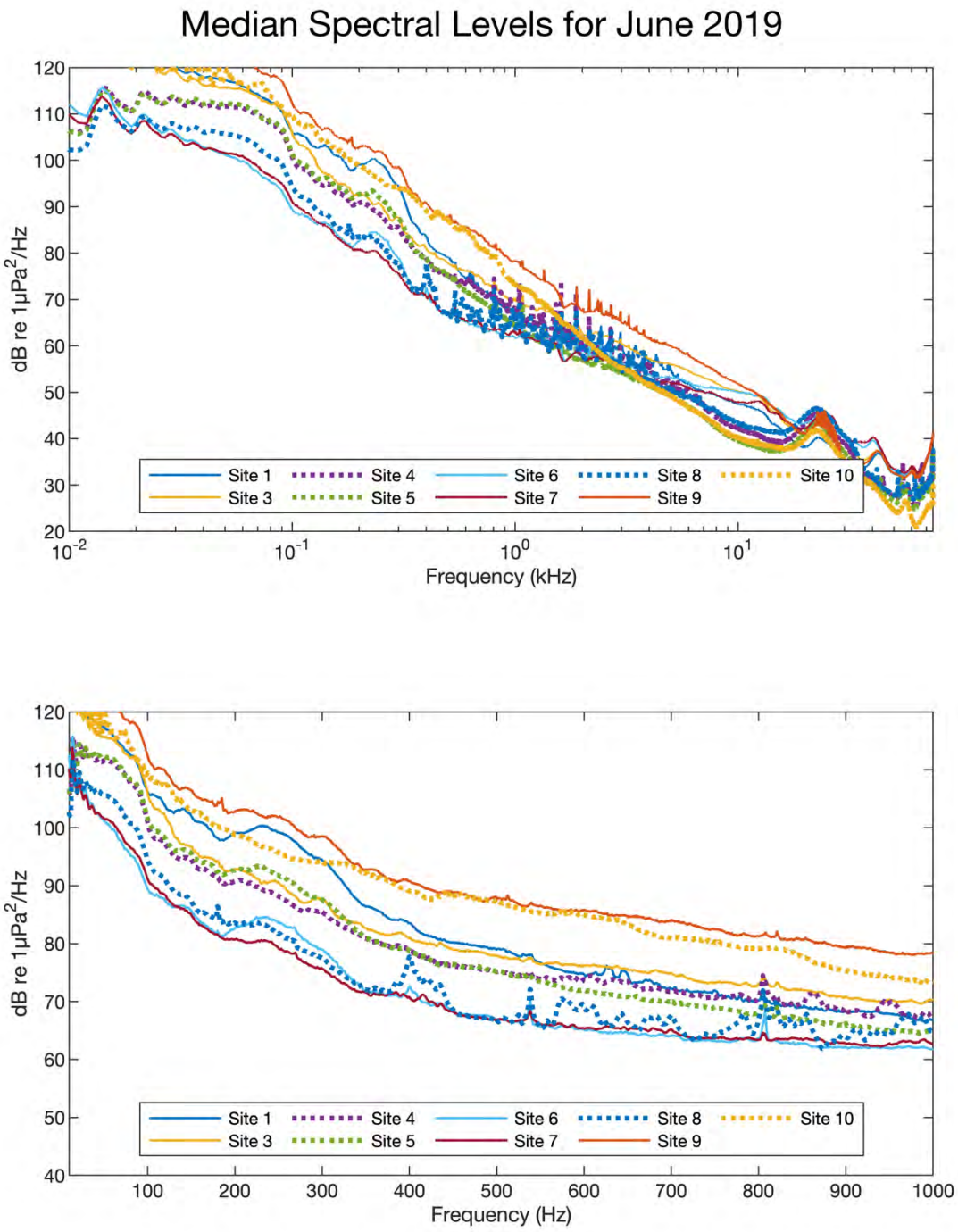

Figure E-C14. Median spectral values for June 2019

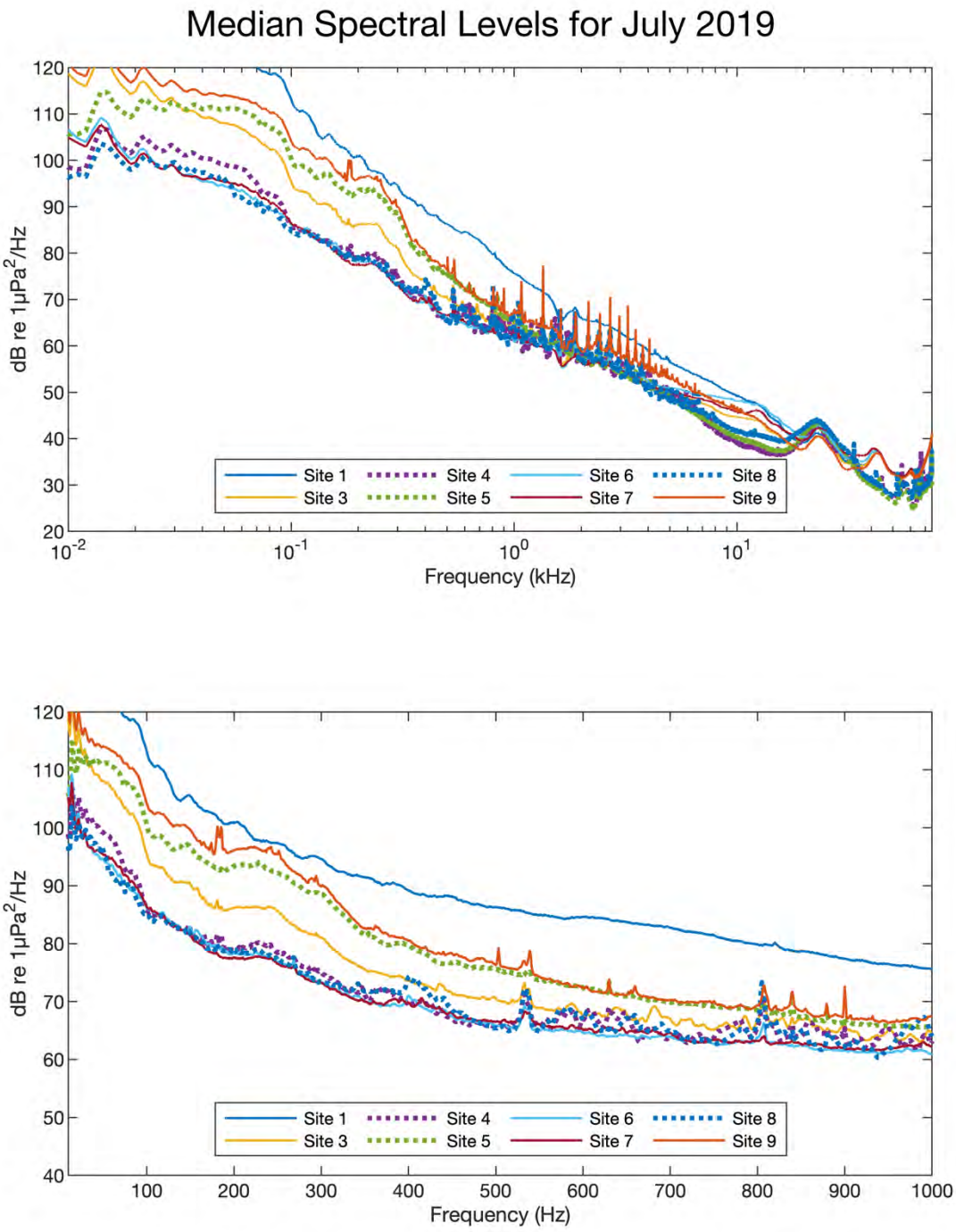

Figure E-C15. Median spectral values for July 2019

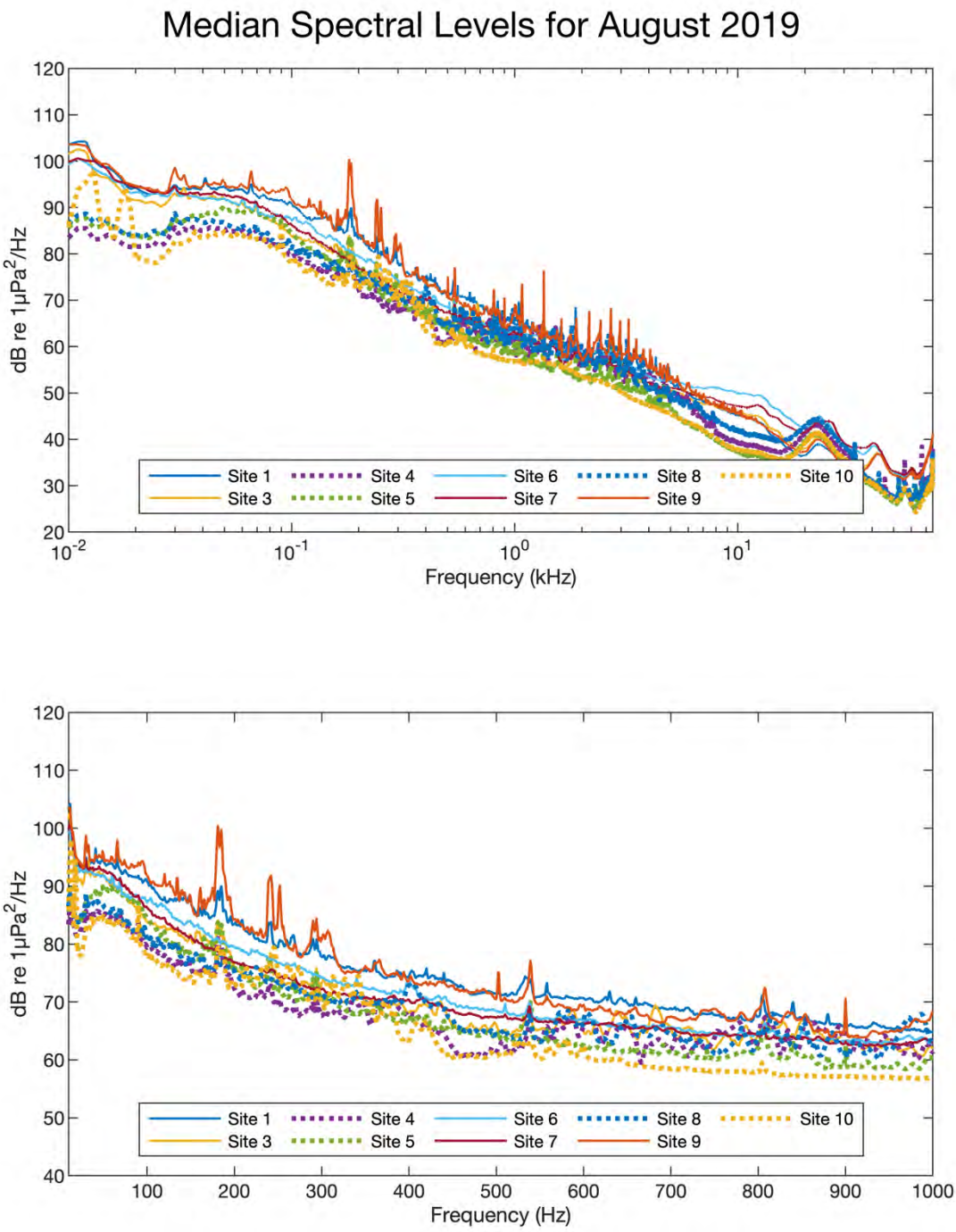

Figure E-C16. Median spectral values for August 2019

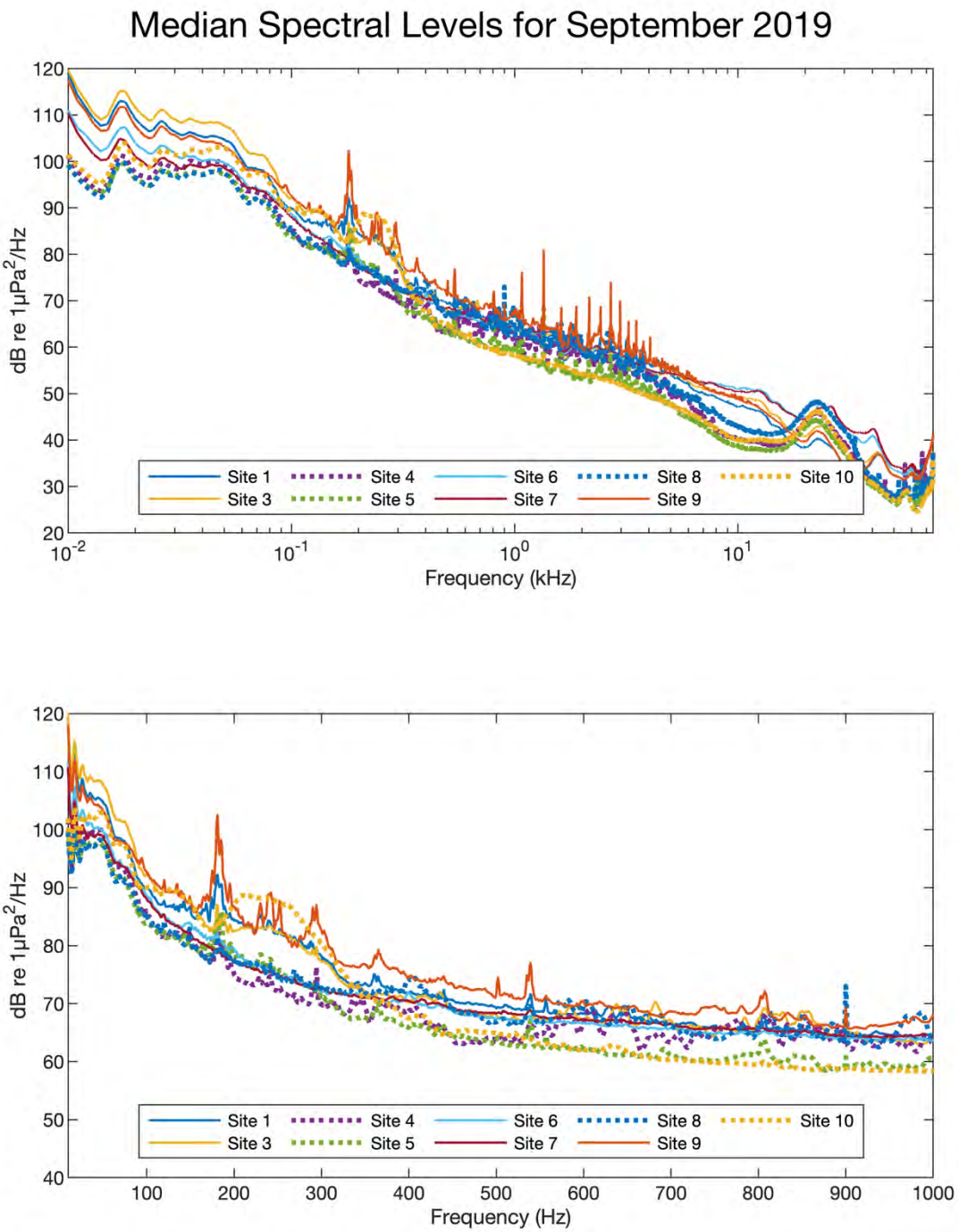

Figure E-C17. Median spectral values for September 2019

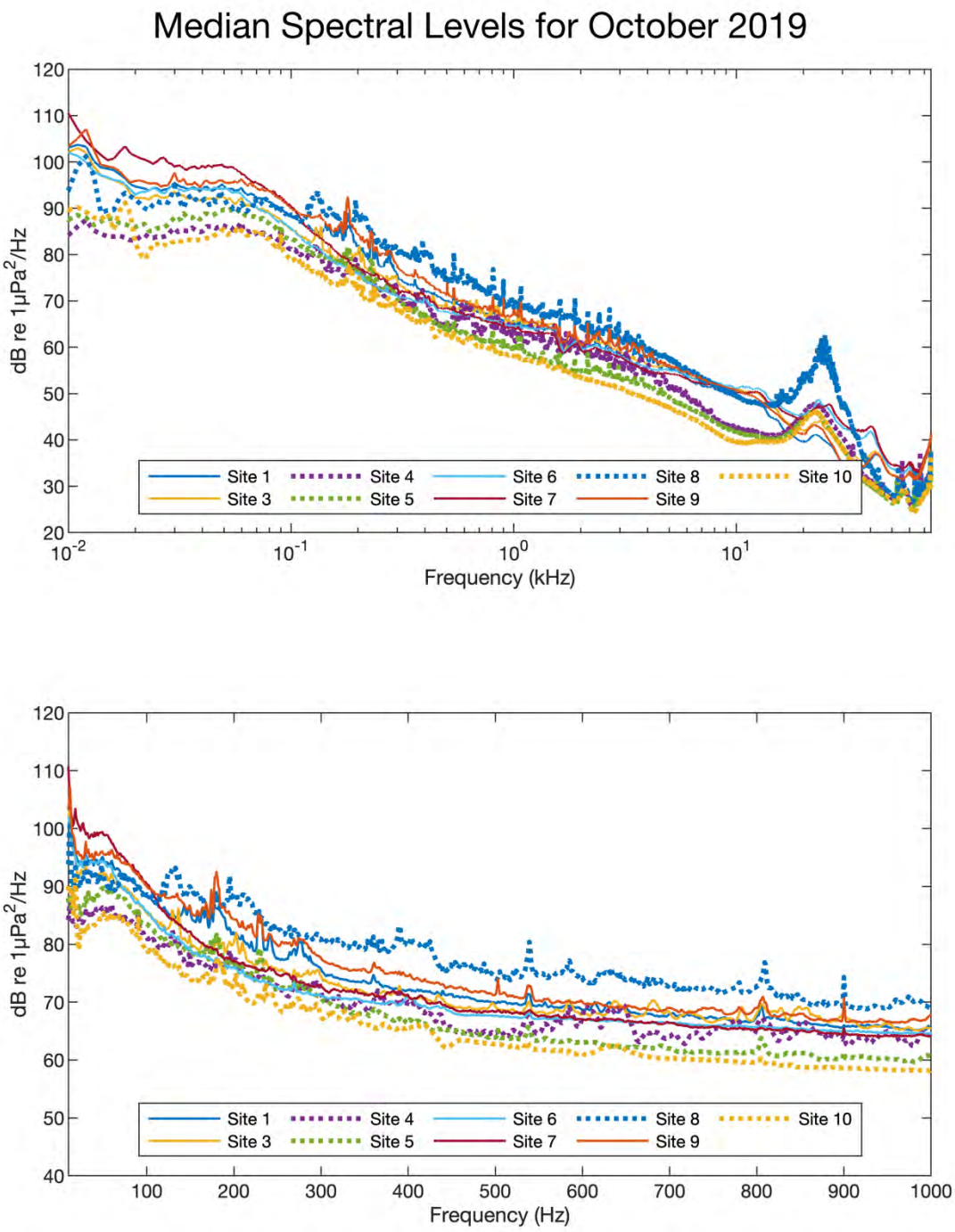

Figure E-C18. Median spectral values for October 2019

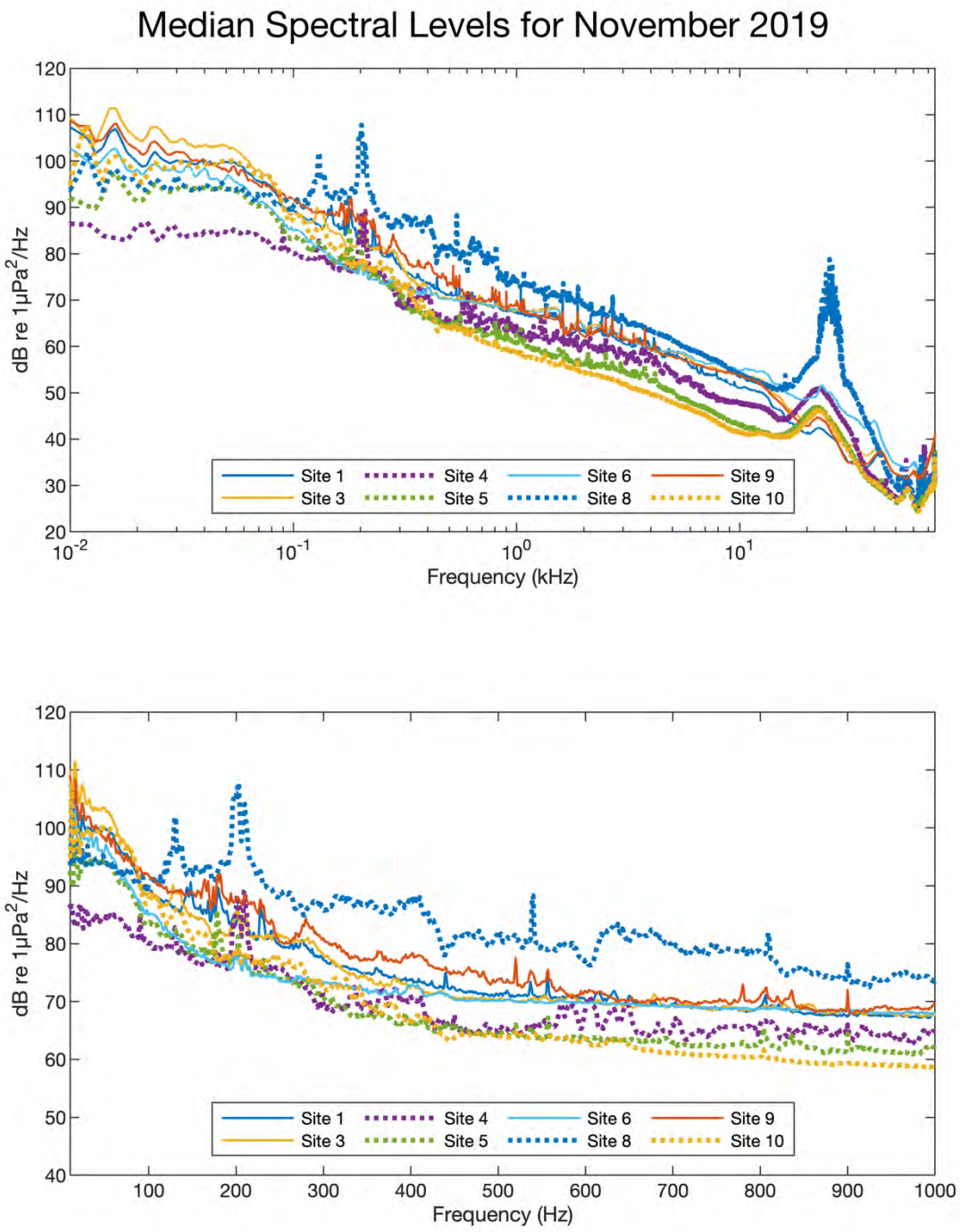

Figure E-C19. Median spectral values for November 2019

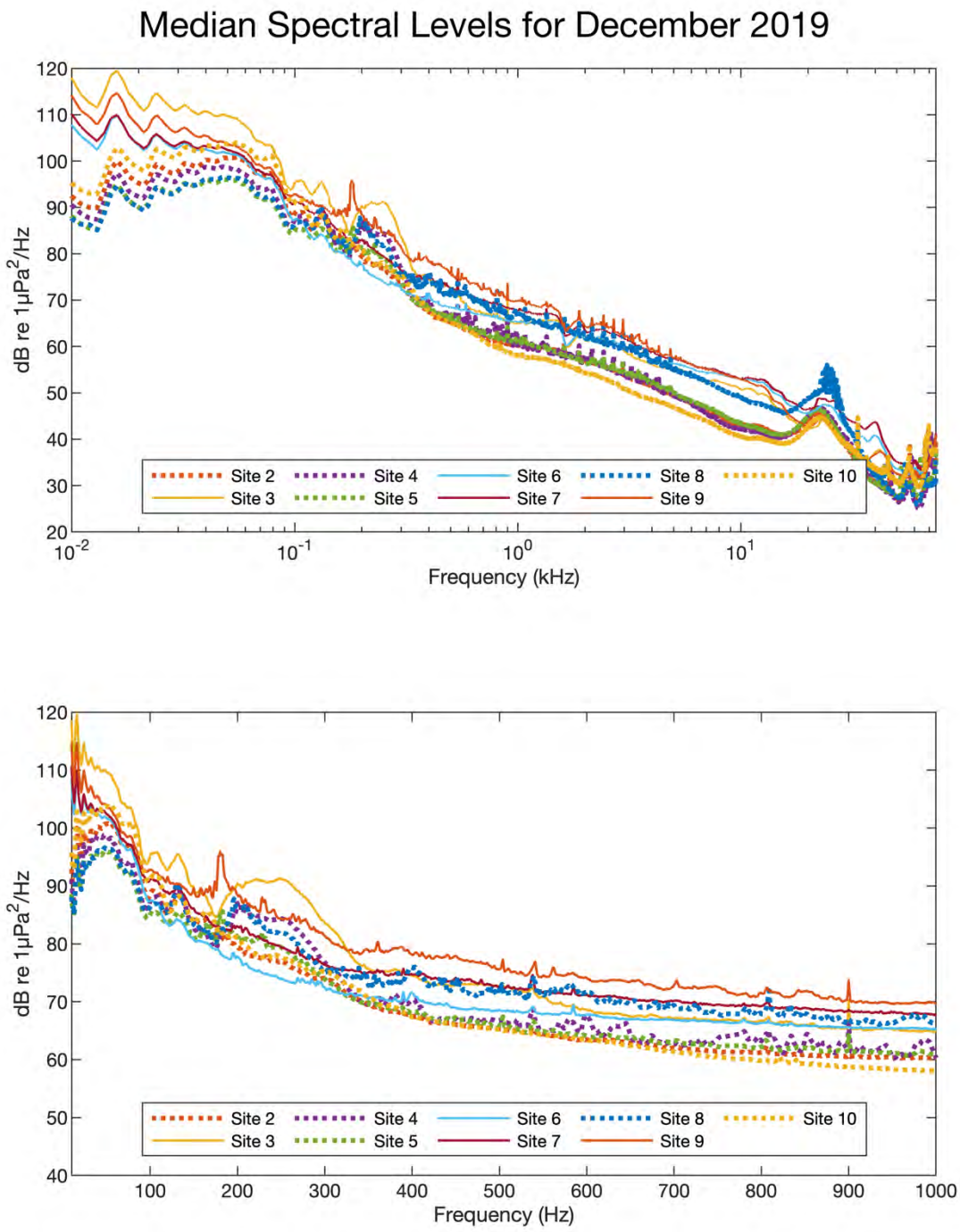

Figure E-C20. Median spectral values for December 2019

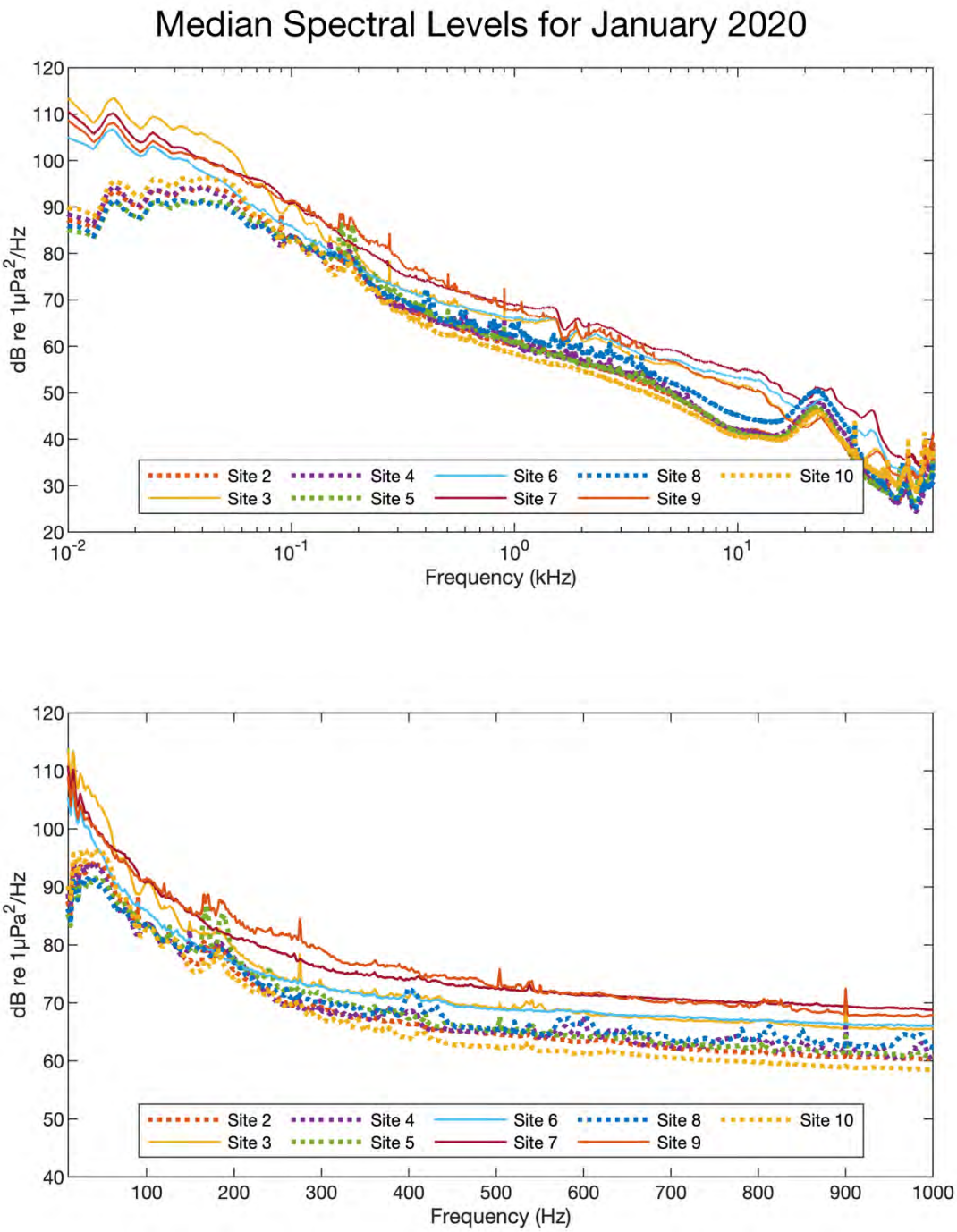

Figure E-C21. Median spectral values for January 2020

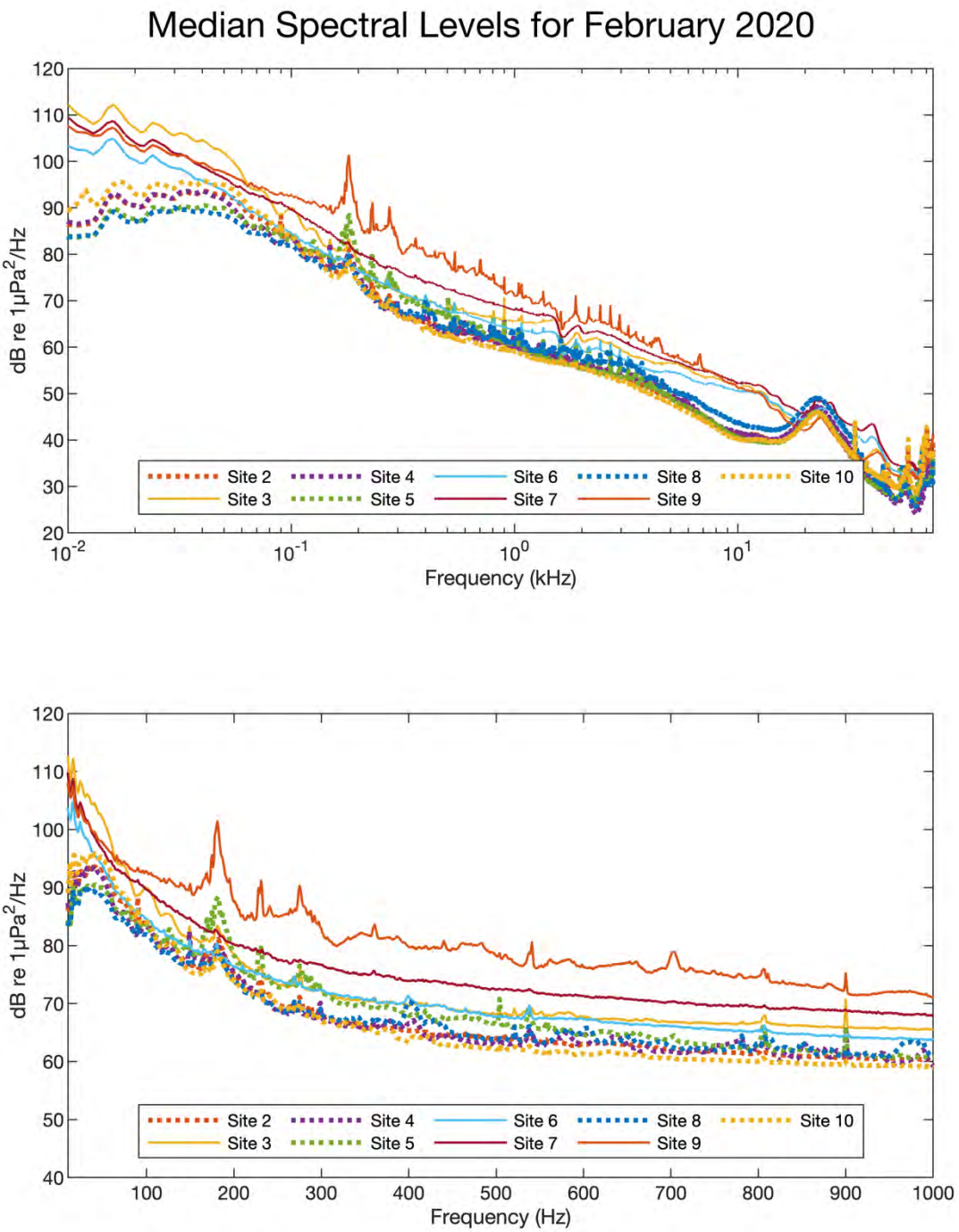

Figure E-C22. Median spectral values for February 2020

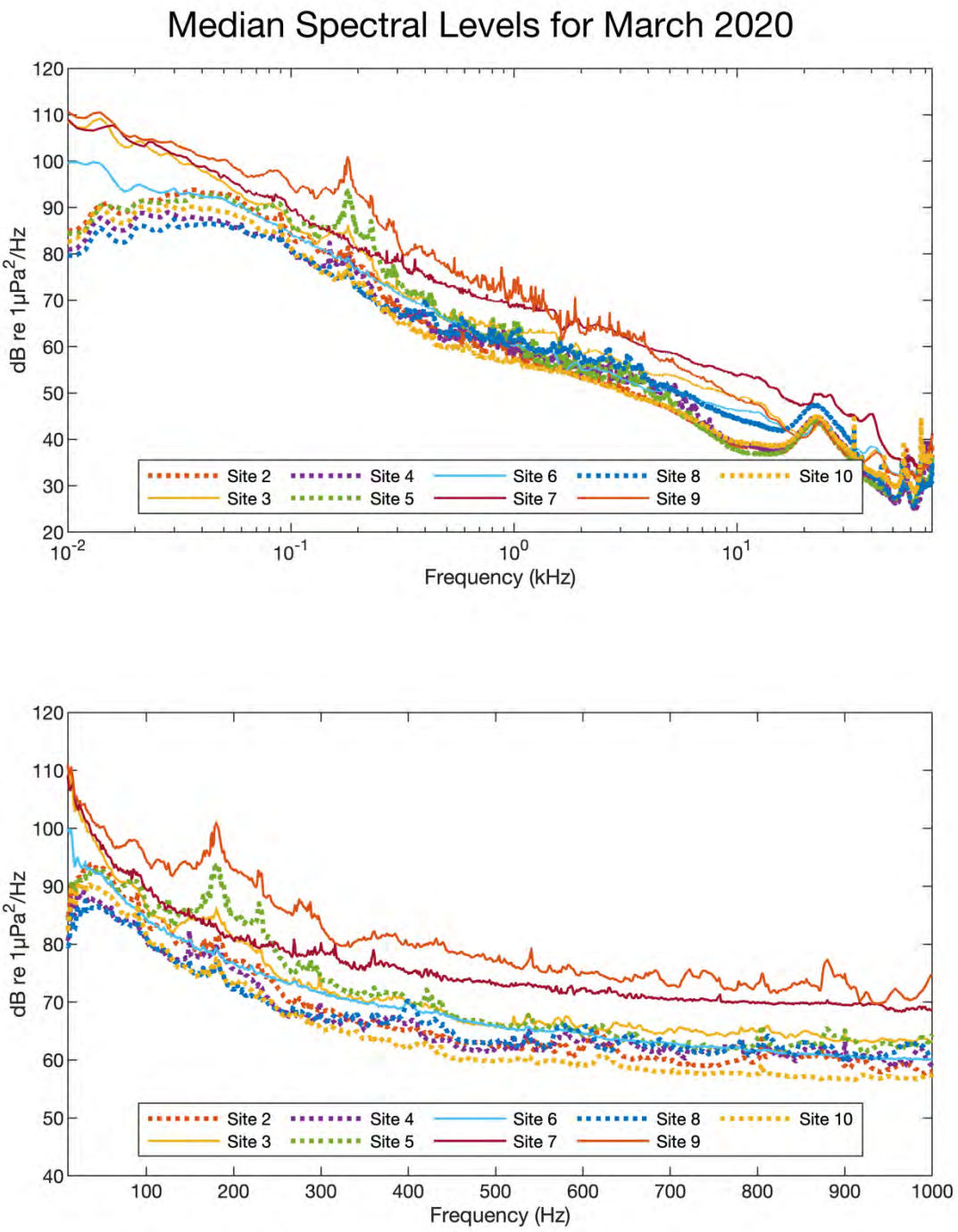

Figure E-C23. Median spectral values for March 2020

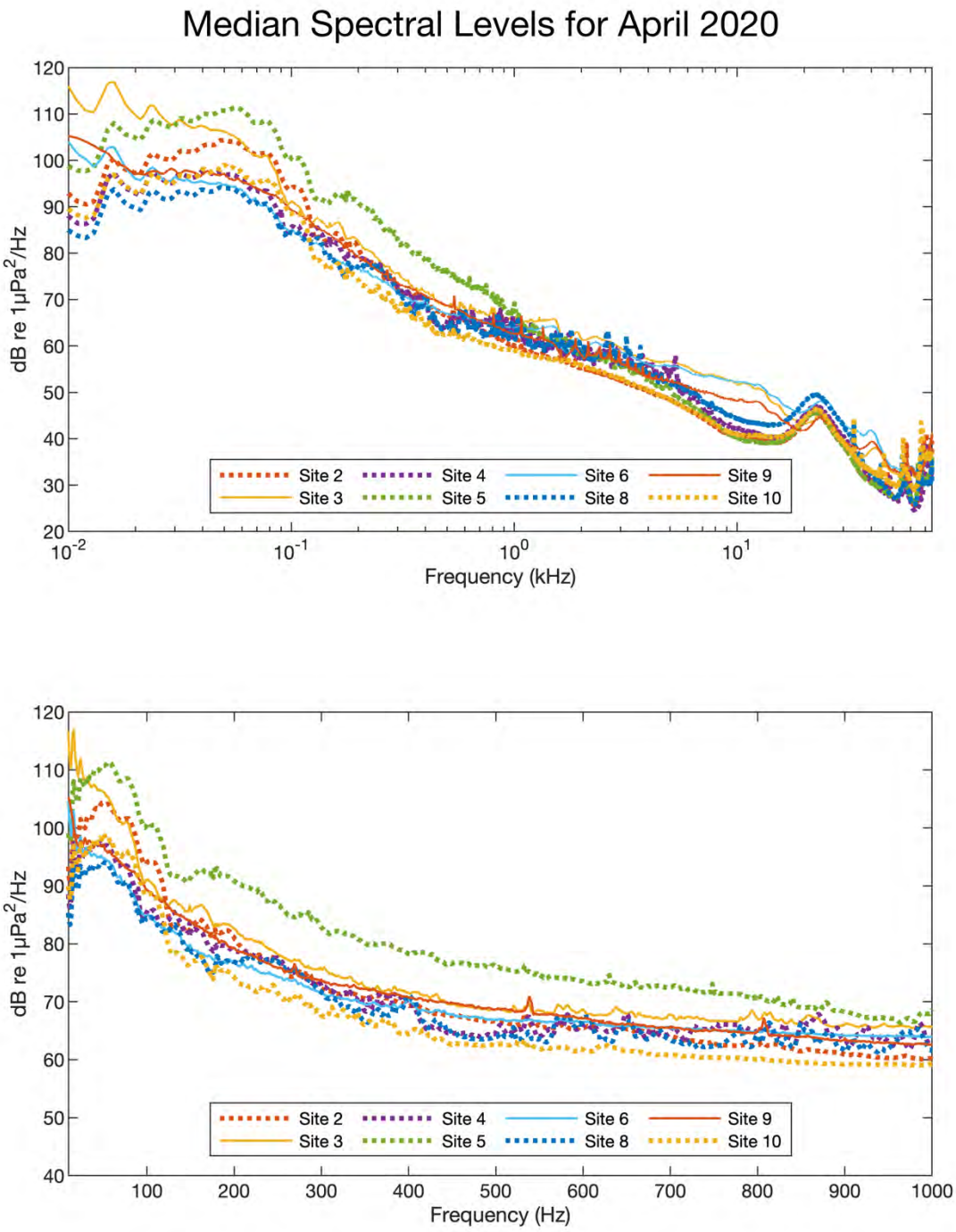

Figure E-C24. Median spectral values for April 2020

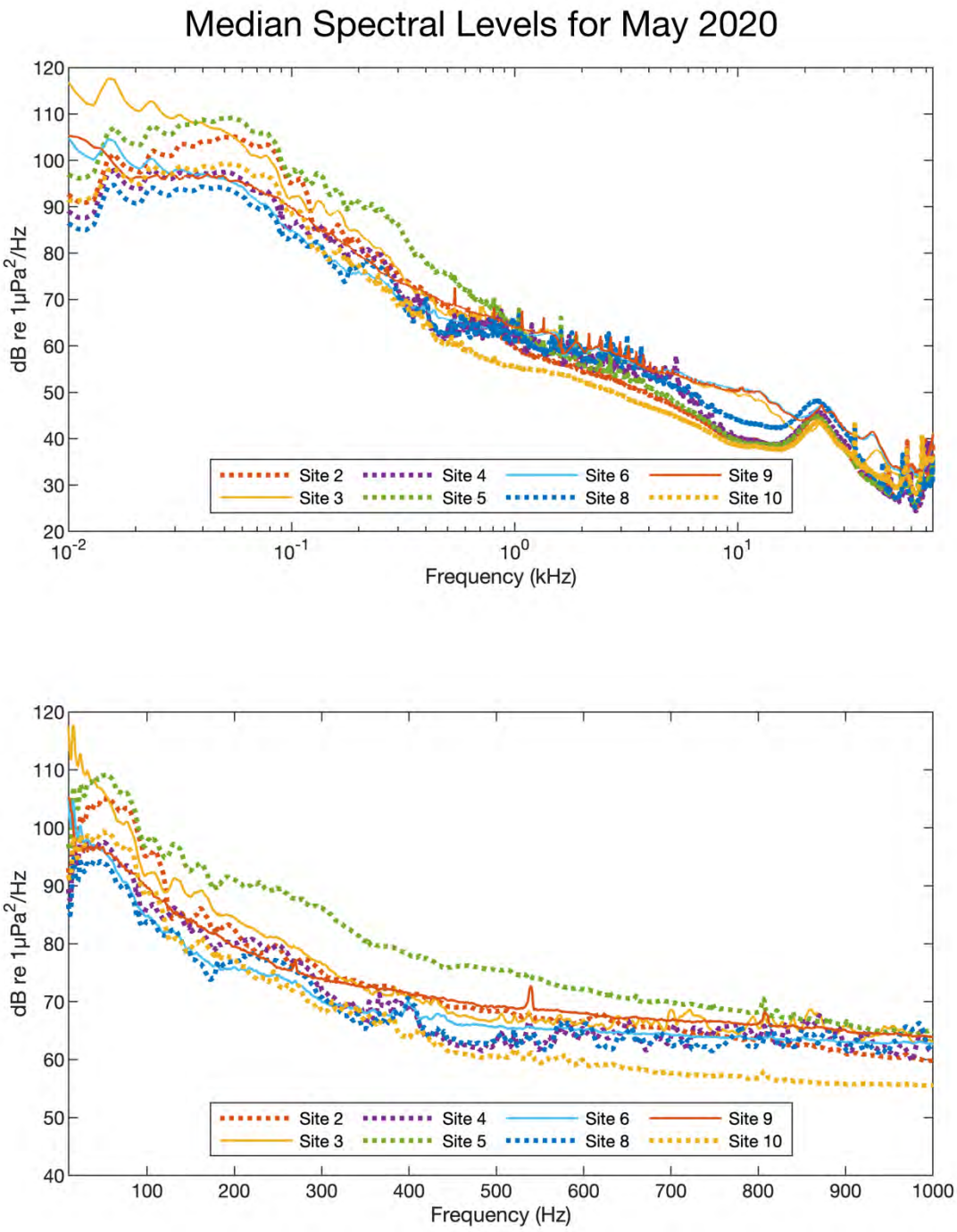

Figure E-C25. Median spectral values for May 2020

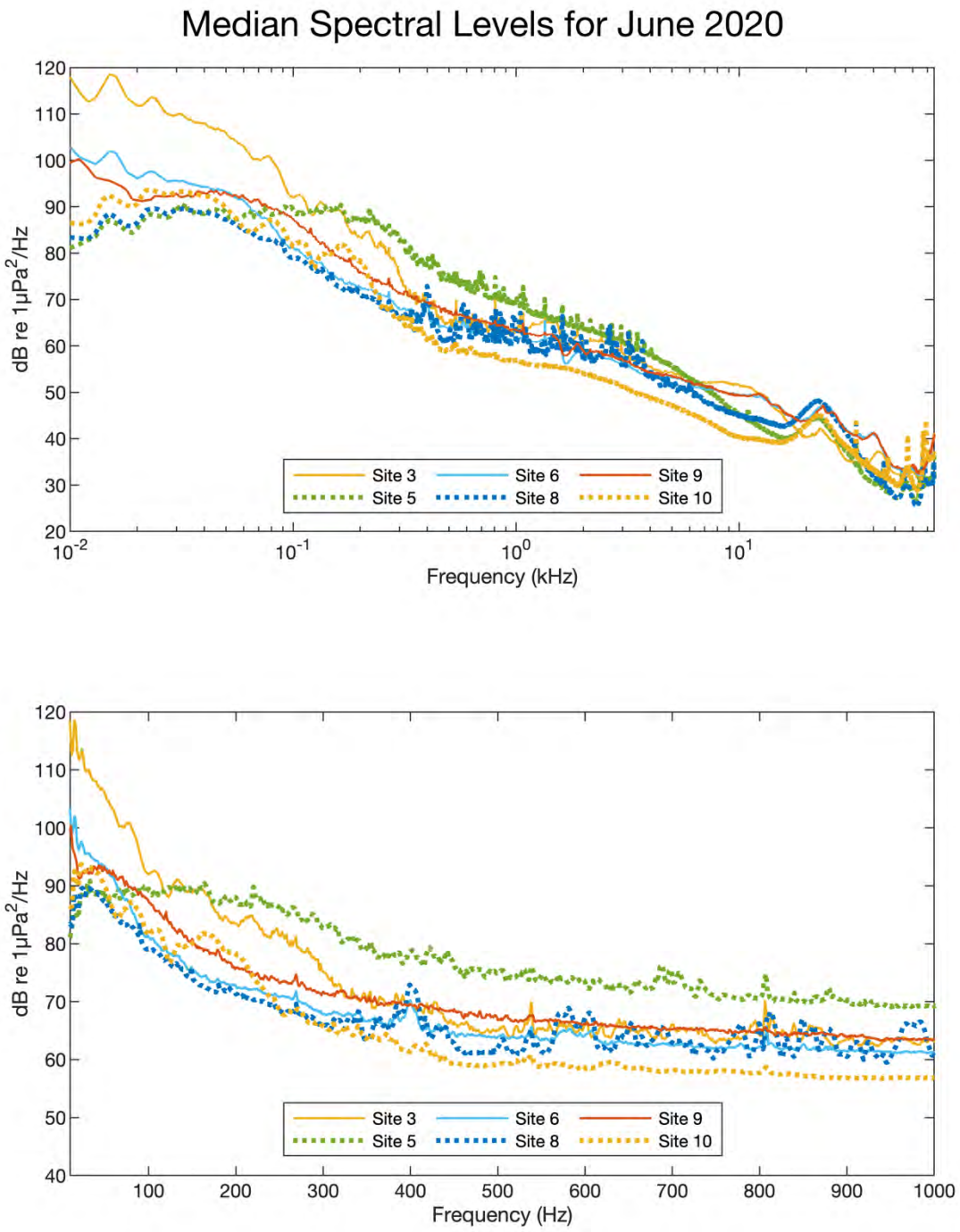

Figure E-C26. Median spectral values for June 2020

Department of the Interior (DOI)
The Department of the Interior protects and manages the Nation's natural resources and cultural heritage; provides scientific and other information about those resources; and honors the Nation’s trust responsibilities or special commitments to American Indians, Alaska Natives, and affiliated island communities.

Bureau of Ocean Energy Management (BOEM)
The mission of the Bureau of Ocean Energy Management is to manage development of U.S. Outer Continental Shelf energy and mineral resources in an environmentally and economically responsible way.

BOEM Environmental Studies Program
The mission of the Environmental Studies Program is to provide the information needed to predict, assess, and manage impacts from offshore energy and marine mineral exploration, development, and production activities on human, marine, and coastal environments. The proposal, selection, research, review, collaboration, production, and dissemination of each of BOEM’s Environmental Studies follows the DOI Code of Scientific and Scholarly Conduct, in support of a culture of scientific and professional integrity, as set out in the DOI Departmental Manual (305 DM 3).